C-H Functionalization of Imidazo-Heterocycles and Exploration of Imidazolium-Supported Benzotriazole Reagent for Selective Organic Transformations

THESIS

Submitted in partial fulfillment

of the requirements for the degree of

DOCTOR OF PHILOSOPHY

by

S M ABDUL SHAKOOR

ID. NO. 2012PHXF0018P

Under the supervision of

DR. RAJEEV SAKHUJA

DEPARTMENT OF CHEMISTRY
BIRLA INSTITUTE OF TECHNOLOGY AND SCIENCE
PILANI (RAJASTHAN) INDIA
2017

BIRLA INSTITUTE OF TECHNOLOGY AND SCIENCE
PILANI (RAJASTHAN)

CERTIFICATE

This is to certify that the thesis entitled **"C-H Functionalization of Imidazo-Heterocycles and Exploration of Imidazolium-Supported Benzotriazole Reagent for Selective Organic Transformations"** submitted by **Mr. S. M. ABDUL SHAKOOR**, ID No. **2012PHXF0018P** for the award of Ph.D. Degree of the Institute embodies the original work done by him under my supervision.

Signature in full of the Supervisor

Name in capital block letters: **Dr. RAJEEV SAKHUJA**
Designation: Assistant Professor, Birla Institute of Technology and Science Pilani, Pilani Campus, Rajasthan India.

Date:

Dedicated to

My Parents,

Wife and

Sister

ACKNOWLEDGEMENTS

First of all, I want to submit myself to the creator of everything ***"The Almighty Allah"*** who bestowed me with abundance of blessings and enabling me to make a material contribution in the field of research. Next, with humble submission and a deep sense of gratitude I want to extend my sincere thanks to my beloved family for their continuous love, support, and confidence. Their love and affection has really gone a long way in successful completion of thesis. It is their faith in me which has seen in this work through. A special thanks to my grandparents for their countless love and blessing. May Allah grant peace to their departed souls and provide special place in heaven.

Heartfelt thanks are extended to my research supervisor Dr. Rajeev Sakhuja, for his guidance, infrastructural support, and constant encouragement throughout the course of this study. His friendly disposition, constant encouragement, and moral support have always inspired me to go ahead in my research work with confidence and zeal.

I am immensely thankful to the Vice-Chancellor, Director, Dean Administration, Deans and Associate Deans of Birla Institute of Technology & Science, Pilani (BITS Pilani) for giving me the opportunity to pursue my doctoral studies by providing necessary facilities and financial support.

I highly appreciate the cooperation and affection extended by all the faculty members of the Department of Chemistry, BITS Pilani, which has made my stay here very productive. I express my sincere gratitude to my Doctoral Advisory Committee; Prof. Anil Kumar and Dr. Indresh Kumar. I also would like to extend my sincere thankfulness to Prof. S. C. Sivasubramanian, Prof. Subit K. Saha, Prof. Ram. K. Roy, Prof. Dalip Kumar, Prof. Anil Kumar, Prof. Saumi Ray (DRC Convener), Prof. Bharti Khungar (Head), Prof. Ajay K. Sah, Prof. Inamur R. Laskar, Dr. Madhushree Sarkar, Dr. Prashant U. Manohar, Dr. Paritosh Shukla, Dr. Indresh Kumar, Dr. Surojit Pande, Dr. Shamik Chakraborty, Dr. Bibhas R. Sarkar and staff members (Department of Chemistry, BITS Pilani, Pilani Campus) for their constant guidance. I am highly thankful to Dr. Kiran Bajaj for her valuable suggestion and surveillance. My sincere thanks to Mr. Giridhar Kunkur, Librarian, BITS Pilani and other staff of library for their support and help rendered while utilizing the library services. I acknowledge BITS Pilani for providing me Institute fellowship during the tenure of my Ph.D. In addition DST-FIST is also deeply acknowledged for providing instrumentation facilities in department.

This acknowledgement will be incomplete without mentioning my parents (Mr. Syed Mashkoor Alam and Mrs. Azima Begum). I have been blessed with an exemplary couple, as my parents whose presence has always worked as a solace in the moments of stress. Words and this limited space do not seem adequate enough to express my indebtedness to my venerable parents and sister (Ghazalah Shaheen) for their love, trust, and undeterred support. The acknowledgement of

their contribution has been indelibly imprinted on my mind. I deeply acknowledge a very special person and love of my life, who recently gave entry to my life and will continue the journey with me, my beloved wife Ghazala Nasrin. Completion of this thesis in anticipated time would have been difficult for me without her support.

The great inspiring and congenial atmosphere along with the achievements made in Lab 3110 are one of the most memorable things in my life. I am felling very happy and proud to thanks my compassionate and ever caring juniors (Ms. Santosh Kumari and Mr. Devesh S Agarwal). My heartfelt thanks to my labmates and seniors, Dr. Chandra Sekhar, Dr. Bhupinder Mishra, Dr. Kiran Soni, Dr. Mukund Tantak, Dr. V. Arun, Dr. Meenakshi, Dr. Noorullah Baig, Mr. Manish, Mr. Santosh Khandagale, Mr. Vimal, Mr. Chaitanya, Mr. Bintu Kumar, for their untiring and continued support in last five year. I always had a hearty inspiration from my senior friends, Dr. Parvej Alam, Dr. Kameswara Rao and Dr. Manoj Kumar Muthyala. I extend my heartfelt thanks to my best friends Tabarak Hussain, Ravikanth, Mr. Sheikh Saleem Pasha, Dr. Nisar Ahmed Mir and Mr. P. O. V Ramana Reddy. I am really fortunate and blessed to meet a wonderful couple Mr. Pradeep Choudary and Mrs. Santosh Kumari and I am also thankful to Manth parivaar for their love and affection. It was their love and care which make my stay at pilani more enjoyable and memorable. Words come short to thank number people here in the department of chemistry: (Dr. Ganesh Shelke, Dr. Sunita, Ms. Pankaj Nehra, Dr. Pinku, Mr. Anoop Singh, Mr. Hitesh, Mr. Shiv, Mr. Nitesh, Mr. Fayaz Baig, Mr. Vishal, Ms. Pallavi Rao, Ms. Khima, Ms. Saroj, Ms. Vaishali, Ms. Sonam, Ms. Susheela, Ms. Moyna Das, Ms. Sunita) for their continuous support and charming company during the whole thesis work. I am cheerful in acknowledging a cute baby Master Guddu, who supplemented lots of happiness and joy in my life. My research life in BITS Pilani would have been imperfect without your support deserves my warm thanks for their wonderful helping attitude and for providing an affable environment at the workplace.

Finally, there are many more relatives, friends, and well-wishers whose faith, encouragement, and constant moral support has contributed in a big way in the completion of this work. I express my sincere and special thanks to all of them.

S. M. ABDUL SHAKOOR

ABSTRACT

Synthesis and functionalization of aza-fused heterocycles are considerd as most valuable targets in synthetic chemistry because of their broad range of applications in the field of medicinal and material chemistry. The thesis entitled "**C-H Functionalization of Imidazo-Heterocycles and Exploration of Imidazolium-Supported Benzotriazole Reagent for Selective Organic Transformations**" deals with the functionalization of imidazo[1,2-*a*]pyridine (IP) scaffold *via* conventional heterocyclization, metal-catalyzed C-H activation and metal-free oxidative coupling reactions. In addition, the thesis systematically documents the synthesis and exploration of novel imidazolium-supported benzotriazole reagent as carboxylic acid activator. The thesis is divided into six chapters.

The first chapter of the thesis presents a brief description on recent C-H functionalization reaction on imidazo[1,2-*a*]pyridine, providing a momentary look of imidazo[1,2-*a*]pyridine based works conducted by synthetic chemists in the past.

The second chapter of thesis presents a microwave-assisted strategy for the synthesis of imidazo[1,2-*a*]pyridyl appended quinoxalin-2(1*H*)-ones. The desired products were synthesized by reacting prior synthesized imidazo[1,2-*a*]pyridine-3-glyoxalates and *ortho*-phenylene diamine using montmorillonite K-10 under solvent-free condition or $Yb(OTf)_3$ in THF. This Hinsberg heterocyclization reaction showcased good compatibility with a wide variety of substituted imidazo[1,2-*a*]pyridines resulting in the formation of described products in 20-82% yields, under environmentally being reaction conditions.

The third chapter of the thesis describes a significant exploration of transition metal-catalyzed strategies towards the direct synthesis of functionalized imidazo-heterocycles. The chapter is divided into two parts: **Part A:** presents the copper-catalyzed direct aerobic cross-dehydrogenative coupling of imidazo-heterocycles and aryl acetaldehydes, synthesizing dicarbonylated imidazo-heterocycles in 55-85% yields. The scope of the reaction was generalized with differently substituted electron-rich and electron-deficient imidazo[1,2-*a*]pyridines and aryl acetaldehydes. Wherein the **Part B:** describes a regioselective Ru(II)-catalyzed strategy for the *ortho*-amidation of 2-arylimidazo[1,2-*a*]pyridines with aryl isocyanates *via* Csp^2–H bond activation in 30-78% yields. An array of *ortho*-amidated 2-arylimidazo[1,2-*a*]pyridines with different functionalities on aryl and pyridyl rings were

synthesized in good-to-excellent yields. The scope of the methodology was further expanded with phenylimidazo[2,1-*b*]thiazole, 2-phenylbenzo[*d*]imidazo[2,1-*b*]thiazole, and 2-phenyl imidazo[1,2-*a*]pyrimidines by synthesizing respective *ortho*-amidated products in appreciable yields.

The fourth chapter of the thesis describes the significant exploration of metal-free strategies towards the homocoupling of imidazo-heterocycles. This chapter is also divided into two parts: **Part A:** describes an efficient transition metal-free, phenyliodine diacetate (PIDA)-mediated, $BF_3{\cdot}OEt_2$-accelerated oxidative homocoupling of 2-arylimidazo[1,2-*a*]pyridines for the synthesis of 3,3′-biimidazo[1,2-*a*]pyridines in moderate-to-good yields. The methodology was also extended by synthesizing, biimidazo[2,1-*b*]thiazoles and bibenzo[*d*]imidazo[2,1-*b*]thiazoles under similar reaction conditions. In addition, an organocatalytic approach for the desired transformation employing catalytic amount of iodobenzene with *m*-CPBA/AcOH was also executed. On other way **Part B:** describes the utility of molecular iodine for the oxidative direct homocoupling of imidazo-heterocycles using Na_2S as a sulfur source for predominant synthesis of bis(imidazo[1,2-*a*]pyridin-3-yl)sulfanes and bis(imidazo[1,2-*a*]pyridin-3-yl)disulfanes under variable solvent conditions. These direct oxidative strategies for the synthesis of bis-sulfanes and bis-disulfanes were well exemplified with a broad range of substituted 2-arylimidazo[1,2-*a*]pyridines.

The fifth Chapter of the thesis presents a brief background of different imidazolium-supported reagents, and their application in various organic transformations. Later on, the chapter deals with a detailed synthetic protocol for the synthesis of imidazolium-supported benzotriazole reagent (Im-BtH) as a novel synthetic auxiliary. Thereafter, eight different *N*-acylated imidazolium-supported benzotriazole reagents (Im-BtCOR) were prepared and exemplified as greener carboxyl group activating reagents for the synthesis of library of amides, esters and thioesters in aqueous medium under microwave irradiation. The methodology was proved to be scalable at gram scale by synthesizing Paracetamol in 93% yield. The reagent was successfully recovered and reused five times without any noticeable loss in activity.

Finally, in **the sixth chapter** of the thesis, a summary of the thesis work is presented along with future scope of the research work.

LIST OF TABLES

LIST OF FIGURES

LIST OF ABBREVIATIONS / SYMBOLS

Abbreviation/Symbol	Description
α	Alpha
β	Beta
γ	Gamma
Δ	Delta
°C	Degree centigrade
Å	Angstrom
AcOH	Acetic acid
ACN	Acetonitrile
Ar	Aryl
AMPA	α-amino-3-hydroxy-5-methyl-4-isoxazolepropionic acid
Aq	Aqueous
[Bmim][BF_4]	1-Butyl-3-methylimidazolium tetrafluoroborate
Bn	Benzyl
t-BuOK	Potassium *tert*-butoxide
t-BuONO	*tert*-Butyl nitrite
Cat.	Catalytic
^{13}C	Carbon-13
CDC	Cross-dehydrogenative coupling
m-CPBA	*meta*-Chloroperoxybenzoic acid
d	Doublet
dd	Doublet of doublet
DABCO	1,4-Diazabicyclo[2.2.2]octane

DBU	1,8-Diazabicyclo[5.4.0]undec-7-ene
DCE	1,2-Dichloroethane
DCM	Dichloromethane
DCP	Dicumyl peroxide
DDQ	2,3-Dichloro-5,6-dicyano-1,4-benzoquinone
DIAD	Diisopropyl azodicarboxylate
DLP	Dilauroylperoxide
DMAc	Dimethylacetamide
DMAP	4-Dimethylaminopyridine
DME	Dimethoxyethane
DMF	*N*,*N*-Dimethylformamide
DMSO-d_6	Deuterated dimethylsulfoxide
DMSO	Dimethylsulfoxide
DNA	Deoxyribonucleic acid
DTC	Dithiocarbamate
EI	Electron Ionization
[emim][BF_4]	1-Ethyl-3-methylimidazolium tetrafluoroborate
ESI-MS	Electron Spray Ionization Mass Spectrometry
ESI-TOF	Electron Spray Ionization-Time of Flight
EtOAc	Ethyl acetate
EtOH	Ethanol
equiv.	Equivalent
g	Gram
GABA	Gamma-aminobutyric acid
h	Hours

HFIP	Hexafluoroisopropanol
HRMS	High Resolution Mass Spectra
4-HOTEMPO	4-Hydroxy-2,2,6,6-tetramethylpiperidin-1-oxyl
HTIB	[Hydroxy(tosyloxy)iodo]benzene
IBD	Iodobenzene diacetate
IBX	2-Iodoxybenzoic acid
ILs	Ionic liquids
IR	Infra-red
Hz	Hertz
IP	Imidazo[1,2-*a*]pyridines
J	Coupling constant
KOAc	Potassium acetate
Lit.	Literature
LXR	liver X receptor
mp	Melting point
m	Multiplet
mg	Milligram
MHz	Mega hertz
min	Minutes
mmol	Millimole
MW	Microwave
N_2	Nitrogen
NBS	*N*-bromosuccinimide
NCS	*N*-chlorosuccinimide
NMP	N-Methyl-2-pyrrolidone

NMR	Nuclear Magnetic Resonance
NIP	Naphtho[1′,2′:4,5]imidazo[1,2-*a*]pyridine
Nu	Nucleophile
O_2	Oxygen
PAMs	Positive Allosteric Modulators
PEG400	Polyethylene Glycol400
Phen	1,10-Phenanthroline
PIDA	Phenyl iodonium diacetate
PIFA	(Bis(trifluoroacetoxy)iodo)benzene
PivOH	Pivalic acid
ppm	Parts per million
%	Percentage
r.t.	Room temperature
s	Singlet
SAR	Structure-activity relationship
SET	Single electron transfer
t	Triplet
TEA	Triethyl amine
TFA	Trifluoroacetic acid
TBAB	Tetrabutylammonium bromide
TBHP	*tert*-Butyl hydroperoxide
TEMPO	2,2,6,6-tetramethylpiperidine-1-oxyl
THF	Tetrahydrofuran
TLC	Thin layer chromatography
TMDEA	Tetramethylethylenediamine

TMS	Tetramethylsilane
TMSCl	Trimethylsilyl chloride
TMPMgCl	2,2,6,6-Tetramethylpiperidinylmagnesium chloride
TosMIC	*p*-Toluenesulfonylmethyl isocyanide
-OTf	Triflouromethanesulfonate
δ	Parts per million
Xphos	XPhos [2-Dicyclohexylphosphino-2′,4′,6′-triisopropylbiphenyl]

TABLE OF CONTENTS

CHAPTER 1

Recent Advancements in C-H Functionalization of Imidazo[1,2-*a*]pyridines

1.1 Introduction

Heterocycles constitute the largest classical division of organic compounds. The extensive use of heterocyclic compounds in the pharmaceutical industry is perhaps attributable to the availability of ample range of reactions that facilitate subtle structural modifications in them. In particular, nitrogen-containing heterocycles have gained much attention due to their utility as valuable intermediates for diverse synthetic transformations.[1] Aza-fused heterocycles comprise a family of biological agents with interesting pharmacological properties, and consequently to its DNA intercalating ability that make them suitable candidates as anti-neoplastic and mutagenic agents.[2,3]

Among various aza-fused heterocyclic systems, imidazo[1,2-*a*]pyridine (IP) (**1**) has been recognized as a privileged scaffold because of its versatile biological profile including, anti-HIV, antiviral, antimicrobial, antitumor, anti-inflammatory, anti-parasitic and hypnotic activities.[4-10] In addition, the core skeleton is found in numerous commercially available drugs such as Alpidem, Saripidem, Zolpidem, Nicopidem, Zolimidine, Miroprofen, Minodronic acid (Figure 1.1.1).[11-16] IP derivatives are also used as *β*-amyloid formation inhibitors, GABA and benzodiazepine receptor agonists, and cardiotonic agents.[17-19]

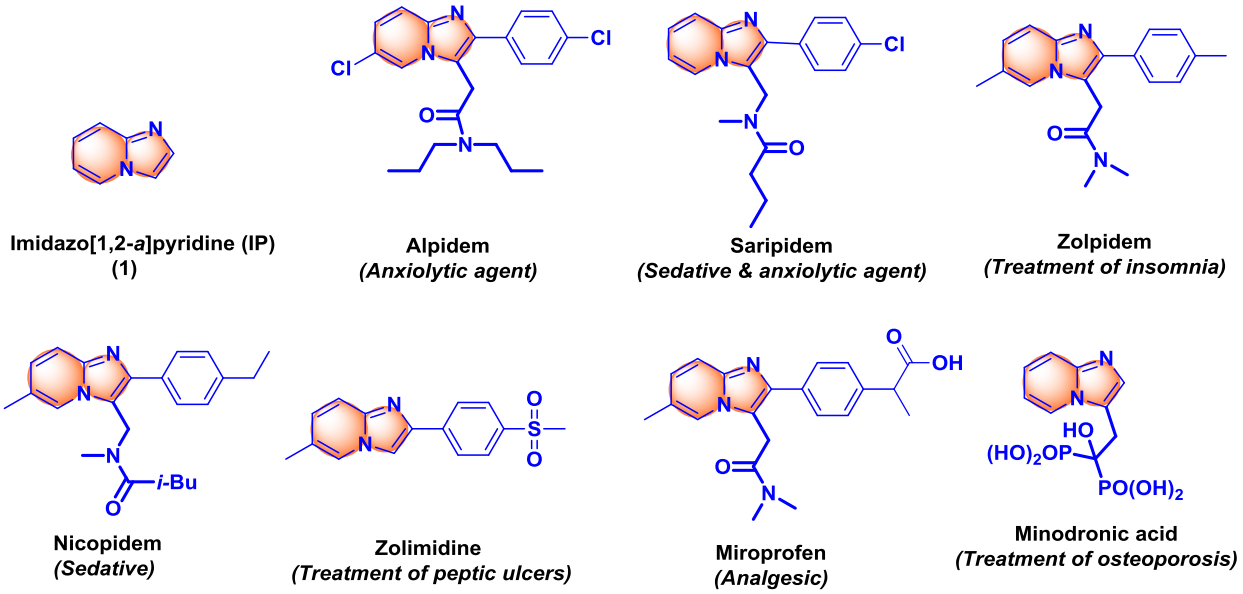

Figure 1.1.1: Currently marketed functionalized imidazo[1,2-*a*]pyridine based drugs

Apart from biological value, imidazo[1,2-*a*]pyridine exhibits profound applications in the field of material science and agro chemistry. Moreover, the structure activity relationship (SAR) studies on functionalized imidazo[1,2-*a*]pyridines (**1**) unveil the great dependency of

substituents at the C-2 and C-3 positions.[20] The applicative value of substituted IPs has stimulated considerable attention of our group, and other organic chemists toward the construction of functionalized imidazo[1,2-*a*]pyridines.

Chemically, imidazo[1,2-*a*]pyridine is an electron-rich hetero-aromatic compound that readily undergo electrophilic substitution reaction preferably at the C-3 position. The functionalizations at C-3 position of the imidazo[1,2-*a*]pyridine scaffold have been exemplified *via* four major strategies:

1. Direct electrophilic substitution
2. Metal-catalyzed cross-coupling reaction
3. Metal-catalyzed direct C-H activation
4. Metal-free C-H activation

A broad classification on various C-H functionalizations of imidazo[1,2-*a*]pyridine (**1**) is depicted in Figure 1.1.2

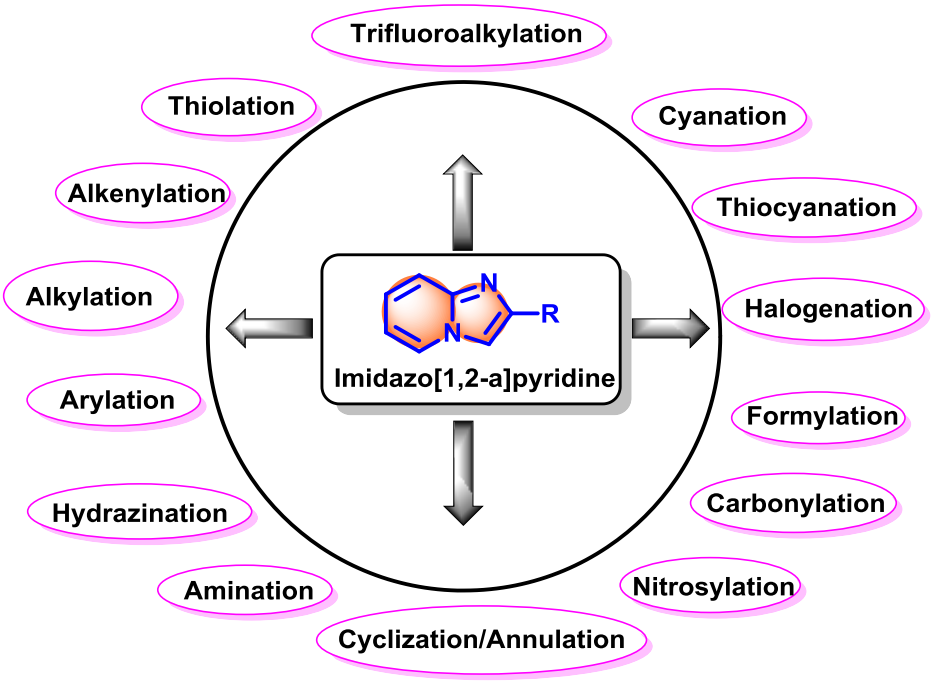

Figure 1.1.2: A representative diagram depicting various functionalizations on imidazo[1,2-*a*]pyridine

This chapter briefly describes some recent developments in C-H functionalizations of imidazo[1,2-*a*]pyridines on the basis of nascent bond formation *via* Csp^2-H bond activation.

1.2 C-C Bond formations

Csp^2-Csp^2 bond formation: C-H arylation of imidazo[1,2-*a*]pyridines

Cross-coupling reactions have received remarkable attention of organic chemists. The considerable interest in this approach towards constructing aryl-(hetero)aryl C-C bonds have been successfully employed for the syntheses of natural products, agrochemicals, polymers, pharmaceuticals, and their precursors. In particular, 3-arylimidazo[1,2-*a*]pyridine is often cited as the core structural framework of various bioactive compounds, such as liver X receptor (LXR) agonists,[21] GABAAα2/α3[22] agonists, γ-secretase modulators (GSMs),[23] and positive allosteric modulators (PAMs) of metabotropic glutamate 2 receptor (Figure 1.2.1).[24]

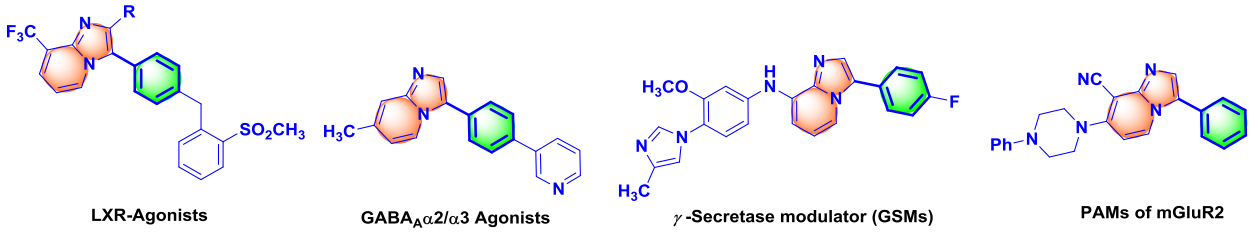

Figure 1.2.1: Selective examples of biologically active 3-arylimidazo[1,2-*a*]pyridines

In this regard, various metal-catalyzed strategies have been developed toward the C-3 arylation of imidazo[1,2-*a*]pyridine (**1**) in recent times. Chakravarty *et al.* documented phosphine-free Pd-catalyzed direct arylation of 2-arylimidazo[1,2-*a*]pyridines (**1**) with different aryl iodides (**2**) using silver(I) carboxylate. The presented C-H arylation was equally effective with a variety of electron-rich and electron-deficient 2-arylimidazo[1,2-*a*]pyridines (**1**), yielding C-3 arylated products in moderate-to-good yields (Scheme 1.2.1a).[25] Similarly, Doucet and coworkers also reported phosphine-free direct arylation of substituted imidazo[1,2-*a*]pyridines (**1**) with aryl bromides (**3**) using palladium catalyst in dimethylacetamide. In this case, electron-deficient aryl bromides (**3**) offered high yields of arylated products (Scheme 1.2.1b).[26] Cao *et al.* used aryl chlorides **4** as coupling partner for the direct arylation of substituted imidazo[1,2-*a*]pyridines (**1**) using $Pd(OAc)_2$ in association with 10 mol % of $BuAd_2P$. The methodology was effective with various substituted aryl chlorides (**4**), albeit failed with strong electron-withdrawing and strong electron-donating groups such as nitro and methoxy, respectively (Scheme 1.2.1c).[27] Wang and Kwong group achieved C-3 arylation with aryl tosylates (**5**) or mesylates (**6**) by employing $Pd(OAc)_2$ associated with **L1** SPhos (2-dicyclohexylphosphino-2′,6′-dimethoxybiphenyl) or **L2** (2-(2-(diisopropylphosphino)-phenyl)-1-methyl-1*H*-indole) (Scheme 1.2.1d).[28] Raboin *et al.*

described C-3 arylation of substituted imidazo[1,2-*a*]pyridines (**1**) under microwave-induced condition using palladium catalyst in the presence of triphenylphosphine. Various substituted aryl or heteroaryl bromides (**3**) were treated with a ample range of substituted imidazo[1,2-*a*]pyridines (**1**) to give 2,3,6-trisubstituted imidazo[1,2-*a*]pyridines **7** in good-to-excellent yields (Scheme 1.2.1e).[29] Lee and coworkers used magnetically recyclable Pd-Fe_3O_4 nanoparticles for the regioselective C-3 direct arylation of substituted imidazo[1,2-*a*]pyridines (**1**) with aryl bromides (**3**). The scope of the reaction was examined with different electron-deficient and electron-rich as well as sterically-hindered aryl bromides (**3**) (Scheme 1.2.1f).[30] Recently, Cao and his teammate reported Pd-catalyzed direct cross-coupling of substituted imidazo[1,2-*a*]pyridines (**1**) with aryl boronic acids (**8**) using $Cu(OAc)_2$ in presence of palladium catalyst forming a multi-substituted imidazo[1,2-*a*]pyridines **7**. Presence of electron-donating and electron-withdrawing groups on imidazo[1,2-*a*]pyridines did not altered the product yield, albeit the reactivity was dependent on the position of substituents (Scheme 1.2.1g).[31]

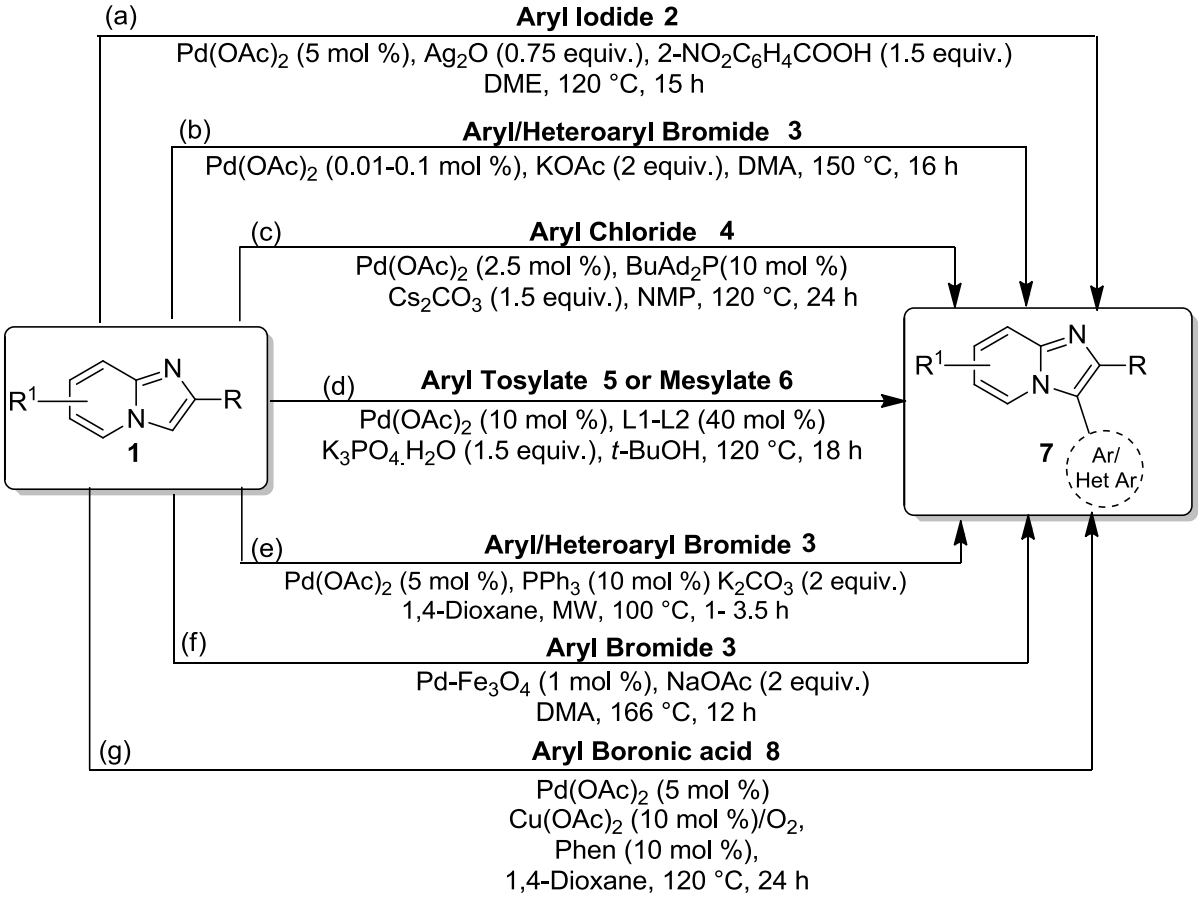

Scheme 1.2.1: Pd-catalyzed C-3 arylation of imidazo[1,2-*a*]pyridines (**1**)

Ruthenium(II) catalyst was elegantly employed by Yang *et al.* towards the regioselective C-3 arylation of substituted imidazo[1,2-*a*]pyridines (**1**) with different aryl halides, affording C-3 arylated imidazo[1,2-*a*]pyridines (**7**) (Scheme 1.2.2a). The developed methodology preceded by insertion of Ru complex to C–H bond followed by formation of a cationic three-member cyclic intermediate.[32] Thereafter, Cui and coworkers utilized Rhodium(III) catalyst for the same transformation. A variety of aryl halides or triflates **9** were evaluated under the described conditions, affording the corresponding C-3 arylated product in good-to-excellent yields (Scheme 1.2.2b).[33]

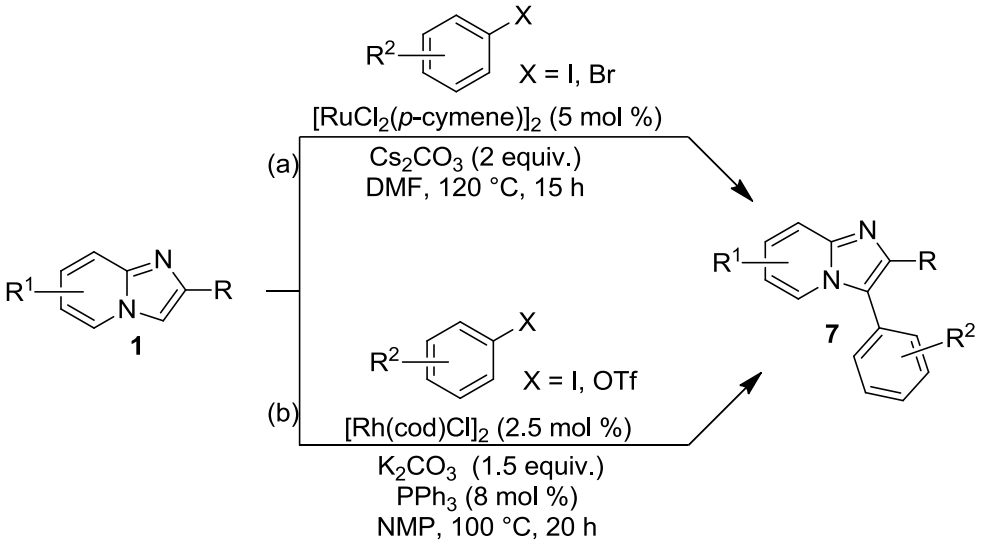

Scheme 1.2.2: Ru/Rh-catalyzed C-3 arylation of imidazo[1,2-*a*]pyridines (**1**)

Further in 2012, Cao and coworkers improved the direct C-3 arylation methodology by employing inexpensive copper(I) catalytic system. Reaction of different aryl iodides (**2**), aryl bromides (**3**), and triflates (**9**) with a range of substituted imidazo[1,2-*a*]pyridines (**1**) gave the C-3 arylated products **7** in good-to-excellent yields (Scheme 1.2.3). Unfortunately, arylation using heteroaryl halides could not flourish the desired products. The reaction was described to proceed through base-mediated C–H proton abstraction followed by transmetalation with copper, which further undergoes oxidative addition of aryl halide.[34]

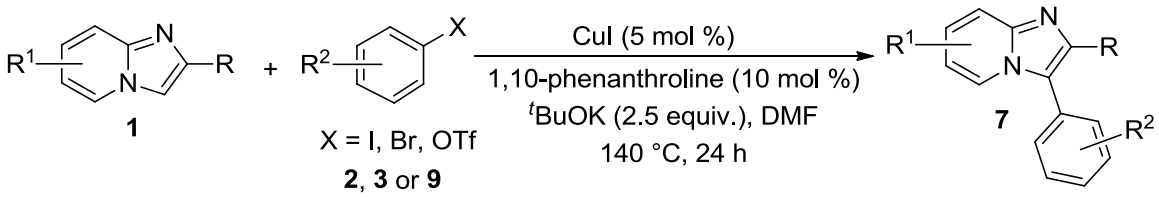

Scheme 1.2.3: Cu-catalyzed C-3 arylation of imidazo[1,2-*a*]pyridines (**1**)

Zhan *et al.* achieved C-3 arylation *via* direct oxidative coupling reaction of imidazo[1,2-*a*]pyridines (**1**) with completely unactivated arenes **10,** employing palladium catalyst with suitable oxidant Ag_2CO_3 and additive. The reaction exhibited excellent selectivity and broad range of functional group tolerance including different electron-rich and electron-deficient substrates (Scheme 1.2.4).[35]

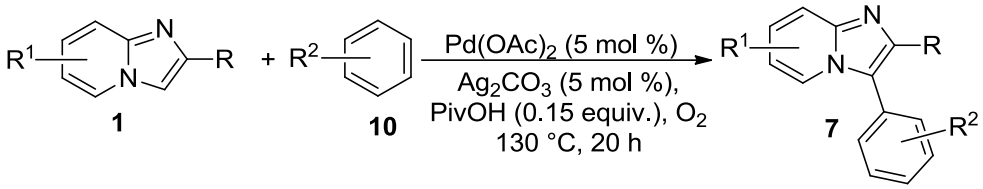

Scheme 1.2.4: Pd-catalyzed direct oxidative C-3 arylation of imidazo[1,2-*a*]pyridines (**1**)

Recently, Tang *et al.* reported metal-free heteroarylation *via* deaminative cross-coupling of substituted imidazo[1,2-*a*]pyridines (**1**) with 2-aminobenzothiazole (**11**) in presence of KOAc and *t*-butylnitrite in 1,2-dichloroethane. A wide substrate array of imidazo[1,2-*a*]pyridines with electron-deficient, electron-rich and sterically hindered groups were examined (Scheme 1.2.5). The reaction was proposed to proceed through the formation of diazonium salt, followed by deamination and subsequent coupling with substituted imidazo[1,2-*a*]pyridines (**1**).[36]

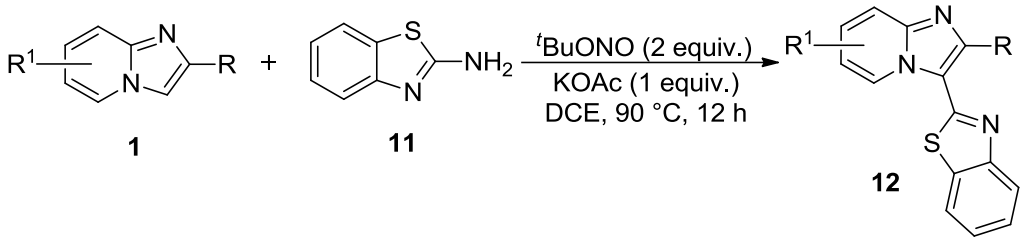

Scheme 1.2.5: Metal-free heteroarylation of imidazo[1,2-*a*]pyridines (**1**)

Csp^2-Csp^2 bond formation: C-H alkenylation of imidazo[1,2-*a*]pyridines

C-H Alkenylation of arenes and hetroarenes has been an important step in the synthesis of numerous natural products and pharmaceuticals. Within this relam, Fujiwara-Moritani reaction[37] is one of the most important Pd-catalyzed oxidative coupling reaction of arenes with olefins that has proven to be a valuable tool for the steroselective synthesis of substituted alkenes in recent years. In this regard, Raboin *et al.* synthesized C-3-alkenylated imidazo[1,2-*a*]pyridines **16** by reacting various substituted bromoalkenes **13** with substituted imidazo[1,2-*a*]pyridines (**1**) *via* C-H activation process using palladium as catalyst and triphenylarsine as ligand under basic conditions (Scheme 1.2.6a).[38] Later, same group improved the strategy by employing vinyl

ketones (**14**) and alkyl acrylates (**15**) for *β*-selective oxidative C-3 alkenylation of imidazo[1,2-*a*]pyridines (**1**) under Pd-catalyzed conditions using copper acetate as external oxidant.[39]

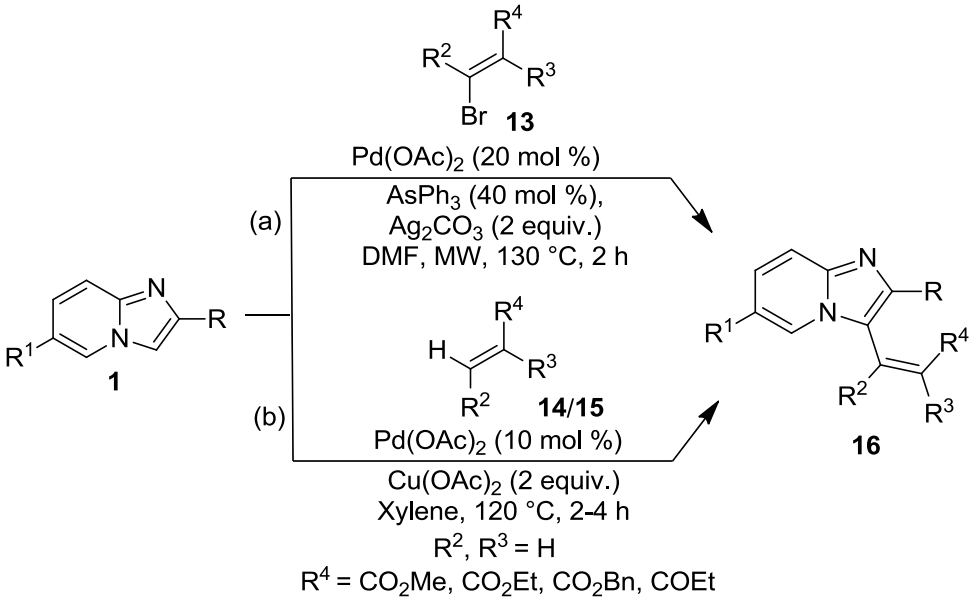

Scheme 1.2.6: Pd-catalyzed regioselective C-3 alkenylation of imidazo[1,2-*a*]pyridines (**1**)

Moreover, Hajra group synthesized alkenylated imidazo[1,2-*a*]pyridines **18** *via* aerobic cross-dehydrogenative coupling between substituted imidazo[1,2-*a*]pyridines (**1**) and alkenes **17** under Pd-catalyzed ligand-free conditions using TBAB. (Scheme 1.2.7).[40]

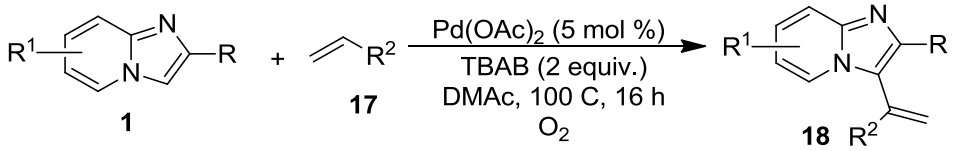

Scheme 1.2.7: Pd-catalyzed *α*-selective alkenylation of imidazo[1,2-*a*]pyridines (**1**)

Interestingly, Ru(II) complex was effectively utilized by Sawant and Pardasani *et al.* for the regioselective *ortho* C–H bond alkenylation of 2-arylimidazo[1,2-*a*]pyridines (**1**) *via* internal coordination of imidazolyl nitrogen (N1), yielding 2-(2′-alkenylphenyl)imidazo[1,2-*a*]pyridines (**19**) in moderate-to-excellent yields (Scheme 1.2.8).[41]

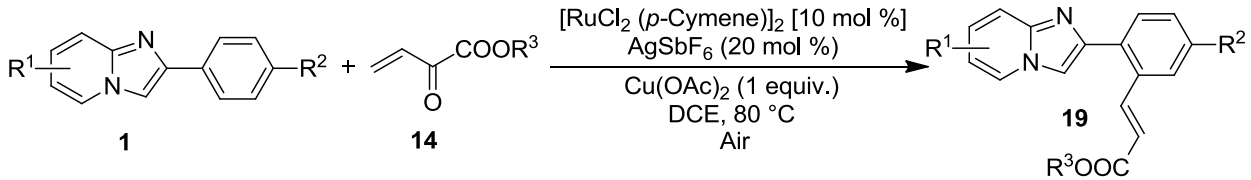

Scheme 1.2.8: Ru-catalyzed *ortho*-alkenylation of 2-arylimidazo[1,2-*a*]pyridines (**1**)

Hajra and coworkers also synthesized allenes decorated imidazo[1,2-*a*]pyridines by the reaction of 1,1,3-triphenylprop-2-yn-1-ol (**20**) and substituted imidazo[1,2-*a*]pyridines in the presence of $Zn(OTf)_2$ in toluene (Scheme 1.2.9). The general substrate variability were examined by varying substituents on pyridine and 2-aryl ring of imidazo[1,2-*a*]pyridines. The reaction mechanism was described to proceed *via* S_N2' pathway.[42]

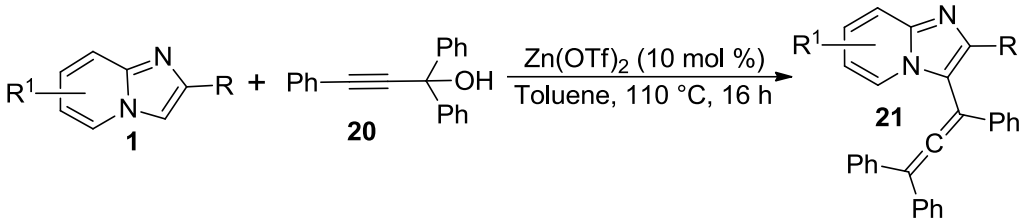

Scheme 1.2.9: Zn-catalyzed C-3 allenylation of imidazo[1,2-*a*]pyridines (**1**)

Csp^2-Csp^2 bond formation: C-H formylation/carbonylation of imidazo[1,2-*a*]pyridines

Owing to the remarkable applicative value of formylated (hetero)arenes in synthetic chemistry, and to replace the classical Vilsmeier–Haack,[43,44] Reimer–Tiemann,[45,46] Rieche,[47] and Friedel–Crafts acylations reactions,[48] Cao *et al*. reported a Cu-catalyzed C-3 formylation of imidazo[1,2-*a*]pyridines (**1**) with dimethyl sulfoxide (**22**), utilizing molecular oxygen as the terminal oxidant (Scheme 1.2.10a).[49] The reaction was described to proceed *via* single electron transfer (SET) radical pathway. Afterwards, Liu and coworkers prepared the same C-3 formylated products (**23**) under Fe(III)-catalyzed conditions using dimethyl sulfoxide (**22**) as the carbon source. A similar single electron transfer oxidation process involvement was proposed with the assistance of ferric chloride and molecular oxygen (Scheme 1.2.10b).[50]

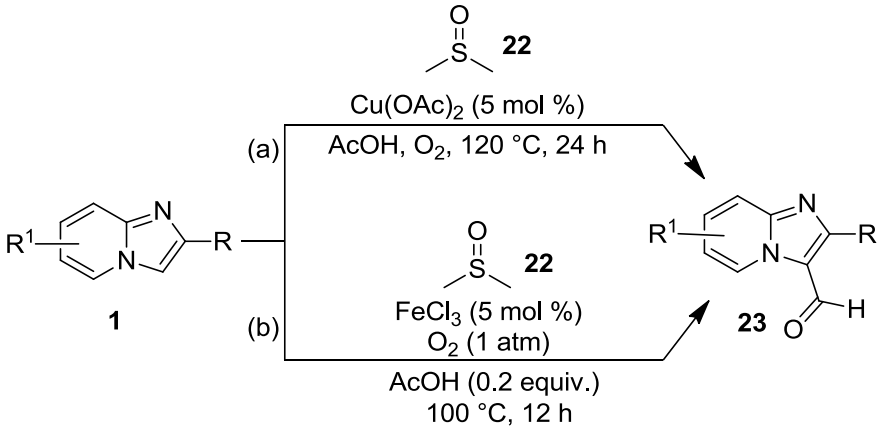

Scheme 1.2.10: Cu/Fe-catalyzed C-3 formylation of imidazo[1,2-*a*]pyridines (**1**)

The direct introduction of carbonyl group in a heterocyclic system is highly desirable due its prevalent presence in various natural products, commercialized drugs and synthetic materials. Cao *et al.* developed a Cu-catalyzed cross-coupling strategy for amalgamation of C(sp^2)-H and Csp^3-H bonds between substituted imidazo[1,2-*a*]pyridines (**1**) and methyl heteroarenes **24** to obtain C-3 carbonylated imidazo[1,2-*a*]pyridines **25**. Other heterocycles such as 2-methylquinoline, 2-methylpyrazine, 2-chloro-3-methylpyrazine, and 2,5-dimethylthiazole were also used to carbonylate imidazo[1,2-*a*]pyridines in moderate-to-good yields (Scheme 1.2.11). The reaction was described to proceed through the formation of peroxo radical species in TFA under oxygen environment *via* SET mechanism.[51]

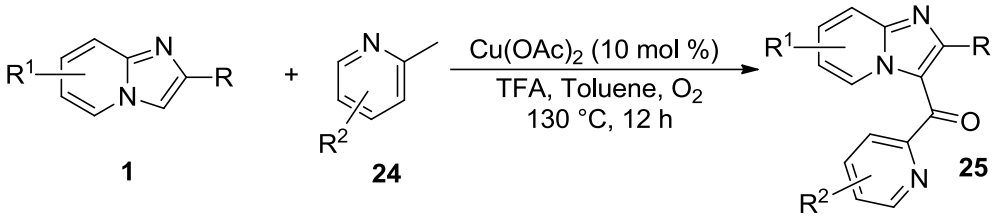

Scheme 1.2.11: Cu-catalyzed C-3 carbonylation of imidazo[1,2-*a*]pyridines (**1**)

Similarly, direct introduction of ester group to organic molecule is undoubtly appreciable as it can be easily converted into diverse functional groups such as hydroxymethyl, carbonyl, amide, *etc*. With this anticipation, Sun and coworkers developed a regioselective Fe-catalyzed strategy for the alkoxycarbonylation of substituted imidazo[1,2-*a*]pyridines (**1**) using carbazates **26**, in presence of oxidant $(NH_4)_2S_2O_8$ in DMSO (Scheme 1.2.12). The scope of the reaction was efficiently evaluated by investigating a variety of 2-arylimidazo[1,2-*a*]pyridines possessing electron-donating and electron-withdrawing groups. The reaction was depicted to proceed through radical mechanism by the formation of alkoxycarbonyl radical intermediate *via* sequential SET process followed by deprotonation steps to afford the described products **27** in the presence of Fe(II) and $S_2O_8^{2-}$.[52]

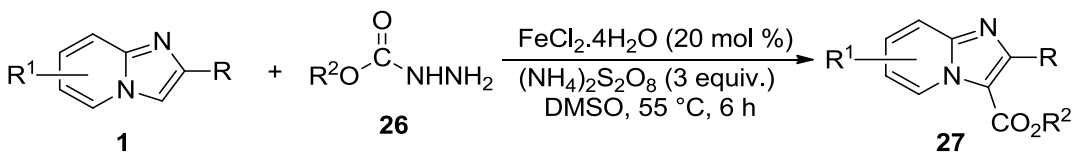

Scheme 1.2.12: Fe-catalyzed C-3 alkoxycarbonylation of imidazo[1,2-*a*]pyridines (**1**)

Csp^2-Csp^3 bond formation: Alkylation of imidazo[1,2-*a*]pyridines

Li and coworkers reported metal-free protocol for C-3 alkylation of substituted imidazo[1,2-*a*]pyridines (**1**) with xanthates **28** in presence of oxidant dilauroyl peroxide (DLP) *via* radical mechanism. The scope of the reaction was examined with a series of imidazo[1,2-*a*]pyridines possessing different substituents at different positions; albeit not much effect on the yield of the product either using electron-donating or electron-withdrawing substituents was noticed (Scheme 1.2.13). The utility of reaction was further extended towards the synthesis of Alpidem and Zolpidem using amide containing xanthate.[53]

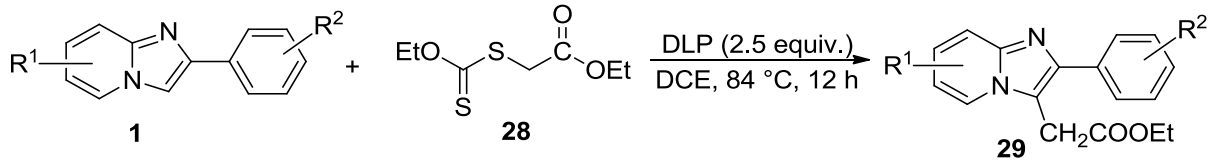

Scheme 1.2.13: Metal-free C-3 alkoxycarbonylation of imidazo[1,2-*a*]pyridines (**1**)

Csp^2- Csp^3 bond formation: Tosylmethylation of imidazo[1,2-*a*]pyridines

Song *et al.* utilized *p*-toluenesulfonylmethyl isocyanide (TosMIC) (**30**) for the first time as a tosylmethylating reagent, and decorated the C-3 position of substituted imidazo[1,2-*a*]pyridines (**1**) with tosyl methylene group to yield **31,** in a solvent mixture of H_2O and PEG 400 under an argon atmosphere. The protocol offered broad range of substrate compatibility with halogen, methyl, methoxy, and ester functionalities (Scheme 1.2.14). The authors recognized the crucial involvement of $FeCl_3$ for this selective transformation. The reaction was believed to proceed either through formation of radical intermediate or carbonium ion, accompanied by the generation of $Fe(CN)_3$ and $Cl^{\bullet}$ or Cl^- species. The exact mechanism was unclear in the report.[54]

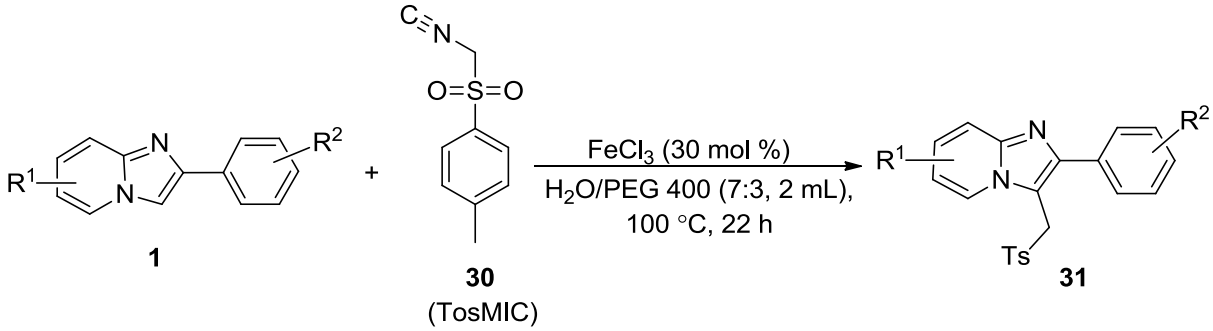

Scheme 1.2.14: Fe-catalyzed tosylmethylation of imidazo[1,2-*a*]pyridines (**1**)

Csp^2-Csp^3 bond formation: Trifluoroalkylation of imidazo[1,2-*a*]pyridines

The incorporation of a trifluoroalkyl group into organic molecules has gained much attention due its chemical and biochemical altering capability in term of solubility, metabolic stability, and bioavailability.[55,56] As a consequence, fluorinated compounds are widely explored in pharmaceutical and agrochemical industries, as well as in material science.[57,58] In a continuous program towards the decoration of imidazo[1,2-*a*]pyridines, Hajra *et al.* reported catalytic oxidative trifluoromethylation of substituted imidazo[1,2-*a*]pyridines (**1**), employing Langlois reagent (CF_3SO_2Na) (**32**) under ambient condition in presence of catalytic amount of $AgNO_3$ and TBHP at room temperature (Scheme 1.2.15a). C-2 Aryl groups possessing electron-donating substituents gave higher yields as compared to electron-withdrawing substituents. The reaction was believed to proceed *via* radical pathway.[59] In addition, Tang *et al*. also succeeded in trifluoromethylation of substituted imidazo[1,2-*a*]pyridines (**1**) with same reagent using $Cu(OAc)_2$ in presence of TBHP oxidant under ionic liquid/water media for which a radical pathway was proposed (Scheme 1.2.15b).[60]

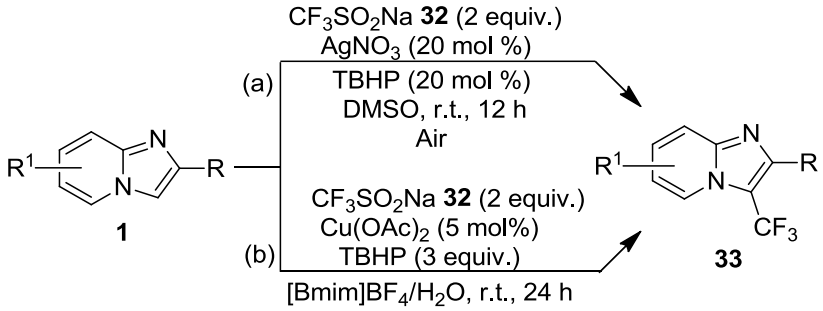

Scheme 1.2.15: Metal-catalyzed C-3 trifluoromethylation of imidazo[1,2-*a*]pyridines (**1**)

Xu *et al.* successfully achieved regioselective trifluoroethylation of substituted imidazo[1,2-*a*]pyridines (**1**) using 1,1,1-trifluoro-2-iodoethane (**34**) as a trifluoroethyl radical source in presence of iridium catalyst under visible light (Scheme 1.2.16). A variety of substituents on the aromatic rings were compatible under the standard reaction conditions, albeit halogen containing imidazo[1,2-*a*]pyridines showed sluggish reactivity. The reaction mechanism followed radical pathway through the formation of $CH_2CF_3^{\bullet}$ radical species *via* visible-light photocatalysis.[61]

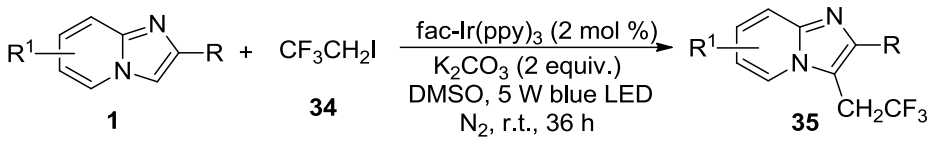

Scheme 1.2.16: Ir-catalyzed C-3 trifluoromethylation of imidazo[1,2-*a*]pyridines (**1**)

Recently, Hajra group developed a Cu-catalyzed ethoxycarbonyl-difluoromethylation of imidazo[1,2-*a*]pyridines (**1**) with $BrCF_2CO_2Et$ (**36**) under basic conditions in acetonitrile. A wide range of imidazo[1,2-*a*]pyridines and other imidazo-heterocycles were treated under the optimized reaction conditions to obtain the targeted products **37** (Scheme 1.2.17). The reaction was described to proceed *via* oxidative addition of Cu(I)-catalyst to $BrCF_2CO_2Et$ to *via* oxidative addition, followed by nucleophilic addition of imidazo[1,2-*a*]pyridine generating stable carbocation species, which upon reductive elimination under basic conditions yielded the desired product.[62]

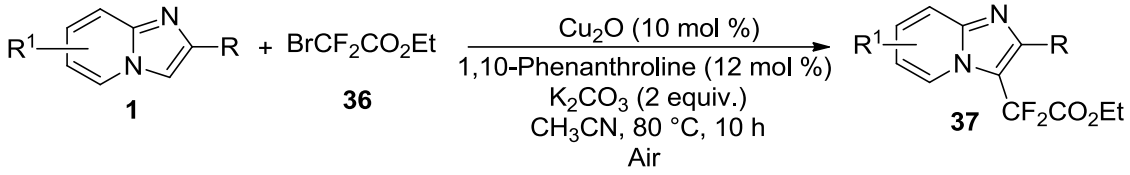

Scheme 1.2.17: Cu-catalyzed ethoxycarbonyl-difluoromethylation of imidazo[1,2-*a*]pyridines (**1**)

Csp^2- Csp^3 bond formation: Hydroxyalkylation of imidazo[1,2-*a*]pyridines

Hao and coworkers disclosed a simple and mild method for hydroxyalkylation of substituted imidazo[1,2-*a*]pyridines (**1**) through Friedel-Crafts reaction with ethyl trifluoropyruvate (**38)** (Scheme 1.2.18). The optimized reaction conditions exhibited good functional group tolerance with electron-rich as well as electron-deficient species.[63]

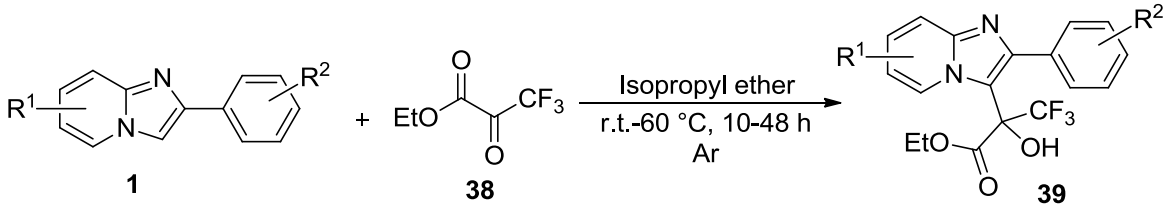

Scheme 1.2.18: C-3 Hydroxyalkylation of imidazo[1,2-*a*]pyridines (**1**)

Csp^2-Csp^3 bond formation: Synthesis of bis(imidazo[1,2-*a*]pyrid-3-yl)methanes

Biheteroaryls connected *via* methylene bridge are interesting targets, and are frequently found in many natural products, pharmaceutical motifs, and functional materials. Inspiring from the eye catching biological profile of several bis(heteroaryl)methanes, Kumar *et al.* described an

efficient protocol for the synthesis of methylene-bridged bis-imidazo[1,2-*a*]pyridines **40** using vanadium catalyst and DMA as a solvent cum methylene source. The reaction was believed to proceed through the formation of iminium intermediate by the action of vanadium and IBD, followed by electrophilic substitution (Scheme 1.2.19a).[64] Likewise, Patel and coworkers employed $Cu(OAc)_2$ and oxidant $K_2S_2O_8$ in DMA towards the formation of methylene-bridged bis-imidazo[1,2-*a*]pyridines **40** (Scheme 1.2.19b).[65] Sun *et al.* demonstrated metal-free H_3PO_4-promoted strategy for the synthesis of symmetrical methylene-bridged bis-imidazo[1,2-*a*]pyridines **40** using DMSO as methylene synthon. The reaction mechanism was believed to proceed with the thermal decomposition of DMSO into CH_2O in presence of H_3PO_4 (Scheme 1.2.19c).[66] Moreover, Yadav *et al.* also synthesized methylene-bridged bis-imidazo[1,2-*a*]pyridines **40** using DMSO as a methylene source and H_2O_2 as mild oxidant in absence of transition-metal catalyst. The reaction was described to proceed through the formation of methyl radical from DMSO by means of hydroxyl radical of H_2O_2, which thereafter react with imidazo[1,2-*a*]pyridine in sequential manner to offer the desired product (Scheme 1.2.19d).[67]

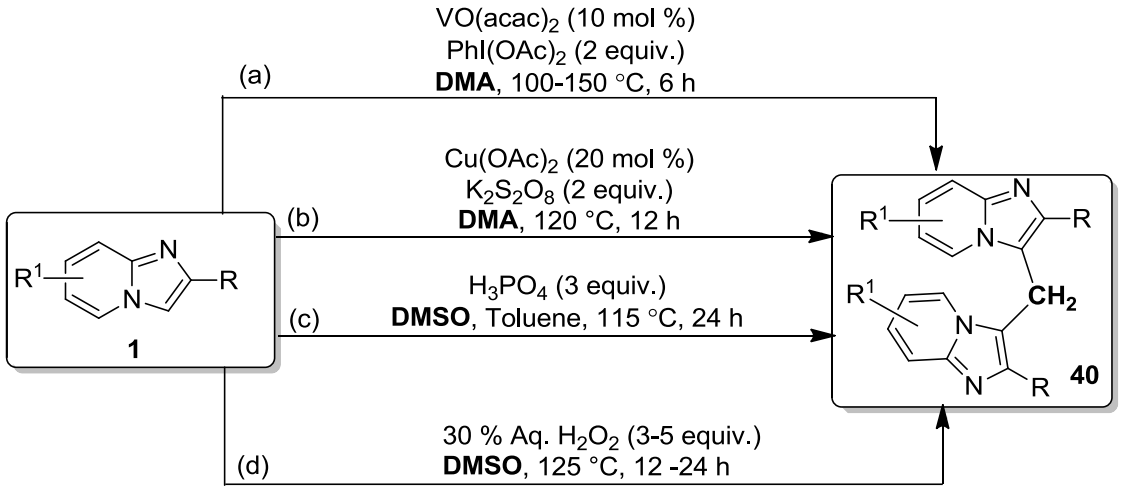

Scheme 1.2.19: Metal-catalyzed and metal-free protocols for the synthesis of methylene-bridged bis-imidazo[1,2-*a*]pyridines (**40**)

In addition, Cu-catalyzed strategy was applied by Hajra group to synthesize unsymmetrical heterodiarylmethanes **43** using DMF as one carbon source. Imidazo[1,2-*a*]pyridines effectively reacted with indole derivatives **41** and electron rich *N*,*N*-dimethylaniline **42** in presence of copper iodide and $K_2S_2O_8$ oxidant in DMF. The substrate scope of the reaction was well studied using variable electron-withdrawing and electron-donating groups on imidazo[1,2-*a*]pyridines

(Scheme 1.2.20).[68] In consistence with the previous report, the reaction mechanism was proposed to proceed with formation of iminium ion followed by nucleophilic attack of imidazo[1,2-*a*]pyridine.

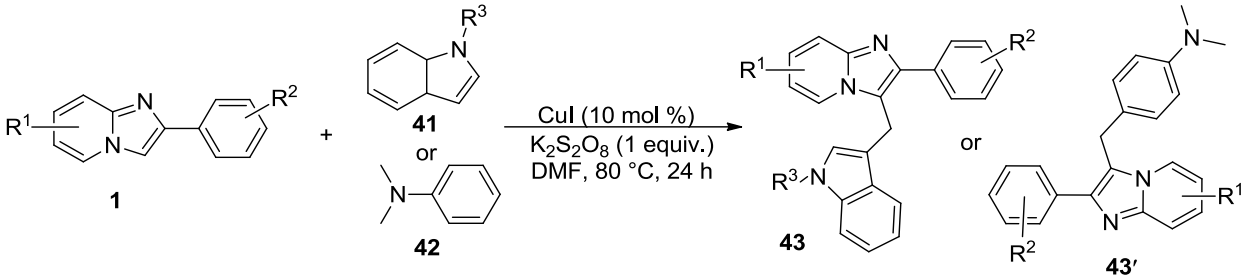

Scheme 1.2.20: Cu-catalyzed synthesis of methylene-bridged unsymmetrical heteroarenes (**43** & **43'**)

Csp^2-Csp^3 bond formation: Synthesis of imidazopyridyl acetonitriles

Aryl/heteroaryl acetonitriles are valuable synthons in many organic transformation,[69] and are also foremost important in medicinal chemistry due to the occurrence of (hetero)aryl acetonitrile units in various pharmaceutically active molecules, such as Levocabastine, Verapamil, Isoaminile, Anastrozole, Diphenoxylate, and Cilomilast.[70] Looking at the valuable pharmacological importance, Xu *et al.* developed a Fe-catalyzed cross-dehydrogenative protocol for the coupling of 2-arylimidazo[1,2-*a*]pyridines (**1**) and acetonitrile (**44**) to achieve the desired heteroaryl-acetonitriles **45** in moderate-to-good yields using dicumyl peroxide (DCP) as an oxidant. In general, electron-rich 2-arylimidazo[1,2-*a*]pyridines (**1**) showcased better reactivity (Scheme 1.2.21). The strategy was successfully employed for the fast access of Zolpidem. The reaction mechanism was proposed to proceed *via* the formation of cumyloxyl radical in the presence of $FeCp_2$ complex, and finally by the formation of cyanomethyl radical which eventually undergoes radical cross-coupling with 2-arylimidazo[1,2-*a*]pyridine (**1**).[71]

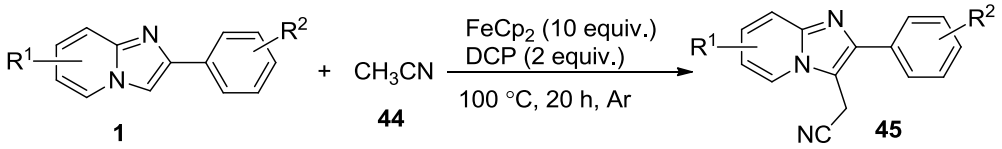

Scheme 1.2.21: Fe-catalyzed synthesis of imidazo[1,2-*a*]pyridyl acetonitriles (**45**)

Csp^2-Csp bond formation: Synthesis of fused imidazo[1,2-*a*]pyridines *via* C-H annulations

Oxidative annulation reaction with internal alkynes is one of the important methods to synthesize fused polycyclic heteroarenes.[72] This is due to the potential utility of ladder type π-conjugated systems as organic electronic materials.[73] Thus, noticeable efforts have been devoted by various

research groups towards the insertion of alkynes into C–H and heteroatom–hydrogen bonds in different organic scaffolds.

Li group recently reported Rh(III)-catalyzed C−H activation of substituted 2-arylimidazo[1,2-*a*]pyridines (**1**) in divergent oxidative coupling with alkynes **46**. Interestingly, the Rh(III)-catalyzed methodology provides an easy access to 5,6-disubstituted naphtho[1′,2′:4,5]imidazo-[1,2-*a*]pyridines (**47**) and fused isoquinolinium derivatives **48** by varying the external oxidant from $AgSbF_6$ to $AgBF_4$, respectively. The reaction was adequately explored with a broad range of substituted 2-arylimidazo[1,2-*a*]pyridines substrates with variable electronic substituent, affording their corresponding 5,6-disubstituted naphtho[1′,2′:4,5]imidazo-[1,2-*a*]pyridines (**47**) in moderate-to-good yields (Scheme 1.2.21).[74]

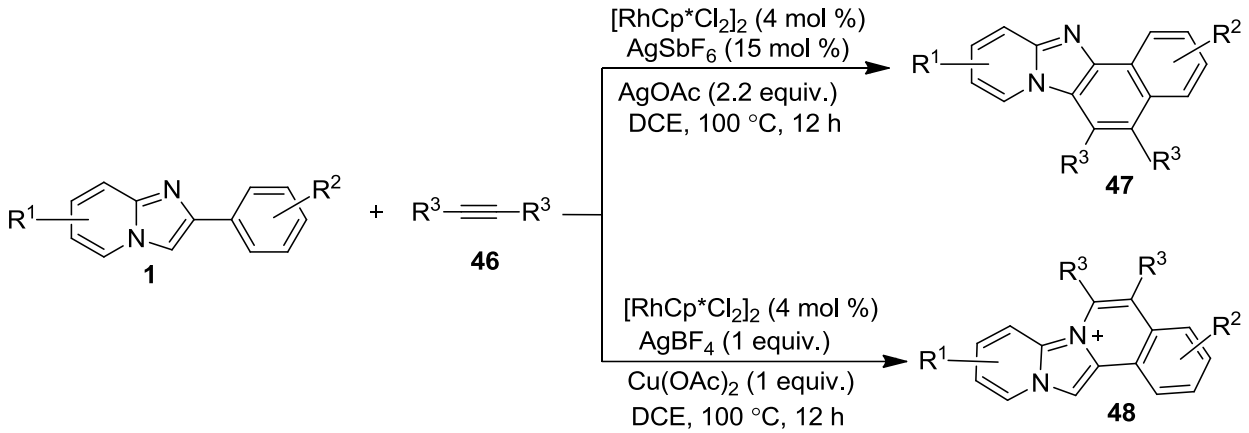

Scheme 1.2.21: Rh-catalyzed synthesis of naphtho-fused imidazo[1,2-*a*]pyridines (**47**) and fused isoquinolinium derivatives (**48**)

With prospect to synthesize naphtho[1′,2′:4,5]imidazo[1,2-*a*]pyridines (NIP) (**47**), Fan *et al.* subsequently utilized Pd-catalyst for the oxidative cycloaromatization of substituted 2-arylimidazo[1,2-*a*]pyridines (**1**) with internal alkyne **46**. However, imidazo[5,1,2-*cd*]indolizine (**49**) was also obtained albeit in lower yield along with **47** (Scheme 1.2.22a). Interestingly, the authors modified the strategy for exclusively obtaining imidazo[5,1,2-*cd*]indolizines (**49**) using 5-methyl-2-phenylimidazo[1,2-*a*]pyridine (Scheme 1.2.22b). Similarly, the selective formation of **49** was also elegantly achieved with 2-mesitylimidazo[1,2-*a*]pyridine (Scheme 1.2.22c). Moreover, the reaction showcased a wide range of substituent tolerance with various substituted alkynes.[75]

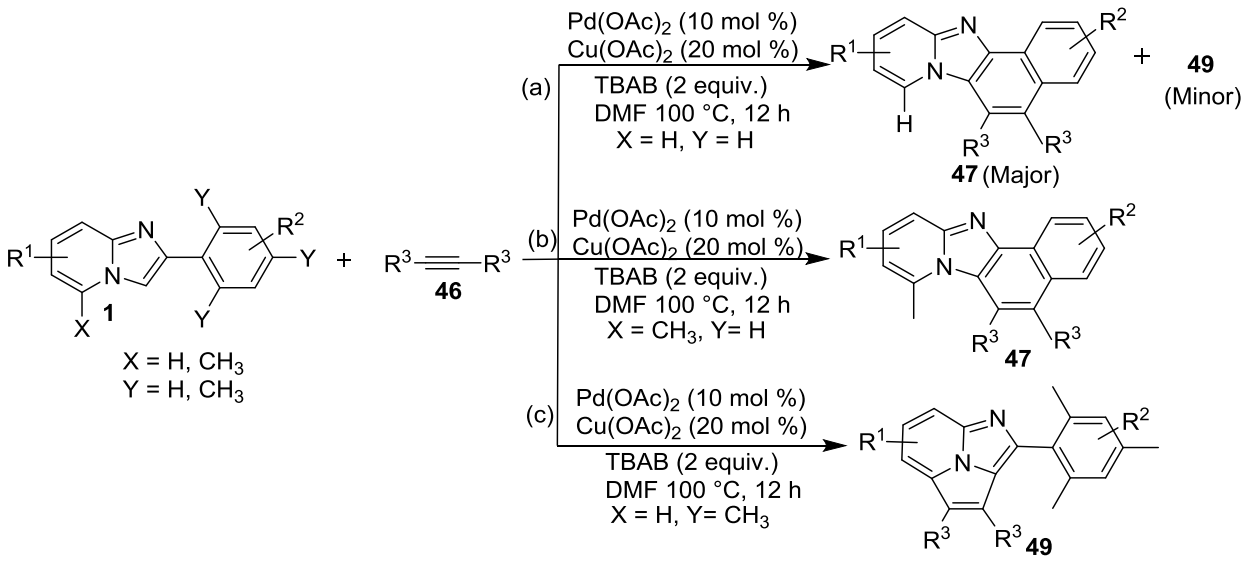

Scheme 1.2.22: Pd-catalyzed annulative synthesis of fused imidazo[1,2-*a*]pyridines (**47** & **49**)

In the same year, Hajra and team documented Pd-catalyzed direct dehydrogenative annulation of imidazo[1,2-*a*]pyridines (**1**) with diarylalkynes (**46**), providing a gallery of imidazo[5,1,2-*cd*]indolizines (**49**) in moderate-to-excellent yields (Scheme 1.2.23).[76]

Scheme 1.2.23: Pd-catalyzed annulative synthesis of **49** from imidazo[1,2-*a*]pyridines (**1**) and diarylalkynes (**46**)

In addition, similar reactions have been also documented by Cheng, Song and Verma's group independently using various internal alkynes, producing various substituted naphtho[1′,2′:4,5]imidazo[1,2-*a*]pyridines **47** in moderate-to-excellent yields. Cheng and coworkers used [Cp*Rh(CH_3CN)$_3$](SbF_6)$_2$] as a highly effective catalyst for the expected annulation reaction (Scheme 1.2.24a).[77] Whereas, Song[78] and Verma[79] groups utilized [RhCp*Cl_2]$_2$ catalyst with Co(OAc)$_2$.4H_2O and Cu(OAc)$_2$.H_2O respectively, to achieve the annulated products **47** in good-to-excellent yields (Scheme 1.2.24b and 1.2.24c).

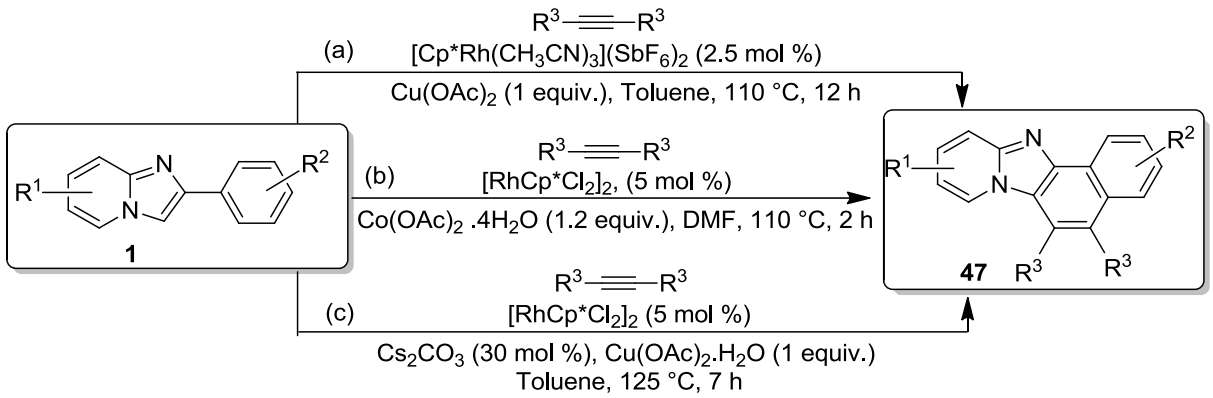

Scheme 1.2.24: Rh-catalyzed oxidative annulation protocols for the synthesis of naphtho-fused imidazo[1,2-*a*]pyridines (**47**)

With an anticipation to insert arenes into carbene precursors, Li and coworkers documented an articulate Rh(III) and Ir(III)-catalyzed carbocyclization between substituted 2-arylimidazo[1,2-*b*]pyridines (**1**) and *α*-diazo esters (**50**) yielding naphtho-fused imidazo[1,2-*a*]pyridines **51** & **52**. Iridium and Rhodium catalysts exhibited complementary scope of the diazo substrates (Scheme 1.2.25). The Rh(III)-catalyzed reaction proceeded by nitrogen coordination, cyclometalation (rhodacycle intermediate), and by eventual formation of rhodium carbene species *via* dediazoniation of coordinized diethyl diazo malonate (Scheme 1.2.25a). While the iridacycle complex of $[Cp^*IrCl_2]_2$ and 2-arylimidazo[1,2-*a*]pyridine has been isolated and acclaimed to be the active catalyst for the depicted transformation (Scheme 1.2.25b).[80]

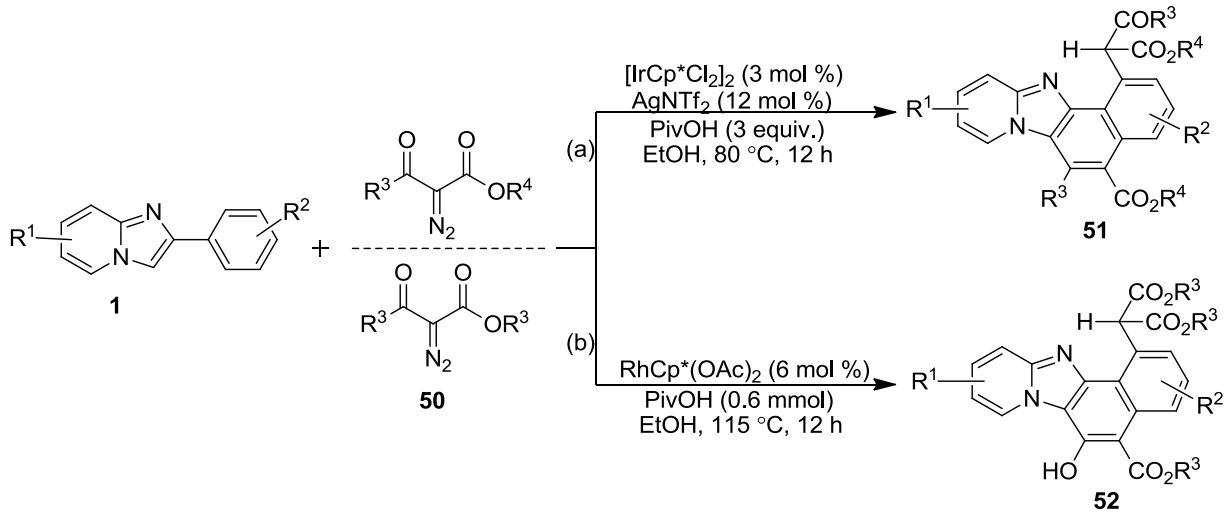

Scheme 1.2.25: Ir- and Rh-catalyzed synthesis of naphtho-fused imidazo[1,2-*a*]pyridines (**51**) and (**52**)

Csp^2-Csp bond formation: Synthesis of bis-cyanated 2-arylimidazo[1,2-*a*]pyridines

Introduction of nitrile group in heterocyclic frameworks are highly desirable, because of their synthetic potential in transformation to useful functionalities; thus they have received great importance in natural product synthesis.[70,81] In this regard, Hao and coworkers documented a Rh(III)-catalyzed bis-cyanation of substituted 2-arylimidazo[1,2-*a*]pyridines (**1**) with *N*-cyano-*N*-phenyl-*p*-methylbenzenesulfonamide (**53**) *via* *N*-directed *ortho* double C-H activation in the presence of catalytic $AgSbF_6$. A broad range of substituted 2-arylimidazo[1,2-*a*]pyridines (**1**) and other related heterocycles were reacted under the optimized conditions to afford the desired products **54** (Scheme 1.2.26). The double C-H activation mechanism proceeded by the formation of active Rh(III) complex using $[RhCp^*Cl_2]_2$ in the presence of $AgSbF_6$ and $NaHCO_3$ *via* the formation of five-membered rhodacycle intermediate.[82]

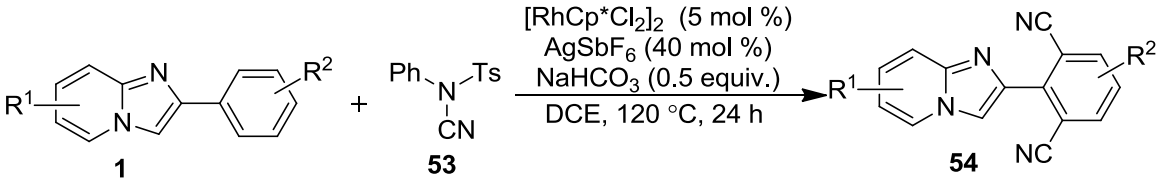

Scheme 1.2.26: Rh-catalyzed bis-cyanation of 2-arylimidazo[1,2-*a*]pyridines (**1**)

1.3 C-S/Se Bond formations

Csp^2-S/Se, Csp^2-S/Se-Csp^2 bond formation: Thiolation and selenylation of imidazo[1,2-*a*]pyridines

Thioethers are the most noticed organosulfur compounds in organic synthesis due to their significant applications as pharmaceuticals, agrochemicals, organic-dyes and materials.[83-85] As a consequence, the development of novel, efficient, and practical methods for C–S bond formation is still a prime topic in organic chemistry.[86-89] In conjuction to this, several methodologies have been periodically published in last couple of years towards the C-3 thiolation of imidazo[1,2-*a*]pyridines under metal-catalyzed and metal-free conditions.

In 2011, Zhou group reported an efficient Cu-catalyzed aerobic process for C-3 sulfenylation and selenylation of 2-arylimidazo[1,2-*a*]pyridines (**1**) using disulfides (**55a**) and diselenide (**55b**). The methodology was well exemplified with various substituted 2-arylimidazo[1,2-*a*]pyridines (**1**), yielding the desired products up to 98% yield (Scheme 1.3.1). In addition, the authors also extended the thiolation and selenylation strategy on imidazo-pyrimidines and indoles.[90]

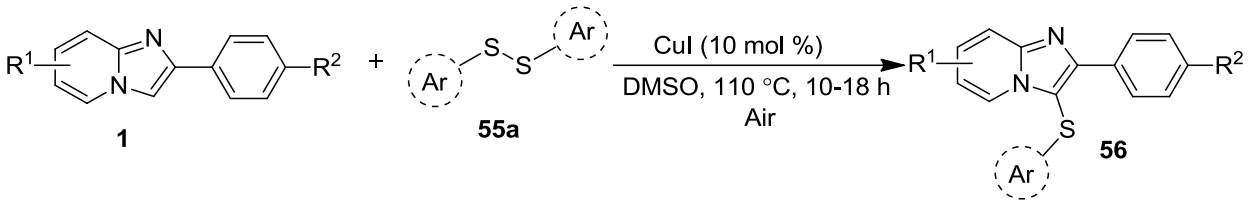

Scheme 1.3.1: Cu-catalyzed C-3 sulfenylation of imidazo[1,2-*a*]pyridines (**1**) with disulfides (**55a**)

Adimurthy and coworkers described the utility of *p*-tosyl chloride (**57**) as benign sulfur source for the regioselective C-3 sulfenylation of substituted imidazo[1,2-*a*]-pyridines (**1**) by employing copper catalyst. CuI (10 mol %)/PPh_3 (3 equiv.) was optimized to be the best catalyst-ligand dyad for the selective C-3 sulfenylation in toluene. The reaction tolerated a wide range of substituted imidazo[1,2-*a*]pyridines (**1**) including electron-donating (Me, Et, OMe and SMe) and electron-withdrawing substituents (CN) on the aryl ring (Scheme 1.3.2).[91]

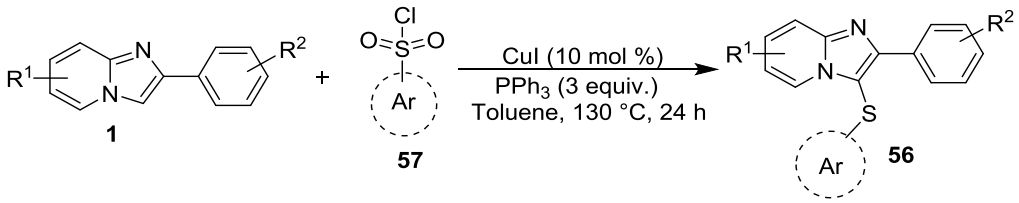

Scheme 1.3.2: Cu-catalyzed C-3 sulfenylation of imidazo[1,2-*a*]pyridines (**1**) with *p*-tosyl chloride (**57**)

In the continuous program for synthesizing functionalized imidazo[1,2-*a*]pyridines, Cao *et al.* prepared thioether-decorated imidazo[1,2-*a*]pyridines **56** in 72-92% yields *via* C–H/S–H cross-coupling of substituted imidazo[1,2-*a*]pyridines (**1**) with aliphatic and aromatic thiols **58** using copper catalyst in the presence of molecular oxygen (Scheme 1.3.3). The reaction mechanism was believed to initiate by the formation of Cu(I)SR species by the reaction between thiol and CuI, which follows usual concerted metalation–deprotonation-reductive elimination to generate the cross-coupling product in the presence of molecular oxygen, along with the regeneration of Cu(I) catalyst.[92]

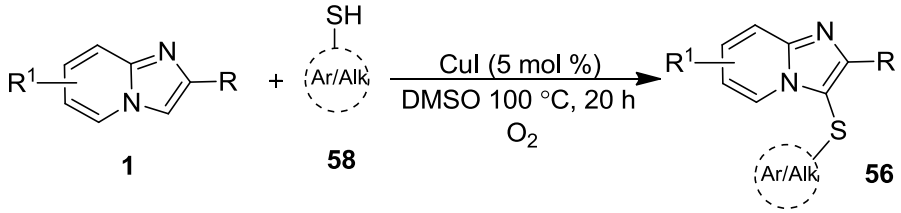

Scheme 1.3.3: Cu-catalyzed C-3 sulfenylation of imidazo[1,2-*a*]pyridines (**1**) with thiols (**58**)

Similarly, Zheng and coworkers disclosed a Cu-catalyzed regioselective cross-dehydrogenative coupling strategy for the C-3 sulfenylation of substituted 2-arylimidazo[1,2-*a*]pyridines (**1**) from a variety of easily available heterocyclic thiols **58** such as benzo[*d*]thiazole-2-thiol, benzo[*d*]oxazole-2-thiol, 1-methyl-1*H*-imidazole-2-thiol and pyrimidine-2-thiol. Under the described conditions, various substituted IP showcased moderate-to-excellent reactivity with aromatic/aliphatic and heterocyclic thiols (Scheme 1.3.4).[93]

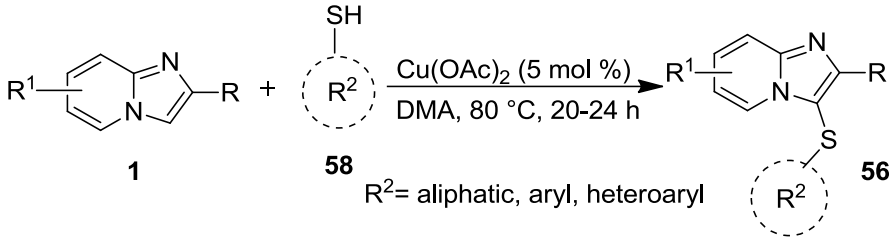

Scheme 1.3.4: Cu-catalyzed C-3 sulfenylation of imidazo[1,2-*a*]pyridines (**1**) with thiols (**58**)

In order to further improve sulfenylation strategy, Adimurthy and coworkers achieved the selective sulfenylation of imidazo[1,2-*a*]pyridines (**1**) through a one-pot three-component Cu-catalyzed protocol using elemental sulfur and haloarenes as a thioarylation source under basic conditions. A broad range of aryl iodides were explored with various imidazo[1,2-*a*]pyridines (**1**) bearing multitude of functional groups such as Br, Cl, CH_3, CN, NO_2, SO_2CH_3 on the aryl ring (Scheme 1.3.5a).[94] Zhou group explored the utilization of sodium thiosulfate as an odour-free sulfur source for the thioarylation of imidazo[1,2-*a*]pyridines (**1**) using copper catalyst with various alkyl and aryl halides in DMF (Scheme 1.3.5b).[95] Similarly, Jiang *et al.* also presented a similar Pd/Cu-catalyzed oxidative strategy for sulfenylation of imidazo[1,2-*a*]pyridines (**1**) using elemental sulfur, as an extended example of sulfenylation chemistry (Scheme 1.3.5c).[88]

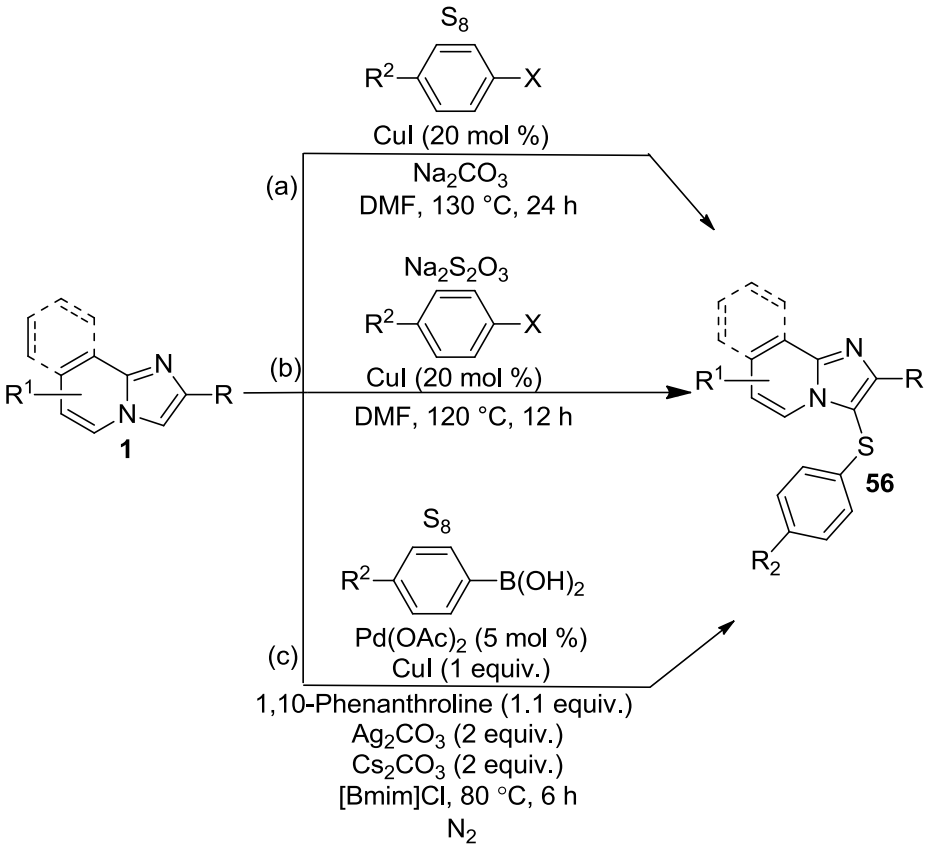

Scheme 1.3.5: Multi-component based Cu/Pd-catalyzed C-3 sulfenylation of imidazo[1,2-*a*]pyridines (**1**)

Adimurthy *et al.* reported an efficient *N*-chlorosuccinimide-promoted metal-free protocol for the sulfenylation of imidazo[1,2-*a*]pyridines (**1**) using thiophenols **58** in DCM at room temperature. 2-Arylimidazo[1,2-*a*]pyridines bearing electron-donating (Me, Et, OMe, and SMe) and electron -withdrawing groups (SO_2Me, Cl, Br, and CN) demonstrated moderate-to-good reactivity (Scheme 1.3.6). The mechanism was proposed to proceed with the formation of sulfenyl chloride intermediate from NCS with thiophenol**,** followed by electrophilic substitution and dehydrochlorination with IP.[96]

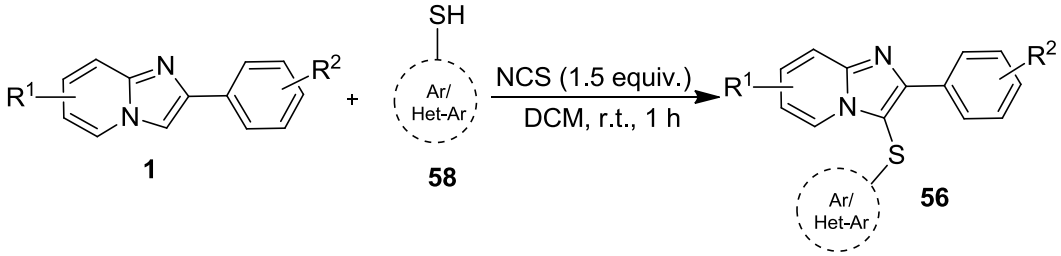

Scheme 1.3.6: Metal-free C-3 sulfenylation of imidazo[1,2-*a*]pyridines **(1)** with thiols (**58**)

Csp^2-S bond formation: Thiocyanation of imidazo[1,2-*a*]pyridines

Organic thiocyanates (RSCN) are important synthetic intermediates to access various valuable sulfur-containing compounds possessing diverse pharmacological profiles. In this regard, Hajra and coworkers reported a eosin Y photoredox-catalyzed metal-free process for the C-3 thiocyanation of substituted imidazo[1,2-*a*]pyridines (**1**) with NH_4SCN at room temperature using blue LED light (Scheme 1.3.7a). The methodology was generalized with varyingly substituted imidazo[1,2-*a*]pyridines (**1**); whereby, almost equal effectiveness for both electron-donating and electron-withdrawing substituents on the aryl and pyridyl ring was observed. The authors also splendidly succeeded in the selenothiocyantion under similar photoredox conditions. The authors proposed the reaction mechanism as radical SET pathway that proceed by mean of photoexitation of eosin Y in the presence of blue LED light [97] Along the same line, Wang *et al*. presented a radical mechanism based approach for the direct catalyst-free C-3 thiocyanation of imidazo[1,2-*a*]pyridines (**1**) with KSCN at room temperature (Scheme 1.3.7b). A wide array of substituted imidazo[1,2-*a*]pyridines were applicable for the regioselective functionalization, showing no obvious electronic effect for the transformation. The reaction proceeded with the generation of $SCN^{\bullet}$ or electrophile thiocyanogen by the oxidation of KSCN which further upon reaction with imidazo[1,2-*a*]pyridine (**1**) yielded the alkyl radical intermediate or carbocation intermediate.[98] Another practically distinct protocol was vividly displayed using a combination of *N*-chlorosuccinimide/NaSCN for the synthesis of 3-thiocyanatoimidazo[1,2-*a*]pyridines **59** in ethanol at room temperature (Scheme 1.3.7c).[99] A broad range of imidazo[1,2-*a*]pyridines (**1**) bearing functional groups such as –OH, –Cl, –Br, $–NO_2$, and $–CF_3$ were well tolerated under the established reaction conditions.

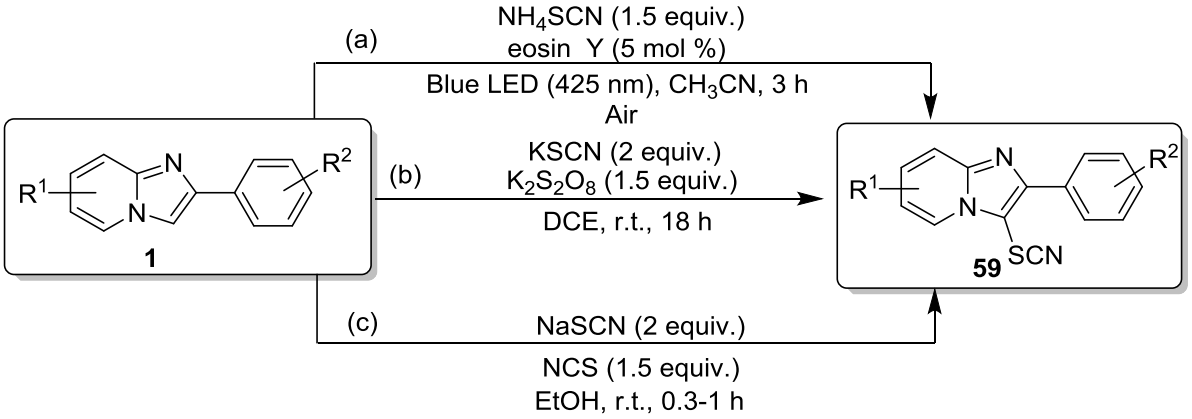

Scheme 1.3.7: Metal-free C-3 thiocyanation of imidazo[1,2-*a*]pyridines (**1**)

Csp^2-S Bond formation: Miscellaneous strategies

Looking at the unique chemical and medicinal versatility of dithiocarbamate (DTC) group in several organic molecules, Hu and Tang *et al.* established an ideal C–H bond functionalization strategy for the introduction of dithiocarbamates on to the imidazo[1,2-*a*]pyridines (**1**) under iron catalyzed/iodine-mediated conditions to afford **61**. Notably, the presence of electron-donating substituent's resulted in better reactivity (Scheme 1.3.8). The reaction mechanism was described to proceed with the generation R-S-I intermediate by the reaction of disulfiram (DFS) and I_2, followed by Friedel–Crafts reaction with 2-arylimidazo[1,2-*a*]pyridine.[100]

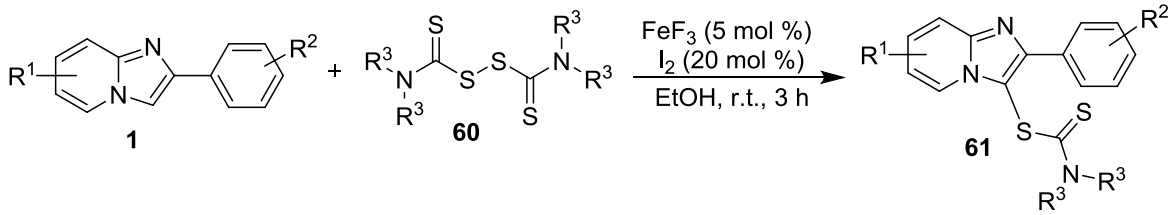

Scheme 1.3.8: Fe catalyzed introduction of dithiocarbamates on to the imidazo[1,2-*a*]pyridines (**1**)

With an anticipation to increase the lipophilicity and transmembrane permeation capability of imidazo[1,2-*a*]pyridines, Li *et al.* reported a trifluoromethylthiolation protocol of imidazo[1,2-*a*]pyridines under Fe-catalyzed conditions using (*N*-trifluoromethylthio)saccharin (**62**) as a SCF_3 source to afford **63**. The methodology was also applied to other (hetero)arenes such as *N*-protected indoles, ester-substituted indolizines, and pyrrolo[1,2-*a*]pyrazines.[101]

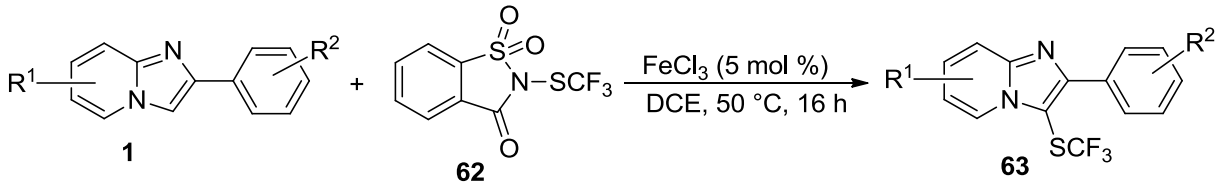

Scheme 1.3.9: Fe-catalyzed C-3 trifluoromethylthiolation of imidazo[1,2-*a*]pyridines (**1**)

1.4 C-N Bond formations

Csp^2- N bond formation: Hydrazination of imidazo[1,2-*a*]pyridines

Li *et al.* disclosed a metal-free regioselective strategy for the hydrazination of imidazo[1,2-*a*]pyridines (**1**) with diethyl azodicarboxylate (DEAD) (**64a**), producing C-3 aminated imidazo[1,2-*a*]pyridines **65** in CH_3CN (Scheme 1.4.1). A variety of substituted imidazo[1,2-*a*]pyridines showcased excellent compatibility within the described reaction conditions, and the reaction was proposed to proceed through *pseudo*-Michael reaction or by concerted mechanism.[102]

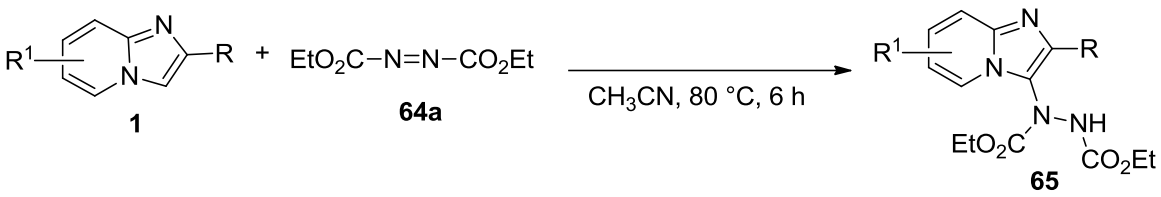

Scheme 1.4.1: Metal-free direct C-3 hydrazination of imidazo[1,2-*a*]pyridines (**1**)

As an extension to above work, Sabitha and coworkers reported an efficient one-pot sequential protocol for the synthesis of novel pyrido[2',1':2,3]imidazo[4,5-*c*]cinnoline derivatives (**66**) through regioselective C-3 hydrazination of substituted 2-arylimidazo[1,2-*a*]pyridines **1** with diisopropyl azodicarboxylate (DIAD) (**64b**) followed by an phenyliodine(III) diacetate (PIDA)-mediated oxidative *N*-arylation (Scheme 1.4.2). This one-pot sequential strategy endured a wide range of substituents on the 2-arylimidazo[1,2-*a*]pyridines (**1**), affording the fused products **66** in good-to-excellent yields.[103]

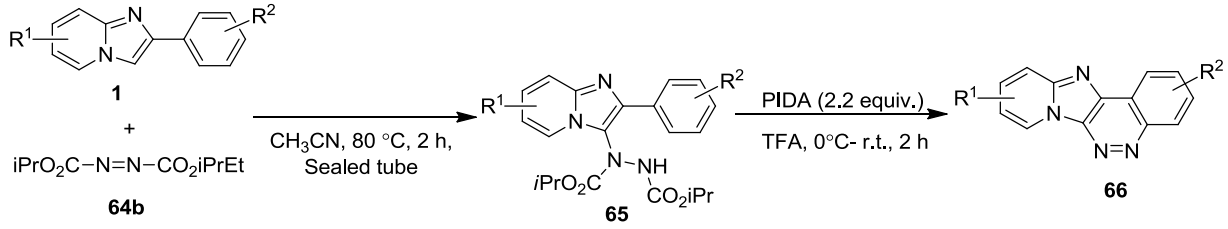

Scheme 1.4.2: Metal-free strategy for the synthesis of pyrido-imidazo-fused cinnolines (**66**)

Csp^2-N bond formation: C-H azotization of imidazo[1,2-*a*]pyridines

Hajra and coworkers presented ^{t}BuONO-mediated synthesis of azo imidazo[1,2-*a*]pyridines (**68**) using aniline **67** at room temperature. A variety of anilines with electron-rich as well as electron-deficient groups were explored, and it was concluded that electron-deficient substrates gave better yields of corresponding product, although no effect was observed in case of substituent on imidazo[1,2-*a*]pyridines (Scheme 1.4.3). The reaction was believed to proceed through formation of diazonium intermediate *via* the reaction of aniline and ^{t}BuONO, which was further attacked by nucleophilic site of imidazo[2,1-*a*]pyridine.[104]

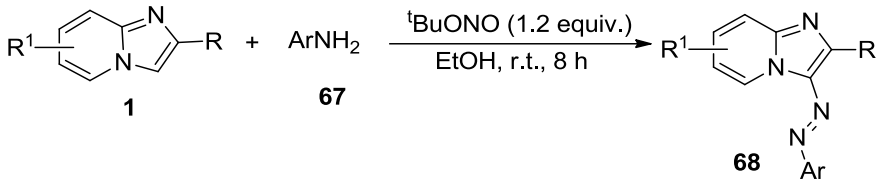

Scheme 1.4.3: Metal-free ^{t}BuONO-mediated synthesis of azo imidazo[1,2-*a*]pyridines (**68**)

With the advent interest to develop ladder type π-expanded aromatic frameworks, Gryko *et al.* recently synthesized 5*H*-pyrido[2',1':2,3]imidazo[4,5-*b*]indoles (**71**) in few steps through intramolecular C–H bond oxidative amination of prior synthesized imidazo[1,2-*a*]pyridyl tosyl amides (**70**) using $Cu(OTf)_2$–PIDA–TFA (Scheme 1.4.4). The authors disclosed another apparently effective PIFA-TFA mediated method for the described cyclization.[105]

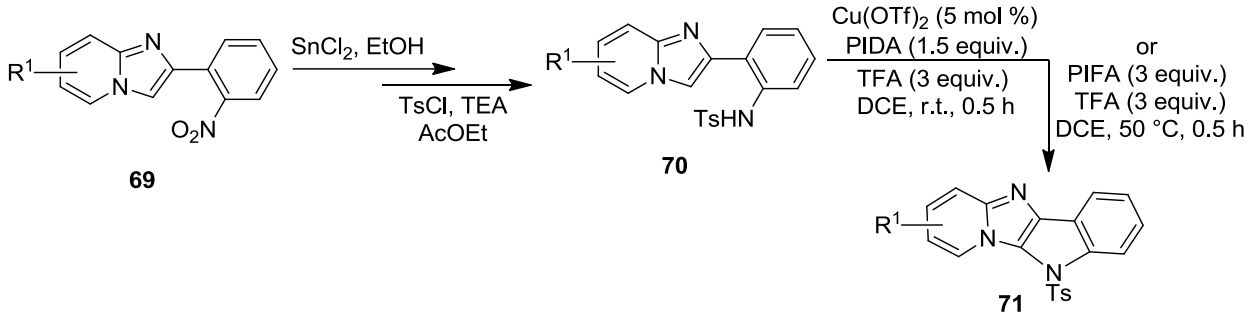

Scheme 1.4.4: Cu-catalyzed synthesis of pyrido-imidazo-fused indole derivatives (**71**)

Csp^2-N bond formation: Nitrosylation of imidazo[1,2-*a*]pyridines

Hajra[106] and Wang[107] *et al.* independently described simple and elegant methods for synthesis of 3-nitrosoimidazo[1,2-*a*]pyridines (**72**) through C(sp^2)–H bond functionalization, employing *tert*-butyl nitrite as a NO source under metal-free conditions (1.4.5a,b). The reaction was presumed to occur through homolytic cleavage of ^{t}BuONO giving NO radical, which in turn reacted with IP to afford the described product.

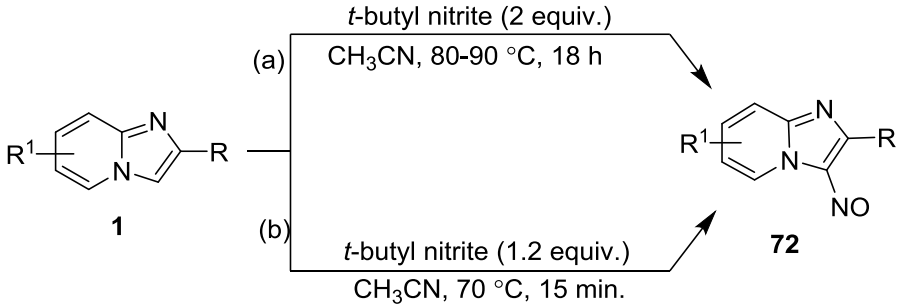

Scheme 1.4.5: Metal-free C-3 direct nitrosylation of imidazo[1,2-*a*]pyridines (**1**)

Csp^2- N bond formation: Synthesis of aminated imidazo[1,2-*a*]pyridines

Recently, Hajra *et al.* demonstrated PIDA-mediated direct oxidative C−H amination of 2-arylimidazo[1,2-*a*]pyridines (**1**) with morpholine, thiomorpholine and piperidine (**73**) at room temperature in very shorter reaction time (Scheme 1.4.6). The reaction was proposed to proceed *via* radical pathway through the formation of morpholine radical by means of PIDA.[108]

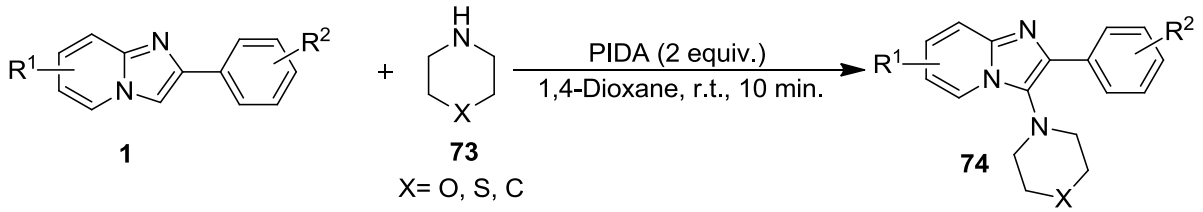

Scheme 1.4.6: Metal-free synthesis of C-3 aminated imidazo[1,2-*a*]pyridines (**74**)

1.5 C-P Bond formations

Csp^2- P bond formation: Phosphonylation of imidazo[1,2-*a*]pyridines

Singh *et al.* disclosed an efficient Mn(III)-catalyzed regioselective synthesis of 3-phosphonated imidazo[1,2-*a*]pyridines (**76**) using dialkyl phosphites (**75**). A wide range of substituted imidazo[1,2-*a*]pyridines (**1**) were tolerated under the optimized reaction conditions (Scheme 1.5.1). Few other heteroarenes such as indole, azaindole, pyrrole and *N*-protected pyrrole were also evaluated, and the reaction was believed to proceed through radical pathway.[109]

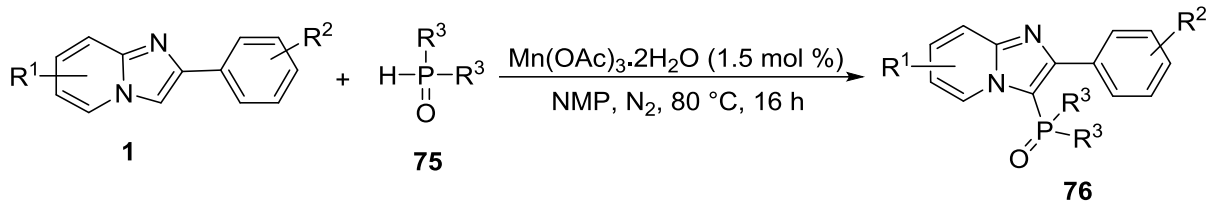

Scheme 1.5.1: Mn-catalyzed C-3 phosphonylation of imidazo[1,2-*a*]pyridines (**1**)

1.6 C-X Bond formations

Csp^2-F bond formation: Fluorination of imidazo[1,2-*a*]pyridines

C-3-Fluorinated imidazo[1,2-*a*]pyridines (**77**) were regioselectively synthesized by Sun *et al.* using Selectfluor (1-chloromethyl-4-fluoro-1,4-diazoniabicyclo[2.2.2]octane (tetrafluoroborate)) as a fluorinating reagent in aqueous media at room temperature. Good functional group tolerance was observed with negligible influence of electronic effects. Moreover, strong electron-withdrawing group such as nitro also gave excellent yield of product. The probable mechanism was believed to proceed through electrophilic fluorination.[110]

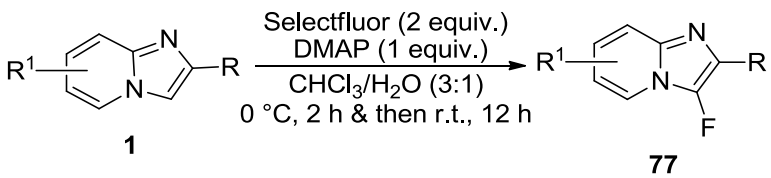

Scheme 1.6.1: Metal-free C-3 fluorination of imidazo[1,2-*a*]pyridines (**77**)

1.7 Tandem Bond formations

Tandem multiple Csp^2-C/S/N/O bond formations: Synthesis of fused imidazo[1,2-*a*]pyridines

Fused heterocyclic skeletons seek great attention of researchers in the field of medicinal chemistry. Tandem/domino approaches have been efficiently involved in the construction of various multifaceted structures with the formation of several new C−C or C−N/S/O bonds in a single action. Within the same realm, Kumar and coworkers disclosed an elegant one-pot tandem protocol for the synthesis of azole-fused imidazo[1,2-*a*]pyridines **79**, evaluating the scope of reaction with various azoles such as imidazole, 4-methylimidazole, benzimidazole, 1,2,4-triazole, and 1*H*-imidazo[4,5-*b*]pyridines with substituted 2-(2-bromophenyl)imidazo[1,2-*a*]pyridines (**1**) *via* sequential C–N bond formation followed by intramolecular dehydrogenative cross-coupling (Scheme 1.7.1). The cross-dehydrogenative coupling reaction was catalyzed by $Pd(OAc)_2$ in the presence of oxidant $Cu(OAc)_2$.[111]

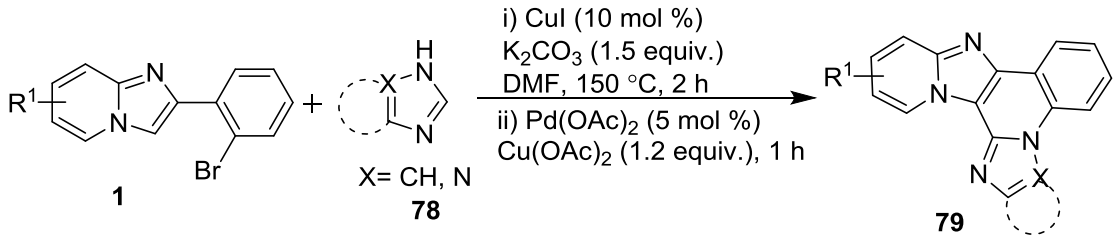

Scheme 1.7.1: Cu-Pd-catalyzed tandem synthesis of azole-fused imidazo[1,2-*a*]pyridines (**79**)

In an extension this report, Fan *et al.* develop an bimetallic relay-catalyzed cascade synthesis of pyrido[2′,1′:2,3]imidazo[4,5-*c*][1,2,3]triazolo[1,5-*a*]quinolone (**81**) derivatives from 2-(2-bromophenyl)imidazo[1,2-*a*]pyridines (**1'**), alkynes (**80**), and sodium azide. The process involves azide-alkyne cycloaddition, and subsequent C−N cross-coupling between the *in-situ* generated 1,2,3-triazole and aryl bromide. This eventually undergoes oxidative cross-dehydrogenative coupling at the C-3 position of imidazo[1,2-*a*]pyridine to afford the targeted product *via* the formation of seven-membered palladacycle intermediate under Pd/Cu-catalyzed conditions (Scheme 1.7.2). The influence of steric and electronic parameters on the efficiency of this cascade transformation were evaluated with a broad range of electron-donating and electron-withdrawing substituents on phenyl acetylene and 2-(2-bromophenyl)imidazo[1,2-*a*]pyridines (**1**).[112]

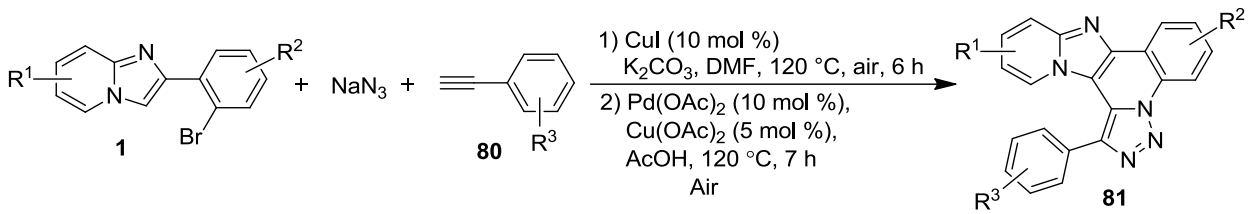

Scheme 1.7.2: Cu-Pd-catalyzed tandem synthesis of pyrido[2′,1′:2,3]imidazo[4,5-*c*][1,2,3]-triazolo[1,5-*a*]quinolone derivatives (**81**)

Fan *et al.* later also reported efficient Pd-catalyzed methodologies for the coupling of indenone and chromenone with imidazo[1,2-*a*]pyridines, affording 11*H*-indeno[1′,2′:4,5] imidazo[1,2-*a*]pyridin-11-one (**82**) and 6*H*-chromeno[4′,3′:4,5]imidazo[1,2-*a*]pyridin-6-one (**83**), respectively in moderate-to-good yields (Scheme 1.7.3). The first strategy proceeded through Pd-catalyzed CO insertion followed by C−H bond activation with carbon monoxide, whereas the second strategy was driven with the crucial participation of $Cu(OAc)_2$, and was proposed to proceed through several cascade processes including acetoxylation, deacetylation, CO insertion, and C−H bond activation.[113]

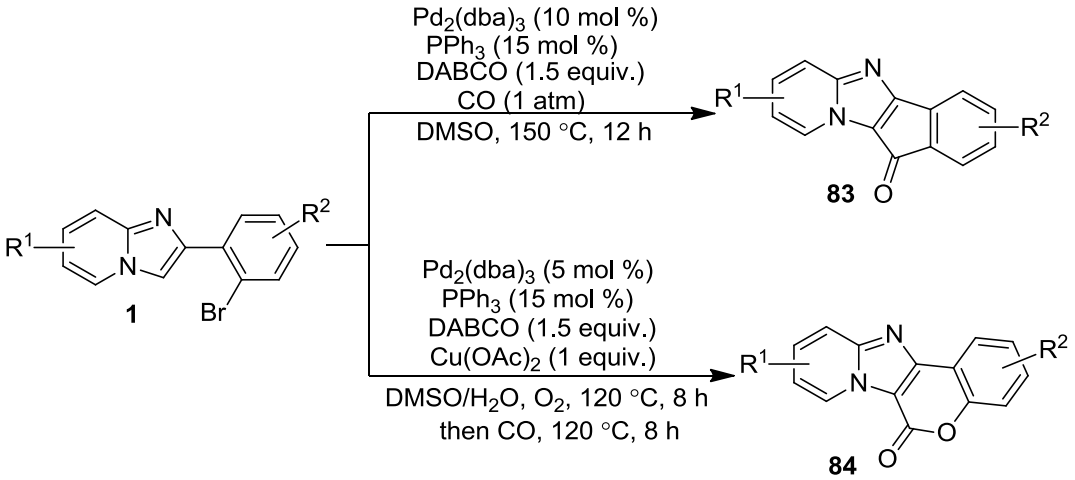

Scheme 1.7.3: Pd-catalyzed synthesis of 11*H*-indeno[1′,2′:4,5]imidazo[1,2-*a*]pyridin-11-one (**83**) and 6*H*-chromeno[4′,3′:4,5]imidazo[1,2-*a*]pyridin-6-one derivatives (**84**)

Synthesis of benzo[*b*]thiophene-fused imidazo-pyridines (**85a**) was independently reported by Liu and Wang groups under Cu-catalyzed conditions. The methodologies described the double C–S bond formation *via* Ullmann-type *S*-arylation followed by C–H thiolation using K_2S as a sulfur source. Both the strategies were effective with a wide range of substituents such as; CH_3, OCH_3, F, Cl, Br, CF_3, $COOCH_3$ on 2-arylimidazo[1,2-*a*]pyridine to furnish the desired products (Scheme 1.7.4a,b).[114,115] Within the same realm, Yasuike *et al.* documented a Cu-catalyzed

tandem approach involving Ullmann-type *Se*-arylation and Csp^2–H selenation for the synthesis of benzo[*b*]selenophene-fused imidazo[1,2-*a*]pyridines (**85b**) using Se powder (Scheme 1.7.4c)[116]

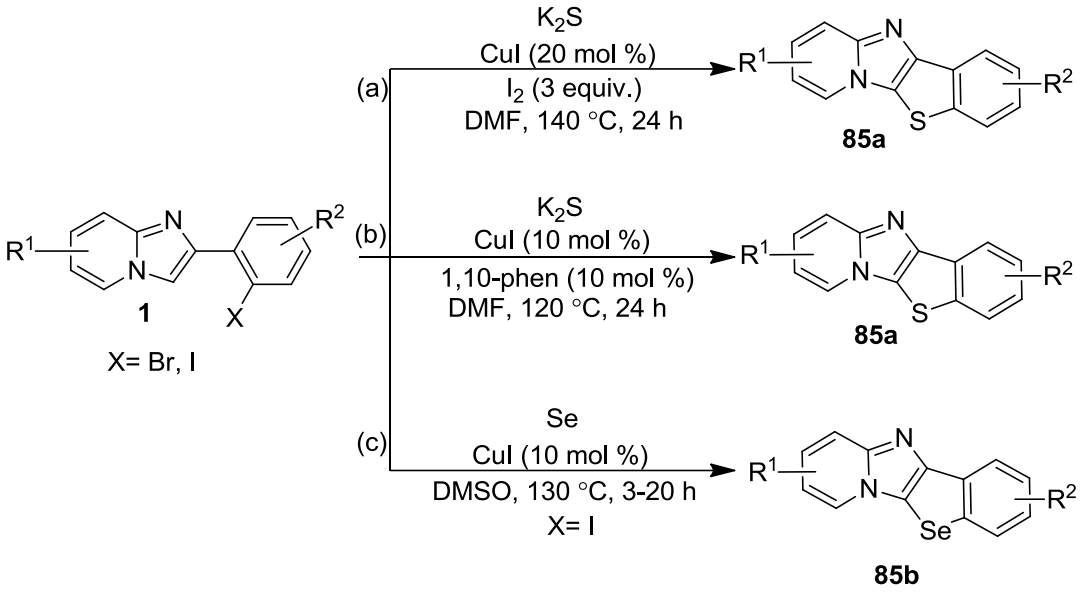

Scheme 1.7.4: Cu-catalyzed synthesis of benzo[*b*]thiophene/benzo[*b*]selenophene-fused imidazo[1,2-*a*]pyridines (**85a** & **85b**)

Gryko and collaborators developed an articulate approach for the construction of fused bis-imidazo[1,2-*a*]-pyridine (2,2*a*1,5*b*1,7-tetraazacyclopenta[*hi*]aceanthrylene) (**87**) under Pd-catalyzed conditions (Scheme 1.7.5). The authors described the strategy to be first case of double head-to-tail direct arylation of aromatic compounds. The unusual photophysical properties of the presented compound were briefly described.[117]

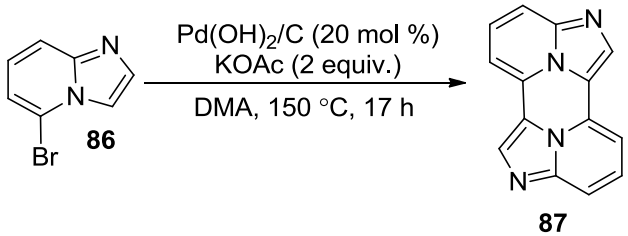

Scheme 1.7.5: Pd-catalyzed synthesis of fused bis-imidazo[1,2-*a*]pyridines (**87**)

In the striking contrast, Peng and coworkers documented a Pd-catalyzed strategy involving intermolecular C-3-arylation and intramolecular C-5-arylation of 2-arylimidazo[1,2-*a*]pyridines (**1**) with *o*-dihaloarenes (**88**). The use of $Pd(OAc)_2$/Xphos as suitable catalyst and ligand dayd

effectively leads to the regioselective formation of benzo[*a*]imidazo[5,1,2-*cd*]indolizines (**89**) derivatives in good to excellent yields (Scheme 1.7.6).[118]

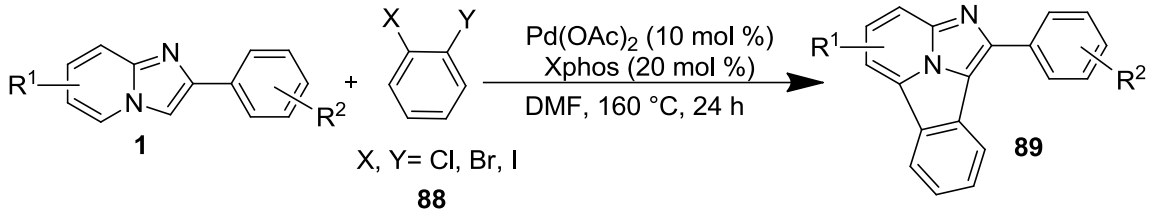

Scheme 1.7.6: Pd-catalyzed synthesis of benzo[*a*]imidazo[5,1,2-*cd*]indolizines (**89**)

Wu and coworkers reported an efficient synthesis of novel 6*H*-benzo[*b*]imidazo[5,1,2-*de*]quinolizin-6-ones (**91**) derivatives *via* Pd-catalyzed tandem cyclization of imidazo[1,2-*a*]pyridines (**1**) with 2-chlorobenzaldehydes (**90**). The reaction was proposed to proceed through C-3 arylation, followed by acylation at C-8 position *via* C−H bond activation without the assistance of directing group in air under the described reaction conditions. Imidazo[1,2-*a*]pyridines bearing sustituents such as CF_3, Ph, CH_3, and Cl at diffrent positions, were compatible under the optimized reaction conditions, and the corresponding regioselective products (**91**) were isolated in moderate-to-good yields (Scheme 1.7.7).[119]

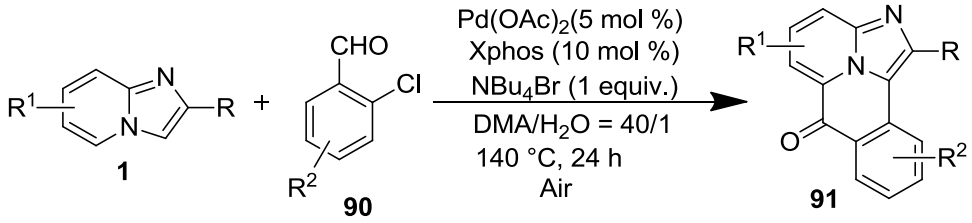

Scheme 1.7.7: Pd-catalyzed tandem synthesis of 6*H*-benzo[*b*]imidazo[5,1,2-*de*]quinolizin-6-ones (**91**)

Inspired by the fascinating biological profile and the fluorishing modern chemistry on imidazo[1,2-*a*]pyridines, we anticipated to functionalize this amazing heterocycle either under transition-metal catalyzed or metal-free conditions.

1.8 References

(1) Welsch, M. E.; Snyder, S. A.; Stockwell, B. R. *Current Opinion in Chemical Biology* **2010**, *14*, 347-361.

(2) Ebrahimlo, A. R. M.; Khalafy, J.; Marjani, A. P.; Prager. R. F. *Arkivok* **2009**, *12*, 17-30.

(3) Garuti, L.; Roberti, M.; Pizzirani, D. *Mini Reviews in Medicinal Chemistry* **2007**, *7*, 481-489.

(4) Enguehard-Gueiffier, C.; Gueiffier, A. *Mini Reviews in Medicinal Chemistry* **2007**, *7*, 888-899.

(5) Rival, Y.; Grassy, G.; Taudou, A.; Ecalle, R. *European Journal of Medicinal Chemistry* **1991**, *26*, 13-18.

(6) Rival, Y.; Grassy, G.; Micheal, G. *Chemical and Pharmaceutical Bulletin* **1992**, *40*, 1170-1176.

(7) Kim, O.; Jeong, Y.; Lee, H.; Hong, S. -S.; Hong, S. *Journal of Medicinal Chemistry* **2011**, *54*, 2455-2466.

(8) Bode, M. L.; Gravestock, D.; Moleele, S. S.; vander Westhuyzen, C. W.; Pelly, S. C.; Steenkamp, P. A.; Hoppe, H. C.; Khan, T.; Nkabinde, L. A. *Bioorganic & Medicinal Chemistry* **2011**, *19*, 4227-4237.

(9) Cheng, D.; Croft, L.; Abdi, M.; Lightfoot, A.; Gallagher, T. *Organic Letters* **2007**, *9*, 5175-5178.

(10) Kamal, A.; Reddy, J. S.; Ramaiah, M. J.; Dastagiri, D.; Bharathi, E. V.; Sagar, M. V. P.; Pushpavalli, S.; Ray, P.; Pal-Bhadra, M. *MedChemComm* **2010**, *1*, 355-360.

(11) Harrison, T. S.; Keating, G. M. *CNS drugs* **2005**, *19*, 65-89.

(12) Jain, A. N. *Journal of Medicinal Chemistry* **2004**, *47*, 947-961.

(13) Abe, Y.; Kayakiri, H.; Satoh, S.; Inoue, T.; Sawada, Y.; Inamura, N.; Asano, M.; Aramori, I.; Hatori, C.; Sawai, H. *Journal of Medicinal Chemistry* **1998**, *41*, 4587-4598.

(14) Almirante, L.; Polo, L.; Mugnaini, A.; Provinciali, E.; Rugarli, P.; Biancotti, A.; Gamba, A.; Murmann, W. *Journal of Medicinal Chemistry* **1965**, *8*, 305-312.

(15) Mikami, T.; Ochi, Y.; Suzuki, K.; Saito, T.; Sugie, Y.; Sakakibara, M. *Journal of Pharmacology and Experimental Therapeutics* **2008**, *325*, 190-199.

(16) Wafford, K.; Van Niel, M.; Ma, Q.; Horridge, E.; Herd, M.; Peden, D.; Belelli, D.; Lambert, *Neuropharmacology* **2009**, *56*, 182-189.

(17) Stasyuk, A. J.; Banasiewicz, M.; Cyrański, M. K.; Gryko, D. T. *The Journal of Organic Chemistry* **2012**, *77*, 5552-5558.

(18) Fookes, C. J.; Pham, T. Q.; Mattner, F.; Greguric, I.; Loc'h, C.; Liu, X.; Berghofer, P.; Shepherd, R.; Gregoire, M.-C.; Katsifis, A. *Journal of Medicinal Chemistry* **2008**, *51*, 3700-3712.

(19) Davey, D.; Erhardt, P. W.; Lumma Jr, W. C.; Wiggins, J.; Sullivan, M.; Pang, D.; Cantor, E. *Journal of Medicinal Chemistry* **1987**, *30*, 1337-1342.

(20) Reddy, K. R.; Reddy, A. S.; Shankar, R.; Kant, R.; Das, P. *Asian Journal of Organic Chemistry* **2015**, *4*, 573-583.

(21) Singhaus, R. R.; Bernotas, R. C.; Steffan, R.; Matelan, E.; Quinet, E.; Nambi, P.; Feingold, I.; Huselton, C.; Wilhelmsson, A.; Goos-Nilsson, A. *Bioorganic & Medicinal Chemistry Letters* **2010**, *20*, 521-525.

(22) Goodacre, S. C.; Street, L. J.; Hallett, D. J.; Crawforth, J. M.; Kelly, S.; Owens, A. P.; Blackaby, W. P.; Lewis, R. T.; Stanley, J.; Smith, A. J. *Journal of Medicinal Chemistry* **2006**, *49*, 35-38.

(23) Bischoff, F.; Berthelot, D.; De Cleyn, M.; Macdonald, G.; Minne, G.; Oehlrich, D.; Pieters, S.; Surkyn, M.; Trabanco, A. S. A.; Tresadern, G. *Journal of Medicinal Chemistry* **2012**, *55*, 9089-9106.

(24) Tresadern, G.; Cid, J. M.; Macdonald, G. J.; Vega, J. A.; de Lucas, A. I.; García, A.; Matesanz, E.; Linares, M. L.; Oehlrich, D.; Lavreysen, H. *Bioorganic & Medicinal Chemistry Letters* **2010**, *20*, 175-179.

(25) Kona, S.; Ravi, R. S.; Chakravarty, M.; Chava, V. N. R. *Journal of Chemistry* **2013**, 1- 7.

(26) Fu, H. Y.; Chen, L.; Doucet, H. *The Journal of Organic Chemistry* **2012**, *77*, 4473-4478.

(27) Cao, H.; Lin, Y.; Zhan, H.; Du, Z.; Lin, X.; Liang, Q. -M.; Zhang, H. *RSC Advances* **2012**, *2*, 5972-5975.

(28) Choy, P. Y.; Luk, K. C.; Wu, Y.; So, C. M.; Wang, L.-l.; Kwong, F. Y. *The Journal of Organic Chemistry* **2015**, *80*, 1457-1463.

(29) Koubachi, J.; El Kazzouli, S.; Berteina-Raboin, S.; Mouaddib, A.; Guillaumet, G. *Synlett* **2006**, 3237-3242.

(30) Lee, J.; Chung, J.; Byun, S. M.; Kim, B. M.; Lee, C. *Tetrahedron* **2013**, *69*, 5660-5664.

(31) Zhao, L.; Zhan, H.; Liao, J.; Huang, J.; Chen, Q.; Qiu, H.; Cao, H. *Catalysis Communications* **2014**, *56*, 65-67.

(32) Yang, H.; Yang, L.; Li, Y.; Zhang, F.; Liu, H.; Yi, B. *Catalysis Communications* **2012**, *26*, 11-14.

(33) Liu, Y.; He, L.; Yin, G.; Wu, G.; Cui, Y. *Bulletin of the Korean Chemical Society* **2013**, *34*, 2340-2342.

(34) Cao, H.; Zhan, H.; Lin, Y.; Lin, X.; Du, Z.; Jiang, H. *Organic Letters* **2012**, *14*, 1688-1691.

(35) Wang, S.; Liu, W.; Cen, J.; Liao, J.; Huang, J.; Zhan, H. *Tetrahedron Letters* **2014**, *55*, 1589-1592.

(36) Ji, X. -M.; Xu, L.; Yan, Y.; Chen, F.; Tang, R. -Y. *Synthesis* **2016**, 687-696.

(37) Zhou, L.; Lu, W. *Chemistry-A European Journal* **2014**, *20*, 634-642.

(38) Koubachi, J.; El Kazzouli, S.; Berteina-Raboin, S.; Mouaddib, A.; Guillaumet, G. *Synthesis* **2008**, 2537-2542.

(39) Koubachi, J.; Berteina-Raboin, S.; Mouaddib, A.; Guillaumet, G. *Synthesis* **2009**, 271-276.

(40) Ghosh, M.; Naskar, A.; Mitra, S.; Hajra, A. *European Journal of Organic Chemistry* **2015**, 715-718.

(41) Sawant, D.; Singh, I.; Tulsyan, G.; Abbagani, K.; Pardasani, R. T. *Synlett* **2015**, 1671-1676.

(42) Jana, S.; Dey, A.; Singsardar, M.; Bagdi, A. K.; Hajra, A. *The Journal of Organic Chemistry* **2016**, *81*, 9489-9493.

(43) Vilsmeier, A.; Haack, A. *European Journal of Inorganic Chemistry* **1927**, *60*, 119-122.

(44) Li, Q.; Zhou, M.; Han, L.; Cao, Q.; Wang, X.; Zhao, L.; Zhou, J.; Zhang, H. *Chemical Biology & Drug Design* **2015**, *86*, 849-856.

(45) Reimer, K.; Tiemann, F. *European Journal of Inorganic Chemistry* **1876**, *9*, 1268-1278.

(46) Wynberg, H. *Chemical Reviews* **1960**, *60*, 169-184.

(47) Meth-Cohn, O.; Ashton, M. *Tetrahedron Letters* **2000**, *41*, 2749-2752.

(48) Olah, G. A.; Ohannesian, L.; Arvanaghi, M. *Chemical Reviews* **1987**, *87*, 671-686.

(49) Cao, H.; Lei, S.; Li, N.; Chen, L.; Liu, J.; Cai, H.; Qiu, S.; Tan, J. *Chemical Communication* **2015**, *51*, 1823-1825.

(50) Xiang, S.; Chen, H.; Liu, Q. *Tetrahedron Letters* **2016**, *57*, 3870-3872.

(51) Lei, S.; Mai, Y.; Yan, C.; Mao, J.; Cao, H. *Organic Letters* **2016**, *18*, 3582-3585.

(52) Gao, Y.; Lu, W.; Liu, P.; Sun, P. *The Journal of Organic Chemistry* **2016**, *81*, 2482-2487.

(53) Wang, S.; Huang, X.; Ge, Z.; Wang, X.; Li, R. *RSC Advances* **2016**, *6*, 63532-63535.

(54) Lu, S.; Zhu, X.; Li, K.; Guo, Y. -J.; Wang, M. -D.; Zhao, X. -M.; Hao, X. -Q.; Song, M. -P. *The Journal of Organic Chemistry* **2016**, *81*, 8370-8377.

(55) Purser, S.; Moore, P. R.; Swallow, S.; Gouverneur, V. *Chemical Society Reviews* **2008**, *37*, 320-330.

(56) Kirk, K. L. *Organic Process Research & Development* **2008**, *12*, 305-321.

(57) Langlois, B. R.; Billard, T.; Roussel, S. *Journal of Fluorine Chemistry* **2005**, *126*, 173-179.

(58) Müller, K.; Faeh, C.; Diederich, F. *Science* **2007**, *317*, 1881-1886.

(59) Monir, K.; Bagdi, A. K.; Ghosh, M.; Hajra, A. *The Journal of Organic Chemistry* **2015**, *80*,1332-1337.

(60) Ji, X. -M.; Wei, L.; Chen, F.; Tang, R. -Y. *RSC Advances* **2015**, *5*, 29766-29773.

(61) Zhu, M.; Han, X.; Fu, W.; Wang, Z.; Ji, B.; Hao, X. -Q.; Song, M. -P.; Xu, C. *The Journal of Organic Chemistry* **2016**, *81*, 7282-7287.

(62) Mishra, S.; Mondal, P.; Ghosh, M.; Mondal, S.; Hajra, A. *Organic & Biomolecular Chemistry* **2016**, *14*, 1432-1436.

(63) Li, K.; Zhao, X. -M.; Yang, F. -L.; Hou, X.-H.; Xu, Y.; Guo, Y. -C.; Hao, X. -Q.; Song, M. -P. *RSC Advances* **2015**, *5*, 90478-90481.

(64) Kaswan, P.; Nandwana, N. K.; DeBoef, B.; Kumar, A. *Advanced Synthesis & Catalysis* **2016**, *358*, 2108-2115.

(65) Modi, A.; Ali, W.; Patel, B. K. *Advanced Synthesis & Catalysis* **2016**, *358*, 2100-2107.

(66) Liu, P.; Shen, Z.; Yuan, Y.; Sun, P. *Organic & Biomolecular Chemistry* **2016**, *14*, 6523-530.

(67) Patel, O. P.; Anand, D.; Maurya, R. K.; Yadav, P. P. *The Journal of Organic Chemistry* **2016**, *81*, 7626-7634.

(68) Mondal, S.; Samanta, S.; Santra, S.; Bagdi, A. K.; Hajra, A. *Advanced Synthesis & Catalysis* **2016**, *358*, 3633-3641.

(69) Sodeoka, M.; Todd, M.; Kraus, G. A.; Darcel, C.; Stankiewicz, A.; Seidl, P. R.; De Boef, B.; Kou, Y.; Itami, K.; Li, Z. *From C-H to C-C Bonds: Cross-dehydrogenative-coupling*; Royal Society of Chemistry, **2014**.

(70) Fleming, F. F.; Yao, L.; Ravikumar, P.; Funk, L.; Shook, B. C. *Journal of Medicinal Chemistry* **2010**, *53*, 7902-7917.

(71) Su, H.; Wang, L.; Rao, H.; Xu, H. *Organic Letters* **2017**, *19*, 2226-2229.

(72) Ackermann, L. *Accounts of Chemical Research* **2013**, *47*, 281-295.

(73) Guo, X.; Baumgarten, M.; Müllen, K. *Progress in Polymer Science* **2013**, *38*, 1832-1908.

(74) Qi, Z.; Yu, S.; Li, X. *The Journal of Organic Chemistry* **2015**, *80*, 3471-3479.

(75) Li, P.; Zhang, X.; Fan, X. *The Journal of Organic Chemistry* **2015**, *80*, 7508-7518.

(76) Ghosh, M.; Naskar, A.; Mishra, S.; Hajra, A. *Tetrahedron Letters* **2015**, *56*, 4101-4104.

(77) Peng, H.; Yu, J. -T.; Jiang, Y.; Wang, L.; Cheng, J. *Organic & Biomolecular Chemistry* **2015**, *13*, 5354-5357.

(78) Wang, W.; Niu, J. -L.; Liu, W.-B.; Shi, T. -H.; Hao, X.-Q.; Song, M. -P. *Tetrahedron* **2015**, *71*, 8200-8207.

(79) Kotla, S. K. R.; Choudhary, D.; Tiwari, R. K.; Verma, A. K. *Tetrahedron Letters* **2015**, *56*,4706-4710.

(80) Li, Y.; Wang, F.; Yu, S.; Li, X. *Advanced Synthesis & Catalysis* **2016**, *358*, 880-886.

(81) Liskey, C. W.; Liao, X.; Hartwig, J. F. *Journal of the American Chemical Society* **2010**, *132*, 11389-11391.

(82) Zhu, X.; Shen, X. -J.; Tian, Z.-Y.; Lu, S.; Tian, L. -L.; Liu, W.-B.; Song, B.; Hao, X. -Q. *The Journal of Organic Chemistry* **2017**, *82*, 6022-6031.

(83) Herradura, P. S.; Pendola, K. A.; Guy, R. K. *Organic Letters* **2000**, *2*, 2019-2022.

(84) Faucher, A. -M.; White, P. W.; Brochu, C.; Grand-Maître, C.; Rancourt, J.; Fazal, G. *Journal of Medicinal Chemistry* **2004**, *47*, 18-21.

(85) Paramashivappa, R.; Kumar, P. P.; Rao, P. S.; Rao, A. S. *Bioorganic & Medicinal Chemistry Letters* **2003**, *13*, 657-660.

(86) Kondo, T.; Mitsudo, T.-A. *Chemical Reviews* **2000**, *100*, 3205-3220.

(87) Zhou, Z.; Liu, Y.; Chen, J.; Yao, E.; Cheng, J. *Organic Letters* **2016**, *18*, 5268-5271.

(88) Li, J.; Li, C.; Yang, S.; An, Y.; Wu, W.; Jiang, H. *The Journal of Organic Chemistry* **2016**, *81*, 7771-7783.

(89) Chen, F. -J.; Liao, G.; Li, X.; Wu, J.; Shi, B. -F. *Organic Letters* **2014**, *16*, 5644-5647.

(90) Li, Z.; Hong, J.; Zhou, X. *Tetrahedron* **2011**, *67*, 3690-3697.

(91) Ravi, C.; Mohan, D. C.; Adimurthy, S. *Organic & Biomolecular Chemistry* **2016**, *14*, 2282-2290.

(92) Cao, H.; Chen, L.; Liu, J.; Cai, H.; Deng, H.; Chen, G.; Yan, C.; Chen, Y. *RSC Advances* **2015**, *5*, 22356-22360.

(93) Zheng, Z.; Qi, D.; Shi, L. *Catalysis Communications* **2015**, *66*, 83-86.

(94) Ravi, C.; Reddy, N. N. K.; Pappula, V.; Samanta, S.; Adimurthy, S. *The Journal of Organic Chemistry* **2016**, *81*, 9964-9972.

(95) Ding, Y.; Xie, P.; Zhu, W.; Xu, B.; Zhao, W.; Zhou, A. *RSC Advances* **2016**, *6*, 81932-81935.

(96) Ravi, C.; Mohan, D. C.; Adimurthy, S. *Organic Letters* **2014**, *16*, 2978-2981.

(97) Mitra, S.; Ghosh, M.; Mishra, S.; Hajra, A. *The Journal of Organic Chemistry* **2015**, *80*, 75-8281.

(98) Yang, D.; Yan, K.; Wei, W.; Li, G.; Lu, S.; Zhao, C.; Tian, L.; Wang, H. *The Journal of Organic Chemistry* **2015**, *80*, 11073-11079.

(99) Zhang, H.; Wei, Q.; Wei, S.; Qu, J.; Wang, B. *European Journal of Organic Chemistry* **2016**, 3373-3379.

(100) Jiao, J.; Wei, L.; Ji, X. M.; Hu, M. L.; Tang, R. Y. *Advanced Synthesis & Catalysis* **2016**, *58*, 268-275.

(101) Wang, Q.; Qi, Z.; Xie, F.; Li, X. *Advanced Synthesis & Catalysis* **2015**, *357*, 355-360.

(102) Wang, Y.; Frett, B.; McConnell, N.; Li, H. -Y. *Organic & Biomolecular Chemistry* **2015**, *13*, 2958-2964.

(103) Kandimalla, S. R.; Sabitha, G. *RSC Advances* **2016**, *6*, 67086-67095.

(104) Chakraborty, A.; Jana, S.; Kibriya, G.; Dey, A.; Hajra, A. *RSC Advances* **2016**, *6*, 34146 34152.

(105) Kielesiński, Ł.; Tasior, M.; Gryko, D. T. *Organic Chemistry Frontiers* **2015**, *2*, 21-28.

(106) Monir, K.; Ghosh, M. Jana, S.; Mondal, P.; Majee, A.; Hajra, A. *Organic & Biomolecular Chemistry* **2015**, *13*, 8717-8722.

(107) Yang, D.; Yan, K.; Wei, W.; Liu, Y.; Zhang, M.; Zhao, C.; Tian, L.; Wang, H. *Synthesis* **2016,** *48*, 122–130.

(108) Mondal, S.; Samanta, S.; Jana, S.; Hajra, A. *The Journal of Organic Chemistry* **2017**, *82*, 504-4510.

(109) Yadav, M.; Dara, S.; Saikam, V.; Kumar, M.; Aithagani, S. K.; Paul, S.; Vishwakarma, R. A.; Singh, P. P. *European Journal of Organic Chemistry* **2015**, *2015*, 6526-6533.

(110) Liu, P.; Gao, Y.; Gu, W.; Shen, Z.; Sun, P. *The Journal of Organic Chemistry* **2015**, *80*, 11559-11565.

(111) Pericherla, K.; Khedar, P.; Khungar, B.; Kumar, A. *Chemical Communications* **2013**, *49*, 924-2926.

(112) Wang, Z.; Li, B.; Zhang, X.; Fan, X. *The Journal of Organic Chemistry* **2016**, *81*, 6357-6363.

(113) Zhang, J.; Zhang, X.; Fan, X. *The Journal of Organic Chemistry* **2016**, *81*, 3206-32013.

(114) Huang, H.; Dang, P.; Wu, L.; Liang, Y.; Liu, J. *Tetrahedron Letters* **2016**, *57*, 574-577.

(115) Yan, K.; Yang, D.; Wei, W.; Lu, S.; Li, G.; Zhao, C.; Zhang, Q.; Wang, H. *Organic Chemistry Frontiers* **2016**, *3*, 66-70.

(116) Matsumura, M.; Sakata, Y.; Iwase, A.; Kawahata, M.; Kitamura, Y.; Murata, Y.; Kakusawa, N.; Yamaguchi, K.; Yasuike, S. *Tetrahedron Letters* **2016**, *57*, 5484-5488.

(117) Firmansyah, D.; Deperasińska, I.; Vakuliuk, O.; Banasiewicz, M.; Tasior, M.; Makarewicz, ; Cyrański, M. K.; Kozankiewicz, B.; Gryko, D. T. *Chemical Communications* **2016**, *52*, 1262-1265.

(118) Wang, H.; Chen, C.; Huang, Z.; Yao, L.; Li, B.; Peng, J. *Synthesis* **2015**, *47*, 2457-2466.

(119) Mu, B.; Li, J.; Zou, D.; Wu, Y.; Chang, J.; Wu, Y. *Organic Letters* **2016**, *18*, 5260-5263.

CHAPTER 2

Microwave-Assisted Expedite Synthesis of Imidazo[1,2-*a*]pyridyl Quinoxalin-2(1*H*)-ones

2.1 Introduction

As described in chapter 1, imidazo[1,2-*a*]pyridine (IP) is a highly privileged and potentially bioactive heterocycle possessing strong antiviral, antimicrobial, antitumor, anti-inflammatory, antiparasitic, hypnotic and anticancer activities in its various functionalized forms.[1-6] Interestingly, several drugs and prodrugs based on imidazo[1,2-*a*]pyridine nucleus such as Olprinone (the PDE 3 inhibitor),[7] Soraprazan (antiulcer, clinical trial phase I, II compound)[8] optically active GSK812397 (anti-HIV agent),[9] WO2015200341 (tropomyosin receptor kinase inhibitor)[10] contains different heterocyclic systems intact to its structural periphery (Figure 2.1.1).

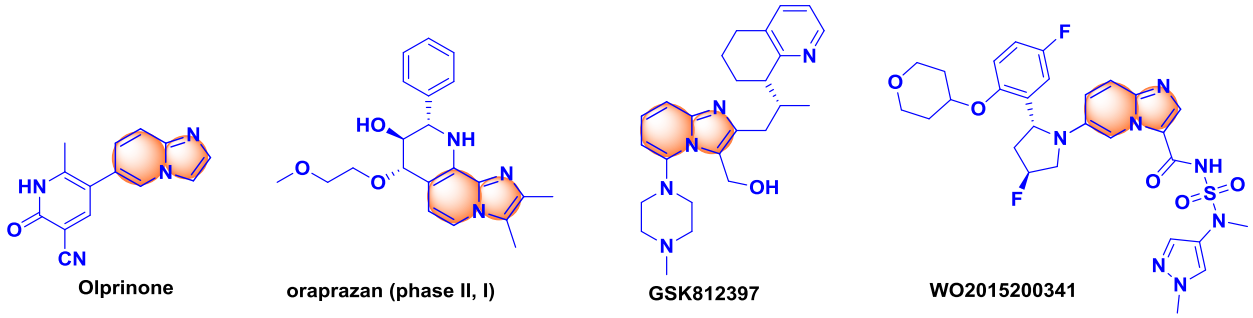

Figure 2.1.1: Selective examples of bioactive imidazo[1,2-*a*]pyridines containing different heterocyclic skeletons intact

The profound importance of these bioactive molecules has opened up new gateways for the medicinal chemists to synthesize various biologically potent imidazo-pyridine conjugates with other heterocycles. In conjunction to this ideology, Purohit *et al*. prepared 2-[(4'-chlorophenyl)-6- methyl imidazo[1,2-*a*]pyridin-3-yl]-(1"-propene-3"-aryl-3"-yl)-pyrimidine-2"',4"',6"'-(3"'*H*,5"'*H*)-triones (**3**) by the cyclocondensation of 2-(4'-chlorophenyl)-6-methyl-3-(1"-aryl-2"-propene-1"-one-3-yl)-imidazo[1,2-*a*]pyridines (**1**) with barbituric acid (**2**) in glacial acetic acid at 110 °C (Scheme 2.1.1).[11] Interestingly, compound **3** was found to possess remarkable antibacterial and antifungal activities.

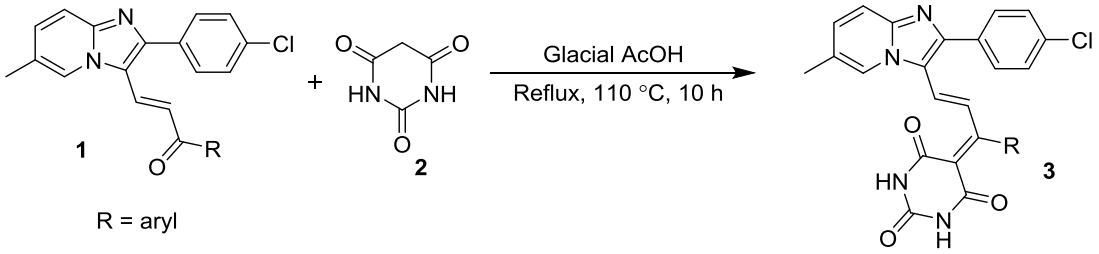

Scheme 2.1.1: Synthesis of imidazo[1,2-*a*]pyridine–barbituric acid conjugates (**3**)

The same authors further reported the synthesis of methylene bridged imidazo[1,2-*a*]pyridyl-oxaindazolines (**8**) from substituted imidazo[1,2-*a*]pyridine-3-carbaldehydes **(4**) in two steps. The first step involves the reaction of **4** with benzoylglycine (**5**) to yield methylene-bridged imidazo[1,2-*a*]pyridyl-phenyl-5''-oxazolone (**6**), which upon further reaction with aryl amines (**7**) afforded **8** in descent yields. The synthesized derivatives were tested against Gram +ve, Gram -ve bacteria and fungi. Notably, some of the products showed moderate activity in concentration up to 50 µg/mL (Scheme 2.1.2).[12]

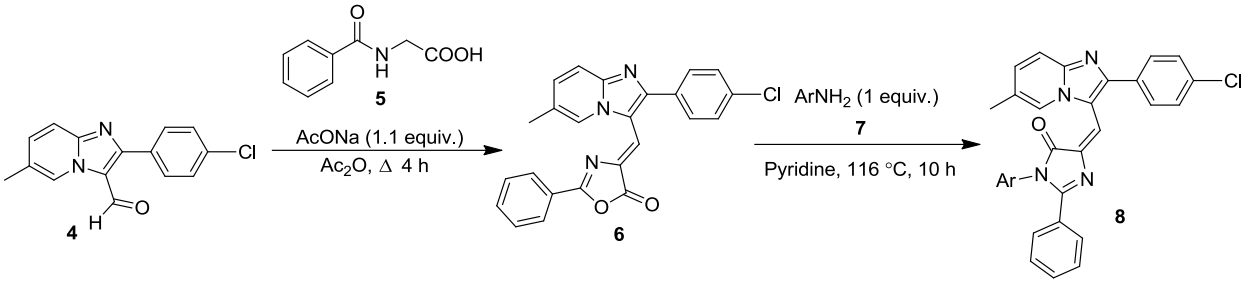

Scheme 2.1.2: Synthesis of methylene-bridged imidazo[1,2-*a*]pyridyl-oxaindazolines (**8**)

Bavantula *et al.* documented a one-pot multi-component synthesis of thiazolyl linked imidazo[1,2-*a*]pyridine-coumarin conjugates **11** from substituted imidazo[1,2-*a*]pyridine-3-carbaldehydes **4**, thiosemicarbazide (**9**) and substituted 3-(2-bromoacetyl)-2*H*-chromen-2-ones/ 2-(2-bromoacetyl)-3*H*-benzo[*f*]chromen-3-ones (**10**) in ethanol by employing catalytic amount of acetic acid. The synthesized compounds were evaluated for their *in-vitro* antimicrobial activity against different bacterial and fungal strains, Interestingly, some of the compounds displayed antibacterial activity with minimum inhibitory concentration of 150 µg/mL (Scheme 2.1.3).[13]

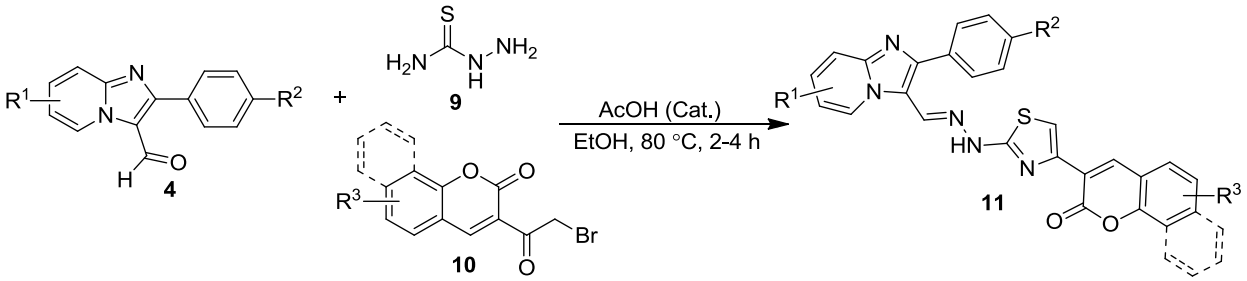

Scheme 2.1.3: One-pot multi-component synthesis of thiazolyl linked imidazo[1,2-*a*]pyridine- coumarin conjugates (**11**)

Gudmundsson and coworkers reported a series of 2-aryl-3-pyrimidyl-imidazo[1,2-*a*]pyridines (**15**) with potent antiviral activity against herpes simplex viruses. The compounds were synthesized in multiple synthetic steps, starting from substituted

8-chloro-2-(4-methoxyphenyl)imidazo[1,2-*a*]pyridine-3-carbaldehyde (**12**) *via* the formation of its alkynyl ketone using ethynyl magnesium bromide and finally cyclopentyl guanidine skeleton was introduced into the core imidazo[1,2-*a*]pyridine (IP) moiety using cyclopentyl guanidine (**13**) (Scheme 2.1.4).[14]

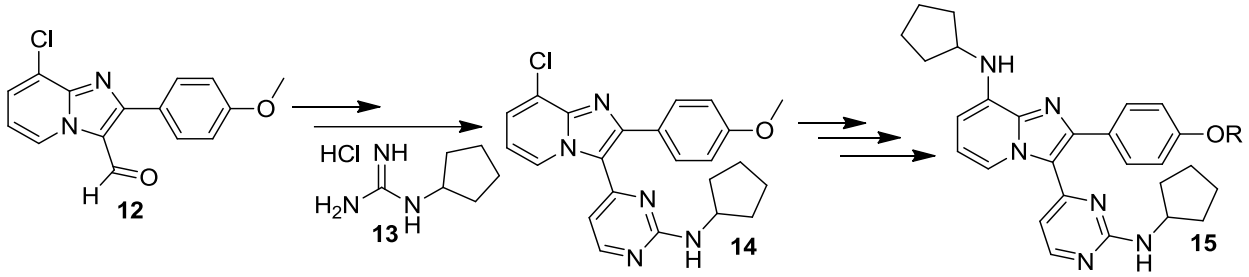

Scheme 2.1.4: Multistep synthesis of 2-aryl-3-pyrimidyl-imidazo[1,2-*a*]pyridines conjugates (**15**)

Kamal *et al.* synthesized imidazo[1,2-*a*]pyridine/imidazo[1,2-*a*]pyrimidine-benzimidazole conjugates (**17)**, by the oxidative cyclization of substituted *ortho*-phenylene diamine (**16)** and imidazo[1,2-*a*]pyridine/imidazo[1,2-*a*]pyrimidine-3-carbaldehyde (**4)** in ethanol using sodium metabisulphite. The compounds showcased moderate to good cytotoxic activity against the human cervical (Hela), lung (A549), prostate (DU-145) and melanoma (B-16) cancer cell lines (Scheme 2.1.5).[15]

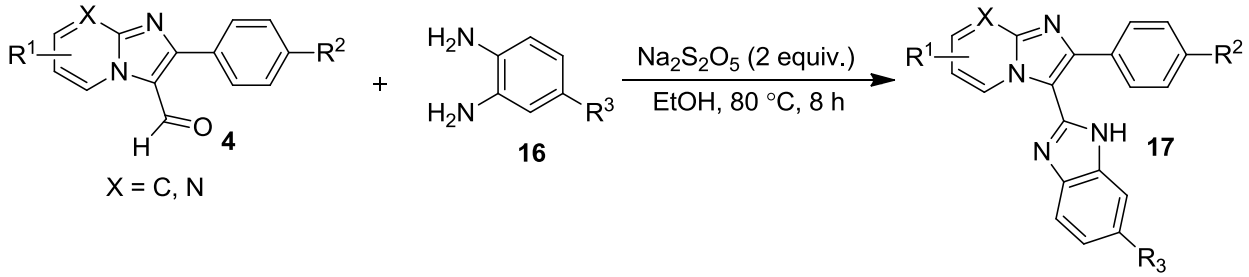

Scheme 2.1.5: Synthesis of imidazopyridine/imidazopyrimidine-benzimidazole conjugates (**17**)

The authors also developed an efficient protocol for the synthesis of imidazopyridine–oxindole conjugates (**19)** through Knoevenagel reaction between imidazo[1,2-*a*]pyridine-3-carbaldehyde (**4**) and oxindole derivatives (**18**). The anticancer activities of these synthesized compounds were studied against selected human cancer cell lines. Some of the compound exhibited promising anti-proliferative activity with GI_{50} values ranging from 0.17 to 9.31 μM (Scheme 2.1.6).[16]

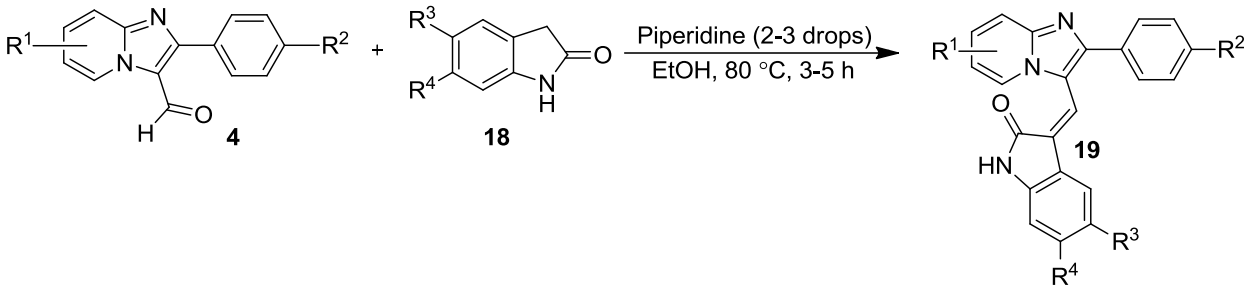

Scheme 2.1.6: Synthesis of imidazopyridine–oxindole conjugates (**19**)

Hayakawa *et al.* synthesized sulfonyl pyrazole derivatives of imidazo[1,2-*a*]pyridine (**24**) starting from 1-(imidazo[1,2-*a*]pyridin-3-yl)ethanones **20** in multiple steps. The methodology involves the condensation of **20** with 1,1-dimethoxy-*N*,*N*-dimethylmethanamine (**21)**, followed by cyclization of resulted enamines with hydrazine hydrate **22** to yield pyrazole derivatives **23**. Finally sulfonylation of **23** with aryl sulfonyl chlorides afforded corresponding **24** (Scheme 2.1.7a). Interestingly, one of the synthesized derivative, 3-(1-[(4-fluorophenyl)sulfonyl]-1*H*-pyrazol-3-yl)-2-methylimidazo[1,2-*a*]pyridine was found as a novel p110*α* inhibitor with an IC_{50} of 0.67l M (Scheme 2.1.7a).[17] The author also presented the synthesis of bioactive thiazole linked imidazo[1,2-*a*]pyridine **26** *via* a multistep protocol (Scheme 2.1.7b).

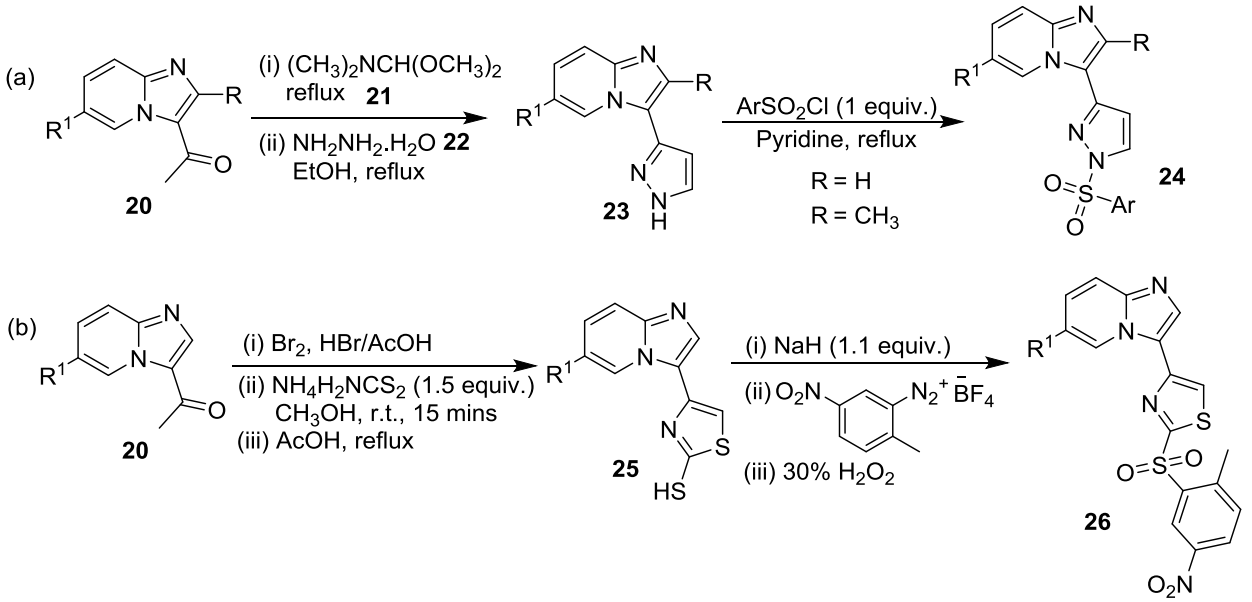

Scheme 2.1.7: Synthesis of pyrazolyl- and thiazolyl-imidazo[1,2-*a*]pyridine sulfones (**24**) and (**26**)

On the other hand, quinoxaline represent an important class of azaheterocycle possessing versatile biological activities such as antibacterial,[18] antihistaminic,[19] antitrypanosomal,[20]

antiplasmodial,[21] and antiinflammatory.[22] In addition, quinoxaline derivatives are reported for their applications as dyes,[23] electroluminescent materials,[24] organic semiconductors[25] and DNA cleaving agents.[26] In particular, 1,2-dihydroquinoxaline-2-ones represent a sub-family with interesting applications in drug discovery. One such application is their antagonism behaviour towards glutamate AMPA (*α*-amino-3-hydroxy-5-methyl-4-isoxazolepropionic acid) receptors, which is quite effective in the therapy of neurodegenerative disorders such as ischemic stroke, epilepsy, head trauma, and Alzheimer's disease, without showing any side effects such as schizophrenia.[27] GRA-293 is one such example that possess imidazole attached to 1,2-dihydroquinoxaline-2-one skeleton (Figure 2.1.2a) showing excellent third generation AMPA receptor antagonist activity *in vitro* and *in vivo* as compared to the known first and second generation AMPA receptor antagonists such as YM-90K, YM-872 (Figure 2.1.2b).[28] Aoki *et al.* reported 3-(indol-2-yl)quinoxalin-2-ones as anti-angiogenesis agents that showed a potent inhibitory activity toward the VEGF-induced proliferation of human mesangial cells and the VEGF-induced auto-phosphorylation of human umbilical vein endothelial cells (Figure 2.1.2c).[29] Ruthenium(II) arene complexes of 3-(1*H*-benzimidazol-2-yl)-1*H*-quinoxalin-2-one have been reported to possess anti proliferative activity in three human cancer cell lines (A549, CH1, SW480).[30] Apart from quinoxalin-2-ones derivatives, several other quinoxaline derivatives (Figure 2.1.2) are also potentially bioactive compounds and are marketed as drugs (Figure 2.1.2).[31]

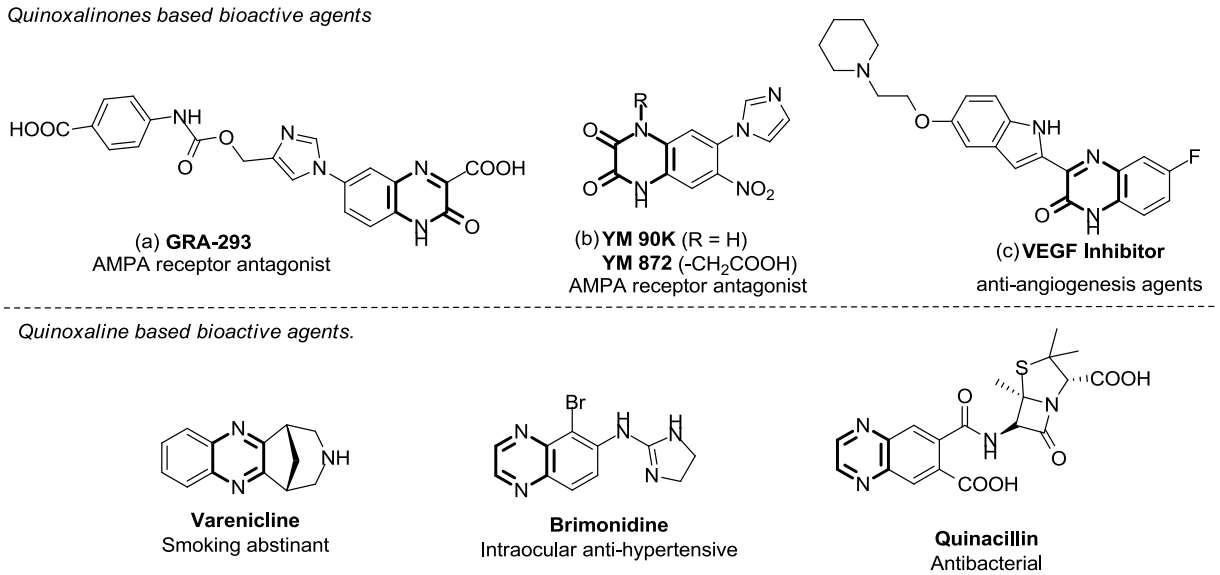

Figure 2.1.2: Selective examples of biologically active quinoxalinone and quinoxaline derivatives

Recently, Mamedov *et al.* have synthesized a series of antibacterial and antifungal active 1-pyridylimidazo[1,5-*a*]quinoxalin-4(5*H*)-ones and their *N*-alkylated derivatives **29** from 3-acylquinoxalin-2(1*H*)-ones/*N*-alkyl derivatives **27** and aminomethylpyridines (**28**) in DMSO at elevated temperature (Scheme 2.1.8).[32]

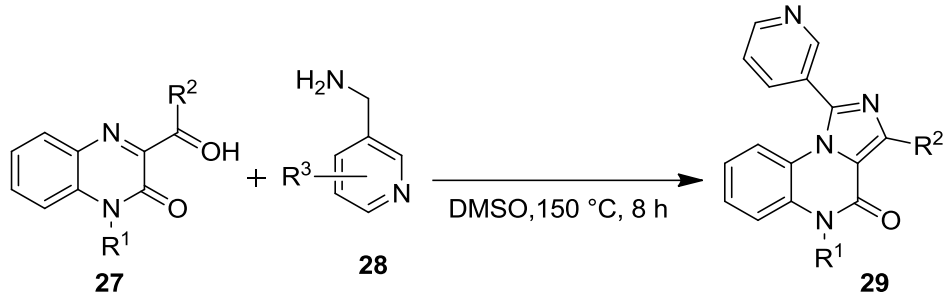

Scheme 2.1.8: Synthesis of 1-pyridylimidazo[1,5-*a*]quinoxalin-4(5*H*)-ones (**29**) and their *N*-alkylated derivatives.

Inspired from the valuable medicinal importance of imidazo[1,2-*a*]pyridyl-heterocyclic conjugates, we aimed to synthesize quinoxalinones linked imidazo[1,2-*a*]pyridines as a potential pharmaceutical lead. To the best of our knowledge, only one patent describes the application of imidazo[1,2-*a*]pyridyl-quinoxalinones as selective inhibitors of platelet-derived growth factor and inhibitors of human ileal bile acid transporter.[33]

2.2 Results and Discussion

The starting material, 2-methyl/2-arylimidazo[1,2-*a*]pyridines (**32)** required for this work, and subsequent works were synthesized by the reaction of substituted *α*-bromo acetone/phenacyl bromides (**30**) and 2-aminopyridines (**31**) in ethanol or ethanol/1,4-dioxane mixture under reflux conditions using reported literature procedures (Scheme 2.2.1).[34,35]

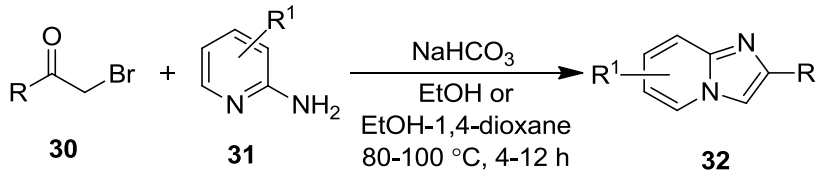

Scheme 2.2.1: Synthesis of 2-methyl/2-arylimidazo[1,2-*a*]pyridines (**32**)

With an anticipation to synthesize quinoxalinone anchored imidazo[1,2-*a*]pyridines, we directly focused our attention towards the exemplification of Hinsberg cyclization reaction with appropriately functionalized imidazo[1,2-*a*]pyridines. Hinsberg reaction[36] is a straightforward high-yielding strategy that involves the hetero-cyclization of *o*-phenylene diamine with *α*-ketoesters in the presence of a catalyst such as acetic acid,[37] sulfuric acid,[38] citric acid,[39]

gallium triflate,[40] polyaniline-sulfate salt.[41] However, the general applicability of catalyst for different alkyl/aryl/heteroaryl *α*-ketoesters substrates remains doubtful, and thus synthesizing novel heterocyclic quinoxalinones *via* Hinsberg reaction remains a challenging task. To the best our knowledge, Hinsberg cyclization of sterically hindered substrates such as imidazo-heterocycles has not been reported. For this purpose, 2-arylimidazo[1,2-*a*]pyridyl-3-glyoxalates (**34**), were synthesized by reacting ethyl oxalyl chloride (**33**) with substituted 2-arylimidazo[1,2-*a*]pyridines (**32**) in 1,4-dioxane under reflux conditions (Scheme 2.2.2).

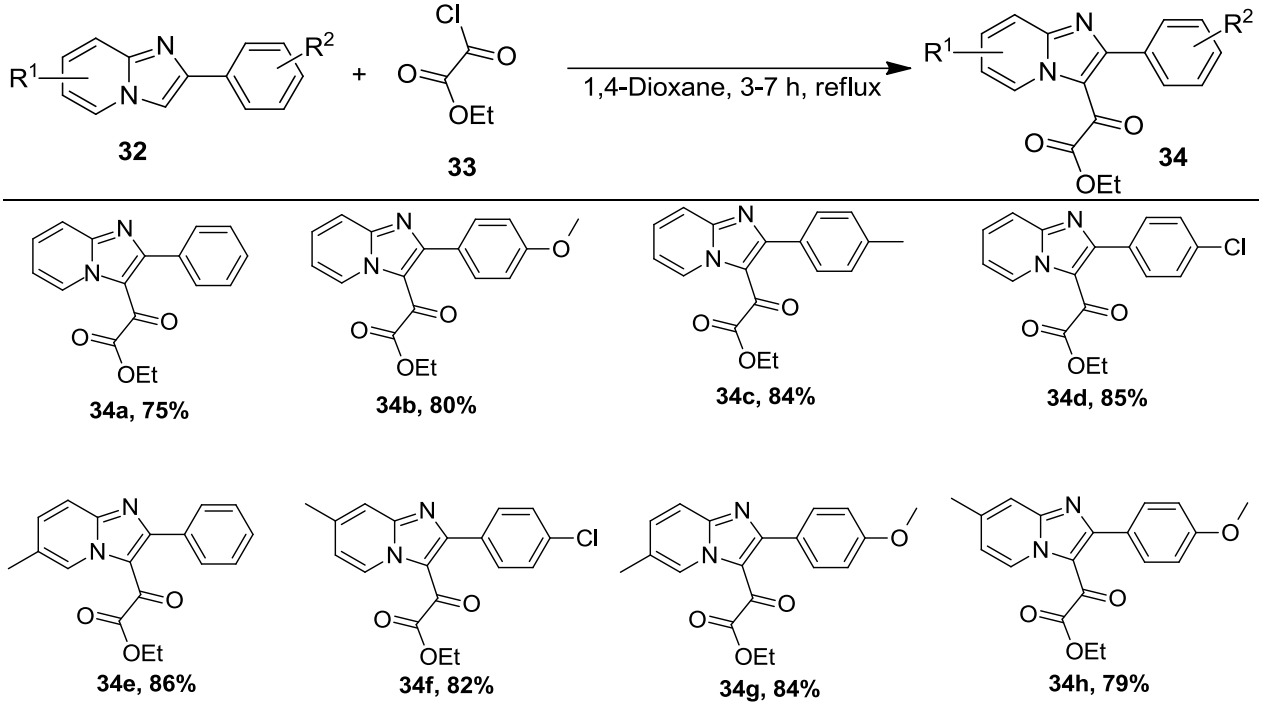

Scheme 2.2.2: Synthesis of 2-arylimidazo[1,2-*a*]pyridyl-3-glyoxalates (**34**)

Thereafter, the heterocyclization reaction between 2-arylimidazo[1,2-*a*]pyridyl-3-glyoxalate (**34a**) and *ortho*-phenylene diamine (**16**) was carried out as a model reaction (Table 2.2.1, entries 1-17). The condensation between **34a** and **16** failed to afford the desired product 3-(2-phenylimidazo[1,2-*a*]pyridin-3-yl)quinoxalin-2(1*H*)-one (**35a**) under classical reflux conditions even up to 120 h in several solvents including CH_3CN, THF, EtOH and DMF (Table 2.2.1, entry 1). In addition, **34a** and **16** also failed to react in any of the aforementioned solvents, even under microwave irradiation at 100 °C up to 2.5 h (Table 2.2.1, entry 2). It is worth to mention that, some of the glyoxalate got decomposed to its starting imidazo[1,2-*a*]pyridine **32a** upon prolonged heating under conventional/microwave conditions. Interestingly, employment of

$Yb(OTf)_3$ (10 mol %) catalyzed the reaction under microwave conditions, affording the desired **35a** in low to moderate yields in THF, CH_3CN, 1,4-dioxane under independent reaction conditions (Table 2.2.1, entry 3). Surprisingly, AgOTf and $Bi(OTf)_3$ were ineffective for the desired transformation resulting in trace product formation (Table 2.2.1, entries 5 and 7).

Table 2.2.1: Selected optimization of reaction conditions for the synthesis of **35a**[a]

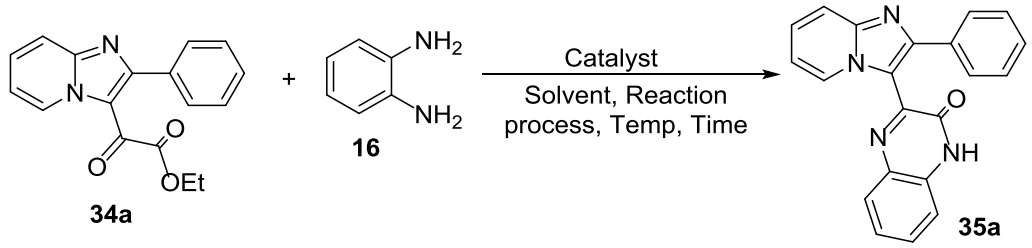

Entry	Catalyst	Solvent	Reaction Process[b]	Temp.[b] (°C)	Time[b] (h)	Yield[c] (%)
1.	-	CH_3CN/THF/EtOH/DMF	Conventional	Reflux	120	-
2.		CH_3CN/THF/EtOH/DMF	Microwave	100	2.5	-
3.	$Yb(OTf)_3$	THF/CH_3CN/Dioxane	Microwave	110	2	55/25/40
4.	$In(OTf)_3$	THF/CH_3CN	Microwave	90	2	40/46
5.	AgOTf	THF/CH_3CN	Microwave	90	2	Trace
6.	$Cu(OTf)_2$	THF/CH_3CN	Microwave	90	2	20/trace
7.	$Bi(OTf)_3$	THF/CH_3CN	Microwave	90	2	Trace
8.	$Sc(OTf)_3$	THF/CH_3CN	Microwave	100	2	40/18
9.	$InBr_3$	THF/CH_3CN	Microwave	100	2.5	32/trace
10.	$InCl_3$	THF/CH_3CN	Microwave	130	2.5	28/trace
11.	**$Yb(OTf)_3$**	**THF**	**Microwave**	**100**	**1.5**	**58**
12.	Neutral Alumina	-	Microwave	150	2	50
13.	Acidic Alumina	-	Microwave	150	2	42
14.	**Mont. K-10**	**-**	**Microwave**	**100**	**1**	**72**
15.	Mont. K-10	-	Microwave	100	2.5	60
16.	Mont. K-10	-	Microwave	130	1.5	58
17.	Acidic Silica gel	-	Microwave	160	2.5	45

[a]Reaction conditions: Imidazo[1,2-*a*]pyridine (**34a**) (0.25 mmol), *o*-phenylene diamine (**16**) (0.30 mmol), catalyst (10 mol %), solvent (2 mL);[b] The reactions were performed as per the conditions mentioned under classical reflux and microwave irradiation at different temperature for different interval of time;[c] Isolated yield; Microwave power was applied at 80W for the standardization.

The usage of other Lewis acids such as $In(OTf)_3$, $Cu(OTf)_2$, $Sc(OTf)_3$, $InBr_3$, $InCl_3$ in THF/CH_3CN under microwave irradiation were also successful, resulting **35a** albeit in lower

yields (Table 2.2.1, entries 4, 6, 8-10). Gratifyingly $Yb(OTf)_3$ (10 mol %) was found to be the best catalyst for desired transformation, resulting **35a** in 58% in THF at 100 °C under microwave irradiation in 1.5 h (Table 2.2.1, entry 11). To further increase the yield of the product, we employed solid supports such as neutral alumina, acidic alumina, silica gel and montmorillonite K-10 for the above transformation (Table 2.2.1, entries 12-17). Delightfully, montmorillonite K-10 support offered **35a** in 72% yield at 100 °C in 1.0 h, under microwave irradiation (Table 2.2.1, entry 14).

With optimized reaction conditions in hand, the substrate scope of imidazo[1,2-*a*]pyridines was explored towards the synthesis of substituted imidazo[1,2-*a*]pyridyl quinoxalinones (**35a-j)** (Scheme 2.2.3). The reaction tolerated a wide range of electron-donating and electron-withdrawing substituents on imidazo[1,2-*a*]pyridyl system, affording the corresponding quinoxalinones **35a-j** in moderate to good (20-75%) yields (Scheme 2.2.3). The presence of electron-withdrawing group on phenyl ring attached at the C-2 position of imidazo[1,2-*a*]pyridine system decreased its reactivity towards the expected heterocyclization. For example; 2-(4′-nitrophenyl)imidazo[1,2-*a*]pyridyl-3-glyoxalate (**34i**) gave poor yield (20%) of corresponding 3-(2-(4-nitrophenyl)imidazo[1,2-*a*]pyridin-3-yl)quinoxalin-2(1*H*)-one (**35i**), probably because **34i** was not obtained as a pure intermediate, and rather was isolated as a mixture along with the starting 2-(4′-nitrophenyl)imidazo[1,2-*a*]pyridine (Scheme 2.2.3).

Notably, the use of $Yb(OTf)_3$ in THF under microwave irradiation gave the desired products in relatively lesser yields over the montmorillonite K-10-supported synthetic protocol for all the derivatives (Scheme 2.2.3). After completion of the reaction, the desired products were isolated either by flash column chromatography or by re-crystallization using $MeOH/CH_2Cl_2$. All the synthesized compounds were characterized by detailed spectroscopic analysis including ^1H NMR, ^{13}C NMR and HRMS. A representative ^1H NMR and ^{13}C NMR spectrum of **35c** is shown in figures 2.2.1 and 2.2.2.

In the recycling study, both $Yb(OTf)_3$ and montmorillonite K-10 were recovered and reused up to three times, without any appreciable loss of catalytic activity. No significant declination in the yield of the product was noticed.

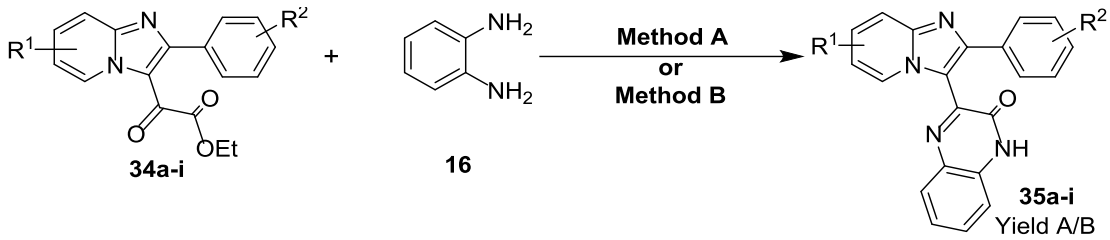

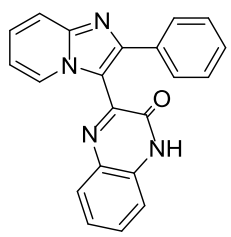

35a
72%^{A}/58%^{B}

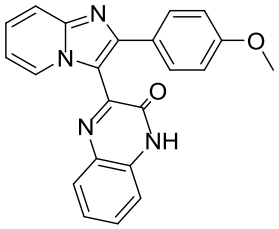

35b
75%^{A}/61%^{B}

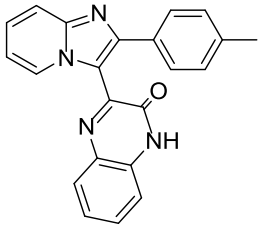

35c
70%^{A}/56%^{B}

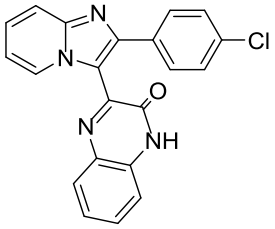

35d
65%^{A}/58%^{B}

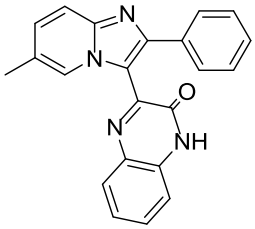

35e
60%^{A}/49%^{B}

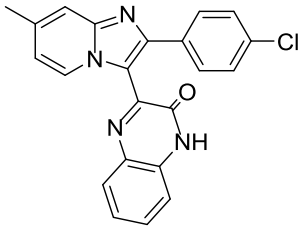

35f
58%^{A}/47%^{B}

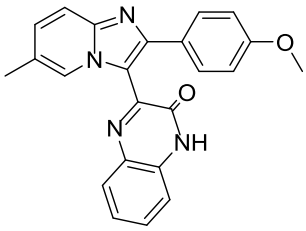

35g
62%^{A}/54%^{B}

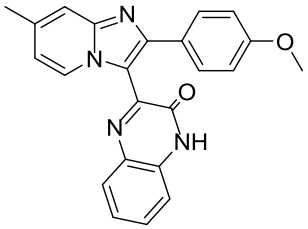

35h
60%^{A}/48%^{B}

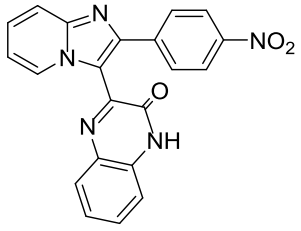

35i
20%^{A}

Method A: 2-arylimidazo[1,2-*a*]pyridyl glyoxalate (**34a-j**) (0.6 mmol), *o*-phenylene diamine (**16**) (0.72 mmol), Montmorillonite K-10 (300 mg) under microwave irradiation at 100 °C.

Method B: 2-arylimidazo[1,2-*a*]pyridyl glyoxalate (**34a-h**) (0.6 mmol), *o*-phenylene diamine (**16**) (0.72 mmol), $Yb(OTf)_3$ (0.06 mmol) in THF (3 mL) under microwave irradiation at 100 °C.

Scheme 2.2.3: Montmorillonite K-10/$Yb(OTf)_3$-catalyzed synthesis of imidazo[1,2-*a*]pyridyl quinoxalinones (**35a-i**)

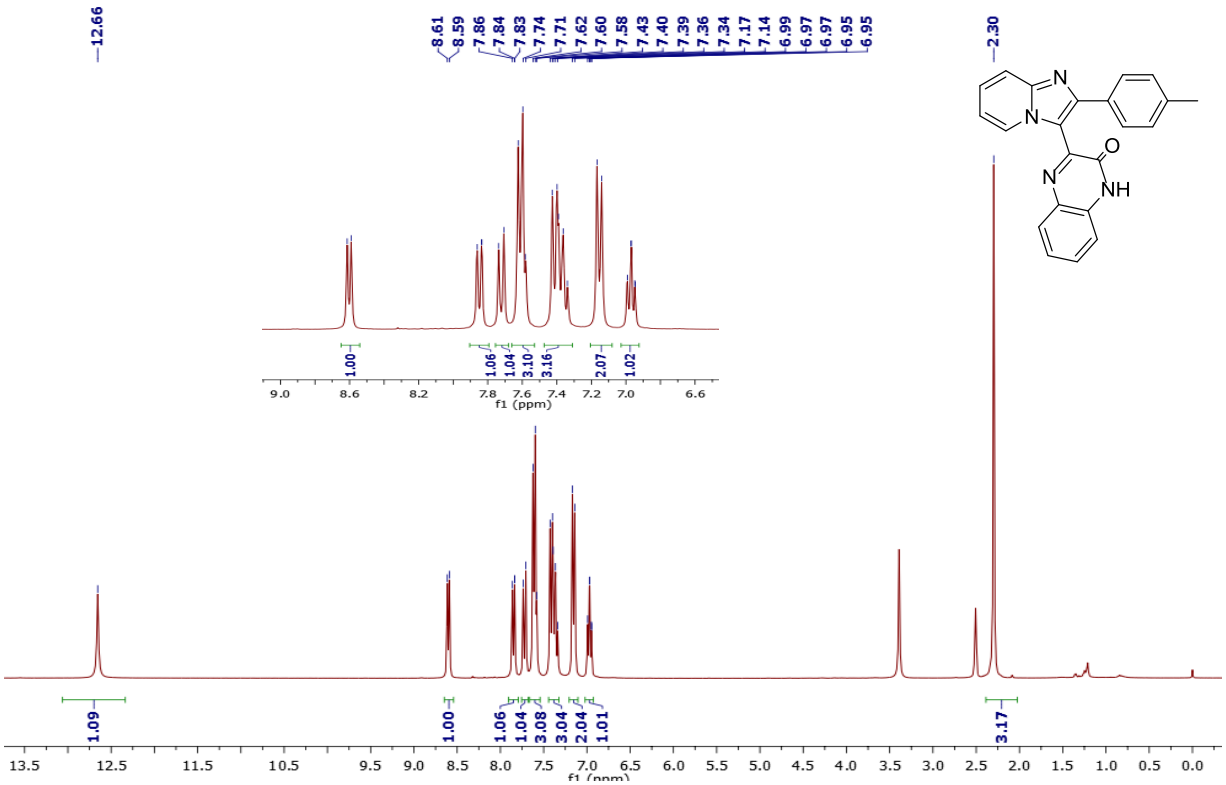

Figure 2.2.1: ^{1}H NMR spectrum of **35c**

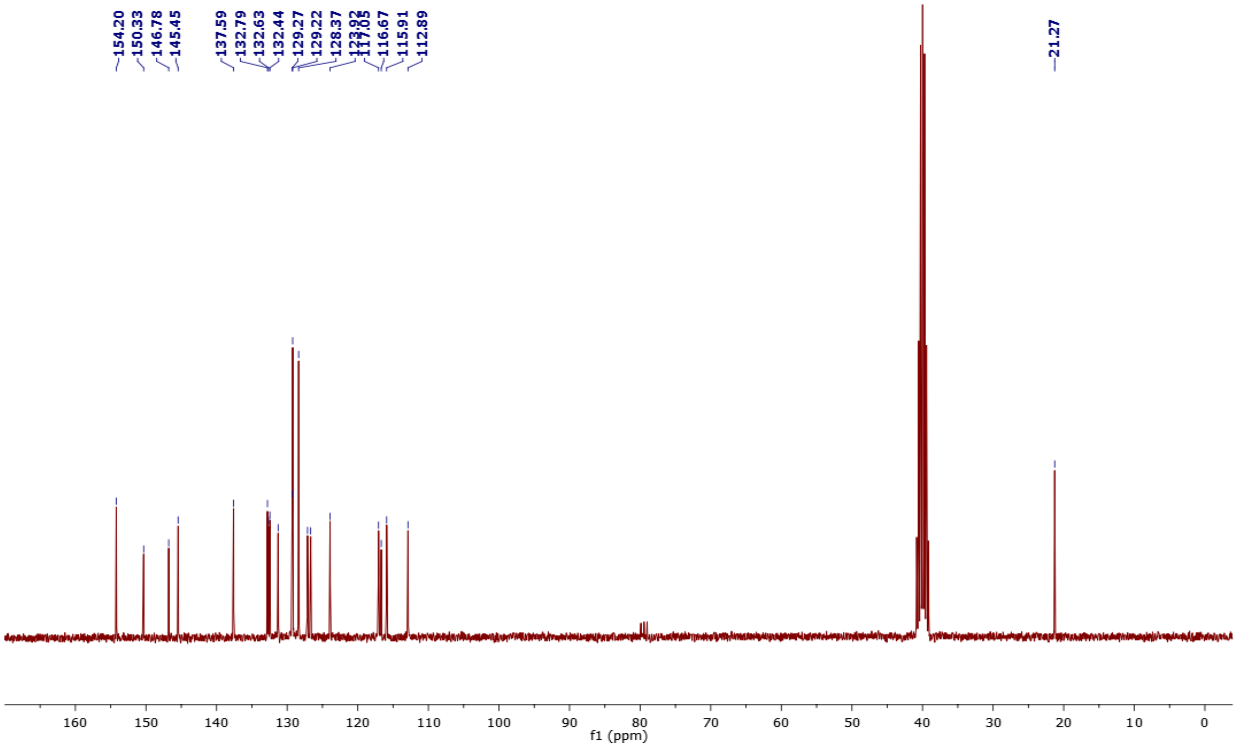

Figure 2.2.2: ^{13}C NMR spectrum of **35c**

The use of montmorillonite K-10 using microwave heating at 100 ^{o}C was further applied to a mixture of 2-methylimidazo[1,2-*a*]pyridyl glyoxalate (**34j**) and *o*-phenylene diamine (**16)** to yield 3-(2-methylimidazo[1,2-*a*]pyridin-3-yl)quinoxalin-2(1*H*)-one (**35j**)[42] in 82% yield in 45 minutes (Scheme 2.2.4). The present method not only reduced the reaction time from 2 days (classical refluxing in CH_3CN) to 45 minutes[42] but also gave comparable yield under environmentally benign reaction conditions.

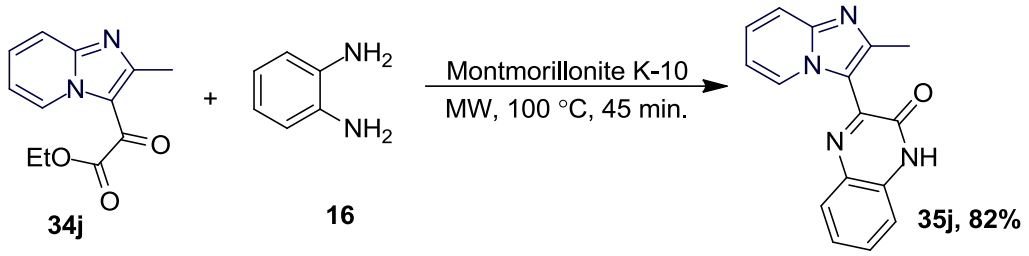

Scheme 2.2.4: Montmorillonite K-10-supported synthesis of **35j**

In summary, we have developed a microwave-assisted, efficient and convenient protocol for the synthesis of imidazo[1,2-*a*]pyridyl quinoxalinones under montmorillonite K-10 or $Yb(OTf)_3$-catalyzed conditions.

2.3 Experimental Section

2.3.1 General Materials and Methods

Commercially available reagents were used without purification. Commercially available solvents were dried by standard procedures prior to use. Melting points were determined in open capillary tubes on a MPA120-automated melting point apparatus and are uncorrected. The microwave-assisted reactions were carried in a CEM Discover Bench Mate Reactor in 10 mL pressure vials at a power of 80W. Reactions were monitored by using thin layer chromatography (TLC) on 0.2 mm silica gel F254 plates (Merck). The chemical structures of final products and intermediates were characterized by nuclear magnetic resonance spectra (^{1}H NMR, ^{13}C NMR) recorded on a Bruker NMR spectrometer (300 MHz, 75 MHz). ^{13}C NMR spectra are fully decoupled. Chemical shifts were reported in parts per million (ppm) using deuterated solvent peak tetramethylsilane (internal) as the standard. High resolution mass spectra were recorded with a TOF analyzer spectrometer by using electrospray mode.

General procedure for the synthesis of 2-arylimidazo[1,2-*a*]pyridyl glyoxalates

To a solution of substituted 2-arylimidazo[1,2-*a*]pyridine (**32a-j**) (2 mmol) in 1,4-dioxane (20 mL), ethyl oxalyl chloride (**33)** (3.5 mmol) was added under an inert atmosphere of nitrogen gas.

The mixture was refluxed for 3–7 h. On completion of the reaction as indicated by TLC, the mixture was allowed to cool and then concentrated under reduced pressure. The residue was triturated with water (80 mL), and the resulting precipitate was either obtained by filtration and washed with water (20 mL) or extracted with dichloromethane (50 mL × 3). In the latter case, the combined organic extracts were dried over sodium sulfate and concentrated to afford crude product, which was recrystallized from ethanol to give pure glyoxalate (**34a-j)**.

Ethyl 2-oxo-2-(2-phenylimidazo[1,2-*a*]pyridin-3-yl)acetate (34a): White solid; yield: 440 mg

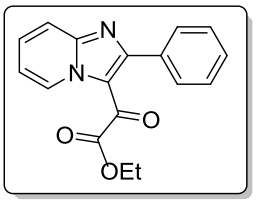

(75%); mp 177-179 °C; ^{1}H NMR (400 MHz, $CDCl_3$) δ 9.67 (d, J = 6.8 Hz, 1H), 7.83 (d, J = 8.8 Hz, 1H), 7.69 – 7.58 (m, 3H), 7.55 – 7.42 (m, 3H), 7.18 (t, J = 6.9 Hz, 1H), 3.69 (q, J = 7.2 Hz, 2H), 1.00 (t, J = 7.2 Hz, 3H); ^{13}C NMR (100 MHz, $CDCl_3$) δ 176.8, 163.5, 158.3, 148.1, 133.6, 131.1, 129.6, 129.0, 128.4, 117.9, 117.5, 115.8, 62.1, 13.4; HRMS (ESI-TOF) (*m/z*) calculated $C_{17}H_{15}N_2O_3^+$: 295.1082; found 295.1068 $[M + H]^+$.

Ethyl 2-(2-(4-methoxyphenyl)imidazo[1,2-*a*]pyridin-3-yl)-2-oxoacetate (34b): Yellow solid;

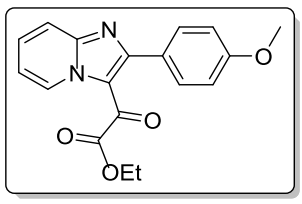

yield: 520 mg (80%); mp 131-133 °C; ^{1}H NMR (400 MHz, $CDCl_3$) δ 9.63 (d, J = 6.9 Hz, 1H), 7.85 – 7.72 (m, 1H), 7.65 – 7.53 (m, 3H), 7.15 (td, J = 6.9, 1.2 Hz, 1H), 7.06 – 6.98 (m, 2H), 3.86 (s, 3H), 3.78 (q, J = 7.2 Hz, 2H), 1.05 (t, J = 7.2 Hz, 3H); ^{13}C NMR (100 MHz, $CDCl_3$) δ 176.7, 163.6, 160.9, 158.1, 148.1, 130.9, 128.9, 125.9, 117.7, 117.2, 115.6, 113.8, 62.1, 55.3, 13.4; HRMS (ESI-TOF) (*m/z*) calculated $C_{18}H_{17}N_2O_4^+$: 325.1189; found 325.1147 $[M + H]^+$.

Ethyl 2-oxo-2-(2-(4-methylphenyl)imidazo[1,2-*a*]pyridin-3-yl)acetate (34c): Brown solid;

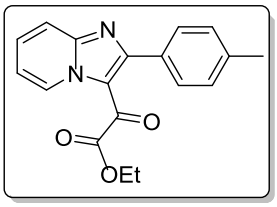

yield: 490 mg (84%); mp 110-112 °C; ^{1}H NMR (400 MHz, $CDCl_3$) δ 9.52 (d, J = 6.8 Hz, 1H), 7.69 (d, J = 8.8 Hz, 1H), 7.48 (t, J = 7.7 Hz, 1H), 7.41 (d, J = 8.0 Hz, 2H), 7.17 (d, J = 7.9 Hz, 2H), 7.03 (t, J = 6.7 Hz, 1H), 3.61 (q, J = 7.2 Hz, 2H), 2.30 (s, 3H), 0.91 (t, J = 7.2 Hz, 3H); ^{13}C NMR (100 MHz, $CDCl_3$) δ 176.8, 163.6, 158.5, 148.1, 139.7, 130.9, 130.7, 129.5, 129.0, 128.9, 117.8, 117.4, 115.7, 62.0, 21.3, 13.4; HRMS (ESI-TOF) (*m/z*) calculated $C_{18}H_{17}N_2O_3^+$: 309.1239; found 309.1257 $[M + H]^+$.

Ethyl 2-(2-(4-chlorophenyl)imidazo[1,2-*a*]pyridin-3-yl)-2-oxoacetate (34d): Pale brown solid;

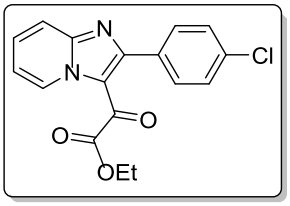

yield: 530 mg (85%); mp 109-112 °C; ^{1}H NMR (400 MHz, $CDCl_3$) δ 9.67 (d, J = 6.9 Hz, 1H), 7.84 (d, J = 8.9 Hz, 1H), 7.66 (t, J = 7.9 Hz, 1H), 7.57 (d, J = 9.0 Hz, 2H), 7.47 (d, J= 9.0 Hz, 2H), 7.23 (t, J = 9.0 Hz, 1H), 3.79 (q, J = 7.2 Hz, 2H), 1.07 (t, J = 7.2 Hz, 3H); ^{13}C NMR (100 MHz, $CDCl_3$) δ 176.6, 163.4, 157.0, 148.2, 136.0, 132.1, 131.2, 130.9, 129.1, 128.7, 117.9, 117.7, 115.9, 62.3, 13.5; HRMS (ESI-TOF) (*m/z*) calculated $C_{17}H_{14}ClN_2O_3^+$: 329.0692; found 329.0712 $[M + H]^+$.

Ethyl 2-(6-methyl-2-phenylimidazo[1,2-*a*]pyridin-3-yl)-2-oxoacetate (34e): Brown solid;

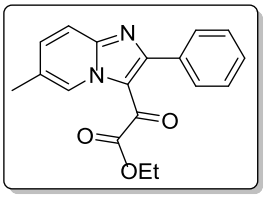

yield: 530 mg (86%); mp 179-181 °C; ^{1}H NMR (400 MHz, $CDCl_3$) δ 9.48 (s, 1H), 7.76 (d, J = 9.0 Hz, 1H), 7.62 (dd, J = 6.5, 2.8 Hz, 2H), 7.53 – 7.42 (m, 4H), 3.66 (q, J = 7.2 Hz, 2H), 2.46 (s, 3H), 1.00 (t, J = 7.2 Hz, 3H); ^{13}C NMR (100 MHz, $CDCl_3$) δ 176.7, 163.6, 157.9, 146.9, 133.9, 133.4, 129.6, 128.4, 127.1, 126.2, 117.7, 116.7, 62.1, 18.4, 13.4; HRMS (ESI-TOF) (*m/z*) calculated $C_{18}H_{17}N_2O_3^+$: 309.1239; found 309.1208 $[M + H]^+$.

Ethyl 2-(2-(4-chlorophenyl)-7-methylimidazo[1,2-*a*]pyridin-3-yl)-2-oxoacetate (34f): White

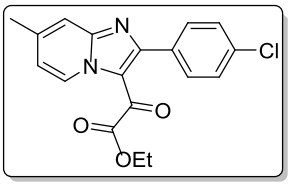

solid; yield: 560 mg (82%); mp 135-137 °C; ^{1}H NMR (400 MHz, $CDCl_3$) δ 9.37 (d, J = 7.1 Hz, 1H), 7.49 – 7.40 (m, 3H), 7.33 (d, J = 8.4 Hz, 2H), 6.88 (dd, J = 7.0, 1.8 Hz, 1H), 3.66 (q, J = 7.1 Hz, 2H), 2.39 (s, 3H), 0.94 (t, J = 7.1 Hz, 3H); ^{13}C NMR (100 MHz, $CDCl_3$) δ 176.0, 163.5, 157.1, 148.5, 143.1, 135.8, 132.2, 130.8, 128.5, 128.1, 118.3, 117.6, 116.3, 62.1, 21.6, 13.4; HRMS (ESI-TOF) (*m/z*) calculated $C_{18}H_{16}ClN_2O_3^+$: 343.0849; found 343.0861 $[M + H]^+$.

Ethyl 2-(2-(4-methoxyphenyl)-6-methylimidazo[1,2-*a*]pyridin-3-yl)-2-oxoacetate (34g):

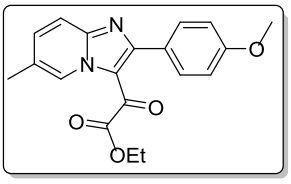

Brown solid; yield: 570 mg (84%); mp 117-118 °C; ^{1}H NMR (400 MHz, $CDCl_3$) δ 9.45 (s, 1H), 7.81 (d, J = 9.0 Hz, 1H), 7.57 (d, J = 8.7 Hz, 2H), 7.51 (d, J = 9.1 Hz, 1H), 7.01 (d, J = 8.7 Hz, 2H), 3.86 (s, 3H), 3.77 (q, J = 7.2 Hz, 2H), 2.45 (s, 3H), 1.05 (t, J = 7.2 Hz, 3H); ^{13}C NMR (100 MHz, $CDCl_3$) δ 177.4, 164.2, 161.3, 160.7, 160.1, 157.4, 146.8, 134.7, 131.4, 127.7, 126.8, 125.7, 117.9, 116.5, 114.7, 62.1, 55.1, 18.1, 13.1; HRMS (ESI-TOF) (*m/z*) calculated $C_{19}H_{19}N_2O_4^+$: 339.1344; found 339.1327 $[M + H]^+$.

Ethyl 2-(2-(4-methoxyphenyl)-7-methylimidazo[1,2-*a*]pyridin-3-yl)-2-oxoacetate (34h):

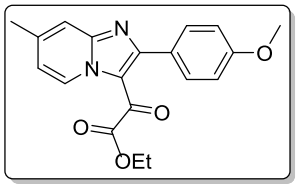

Brown solid; yield: 530 mg (79%); mp 131-132 °C; ^{1}H NMR (400 MHz, $CDCl_3$) δ 9.52 (d, J = 7.0 Hz, 1H), 7.62 (s, 1H), 7.57 (d, J = 8.6 Hz, 2H), 7.06 – 6.94 (m, 3H), 3.86 (s, 3H), 3.77 (q, J = 7.2 Hz, 2H), 2.52 (s, 3H), 1.05 (t, J = 7.2 Hz, 3H); ^{13}C NMR (100 MHz, $CDCl_3$) δ 176.5, 163.7, 161.5, 160.9, 158.04, 148.3, 143.3, 131.3, 128.2, 125.5, 118.2, 117.5, 116.0, 113.9, 62.1, 55.4, 21.7, 13.5; HRMS (ESI-TOF) (*m/z*) calculated $C_{19}H_{19}N_2O_4^+$: 339.1344; found 339.1368 $[M + H]^+$.

Ethyl 2-(2-(4-nitrophenyl)imidazo[1,2-*a*]pyridin-3-yl)-2-oxoacetate (34i): It was not isolated and used as such for the next cyclization step because of the overlapping nature of its spot on TLC with the starting 2-(4′-nitrophenyl)imidazo[1,2-*a*]pyridine (**32i**).

General procedure for the synthesis of 2-arylimidazo[1,2-*a*]pyridyl quinoxalin-2-ones

Method A: A mixture of substituted 2-arylimidazo[1,2-*a*]pyridyl glyoxalate (**34a-j**) (0.6 mmol) and *o*-phenylene diamine (**16**) (0.72 mmol) were dissolved in CH_2Cl_2 (10 mL). Montmorillonite K-10 (300 mg) was added to the mixture, and the solvent was evaporated under reduced pressure. The dry mixture was then transferred to a microwave reaction vial and irradiated in focused microwave oven (CEM) at a 100 °C. The reaction was monitored *via* TLC. After the completion of the reaction, the reaction mixture was diluted with CH_2Cl_2 (50 mL × 3) and the organic layer was separated from catalyst by filtration. The organic layer was concentrated and subjected to flash column chromatography [SiO_2 (100–200 mesh), hexanes/EtOAc, 6:4 v/v] or recrystallization using MeOH/CH_2Cl_2 to yield pure quinoxaline-2-one (**35a-j**).

Method B: A mixture of substituted 2-arylimidazo[1,2-*a*]pyridyl glyoxalate (**34a-h**) (0.6 mmol), *o*-phenylene diamine (**16)** (0.72 mmol) and $Yb(OTf)_3$ (0.06 mmol) were dissolved in THF (3 mL) in a microwave reaction vial. The reaction vial was irradiated in focused microwave oven (CEM) at temperatures 100 °C for 1.5-3 h, and monitored *via* TLC. After the completion of the reaction, THF was evaporated and the reaction mixture was diluted with water and extracted with ethyl acetate (50 mL × 3). The organic layer was concentrated under reduced pressure, and the crude product was subjected to flash column chromatography [SiO_2(100–200 mesh), hexanes/EtOAc, 6:4 v/v], to yield pure quinoxalin-2-one (**35a-h**).

3-(2-Phenylimidazo[1,2-*a*]pyridin-3-yl)quinoxalin-2(1*H*)-one (35a): Brownish yellow solid;

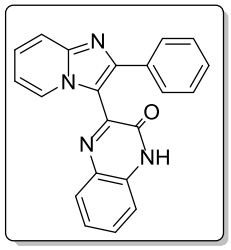

yield: 146 mg (72%, Method A); mp 273-274 °C; ^{1}H NMR (400 MHz, $CDCl_3$ + CD_3OD) δ 8.75 (d, J = 7.0 Hz, 1H), 7.90 (d, J = 6.9 Hz, 1H), 7.79 – 7.63 (m, 3H), 7.51 (t, J = 8.4 Hz, 1H), 7.42 – 7.25 (m, 5H), 7.02 (d, J = 9.0 Hz, 1H), 6.94 (t, J = 7.5 Hz, 1H); ^{13}C NMR (100 MHz, $CDCl_3$ + CD_3OD) δ 154.6, 148.9, 148.7, 146.3, 135.1, 132.7, 131.1, 130.8, 128.8, 128.4, 128.2, 128.1, 126.9, 125.7, 124.5, 117.0, 115.8, 113.2; HRMS (ESI-TOF) (*m/z*) calculated $C_{21}H_{15}N_4O^+$: 339.1245; found 339.1223 $[M + H]^+$.

3-(2-(4-Methoxyphenyl)imidazo[1,2-*a*]pyridin-3-yl)quinoxalin-2(1*H*)-one (35b): Yellow

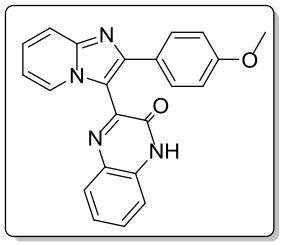

solid; yield: 152 mg (75%, Method A); mp 238-240 °C; ^{1}H NMR (400 MHz, DMSO-d_6) δ 12.64 (s, 1H), 8.57 (d, J = 6.9 Hz, 1H), 7.84 (d, J = 7.9 Hz, 1H), 7.72 – 7.62 (m, 3H), 7.58 (d, J = 8.0 Hz, 1H), 7.44 – 7.32 (m, 3H), 6.99 – 6.85 (m, 3H), 3.76 (s, 3H); ^{13}C NMR (100 MHz, DMSO-d_6 + $CDCl_3$) δ 159.6, 154.2 150.3, 146.7, 145.4, 132.8, 132.6, 131.2, 129.7, 129.2, 127.7, 127.0, 126.5, 123.8, 116.9, 116.2, 115.9, 114.0, 112.7, 55.5; HRMS (ESI-TOF) (*m/z*) calculated $C_{22}H_{17}N_4O_2^+$: 369.1351; found 369.1323 $[M + H]^+$.

3-(2-(4-Methylphenyl)imidazo[1,2-*a*]pyridin-3-yl)quinoxalin-2(1*H*)-one (35c): Yellow solid;

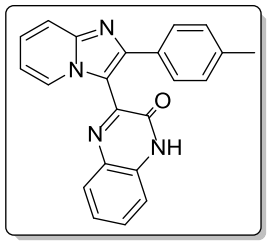

yield: 148 mg (70%, Method A); mp 174-175 °C; ^{1}H NMR (400 MHz, DMSO-d_6) δ 12.66 (s, 1H), 8.60 (d, J = 6.9 Hz, 1H), 7.85 (d, J = 7.3 Hz, 1H), 7.72 (d, J = 9.0 Hz, 1H), 7.66 – 7.54 (m, 3H), 7.47 – 7.32 (m, 3H), 7.15 (d, J = 8.0 Hz, 2H), 6.97 (t, J = 6.4 Hz, 1H), 2.30 (s, 3H); ^{13}C NMR (100 MHz, DMSO-d_6) δ 154.2, 150.3, 146.8, 145.5, 137.6, 132.8, 132.6, 132.4, 131.3, 129.3, 129.2, 128.4, 127.2, 126.7, 123.9, 117.5, 116.7, 115.9, 112.9, 21.3; HRMS (ESI-TOF) (*m/z*) calculated $C_{22}H_{17}N_4O^+$: 353.1402; found 353.1423 $[M + H]^+$.

3-(2-(4-Chlorophenyl)imidazo[1,2-*a*]pyridin-3-yl)quinoxalin-2(1*H*)-one (35d): Yellow solid;

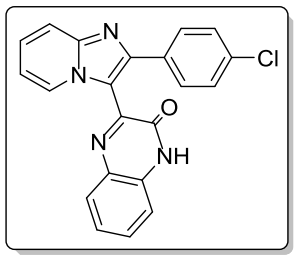

yield: 145 mg (65%, Method A); mp >290 °C; ^{1}H NMR (400 MHz, DMSO-d_6) δ 12.66 (s, 1H), 8.66 (d, J = 6.6 Hz, 1H), 7.85 (d, J = 7.8 Hz, 1H), 7.80 – 7.68 (m, 3H), 7.62 (t, J = 7.4 Hz, 1H), 7.51 – 7.30 (m, 5H), 7.01 (t, J = 6.5 Hz, 1H); ^{13}C NMR (100 MHz, DMSO-d_6) δ 154.1, 149.9, 145.6, 134.2, 132.9, 132.8, 132.6, 131.4, 130.1, 129.3, 128.7,

127.3, 127.1, 123.9, 117.2, 117.1, 115.9, 113.2; HRMS (ESI-TOF) (*m/z*) calculated $C_{21}H_{14}ClN_4O^+$: 373.0856; found 373.0823 $[M + H]^+$.

3-(6-Methyl-2-phenylimidazo[1,2-*a*]pyridin-3-yl)quinoxalin-2(1*H*)-one (35e): Yellow solid;

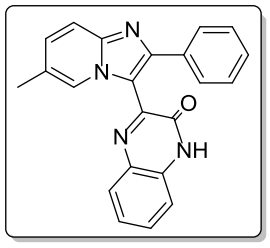

yield: 126 mg (60%, Method A); mp >290 °C; ^{1}H NMR (400 MHz, DMSO-d_6) δ 12.65 (s, 1H), 8.39 (s, 1H), 7.86 (d, J = 7.9 Hz, 1H), 7.74 – 7.58 (m, 4H), 7.44 – 7.23 (m, 6H), 2.29 (s, 3H); ^{13}C NMR (100 MHz, DMSO-d_6 + $CDCl_3$) δ 154.3, 150.5, 146.1, 144.4, 135.2, 132.9, 132.7, 131.4, 129.6, 129.4, 128.6, 128.2, 128.1, 124.5, 123.9, 122.2, 116.7, 116.5, 115.9, 18.2; HRMS (ESI-TOF) (*m/z*) calculated $C_{22}H_{17}N_4O^+$: 353.1402; found 353.1378 $[M + H]^+$.

3-(2-(4-Chlorophenyl)-7-methylimidazo[1,2-*a*]pyridin-3-yl)quinoxalin-2(1*H*)-one (35f):

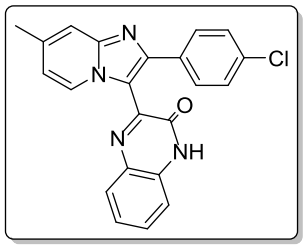

Yellow solid; yield: 134 mg (58%, Method A); mp >290 °C; ^{1}H NMR (400 MHz, $CDCl_3$ + CD_3OD) δ 8.61 (d, J = 7.1 Hz, 1H), 7.90 (dd, J = 8.1, 1.4 Hz, 1H), 7.64 – 7.53 (m, 3H), 7.48 (dt, J = 2.0, 1.1 Hz, 1H), 7.48 – 7.37 (m, 1H), 7.35 – 7.30 (m, 2H), 7.26 (dd, J = 8.2, 1.4 Hz, 1H), 6.80 (dd, J = 7.2, 1.7 Hz, 1H), 2.48 (brs, 3H); ^{13}C NMR (100 MHz, $CDCl_3$ + CD_3OD) δ 154.2, 148.6, 147.4, 146.7, 138.6, 134.0, 133.6, 132.7, 130.9, 129.5, 128.8, 128.2, 125.7, 124.3, 115.9, 115.5, 115.3, 21.4; HRMS (ESI-TOF) (*m/z*) calculated $C_{22}H_{16}ClN_4O^+$: 387.1012; found 387.1049 $[M + H]^+$.

3-(2-(4-Methoxyphenyl)-6-methylimidazo[1,2-*a*]pyridin-3-yl)quinoxalin-2(1*H*)-one (35g):

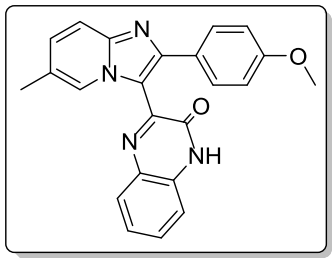

Yellow solid; yield: 142 mg (62%, Method A); mp 285-287 °C; ^{1}H NMR (400 MHz, DMSO-d_6) δ 12.64 (s, 1H), 8.34 (s, 1H), 7.90 – 7.82 (m, 1H), 7.68 – 7.55 (m, 4H), 7.45 – 7.33 (m, 2H), 7.24 (dd, J = 9.1, 1.7 Hz, 1H), 6.94 – 6.85 (m, 2H), 3.75 (s, 3H), 2.29 (s, 3H); ^{13}C NMR (100 MHz, DMSO-d_6 + $CDCl_3$) δ 159.4, 154.2, 150.4, 146.2, 144.4, 132.7, 132.7, 131.2, 129.5, 129.4, 129.2, 127.7, 124.3, 123.9, 122.0, 116.3, 115.9, 115.6, 113.9, 55.5, 18.2; HRMS (ESI-TOF) (*m/z*) calculated $C_{23}H_{19}N_4O_2^+$: 383.1508; found 383.1542 $[M + H]^+$.

3-(2-(4-Methoxyphenyl)-7-methylimidazo[1,2-*a*]pyridin-3-yl)quinoxalin-2(1*H*)-one (35h):

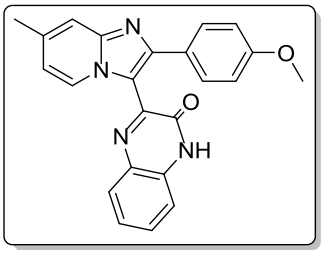

Yellow solid; yield: 137 mg (60%, Method A); mp >290 °C; ^{1}H NMR (400 MHz, $CDCl_3$) δ 8.64 (d, J = 6.7 Hz, 1H), 7.77 (d, J = 7.8 Hz, 1H), 7.59 (d, J = 8.3 Hz, 2H), 7.38 (s, 1H), 7.33 – 7.26 (m, 1H), 7.07 (dd, J = 16.8, 6.2 Hz, 1H), 6.78 – 6.65 (m, 3H), 6.62 (d, J = 7.3 Hz, 1H), 3.47 (s, 3H), 2.33 (s, 3H); ^{13}C NMR (100 MHz, $CDCl_3$) δ 159.6, 155.2, 148.7, 147.0, 138.0, 132.9, 130.8, 130.4, 129.7, 128.5, 128.3, 125.1, 124.4, 116.1, 115.5, 114.9, 113.5, 55.0, 21.4; HRMS (ESI-TOF) (*m/z*) calculated $C_{23}H_{19}N_4O_2^+$: 383.1508; found 383.1482 $[M + H]^+$.

3-(2-(4-Nitrophenyl)imidazo[1,2-*a*]pyridin-3-yl)quinoxalin-2(1*H*)-one (35i): Pale yellow solid; yield: 46 mg (20%, Method A); mp 240-242 °C; ^{1}H NMR (400 MHz, $CDCl_3$) δ 8.77 (d, J = 7.0 Hz, 1H), 8.24 (d, J = 8.4 Hz, 2H), 7.98 –7.84 (m, 3H), 7.77 (d, J = 9.0 Hz, 1H), 7.60 (t, J = 7.7 Hz, 1H), 7.43 (t, J = 7.8 Hz, 2H), 7.13 – 6.94 (m, 2H); HRMS (ESI-TOF) (*m/z*) calculated $C_{21}H_{14}N_5O_3^+$: 384.1096; found 384.1125 $[M + H]^+$.

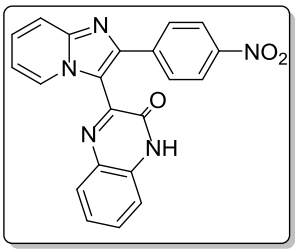

3-(2-Methylimidazo[1,2-*a*]pyridin-3-yl)quinoxalin-2(1*H*)-one (35j): Yellow solid; yield: 172 mg (82%, Method A); mp 222-224 °C; ^{1}H NMR (400 MHz, DMSO-d_6) δ 12.61 (s, 1H), 8.71 (d, J = 6.9 Hz, 1H), 7.82 (d, J = 7.7 Hz, 1H), 7.64 – 7.51 (m, 2H), 7.42 – 7.30 (m, 3H), 6.96 (t, J = 6.7 Hz, 1H), 2.50 (s, 3H); ^{13}C NMR (100 MHz, DMSO-d_6) δ 154.3, 149.6, 147.3, 145.6, 135.4, 132.6, 132.1, 130.5, 128.8, 127.9, 126.3, 123.9, 118.2, 116.4, 115.7, 112.4, 16.2; HRMS (ESI-TOF) (*m/z*) calculated $C_{16}H_{13}N_4O^+$: 277.1089; found 277.1181$[M + H]^+$.

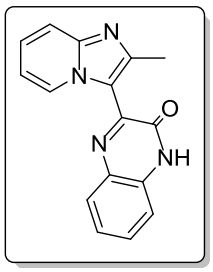

2.4. References

(1) Bode, M. L.; Gravestock, D.; Moleele, S. S.; van der Westhuyzen, C. W.; Pelly, S. C.; Steenkamp, P. A.; Hoppe, H. C.; Khan, T.; Nkabinde, L. A. *Bioorganic and Medicinal Chemistry* **2011**, *19*, 4227-4237.

(2) Cheng, D.; Croft, L.; Abdi, M.; Lightfoot, A.; Gallagher, T. *Organic Letters* **2007**, *9*, 5175-5178.

(3) Kamal, A.; Reddy, J. S.; Ramaiah, M. J.; Dastagiri, D.; Bharathi, E. V.; Sagar, M. V. P.;Pushpavalli, S.; Ray, P.; Pal-Bhadra, M. *Medicinal Chemical Communications* **2010**, *1*, 355-360.

(4) Kim, O.; Jeong, Y.; Lee, H.; Hong, S. -S.; Hong, S. *Journal of Medicinal Chemistry* **2011**, *54*, 2455-2466.

(5) Rival, Y.; Grassy, G.; Taudou, A.; Ecalle, R. *European Journal of Medicinal Chemistry* **1991** *26*, 13-18.

(6) Rival, Y.; Grassy, G.; Micheal, G. *Chemical and Pharmaceutical Bulletin* **1992**, *40*, 1170-1176.

(7) Mizushige, K.; Ueda, T.; Yukiiri, K.; Suzuki, H. *Cardiovascular Therapeutics* **2002**, *20*, 163-174.

(8) Simon, W.; Herrmann, M.; Klein, T.; Shin, J.; Huber, R.; Senn-Bilfinger, J. Postius, S. *Journal of Pharmacology and Experimental Therapeutics* **2007**, *321*, 866-874.

(9) Jenkinson, S.; Thomson, M.; McCoy, D.; Edelstein, M.; Danehower, S.; Lawrence, W.; Wheelan, P.; Spaltenstein, A.; Gudmundsson, K. *Antimicrobial Agents and Chemotherapy* **2010**, *54*, 817-824.

(10) Bailey, J. J.; Schirrmacher, R.; Farrell, K.; Bernard-Gauthier, V. *Expert Opinion on Therapeutic Patents* **2017**, 1-19.

(11) Bhuva, V.; Patolia, V.; Patel, A.; Purohit, D. *Organic Chemistry: An Indian Journal* **2009**, *5*, 264-268.

(12) Bhuva, V.; Patolia, V.; Patel, A.; Purohit, D. *Organic Chemistry: An Indian Journal* **2012**, *8*, 259-263.

(13) Gali, R.; Banothu, J.; Bavantula, R. *Journal of Heterocyclic Chemistry* **2015**, *52*, 641-646.

(14) Gudmundsson, K. S.; Johns, B. A. *Bioorganic & Medicinal Chemistry Letters* **2007**, *17*, 2735-2739.

(15) Kamal, A.; Kumar, G. B.; Nayak, V. L.; Reddy, V. S.; Shaik, A. B.; Reddy, M. K. *Medicinal Chemical Communications* **2015**, *6*, 606-612.

(16) Kamal, A.; Reddy, V. S.; Karnewar, S.; Chourasiya, S. S.; Shaik, A. B.; Kumar, G. B.; Kishor, C.; Reddy, M. K.; Narasimha Rao, M.; Nagabhushana, A. *ChemMedChem* **2013**, *8*, 2015-2025.

(17) Hayakawa, M.; Kaizawa, H.; Kawaguchi, K. -I.; Ishikawa, N.; Koizumi, T.; Ohishi, T.; Yamano, M.; Okada, M.; Ohta, M.; Tsukamoto, S. -I. *Bioorganic & Medicinal Chemistry* **2007**, *15*, 403-412.

(18) Parhi, A. K.; Zhang, Y.; Saionz, K. W.; Pradhan, P.; Kaul, M.; Trivedi, K.; Pilch, D. S.; LaVoie, E. J. *Bioorganic & Medicinal Chemistry Letters* **2013**, *23*, 4968-4974.

(19) Pereira, J. A.; Pessoa, A. M.; Cordeiro, M. N. D. S.; Fernandes, R.; Prudêncio, C.; Noronha, J. P.; Vieira, M. *European Journal of Medicinal Chemistry* **2015**, *97*, 664-672.

(20) Urquiola, C.; Vieites, M.; Aguirre, G.; Marín, A.; Solano, B.; Arrambide, G.; Noblía, P.; Lavaggi, M. L.; Torre, M. H.; González, M. *Bioorganic & Medicinal Chemistry* **2006**, *14*, 5503-5509.

(21) Zarranz, B.; Jaso, A.; Lima, L. M.; Aldana, I.; Monge, A.; Maurel, S.; Sauvain, M. *Revista Brasileira de Ciências Farmacêuticas* **2006**, *42*, 357-361.

(22) Kim, Y. B.; Kim, Y. H.; Park, J. Y.; Kim, S. K. *Bioorganic & Medicinal Chemistry Letters* **2004**, *14*, 541-544.

(23) Jung, C. Y.; Song, C. J.; Yao, W.; Park, J. M.; Hyun, I. H.; Seong, D. H.; Jaung, J. Y. *Dyes and Pigments* **2015**, *121*, 204-210.

(24) Kulkarni, A. P.; Zhu, Y.; Jenekhe, S. A. *Macromolecules* **2005**, *38*, 1553-1563.

(25) Iyer, A.; Bjorgaard, J.; Anderson, T.; Köse, M. E. *Macromolecules* **2012**, *45*, 6380-6389.

(26) Ganley, B.; Chowdhury, G.; Bhansali, J.; Daniels, J. S.; Gates, K. S. *Bioorganic & Medicinal Chemistry* **2001**, *9*, 2395-2401.

(27) Takano, Y.; Shiga, F.; Asano, J.; Ando, N.; Uchiki, H.; Fukuchi, K.; Anraku, T. *Bioorganic & Medicinal Chemistry* **2005**, *13*, 5841-5863.

(28) Takano, Y.; Shiga, F.; Asano, J.; Hori, W.; Fukuchi, K.; Anraku, T.; Uno, T. *Bioorganic & Medicinal Chemistry* **2006**, *14*, 776-792.

(29) Aoki, K.; Koseki, J. -I.; Takeda, S.; Aburada, M.; Miyamoto, K. -I. *Chemical and Pharmaceutical Bulletin* **2007**, *55*, 922-925.

(30) Ginzinger, W.; Mühlgassner, G.; Arion, V. B.; Jakupec, M. A.; Roller, A.; Galanski, M.; Reithofer, M.; Berger, W.; Keppler, B. K. *Journal of Medicinal Chemistry* **2012**, *55*, 3398-3413.

(31) Rao, K. R.; Raghunadh, A.; Kalita, D.; Laxminarayana, E.; Pal, M.; Meruva, S. B. *Journal of Heterocyclic Chemistry* **2015**, *53*, 901-908.

(32) Kalinin, A. A.; Voloshina, A. D.; Kulik, N. V.; Zobov, V. V.; Mamedov, V. A. *European Journal of Medicinal Chemistry* **2013**, *66*, 345-354.

(33) Aoki, K.; Koseki, J.; Hirokawa, H.; Obata, T.; Watanabe, T. T. *Japan Kokai Tokkyo Koho JP* **2007**, *2007099642*.

(34) Vilchis-Reyes, M. A.; Zentella, A.; Martínez-Urbina, M. A.; Guzman, A.; Vargas, O.; Apan, M. T. R.; Gallegos, J. L. V.; Díaz, E. *European Journal of Medicinal Chemistry* **2010**, *45*, 379-386.

(35) Fisher, M. H.; Lusi, A. *Journal of Medicinal Chemistry* **1972**, *15*, 982-985.

(36) Hinsberg, O. *European Journal of Organic Chemistry* **1896**, *293*, 245-259.

(37) Kawanishi, N.; Sugimoto, T.; Shibata, J.; Nakamura, K.; Masutani, K.; Ikuta, M.; Hirai, H. *Bioorganic & Medicinal Chemistry Letters* **2006**, *16*, 5122-5126.

(38) Abasolo, M. I.; Gaozza, C. H.; Fernández, B. M. *Journal of Heterocyclic Chemistry* **1987**, *24*, 1771-1775.

(39) Mahesh, R.; Dhar, A. K.; Tvnv, T. S.; Thirunavukkarasu, S.; Devadoss, T. *Chinese Chemical Letters* **2011**, *22*, 389-392.

(40) Prakash, G. S.; Vaghoo, H.; Venkat, A.; Panja, C.; Chacko, S.; Mathew, T.; Olah, G. A. *Future Medicinal Chemistry* **2009**, *1*, 909-920.

(41) Srinivas, C.; Kumar, C. N. S. S. P.; Rao, V. J.; Palaniappan, S. *Journal of Molecular Catalysis A: Chemical* **2007**, *265*, 227-230.

(42) Zamkova, I. A.; Chekotylo, O. O.; Geraschenko, O. V.; Grygorenko, O. O.; Mykhailiuk, P. K.; Tolmachev, A. A. *Synthesis* **2010**, 1692-1696.

CHAPTER 3A

Copper-Catalyzed Direct Dicarbonylation of Imidazo-heterocycles *via* C-H Bond Activation

3A.1 Introduction

Transition-metal catalyzed direct cross-dehydrogenative C-H transformation has attracted considerable attention, and the strategy has been explored for the formation of nascent C-C and C-X (X = S, N, O) bond (Figure 3A.1.1).[1-8]

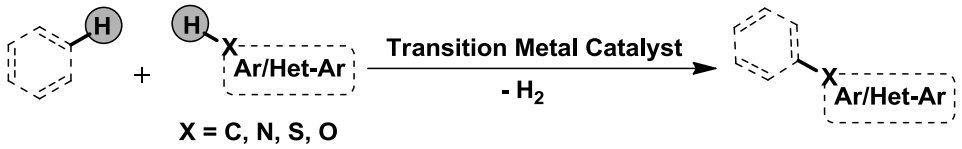

Figure 3A.1.1: A generalized representation of cross-dehydrogenative coupling

To date, within the field of homogeneous catalysis, Pd-catalyzed reactions are perhaps the most versatile methods for the oxidative C-C, C-N and C-O bond formations. However, palladium chemistry is associated with some serious drawbacks such as its cost, high toxicity and restrictions in substrate scope, thereby opening new doors for the investigation of other metal catalysts as an alternative to palladium.[9-11] In this regard, copper has received increasing attention towards the construction of various bonds in organic synthesis *via* C–H bond activation.[10,12-16] Intriguingly, copper can exchange its oxidation state from Cu (0) to Cu (III) through one-electron or two-electron processes.[13] As a result, the radical pathway and two-electron bond-forming pathway *via* organometallic intermediates can occur. The single-electron transfer (SET) from the electron-rich substrates to Cu(II) species is proposed to initiate a sequence of steps that ultimately affords the oxidative coupled products.[13,17] In recent years, oxygen has been predominately used as an ideal and abundant oxidant in various organic transformation under the Cu-catalyzed conditions.[18] Pleasingly, the performance of Cu-catalyzed reaction exponentially increases in the presence of "oxygen" either by acting as a pool for electrons (oxidase activity) or as a source of oxygen atoms that are incorporated into the product (oxygenase activity), or both.[19,20] The oxidation of copper with oxygen is a facile process allowing catalytic turnover in net oxidative processes and ready access to the higher Cu(III) oxidation state, which enables a range of powerful transformations including two-electron reductive elimination to Cu(I).

Tremendous hikes from 30 citations per year in the 1980s to over 300 citations per year in the 2000s were noticed in the employment of copper catalysis using molecular oxygen/aerial oxygen. Contentedly, aerobic Cu-catalyzed dehydrogenative functionalizations have been embarked as a powerful synthetic tool in the domain of green and sustainable chemistry *via* a

single electron transfer (SET) process. The cost-effectiveness, relatively better stability, easy-usability and the accessibility to synthesize complex molecule from simple starting material in minimum actions have popularized the Cu-catalyzed CDC reactions in numerous ways.[13] In recent years, extended efforts have been made by various research groups towards the construction nascent C-C and C-X (hetero atom) bonds *via* Cu-catalyzed CDC approach under aerobic condition.[13,18] A brief over view of Cu-catalyzed aerobic CDC methodologies is depicted in a pictorial representation (Figure 3A.1.1).

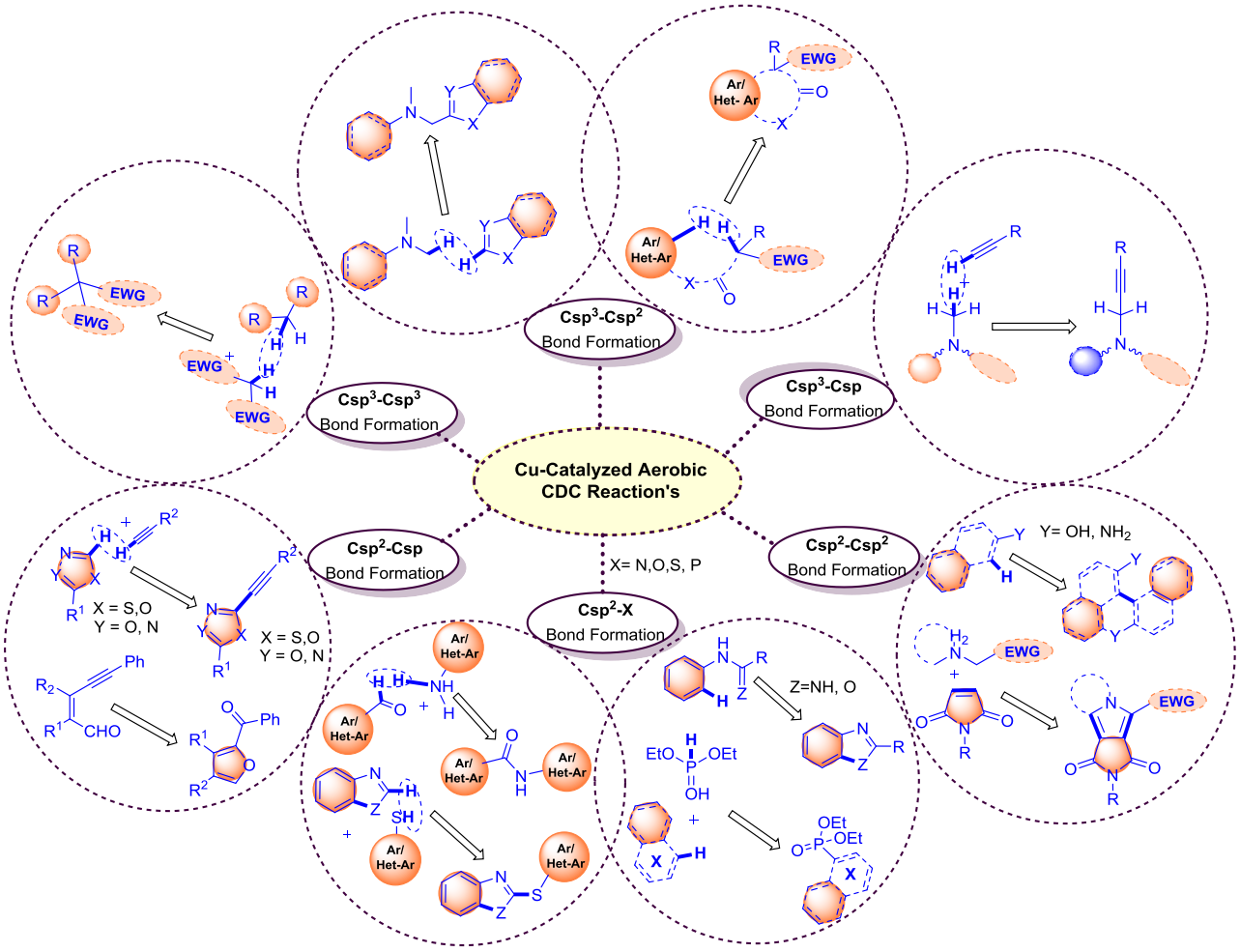

Figure 3A.1.2: A brief overview of Cu-catalyzed aerobic CDC methodologies

Aldehydes **2** have also been explored for metal-catalyzed *ortho*-aroylation of aromatic and heteroaromatic systems *via* Csp^2-Csp^2 cross-dehydrogenative coupling. In this context, Li and Kwong *et al.* independently reported Pd-catalyzed *ortho*-acylation of acetanilides (**1**) with aldehydes **2** in the presence of *tert*-butyl hydroperoxide (TBHP) in toluene, affording the *ortho*-acyl acetanilides (**3**) in moderate to good yields (Scheme 3A.1.1).[21,22]

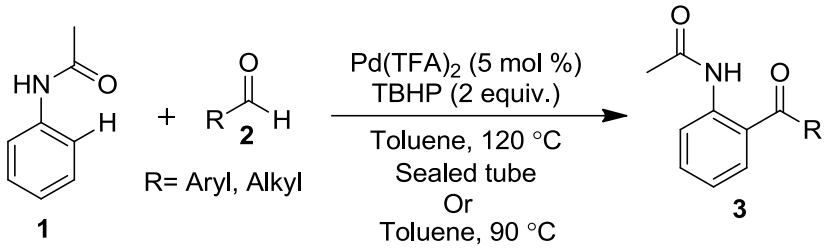

Scheme 3A.1.1: Pd-catalyzed *ortho*-acylation of acetanilides (**1**) with aldehydes (**2**)

Wang *et al.* reported a convergent and straightforward Pd-catalyzed protocol for the synthesis of *ortho*-acylated azobenzenes **5** from aromatic azo compounds **4** and aldehydes **2** *via* an azo-directed C-H bond activation process in the presence of TBHP as an oxidant. The obtained acylated azobenzenes **5** were further transformed into corresponding indazoles derivative (**6**) through reduction using Zn/NH_4Cl in methanol at room temperature (Scheme 3A.1.2).[23]

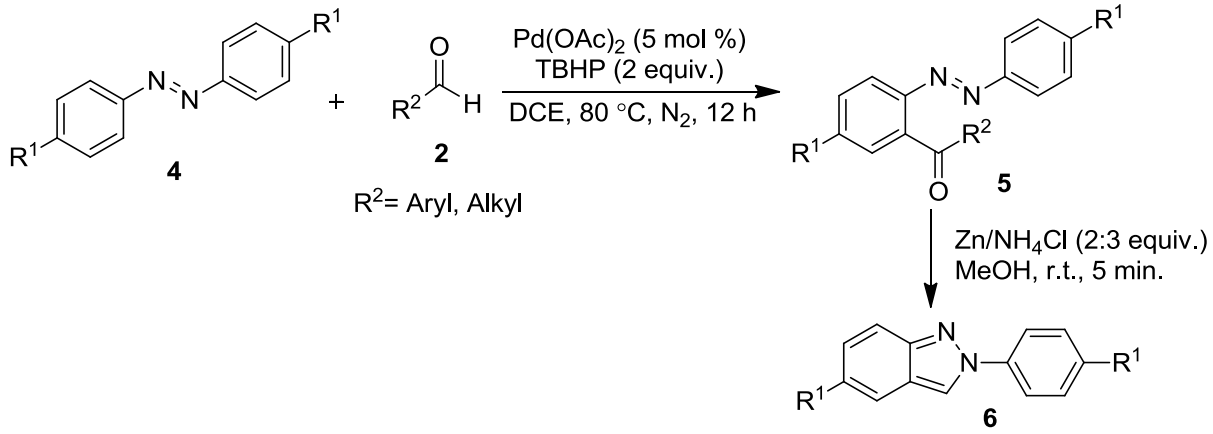

Scheme 3A.1.2: Pd-catalyzed *ortho*-acylation of azobenzenes (**4**) with aldehydes (**2**)

Kim *et al.* developed an efficient protocol for the Pd-catalyzed oxidative *ortho*-acylation of *N*-benzyltriflamides (**7**) with aldehydes **2** *via* C-H bond activation using acetic acid/TBHP in DMF:CH_3CN (1:1) at 100 °C for 40 h. The methodology was successfully utilized for the preparation of analgesic Nefopam (**9**) in multiple steps. (Scheme 3A.1.3).[24]

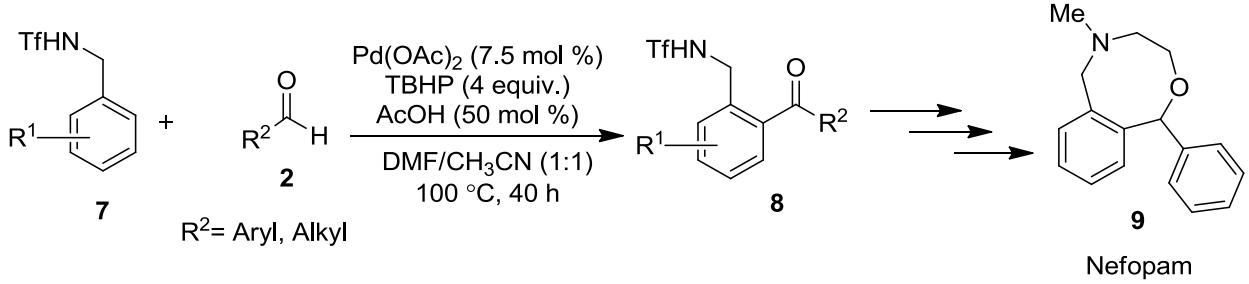

Scheme 3A.1.3: Pd-catalyzed *ortho*-acylation of *N*-benzyltriflamides (**7**) with aldehydes (**2**)

In 2013, Pan *et al.* presented a simple and efficient Pd-catalyzed strategy for direct C-3 acylation of benzofurans and benzothiophenes (**10**) with aromatic aldehydes **2** in air to yield **11** by a cross-dehydrogenative coupling (CDC) reaction (Scheme 3A.1.4).[25]

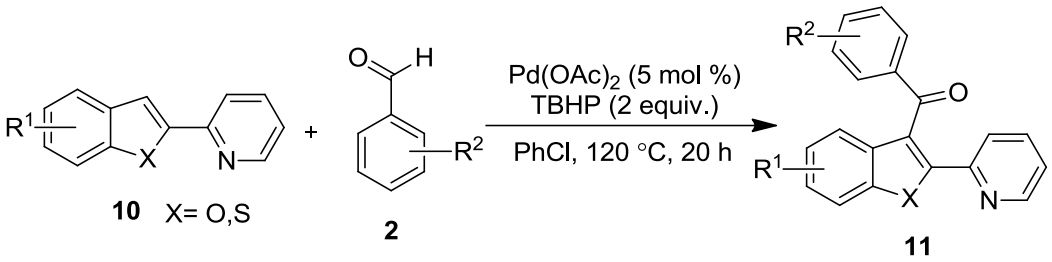

Scheme 3A.1.4: Pd-catalyzed C-3 acylation of benzofurans and benzothiophenes (**10**) with aldehydes (**2**)

In the same year, Patel and Wu groups independently documented elegant protocols for the *ortho*-aroylation of 2-arylbenzothiazoles and 2-arylbenzoxazoles (**12**), respectively by self-direction of the substrate nitrogen in the presence of $Pd(OAc)_2$ and TBHP as an oxidant (Scheme 3A.1.5).[26,27]

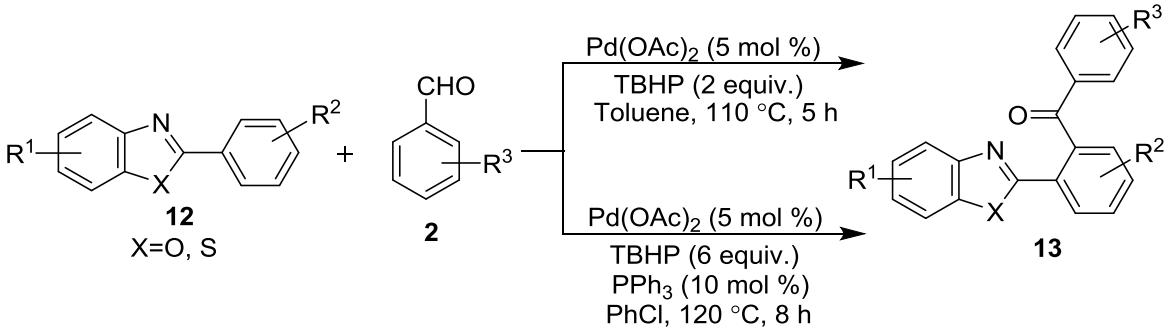

Scheme 3A.1.5: Pd-catalyzed *ortho*-aroylation of 2-arylbenzothiazoles and 2-arylbenzoxazoles (**12**) with aldehydes (**2**)

Surprisingly, aroylation of aryl and hetroaryls under Cu-catalyzed conditions are very scarce. Oxidative amidation of various amines with aldehydes have been successfully achieved in the presence of copper catalysts. In this regard, Jiao and coworkers described CuBr-catalyzed oxidative cross-dehydrogenative Csp^2-N bond formation strategy between aryl acetaldehyde (**14**) and aromatic amines (**15**) for synthesizing α-ketoamides **17**.[28] Later, the same group also synthesized α-ketoamides **17** from phenyl glyoxals (**16**) and anilines (**15**) under CuBr-catalyzed reaction conditions (Scheme 3A.1.6).[29]

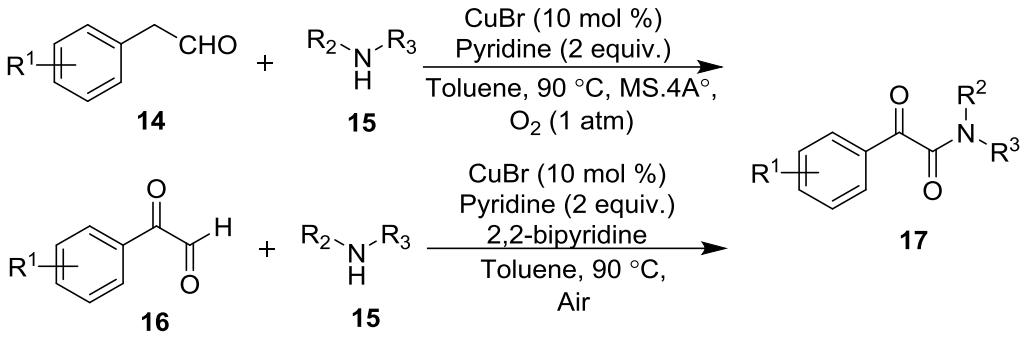

Scheme 3A.1.6: Cu-catalyzed synthesis of *α*-ketoamides (**17**) from anilines (**15**)

Very recently, Deng *et al.* disclosed a paradoxical regioselective Cu-catalyzed oxygenative cross-dehydrogenative dicarbonylation strategy at the *para*-C-H of primary anilines (**15**) with methyl ketones **18** to obtain **19** using catalytic amount of $BF_3{\cdot}OEt_2$ in the presence of oxygen (Scheme 3A.1.7).[30]

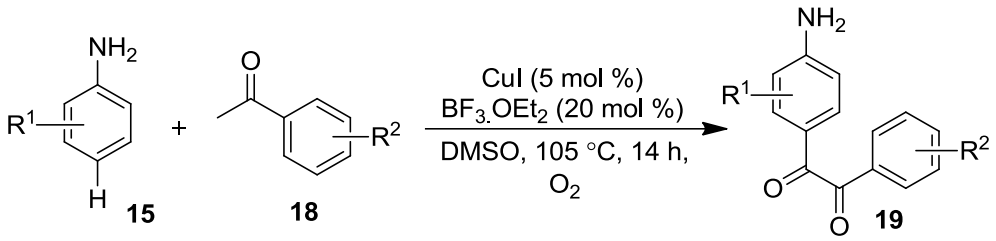

Scheme 3A.1.7: Cu-catalyzed oxygenative dicarbonylation of anilines (**15**) with methyl ketones

In resemblance to the above protocol, Ahmed and team described an efficient Cu(II)-catalyzed protocol for the *ortho*-functionalization of phenols (**20**) with phenyl glyoxal (**16**) at lower temperature in toluene (Scheme 3A.1.8).[31]

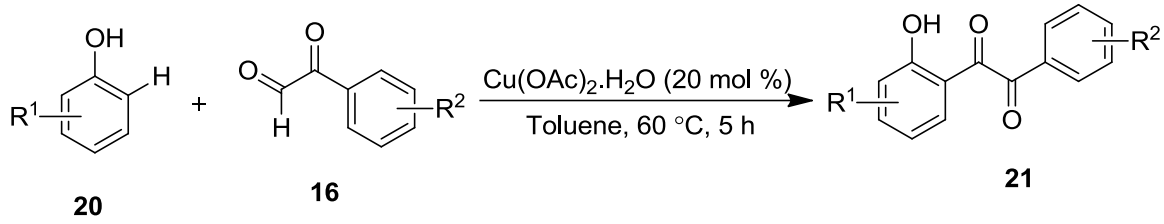

Scheme 3A.1.8: Cu-catalyzed *o*-dicarbonylation of phenol (**20**) with phenyl glyoxal

Li and co-workers presented a unique and novel Cu-catalyzed intramolecular C-H oxidation/acylation *via* a cross-dehydrogenative strategy for constructing substituted indoline-2,3-diones (**23**) with good functional groups tolerance in THF at 100 °C under oxygen environment (Scheme 3A.1.9).[32]

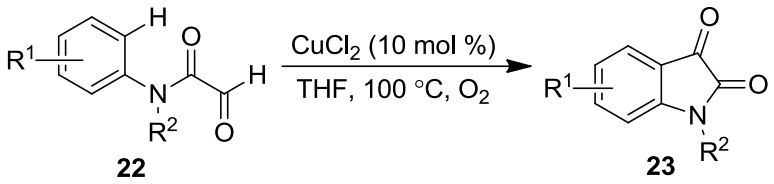

Scheme 3A.1.9: Cu-catalyzed synthesis of indoline-2,3-diones (**23**)

Jiao *et al.* described a Cu-catalyzed oxidative dehydrogenative coupling reaction of alcohols **24** and phenyl glyoxal (**16**) in the presence of air affording *α*-ketoesters **25** in moderate-to-good yields (Scheme 3A.1.10).[33]

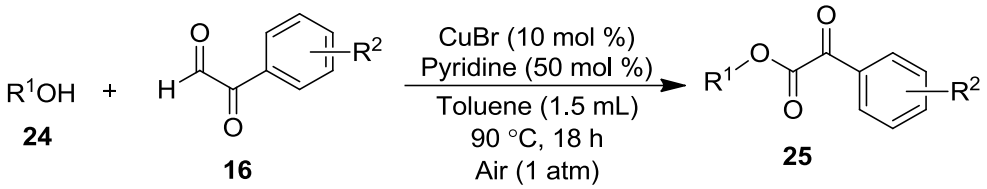

Scheme 3A.1.10: Cu-catalyzed synthesis of *α*-ketoesters from alcohols **24** and phenyl glyoxal

Interestingly, Li and coworkers reported a highly regio- and stereoselective synthesis of *E*-1,2-dicarbonyl-3-ene derivatives (**27**) in good yields by CuBr-catalyzed cross-dehydrogenative coupling between terminal alkynes **26** and phenyl glyoxal (**16**) in presence of morpholine (Scheme 3A.1.11).[34]

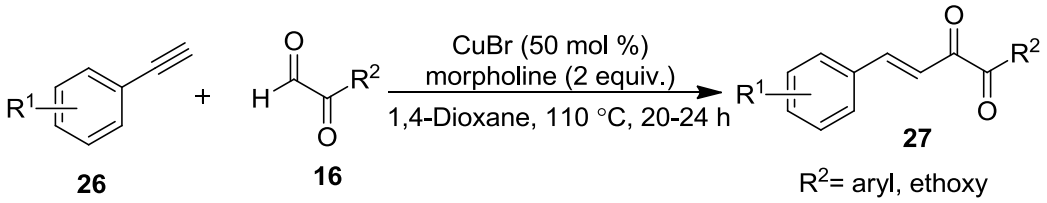

Scheme 3A.1.11: Cu-catalyzed synthesis of *E*-1,2-dicarbonyl-3-ene derivatives (**27**) from terminal alkyne (**26**) and phenyl glyoxal (**16**)

Yang and coworkers developed an efficient and practical protocol for Cu-catalyzed aerobic oxidative dicarbonylation of indoles (**28**) using phenyl glyoxal (**16**) to obtain C-3 dicarbonylated indoles **29** under the described conditions (Scheme 3A.1.12).[35]

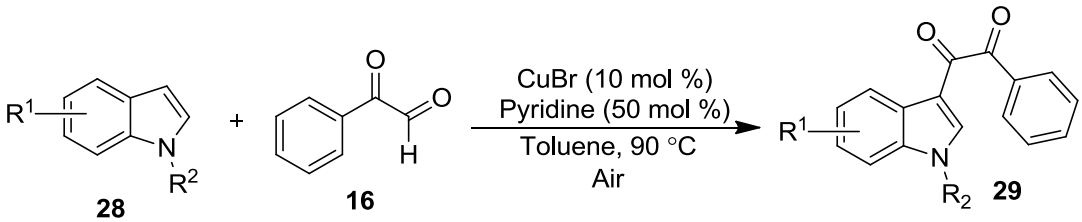

Scheme 3A.1.12: Cu-catalyzed C-3 dicarbonylation of indole (**28**) with phenyl glyoxal

On the other hand, the increasing citation of imidazo[1,2-*a*]pyridines in recent articles have allude the interest of organic chemists towards the construction of newer bioactive functionalized imidazo[1,2-*a*]pyridines. More specifically, the transition-metal catalyzed functionalization of imidazo[1,2-*a*]pyridines in recent years have opened new doors for the synthesis of novel heterocyclic systems.[36]

Despite significant progress for C-3 functionalization of imidazo[1,2-*a*]pyridines, there was no report on the direct cross-dehydrogenative coupling (CDC) between aldehydic Csp^2-H and C3(sp^2)–H of imidazo[1,2-*a*]pyridines at the time of initiation of the present work. Thus, we planned to develop an efficient strategy for the cross-dehydrogenative coupling of aryl acetaldehydes and imidazo[1,2-*a*]pyridines. However, during the progress of this work, Atmakur *et al.* reported I_2-DMSO-PTSA catalyzed C-3 dicarbonylation of imidazo[1,2-*a*]pyridines (**30**) using acetophenones (**18**) (Scheme 3A.1.13a).[37] During the review of the present work, Cao and coworkers illustrated the use of *N*,*N*-disubstituted acetamide or acetone for the dicarbonylation of imidazo[1,2-*a*]pyridines (**30**) in presence of copper salt using molecular oxygen as oxidant in acetic acid and toluene at 140 °C (Scheme 3A.1.13b).[38] Later, in addition to our report on C-3 dicarbonylation of imidazo[1,2-*a*]pyridines Cao group again reported Cu-catalyzed regioselective synthesis of 1,2-dicarbonylated imidazo[1,2-*a*]pyridines, (**31**) using methyl ketones (**18**) as a dicarbonyl source in acetic acid and *t*-amyl alcohol under the environment of molecular oxygen (Scheme 3A.1.13c).[39] Recently, Hajra group also synthesized 1,2-dicarbonylated imidazo[1,2-*a*]pyridines (**31**) using $FeCl_3$ catalyst and arylglyoxal (**16**) (Scheme 3A.1.13d).[40]

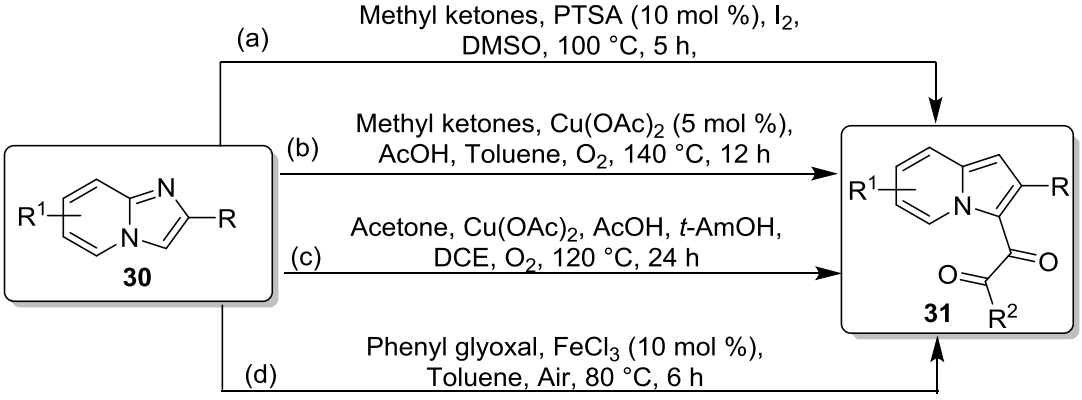

Scheme 3A.1.13: Various other synthetic reports for the synthesis of C-3 dicarbonylated imidazo[1,2-*a*]pyridines (**31**)

3A.2 Results and Discussion

Our preliminary investigation started with the reaction of imidazo[1,2-*a*]pyridine (**30a**) and phenyl acetaldehyde (**14a**) in the presence of catalytic amount of copper acetate (10 mol %) and TBHP (1 equiv.) as oxidant in toluene at 100 °C. To our delight, the expected product, 1-phenyl-2-(2-phenylimidazo[1,2-*a*]pyridin-3-yl)ethane-1,2-dione (**31a**) was obtained in 46% yield after 20 h. (Table 3A.2.1, entry 1) The structure of the **31a** was confirmed by its detailed spectroscopic analysis. The ^{1}H NMR of compound **31a** exhibited 14 protons in the aromatic region between δ 7.03-9.78, with the C5-H deshielded at δ 9.78, accounting for the coupling between imidazo[1,2-*a*]pyridine and phenyl acetaldehyde moieties. Absence of a peak for methylene protons and the corresponding carbon in the ^{1}H NMR and ^{13}C spectra's respectively, indicated that during coupling functional transformation of methylene group has taken place (Figure 3A.2.2 and Figure 3A.2.3). This got support from the presence of two carbonyl peaks at δ 190.4 and 183.7 in the ^{13}C NMR spectrum of **31a**. The final confirmation was obtained by HRMS of **31a**.

Several experiments were performed to further optimize the reaction condition, and the results are summarized in Table 3A.2.1. Screening of different copper catalysts revealed that the best yield (60%) was obtained by using CuBr whereas other copper catalyst such as CuI, CuCl, and CuO gave similar yields as that of $Cu(OAc)_2$ (Table 3A.2.1, entries 2-4). Lower yield of **31a** was obtained by using $CuSO_4.5H_2O$ (Table 3A.2.1, entry 6). We next undertook the process of solvent screening. It was noticed that **31a** was isolated in comparatively lesser yield in DCM, DCE and xylene (Table 3A.2.1, entries 7-9). Subsequently, the effect of varying oxidant on the coupling between **30a** and **14a** in toluene was studied. An improvement in the yield of **31a** was observed by using oxidants such as $K_2S_2O_8$, CAN (Table 3A.2.1, entries 10-11), however comparatively lesser yields were obtained with *m*-CPBA and BPO (benzoyl peroxide) (Table 3A.2.1, entries 12-13). Delightfully, the substitution of external oxidants with air resulted in almost similar yield of **31a** (Table 3A.2.1, entry 14). We next attempted the coupling reaction in air using a couple of ligands including 1,10-phenanthroline, TMDEA and 2,2-bipyridine (Table 3A.2.1, entries 15-17). Among these ligands, the use of 2,2-bipyridine along with CuBr produced 80% of **31a** in toluene, even when the time of the reaction was reduced from 20 h to 12 h (Table 3A.2.1, entries 17 & 18). Notably, $InCl_3$, $RuCl_3$ and $FeCl_3$ were able to catalyze the reaction, albeit in lower yields (Table 3A.2.1, entries 19-21). Employment of other transition

metal catalysts, such as $Pd(OAc)_2$, $PdCl_2$ and $Pd(PPh_3)Cl_2$ did not yield **31a** in noticeable amounts (Table 3A.2.1, entries 22-24).

Table 3A.2.1: Selected optimization[a] of reaction conditions for the synthesis of **31a**

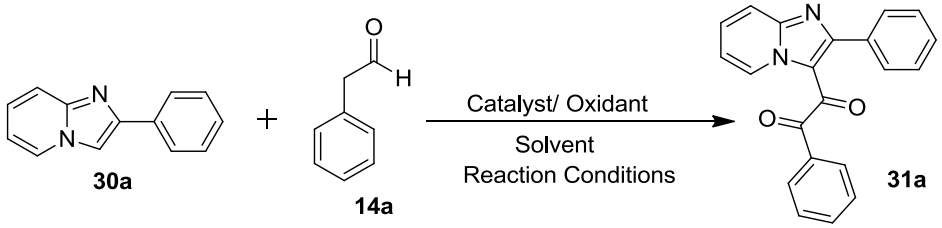

Entry	Catalysts	Solvent	Oxidant	Ligand	Yield[c] (%)
1.	$Cu(OAc)_2$	Toluene	TBHP	-	46
2.	CuI	Toluene	TBHP	-	42
3.	CuCl	Toluene	TBHP	-	45
4.	CuO	Toluene	TBHP	-	38
5.	CuBr	Toluene	TBHP	-	60
6.	$CuSO_4.5H_2O$	Toluene	TBHP	-	20
7.	CuBr	DCE	TBHP	-	55
8.	CuBr	DCM	TBHP	-	30
9.	CuBr	Xylene	TBHP	-	56
10.	CuBr	Toluene	$K_2S_2O_8$	-	63
11.	CuBr	Toluene	CAN	-	64
12.	CuBr	Toluene	*m*-CPBA	-	42
13.	CuBr	Toluene	BPO	-	46
14.	CuBr	Toluene	Air	-	66
15.	CuBr	Toluene	Air	1,10-phenanthroline	72
16.	CuBr	Toluene	Air	TMDEA	67
17.	CuBr	Toluene	Air	2,2-bipyridine	80
18.	**CuBr**	**Toluene** [b]	**Air**	**2,2-bipyridine**	**80**
19.	$InCl_3$	Toluene	Air	2,2-bipyridine	52
20.	$RuCl_3$	Toluene	Air	2,2-bipyridine	58
21.	$FeCl_3.6H_2O$	Toluene	Air	2,2-bipyridine	70
22.	$Pd(OAc)_2$	Toluene	TBHP	2,2-bipyridine	-
23.	$PdCl_2$	Toluene	TBHP	2,2-bipyridine	-
24.	$Pd(PPh_3)Cl_2$	Toluene	TBHP	2,2-bipyridine	-

[a]Reaction conditions: Imidazo[1,2-*a*]pyridine (**30a**) (0.25 mmol), phenyl acetaldehyde (**14a**) (0.30 mmol), catalyst (10 mol %), oxidant (0.25 mmol), ligand (10 mol %), solvent (4 mL). The reactions were performed and monitored at 100 °C [except for entry 7 (80 °C) and entry 8 (40 °C)] for 20 h; [b]After 12 h; [c]Isolated yield; TMDEA: tetramethylethylenediamine; BPO: benzoyl peroxide; TBHP: *tert*-butyl hydroperoxide.

After a great deal of screening different parameters, the highest yield (80%) of C-3 dicarbonylated product **31a** was obtained when 1.2 equiv. of phenyl acetaldehyde was coupled with 1 equiv. imidazo[1,2,*a*]pyridine using CuBr/2,2'-bipyridine (10 mol % each) in toluene at

100 °C under an atmosphere of air. Under the optimized conditions, the scope of aryl acetaldehydes was investigated (Scheme 3A.2.1). Both the electron-rich and electron-deficient aryl acetaldehydes (**14a-g**) efficiently reacted with 2-phenylimidazo[1,2-*a*]pyridine (**30a**) to give corresponding C-3 dicarbonylated products (**31a-g**) in 70-85% isolated yield. Among aryl acetaldehydes, 4-fluorophenyl acetaldehyde **14f** displayed highest reactivity when reacted with **30a,** yielding 85% of the corresponding dicarbonylated product **31f** as compared to other halo derivatives (4-Br, 4-Cl). Naphthyl-substituted acetaldehyde also successfully afforded **31g** in 76% isolated yield. Relatively lesser yields of C-3 dicarbonylated products (**31b** & **31c**) were obtained when 4-methyl and 4-methoxy substituted phenyl acetaldehydes were employed. Unfortunately, acetaldehyde and propionaldehyde failed to react with **30a**.

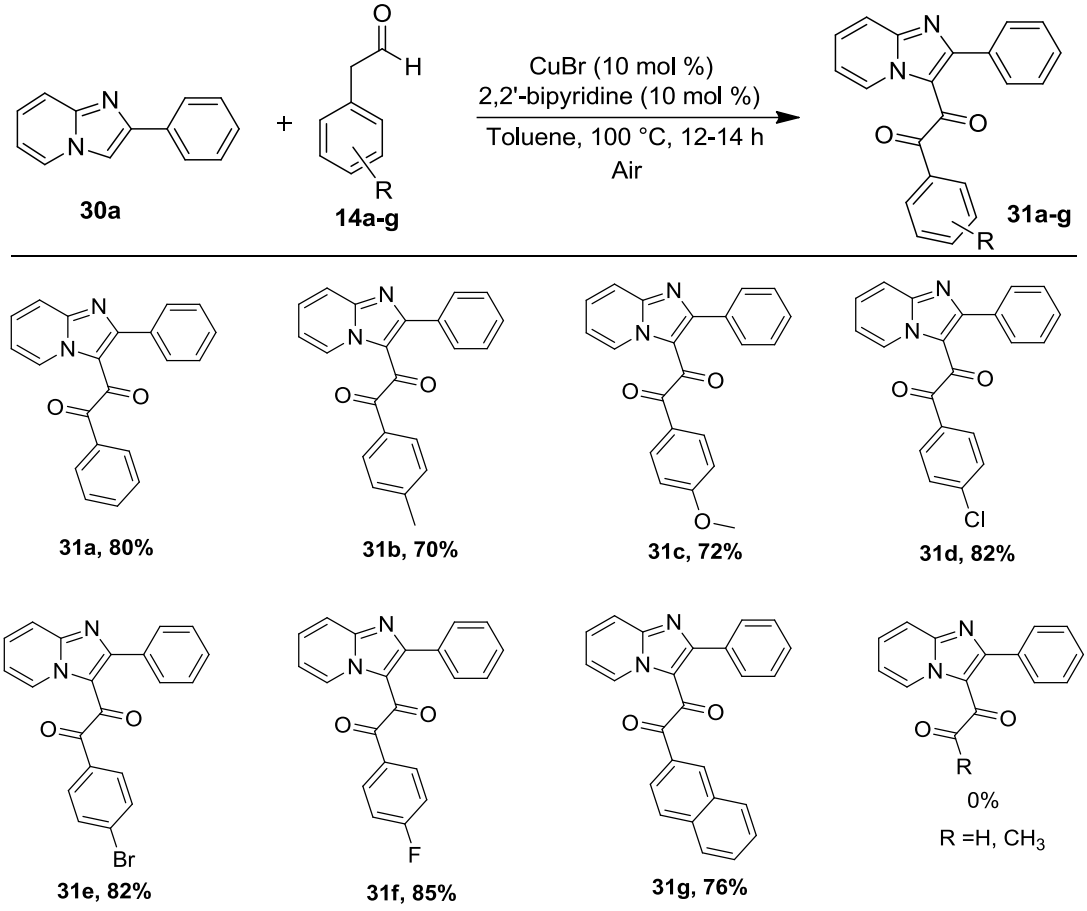

Scheme 3A.2.1: Scope of aryl acetaldehydes (**14a-g**) for the synthesis of C-3 dicarbonylated imidazo[1,2-*a*]pyridines

The scope of reaction was further expanded to a variety of substituted 2-arylimidazo[1,2-*a*]pyridines with substituted aryl acetaldehydes (Scheme 3A.2.2).

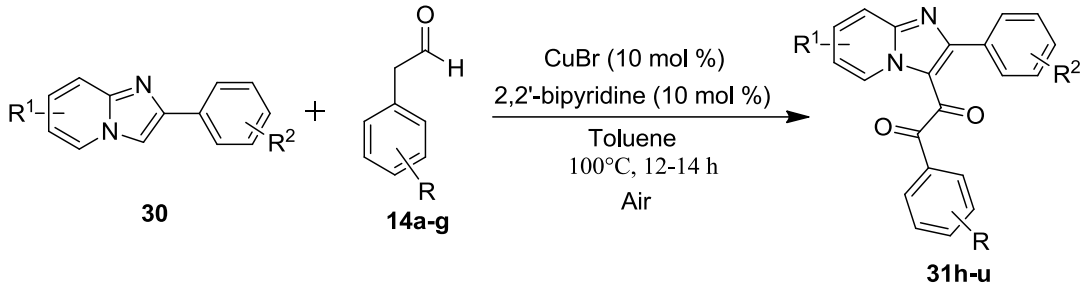

30 14a-g 31h-u

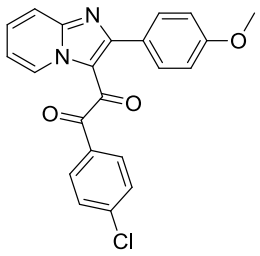

31h, 78%

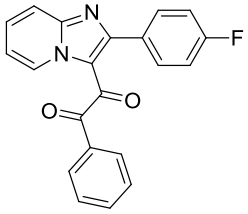

31i, 75%

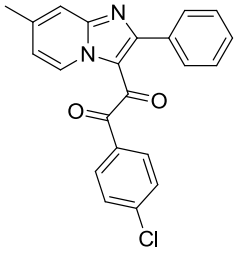

31j, 80%

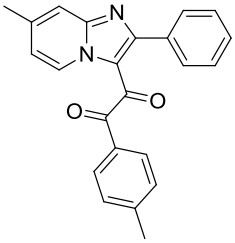

31k, 72%

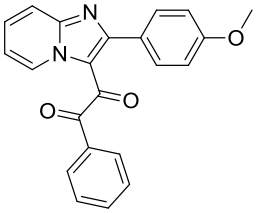

31l, 70%

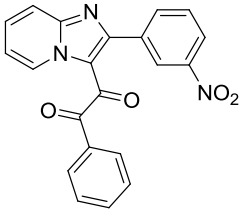

31m, 55%

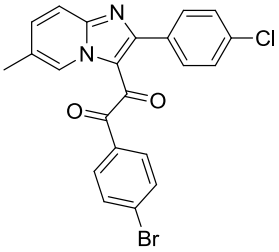

31n, 77%

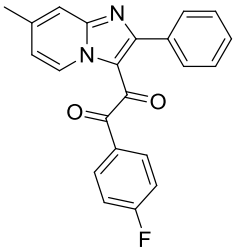

31o, 82%

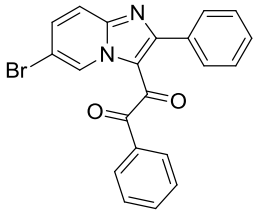

31p, 75%

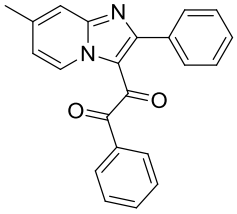

31q, 72%

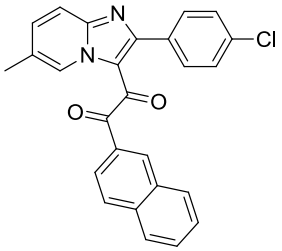

31r, 74%

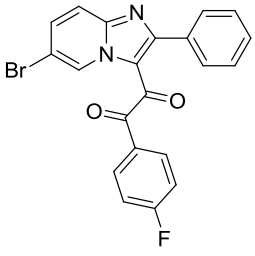

31s, 78%

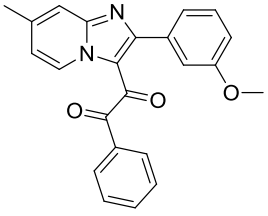

31t, 73%

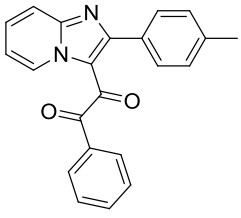

31u, 71%

Scheme 3A.2.2: Scope of imidazo[1,2-*a*]pyridines (**30**) and aryl acetaldehydes (**14**)

Presence of both electron-donating and electron-withdrawing substituents on the aryl and pyridyl ring of 2-phenylimidazo[1,2-*a*]pyridines showcased a marked difference in their reactivity towards aerial oxidative cross-dehydrogenative coupling with aryl acetaldehydes. Interestingly, presence of nitro group at phenyl of 2-phenylimidazo[1,2-*a*]pyridine yielded the corresponding product **31m** in 55% yield.

To extend the scope of our methodology, few other imidazo-heterocyles such as imidazo[1,2-*a*]pyrimidine (**32a**), imidazo[2,1-*b*]thiazole (**32b**) and benzo[*d*]imidazo[2,1-*b*]thiazole (**32c**) were reacted with phenyl acetaldehyde (**14a**) under optimized conditions to yield their corresponding dicarbonylated products (**33a-c**) in 68-74% isolated yields (Scheme 3A.2.3). It is noteworthy that these imidazo-heterocycles yielded the corresponding C-3 dicarbonylated products in longer reaction time as compared to imidazo[1,2-*a*]pyridines.

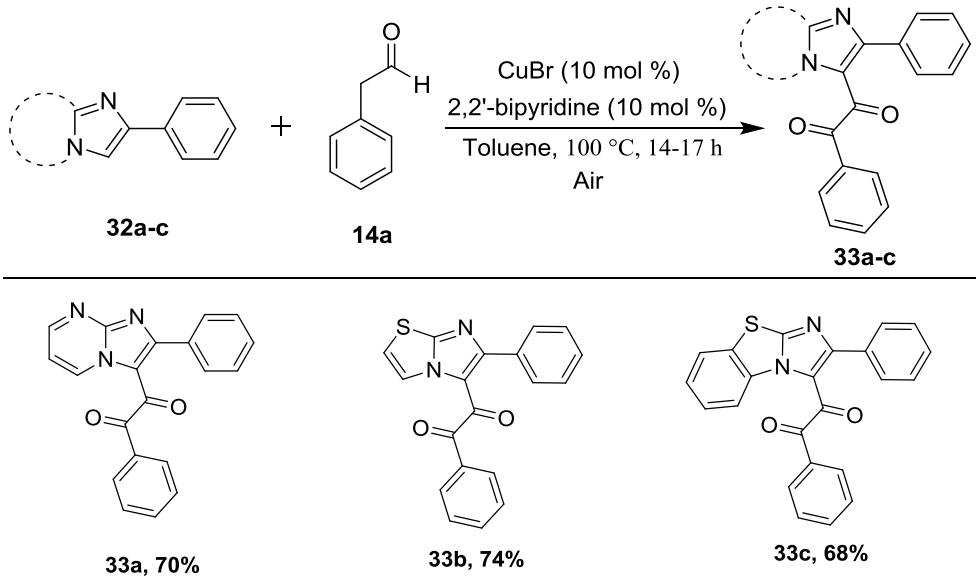

Scheme 3A.2.3: Scope of imidazo-heterocycles (**33a-c**) for the synthesis of C-3 dicarbonylated imidazo-heterocycles

To gain some insight into reaction mechanism, a few control experiments were performed (Scheme 3A.2.4). The reaction did not yield the expected product at all in the presence of radical scavenger TEMPO (3 equiv.), thereby suggesting an evidence for the radical mechanism (Scheme 3A.2.4a). When the reaction was performed under nitrogen atmosphere, the product was observed in traces on TLC, thereby indicating a crucial participation of aerial oxygen not only as an oxidant but also as an initiator to trigger the catalytic process. The reaction of phenyl

acetaldehyde under copper bromide catalyzed conditions in air did not yield phenyl glyoxal at all, thereby suggesting that the oxidation of phenyl acetaldehyde to phenyl glyoxal (**16**) may not be involved in the reaction (Scheme 3A.2.4b). The reaction did not proceed in the absence of copper bromide emphasizing the role of copper as an oxidant (Scheme 3A.2.4a). Interestingly, benzaldehyde (**2**) failed to give the corresponding oxidized product (**34a**), rather the TLC of the reaction mixture shows major un-reacted imidazo[1,2-*a*]pyridine along even after refluxing for 12 h under similar Cu-catalyzed conditions, in presence/absence of external oxidants. Some faint spots were observed on TLC, which were not isolated. Assuming that C-3 alkenyl or alkynyl substituted imidazo[1,2-*a*]pyridine might be formed as intermediates in the reaction between **30a** and **14a**, compounds **35** or **36** were synthesized by standard procedures[41,42] as model substrates. Surprisingly **35** or **36** did not afford the dicarbonylated product **31a** under optimized condition, (Scheme 3A.2.4d) indicating that their formation is not involved in the mechanism.

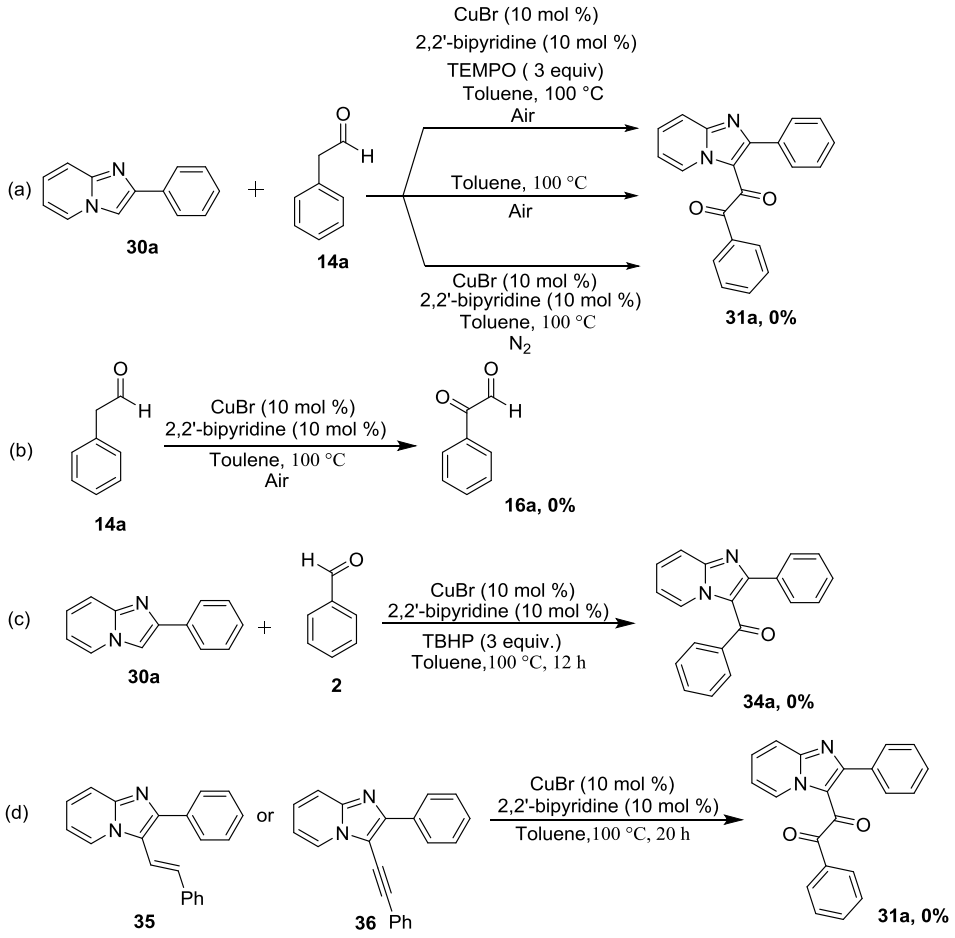

Scheme 3A.2.4: Control experiments

From the control experiments and literature reports,[13,43-45] the plausible mechanism of the reaction is believed to be initiated by the attack of 2-arylimidazo[1,2-*a*]pyridine (**30b**) on carbonyl of phenyl acetaldehyde (**14a**) to give **C**, probably by radical mechanism in presence of $CuBr/O_2$ *via* single electron transfer[13] (SET). Further, CuBr-catalyzed oxidation of **C** to **D**, and subsequently to **E** with the removal of HBr, followed by oxygen insertion yields super oxide radical **F**.[46] Finally **F** forms the C-3 dicarbonylated product **31b** (Scheme 3A.2.5). To provide analytical support to our proposed mechanism, the LC/HRMS of the reaction mixture was recorded after 2 h. Presence of the peaks at *m/z* 329.1378 and 357.1294 corresponding to the molecular formula $C_{22}H_{21}N_2O$ $[M+H]^+$ and $C_{22}H_{17}N_2O_3$ $[M-Cu]^+$ respectively, indicated the formation of intermediates **C** and **F** (Figure 3A.2.1).

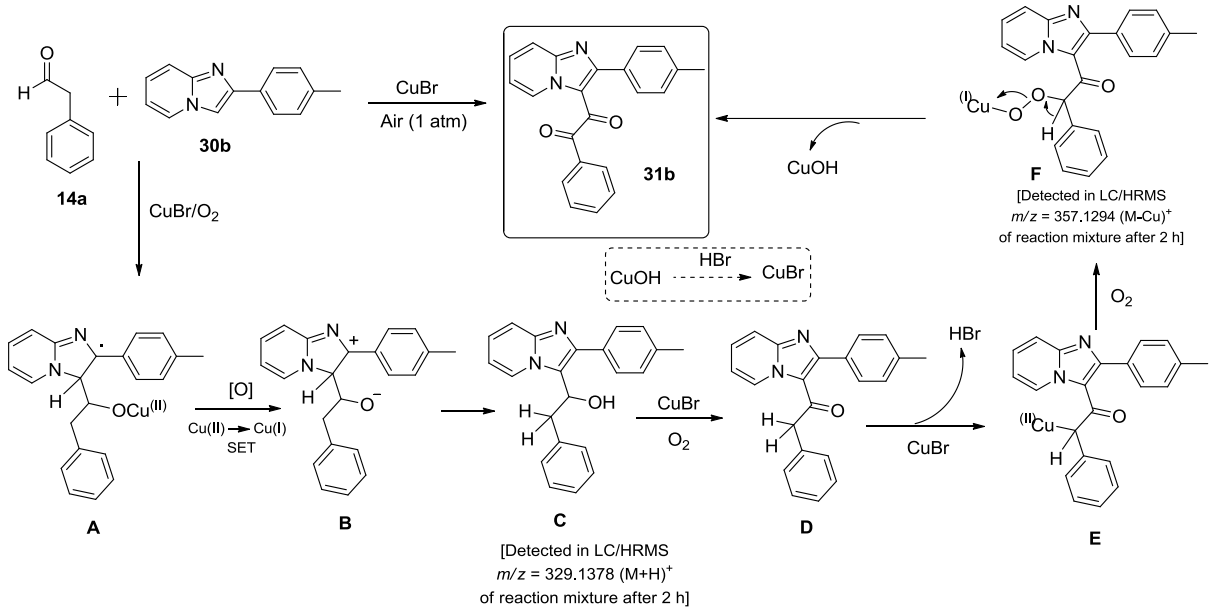

Scheme 3A.2.5: Plausible mechanism

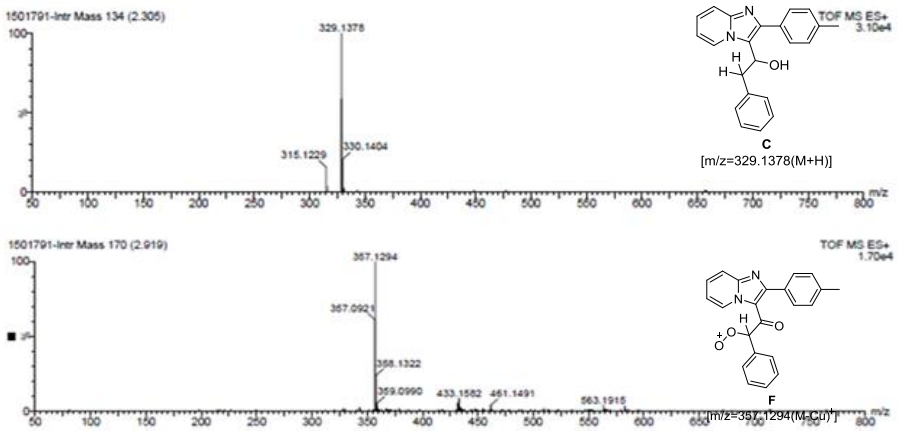

Figure 3A.2.1: LC-HRMS of crude reaction mixture (**31b**) after 2 h of the reaction

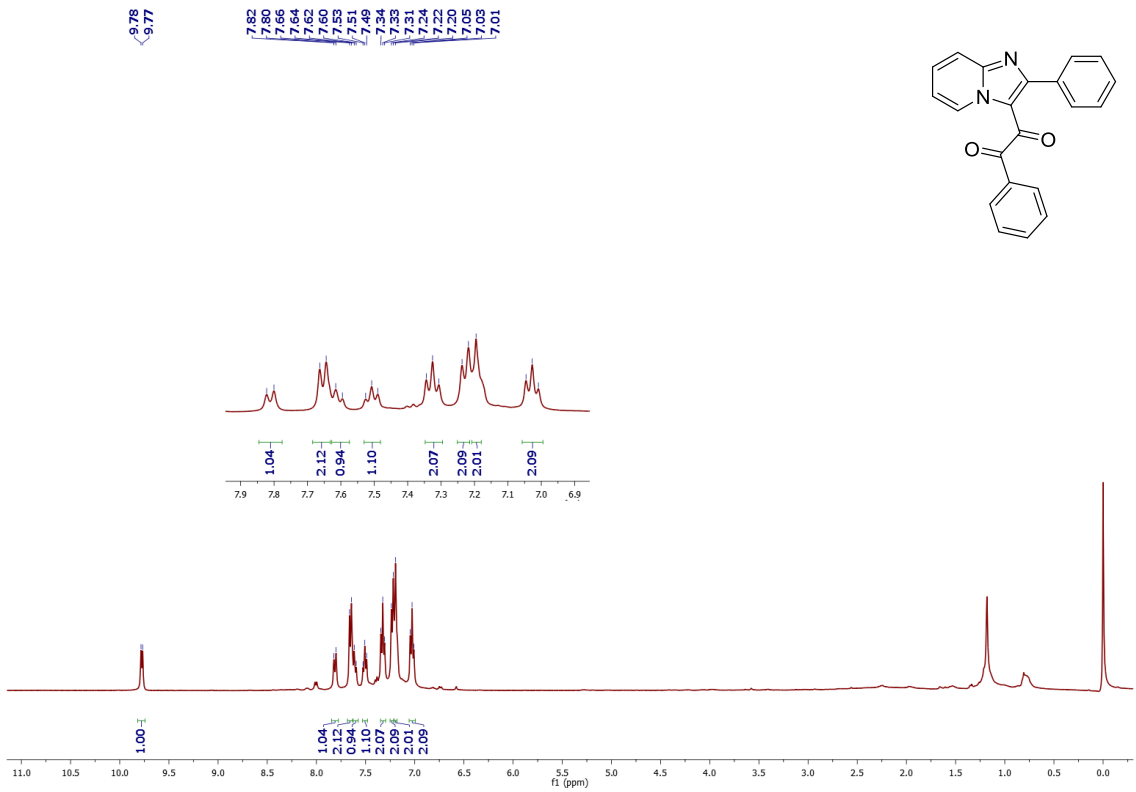

Figure 3A.2.2: ^{1}H NMR spectrum of **31a**

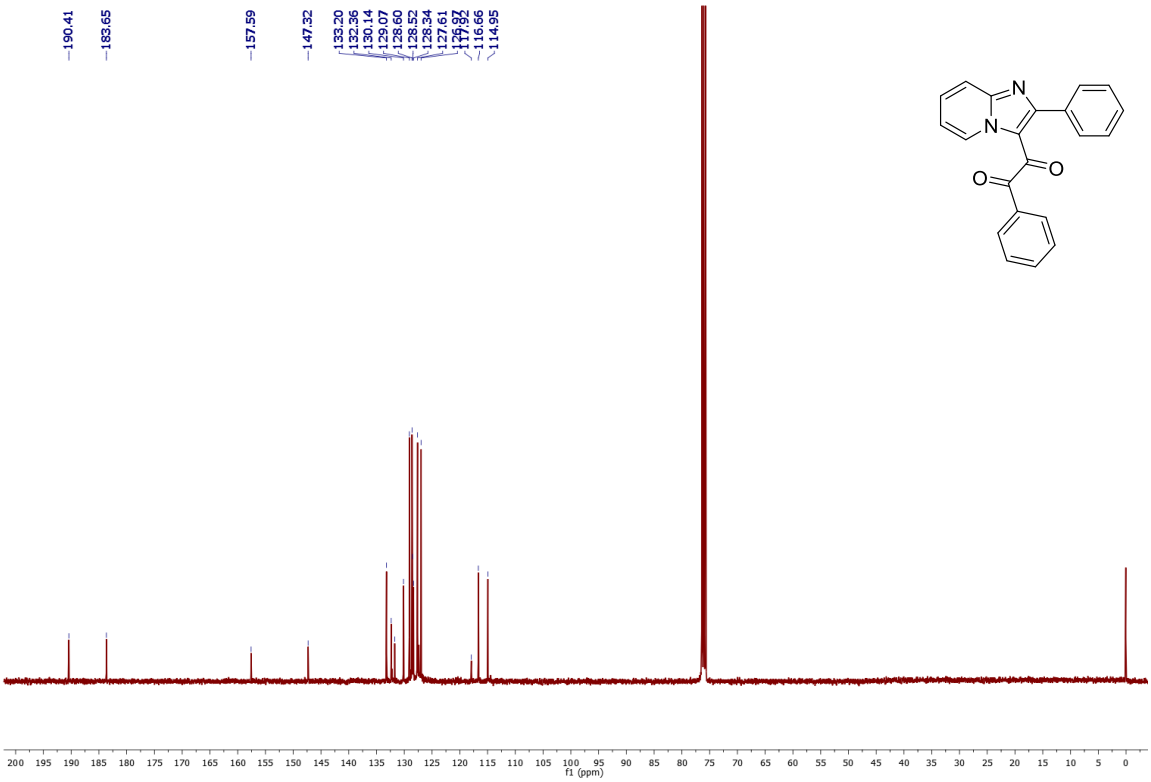

Figure 3A.2.3: ^{13}C NMR spectrum of **31a**

In summary we have developed an efficient and atom-economical Cu-catalyzed strategy for the cross-dehydrogenative coupling between aryl acetaldehydes and imidazo-heterocycles, yielding C-3 dicarbonylated imidazo-heterocycles in moderate-to-good yields.

3A.3 Experimental Section

3A.3.1 General Materials and Methods

All the chemicals were purchased from Sigma-Aldich, Alfa Aesar, and Spectrochem India Pvt. Ltd and used without further purification. The solvents used were purchased from Merck (India) and were distilled and dried before use. Nuclear magnetic resonance spectra were recorded on Bruker 400 spectrometer. All ^{1}H NMR experiments were reported in δ units, parts per million (ppm), and were measured relative to residual chloroform (7.26 ppm) or DMSO (2.5 ppm) in the deuterated solvent. All ^{13}C NMR spectra were reported in ppm relative to deuterochloroform (77.0 ppm) or [d_6] DMSO (39.5 ppm). All coupling constants J were reported in Hz. The following abbreviations were used to describe peak splitting patterns when appropriate: s = singlet, d = doublet, t = triplet, dd = doublet of doublet, m = multiplet and br s = broad singlet. Melting points were determined on a capillary point apparatus equipped with a digital thermometer and are uncorrected. High resolution mass spectra were recorded with a TOF analyzer spectrometer by using electrospray mode.

General procedure for dicarbonylation of imidazo-heterocycles

A mixture of imidazo-heterocycle (**30a-h**, **32a-c**) (0.52 mmol), aryl acetaldehyde (**14a-g**) (0.62 mmol), CuBr (0.052 mmol), 2,2-bipyridine (0.052 mmol) in toluene (8 mL) were heated at 100 °C for 12-17 h. The progress of reaction was monitored by TLC. Thereafter, toluene was evaporated and the reaction mixture was subjected to silica gel column chromatography (hexanes/EtOAc, 9:1) to yield the dicarbonylated product (**31a-u** and **33a-c**).

1-Phenyl-2-(2-phenylimidazo[1,2-*a*]pyridin-3-yl)ethane-1,2-dione (31a): Yellow solid; yield:

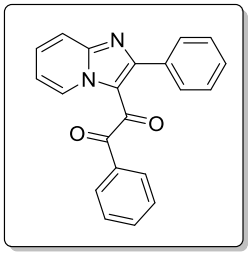

134 mg (80%); mp 122–124 °C (lit.[37] mp 122-123 °C); ^{1}H NMR (400 MHz, $CDCl_3$) δ 9.78 (d, J = 6.7 Hz, 1H), 7.81 (d, J = 8.7 Hz, 1H), 7.65 (d, J = 7.7 Hz, 2H), 7.61 (d, J = 8.0 Hz, 1H), 7.51 (t, J = 7.3 Hz, 1H), 7.33 (t, J = 7.5 Hz, 2H), 7.23 (d, J = 7.7 Hz, 2H), 7.21 – 7.15 (m, 2H), 7.03 (t, J = 7.4 Hz, 2H); ^{13}C NMR (100 MHz, $CDCl_3$) δ 190.4, 183.6, 157.6, 147.3, 133.2, 132.4, 131.7, 130.1, 129.0, 128.6, 128.5, 128.3, 127.6, 127.0, 117.9, 116.7, 114.9; IR (KBr): 2930, 2902, 1675, 1596, 1402, 1129, 859, 720 cm^{-1}.

1-(2-Phenylimidazo[1,2-*a*]pyridin-3-yl)-2-(*p*-tolyl)ethane-1,2-dione (31b): Light yellow solid;

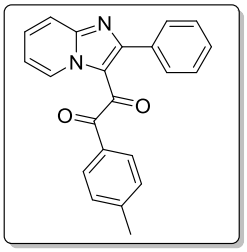

yield: 117 mg (70%); mp 152–154 °C (lit.[37] mp 152-155 °C); ^{1}H NMR (400 MHz, $CDCl_3$) δ 9.85 (d, J = 6.9 Hz, 1H), 7.87 (d, J = 8.9, 1H), 7.71 – 7.67 (m, 1H), 7.65 (d, J = 8.2 Hz, 2H), 7.35 – 7.31 (m, 1H), 7.32 (d, J = 1.3 Hz, 1H), 7.29 (dd, J = 7.4, 0.9 Hz, 1H), 7.26 (dd, J = 7.1, 1.2 Hz, 1H), 7.21 (d, J = 8.0 Hz, 2H), 7.15 – 7.10 (m, 2H), 2.43 (s, 3H); ^{13}C NMR (100 MHz, $CDCl_3$) δ 191.1, 184.8, 158.6, 148.3, 145.3, 132.9, 131.0, 130.9, 130.0, 129.7, 129.4, 129.4, 127.9, 118.9, 117.6, 115.8, 21.9; IR (KBr): 3016, 1678, 1593, 1526, 1467, 1341, 730 cm^{-1}.

1-(4-Methoxyphenyl)-2-(2-phenylimidazo[1,2-*a*]pyridin-3-yl)ethane-1,2-dione (31c): Brown

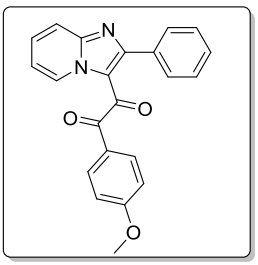

solid; yield: 132 mg (72%); mp 165–168 °C (lit.[37] mp 166-168 °C); ^{1}H NMR (400 MHz, $CDCl_3$) δ 9.85 (d, J = 6.9 Hz, 1H), 7.86 (d, J = 8.9 Hz, 1H), 7.72 (d, J = 8.9 Hz, 2H), 7.70 – 7.64 (m, 1H), 7.38 – 7.31 (m, 2H), 7.26 (m, 2H), 7.14 (t, J = 7.6 Hz, 2H), 6.88 (d, J = 8.9 Hz, 2H), 3.90 (s, 3H); ^{13}C NMR (100 MHz, $CDCl_3$) δ 190.1, 185.0, 164.4, 158.5, 148.3, 133.0, 132.0, 130.8, 130.0, 129.3, 127.8, 126.7, 119.0, 117.6, 115.7, 113.9, 55.6; IR (KBr): 2930, 1658, 1599, 1460, 1260, 1180, 748, 753 cm^{-1}.

1-(4-Chlorophenyl)-2-(2-phenylimidazo[1,2-*a*]pyridin-3-yl)ethane-1,2-dione (31d): Yellow

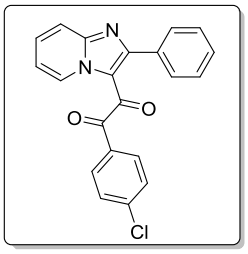

solid; yield: 152 mg (82%); mp 122–125 °C (lit.[37] mp 120-125 °C); ^{1}H NMR (400 MHz, $CDCl_3$) δ 9.81 (d, J = 6.7 Hz, 1H), 7.87 (d, J = 8.1 Hz, 1H), 7.68 (d, J = 8.1 Hz, 2H), 7.49 – 7.42 (m, 1H), 7.38 (d, J = 8.3 Hz, 2H), 7.31 (d, J = 7.5 Hz, 3H), 7.26 (brs, 1H), 7.15 (t, J = 7.5 Hz, 2H); ^{13}C NMR (100 MHz, $CDCl_3$) δ 190.1, 183.9, 158.8, 148.5, 40.7, 131.8, 131.2, 130.9, 130.0, 129.6, 129.3, 129.0, 128.0, 118.9, 117.7, 116.0; IR (KBr): 2953, 2806, 1676, 1592, 1400, 1253, 753 cm^{-1}.

1-(4-Bromophenyl)-2-(2-phenylimidazo[1,2-a]pyridin-3-yl)ethane-1,2-dione (31e): White

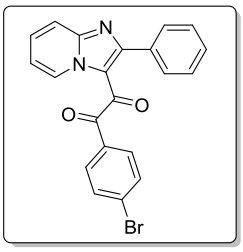

solid; yield: 171 mg (82%); mp 137–140 °C (lit.[37] mp 138-140 °C); ^{1}H NMR (400 MHz, $CDCl_3$) δ 9.81 (d, J = 6.9 Hz, 1H), 7.87 (d, J = 8.9 Hz, 1H), 7.72 – 7.66 (m, 1H), 7.62 – 7.52 (m, 4H), 7.31 – 7.27 (m, 3H), 7.26 (dd, J = 6.9, 1.1 Hz, 1H), 7.14 (t, J = 7.7 Hz, 2H); ^{13}C NMR (100 MHz, $CDCl_3$) δ 190.3, 183.8, 158.8, 148.5, 132.8, 132.2, 132.0, 131.2, 130.9,

130.0, 129.6, 129.6, 129.3, 128.1, 118.9, 117.7, 116.0; IR (KBr): 3067, 2932, 1676, 1590, 1400, 1254, 753 cm^{-1}.

1-(4-Fluorophenyl)-2-(2-phenylimidazo[1,2-*a*]pyridin-3-yl)ethane-1,2-dione (31f): Yellow solid; yield: 151 mg (85%); mp 165–167 °C (lit.[37] mp 165–168 °C); ^{1}H NMR (400 MHz, $CDCl_3$) δ 9.83 (d, J = 6.7 Hz, 1H), 7.88 (d, J = 8.8 Hz, 1H), 7.83 – 7.73 (m, 2H), 7.73 – 7.66 (m, 1H), 7.32 (brs, 1H), 7.31 – 7.24 (m, 3H), 7.15 (t, J = 7.5 Hz, 2H), 7.09 (t, J = 8.4 Hz, 2H); ^{13}C NMR (100 MHz, $CDCl_3$) δ 189.8, 184.2, 167.6, 165.0, 158.7, 148.4, 132.9, 132.3, 132.2, 131.1, 130.1, 129.5, 129.3, 128.0, 118.0, 115.9; IR (KBr): 2943, 2816, 1666, 1582, 1400, 1233, 763 cm^{-1}.

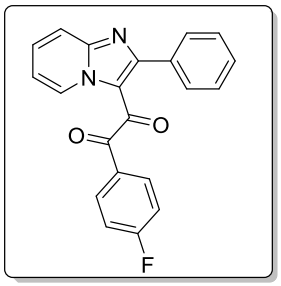

1-(Naphthalen-2-yl)-2-(2-phenylimidazo[1,2-*a*]pyridin-3-yl)ethane-1,2-dione (31g): Yellow solid; yield: 147 mg (76%); mp 159–162 °C (lit.[37] mp 158–162 °C); ^{1}H NMR (400 MHz, $CDCl_3$) δ 9.89 (d, J = 6.9 Hz, 1H), 8.37 (s, 1H), 7.93 – 7.85 (m, 3H), 7.82 (d, J = 8.6 Hz, 1H), 7.72 – 7.68 (m, 1H), 7.68 – 7.60 (m, 2H), 7.55 (dd, J = 11.1, 3.9 Hz, 1H), 7.34 – 7.28 (m, 2H), 7.28 – 7.24 (m, 1H), 7.24 – 7.20 (m, 1H), 7.02 (t, J = 7.7 Hz, 2H); ^{13}C NMR (100 MHz, $CDCl_3$) δ 191.4, 184.6, 158.7, 148.4, 136.0, 133.0, 132.6, 132.3 ,131.1, 130.9, 130.0, 129.9, 129.4, 129.4, 129.2, 128.7, 127.9, 127.0, 124.0, 119.0, 117.7, 115.9; IR (KBr): 2939, 2844, 1625, 1609, 1409, 1228, 739 cm^{-1}.

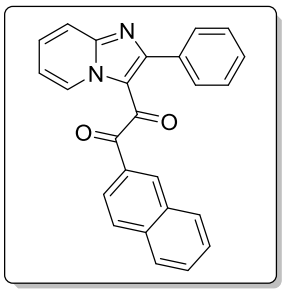

1-(4-Chlorophenyl)-2-(2-(4-methoxyphenyl)imidazo[1,2-*a*]pyridin-3-yl)ethane-1,2-dione:

(31h): Yellow solid; yield: 136 mg (78%); mp 162–165 °C; ^{1}H NMR (400 MHz, $CDCl_3$) δ 9.80 (d, J = 6.7 Hz, 1H), 7.84 (d, J = 8.8 Hz, 1H), 7.70 (d, J = 8.1 Hz, 2H), 7.66 (d, J = 8.6 Hz, 1H), 7.38 (d, J = 8.3 Hz, 2H), 7.27 – 7.19 (m, 3H), 6.65 (d, J = 8.3 Hz, 2H), 3.77 (s, 3H); ^{13}C NMR (100 MHz, $CDCl_3$) δ 190.3, 183.9, 160.8, 158.8, 148.6, 140.7, 131.9, 131.5, 131.1, 130.9, 129.3, 129.0, 125.2, 118.8, 117.6, 115.8, 113.5, 55.3; IR (KBr): 3089, 2910, 1686, 1642, 1409, 1252, 895 cm^{-1}; HRMS (ESI-TOF) (m/z) calculated $C_{22}H_{16}ClN_2O_3^+$: 391.0849; found 391.0863 $[M+H]^+$ and 393.1009 $[M+H+2]^+$.

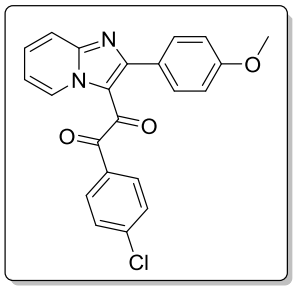

1-(2-(4-Fluorophenyl)imidazo[1,2-*a*]pyridin-3-yl)-2-phenylethane-1,2-dione (31i): White solid; yield: 121 mg (75%); mp 175–178 °C; ^{1}H NMR (400 MHz, $CDCl_3$) δ 9.85 (d, J = 6.9 Hz, 1H), 7.87 (d, J = 8.9 Hz, 1H), 7.78 – 7.73 (m, 2H), 7.72 – 7.67 (m, 1H), 7.61 (t, J = 7.4 Hz, 1H), 7.43 (t, J = 7.8 Hz, 2H), 7.31 – 7.29 (m, 1H), 7.29 – 7.26 (m, 2H), 6.81 (t, J = 8.6 Hz, 2H); ^{13}C NMR (100 MHz, $CDCl_3$) δ 191.5, 184.5, 164.7, 162.3, 157.5, 148.3, 134.4, 132.0, 132.0, 131.2, 129.5, 129.1, 129.7, 119.9, 117.6, 116.0, 115.1, 114.9; IR (KBr): 2983, 2890, 1686, 1624, 1409, 1382, 792 cm^{-1}; HRMS (ESI-TOF) (*m/z*) calculated $C_{21}H_{14}FN_2O_2^+$: 345.1039; found 345.1026 $[M+H]^+$.

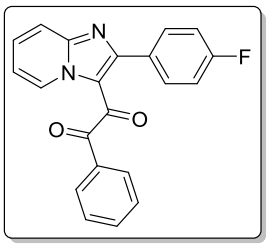

1-(4-Chlorophenyl)-2-(7-methyl-2-phenylimidazo[1,2-*a*]pyridin-3-yl)ethane-1,2-dione (31j): Brown solid, yield: 143 mg (80%); mp 178–180 °C; ^{1}H NMR (400 MHz, $CDCl_3$) δ 9.69 (d, J = 7.0 Hz, 1H), 7.70 – 7.65 (m, 2H), 7.63 (s, 1H), 7.38 (d, J = 8.6 Hz, 2H), 7.30 (d, J = 0.7 Hz, 1H), 7.31 – 7.27 (m, 2H), 7.15 (dd, J = 10.1, 5.2 Hz, 2H), 7.10 (dd, J = 7.0, 1.6 Hz, 1H), 2.58 (s, 3H); ^{13}C NMR (100 MHz, $CDCl_3$) δ 190.3, 183.5, 159.1, 148.9, 143.2, 140.6, 133.0, 131.9, 130.8, 130.0, 129.5, 129.0, 128.5, 128.0, 118.3, 116.5, 21.8; IR (KBr): 3032, 2924, 1682, 1643, 1412, 1250, 903 cm^{-1}; HRMS (ESI-TOF) (*m/z*) calculated $C_{22}H_{16}ClN_2O_2^+$: 375.0900; found 375.0923 $[M+H]^+$ and 377.1061 $[M+H+2]^+$.

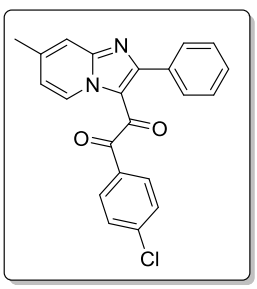

1-(7-Methyl-2-phenylimidazo[1,2-*a*]pyridin-3-yl)-2-(*p*-tolyl)ethane-1,2-dione (31k): Brown solid; yield: 122 mg (72%); mp 179–181 °C; ^{1}H NMR (400 MHz, $CDCl_3$) δ 9.70 (d, J = 7.0 Hz, 1H), 7.66 – 7.59 (m, 3H), 7.32 – 7.28 (m, 2H), 7.27 (brs, 1H), 7.19 (d, J = 8.0 Hz, 2H), 7.11 (d, J = 7.7 Hz, 2H), 7.08 – 7.05 (m, 1H), 2.56 (s, 3H), 2.42 (s, 3H); ^{13}C NMR (100 MHz, $CDCl_3$) δ 191.3, 184.4, 158.9, 148.8, 145.2, 142.9, 133.0, 131.1, 130.0, 129.7, 129.4, 129.3, 128.5, 127.9, 118.7, 118.1, 116.4, 21.9, 21.8; IR (KBr): 3032, 1682, 1597, 1412, 1250, 903 cm^{-1}; HRMS (ESI-TOF) (*m/z*) calculated $C_{23}H_{19}N_2O_2^+$: 355.1446; found 355.1477 $[M+H]^+$.

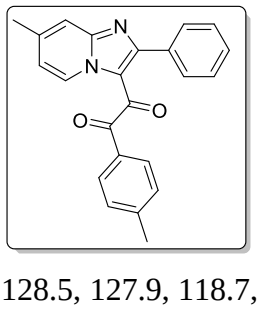

1-(2-(4-Methoxyphenyl)imidazo[1,2-*a*]pyridin-3-yl)-2-phenylethane-1,2-dione (31l): Brown solid; yield: 111 mg (70%); mp 166–167 °C (lit.[37] mp 166-168 °C); ^{1}H NMR (400 MHz, $CDCl_3$) δ 9.84 (d, J = 6.8 Hz, 1H), 7.85 (d, J = 8.9 Hz, 1H), 7.79 – 7.74 (m, 2H), 7.70 – 7.65 (m, 1H), 7.58 (d, J = 7.4 Hz, 1H), 7.42 (t, J = 7.7 Hz, 2H), 7.27 – 7.25 (m, 1H), 7.23 (t, J = 2.7 Hz, 2H), 6.63

(d, *J* = 8.7 Hz, 2H), 3.76 (s, 3H); ^{13}C NMR (100 MHz, $CDCl_3$) δ 191.6, 184.6, 161.0, 158.6, 148.4, 134.1, 133.4, 131.5, 131.0, 129.6, 129.3, 128.5, 125.1, 118.9, 117.5, 115.7, 113.5, 55.3; IR (KBr): 3060, 2933, 2751, 1684, 1615, 1239, 658 cm^{-1}.

1-(2-(3-Nitrophenyl)imidazo[1,2-*a*]pyridin-3-yl)-2-phenylethane-1,2-dione (31m): White

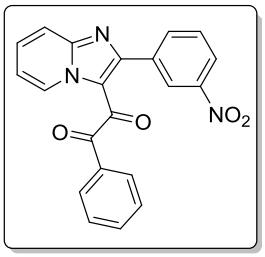

solid; yield: 85 mg (55%); mp 199–200 °C; ^{1}H NMR (400 MHz, $CDCl_3$) δ 9.85 (d, *J* = 6.8 Hz, 1H), 8.14 (d, *J* = 8.1 Hz, 1H), 8.04 (s, 1H), 7.89 (d, *J* = 8.9 Hz, 1H), 7.80 – 7.71 (m, 4H), 7.61 (t, *J* = 7.4 Hz, 1H), 7.45 (d, *J* = 3.3 Hz, 1H), 7.45 – 7.40 (m, 2H), 7.32 (t, *J* = 6.8 Hz, 1H); ^{13}C NMR (100 MHz, $CDCl_3$) δ 191.4, 184.0, 155.6, 148.3, 147.2, 135.8, 134.9, 132.9, 131.5, 129.5, 129.4, 129.0, 125.1, 124.1, 119.1 117.9, 116.4; IR (KBr): 3078, 1674, 1589, 1404, 1250, 856 cm^{-1}; HRMS (ESI-TOF) (m/z) calculated $C_{21}H_{14}N_3O_4^+$: 372.0984; found 372.0998 $[M+H]^+$.

1-(4-Bromophenyl)-2-(2-(4-chlorophenyl)-6-methylimidazo[1,2-*a*]pyridin-3-yl)ethane-1,2-

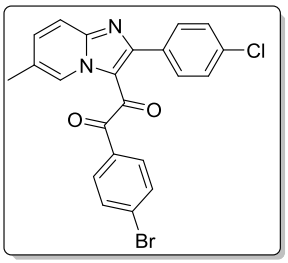

dione (31n): White solid; yield 143 mg (77%); mp 159–160 °C; ^{1}H NMR (400 MHz, $CDCl_3$) δ 9.64 (s, 1H), 7.77 (d, *J* = 9.0 Hz, 1H), 7.63 – 7.57 (m, 4H), 7.58 – 7.54 (m, 1H), 7.22 (d, *J* = 8.4 Hz, 2H), 7.13 (d, *J* = 8.4 Hz, 2H), 2.53 (s, 3H); ^{13}C NMR (100 MHz, $CDCl_3$) δ 190.4, 183.4, 157.1, 147.3, 135.8, 134.2, 132.1, 131.5, 131.3, 130.8, 129.9, 128.2, 127.3, 126.5, 116.9, 18.5; IR (KBr): 3094, 2924, 1674, 1620, 1409, 1396, 1273, 872 cm^{-1}; HRMS (ESI-TOF) (*m/z*) calculated $C_{22}H_{15}BrClN_2O_2^+$: 453.0005; found 453.0018 $[M+H]^+$ and 455.0164 $[M+H+2]^+$.

1-(4-Fluorophenyl)-2-(7-methyl-2-phenylimidazo[1,2-*a*]pyridin-3-yl)ethane-1,2-dione (31o):

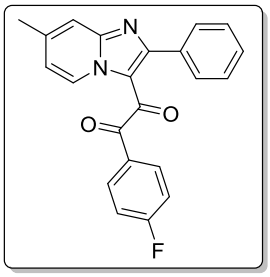

Yellow solid; yield: 141 mg (82%); mp 191–192 °C; ^{1}H NMR (400 MHz, $CDCl_3$) δ 9.69 (d, *J* = 6.9 Hz, 1H), 7.76 (dd, *J* = 8.1, 5.6 Hz, 2H), 7.62 (s, 1H), 7.30 – 7.24 (m, 3H), 7.14 (t, *J* = 7.6 Hz, 2H), 7.11 – 7.04 (m, 3H), 2.57 (s, 3H); ^{13}C NMR (100 MHz, $CDCl_3$) δ 190.0, 183.7, 167.5, 164.9, 159.1, 148.9, 143.1, 133.0, 132.3, 130.0, 129.5, 128.5, 127.9, 118.3, 116.5, 116.5, 115.8, 21.8; IR (KBr): 3032, 1674, 1620, 1412, 1242, 903 cm^{-1}; HRMS (ESI-TOF) (*m/z*) calculated $C_{22}H_{16}FN_2O_2^+$: 359.1195; found 359.1206 $[M+H]^+$.

1-(6-Bromo-2-phenylimidazo[1,2-*a*]pyridin-3-yl)-2-phenylethane-1,2-dione (31p): Light yellow solid; yield: 111 mg (75%); mp 152–154 °C (lit.[37] mp 153-155 °C); ^{1}H NMR (400 MHz, $CDCl_3$) δ 10.04 (t, J = 1.3 Hz, 1H), 7.77 – 7.74 (m, 3H), 7.73 (d, J = 1.3 Hz, 1H), 7.63 – 7.58 (m, 1H), 7.48 – 7.37 (m, 3H), 7.38 – 7.32 (m, 2H), 7.12 (t, J = 6.2 Hz, 2H); ^{13}C NMR (100 MHz, $CDCl_3$) δ 191.1, 184.8, 158.6, 146.7, 134.3, 134.2, 133.2, 132.5, 130.0, 129.7, 129.6, 129.4, 128.7, 128.0, 118.9, 118.2, 110.6; IR (KBr): 3160, 2963, 2851, 1644, 1615, 1239, 678 cm^{-1}.

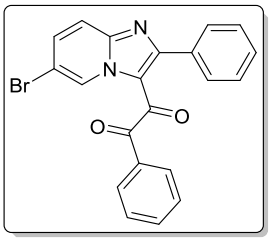

1-(7-Methyl-2-phenylimidazo[1,2-*a*]pyridin-3-yl)-2-phenylethane-1,2-dione (31q): White solid; yield: 118 mg (72%); mp 142–145 °C; ^{1}H NMR (400 MHz, $CDCl_3$) δ 9.71 (d, J = 7.0 Hz, 1H), 7.73 (dd, J = 8.3, 1.1 Hz, 2H), 7.63 (s, 1H), 7.61 – 7.55 (m, 1H), 7.40 (t, J = 7.8 Hz, 2H), 7.32 – 7.29 (m, 2H), 7.28 – 7.24 (m, 1H), 7.13 – 7.07 (m, 3H), 2.57 (s, 3H); ^{13}C NMR (100 MHz, $CDCl_3$) δ 191.6, 184.2, 159.0, 148.8, 143.0, 134.1, 133.5, 132.9, 130.0, 129.5, 128.5, 127.9, 118.7, 118.2, 116.4, 21.8; IR (KBr): 3018, 1690, 1598, 1471, 1345, 730 cm^{-1}; HRMS (ESI-TOF) (m/z) calculated $C_{22}H_{17}N_2O_2^+$: 341.1290; found 341.1317 $[M+H]^+$.

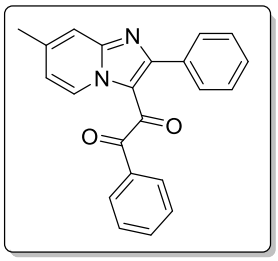

1-(2-(4-Chlorophenyl)-6-methylimidazo[1,2-*a*]pyridin-3-yl)-2-(naphthalen-2-yl)ethane-1,2-dione (31r): Yellow solid; yield: 129 mg (74%); mp 120–122 °C; ^{1}H NMR (400 MHz, $CDCl_3$) δ 9.72 (s, 1H), 8.34 (s, 1H), 7.92 – 7.85 (m, 3H), 7.76 (d, J = 9.0 Hz, 1H), 7.71 (dd, J = 8.6, 1.6 Hz, 1H), 7.68 – 7.62 (m, 1H), 7.57 (d, J = 7.9 Hz, 1H), 7.55 – 7.51 (m, 1H), 7.21 (d, J = 8.4 Hz, 2H), 7.00 (d, J = 8.4 Hz, 2H), 2.52 (s, 3H); ^{13}C NMR (100 MHz, $CDCl_3$) δ 191.7, 184.2, 157.1, 147.3, 136.0, 135.6, 134.0, 132.5, 132.2, 131.6, 131.3, 130.8, 129.8, 129.3, 128.7, 128.0, 127.4, 127.1, 126.4, 123.8, 118.8, 116.9, 18.6; IR (KBr): 2942, 2856, 1628, 1612, 1411, 1228, 739 cm^{-1}; HRMS (ESI-TOF) (*m/z*) calculated $C_{26}H_{18}ClN_2O_2^+$: 425.1056; found 425.1033 $[M+H]^+$ and 427.1217 $[M+H+2]^+$.

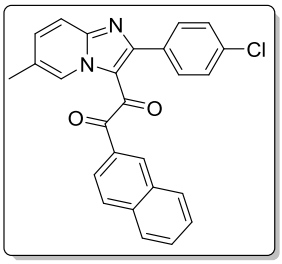

1-(6-Bromo-2-phenylimidazo[1,2-*a*]pyridin-3-yl)-2-(4-fluorophenyl)ethane-1,2-dione (31s):

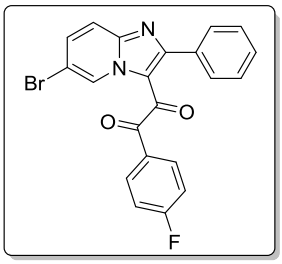

Yellow solid; yield: 121 mg (78%); mp 202–204 °C; ^{1}H NMR (400 MHz, $CDCl_3$ + DMSO-d_6) δ 9.87 (s, 1H), 7.84 – 7.72 (m, 4H), 7.34 – 7.27 (m, 1H), 7.16 (d, J = 7.1 Hz, 2H), 7.08 – 7.01 (m, 4H); ^{13}C NMR (100 MHz, $CDCl_3$ + DMSO-d_6) δ 194.3, 189.0, 172.3, 169.7, 163.2, 151.5, 139.3, 137.3, 134.7, 134.5, 133.9, 132.7, 123.5, 123.0, 121.0, 120.7, 115.4; IR (KBr): 3132, 2950, 1674, 1612, 1481, 1412, 1250, 872 cm^{-1}; HRMS (ESI-TOF) (*m/z*) calculated $C_{21}H_{13}BrFN_2O_2^+$: 423.0144; found 423.0138 $[M+H]^+$ and 425.0308 $[M+H+2]^+$.

1-(2-(3-Methoxyphenyl)-7-methylimidazo[1,2-*a*]pyridin-3-yl)-2-phenylethane-1,2-dione (31t):

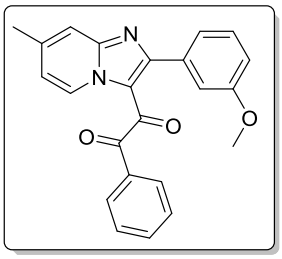

White solid; yield 113 mg (73%); mp 153–155 °C; ^{1}H NMR (400 MHz, $CDCl_3$) δ 9.69 (s, 1H), 7.79 (d, J = 9.1 Hz, 1H), 7.77 – 7.74 (m, 2H), 7.59 – 7.53 (m, 2H), 7.42 (t, J = 7.8 Hz, 2H), 7.03 – 6.98 (m, 1H), 6.88 (dd, J = 7.5, 1.1 Hz, 1H), 6.84 – 6.79 (m, 2H), 3.54 (s, 3H), 2.53 (s, 3H); ^{13}C NMR (100 MHz, $CDCl_3$) δ 191.3, 184.4, 158.9, 158.3, 147.2, 134.2, 133.5, 129.5, 129.1, 128.6, 127.4, 126.2, 122.7, 118.7, 116.9, 116.4, 114.2, 54.9, 18.5; IR (KBr): 3132, 2948, 1674, 1614, 1481, 1250, 873 cm^{-1}; HRMS (ESI-TOF) (*m/z*) calculated $C_{23}H_{19}N_2O_3^+$: 371.1395; found 371.1364 $[M+H]^+$.

1-Phenyl-2-(2-(*p*-tolyl)imidazo[1,2-*a*]pyridin-3-yl)ethane-1,2-dione (31u): Yellow solid;

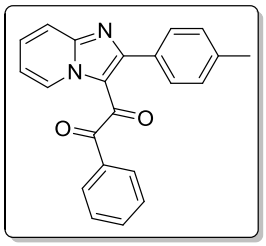

yield: 119 mg (71%); mp 109–110 °C (lit.[37] mp 110 °C); ^{1}H NMR (400 MHz, $CDCl_3$) δ 9.85 (d, J = 6.9 Hz, 1H), 7.86 (d, J = 8.9 Hz, 1H), 7.80 – 7.72 (m, 2H), 7.72 – 7.64 (m, 1H), 7.60 (t, J = 7.4 Hz, 1H), 7.42 (t, J = 7.8 Hz, 2H), 7.25 (td, J = 6.9, 1.0 Hz, 1H), 7.20 (d, J = 8.0 Hz, 2H), 6.91 (d, J= 7.8 Hz, 2H), 2.29 (s, 3H); ^{13}C NMR (100 MHz, $CDCl_3$) δ 191.5, 184.6, 158.9, 148.4, 139.5, 134.1, 133.5, 131.0, 129.9, 129.6, 129.3, 128.7, 118.9, 117.6, 115.7, 21.3 ; IR (KBr): 3065, 2921, 2841, 1674, 1605, 1229, 758 cm^{-1}.

1-Phenyl-2-(2-phenylimidazo[1,2-*a*]pyrimidin-3-yl)ethane-1,2-dione (33a): White solid;

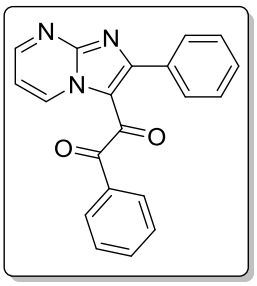

yield: 117 mg (70%); mp 170–171 °C (lit.[37] mp 171 °C); ^{1}H NMR (400 MHz, $CDCl_3$) δ 10.07 (dd, J = 6.8, 1.8 Hz, 1H), 8.92 (dd, J = 4.1, 1.9 Hz, 1H), 7.76 (d, J = 7.4 Hz, 2H), 7.62 (t, J = 7.4 Hz, 1H), 7.44 (t, J = 7.7 Hz, 2H), 7.38 (d, J = 7.3 Hz, 2H), 7.31 (dd, J = 9.4, 5.3 Hz, 2H), 7.13 (t, J = 7.6 Hz, 2H); ^{13}C NMR (100 MHz, $CDCl_3$) δ 190.8, 185.3, 159.9, 154.9,

150.9, 136.9, 134.5, 133.0, 132.3, 130.0, 129.6, 128.7, 128.1, 117.2, 111.8; IR (KBr): 3068, 2924, 1682, 1595, 1493, 1392, 1347, 1138, 874, 685 cm^{-1}.

1-Phenyl-2-(6-phenylimidazo[2,1-*b*]thiazol-5-yl)ethane-1,2-dione (33b): Light yellow solid; yield: 129 mg (74%); mp 160–161 °C (lit.[37] mp 160-162 °C); ^{1}H NMR (400 MHz, $CDCl_3$) δ 8.58 (d, J = 4.4 Hz, 1H), 7.78 (dd, J = 8.3, 1.2 Hz, 2H), 7.64 – 7.57 (m, 1H), 7.43 (dd, J = 10.8, 4.8 Hz, 2H), 7.34 – 7.32 (m, 1H), 7.31 (d, J = 1.3 Hz, 1H), 7.28 (dd, J = 6.2, 1.3 Hz, 1H), 7.17 (d, J = 4.4 Hz, 1H), 7.13 (t, J = 7.7 Hz, 2H); ^{13}C NMR (100 MHz, $CDCl_3$) δ 191.7, 183.1, 158.6, 156.2, 134.4, 133.2, 132.7, 129.8, 129.6, 129.5, 128.7, 128.0, 122.0, 115.0; IR (KBr): 3163, 2963, 2851, 1644, 1615, 1229, 658 cm^{-1}.

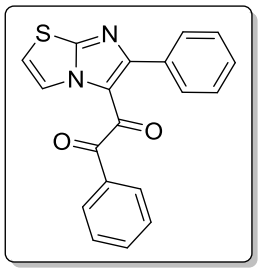

1-Phenyl-2-(2-phenylbenzo[*d*]imidazo[2,1-*b*]thiazol-3-yl)ethane-1,2-dione (33c): Light yellow solid; yield: 104 mg (68%); mp 177-178 °C; ^{1}H NMR (400 MHz, $CDCl_3$) δ 9.23 (dd, J = 8.5, 0.6 Hz, 1H), 7.81 (dd, J = 8.0, 0.9 Hz, 1H), 7.76 – 7.71 (m, 2H), 7.59 (m, 2H), 7.53 – 7.47 (m, 1H), 7.44 – 7.37 (m, 2H), 7.32 – 7.28 (m, 2H), 7.27 – 7.22 (m, 1H), 7.11 – 7.04 (m, 2H); ^{13}C NMR (100 MHz, $CDCl_3$) δ 191.4, 183.4, 160.6, 155.4, 134.2, 133.1, 133.3, 132.7, 130.3, 130.0, 129.6, 128.5, 127.9, 126.9, 126.0, 125.2, 123.8, 118.8; IR (KBr): 3158, 2950, 1697, 1645, 1239, 698 cm^{-1}; HRMS (ESI-TOF) (*m/z*) calculated $C_{23}H_{15}N_2O_2S^+$: 383.0854; found 383.0861 $[M+H]^+$.

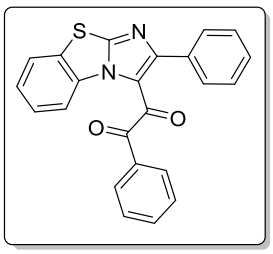

3A.4 References

(1) Miao, J.; Ge, H. *European Journal of Organic Chemistry* **2015**, 7859-7868.

(2) Li, C.-J. *Accounts of Chemical Research* **2008**, *42*, 335-344.

(3) Wendlandt, A. E.; Suess, A. M.; Stahl, S. S. *Angewandte Chemie International Edition* **2011**, *50*, 11062-11087.

(4) Scheuermann, C. J. *Chemistry–An Asian Journal* **2010**, *5*, 436-451.

(5) Alberico, D.; Scott, M. E.; Lautens, M. *Chemical Reviews* **2007**, *107*, 174-238.

(6) Li, B. -J.; Shi, Z. -J. *Chemical Society Reviews* **2012**, *41*, 5588-5598.

(7) Gini, A.; Brandhofer, T.; Mancheño, O. G. *Organic & Biomolecular Chemistry* **2017**, *15*, 1294-1312.

(8) Lyons, T. W.; Sanford, M. S. *Chemical Reviews* **2010**, *110*, 1147-1169.

(9) Yang, Y.; Lan, J.; You, J. *Chemical Reviews* **2017**, *117*, 8787-8863.

(10) Shang, R.; Ilies, L.; Nakamura, E. *Chemical Reviews* **2017**, *117*, 9086-9139.

(11) Lv, L.; Li, Z. *Topics in Current Chemistry* **2016**, *374*, 1-39.

(12) Rao, W. -H.; Shi, B. -F. *Organic Chemistry Frontiers* **2016**, *3*, 1028-1047.

(13) Zhang, C.; Tang, C.; Jiao, N. *Chemical Society Reviews* **2012**, *41*, 3464-3484.

(14) Huang, X. -F.; Salman, M.; Huang, Z. Z.; *Chemistry - A European Journal* **2014,** *20*, 6616-6621.

(15) Guo, X. -X.; Gu, D. -W.; Wu, Z.; Zhang, W. *Chemical Reviews* **2014**, *115*, 1622-1651.

(16) Hirano, K.; Miura, M. *Chemical Communications* **2012**, *48*, 10704-10714.

(17) King, A. E.; Huffman, L. M.; Casitas, A.; Costas, M.; Ribas, X.; Stahl, S. S. *Journal of the American Chemical Society* **2010**, *132*, 12068-12073.

(18) Allen, S. E.; Walvoord, R. R.; Padilla-Salinas, R.; Kozlowski, M. C. *Chemical Reviews* **2013**, *113*, 6234-6458.

(19) Cavani, F.; Teles, J. H. *ChemSusChem* **2009**, *2*, 508-534.

(20) Kuppinger, M.; Obermüller, I.; Peterhans, B. *Chimia International Journal for Chemistry* **2005**, *59*, 693-697.

(21) Li, C.; Wang, L.; Li, P.; Zhou, W. *Chemistry-A European Journal* **2011**, *17*, 10208-10212.

(22) Wu, Y.; Li, B.; Mao, F.; Li, X.; Kwong, F. Y. *Organic Letters* **2011**, *13*, 3258-3261.

(23) Li, H.; Li, P.; Wang, L. *Organic Letters* **2013**, *15*, 620-623.

(24) Sharma, S.; Park, J.; Park, E.; Kim, A.; Kim, M.; Kwak, J. H.; Jung, Y. H.; Kim, I. S. *Advanced Synthesis & Catalysis* **2013**, *355*, 332-336

(25) Zhao, J.; Fang, H.; Xie, C.; Han, J.; Li, G.; Pan, Y. *Asian Journal of Organic Chemistry* **2013**, *2*, 1044-1047.

(26) Banerjee, A.; Santra, S. K.; Guin, S.; Rout, S. K.; Patel, B. K. *European Journal of Organic Chemistry* **2013**, 1367-1376.

(27) Zhang, Q.; Li, C.; Yang, F.; Li, J.; Wu, Y. *Tetrahedron* **2013**, *69*, 320-326.

(28) Zhang, C.; Xu, Z.; Zhang, L.; Jiao, N. *Angewandte Chemie International Edition* **2011**, *123*, 11284-11288.

(29) Zhang, C.; Zong, X.; Zhang, L.; Jiao, N. *Organic Letters* **2012**, *14*, 3280-3283.

(30) Ji, X.; Li, D.; Zhou, X.; Huang, H.; Deng, G.-J. *Green Chemistry* **2017**, *19*, 619-622.

(31) Battini, N.; Battula, S.; Ahmed, Q. N. *European Journal of Organic Chemistry* **2016**, 658-662.

(32) Tang, B. -X.; Song, R. -J.; Wu, C. -Y.; Liu, Y.; Zhou, M. -B.; Wei, W. -T.; Deng, G. -B.; in, D. -L.; Li, J. -H. *Journal of the American Chemical Society* **2010**, *132*, 8900-8902.

(33) Zhang, C.; Jiao, N. *Organic Chemistry Frontiers* **2014**, *1*, 109-112.

(34) Chen, S.; Li, X.; Zhao, H.; Li, B. *The Journal of Organic Chemistry* **2014**, *79*, 4137-4141.

(35) Yang, J. -M.; Cai, Z. -J.; Wang, Q. -D.; Fang, D.; Ji, S. -J. *Tetrahedron* **2015**, *71*, 7010-7015.

(36) Koubachi, J.; El Kazzouli, S.; Bousmina, M.; Guillaumet, G. *European Journal of Organic Chemistry* **2014**, 5119-5138.

(37) Chennapuram, M.; Emmadi, N. R.; Bingi, C.; Atmakur, K. *RSC Advances* **2015**, *5*, 19418-19425.

(38) Wang, C.; Lei, S.; Cao, H.; Qiu, S.; Liu, J.; Deng, H.; Yan, C. *The Journal of Organic Chemistry* **2015**, *80*, 12725-12732.

(39) Lei, S.; Chen, G.; Mai, Y.; Chen, L.; Cai, H.; Tan, J.; Cao, H. *Advanced Synthesis & Catalysis* **2016**, *358*, 67-73.

(40) Samanta, S.; Mondal, S.; Santra, S.; Kibriya, G.; Hajra, A. *The Journal of Organic Chemistry* **2016**, *81*, 10088-10093.

(41) Koubachi, J.; El Kazzouli, S.; Berteina-Raboin, S.; Mouaddib, A.; Guillaumet, G. *Synthesis* **2008**, 2537-2542.

(42) El Akkaoui, A.; Bassoude, I.; Koubachi, J.; Berteina-Raboin, S.; Mouaddib, A.; Guillaumet, G. *Tetrahedron* **2011**, *67*, 7128-7138.

(43) Naveen, T.; Kancherla, R.; Maiti, D. *Organic Letters* **2014**, *16*, 5446-5449.

(44) Donthiri, R. R.; Samanta, S.; Adimurthy, S. *Organic & Biomolecular Chemistry* **2015**, *13*, 10113-10116.

(45) Modak, A.; Dutta, U.; Kancherla, R.; Maity, S.; Bhadra, M.; Mobin, S. M.; Maiti, D. *Organic Letters* **2014**, *16*, 2602-2605.

(46) Costas, M. *ChemCatChem* **2012**, *4*, 175-176.

CHAPTER 3B

Ruthenium(II)-Catalyzed Regioselective *o*-Amidation of 2-Arylimidazo-Heterocycles *via* C-H Bond Activation

3B.1 Introduction

Transition metal-catalyzed direct C-H functionalization at non-activated C-H bonds with various coupling partners *via* chelation-assisted activation has streamlined the chemical synthesis by ceasing tedious and expensive substrate pre-activation steps.[1-5] Within this domain, immense progress has been documented towards the formation of pivotal C-C bonds in recent years. Chelation-assisted direct C−H bond activation by mean of suitably placed directing groups was initially showcased by Pd or Rh catalysts,[6-13] however, at present the usage of a large variety of other metal catalysts including the environmentally benign Ru catalysts are well exemplified (Figure 3B.1.1).[14-21]

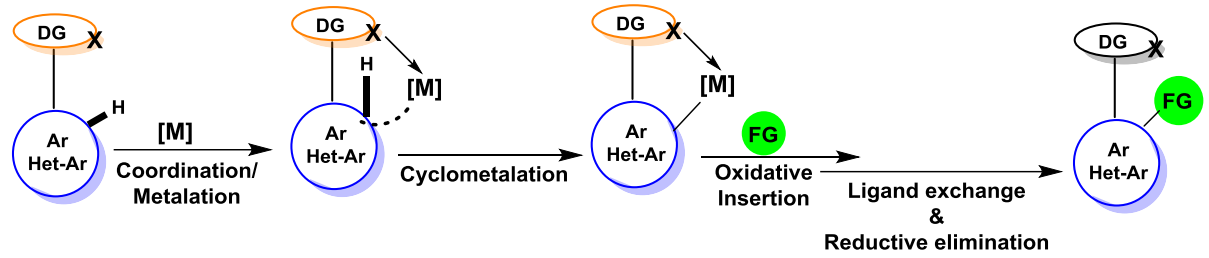

Figure 3B.1.1: Generalized mechanism for transition metal-catalyzed chelation-assisted C-H functionalization

Ruthenium (Ru) is the 74th most abundant metal on earth (Z = 44), with an electronic configuration [Kr] $4d^7$ $5s^1$. Ruthenium was discovered and isolated by Karl Ernst Claus in 1844. It displays a broad range of oxidation states in its various complexes such as -2: $[Ru(CO)_4]^{2-}$, 0: $[Ru(PPh_3)_3(MeCN)]$, +1: $[RuCl(dppp)_2]$, +2: $[RuCl_2(PPh_3)_3]$, +3: $[RuCl_3]$, +4: $[RuCl_4(bipy)]$, +5: $[RuF_6]^-$, +6: $[RuO_4]^{2-}$, +7: $[RuO_4]^-$, +8: $[RuO_4]$, however +2, +3 and +4 states are most common (Figure 3B.1.2).[22]

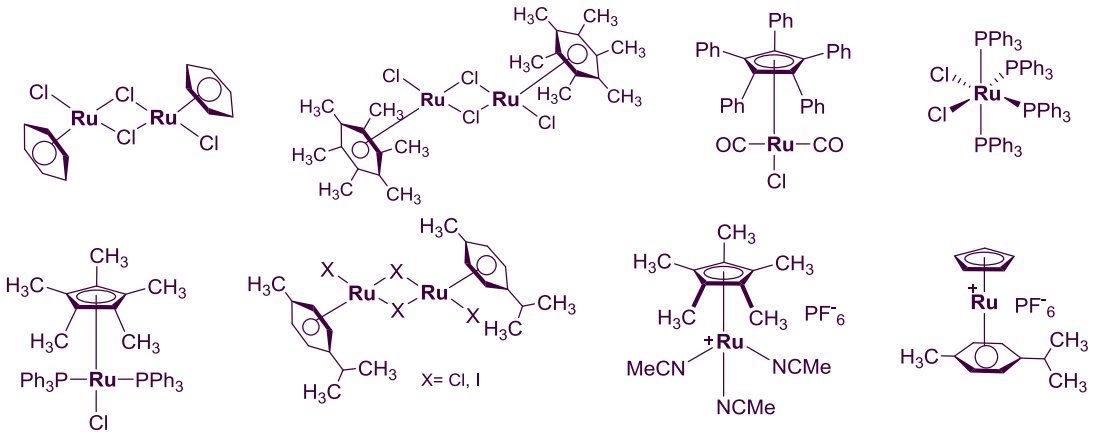

Figure 3B.1.2: Selective examples of ruthenium complexes used in organic synthesis

Ruthenium complexes are powerful and versatile synthetic tool for the selective catalysis of various oxidative transformations such as asymmetric epoxidation of alkenes,[23] generation of dioxygen species,[24] dihydroxylation of olefines,[25] and oxidative dehydrogenation of alcohols.[26] In addition, organometallic ruthenium carbene and alkylidene complexes have been found to be highly efficient catalysts for olefin metathesis,[27] along with the most well-known Grubbs′ catalyst.[28] Interestingly, Ru in recent years has been actively involved in several chelation-assisted functionalization methodologies, such as hydroarylation of alkyenes[29,30] catalytic alkylation of Csp^2–H bonds with alkyl halides,[31] alkylation of alkene and arene Csp^2–H bonds with alcohols,[31] oxidative cross-coupling reaction,[32] amination,[33] amidation,[32,34] cyanation[35] and hydroxylation of Csp^2–H bonds (Figure 3B.1.3).[36]

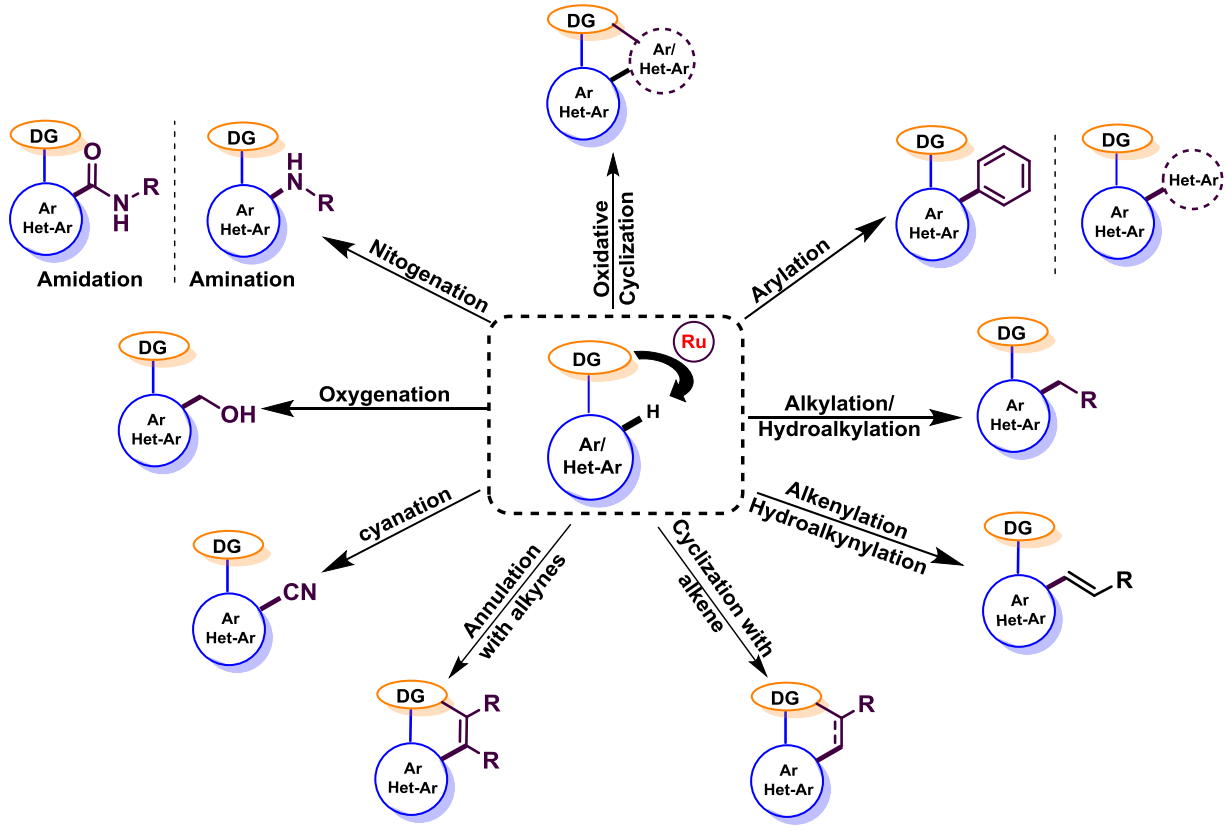

Figure 3B.1.3: A pictorial representation of Ru-catalyzed functionalization *via* chelation-assisted C-H activation

In particular, the role of ruthenium in chelation assisted C-H activation strategies is highly admirable. The ongoing employment of ruthenium (II) catalyst for various selective transformations is likely due to their easy transformation into cyclometalated species *via* C–H bond cleavage, their compatibility with currently used oxidants, and the stability of some of them

to both air and water. A multitude of functionalities, including amide, amine, ketone, ester, alcohol and azo group have acted as directing groups in C–H functionalization *via* metal chelation-assisted strategy.[1,5,36-39] The heteroatom of the directing group coordinates with the ruthenium *via* either σ or π bond and allows bringing the ortho C–H bond of aromatics in close proximity to the active metal centre. During this time, the C–H bond activation takes place very selectively at the ortho position providing a five-membered cyclometalated intermediate.

Exploring this mechanistic approach, Murai's group utilized a Ru(0)-catalyst precursor for chelation-assisted *ortho*-alkylation of ketones with vinyl silanes *via* C–H bond activation in 1993 (Scheme 3B.1.1).[40]

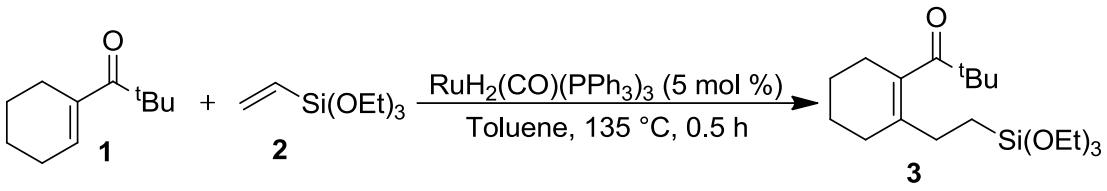

Scheme 3B.1.1: Ru-catalyzed *ortho*-alkylation of ketones (**1**) with vinyl silanes (**2**)

Ever since this work, chelation-assisted Ru(II)-catalyzed addition to C-C π-bonds *via* cyclometalation-migratory insertion mechanism has witnessed enormous progress over Rh or Re catalysis.[40-48] However, such reactions have not been extended to systems incorporating polar C-N bond, and only proceed in presence of strongly coordinating aryl pyridines or aryl pyrazoles.[49,50]

Along this line, the direct insertion of activated or non-activated C−H bonds into the polar C−N π-bond of isocyanates is a highly auspicious methodology for providing synthetically and biologically important amides using Ru, Rh and Re catalysts. Pioneering efforts have been made by Ackermann, Kuninobu and Takai, Bergman and Ellman, Cheng and Li towards introducing amide functionalities[49-56] on various biologically important heterocyclic scaffolds, by virtue of versatile directing groups.

In 2011, Ellman *et al.* described a Rh(III)-catalyzed protocol for the amidation of enamide **4** and anilide **5** C-H bonds with a broad range of isocyanates (**6**), yielding enamine amides **7** and *N*-acyl anthranilamides (**8**) in good-to-excellent yields (Scheme 3B.1.2).[50]

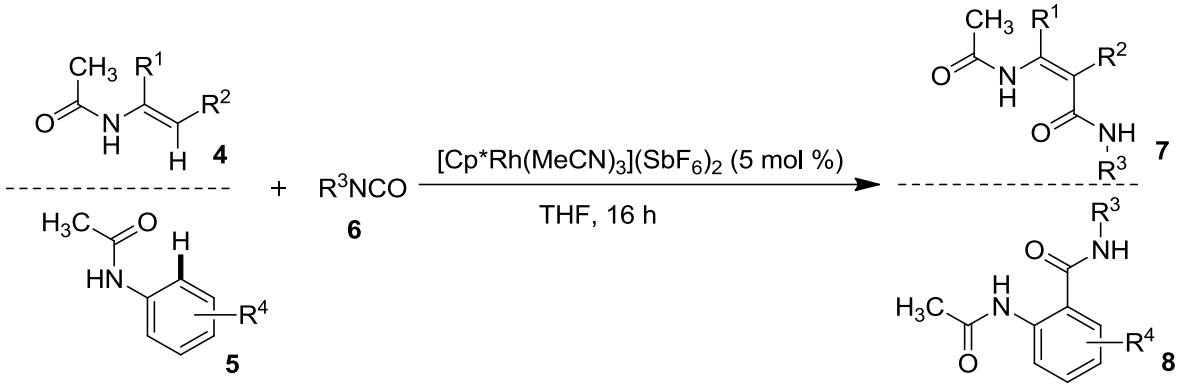

Scheme 3B.1.2: Rh(III)-catalyzed synthesis of enamine amides (**7**) and *N*-acyl anthranilamides (**8**) with isocyanates (**6**)

The authors also demonstrated the feasibility of the reaction by successful amidation of 2-aryl pyridines (**9**) using $[Cp^*RhCl_2]_2/AgSbF_6$ catalytic combination in dichlomethane in 24 h (Scheme 3B.1.3a).[50] However later, Cheng and coworkers presented an easy and convenient Ru(II)-catalyzed amidation of 2-aryl pyridines (**9**) with isocyanates (**6**) in the presence of NaOAc in *ortho*-xylene *via* C-H bond activation strategy (Scheme 3B.1.3b).[49]

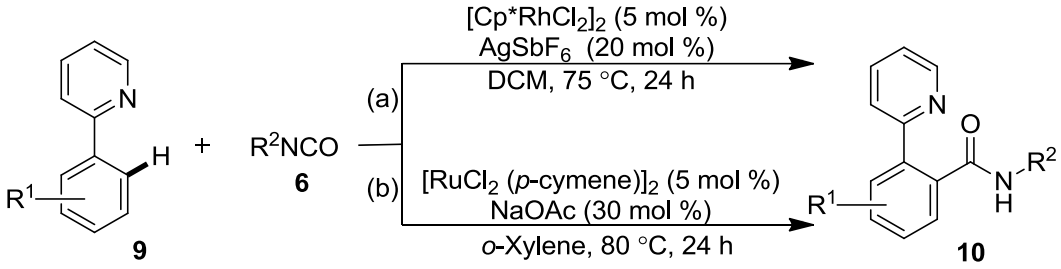

Scheme 3B.1.3: Rh(III)/Ru(II)-catalyzed amidation of 2-phenyl pyridines (**9**) with isocyanates (**6**)

Very recently, Ellman *et al.* achieved a robust Co(III)-catalyzed *ortho* C−H bond amidation with isocyanates (**6**) on the aryl ring of the different substrates by mean of nitrogen containing heterocyclic directing groups such as 1-pyrazoles, 2-pyridyl and 2-pyrimidinyl. Particularly, *N*-aryl-1*H*-pyrazole (**11**) was found to be more reactive towards the desired transformation in the presence of preformed cationic cobalt complex $[Cp^*Co(C_6H_6)][PF_6]_2$ (Scheme 3B.1.4).[57]

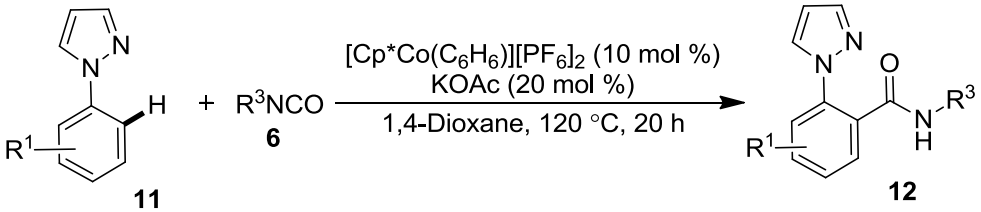

Scheme 3B.1.4: Co(III)-catalyzed amidation of *N*-aryl-1*H*-pyrazole (**11**) with isocyanates (**6**)

Ackermann *et al.* used cationic ruthenium(II)-complex as an efficient catalytic system for the synthesis of phthalimide derivatives **15** *via* amidation of amides **13** with various isocyanates. Moreover, amidation was also successfully carried out to other heteroaromatic substrates **14** offering unsymmetrical diamides **16** using $[RuCl_2(p\text{-cymene})]_2$. The methodology was also applied towards the synthesis of a potent COX-2 enzyme inhibitor (Scheme 3B.1.5).[51]

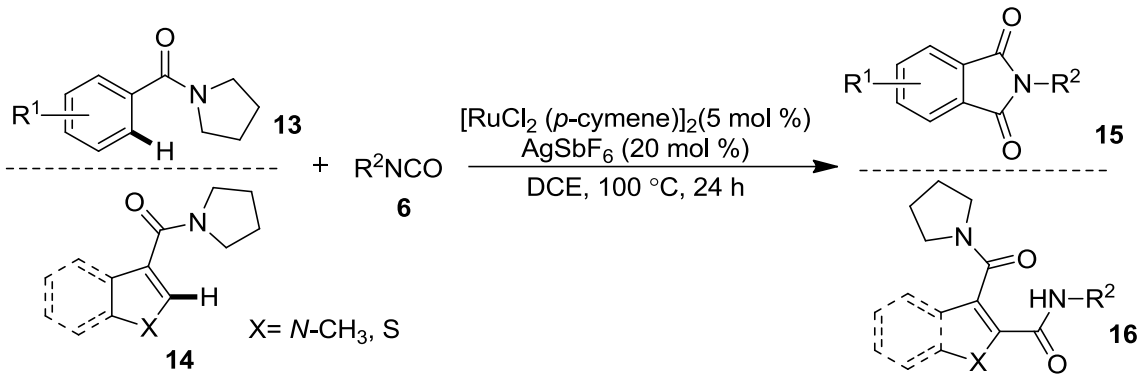

Scheme 3B.1.5: Ru(II)-catalyzed synthesis of phthalimide derivatives (**15**) and selective amidation of (**14**)

Rh(III)-catalyzed C-2 amidation of *N*-substituted indoles and pyrroles (**17**) with aryl and alkyl isocyanates was successfully achieved by Kim *et al.* by using cationic Rh(III) complex, yielding **18** in excellent yields *via* C−H bond activation mechanism (Scheme 3B.1.6).[58]

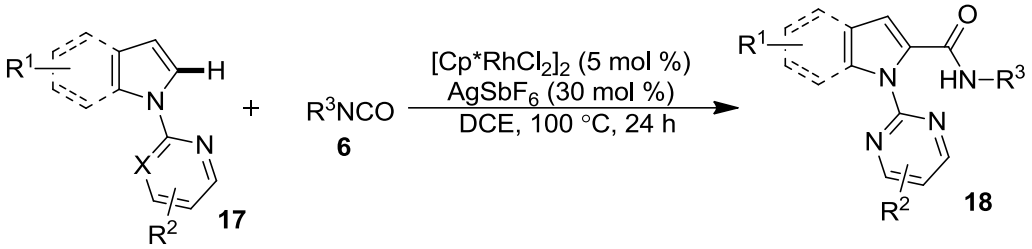

Indole and pyrrole

Scheme 3B.1.6: Rh(III)-catalyzed amidation of *N*-substituted indoles and pyrroles (**17**) with isocyanates (**6**)

Ackermann group reported the first Mn(I)-catalyzed aminocarbonylation of *N*-substituted indoles and pyrroles **17** *via* C-H bond activation. $[MnBr(CO)_5]$ independently catalyzes the reaction without the use of any ligand. The catalyst displayed high functional group tolerance, thereby demonstrating the *ortho*-amidation of some valuable synthetic heteroarenes with ample substrate scope (Scheme 3B.1.7).[56]

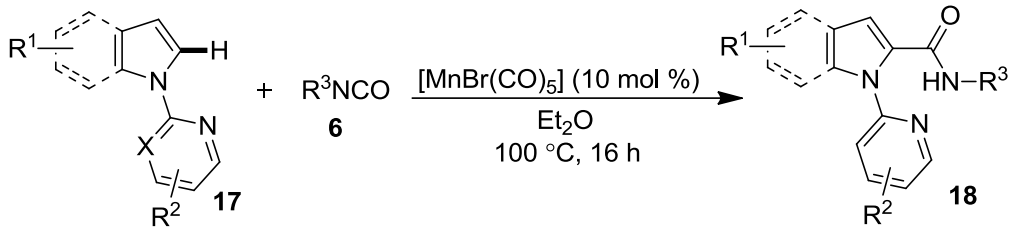

Scheme 3B.1.7: Mn(I)-catalyzed aminocarbonylation of *N*-substituted indoles and pyrroles (**17**) with isocyanates (**6**)

As an application to chelate-assisted *ortho*-amidation reactions, Li and coworkers developed a one-pot cascade cyclization process for the synthesis of *N*-substituted phthalimides **15** from benzoic acids (**19**) and isocyanates (**6**) *via* direct ortho C-H bond amidation, followed by intramolecular cyclization using $[Cp^*RhCl_2]_2$ in the presence of sodium acetate (Scheme 3B.1.8).[53]

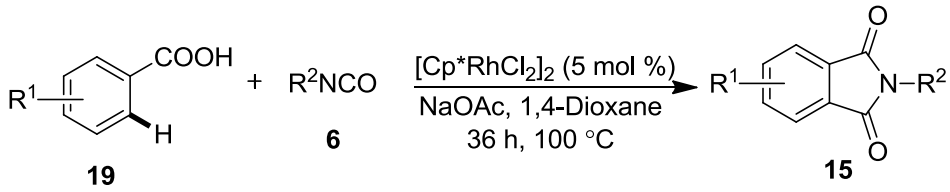

Scheme 3B.1.8: Rh(III)-catalyzed synthesis of *N*-substituted phthalimides (**15**) from substituted benzoic acids (**19**) and isocyanates (**6**)

Kim *et al.* implemented the Rh(III)-catalyzed strategy for the *ortho*-C-H amidation of azobenzenes (**20**) with aryl/alkyl isocyanates (**6**) and arylsulfonyl isocyanates (**22**) under similar reaction conditions using $[Cp^*RhCl_2]_2$ with $AgNTf_2$ and NaOAc (Scheme 3B.1.9).[59]

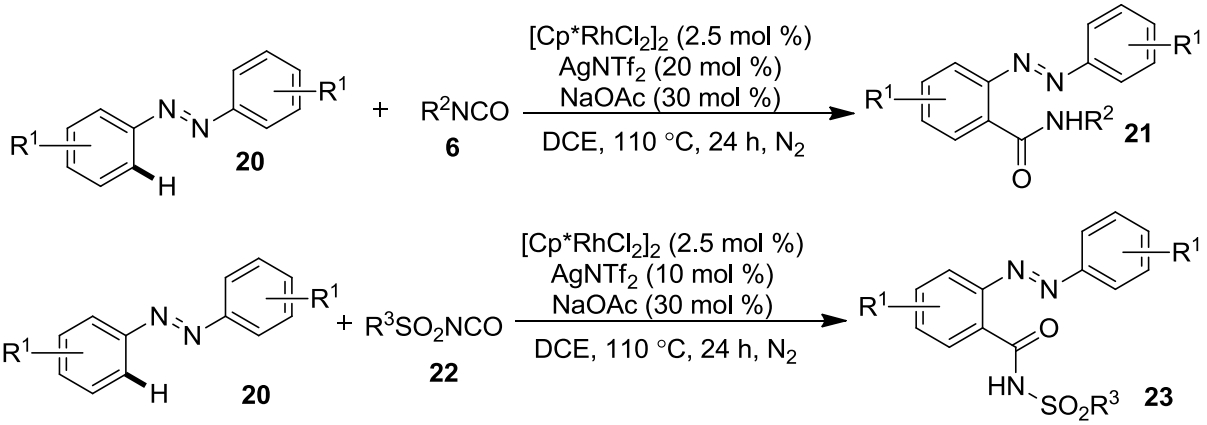

Scheme 3B.1.9: Rh(III)-catalyzed synthesis of amidated azobenzenes (**21**) and *N*-sulfonylamidated (**23**)

Moreover, Wang *et al.* documented a chemo- and regioselective approach towards the synthesis of mono C–H functionalized *o*-azobenzamides (**21**) from azobenzenes (**20**) by employment of rhenium catalyst in the presence of NaOAc in toluene. The mechanism was proved to proceed *via* a five-membered rhenacycle reaction intermediate (Scheme 3B.1.10).[54]

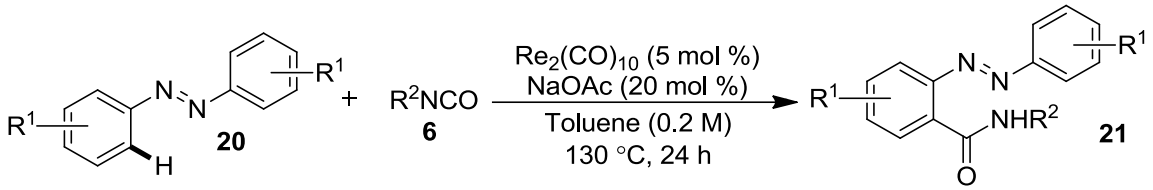

Scheme 3B.1.10: Re-catalyzed synthesis of *ortho*-azobenzamides (**21**) from azobenzenes (**20**) with isocyanates (**6**)

In most of the above described strategies, the directing group (DG) is introduced in the parent aryl moiety to accomplish its *ortho*-amidation, while in very few substrate-directed motifs, the *ortho*-amidation proceeds through an inbuilt coordinating site. Being fascinated by the biological activities of amido functionalized imidazo[1,2-*a*]pyridines such as DS-1, CJ-033466, Q203 (Figure 3B.1.4), [61-67] and recognizing imidazo[1,2-*a*]pyridine to be a potential substrate-directed motif, we spurred our interest towards developing an efficient strategy for the synthesis of new amido functionalized IPs as potential drug pharmacophores.

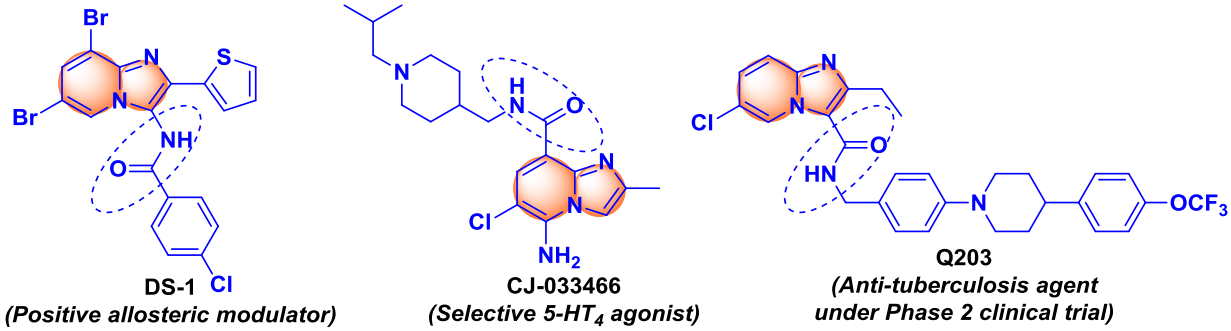

Figure 3B.1.4 Selective examples of biologically active amido functionalized imidazo[1,2-*a*]pyridines

3B.2 Results and discussion

Our investigation commenced with the identification of a suitable catalyst and appropriate reaction conditions that would allow selective *ortho*-amidation using phenyl isocyanate (**6a**) on the aryl ring of 6-bromo-2-phenylimidazo[1,2-*a*]pyridine **(24a)**. To identify an efficient catalyst for developing the above strategy, we initially employed 5 mol % of $[RuCl_2$ (*p*-cymene)$]_2$ in a variety of solvents such as dichloromethane, toluene, xylene, 1,2-dichloroethane under reflux

conditions (Table 3B.2.1, entry 1). However, the reaction failed to furnish the expected product (**25a**) in absence or presence of a variety of additives such as NaOAc, KOAc and CsOAc (Table 3B.2.1, entries 1-4). Delightfully, the use of $AgSbF_6$ (30 mol %) with [$RuCl_2$ (*p*-cymene)]$_2$ (5 mol %) gave 56% of the expected mono *ortho*-amidated product (**25a**) along with 25% of *bis ortho*-amidated product (**25a'**) in DCE at 100 ^oC after 18 h (Table 3B.2.1, entry 5).

Table 3B.2.1: Selected optimization[a] of reaction conditions for the synthesis of **25a**

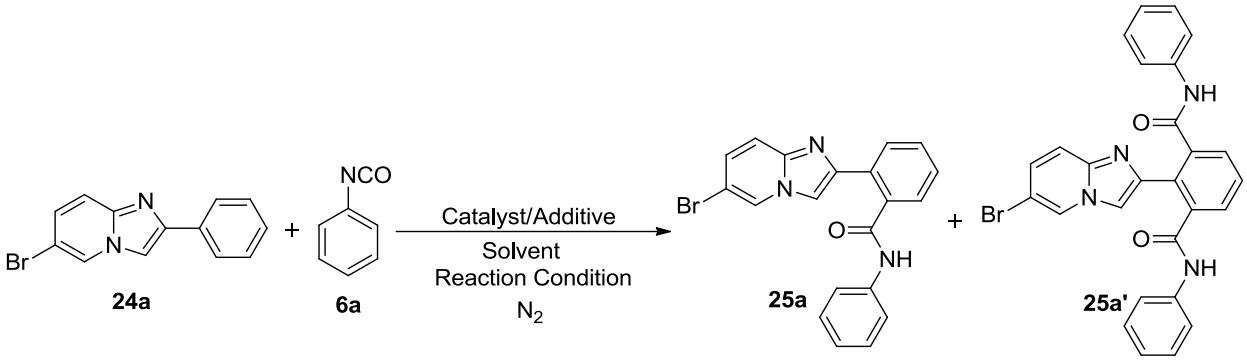

Entry	Catalyst	Additive	Reaction Condition	Yield 25a (%)	Yield[f] 25a'(%)
1.	[$RuCl_2$ (*p*-cymene)]$_2$	-	DCE/DCM/xylene/toluene Reflux, 24 h	NR	-
2.	[$RuCl_2$ (*p*-cymene)]$_2$	NaOAc	DCE/ xylene, 100 °C, 24 h	NR	-
3.	[$RuCl_2$ (*p*-cymene)]$_2$	KOAc	DCE/ xylene, 100 °C, 24 h	NR	-
4[a].	[$RuCl_2$ (*p*-cymene)]$_2$	CsOAc	DCE/ xylene, 100 °C, 24 h	NR	-
5.	[$RuCl_2$ (*p*-cymene)]$_2$	$AgSbF_6$	DCE, 100 °C, 18 h	56	25
6.	[$RuCl_2$ (*p*-cymene)]$_2$	$Cu(OAc)_2$	DCE, 100 °C, 18 h	55	22
7.	[$RuCl_2$ (*p*-cymene)]$_2$	KPF_6	DCE, 100 °C, 18 h	62	20
8.	[$RuCl_2$ (*p*-cymene)]$_2$	KPF_6	DCE, 100 °C, 14 h	72	trace
9[b].	[$RuCl_2$ (*p*-cymene)]$_2$	KPF_6	DCE, 100 °C, 14 h	73	trace
10[c].	[$RuCl_2$ (*p*-cymene)]$_2$	KPF_6	DCE, 100 °C, 14 h	70	trace
11[d].	[$RuCl_2$ (*p*-cymene)]$_2$	KPF_6	DCE, 100 °C, 14 h	62	trace
12[e].	**[$RuCl_2$ (*p*-cymene)]$_2$**	**KPF_6**	**DCE, 100 °C, 14 h**	**75**	trace
13[e].	[$RuCl_2$ (*p*-cymene)]$_2$	KPF_6	Toluene, 100 °C, 14 h	54	trace
14[e].	[$RuCl_2$ (*p*-cymene)]$_2$	KPF_6	Benzene, 80 °C, 14 h	46	trace
15[e].	[$RuCl_2$ (*p*-cymene)]$_2$	KPF_6	DCM, 40 °C, 14 h	48	15
16[e].	$RuCl_2(PPh_3)_3$	KPF_6	DCE, 100 °C, 14 h	NR	-
17[e].	$RuCl_3$. xH_2O	KPF_6	DCE, 100 °C, 14 h	NR	-
18[e].	$Rh(OAc)_2$	KPF_6	DCE, 100 °C, 14 h	NR	-
19[e].	$Pd(OAc)_2$	KPF_6	DCE, 100 °C, 14 h	NR	-

[a]Reaction conditions: **24a** (0.25 mmol), **6a** (0.25 mmol), catalyst (5 mol %), additive (30 mol %), solvent (4 mL). The reactions were performed as per the conditions mentioned; [b]10 mol % of [$RuCl_2$ (*p*-cymene)]$_2$; [c]50 mol % of KPF_6; [d]20 mol % of KPF_6; [e]**6a** (0.37 mmol); [f]Isolated yield; NR: No Reaction.

Replacing $AgSbF_6$ with $Cu(OAc)_2$ also resulted in similar yields of **25a** and **25a'** (Table 3B.2.1, entry 6). Interestingly, an employment of comparatively cheaper and stable KPF_6 (30 mol %) resulted in the formation of **25a** and **25a'** in 62% and 20% yields respectively, after 18 h (Table 3B.2.1, entry 7). Gratifyingly, performing the above reaction for lesser time period (14 h) yielded 72% of **25a** as a major product (Table 3B.2.1, entry 8). An increment in the catalyst loading from 5 mol % to 10 mol % or additive loading to 50 mol % did not show any noticeable amelioration in the yield of **25a** (Table 3B.2.1, entries 9-10). On the other hand, reduction in the yield of **25a** was observed when 20 mol % of KPF_6 was used with 5 mol % of the ruthenium catalyst (Table 3B.2.1, entry 11). Further, an enhancement in the yield of **25a** up to 75% was observed by using 1.5 equivalents of phenyl isocyanate (**6a**) possibly due to the unstable behavior of isocyanate (Table 3B.2.1, entry 12). Albeit, the change of solvents to toluene, benzene and dichloromethane were less effective for the catalytic reaction giving **25a** in 54%, 46% and 48% yields, respectively (Table 3B.2.1, entries 13-15). The use of other ruthenium catalyst such as $RuCl_2(PPh_3)_3$ and $RuCl_3{\cdot}\times H_2O$ and other available transition-metal catalyst including $Rh(OAc)_2$ and $Pd(OAc)_2$ were found to be completely inactive for the above transformation (Table 3B.2.1, entries 16-19).

With the optimized conditions in hand, the scope of the developed strategy was applied to a variety of aryl isocyanates, and a wide range of 2-arylimidazo[1,2-*a*]pyridines (Scheme 3B.2.1). Among the isocyanates used, chloro substituted aryl isocyanates (**6b-e**) showed fairly good reactivity with substituted and unsubstituted imidazo[1,2-*a*]pyridines. For example, 4-chlorophenyl isocyanate (**6b**) resulted in the formation of corresponding imidazo[1,2-*a*]pyridin-2-yl benzamides (**25b**, **25c** and **25d**), in 74%, 76% and 72% isolated yields, respectively. While, 3-chlorophenyl isocyanate (**6c**) showed slightly lower reactivity affording **25e** and **25f** in 66% and 69% isolated yields with **24e** and **24a** respectively. The use of 2,5-dichlorophenyl isocyanate (**6d**) gave comparatively better yield of the desired *ortho*-amidated product (**25h**, 77%) as compared to 2,3-dichlorophenyl isocyanate (**6e**). A reduction in the yield of amidated product (**25i**, 59%) was noticed when 2-fluorophenyl isocyanate (**6f**) was allowed to react with **24a** as compared to phenyl isocyanate (**6a**). 4-Methoxyphenyl isocyanate (**6g**) showed comparative reluctance to react with **24g-h** under the optimized reaction conditions, resulting **25j** and **25k** in 50% and 58% yields respectively. 1-Napthyl isocyanate (**6h**) also reacted well with **24i** to give the corresponding product, **25l** in 65% isolated yield. The presence of electron-

donating groups such as methyl and methoxy on the aryl ring of 2-arylimidazo[1,2-*a*]pyridines underwent *ortho*-amidation affording **25m-p** in fairly good yields. 2-Naphthylimidazo[1,2-*a*]pyridine (**24j**) also showed similar affinity towards the formation of desired product **25r** in 70% isolated yield. Imidazo[1,2-*a*]pyridine (**24k**) bearing bromo substitution on the aryl ring showcased retardation in its reactivity resulting in 60% of **25s**. Albeit, the *ortho*-amidated product **25t** was isolated in poor yield when 2-furyl isocyanate (synthesized *in-situ*) was used under similar conditions. Unfortunately nitro substituted imidazo[1,2-*a*]pyridine **24l** failed to yield the desired amidated product **25u** under our optimized conditions.

All the synthesized compounds were isolated by column chromatography and characterized by detailed spectroscopic analysis. The ^{1}H NMR spectrum of **25d** showed three characteristic singlets, for one proton each at δ 10.72, 7.88 and 7.60 for the amidic (*N-H*), C-5 *H* and C-3 *H* respectively along with other expected signals, evidencing the presence of an amidic group at the 2-phenyl ring. The ^{1}H and ^{13}C NMR spectrum of **25d** is depicted in Figure 3B.2.1 and 3B.2.2.

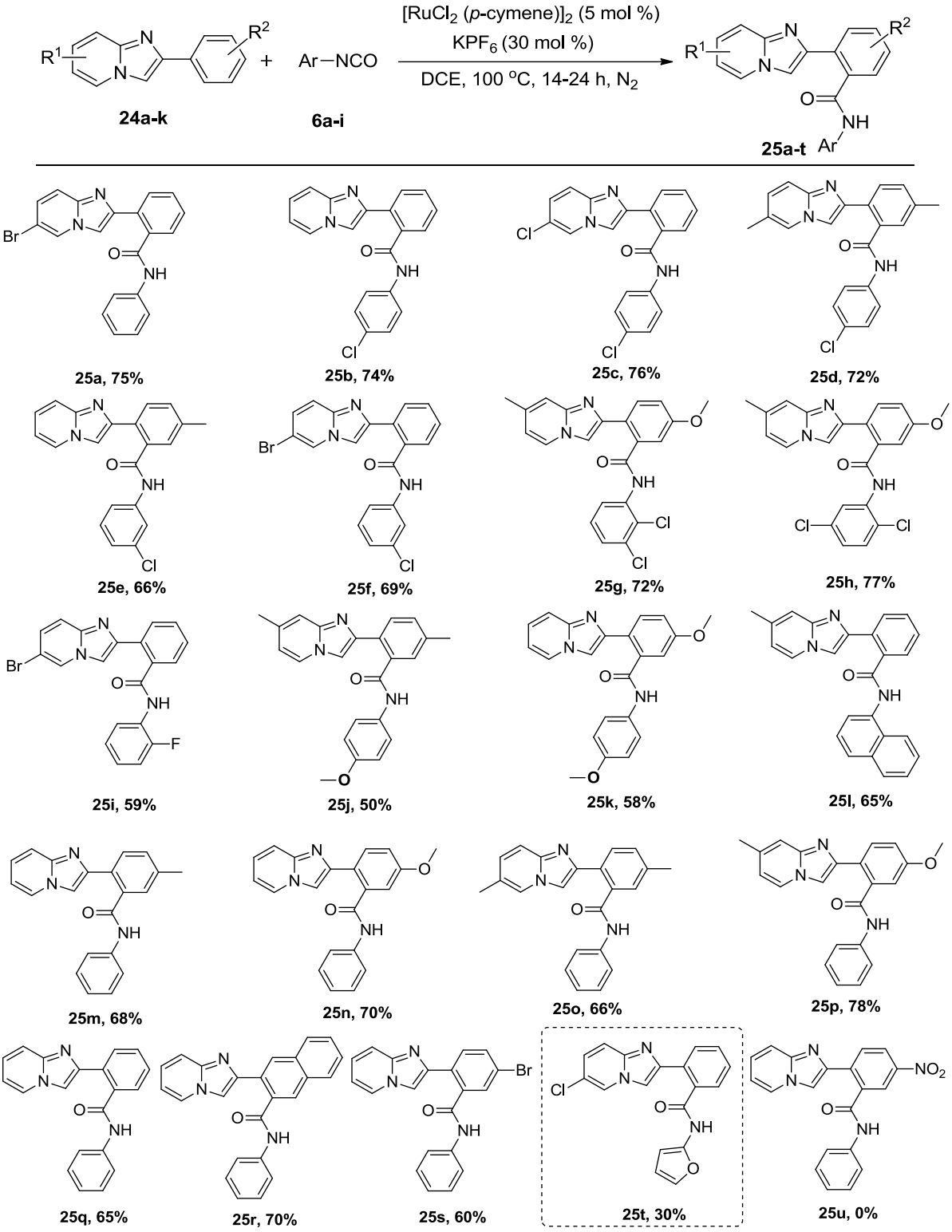

Scheme 3B.2.1: Substrate scope of 2-arylimidazo[1,2-*a*]pyridines (**24**) and isocyanates (**6**)

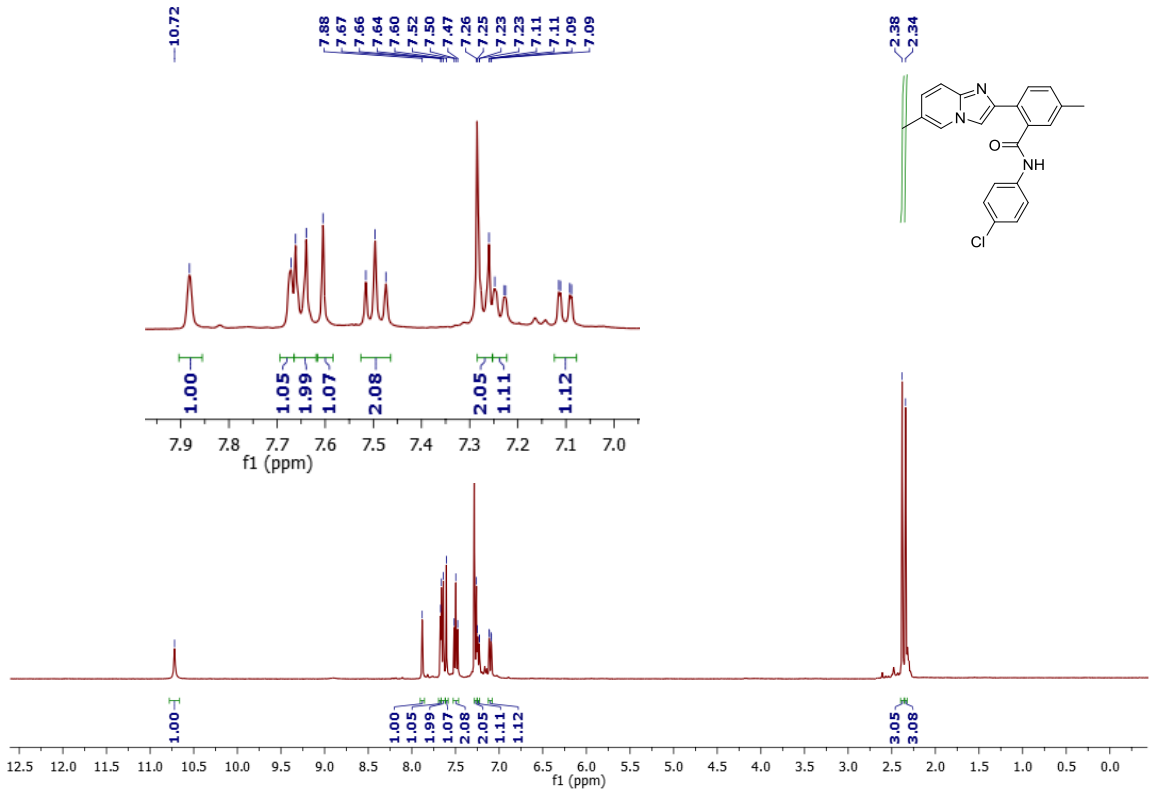

Figure 3B.2.1: ^{1}H NMR spectra of **25d**

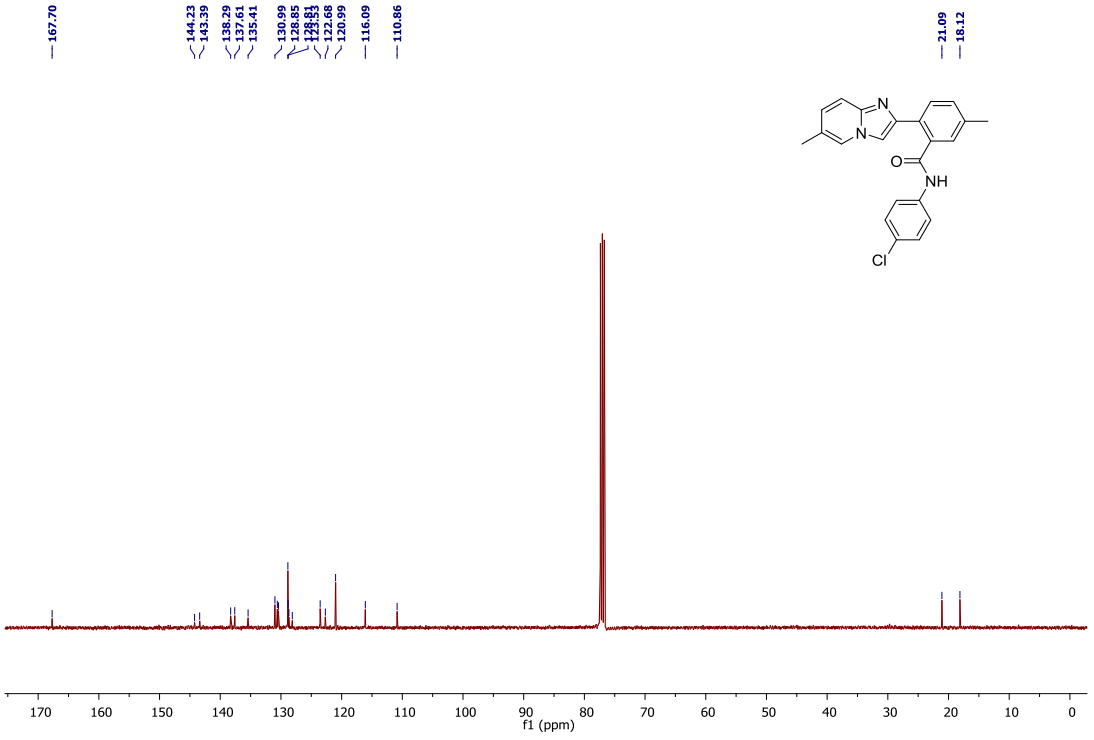

Figure 3B.2.2: ^{13}C NMR spectra of **25d**

As a representative example, single crystals of **25d** were grown using ethyl acetate/hexanes for the X-ray diffraction studies. **25d** crystallizes in the Monoclinic *P*21/*c* space group. An ORTEP diagram of **25d** (CCDC No. 1501223) is shown in Figure 3B.2.3.

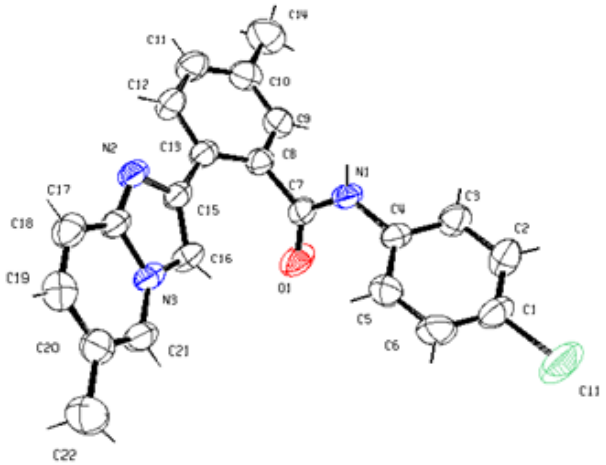

Figure 3B.2.3: An ORTEP diagram of **25d**

The scope of the reaction was further explored towards the selective *ortho*-amidaton of 2-2-(thiophen-2-yl)imidazo[1,2-*a*]pyridine (**26a**) and 2-(furan-2-yl)imidazo[1,2-*a*]pyridine (**26b**) under standardized conditions, affording the corresponding *ortho*-amidated products **27a** and **27b** in 73% and 70% yields, respectively (Scheme 3B.2.2).

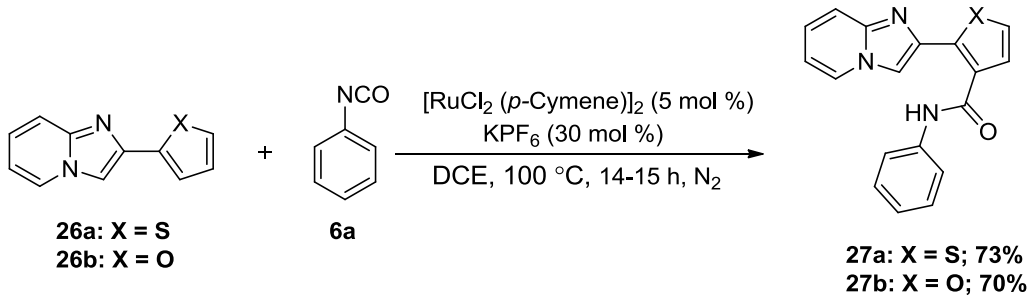

Scheme 3B.2.2: *ortho*-Amidation of 2-heteroarylimidazo[1,2-*a*]pyridines(**26a-b**) with phenyl isocyanate (**6a**)

To extend the scope of our methodology, a few other imidazo-heterocyles such as 2-phenylimidazo[2,1-*b*]thiazole (**28a**), and 2-phenylbenzo[*d*]imidazo[2,1-*b*]thiazole (**28b**) were reacted with phenyl isocyanate (**6a**) under optimized conditions to obtain their corresponding amidated products **29a** and **29b** in 67% and 70% yields, respectively (Scheme 3B.2.3). In addition, it was observed that 2-phenylimidazo[2,1-*b*]thiazole (**28a**) showed excellent reactivity,

and heating for 18 h also resulted in the isolation of *bis ortho*-amidated product (**29a'**) in 18% yield along with **29a**.

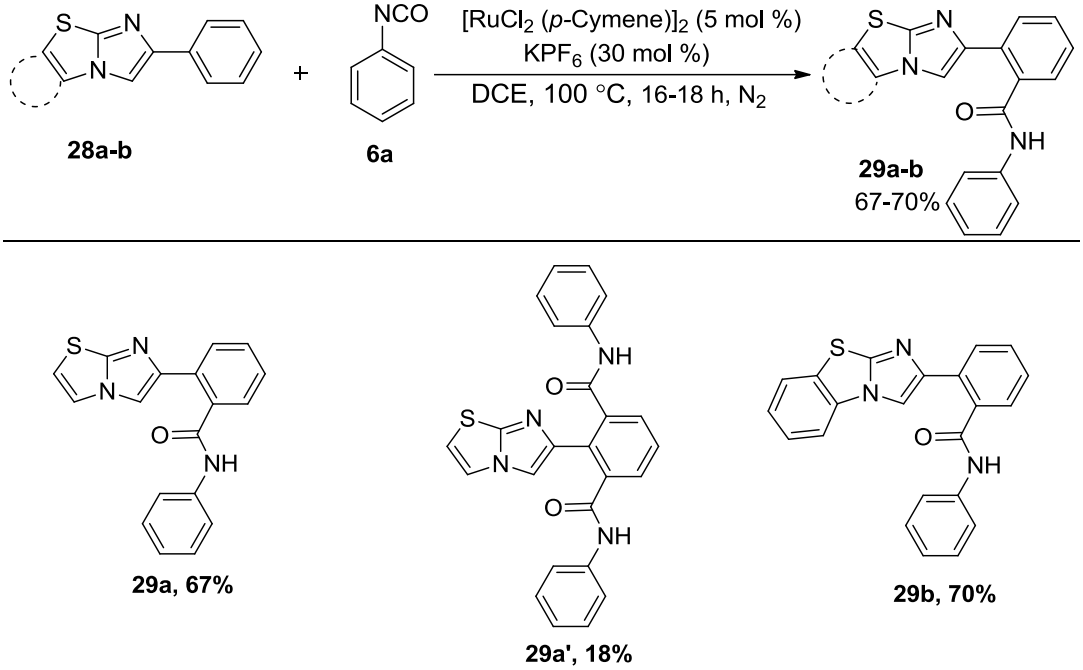

Scheme 3B.2.3: *ortho*-Amidation of 2-phenylimidazolyl thiazoles (**28a-b**)

It is noteworthy that attempts to undergo *ortho*-amidation of 2-arylimidazo[1,2-*a*]pyrimidine (**30a**) with phenyl isocyanate (**6a)** under similar experimental conditions resulted in predominant formation of *bis ortho*-amidated product **31a'** in 80% yield after 10 h. This could possibly be due to presence of an extra nitrogen in the chelating vicinity that enhances its reactivity and restrains the reaction to stop after mono *ortho*-amidation (Scheme 3B.2.4).

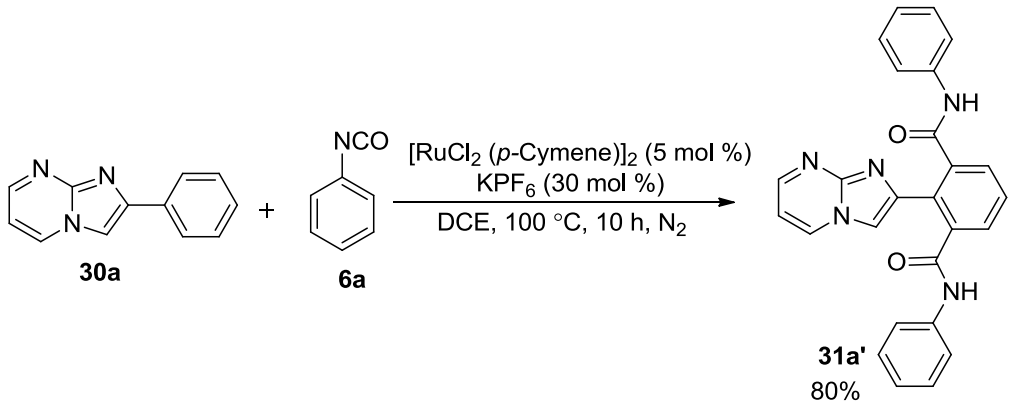

Scheme 3B.2.4: *ortho*-Amidation of 2-phenylimidazo[1,2-*a*]pyrimidine (**30a**) with phenyl isocyanate (**6a**)

To assess the scalability of this Ru(II)-catalyzed C−H bond amidation process, a gram scale reaction was performed between **24f** and **6a** under optimized conditions to yield the desired *ortho*-amidated product **25p** in 70% (1.05 g) yield, which was similar to that obtained on a smaller scale (Scheme 3B.2.5).

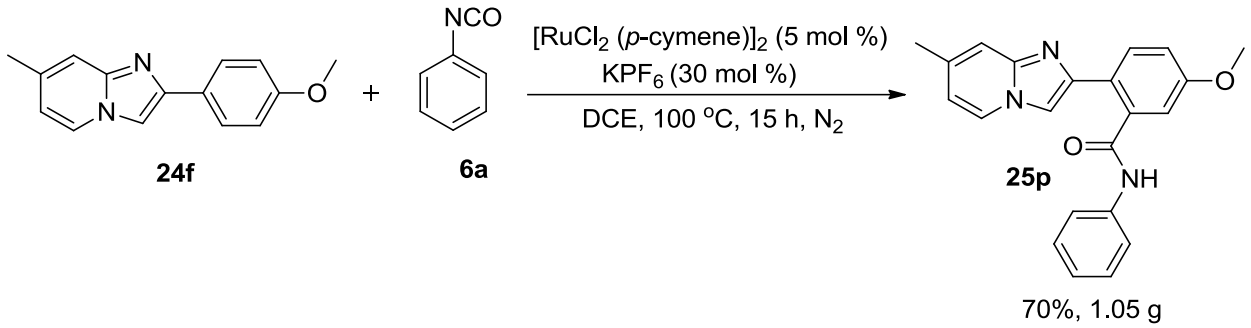

Scheme 3B.2.5: Gram scale synthesis of **25p**

To gain some insights into mechanism, a few control experiments were performed. Stoichiometric reaction between 6-methyl-2-(*p*-tolyl)imidazo[1,2-*a*]pyridine (**24d**) with phenyl isocyanate (**6a**) under catalyst-free conditions failed to yield either C-3 amidated or *ortho*-amidated product, thereby suggesting a vital role of catalyst and additive (Scheme 3B.2.6.i). The inability of imidazo[1,2-*a*]pyridine (**24m**) to give any amidated product with **6a** under optimized conditions further affirmed the non-reactivity of C-3 centre under ruthenium catalysis (Scheme 3B.2.6.ii). Reaction of 1.5 equivalent of **24d** with 1 equivalent of $[RuCl_2$ (*p*-cymene)$]_2$ in the presence of KPF_6 (3 equiv.) in 1,2-dichloroethane resulted in the formation of cyclometalated complex (**C₃**) after 12 h at room temperature (Scheme 3B.2.6iii). Formation of **C₃** was confirmed by ESI-MS analysis is shown in (Figure 3B.2.4), however, it was only partially purified by repeated diethyl ether wash. Attempts to purify **C₃** by undertaking column chromatography (using silica gel or neutral alumina as adsorbents) were unsuccessful probably due to the instability of the complex. The proposed structure of **C₃** was in accordance with the literature reports.[54] Employing catalytic amounts of the isolated complex **C₃** for coupling reaction between **24d** and **6a** in the presence of KPF_6 under optimized conditions, the desired product **25o** was obtained in comparable yields (Scheme 3B.2.6.iv). Finally attempting stoichiometric reaction between isolated **C₃** and **24d** also resulted in the formation of **25o** in 40% yield (Scheme 3B.2.6.v), thereby suggesting **C₃** to be an intermediate and a reservoir of active species **C₂** in the catalytic process.

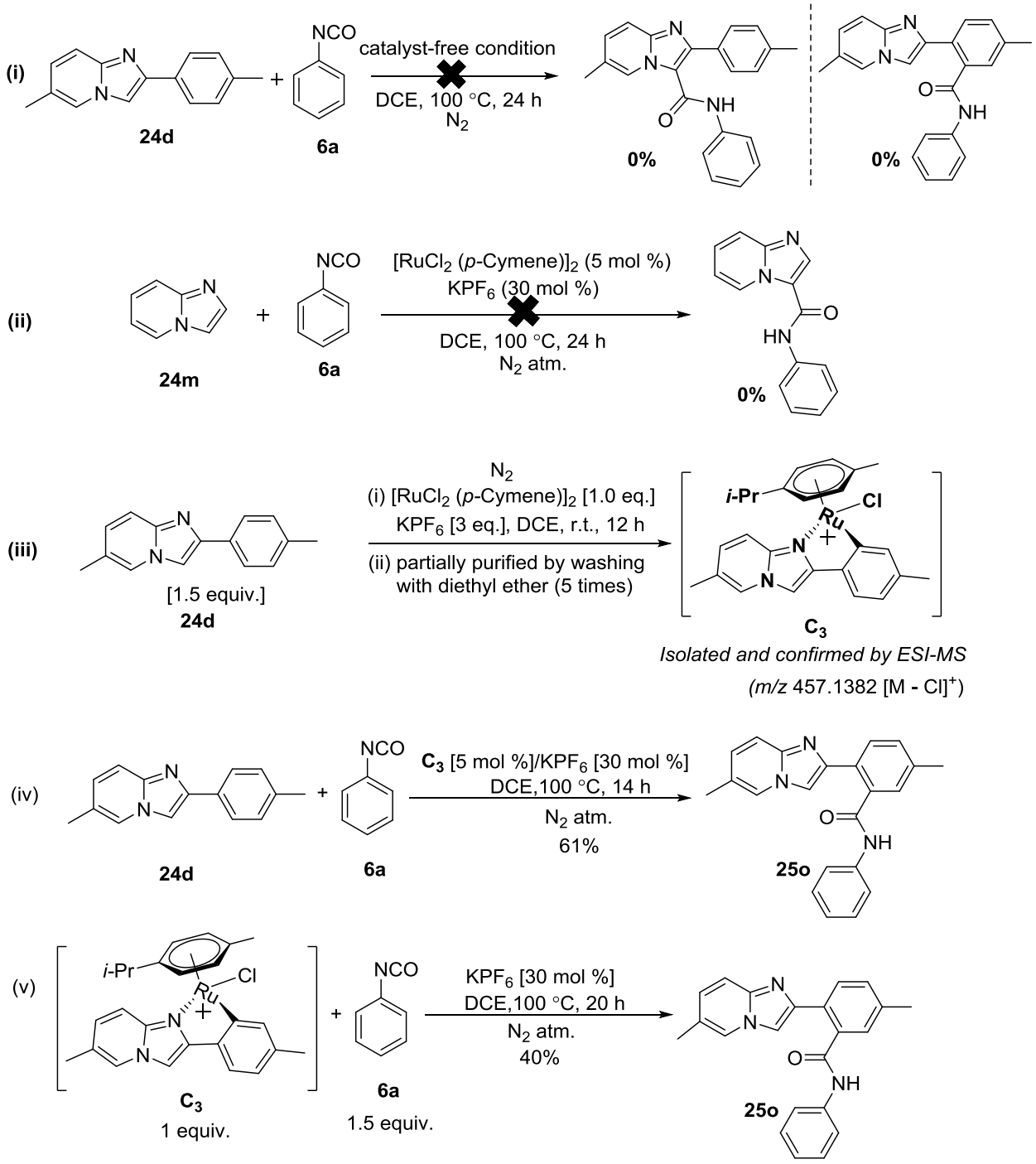

Scheme 3B.2.6: Control experiments

From the control experiments and literature reports[51,68-70] it is proposed that the plausible catalytic process is initiated by the dissociation of the $[RuCl_2(p\text{-cymene})]_2$ dimer (**C₁**) into cationic ruthenium monomeric species **C₂** (active catalyst), most likely by substitution of Cl^- ligand by PF_6^-. Thereafter, reversible C-H ruthenation at the *ortho*-position of aryl ring on

2-phenylimidazo[1,2-*a*]pyridine lead to formation of a cationic intermediate complex **C3**. Coordination of phenyl isocyanate **6a** to **C3**, followed by migratory insertion yielded **C5** *via* **C4**, which on proto-demetalation affords *ortho*-amidated product, along with the regeneration of the cationic ruthenium species **C2** that continues the catalytic process (Scheme 3B.2.7).

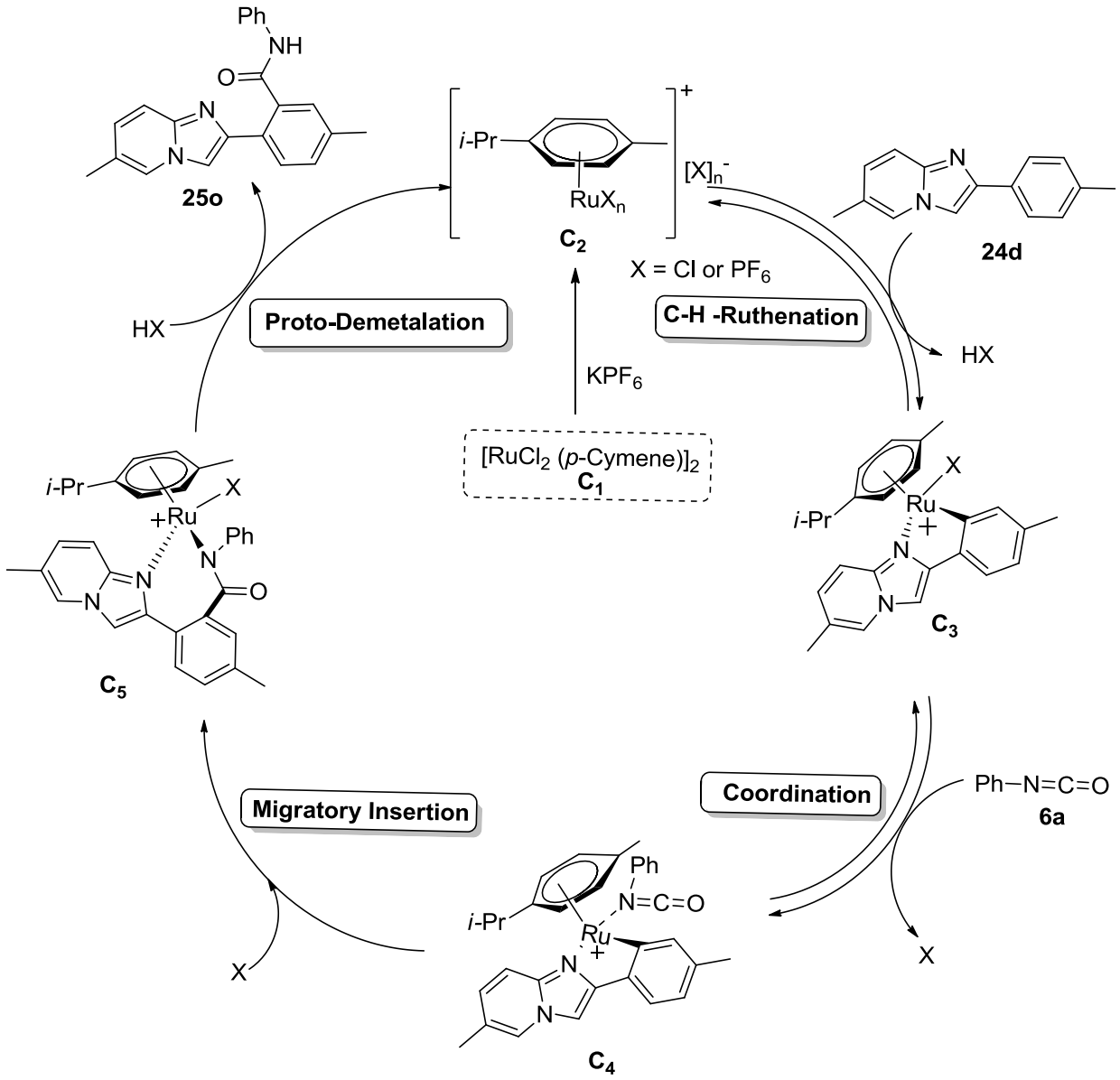

Scheme 3B.2.7 Plausible catalytic pathway for the Ru-catalyzed *ortho*-amidation of **24d** with phenyl isocyanate (**6a**)

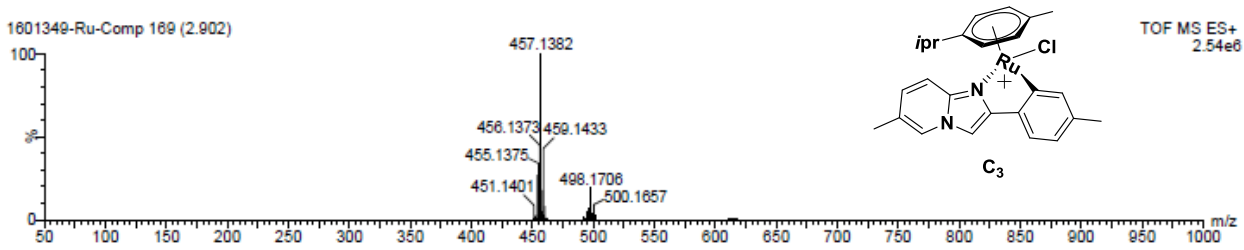

Figure 3B.2.4: ESI-MS of complex **C**$_3$

In summary, we have described a convergent and straightforward method for the regioselective synthesis of *ortho*-amidated imidazo-heterocycles *via* C(sp^2)−H bond activation, and subsequent functionalization with aryl isocyanates employing [RuCl$_2$(*p*-cymene)]$_2$ and KPF$_6$ in catalytic amounts.

3B.3 Experimental section

3B.3.1 General Materials and Methods

Commercially available reagents were used without purification. Commercially available solvents were dried by standard procedures prior to use. Reactions were monitored by using thin layer chromatography (TLC) on 0.2 mm silica gel F254 plates. Nuclear magnetic resonance spectra were recorded on 400 MHz spectrometer and chemical shifts are reported in δ units, parts per million (ppm), relative to residual chloroform (7.26 ppm) or DMSO (2.5 ppm) in the deuterated solvent. The following abbreviations were used to describe peak splitting patterns when appropriate: s = singlet, d = doublet, t = triplet, dd = doublet of doublet and m = multiplet. Coupling constants *J* were reported in Hz. The ^{13}C NMR spectra were reported in ppm relative to deuterochloroform (77.0 ppm) or [d_6] DMSO (39.5 ppm). Melting points were determined on a capillary point apparatus equipped with a digital thermometer and are uncorrected. High resolution mass spectra were recorded with a TOF analyzer spectrometer by using electrospray mode.

General procedure for *ortho*-amidation of imidazo-heterocycles

A mixture of imidazo-heterocycle (**24a-k**, **26a-b**, **28a-b and 30a**) (0.37 mmol), aryl isocyanate (**6a-h**) (0.56 mmol), [RuCl$_2$ (*p*-cymene)]$_2$, (0.02 mmol), KPF$_6$ (0.11 mmol) in dichloroethane (10 mL) was heated at 100 °C under nitrogen atmosphere for 14-20 h. On completion of reaction as indicated by TLC, the reaction mixture was filtered, evaporated and was directly subjected to silica gel column chromatography [SiO$_2$ (100-200 mesh), hexanes/EtOAc, 8:2] to yield the *o*-amidated product (**25a-t**, **27a-b**, **29a-b**). In few cases, the bis *ortho*-amidated product (**25a'**,

29a', **31a'**) were also isolated.

Procedure for the *ortho*-amidation of 24c with furyl isocyanate (6i): Furyl isocyanate was synthesized *in-situ* by heating furan-2-carbonyl azide[71] (0.150 g) in 1,2-dichloroethane at 100 °C for about 45 minutes under nitrogen atmosphere *via* curtius rearrangement. Furyl isocyanate (assuming 100% conversion) was directly used for the *o*-amidation of **24c** (0.100 g, 0.43 mmol) following earlier described procedure to yield **25t**.

2-(6-Bromoimidazo[1,2-*a*]pyridin-2-yl)-*N*-phenylbenzamide (25a): White solid; yield: 109 mg (75%); mp: 198–201 °C; ^{1}H NMR (400 MHz, $CDCl_3$) δ 10.28 (s, 1H), 8.39 (s, 1H), 7.99 (d, J = 7.8 Hz, 1H), 7.92 (s, 1H), 7.67 – 7.63 (m, 2H), 7.52 – 7.44 (m, 2H), 7.41 – 7.35 (m, 2H), 7.23 (t, J = 7.9 Hz, 2H), 7.15 (dd, J = 9.5, 1.8 Hz, 1H), 7.00 (t, J = 7.4 Hz, 1H); ^{13}C NMR (100 MHz, $CDCl_3$) δ 173.4, 148.6, 147.9, 144.3, 141.7, 135.9, 134.4, 134.2, 133.5, 132.9, 132.7, 132.6, 131.9, 128.6, 125.1, 122.6, 116.3, 111.2; HRMS (ESI-TOF) (*m/z*) calculated $C_{20}H_{15}BrN_3O^+$: 392.0398; found 392.0405 $[M+H]^+$ and 394.0555 $[M+H+2]^+$.

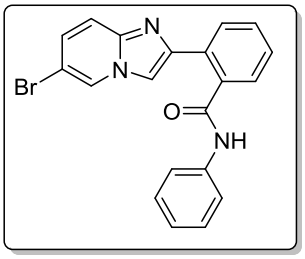

***N*-(4-Chlorophenyl)-2-(imidazo[1,2-*a*]pyridin-2-yl)benzamide (25b):** White solid; yield: 95 mg (74%); mp 225–227 °C; ^{1}H NMR (400 MHz, DMSO-d_6) δ 10.59 (s, 1H), 8.56 (dd, J = 6.8, 1.0 Hz, 1H), 8.09 (s, 1H), 8.04 (d, J = 7.8 Hz, 1H), 7.72 (d, J = 8.9 Hz, 2H), 7.61 – 7.56 (m, 1H), 7.54 – 7.50 (m, 2H), 7.48 – 7.45 (m, 1H), 7.39 (d, J = 8.9 Hz, 2H), 7.25– 7.19 (m, 1H), 6.88 – 6.84 (m, 1H); ^{13}C NMR (100 MHz, DMSO-d_6) δ 168.9, 144.7, 143.0, 138.7, 136.7, 131.7, 129.8, 129.4, 128.9, 128.0, 127.8, 127.4, 125.3, 121.8, 120.2, 117.0, 112.6, 111.0; HRMS (ESI-TOF) (*m/z*) calculated $C_{20}H_{15}ClN_3O^+$: 348.0903; found 348.0910 $[M+H]^+$ and 350.1060 $[M+H+2]^+$.

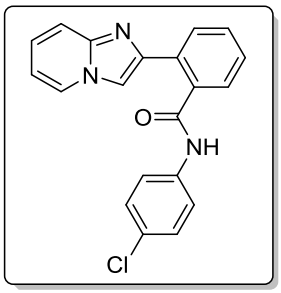

2-(6-Chloroimidazo[1,2-*a*]pyridin-2-yl)-*N*-(4-chlorophenyl)benzamide (25c): White solid; yield: 107 mg (76%); mp 165–166 °C; ^{1}H NMR (400 MHz, DMSO-d_6) δ 10.58 (s, 1H), 8.90 (dd, J = 2.0, 0.8 Hz, 1H), 8.11 (s, 1H), 8.03 (d, J = 7.8 Hz, 1H), 7.74 – 7.69 (m, 2H), 7.61 – 7.55 (m, 2H), 7.53 – 7.47 (m, 2H), 7.41 – 7.37 (m, 2H), 7.28 (dd, J = 9.6, 2.1 Hz, 1H); ^{13}C NMR (100 MHz, DMSO-d_6) δ 168.8, 144.1, 143.1, 136.7, 131.2, 130.1, 129.4, 129.0, 128.3, 128.2, 127.6, 126.4, 125.4, 121.9,

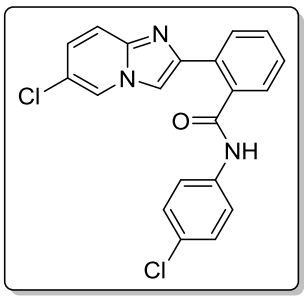

120.3, 119.5, 117.9, 111.7; HRMS (ESI-TOF) (*m/z*) calculated $C_{20}H_{14}Cl_2N_3O^+$: 382.0513; found 382.0521 $[M+H]^+$ and 384.0670 $[M+H+2]^+$.

***N*-(4-Chlorophenyl)-5-methyl-2-(6-methylimidazo[1,2-*a*]pyridin-2-yl)benzamide (25d):**

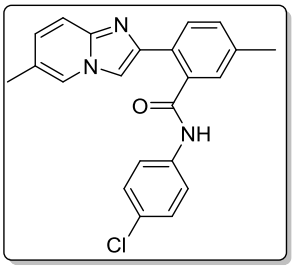

White solid; yield: 100 mg (72%); mp 230–232 °C; ^{1}H NMR (400 MHz, $CDCl_3$) δ 10.72 (s, 1H), 7.88 (s, 1H), 7.67 (s, 1H), 7.65 (d, *J* = 8.8 Hz, 2H), 7.60 (s, 1H), 7.50 (t, *J* = 8.3 Hz, 2H), 7.28 – 7.26 (m, 2H), 7.25 – 7.22 (m, 1H), 7.10 (dd, *J* = 9.2, 1.4 Hz, 1H), 2.38 (s, 3H), 2.34 (s, 3H); ^{13}C NMR (100 MHz, $CDCl_3$) δ 167.7, 144.2, 143.4, 138.3, 137.6, 135.4, 131.0, 130.6, 130.4, 128.9, 128.8, 128.7,128.1, 123.5, 122.7, 121.0, 116.1, 110.9, 21.1, 18.1; HRMS (ESI-TOF) (*m/z*) calculated $C_{22}H_{19}ClN_3O^+$: 376.1216; found 376.1235 $[M+H]^+$ and 378.1370 $[M+H+2]^+$.

***N*-(3-Chlorophenyl)-2-(imidazo[1,2-*a*]pyridin-2-yl)-5-methylbenzamide (25e):** White Solid;

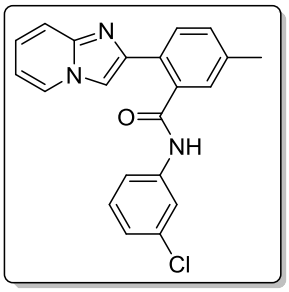

yield: 88 mg (66%); mp 220– 221 °C; ^{1}H NMR (400 MHz, DMSO-d_6) δ 10.62 (s, 1H), 8.56 (d, *J* = 6.7 Hz, 1H), 8.07 (s, 1H), 7.98 – 7.90 (m, 2H), 7.58 – 7.46 (m, 2H), 7.40 (d, *J* = 8.0 Hz, 1H), 7.35 (t, *J* = 8.0 Hz, 2H), 7.24 – 7.18 (m, 1H), 7.14 (d, *J* = 7.86 Hz, 1H), 6.84 (t, *J* = 6.6 Hz, 1H), 2.40 (s, 3H); ^{13}C NMR (100 MHz, DMSO-d_6) δ 169.2, 144.6, 143.1, 141.3, 137.5, 136.4, 133.4, 130.8, 130.7, 129.4, 128.9, 128.5, 127.5, 125.4, 123.6, 119.7, 118.6, 116.9, 112.6, 110.7, 21.0; HRMS (ESI-TOF) (*m/z*) calculated $C_{21}H_{17}ClN_3O^+$: 362.1060; found 362.1079 $[M+H]^+$ and 364.1214 $[M+H+2]^+$.

2-(6-Bromoimidazo[1,2-*a*]pyridin-2-yl)-*N*-(3-chlorophenyl)benzamide (25f): White solid;

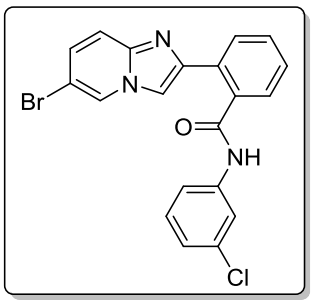

yield: 108 mg (69%); mp 217–219 °C; ^{1}H NMR (400 MHz, DMSO-d_6) δ 10.62 (s, 1H), 8.98 (d, *J* = 1.0 Hz, 1H), 8.12 (s, 1H), 8.04 (d, *J* = 7.7 Hz, 1H), 7.93 (s, 1H), 7.65 – 7.56 (m, 1H), 7.56 – 7.45 (m, 4H), 7.35 (dd, *J* = 9.3, 7.1 Hz, 2H), 7.15 (dd, *J* = 7.9, 1.1 Hz, 1H); ^{13}C NMR (100 MHz, DMSO-d_6) δ 169.0, 143.8, 143.2, 141.1, 136.6, 133.5, 131.2 130.8, 130.1, 129.4, 128.4, 128.3, 128.2, 127.6, 123.7, 119.8, 118.7, 118.1, 111.5, 106.4; HRMS (ESI-TOF) (*m/z*) calculated $C_{20}H_{14}BrClN_3O^+$: 426.0008; found 426.0023 $[M+H]^+$ and 428.0168 $[M+H+2]^+$.

***N*-(2,3-Dichlorophenyl)-5-methoxy-2-(7-methylimidazo[1,2-*a*]pyridin-2-yl)benzamide (25g):**

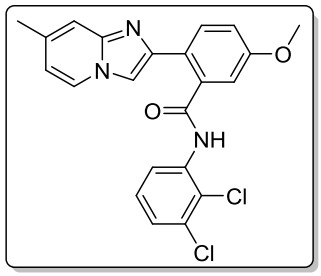

White solid; yield: 113 mg (72%); mp 238–240 °C; ^{1}H NMR (400 MHz, $CDCl_3$) δ 9.50 (d, J = 7.1 Hz, 1H), 8.50 (dd, J = 8.2, 1.5 Hz, 1H), 8.28 (s, 1H), 7.72 – 7.61 (m, 2H), 7.50 (s, 1H), 7.23 (t, J = 8.1 Hz, 1H), 7.17 (dd, J = 8.0, 1.6 Hz, 1H), 7.07 (d, J = 8.7 Hz, 2H), 6.90 (dd, J = 7.2, 1.6 Hz, 1H), 3.90 (s, 3H), 2.50 (s, 3H); ^{13}C NMR (100 MHz, $CDCl_3$ + DMSO-d_6) 160.7, 159.5, 149.1, 146.7, 139.4, 137.0, 132.3, 131.4, 128.6, 127.1, 126.1, 126.1, 121.9, 116.9, 115.7, 114.8, 113.9, 55.8, 21.3; HRMS (ESI-TOF) (*m/z*) calculated $C_{22}H_{18}Cl_2N_3O_2^+$: 426.0776 ; found 426.0793 $[M+H]^+$ and 428.0932 $[M+H+2]^+$.

***N*-(2,5-Dichlorophenyl)-5-methoxy-2-(7-methylimidazo[1,2-*a*]pyridin-2-yl)benzamide (25h):**

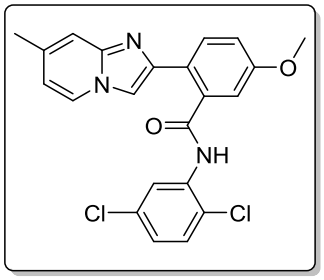

White solid; yield: 121 mg (77%); mp 217–218 °C; ^{1}H NMR (400 MHz, $CDCl_3$) δ 9.50 (d, J = 7.1 Hz, 1H), 8.67 (d, J = 2.4 Hz, 1H), 8.18 (s, 1H), 7.65 (d, J = 8.7 Hz, 2H), 7.50 (s, 1H), 7.16 (d, J = 8.5 Hz, 1H), 7.06 (d, J = 8.7 Hz, 2H), 6.97 (dd, J = 8.5, 2.4 Hz, 1H), 6.94 – 6.86 (m, 1H), 3.89 (s, 3H), 2.51 (s, 3H); ^{13}C NMR (100 MHz, $CDCl_3$) δ 161.1, 159.1, 150.2, 147.4, 139.6, 135.8, 133.3, 131.4, 129.6, 127.6, 125.6, 123.9, 120.8, 120.2, 116.7, 115.9, 114.9, 113.7, 55.5, 21.5; HRMS (ESI-TOF) (*m/z*) calculated $C_{22}H_{18}Cl_2N_3O_2^+$: 426.0776; found 426.0798 $[M+H]^+$ and 428.09338 $[M+H+2]^+$.

2-(6-Bromoimidazo[1,2-*a*]pyridin-2-yl)-*N*-(2-fluorophenyl)benzamide (25i): White solid;

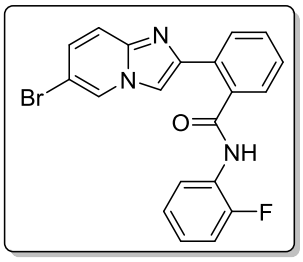

yield: 89 mg (59%); mp 225–227 °C; ^{1}H NMR (400 MHz, DMSO-d_6) δ 10.25 (s, 1H), 9.00 (d, J = 1.1 Hz, 1H), 8.17 (s, 1H), 8.02 (d, J = 7.6 Hz, 1H), 7.84 (dd, J = 9.0, 6.5 Hz, 1H), 7.59 (d, J = 7.3 Hz, 1H), 7.57 – 7.53 (m, 2H), 7.51 – 7.46 (m, 1H), 7.37 (dd, J = 9.5, 1.9 Hz, 1H), 7.27 –7.20 (m, 3H); ^{13}C NMR (100 MHz, DMSO-d_6) δ 169.0, 156.6, 154.2, 143.9, 143.1, 136.5, 131.3, 130.0, 129.4, 128.4, 128.2, 127.5, 126.8, 126.7, 126.3, 124.7, 118.1, 116.2, 111.7, 106.4; HRMS (ESI-TOF) (*m/z*) calculated $C_{20}H_{14}BrFN_3O^+$: 410.0304; found 410.0327 $[M+H]^+$ and 412.0468 $[M+H+2]^+$.

***N*-(4-Methoxyphenyl)-5-methyl-2-(7-methylimidazo[1,2-*a*]pyridin-2-yl)benzamide (25j):**

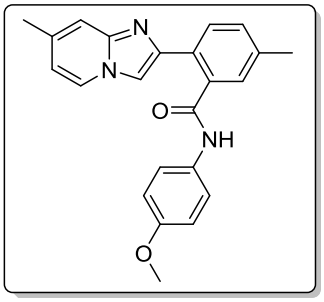

White solid; yield: 68 mg (50%); mp 192–194 °C; ^{1}H NMR (400 MHz, $CDCl_3$) δ 9.91 (s, 1H), 7.96 (d, J = 6.9 Hz, 1H), 7.65 (s, 2H), 7.61 (d, J = 7.9 Hz, 1H), 7.56 (d, J = 9.0 Hz, 2H), 7.36 (s, 1H), 7.26 (d, J = 7.9 Hz, 1H), 6.87 (d, J = 9.0 Hz, 2H), 6.65 (d, J = 6.9 Hz, 1H), 3.81 (s, 3H), 2.43 (s, 3H), 2.40 (s, 3H); ^{13}C NMR (100 MHz, $CDCl_3$) δ 167.6, 156.1, 144.9, 144.0, 138.2, 136.5, 135.8, 132.1, 130.8, 130.4, 130.0, 128.1, 125.0, 121.5, 115.4, 115.3, 114.1, 110.5, 55.5, 21.5, 21.1; HRMS (ESI-TOF) (*m/z*) calculated $C_{23}H_{22}N_3O_2^+$: 372.1712; found 372.1730 $[M+H]^+$.

2-(Imidazo[1,2-*a*]pyridin-2-yl)-5-methoxy-*N*-(4-methoxyphenyl)benzamide (25k): White

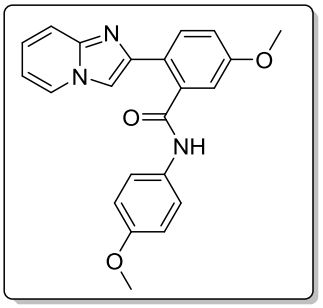

solid; yield: 80 mg (58%); mp 198–201 °C; ^{1}H NMR (400 MHz, MeOH-d_4) δ 8.34 (d, J = 6.8 Hz, 1H), 7.88 (d, J = 10.4 Hz, 2H), 7.53 (d, J = 9.2 Hz, 1H), 7.51 – 7.45 (m, 2H), 7.30 (dd, J = 6.8, 2.2 Hz, 1H), 7.20 – 7.11 (m, 2H), 6.89 (dd, J = 7.1, 2.0 Hz, 2H), 6.86 (dd, J = 4.7, 2.2 Hz, 1H), 3.90 (s, 3H), 3.78 (s, 3H); ^{13}C NMR (100 MHz MeOH-d_4) δ 169.3, 159.5, 156.8, 144.9, 142.6, 137.5, 131.3, 130.8, 126.4, 125.6, 121.9, 121.4, 115.6, 115.2, 113.7, 113.6, 112.7, 110.2, 54.7, 54.4; HRMS (ESI-TOF) (*m/z*) calculated $C_{22}H_{20}N_3O_3^+$: 374.1504; found 374.1523 $[M+H]^+$.

2-(7-Methylimidazo[1,2-*a*]pyridin-2-yl)-*N*-(naphthalen-1-yl)benzamide (25l): White solid;

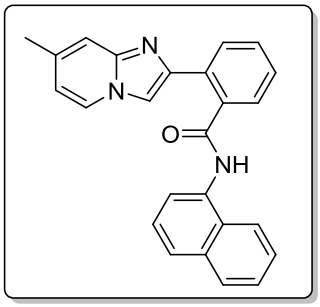

yield: 90 mg (65%); mp 199–203 °C; ^{1}H NMR (400 MHz, DMSO-d_6) δ 10.41 (s, 1H), 8.43 (d, J = 6.7 Hz, 1H), 8.09 (s, 1H), 8.01 – 7.75 (m, 5H), 7.68 (d, J = 7.1 Hz, 1H), 7.62 – 7.47 (m, 4H), 7.36 (s, 1H), 7.30 (t, J = 7.4 Hz, 1H), 6.73 (d, J = 6.6 Hz, 1H), 2.36 (s, 3H); ^{13}C NMR (100 MHz, DMSO-d_6) δ 169.7, 145.2, 143.3, 137.3, 135.9, 134.1, 132.1, 129.8, 129.6, 129.2, 128.3, 127.9, 127.1, 126.8, 126.8, 126.0, 126.0, 123.7, 123.5, 115.2, 110.7, 21.3; HRMS (ESI-TOF) (*m/z*) calculated $C_{25}H_{20}N_3O^+$: 378.1606; found 378.1614 $[M+H]^+$.

2-(Imidazo[1,2-*a*]pyridin-2-yl)-5-methyl-*N*-phenylbenzamide (25m): White solid; yield: 82 mg (68%); mp 188–190 °C; ^{1}H NMR (400 MHz, $CDCl_3$) δ 9.80 (s, 1H), 8.10 (d, J = 6.8 Hz, 1H), 7.75 (s, 1H), 7.71 (s, 1H), 7.68 – 7.61 (m, 4H), 7.35 – 7.30 (m, 3H), 7.26 – 7.21 (m, 1H), 7.10 (t, J = 7.4 Hz, 1H), 6.83 (t, J = 6.8 Hz, 1H), 2.44 (s, 3H); ^{13}C NMR (100 MHz, $CDCl_3$) δ 168.0, 144.6, 138.7, 138.4, 135.8, 131.0, 130.5, 130.0, 129.0, 128.1, 125.9, 125.4, 124.2, 123.2, 120.0, 119.9, 117.0, 112.8, 21.1; HRMS (ESI-TOF) (*m/z*) calculated $C_{21}H_{18}N_3O^+$: 328.1449; found 328.1455 $[M+H]^+$.

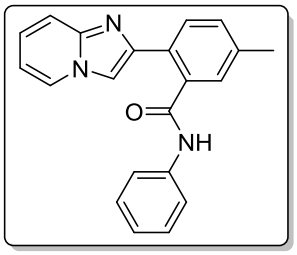

2-(Imidazo[1,2-*a*]pyridin-2-yl)-5-methoxy-*N*-phenylbenzamide (25n): White solid; yield: 89 mg (70%); mp 179–181 °C; ^{1}H NMR (400 MHz, $CDCl_3$) δ 10.07 (s, 1H), 8.12 (d, J = 6.6 Hz, 1H), 7.71 (s, 1H), 7.65 – 7.60 (m, 3H), 7.46 (d, J = 2.2 Hz, 1H), 7.32 (d, J = 7.9 Hz, 2H), 7.25 (d, J = 8.3 Hz, 1H), 7.22 – 7.16 (m, 1H), 7.11 – 7.03 (m, 2H), 6.85 (t, J = 6.6 Hz, 1H), 3.91 (s, 3H); ^{13}C NMR (100 MHz, $CDCl_3$) δ 167.2, 159.6, 144.4, 138.7, 137.1, 132.3, 128.9, 128.8, 125.9, 125.6, 124.1, 119.8, 119.6, 116.9, 116.8, 114.2, 112.9, 111.0, 55.5; HRMS (ESI-TOF) (*m/z*) calculated $C_{21}H_{18}N_3O_2^+$: 344.1399; found 344.1406 $[M+H]^+$.

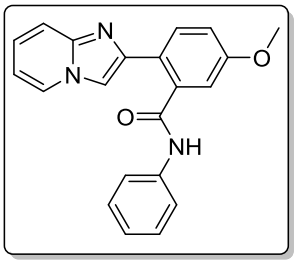

5-Methyl-2-(6-methylimidazo[1,2-*a*]pyridin-2-yl)-*N*-phenylbenzamide (25o): White solid; yield: 75 mg (66%); mp 174–176 °C; ^{1}H NMR (400 MHz, DMSO-d_6) δ 10.44 (s, 1H), 7.96 (s, 1H), 7.88 (dd, J = 7.9, 2.1 Hz, 1H), 7.79 (dd, J = 8.4, 2.4 Hz, 1H), 7.65 (d, J = 7.1 Hz, 2H), 7.36 (d, J = 9.1 Hz, 1H), 7.30 (s, 1H), 7.28 – 7.17 (m, 3H), 7.04 – 6.93 (m, 2H), 2.36 (s, 3H), 2.21 (s, 3H); ^{13}C NMR (100 MHz, DMSO-d_6) δ 168.9, 143.7, 142.9, 139.4, 137.2, 136.4, 130.3, 129.4, 128.8, 128.6, 128.5, 128.2, 124.0, 123.8, 121.9, 120.1, 116.2, 110.3, 21.1, 18.0; HRMS (ESI-TOF) (*m/z*) calculated $C_{22}H_{20}N_3O^+$: 342.1606; found 342.1612 $[M+H]^+$.

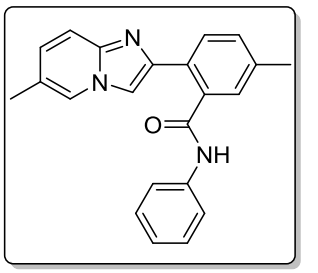

5-Methoxy-2-(7-methylimidazo[1,2-*a*]pyridin-2-yl)-*N*-phenylbenzamide (25p): White solid; yield: 102 mg (78%); mp 189–191 °C; ^{1}H NMR (400 MHz, $CDCl_3$) δ 10.49 (s, 1H), 8.40 (d, J = 6.9 Hz, 1H), 7.97 (d, J = 8.7 Hz, 1H), 7.89 (s, 1H), 7.70 (d, J = 7.8 Hz, 2H), 7.32 (t, J = 7.8 Hz, 2H), 7.28 (s, 1H), 7.13 (dd, J = 8.7, 2.6 Hz, 1H), 7.10 – 7.01 (m, 2H), 6.66 (d, J = 6.9 Hz, 1H), 3.84 (s, 3H), 2.31 (s, 3H); ^{13}C NMR (100 MHz,

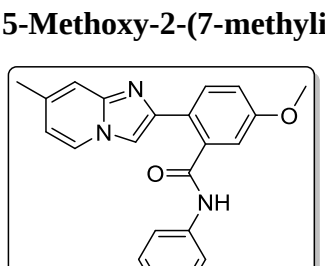

$CDCl_3$) δ 173.2, 163.6, 149.6, 147.5, 144.5, 142.6, 140.4, 135.6, 133.9, 131.3, 129.0, 128.8, 125.1, 120.4, 119.9, 119.7, 117.9, 114.4, 60.7, 26.0; HRMS (ESI-TOF) (*m/z*) calculated $C_{22}H_{20}N_3O_2^+$: 358.1555; found 358.1560 $[M+H]^+$.

2-(Imidazo[1,2-*a*]pyridin-2-yl)-*N*-phenylbenzamide (25q): White solid; yield: 75 mg (65%);

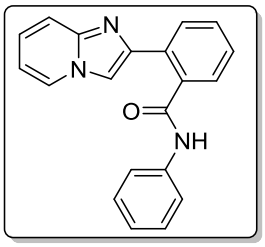

mp 184–186 °C; ^{1}H NMR (400 MHz, DMSO-d_6) δ 10.48 (s, 1H), 8.58 (d, *J* = 6.1 Hz, 1H), 8.11 (s, 1H), 8.05 (d, *J* = 7.5 Hz, 1H), 7.70 (d, *J* = 7.5 Hz, 2H), 7.53 (m, 4H), 7.33 (t, *J* = 7.1 Hz, 2H), 7.28 – 7.23 (m, 1H), 7.08 (t, *J* = 6.8 Hz, 1H), 6.87 (t, *J* = 5.9 Hz, 1H); ^{13}C NMR (100 MHz, DMSO-d_6) δ 168.8, 144.5, 142.9, 139.7, 137.0, 131.4, 129.9, 129.4, 129.1, 128.1, 128.0, 127.9, 125.8, 124.0, 120.3, 117.0, 112.8, 111.1; HRMS (ESI-TOF) (*m/z*) calculated $C_{20}H_{16}N_3O^+$: 314.1293; found 314.1303 $[M+H]^+$.

3-(Imidazo[1,2-*a*]pyridin-2-yl)-*N*-phenyl-2-naphthamide (25r): White solid; yield: 94 mg

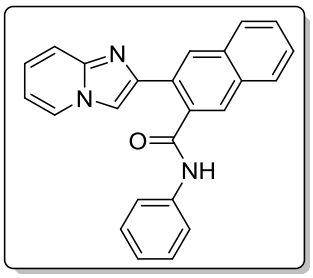

(70%); mp 190–193 °C; ^{1}H NMR (400 MHz, $CDCl_3$) δ 9.81 (s, 1H), 8.12 (d, *J* = 7.4 Hz, 2H), 8.04 (s, 1H), 7.84 (s, 1H), 7.81 – 7.74 (m, 1H), 7.74 – 7.62 (m, 3H), 7.60 (d, *J* = 8.4 Hz, 1H), 7.50 (dd, *J* = 5.9, 2.8 Hz, 2H), 7.38 – 7.29 (m, 3H), 7.12 (t, *J* = 7.3 Hz, 1H), 6.87 (t, *J* = 6.7 Hz, 1H); ^{13}C NMR (100 MHz, DMSO-d_6) δ 206.9, 139.0, 135.7, 133.3, 131.8, 128.76, 128.7, 128.7, 128.2, 127.9, 127.4, 126.9, 126.1, 125.6, 124.2, 123.9, 119.9, 117.6, 116.6, 112.7, 111.2, 111.2; HRMS (ESI-TOF) (*m/z*) calculated $C_{24}H_{18}N_3O^+$: 364.1449; found 364.1454 $[M+H]^+$.

2-(6-Chloroimidazo[1,2-*a*]pyridin-2-yl)-*N*-(furan-2-yl)benzamide (25s): Yellow solid; yield:

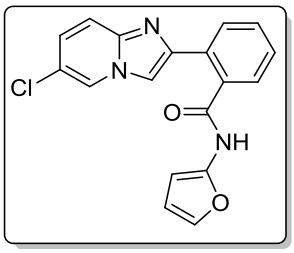

66 mg (30%); mp 200–203 °C; ^{1}H NMR (400 MHz, $CDCl_3$) δ 8.35 (s, 1H), 7.89 (s, 1H), 7.65 (s, 1H), 7.60 (d, *J* = 9.5 Hz, 1H), 7.47 – 7.40 (m, 3H), 7.36 (dd, *J* = 7.3, 5.3 Hz, 2H), 7.27 – 7.24 (m, 1H), 7.23 – 7.19 (m, 1H), 6.69 (dd, *J* = 3.4, 1.7 Hz, 1H); ^{13}C NMR (100 MHz, $CDCl_3$) δ 157.3, 146.5, 145.5, 129.8, 128.8, 128.5, 127.3, 125.2, 121.3, 120.3, 120.3, 117.8, 117.2, 112.9; HRMS (ESI-TOF) (*m/z*) calculated $C_{18}H_{13}ClN_3O_2^+$: 338.0696; found 338.0675 $[M+H]^+$ and 340.0856 $[M+H+2]^+$.

5-Bromo-2-(imidazo[1,2-*a*]pyridin-2-yl)-*N*-phenylbenzamide (25t): White solid; yield: 87 mg (60%); mp 200–203 °C; ^{1}H NMR (400 MHz, $CDCl_3$) δ 10.39 (s, 1H), 8.08 (d, J = 6.8 Hz, 1H), 7.87 (d, J = 2.0 Hz, 1H), 7.78 (s, 1H), 7.72 (d, J = 7.6 Hz, 2H), 7.59 (t, J = 8.4 Hz, 2H), 7.47 (dd, J = 8.3, 2.1 Hz, 1H), 7.36 (t, J = 7.9 Hz, 2H), 7.28 – 7.23 (m, 1H), 7.14 (t, J = 7.4 Hz, 1H), 6.84 (m, 1H); ^{13}C NMR (100 MHz, $CDCl_3$) δ 166.4, 144.6, 142.9, 138.6, 137.4, 132.9, 132.1, 131.6, 129.1, 125.9, 125.9, 124.4, 122.2, 119.9, 117.0, 113.2, 111.3; HRMS (ESI-TOF) (*m/z*) calculated $C_{20}H_{15}BrN_3O^+$: 392.0398; found 392.0403 $[M+H]^+$ and 394.0558 $[M+H+2]^+$.

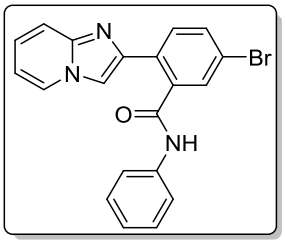

2-(Imidazo[1,2-*a*]pyridin-2-yl)-*N*-phenylthiophene-3-carboxamide (27a): White solid; yield: 86 mg (73%); mp 221–223 °C; ^{1}H NMR (400 MHz, DMSO-d_6) δ 11.52 (s, 1H), 8.65 – 8.60 (m, 1H), 8.43 (s, 1H), 7.80 (d, J = 7.7 Hz, 2H), 7.70 – 7.65 (m, 1H), 7.63 (d, J = 5.3 Hz, 1H), 7.51 (d, J = 5.3 Hz, 1H), 7.42 – 7.30 (m, 3H), 7.14 – 7.08 (m, 1H), 6.96 (td, J = 6.8, 1.0 Hz, 1H); ^{13}C NMR (100 MHz, DMSO-d_6) δ 162.7, 144.3, 139.7, 138.3, 137.9, 133.6, 130.6, 129.3, 127.7, 126.7, 125.7, 124.1, 120.3, 116.7, 113.4, 111.9; HRMS (ESI-TOF) (*m/z*) calculated $C_{18}H_{14}N_3OS^+$: 320.0857; found 320.0885 $[M+H]^+$.

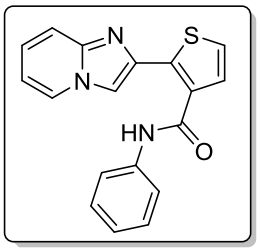

2-(Imidazo[1,2-*a*]pyridin-2-yl)-*N*-phenylfuran-3-carboxamide (27b): White solid; yield: 63 mg (70%); mp 180–182 °C; ^{1}H NMR (400 MHz, DMSO-d_6) δ 13.77 (s, 1H), 8.69 (m, 1H), 8.55 – 8.50 (m, 1H), 7.94 – 7.86 (m, 4H), 7.50 (m, 1H), 7.46 – 7.40 (m, 2H), 7.16 – 7.09 (m, 2H), 7.05 (d, J = 1.9 Hz, 1H); ^{13}C NMR (100 MHz, DMSO-d_6) δ 164.7, 151.4, 148.9, 147.8, 147.7, 144.9, 140.3, 134.3, 132.6, 128.5, 124.9, 124.4, 121.5, 119.1, 118.9, 117.2; HRMS (ESI-TOF) (*m/z*) calculated $C_{18}H_{14}N_3O_2^+$: 304.1086; found 304.1092 $[M+H]^+$.

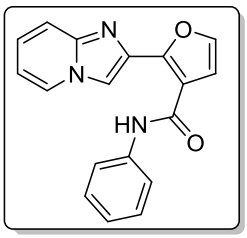

2-(Imidazo[2,1-*b*]thiazol-6-yl)-*N*-phenylbenzamide (29a): Yellow solid; yield: 80 mg (67%); mp 195–198 °C; ^{1}H NMR (400 MHz, DMSO-d_6) δ 10.45 (s, 1H), 7.96 (t, J = 6.7 Hz, 2H), 7.92 (s, 1H), 7.70 (d, J = 7.7 Hz, 2H), 7.56 – 7.50 (m, 1H), 7.46 (d, J = 6.5 Hz, 1H), 7.40 (t, J = 7.0 Hz, 1H), 7.33 (t, J = 7.9 Hz, 2H), 7.24 (d, J = 4.4 Hz, 1H), 7.09 (t, J = 7.4 Hz, 1H); ^{13}C NMR (100 MHz, DMSO-d_6) δ 169.0, 149.2, 144.7, 139.8, 136.2, 131.7, 129.8, 129.1, 128.7,

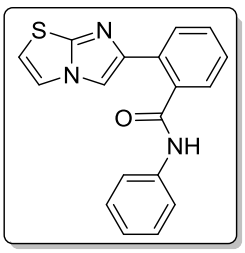

128.0, 127.4, 124.0, 120.6, 120.2, 113.6, 111.4; HRMS (ESI-TOF) (*m/z*) calculated $C_{18}H_{14}N_3OS^+$: 320.0857; found 320.0864 $[M+H]^+$.

2-(Benzo[*d*]imidazo[2,1-*b*]thiazol-2-yl)-*N*-phenylbenzamide (29b): White solid; yield: 95 mg

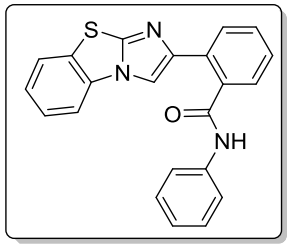

(70%); mp 145–147 °C; ^{1}H NMR (400 MHz, $CDCl_3$) δ 9.16 (s, 1H), 7.92 (s, 1H), 7.80 – 7.72 (m, 2H), 7.68 – 7.63 (m, 3H), 7.55 (d, J = 7.9 Hz, 1H), 7.48 – 7.41 (m, 2H), 7.36 (m, 4H), 7.13 (t, J = 7.4 Hz, 1H); ^{13}C NMR (100 MHz, $CDCl_3$) δ 168.1, 147.5, 145.4, 138.5, 135.6, 132.0, 131.0, 130.2, 130.1, 129.8, 129.0, 128.9, 128.9, 128.0, 126.4, 125.2, 124.3, 120.0, 113.0, 110.2; HRMS (ESI-TOF) (*m/z*) calculated $C_{22}H_{16}N_3OS^+$: 370.1014; found 370.1022 $[M+H]^+$.

2-(6-Bromoimidazo[1,2-*a*]pyridin-2-yl)-*N*^{1},*N*^{3}-diphenylisophthalamide (25a') : White solid;

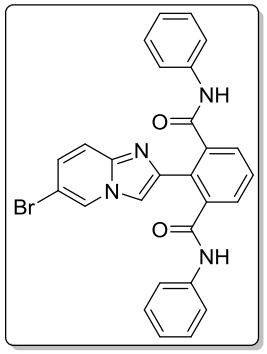

yield: 31 mg (25%); mp 240–242 °C; ^{1}H NMR (400 MHz, DMSO-d_6) δ 10.30 (s, 2H), 8.97 (d, J = 1.1 Hz, 1H), 8.03 (s, 1H), 7.70 – 7.67 (m, 2H), 7.63 – 7.59 (m, 1H), 7.54 (d, J = 7.7 Hz, 4H), 7.39 (d, J = 9.6 Hz, 1H), 7.29 – 7.24 (m, 5H), 7.04 (t, J = 7.4 Hz, 2H); ^{13}C NMR (100 MHz, DMSO-d_6) δ 167.7, 142.7, 142.6, 139.5, 139.3, 129.8, 129.0, 128.9, 128.3, 127.9, 127.3, 123.9, 120.3, 118.1, 112.8, 106.3; HRMS (ESI-TOF) (*m/z*) calculated $C_{27}H_{20}BrN_4O_2^+$: 511.0769; found 511.0778 $[M+H]^+$ and 513.0924 $[M+H+2]^+$.

2-(Imidazo[2,1-*b*]thiazol-6-yl)-*N*^{1},*N*^{3}-diphenylisophthalamide (29a'): Yellow solid; yield: 24

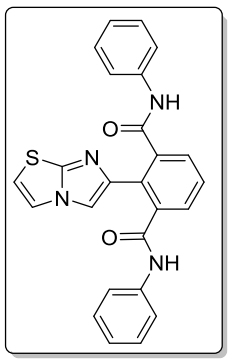

mg (18%); mp 224–225 °C; ^{1}H NMR (400 MHz, DMSO-d_6) δ 10.27 (s, 2H), 7.92 (d, J = 4.5 Hz, 1H), 7.83 (s, 1H), 7.64 – 7.60 (m, 2H), 7.60 – 7.52 (m, 5H), 7.28 (t, J = 7.9 Hz, 4H), 7.16 (d, J = 4.5 Hz, 1H), 7.05 (t, J = 7.4 Hz, 2H); ^{13}C NMR (100 MHz, DMSO-d_6) δ 167.9, 148.5, 142.8, 139.6, 139.0, 130.0, 128.9, 128.7, 127.6, 123.8, 120.3, 120.2, 113.2, 112.6; HRMS (ESI-TOF) (*m/z*) calculated $C_{25}H_{19}N_4O_2S^+$: 439.1228; found 439.1236 $[M+H]^+$.

2-(Imidazo[1,2-*a*]pyrimidin-2-yl)-*N*^{1},*N*^{3}-diphenylisophthalamide (31a'): Yellow solid; yield: 127 mg (80%); mp 273–275 °C; ^{1}H NMR (400 MHz, DMSO-d_6) δ 10.40 (s, 2H), 9.04 – 8.98 (m, 1H), 8.42 (d, J = 1.9 Hz, 1H), 8.00 (s, 1H), 7.70 (d, J = 7.4 Hz, 2H), 7.66 – 7.61 (m, 1H), 7.57 (d, J = 7.9 Hz, 4H), 7.27 (t, J = 7.7 Hz, 4H), 7.04 (t, J = 7.3 Hz, 2H), 6.98 (dd, J = 6.5, 4.2 Hz, 1H); ^{13}C NMR (100 MHz, DMSO-d_6) δ 167.7, 150.5, 147.4, 143.0, 139.6, 139.4, 135.4, 130.0, 129.0, 128.9, 128.4, 124.0, 120.3, 110.7, 109.3; HRMS (ESI-TOF) (*m/z*) calculated $C_{26}H_{20}N_5O_2^+$: 434.1617; found 434.1625 $[M+H]^+$.

Procedure for synthesis of complex C$_3$: A mixture of 6-methyl-2-(*p*-tolyl)imidazo[1,2-*a*]pyridine (**24d**) (0.040 g, 0.17 mmol), $[RuCl_2$-(*p*-cymene)$]_2$, (0.070 g, 0.11 mmol), KPF_6 (3 equiv.) in dichloroethane (5 mL) was stirred for 12 h at room temperature under nitrogen atmosphere. After filtration through celite, the solvent was concentrated under reduced pressure, and the residue was washed with Et_2O (15 mL × 5) to yield partially purified complex **C$_3$**. ESI-MS (*m/z*) calculated $C_{25}H_{27}N_2Ru^+$: 457.1217; found 457.1382 $[M-Cl]^+$.

3B.4 X-ray Crystallography Studies

Initial crystal evaluation and data collection were performed on a Kappa APEX II diffractometer equipped with a CCD detector (with the crystal-to-detector distance fixed at 60 mm) and sealed-tube monochromated MoKα radiation using the program APEX2.[72] By using the program SAINT[72] for the integration of the data, reflection profiles were fitted, and values of F^2 and $\sigma(F^2)$ for each reflection were obtained. Data were also corrected for Lorentz and polarization effects. The subroutine XPREP[72] was used for the processing of data that included determination of space group, application of an absorption correction (SADABS)[72] merging of data, and generation of files necessary for solution and refinement. The crystal structures were solved and refined using SHELX 97.[73] The space group was chosen based on systematic absences and confirmed by the successful refinement of the structure. Positions of most of the non-hydrogen atoms were obtained from a direct methods solution. Several full-matrix least-squares/difference Fourier cycles were performed, locating the remainder of the non-hydrogen atoms. All non-hydrogen atoms were refined with anisotropic displacement parameters. All hydrogen atoms were placed in ideal positions and refined as riding atoms with individual isotropic displacement parameters. All figures were drawn using MERCURY V 3.0[74] and Platon.[75]

3B.4.1 Crystallographic data of 25d (CCDC No. 1501223)

$C_{22}H_{18}ClN_3O$, M_r = 375.84, monoclinic, space group P21/c, a = 10.8372(10) Å, b = 10.5719(5) Å, c = 16.5469(8) Å, α = 90°, β = 90.413(1)°, γ = 90°, V = 1895.7(2) Å3, Z = 4, D_c = 1.317 Mg/cm^3, μ(Mo K_α) = 0.218 mm^{-1}, T = 296(2) K, 48825 reflections collected. Refinement of 2619 reflections (246 parameters) with I > 2σ(I) converged at a final R1 = 0.046, wR2 = 0.1098, and GOF = 1.057.

3B.5 References

(1) Chen, Z.; Wang, B.; Zhang, J.; Yu, W.; Liu, Z.; Zhang, Y. *Organic Chemistry Frontiers* **2015**, *2*, 1107-1295.

(2) Colby, D. A.; Bergman, R. G.; Ellman, J. A. *Chemical Reviews* **2009**, *110*, 624-655.

(3) Colby, D. A.; Tsai, A. S.; Bergman, R. G.; Ellman, J. A. *Accounts of Chemical Research* **2011**, *45*, 814-825.

(4) Ackermann, L.; Lygin, A. V. *Organic Letters* **2012**, *14*, 764-767.

(5) Zhang, M.; Zhang, Y.; Jie, X.; Zhao, H.; Li, G.; Su, W. *Organic Chemistry Frontiers* **2014**, *1*, 843-895.

(6) Sehnal, P.; Taylor, R. J. K.; Fairlamb, I. J. S. *Chemical Reviews* **2010**, *110*, 824-889.

(7) Ackermann, L. *Chemical Reviews* **2011**, *111*, 1315-1345.

(8) Daugulis, O.; Zaitsev, V. G.; Shabashov, D.; Pham, Q. -N.; Lazareva, A. *Synlett*, **2006**, 3382-3388.

(9) Li, S.-S.; Qin, L.; Dong, L. *Organic & Biomolecular Chemistry* **2016**, *14*, 4554-4570.

(10) Song, G.; Li, X. *Accounts of Chemical Research* **2015**, *48*, 1007-1020.

(11) Lewis, J. C.; Bergman, R. G.; Ellman, J. A. *Accounts of Chemical Research* **2008**, *41*, 1013-1025.

(12) Fagnou, K.; Lautens, M. *Chemical Reviews* **2003**, *103*, 169-196.

(13) Song, G.; Wang, F.; Li, X. *Chemical Society Reviews* **2012**, *41*, 3651-3678.

(14) Liu, P. M.; Frost, C. G. *Organic Letters* **2013**, *15*, 5862-5865.

(15) Park, Y.; Jeon, I.; Shin, S.; Min, J.; Lee, P. H. *The Journal of Organic Chemistry* **2013**, *78*, 10209-10220.

(16) Banerjee, A.; Santra, S. K.; Mohanta, P. R.; Patel, B. K. *Organic Letters* **2015**, *17*, 5678-5681.

(17) Ackermann, L.; Lygin, A. V. *Organic Letters* **2011**, *13*, 3332-3335.

(18) Ackermann, L.; Diers, E.; Manvar, A. *Organic Letters* **2012**, *14*, 1154-1157.

(19) Reddy, M. C.; Jeganmohan, M. *Chemical Communications* **2015**, *51*, 10738-10741.

(20) Ziriakus, J.; Pöthig, A.; Drees, M.; Haslinger, S.; Jantke, D.; Kühn, F. E. *Advanced Synthesis & Catalysis* **2013**, *355*, 2845-2859.

(21) Reddy, M. C.; Jeganmohan, M. *European Journal of Organic Chemistry* **2013**, 1150-1157.

(22) Shvo, Y.; Czarkie, D.; Rahamim, Y.; Chodosh, D. F. *Journal of the American Chemical Society* **1986**, *108*, 7400-7402.

(23) Barf, G.; Sheldon, R. *Journal of Molecular Catalysis A: Chemical* **1995**, *102*, 23-39.

(24) Dinger, M. B.; Mol, J. C. *Organometallics* **2003**, *22*, 1089-1095.

(25) Yang, D.; Zhang, C. *The Journal of Organic Chemistry* **2001**, *66*, 4814-4818.

(26) Csjernyik, G.; Éll, A. H.; Fadini, L.; Pugin, B.; Bäckvall, J.-E. *The Journal of Organic Chemistry* **2002**, *67*, 1657-1662.

(27) Hoveyda, A. H.; Zhugralin, A. R. *Nature* **2007**, *450*, 243-251.

(28) Grubbs, R. H.; Trnka, T. M. *Ruthenium in Organic Synthesis* **2004**, 153-177.

(29) Manikandan, R.; Jeganmohan, M. *Organic Letters* **2014**, *16*, 912-915.

(30) Ackermann, L. *Accounts of Chemical Research* **2013**, *47*, 281-295.

(31) Ackermann, L.; Novak, P.; Vicente, R.; Hofmann, N. *Angewandte Chemie International Edition* **2009**, *48*, 6045-6048.

(32) Deng, G.; Zhao, L.; Li, C. J. *Angewandte Chemie International Edition* **2008**, *47*, 6278-6282.

(33) Imm, S.; Bähn, S.; Zhang, M.; Neubert, L.; Neumann, H.; Klasovsky, F.; Pfeffer, J.; Haas, T.; Beller, M. *Angewandte Chemie International Edition* **2011**, *50*, 7599-7603.

(34) Chen, C.; Zhang, Y.; Hong, S. H. *The Journal of Organic Chemistry* **2011**, *76*, 10005-10010.

(35) Murahashi, S.-I.; Komiya, N.; Terai, H.; Nakae, T. *Journal of the American Chemical Society* **2003**, *125*, 15312-15313.

(36) Liu, W.; Ackermann, L. *Organic Letters* **2013**, *15*, 3484-3486.

(37) Wang, W.; Liang, L.; Xu, F.; Huang, W.; Niu, Y.; Sun, Q.; Xu, P. *European Journal of Organic Chemistry* **2014**, *2014*, 6863-6867.

(38) De Sarkar, S.; Liu, W.; Kozhushkov, S. I.; Ackermann, L. *Advanced Synthesis & Catalysis* **2014**, *356*, 1461-1479.

(39) Zhu, R. Y.; Farmer, M. E.; Chen, Y. Q.; Yu, J. Q. *Angewandte Chemie International Edition* **2016**, *55*, 10578–10599.

(40) Murai, S.; Kakiuchi, F.; Sekine, S.; Tanaka, Y.; Kamatani, A.; Sonoda, M.; Chatani, N. *Nature* **1993**, *366*, 529-531.

(41) Ackermann, L.; Althammer, A.; Born, R. *Angewandte Chemie International Edition* **2006**, *45*, 2619-2622.

(42) Ackermann, L.; Lygin, A. V.; Hofmann, N. *Angewandte Chemie International Edition* **2011**, *123*, 6503-6506.

(43) Tlili, A.; Schranck, J.; Pospech, J.; Neumann, H.; Beller, M. *Angewandte Chemie International Edition* **2013**, *52*, 6293-6297.

(44) Nan, J.; Zuo, Z.; Luo, L.; Bai, L.; Zheng, H.; Yuan, Y.; Liu, J.; Luan, X.; Wang, Y. *Journal of the American Chemical Society* **2013**, *135*, 17306-17309.

(45) Li, B.; Dixneuf, P. H. *Chemical Society Reviews* **2013**, *42*, 5744-5767.

(46) Kozhushkov, S. I.; Ackermann, L. *Chemical Science* **2013**, *4*, 886-896.

(47) Arockiam, P. B.; Fischmeister, C.; Bruneau, C.; Dixneuf, P. H. *Angewandte Chemie International Edition* **2010**, *122*, 6779-6782.

(48) Ackermann, L.; Althammer, A.; Born, R. *Angewandte Chemie International Edition* **2006**, *118*, 2681-2685.

(49) Muralirajan, K.; Parthasarathy, K.; Cheng, C.-H. *Organic Letters* **2012**, *14*, 4262-4265.

(50) Hesp, K. D.; Bergman, R. G.; Ellman, J. A. *Journal of the American Chemical Society* **2011**, *133*, 11430-11433.

(51) De Sarkar, S.; Ackermann, L. *Chemistry- A European Journal* **2014**, *20*, 13932-13936.

(52) Shi, X. Y.; Liu, K. Y.; Fan, J.; Dong, X. F.; Wei, J. F.; Li, C. J. *Chemistry- A European Journal* **2015**, *21*, 1900-1903.

(53) Shi, X. Y.; Renzetti, A.; Kundu, S.; Li, C. J. *Advanced Synthesis & Catalysis* **2014**, *356*, 723-728.

(54) Geng, X.; Wang, C. *Organic & Biomolecular Chemistry* **2015**, *13*, 7619-7623.

(55) Kuninobu, Y.; Tokunaga, Y.; Kawata, A.; Takai, K. *Journal of the American Chemical Society* **2006**, *128*, 202-209.

(56) Liu, W.; Bang, J.; Zhang, Y.; Ackermann, L. *Angewandte Chemie International Edition* **2015**, *127*, 14343-14346.

(57) Hummel, J. R.; Ellman, J. A. *Organic Letters* **2015**, *17*, 2400-2403.

(58) Jeong, T.; Han, S.; Mishra, N. K.; Sharma, S.; Lee, S. -Y.; Oh, J. S.; Kwak, J. H.; Jung, Y. H.; Kim, I. S. *The Journal of Organic Chemistry* **2015**, *80*, 7243-7250.

(59) Han, S.; Mishra, N. K.; Sharma, S.; Park, J.; Choi, M.; Lee, S. -Y.; Oh, J. S.; Jung,Y. H.; Kim, I. S. *The Journal of Organic Chemistry* **2015**, *80*, 8026-8035.

(60) Liu, W.; Bang, J.; Zhang, Y.; Ackermann, L. *Angewandte Chemie International Edition* **2015**, *54*, 14137-14140.

(61) Parhi, A. K.; Zhang, Y.; Saionz, K. W.; Pradhan, P.; Kaul, M.; Trivedi, K.; Pilch, D. S.; LaVoie, E. J. *Bioorganic & Medicinal Chemistry Letters* **2013**, *23*, 4968-4974.

(62) Abe, Y.; Kayakiri, H.; Satoh, S.; Inoue, T.; Sawada, Y.; Inamura, N.; Asano, M.; Aramori, I.; Hatori, C.; Sawai, H. *Journal of Medicinal Chemistry* **1998**, *41*, 4587-4598.

(63) Harrison, T. S.; Keating, G. M. *CNS drugs* **2005**, *19*, 65-89.

(64) Almirante, L.; Polo, L.; Mugnaini, A.; Provinciali, E.; Rugarli, P.; Biancotti, A.; Gamba, A.; Murmann, W. *Journal of Medicinal Chemistry* **1965**, *8*, 305-312.

(65) Wafford, K.; Van Niel, M.; Ma, Q.; Horridge, E.; Herd, M.; Peden, D.; Belelli, D.; Lambert, J. *Neuropharmacology.* **2009**, *56*, 182-189.

(66) Pethe, K.; Bifani, P.; Jang, J.; Kang, S.; Park, S.; Ahn, S.; Jiricek, J.; Jung, J.; Jeon, H. K.; Cechetto, J. *Natural Medicine* **2013**, *19*, 1157-1160.

(67) Toga, T.; Kohmura, Y.; Kawatsu, R. *Journal of Pharmacological Sciences* **2007**, *105*, 207-210.

(68) Manikandan, R.; Madasamy, P.; Jeganmohan, M. *ACS Catalysis* **2015**, *6*, 230-234.

(69) Chinnagolla, R. K.; Vijeta, A.; Jeganmohan, M. *Chemical Communications* **2015**, *51*, 12992-12995.

(70) Sawant, D.; Singh, I.; Tulsyan, G.; Abbagani, K.; Pardasani, R. T. *Synlett* **2015**, *26*, 1671-1676.

(71) Padwa, A.; Crawford, K. R.; Rashatasakhon, P.; Rose, M. *The Journal of Organic Chemistry* **2003**, *68*, 2609-2617.

(72) *APEX2*, *SADABS and SAINT*; Bruker AXS inc: Madison, WI, USA, **2008**.

(73) Sheldrick, G. M., *Acta Crystallographica* **2008**, *A64*, 112-122.

(74) Macrae, C. F.; Bruno, I. J.; Chisholm, J. A.; Edginton, P. R.; McCabe, P.; Pidocck, E.; Rodriguez Monge, L.; Taylor, T.; Van de Streek, J.; Wood, P. A *Journal of Applied Crystallography* **2008**, *41*, 466-470.

(75) Spek, A. L. *PLATON, Version 1.62*, University of Utrecht, **1999.**

CHAPTER 4A

Transition Metal-Free Homocoupling of Imidazo-Heterocycles *via* Csp^2–Csp^2 Bond Formation

4A.1 Introduction

Oxidative C–H bond functionalization is the most fascinating and atom-economic process for preparing pharmaceutically and medicinally important compounds in due diligence of sustainable chemistry.[1-4] In this context, transition-metal catalysis plays an unbeatable role,[4-10] however the high cost and toxicity of the heavy metals have fetched the attention of organic chemists toward developing metal-free oxidative C–C bond-forming strategies.[11-13]

In this regard, hypervalent iodine (III) reagents have emerged as elegant and powerful tool for the construction of a plethora of bioactive heterocyclic compounds and natural products.[14-17] The hypervalent iodine (III) reagents are the compounds of iodine in higher oxidation states.[18-20] Even though the oxidizing properties of hypervalent iodine compounds were known since 1893, a renaissance in the field of polyvalent iodine reagents have occurred only in the last two decades.[16,21] This rising fame of hypervalent iodine reagents is because of (i) resemblance of its structure and reactivity with the transition-metal complexes, (ii) ready accessibility, (iii) reduced toxicity, (iv) high reactivity, (v) easy handling (vi) impressive functional group tolerance, and (vii) environmentally benign nature.[19,22,23] Iodine in iodine(III) reagents (aryl-λ^3–iodanes) has a total of ten electrons, and the overall geometry is distorted pseudotrigonal bipyramidal with two heteroatoms ligands (L) occupying the apical positions and the least electronegative carbon ligand and two electron pairs residing in equatorial positions (Figure 4A.1.1).[24,25]

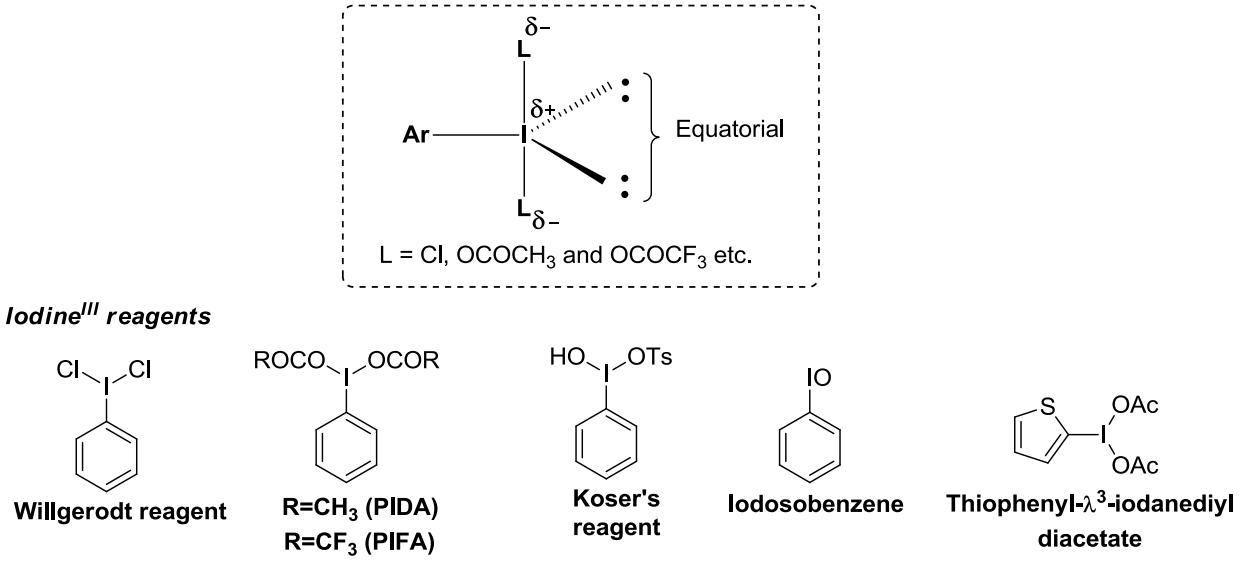

Figure 4A.1.1: Pseudotrigonal bipyramidal structure of aryl-λ^3-iodanes and some commercially available hypervalent iodine (III) reagents

The trivalent organoiodine reagents such as dichloroiodobenzene ($PhICl_2$), diphenyliodine(III) diacetate (PIDA), phenyliodine(III)-bis(trifluoroacetate) (PIFA), iodosobenzene (PhIO), and [hydroxyl(tosyloxy)iodo]benzene(HTIB, Koser's reagent) (Figure 4A.1.1) have been widely utilized in an array of organic reactions including, acetoxylation, oxidative halogenation, oxidative functionalization of unsaturated compounds, arylation, oxidative cationic cyclization, oxidative rearrangements leading to the formation of new carbon–carbon, carbon–heteroatom, and heteroatom–heteroatom bonds (Figure 4A.1.2).[14,18,26-37]

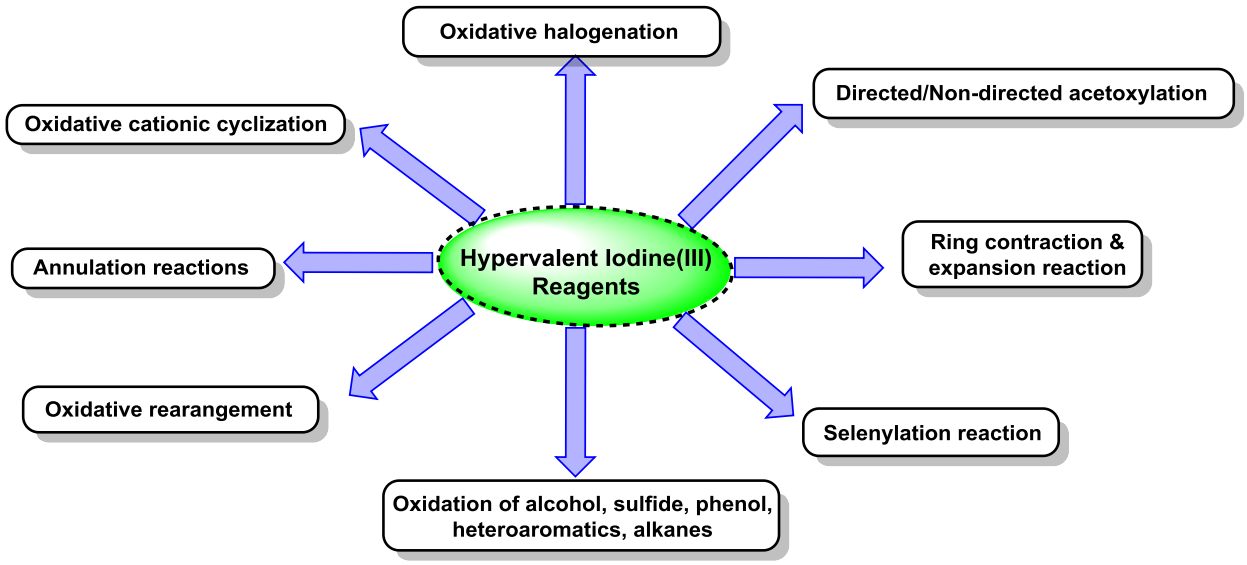

Figure 4A.1.2: Application of hypervalent iodine (III) reagents in various organic transformations

Within the realm of direct oxidative coupling, the $Csp^2–Csp^2$ bond-formation has been immensely explored among all other types of C-C bond forming reactions. Significant contributions have been made towards this end by exploring the reactivity of several metal catalysts ever since the first report on oxidative dimerization of aromatic compounds in 1871. Recently, oxidative biheteroaryl formation has received much citation, and numerous direct homocoupling strategies have been successfully developed with different arenes,[38-42] and (hetero)arenes such as thiophene, indole, indolizine, azole, pyrrole, quinoline, isoquinoline and quinoxaline under metal-catalyzed and metal-free conditions. The occurrence of some of the (hetero)arenes such as bibenzofurans, bipyridines, bi(cyclopenta[*b*]indoles), bipyrroles, bis(pyrido[3,4,5-*kl*]acridinones), biindoles in natural products, pharmaceuticals, and

agrochemicals provided a rationale for such enormous studies to different organic chemists (Figure 4A.1.3).[43,44]

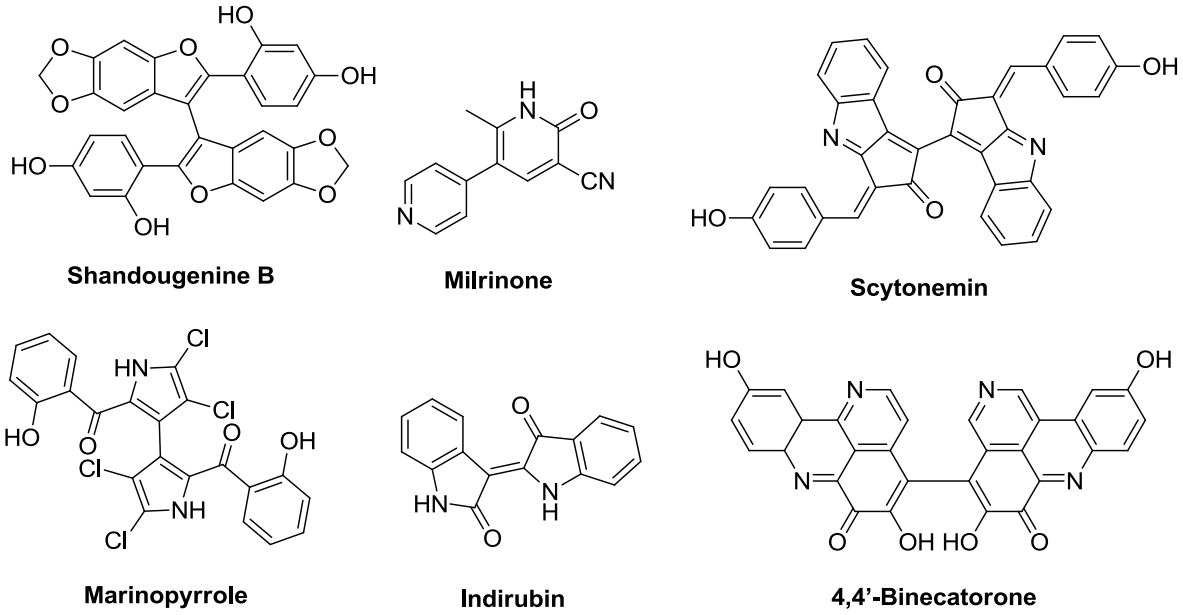

Figure 4A.1.3: Selective examples of biologically active biheteroarenes

In 2004, Mori *et al.* reported the Pd-catalyzed homocoupling of substituted thiophene and benzothiophene (**1**) at the C-2 positions using silver salts AgF/$AgOCOCH_3$ as reaction activators under ambient conditions.[45] Later, the authors developed another cheap activator system, $AgNO_3$/KF for the same chemical transformation (Scheme 4A.1.1).[46]

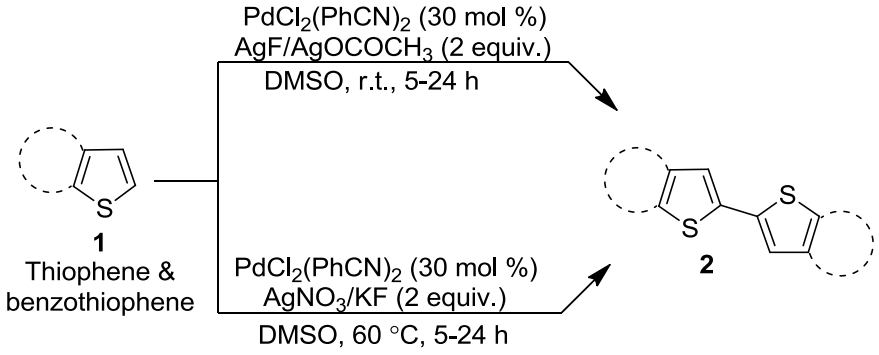

Scheme 4A.1.1: Pd-catalyzed homocoupling of thiophenes and benzothiophenes (**1**)

Tse *et al.* reported a Au-catalyzed strategy for the oxidative homocoupling of 2-methylthiophene (**3**) in 31% yield using $PhI(OAc)_2$ in acetic acid (Scheme 4A.1.2).[47]

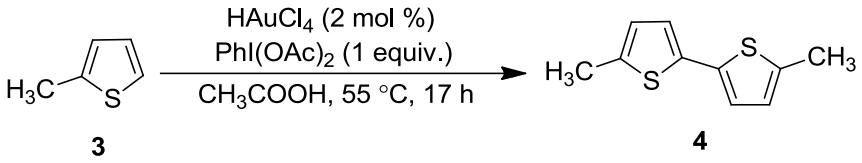

Scheme 4A.1.2: Au-catalyzed oxidative homocoupling of 2-methylthiophene (**3**)

Wang *et al.* presented a high-yielding approach for Pd-catalyzed intermolecular direct C−H homocoupling of thiophenes (**3**) and furans (**5**) using molecular oxygen as the oxidant with TFA in DMSO (Scheme 4A.1.3).[48]

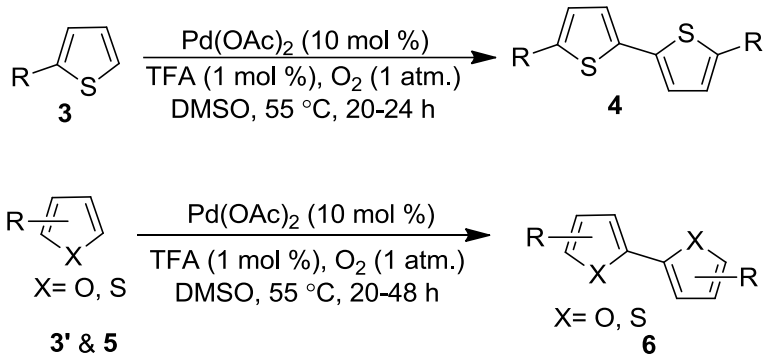

Scheme 4A.1.3: Pd-catalyzed homocoupling of thiophenes (**3**, **3′**) and furans (**5**)

Pd-catalyzed oxidative homocoupling of *N*-substituted indoles **7** was regioselectively achieved by Zhang and coworkers, affording 2,3′-biindoles (**8**) derivatives in high yields using stoichiometric amount of $Cu(OAc)_2.3H_2O$ in DMSO at room temperature (Scheme 4A.1.4a).[49] On the other hand, Shi and coworkers reported oxidative dimerization of *N*-protected and free indoles **7,** affording 3,3'-biindoles (**9**) *via* Pd-catalyzed direct C-H bond activation using $AgNO_3/MgSO_4$ (Scheme 4A.1.4b).[50]

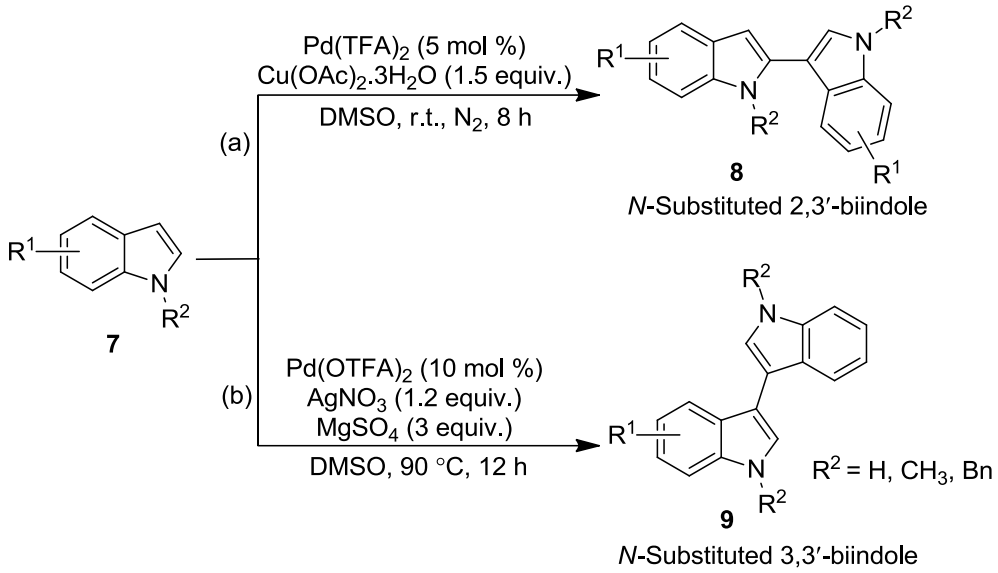

Scheme 4A.1.4: Pd-catalyzed regioselective homocoupling of indoles (**7**)

You *et al.* documented an oxidative Pd-catalyzed approach for homocoupling of indolizines (**10**) to obtain the corresponding biindolizines **11** in good-to-excellent yields using $Cu(OAc)_2$ as an external oxidant. The methodology provides good regioselectivity with broad functional group tolerance (Scheme 4A.1.5).[51]

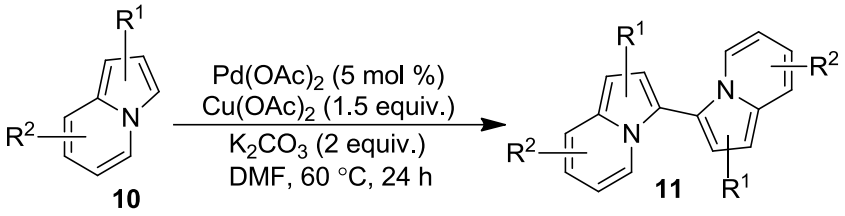

Scheme 4A.1.5: Pd-catalyzed oxidative homocoupling of indolizines (**10**)

Oxidative dimerization of several azole derivatives such as imidazole, thiazole, and oxazole (**12**) *via* copper(II)/silver(I)-catalyzed C-H activation was competently described by Mori *et al.* in 2010, under oxygen atmosphere in xylene at 140 °C (Scheme 4A.1.6a).[52] Subsequently in the same year, Bao and coworkers also employed $Cu(OAc)_2$ for the same transformation without using silver salt under similar reaction conditions, affording the corresponding dimerized product of imidazoles, benzimidazoles, thiazoles, oxadiazoles and benzoxazoles in good-to-excellent yields (**12**) (Scheme 4A.1.6b).[53] Notably, Yamaguchi group reported dimerization of aforementioned azoles (**12**) in an efficient process by using CuCl/2-pyridonate catalytic system (Scheme 4A.1.6c).[54] Daugulis *et al.* presented a deprotonative hetero-arene dimerization using

cobalt, iron, nickel, and manganese catalysis employing oxygen as the oxidant (Scheme 4A.1.6.d).[55]

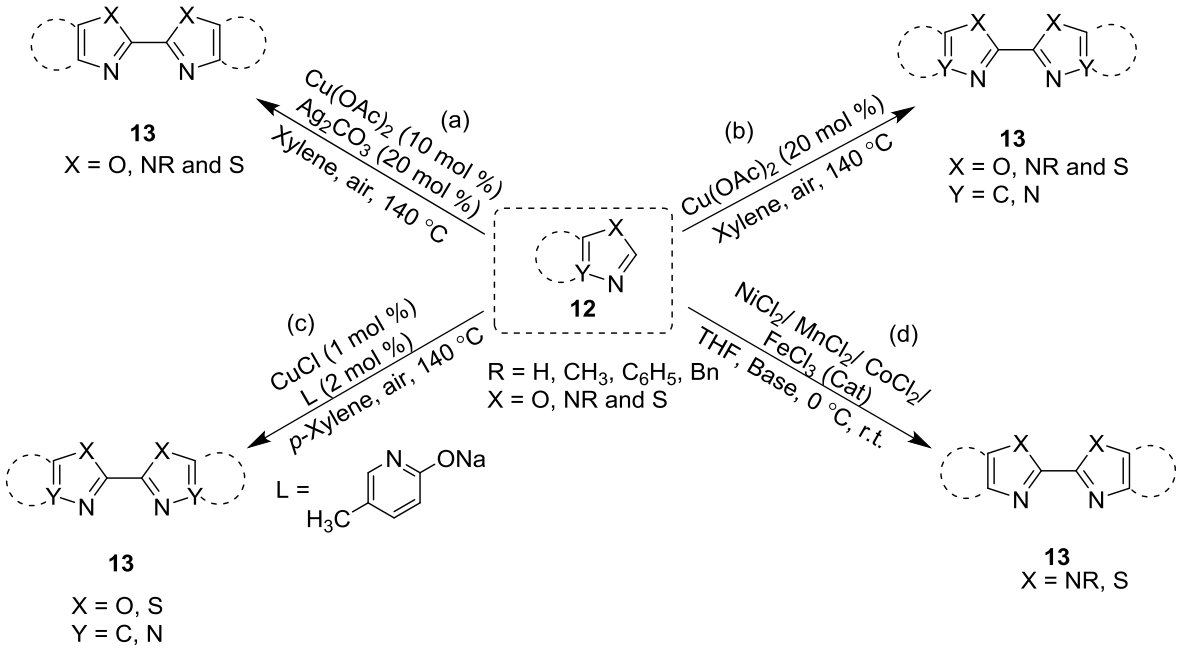

Scheme 4.1.6: Transition metal-catalyzed dimerization of azoles (**12**)

Till date, only a few strategies have been developed for the homocoupling of heterocyclic frameworks under metal-free conditions over the existing metal-catalyzed dimerization protocols. However, the development of metal-free Iodine and hypervalent iodine-induced strategies are gearing up in recent times. Kita and coworkers developed an unprecedented oxidative coupling strategy for the head-to-tail dimerization of alkyl thiophenes **(3)** to selectively obtain 2,2′-bithiophenes (**4**) using phenyliodine bis(trifluoroacetate) (PIFA) in the presence of Lewis acid and trimethylsilyl trifluoromethanesulfonate in DCM (Scheme 4A.1.7a).[56] Later, the authors also reported a regioselective synthesis of head-to-tail affixed unsymmetrical bithiophenes **4** using PhI(OH)OTs (HTIB) reagent in the presence of TMSBr in $(CF_3)_2CHOH$ (HFIP) (Scheme 4A.1.7b).[57]

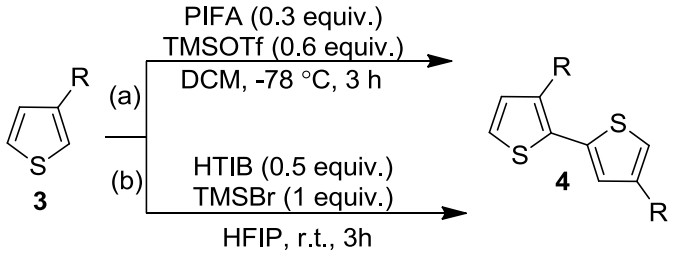

Scheme 4A.1.7: Hypervalent iodine(III) reagent-mediated dimerization of thiophenes (**3**)

Similarly, phenyliodine bis(trifluoroacetate) (PIFA) was efficiently used by Kita *et al.* for the oxidative homocoupling reaction of electron-rich pyrroles (**14**) and indoles (**7**) in presence of TMSBr, affording their corresponding bipyrroles (**15**) and biindoles **16** under described conditions (Scheme 4A.1.8).[58]

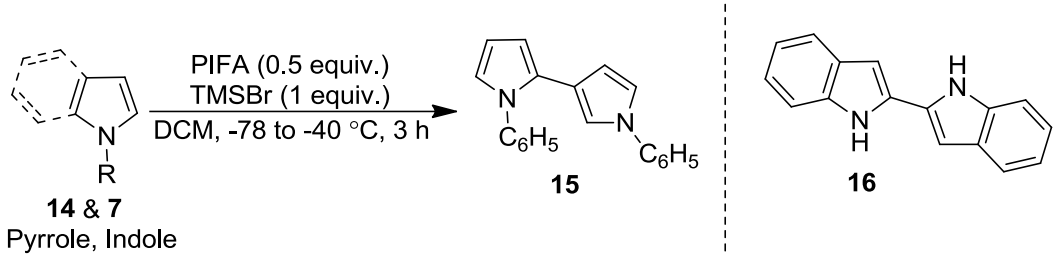

Scheme 4A.1.8: PIFA-mediated oxidative homocoupling reaction of pyrroles (**14**) and indoles (**7**)

Similarly, metal-free intermolecular oxidative dehydrogenative 3,3′-coupling of 2-arylbenzo[*b*]furans (**17**) and 2-arylbenzo[*b*]thiophenes (**18**) was successfully achieved by Helaja and coworkers by using 2,3-dichloro-5,6-dicyano-1,4-quinone (DDQ) in presence of MsOH, yielding bibenzofurans (**19**) and bibenzothiophenes (**20**) (Scheme 4A.1.9).[44]

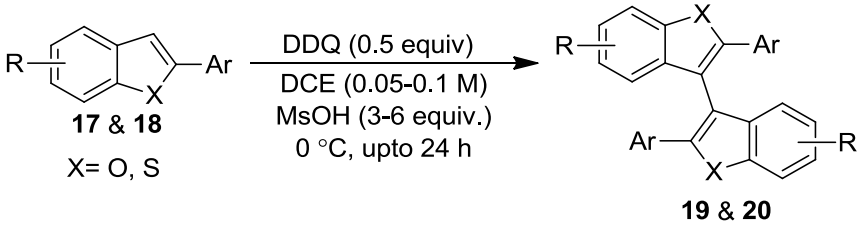

Scheme 4A.1.9: DDQ-induced homocoupling of 2-aryl-benzo[*b*]furans (**17**) and 2-aryl-benzo[*b*]thiophenes (**18**)

Da and coworkers elegantly explored the use of 2,2,6,6-tetramethylpiperidinylmagnesium chloride (TMPMgCl) for the first time towards the direct homocoupling of various electron-deficient azaarenes including quinolines (**21**), isoquinolines (**22**), and quinoxalines (**23**) using tetramethylethylenediamine (TMEDA), affording their corresponding dimerized products (**24-26**) in moderate-to-good yields (Scheme 4A.1.10).[59]

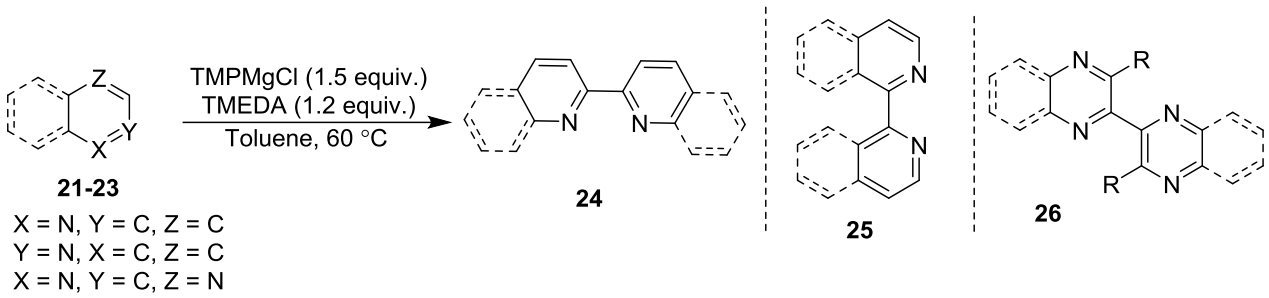

Scheme 4A.1.10: TMPMgCl-promoted homocoupling of various electron-deficient azaarenes (**21**-**23**)

The fascinating biological profiles of the above described bis-heterocycles have drawn the attention of Cao *et al.* towards developing regioselective Cu(I)-catalyzed strategy for intermolecular direct C–H homocoupling of imidazo[1,2-*a*]pyridines (**27**) at the C-3 position using 2,2′-bipyridine as ligand in DMSO in good-to-excellent yields (Scheme 4A.1.11).[60]

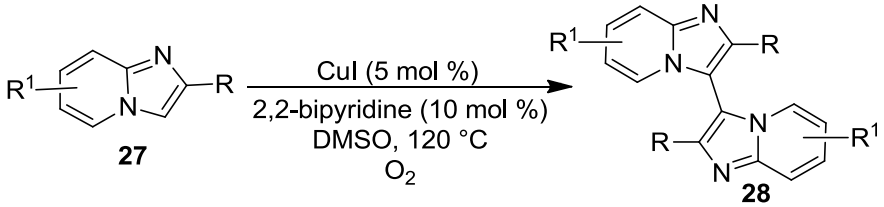

Scheme 4A.1.11: Cu-catalyzed homocoupling of imidazo[1,2-*a*]pyridines (**27**)

Despite some valuable advantages, this homocoupling strategy suffers from certain limitations including the use of metal catalysts, ligands, and high-temperature conditions. As a part of our continuing study on the C–H functionalization of imidazo[1,2-*a*]pyridines, we aimed to develop a complementary transition metal-free strategy for the direct homocoupling of 2-arylimidazo[1,2-*a*]pyridines.

4A.2 Results and Discussion

In contrast to well-exemplified C-3 nucleophilic reactivity of imidazo[1,2-*a*]pyridine, we aimed to explore umpolung reactivity at C-3 for developing a sustainable transition metal-free strategy for synthesizing biimidazo[1,2-*a*]pyridine. Initially, the reaction of 2-phenylimidazo[1,2-*a*]pyridine (**27a**) with 0.5 equiv. of PIDA in 2,2,2-trifluoroethanol (TFE) was carried out at room temperature (Table 4A.2.1). To our delight, the reaction under ambient conditions for 18 h afforded the targeted 2,2′-diphenyl-3,3′-biimidazo[1,2-*a*]pyridine (**28a**) in 32% yield (Table 4A.2.1, entry 1). Interestingly, the use of higher equivalents of PIDA (1 and 1.5 equiv.) under similar conditions increased the isolated yield of **28a** to 50% (Table 4A.2.1,

entries 2 and 3). Unfortunately, when the same reaction was carried out at 50 °C and 80 °C, the yield of **28a** got decreased due to the formation of unidentified by-products (Table A4.2.1, entries 4 and 5). Solvent screening studies showed that the solvent has a crucial role to play in this transformation. Solvents such as CH_3CN, DMF, hexafluoro-2-propanol (HFIP), DCE, and $CHCl_3$ were less effective as compared to 2,2,2-trifluoroethanol (TFE) for the desired transformation (Table 4A.2.1, entries 6–10); however, the use of DCM at room temperature was found to be comparatively better, affording **28a** in 58% yield under the described conditions (Table 4A.2.1, entry 11).

Table 4A.2.1: Selected optimization of reaction conditions for the synthesis of **28a**[a]

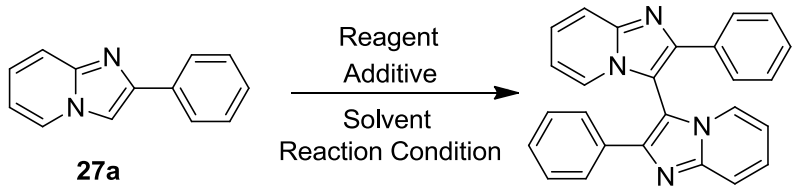

27a **28a**

Entry	Reagent (equiv.)	Additive (equiv.)	Solvent	Yield[b] %
1	$PhI(OAc)_2$ (0.5)	-	TFE	32
2	$PhI(OAc)_2$ (1.0)	-	TFE	46
3	$PhI(OAc)_2$ (1.5)	-	TFE	50
4[c]	$PhI(OAc)_2$ (1.5)	-	TFE	46
5[d]	$PhI(OAc)_2$ (1.5)	-	TFE	42
6	$PhI(OAc)_2$ (1.5)	-	CH_3CN	40
7	$PhI(OAc)_2$ (1.5)	-	DMF	34
8	$PhI(OAc)_2$ (1.5)	-	HFIP	38
9	$PhI(OAc)_2$ (1.5)	-	DCE	49
10	$PhI(OAc)_2$ (1.5)	-	$CHCl_3$	47
11	$PhI(OAc)_2$ (1.5)	-	DCM	58
12	$PhI(O_2CCF_3)_2$ (1.5)	-	DCM	56
13	PhIO (1.5)	-	DCM	28
14	$PhI(OAc)_2$ (1.5)	KI (1)	DCM	43
15	$PhI(OAc)_2$ (1.5)	TBAI (1)	DCM	46
16	**$PhI(OAc)_2$ (1.5)**	**$BF_3.OEt_2$ (0.2)**	**DCM**	**65**
17	$PhI(O_2CCF_3)_2$ (1.5)	$BF_3.OEt_2$ (0.2)	DCM	63

[a]Reaction conditions: 2-Phenylimidazo[1,2-*a*]pyridine (**27a**) (0.2 mmol), oxidant (0.3 mmol), additive, solvent (3 mL), room temperature, 18 h.; [b]Isolated yield; [c]Temperature = 50 °C; [d]Temperature = 80 °C.

In search for a better oxidant for the desired transformation, the use of $PhI(O_2CCF_3)_2$ and PhIO gave **28a** in almost comparable and lower yields, respectively (Table 4A.2.1, entries 12 and 13). In addition, the use of a stoichiometric amount of KI or TBAI as additives under PIDA-mediated

conditions were disappointing (Table 4A.2.1, entries 14 and 15). Gratifyingly, the use of $BF_3.OEt_2$ in catalytic amounts and 1.5 equiv. $PhI(OAc)_2$ in DCM was found to be the optimum reaction condition, affording **28a** in 65% isolated yield (Table 4A.2.1, entry 16). A similar effect was observed for the addition of $BF_3.OEt_2$ and 1.5 equiv. $PhI(O_2CCF_3)_2$ in DCM (Table 4A.2.1,entry 17). No further improvement in the yield of **28a** was observed by increasing the concentration of $BF_3.OEt_2$

With the optimized conditions, the generality of the homocoupling reaction was investigated using a variety of 2-arylimidazo[1,2-*a*]pyridines (**27**) (Scheme 4A.2.1). 2-arylimidazo[1,2-*a*]pyridines bearing a OMe group at the aryl ring showed excellent reactivity, affording the corresponding biimidazo[1,2-*a*]pyridines (**28b-c**) in 69–72% yields. The presence of Me groups either in the aryl or pyridyl ring of **27** resulted in the formation of expected dimers (**28d-e**) in 66% and 59% yields, respectively. Moreover, the presence of Me groups on both the pyridyl and aryl rings also showed a similar reactivity, affording **28f-g** in 65–66% yields, whereas the presence of Me and OMe groups in the pyridyl and aryl rings, respectively, afforded (**28h-i**) in 71 and 74% yields respectively. Interestingly, the presence of two OMe groups on the aryl ring resulted in the formation of **28j** in 78% yield (Scheme 4A.2.1). The introduction of a bulky aryl (naphthyl) or heteroaryl (thienyl) ring at the C-2 position of imidazo[1,2-*a*]pyridine exhibited slightly lower reactivity under the optimized conditions, affording the corresponding dimeric products **28k** and **28l** in 60% and 55% yields, respectively.

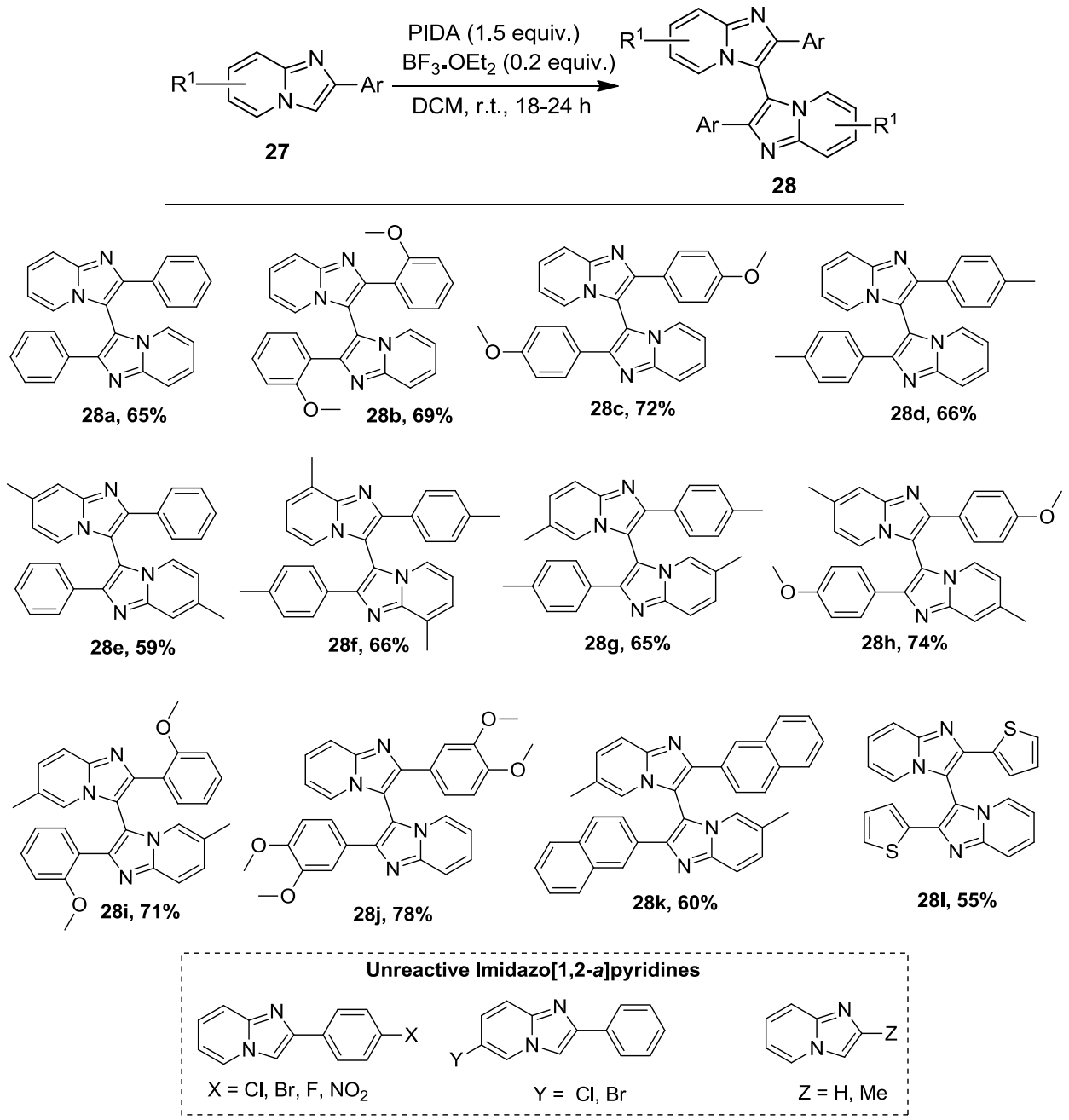

Scheme 4A.2.1: Substrate scope of 2-arylimidazo[1,2-*a*]pyridines (**27**)

Unfortunately, 2-arylimidazo[1,2-*a*]pyridines bearing weak and strong electron-withdrawing groups such as Br, Cl, F, and NO_2 at para position of phenyl ring failed to afford the desired biimidazo[1,2-*a*]pyridines at room temperature or even under reflux conditions (Scheme 4A.2.1). In addition, C-6 chloro- or bromo-substituted 2-arylimidazo[1,2-*a*]pyridines resulted in the trace amount of expected homocoupled products that were not isolated. Although imidazo[1,2-*a*]pyridines possessing aryl group at the C-2 position performed well in this

reaction, unfortunately, unsubstituted and C-2 methyl-substituted imidazo[1,2-*a*]pyridines were found to be completely unreactive, which signifies a crucial necessity of the aryl group at the 2-position under the present conditions (Scheme 4A.2.1). To further extend the scope of our methodology, other imidazo-heterocycles such as 2-arylimidazo[2,1-*b*]thiazole (**29a-b**), and 2-arylbenzo[*d*]imidazo[2,1-*b*]thiazole (**29c**) were allowed to react under optimized conditions. Delightfully, the corresponding biimidazo heteroarenes (**30a**–**c**) were obtained in 57–67% yields (Scheme 4A.2.2).

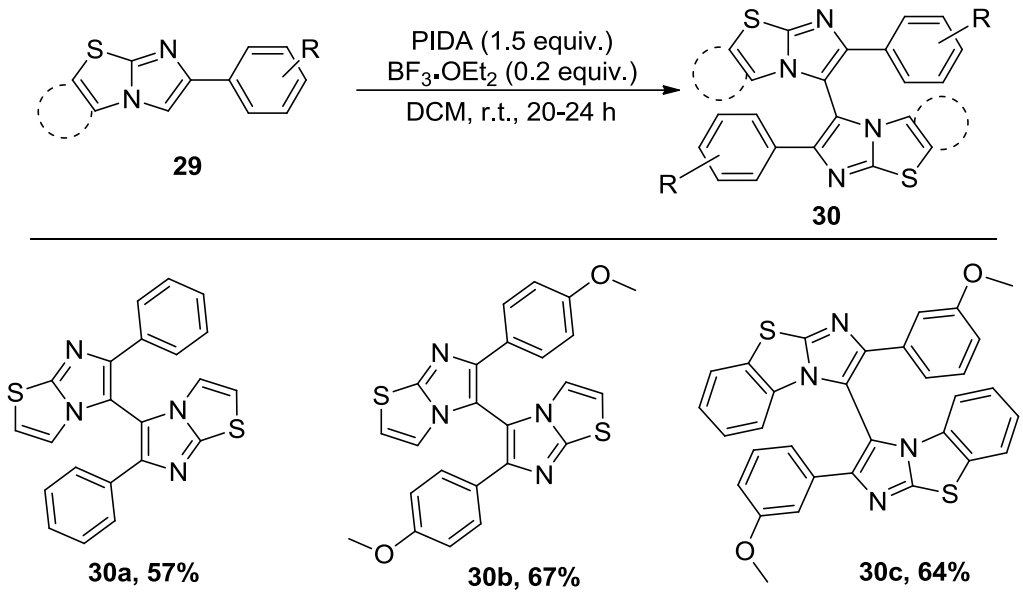

Scheme 4A.2.2: Scope of 2-arylimidazo-heterocycles (**29a-c**)

All the synthesized compounds were isolated by column chromatography and characterized by detailed spectroscopic analysis including ^{1}H and ^{13}C NMR. A representative ^{1}H and ^{13}C NMR spectrums are shown in Figures 4A.2.1 and 4A.2.2, Further to affirm the proposed structure, as a representative example, a single crystal of **30c** was grown in chloroform for X-ray diffraction analysis. Compound **30c** crystallized in the monoclinic space group P21/c. An ORTEP diagram of **30c** is shown in Figure 4A.2.3.

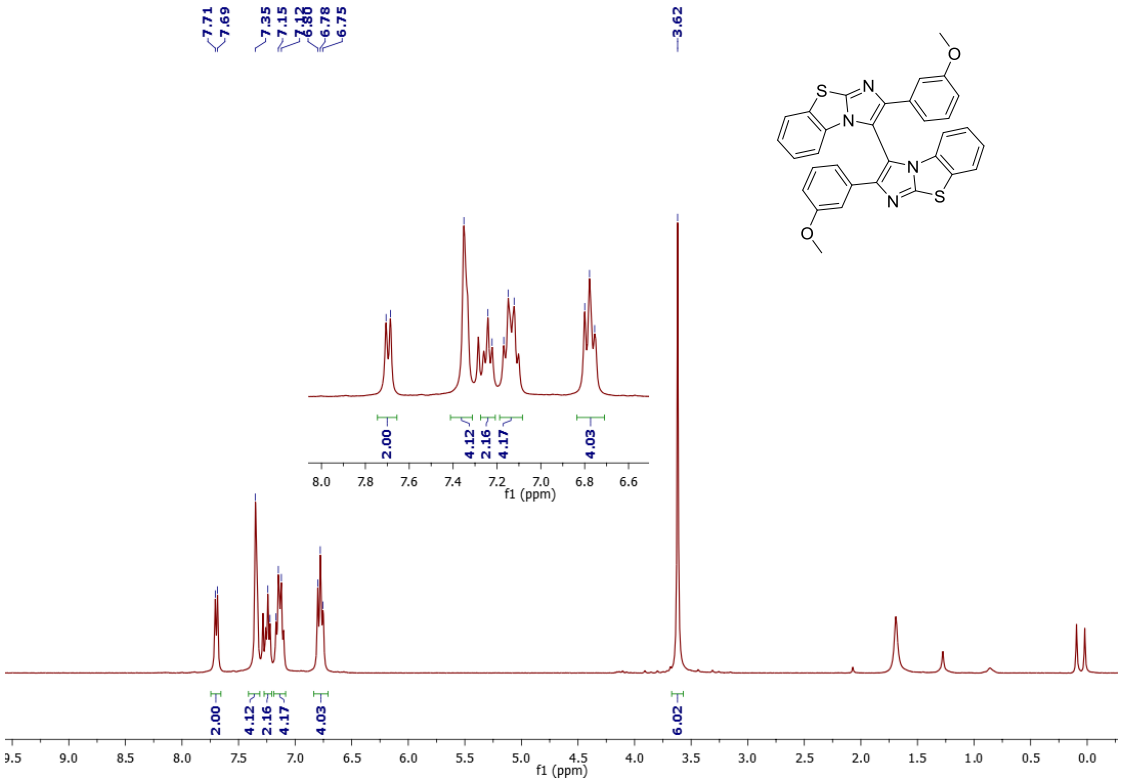

Figure 4A.2.1: ^{1}H NMR spectrum of **30c**

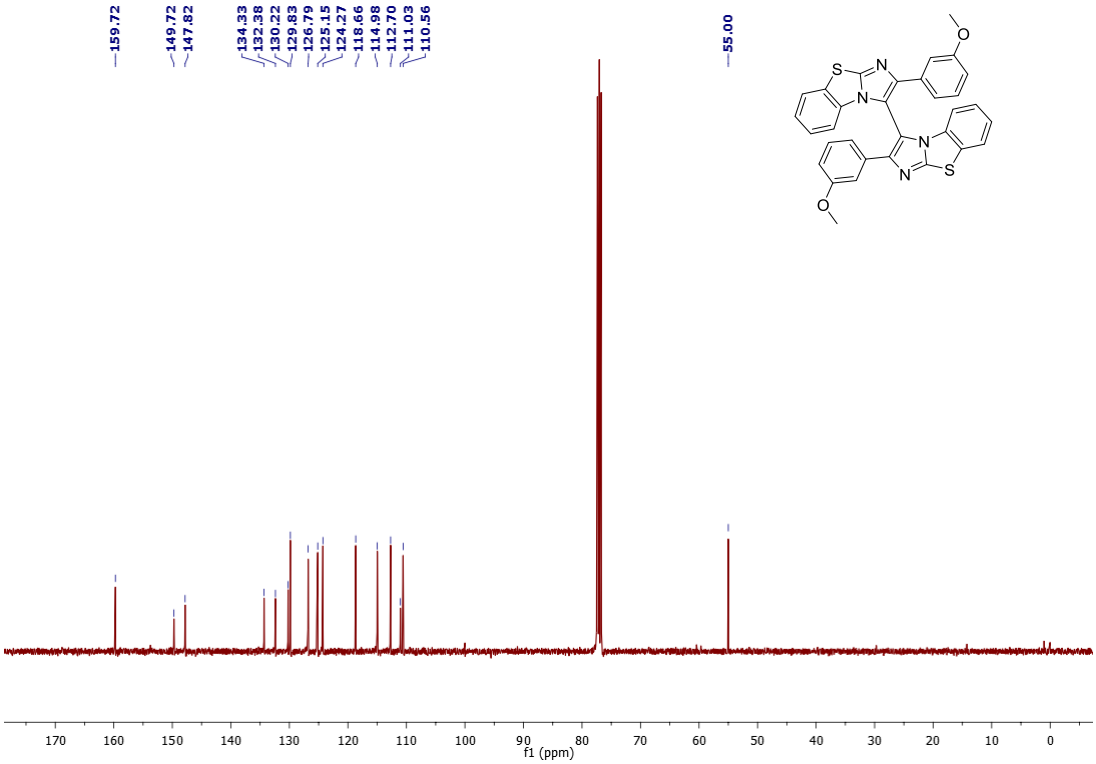

Figure 4A.2.2: ^{13}C NMR spectrum of **30c**

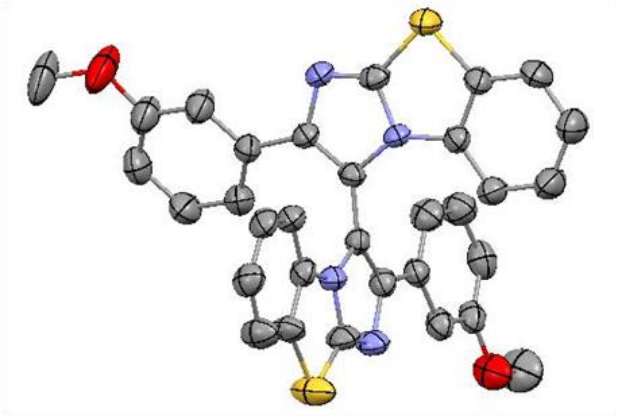

Figure 4A.2.3: An ORTEP diagram of **30c**

To evaluate the scalability of the PIDA-mediated homocoupling strategy, a gram-scale reaction was performed using **27h** under described conditions, affording the desired biimidazo[1,2-*a*]pyridine **28h** in 69% yield, almost the same as that obtained on a smaller scale (Scheme 4A.2.3).

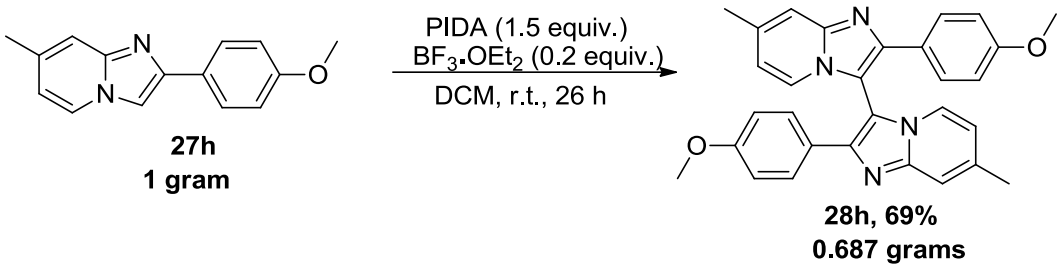

Scheme 4A.2.3: Gram scale synthesis of **28h**

To further advance the synthetic strategy, we attempted to develop an organocatalytic approach for the oxidative homocoupling of imidazo-heterocycles. To our delight, the use of catalytic amounts of iodobenzene and oxidant *m*-CPBA and AcOH facilitated the formation of biimidazo[1,2-*a*]pyridines at room temperature in DCM (Scheme 4A.2.4). This organocatalytic approach was utilized for the synthesis of a few more biimidazo[1,2-*a*]pyridines (**28m**–**o**) along with previously synthesized biimidazo-heterocycles (**28a**, **28j**, and **30b**) (Scheme 4A.2.4). The organocatalytic approach provided previously synthesized biimidazo-heterocycles (**28a**, **28j**, and **30b**) in comparatively lower yields, and longer reaction time (up to 30 h) was required for their synthesis. This methodology could be believed to proceed *via* the *in-situ* generation of $PhI(OAc)_2$ from PhI using *m*-CPBA/AcOH.

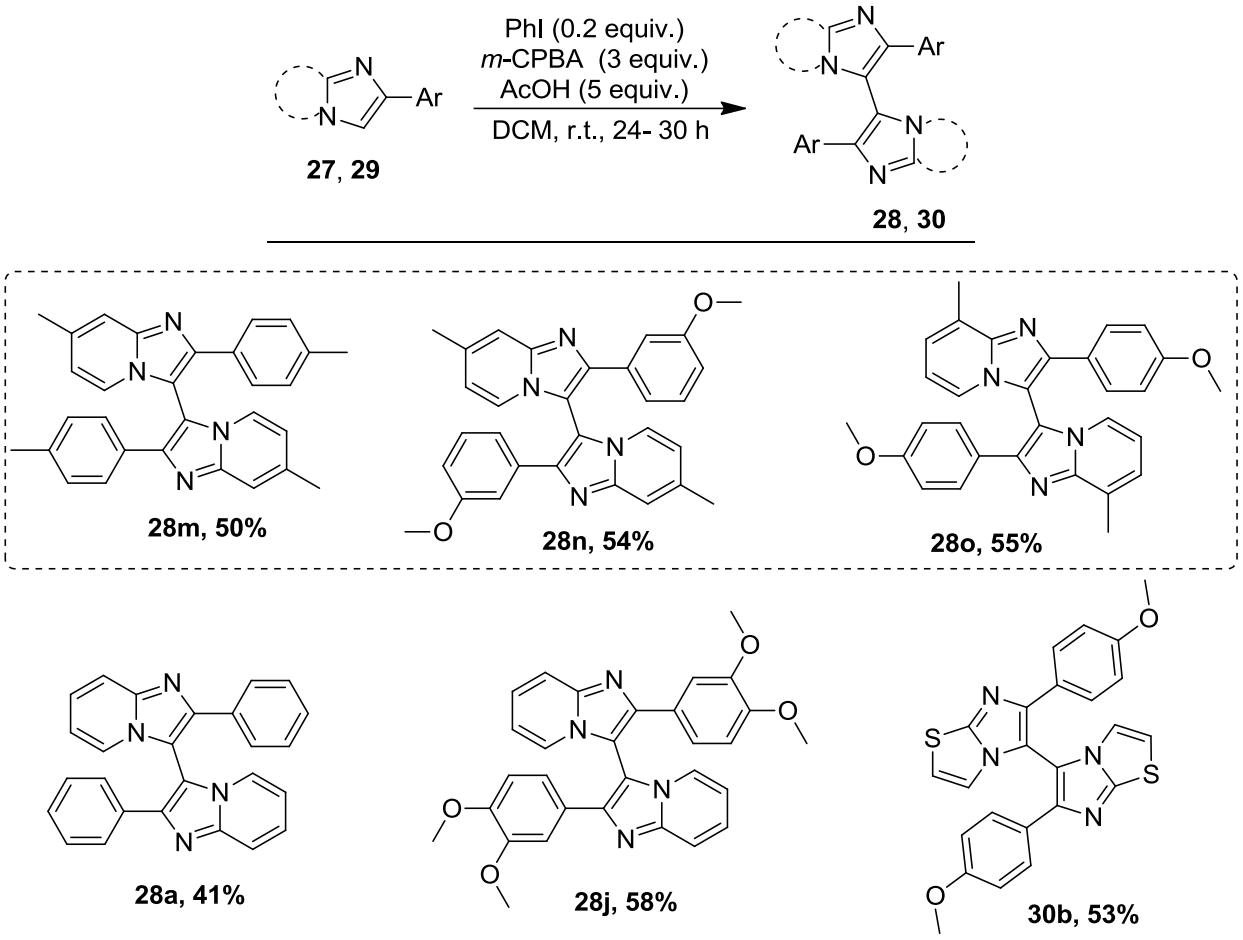

Scheme 4A.2.4: Synthesis of biimidazo-heterocycles (**28m-o**) *via* organocatalytic approach

To gain some insights into the mechanism of the reaction, a few control experiments were performed (Scheme 4A.2.5). The reaction proceeded smoothly in the presence of 3 equivalent of a radical scavenger TEMPO, affording the expected product **28h** in 68% yield. This provides a clear evidence for the non-radical mechanism (Scheme 4A.2.5i). To ascertain the intermolecular nature of the coupling reaction, the reaction of 2-phenylimidazo[1,2-*a*]pyridine (**27a**) and 8-methyl-2-(*p*-tolyl)imidazo[1,2-*a*]pyridine (**27f**) was performed under the standardized reaction conditions (Scheme 4A.2.5ii).

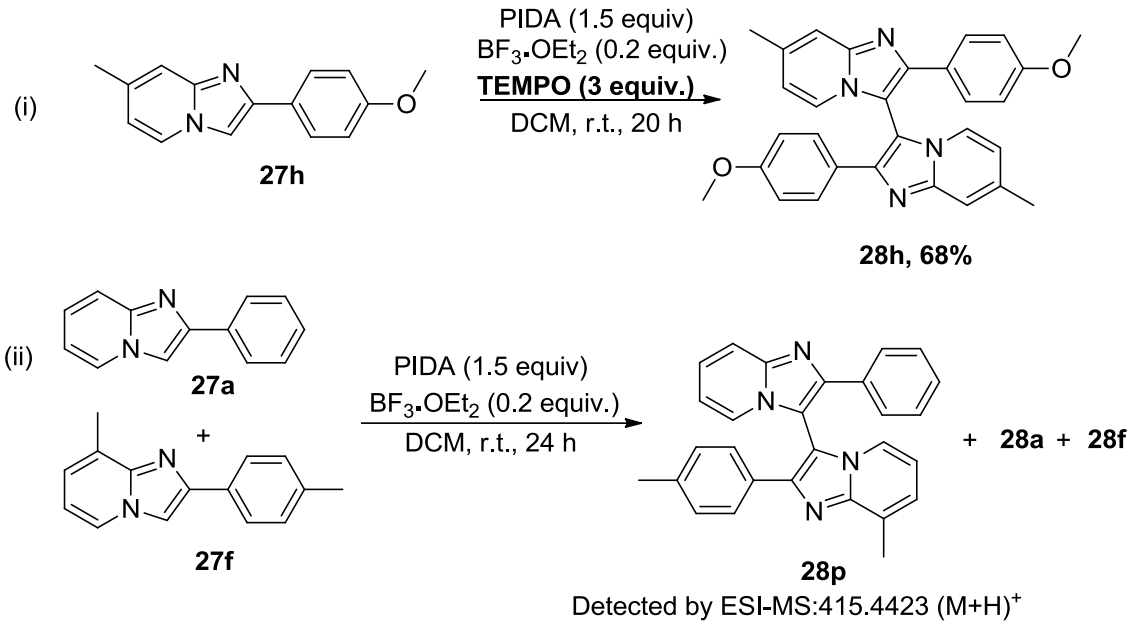

Scheme 4A.2.5: Control experiments

After 24 h, the TLC of the crude mixture showed a number of closely visualized spots. Gratifyingly, the mass of the crude product affirmed the formation of the cross-coupled product (**28p**), in addition to the two expected homocoupled products (**28a** and **28f**) (Figure 4A.2.4).

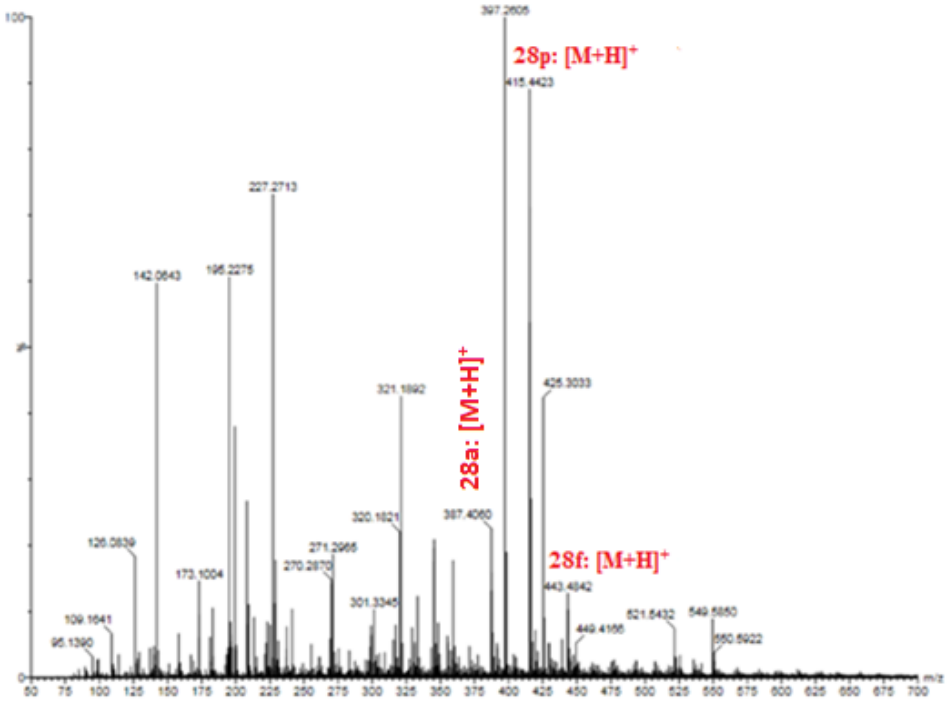

Figure 4A.2.4: ESI-MS of crude reaction mass

Based on the control experiments and previous reports,[6,28,61-63] a plausible mechanism is proposed (Scheme 4A.2.6). The reaction is believed to proceed *via* $BF_3.OEt_2$-accelerated C-3 nucleophilic attack of imidazo[1,2-*a*]pyridine (**27a**) on $PhI(OAc)_2$ (PIDA), forming intermediate **B** through the formation of nitrenium species **A**. The C-3 nucleophilic attack of the second molecule of imidazo[1,2-*a*]pyridine (**27a**) on **B** possibly *via* S_N2' pathway generates species **C**, with the subsequent elimination of iodobenzene (path A). Thereafter, species **C** will eliminate acetic acid to afford biimidazo[1,2-*a*]pyridine (**28a**). Alternatively, the substitution of OAc ion in **B** with **27a** may generate **D**, which upon 1,2-migration and subsequent elimination of PhI yields **28a** (path B).

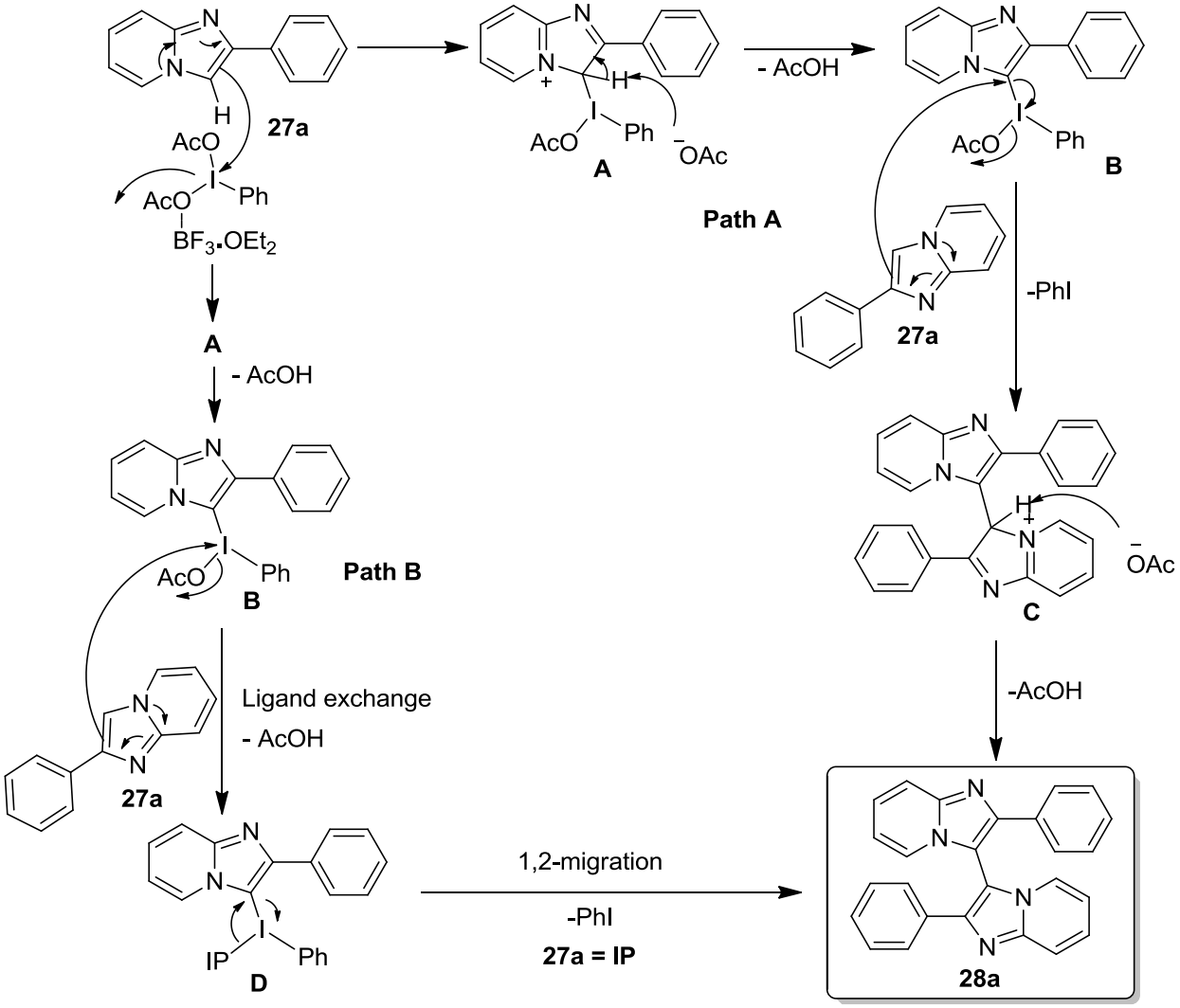

Scheme 4A.2.6: Plausible mechanism for PIDA-mediated homocoupling of imidazo[1,2-*a*]pyridine.

From the proposed mechanism, it is evident that presence of electron-withdrawing groups on aryl or pyridyl rings of imidazo[1,2-*a*]pyridine will disfavor the formation of intermediate species **A**. In addition, it will reduce the nucleophilicity of the second attacking imidazo[1,2-*a*]pyridine molecule, thereby disfavoring the formation of **28a**.

In summary, we have developed a metal-free PIDA-mediated, $BF_3{\cdot}OEt_2$-accelerated oxidative atom-economical process for the synthesis of biimidazo-heterocycles. In addition a complementary organocatalytic approach for the synthesis of biimidazo-heterocycles using 20 mol % of iodobenzene with *m*-CPBA/AcOH was also reported.

4A.3 Experimental Section

4A.3.1 General Materials and Methods

All the chemicals were purchased from Sigma-Aldich, Alfa Aesar, and Spectrochem India Pvt. Ltd and used without further purification. The solvents used were purchased from Merck (India) and were distilled and dried before use. Nuclear magnetic resonance spectra were recorded on Bruker 400 spectrometer. All ^{1}H NMR experiments were reported in δ units, parts per million (ppm), and were measured relative to residual chloroform (7.26 ppm) or DMSO (2.5 ppm) in the deuterated solvent. All ^{13}C NMR spectra were reported in ppm relative to deuterochloroform (77.0 ppm) or [d_6] DMSO (39.5 ppm). All coupling constants *J* were reported in Hz. The following abbreviations were used to describe peak splitting patterns when appropriate: s = singlet, d = doublet, t = triplet, dd = doublet of doublet, m = multiplet and br s = broad singlet. Melting points were determined on a capillary point apparatus equipped with a digital thermometer and are uncorrected. High resolution mass spectra were recorded with a TOF analyzer spectrometer by using electrospray mode.

General procedure for PIDA-mediated synthesis of biimidazo-heterocycles

Method A: A mixture of imidazo-heterocycle (**27a–l** or **29a–c**) (0.4 mmol), PIDA (0.6 mmol), and $BF_3.OEt_2$ (0.08 mmol) in DCM (10 mL) was stirred under ambient conditions at room temperature for 18–24 h. The reaction was monitored *via* TLC. Water (10 mL) was added to the reaction mixture, and the organic layer was washed with a 10% sodium bicarbonate solution (10 mL × 2). The organic layer was concentrated under reduced pressure. The crude product was purified by silica gel column chromatography [SiO_2 (100–200 mesh), hexanes/EtOAc, 8:2 v/v], affording the corresponding biimidazo-heterocycle (**28a–l** or **30a–c**).

General procedure for synthesis of biimidazo-heterocycles *via* an organocatalytic approach

Method B: A mixture of imidazo-heterocycle (**27m–o**, **27a**, **27j**, or **29b**) (0.4 mmol), iodobenzene (0.08 mmol), *m*-CPBA (1.2 mmol), and acetic acid (2 mmol) were added to DCM (10 mL) at 0 ºC; the resulting mixture was stirred under ambient conditions at room temperature for 24–30 h. Water (10 mL) was added to the reaction mixture. The organic layer was separated and washed with a 10% sodium bicarbonate solution (10 mL × 2). The organic layer was concentrated under reduced pressure. The crude product was purified by silica gel column chromatography [SiO_2 (100–200 mesh), hexanes/EtOAc, 8:2 v/v], affording the corresponding biimidazo-heterocycle (**28m–o**, **28a, 28j**, or **30b**).

2,2'-Diphenyl-3,3'-biimidazo[1,2-*a*]pyridine (28a): White solid; yield: 64 mg (65%, Method A); mp: 245–247 °C; ^{1}H NMR (400 MHz, $CDCl_3$) δ 7.81 (d, J = 9.0 Hz, 2H), 7.77 – 7.71 (m, 4H), 7.49 (d, J = 6.8 Hz, 2H), 7.31 (d, J = 7.9 Hz, 2H), 7.28 – 7.24 (m, 6H), 6.68 (t, J = 6.8 Hz, 2H); ^{13}C NMR (100 MHz, $CDCl_3$) δ 146.6, 145.8, 133.2, 128.9, 128.4, 126.7, 126.2, 123.9, 117.7, 112.9, 108.3; HRMS (ESI-TOF) (*m/z*) calculated $C_{26}H_{19}N_4^+$: 387.1609 ; found 387.1617 $[M+H]^+$.

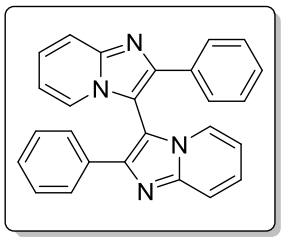

2,2'-Bis(2-methoxyphenyl)-3,3'-biimidazo[1,2-*a*]pyridine (28b): Yellow solid; yield: 68 mg (69%, Method A); mp: 261–263 °C; ^{1}H NMR (400 MHz, $CDCl_3$) δ 7.76 (d, J = 8.9 Hz, 2H), 7.65 (d, J = 6.7 Hz, 2H), 7.37 (d, J = 7.0 Hz, 2H), 7.28 – 7.22 (m, 2H), 7.19 (t, J = 7.4 Hz, 2H), 6.80 (t, J = 7.4 Hz, 2H), 6.71 (d, J = 7.1 Hz, 4H), 3.21 (s, 6H); ^{13}C NMR (100 MHz, $CDCl_3$) δ 156.6, 145.7, 143.4, 130.9, 129.4, 125.0, 124.0, 122.7, 120.6, 117.5, 112.3, 112.0, 110.5, 54.8; HRMS (ESI-TOF) (*m/z*) calculated $C_{28}H_{23}N_4O_2^+$: 447.1821; found 447.1842 $[M+H]^+$.

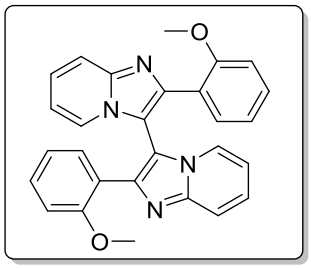

2,2'-Bis(4-methoxyphenyl)-3,3'-biimidazo[1,2-*a*]pyridine (28c): White solid; yield: 71 mg (72%, Method A); mp: 260–262 °C; ^{1}H NMR (400 MHz, $CDCl_3$) δ 7.77 (d, J = 9.0 Hz, 2H), 7.68 (d, J = 8.9 Hz, 4H), 7.47 (d, J = 6.8 Hz, 2H), 7.30 – 7.25 (m, 2H), 6.80 (d, J = 8.9 Hz, 4H), 6.67 (dd, J = 9.8, 3.7 Hz, 2H), 3.77 (s, 6H); ^{13}C NMR (100 MHz, $CDCl_3$) δ 159.8, 146.5, 145.8, 127.9, 126.0, 125.9, 123.9, 117.4, 114.2, 112.7, 107.4, 55.2; HRMS (ESI-TOF) (*m/z*) calculated $C_{28}H_{23}N_4O_2^+$: 447.1821;

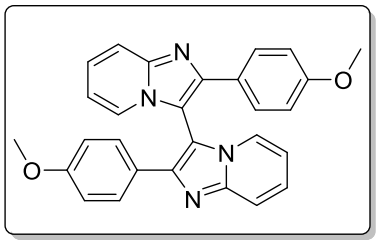

found 447.1845 $[M+H]^+$.

2,2'-Di-*p*-tolyl-3,3'-biimidazo[1,2-*a*]pyridine (28d): White solid; yield: 65 mg (66%, Method A); mp: 277–279 °C; ^{1}H NMR (400 MHz, $CDCl_3$) δ 7.82 – 7.78 (m, 2H), 7.63 (d, J = 8.2 Hz, 4H), 7.50 – 7.46 (m, 2H), 7.32 – 7.29 (m, 2H), 7.07 (d, J = 8.0 Hz, 4H), 6.67 (td, J = 6.8, 1.1 Hz, 2H), 2.30 (s, 6H); ^{13}C NMR (100 MHz, $CDCl_3$) δ 146.5, 145.9, 138.4, 130.4, 129.6, 126.4, 126.1, 123.9, 117.5, 112.8, 107.9, 21.2; HRMS (ESI-TOF) (*m/z*) calculated $C_{28}H_{23}N_4^+$: 415.1922; found 415.1935 $[M+H]^+$.

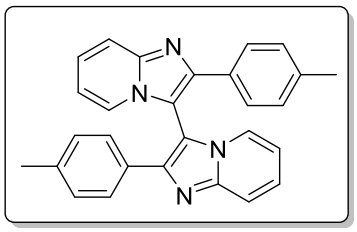

7,7'-Dimethyl-2,2'-diphenyl-3,3'-biimidazo[1,2-*a*]pyridine (28e): Yellow solid; yield: 58 mg (59%, Method A); mp: 263–265 °C; ^{1}H NMR (400 MHz, $CDCl_3$) δ 7.73 (dd, J = 7.2, 2.3 Hz, 4H), 7.55 (s, 2H), 7.36 (d, J = 7.0 Hz, 2H), 7.29 – 7.20 (m, 6H), 6.50 (dd, J = 7.0, 1.3 Hz, 2H), 2.42 (s, 6H); ^{13}C NMR (100 MHz, $CDCl_3$) δ 146.9, 145.4, 137.4, 133.4, 128.8, 128.2, 126.7, 123.1, 116.1, 115.5, 107.8, 29.7; HRMS (ESI-TOF) (*m/z*) calculated $C_{28}H_{23}N_4^+$: 415.1922; found 415.1939 $[M+H]^+$.

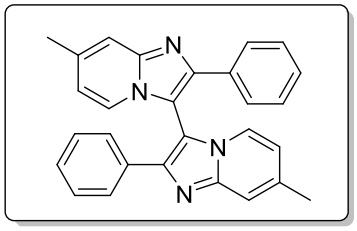

8,8'-Dimethyl-2,2'-di-*p*-tolyl-3,3'-biimidazo[1,2-*a*]pyridine (28f): Yellow solid; yield: 65 mg (66%, Method A); mp: 256–258 °C; ^{1}H NMR (400 MHz, $CDCl_3$) δ 7.66 (d, J = 8.2 Hz, 4H), 7.34 (d, J = 6.7 Hz, 2H), 7.05 (d, J = 7.7 Hz, 6H), 6.55 (t, J = 6.8 Hz, 2H), 2.78 (s, 6H), 2.29 (s, 6H); ^{13}C NMR (100 MHz, $CDCl_3$) δ 146.8, 145.3, 137.9, 130.8, 129.4, 127.5, 126.6, 124.6, 121.7, 112.6, 108.7, 21.2, 17.0; HRMS (ESI-TOF) (*m/z*) calculated $C_{30}H_{27}N_4^+$: 443.2235; found 443.2251 $[M+H]^+$.

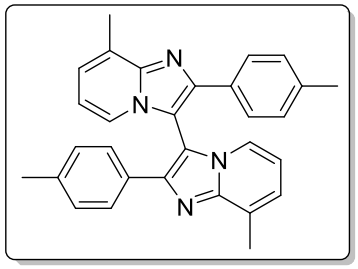

6,6'-Dimethyl-2,2'-di-*p*-tolyl-3,3'-biimidazo[1,2-*a*]pyridine (28g): Yellow solid; yield: 64 mg (65%, Method A); mp: 268–269 °C; ^{1}H NMR (400 MHz, $CDCl_3$) δ 7.69 (d, J = 9.1 Hz, 2H), 7.62 (d, J = 8.1 Hz, 4H), 7.23 (s, 2H), 7.14 (d, J = 9.1 Hz, 2H), 7.06 (d, J = 8.0 Hz, 4H), 2.29 (s, 6H), 2.14 (s, 6H); ^{13}C NMR (100 MHz, $CDCl_3$) δ 145.8, 145.5, 138.1, 130.6, 129.5, 129.2, 126.4, 122.7, 121.5, 116.8, 107.7, 21.2, 18.2; HRMS (ESI-TOF) (*m/z*) calculated $C_{30}H_{27}N_4^+$: 443.2235; found 443.2258 $[M+H]^+$.

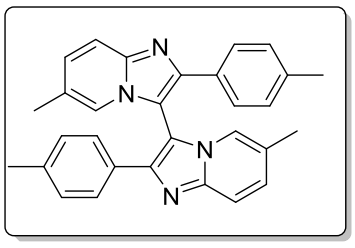

2,2'-Bis(4-methoxyphenyl)-7,7'-dimethyl-3,3'-biimidazo[1,2-*a*]pyridine (28h): Yellow solid;

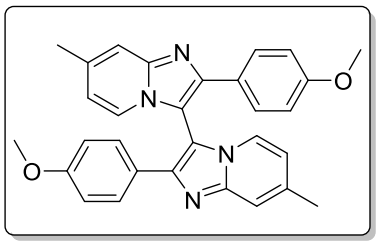

yield: 73 mg (74%, Method A); mp: 248–250 °C; ^{1}H NMR (400 MHz, $CDCl_3$) δ 7.67 (d, J = 8.4 Hz, 4H), 7.51 (s, 2H), 7.35 (d, J = 6.7 Hz, 2H), 6.79 (d, J = 8.3 Hz, 4H), 6.49 (d, J = 6.6 Hz, 2H), 3.77 (s, 6H), 2.42 (s, 6H); ^{13}C NMR (100 MHz, $CDCl_3$) δ 159.6, 146.9, 145.3, 137.0, 127.9, 126.2, 123.1, 115.9, 115.3, 114.2, 106.9, 55.2, 21.4; HRMS (ESI-TOF) (*m/z*) calculated $C_{30}H_{27}N_4O_2^+$: 475.2134; found 475.2147 $[M+H]^+$.

2,2'-Bis(2-methoxyphenyl)-6,6'-dimethyl-3,3'-biimidazo[1,2-*a*]pyridine (28i): White solid;

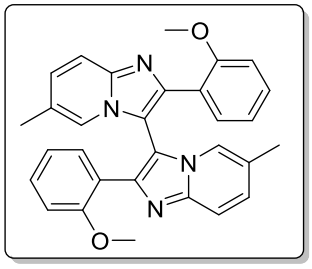

yield: 70 mg (71%, Method A); mp: 231–233 °C; ^{1}H NMR (400 MHz, $CDCl_3$) δ 7.65 (d, J = 9.1 Hz, 2H), 7.43 (s, 2H), 7.35 (dd, J = 7.5, 1.5 Hz, 2H), 7.22 – 7.16 (m, 2H), 7.09 (d, J = 9.1 Hz, 2H), 6.80 (t, J = 7.4 Hz, 2H), 6.73 (d, J = 8.3 Hz, 2H), 3.26 (s, 6H), 2.17 (s, 6H); ^{13}C NMR (100 MHz, $CDCl_3$) δ 156.6, 144.8, 143.1, 131.0, 129.3, 128.0, 123.1, 121.9, 121.8, 120.5, 116.8, 111.9, 110.4, 54.8, 18.1; HRMS (ESI-TOF) (*m/z*) calculated $C_{30}H_{27}N_4O_2^+$: 475.2134; found 475.2141 $[M+H]^+$.

2,2'-Bis(3,4-dimethoxyphenyl)-3,3'-biimidazo[1,2-*a*]pyridine (28j): Yellow solid; yield: 77

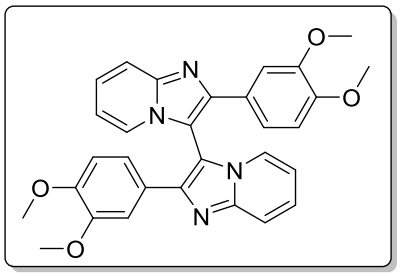

mg (78%, Method A); mp: 254–258 °C; ^{1}H NMR (400 MHz, $CDCl_3$) δ 7.80 (d, J = 9.0 Hz, 2H), 7.51 (d, J = 6.8 Hz, 2H), 7.34 – 7.29 (m, 4H), 7.26 (dd, J = 8.4, 1.9 Hz, 2H), 6.77 – 6.68 (m, 4H), 3.84 (s, 6H), 3.61 (s, 6H); ^{13}C NMR (100 MHz, $CDCl_3$) δ 149.2, 149.0, 146.4, 145.6, 126.2, 125.9, 124.0, 119.3, 117.3, 112.9, 111.3, 109.3, 107.9, 55.8, 55.5; HRMS (ESI-TOF) (*m/z*) calculated $C_{30}H_{27}N_4O_4^+$: 507.2032; found 507.2049 $[M+H]^+$.

6,6'-Dimethyl-2,2'-di(naphthalen-2-yl)-3,3'-biimidazo[1,2-*a*]pyridine (28k): White solid;

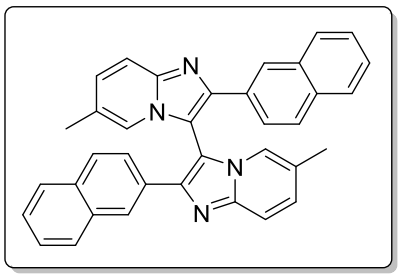

yield: 59 mg (60%, Method A); mp: 264–266 °C; ^{1}H NMR (400 MHz, $CDCl_3$) δ 8.39 (s, 2H), 7.83 – 7.70 (m, 8H), 7.68 (d, J = 8.6 Hz, 2H), 7.42 (dd, J = 5.7, 3.6 Hz, 4H), 7.32 (s, 2H), 7.18 (d, J = 8.2 Hz, 2H), 2.11 (s, 6H); ^{13}C NMR (100 MHz, $CDCl_3$) δ 145.8, 145.8, 133.5, 133.1, 130.9, 129.6, 128.6, 128.5, 127.5, 126.2, 126.1, 125.9, 124.1, 123.0, 121.5, 117.0,

108.4, 18.2; HRMS (ESI-TOF) (*m/z*) calculated $C_{36}H_{27}N_4^+$: 515.2235; found 515.2251 $[M+H]^+$.

2,2'-Di(thiophen-2-yl)-3,3'-biimidazo[1,2-*a*]pyridine (28l): Yellow solid; yield: 54 mg (55%, Method A); mp: 253–254 °C; ^{1}H NMR (400 MHz, $CDCl_3$) δ 7.83 (d, J = 9.1 Hz, 2H), 7.57 (d, J = 6.8 Hz, 2H), 7.39 – 7.32 (m, 2H), 7.23 (d, J = 4.8 Hz, 2H), 7.08 – 6.99 (m, 2H), 6.91 (dd, J = 4.7, 4.0 Hz, 2H), 6.78 (t, J = 6.7 Hz, 2H); ^{13}C NMR (100 MHz, $CDCl_3$) δ 146.8, 142.3, 135.9, 127.9, 126.6, 126.2, 125.2, 124.1, 117.6, 113.3, 106.1; HRMS (ESI-TOF) (*m/z*) calculated $C_{22}H_{15}N_4S_2^+$: 399.0738; found 399.0750 $[M+H]^+$.

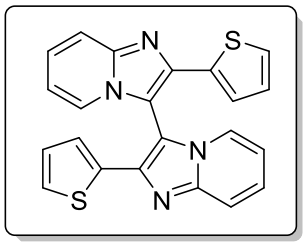

7,7'-Dimethyl-2,2'-di-*p*-tolyl-3,3'-biimidazo[1,2-*a*]pyridine (28m): White solid; yield: 49 mg (50%, Method B); mp: 250–252 °C; ^{1}H NMR (400 MHz, $CDCl_3$) δ 8.03 (d, J = 8.2 Hz, 4H), 7.99 (d, J = 7.0 Hz, 2H), 7.40 (s, 2H), 7.31 (d, J = 8.0 Hz, 4H), 6.77 (dd, J = 7.0, 1.3 Hz, 2H), 2.45 (s, 6H), 2.43 (s, 6H); ^{13}C NMR (100 MHz, $CDCl_3$) δ 144.1, 139.5, 137.9, 135.8, 129.8, 129.2, 127.3, 121.8, 115.9, 115.4, 104.6, 21.4, 21.3; HRMS (ESI-TOF) (*m/z*) calculated $C_{30}H_{27}N_4^+$: 443.2235; found 443.2218 $[M+H]^+$.

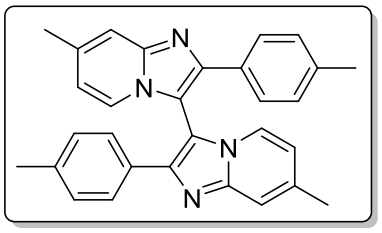

2,2'-Bis(3-methoxyphenyl)-7,7'-dimethyl-3,3'-biimidazo[1,2-*a*]pyridine (28n): Yellow solid; yield: 53 mg (54%, Method B); mp: 247–249 °C; ^{1}H NMR (400 MHz, $CDCl_3$) δ 7.55 (s, 2H), 7.38 (d, J = 7.1 Hz, 2H), 7.35 – 7.32 (m, 2H), 7.24 (d, J = 7.8 Hz, 2H), 7.14 (t, J = 7.9 Hz, 2H), 6.80 (dd, J = 8.2, 1.8 Hz, 2H), 6.53 (dd, J = 7.0, 1.5 Hz, 2H), 3.62 (s, 6H), 2.43 (s, 6H); ^{13}C NMR (100 MHz, $CDCl_3$) δ 159.8, 146.8, 145.3, 137.4, 134.7, 129.8, 123.2, 118.9, 116.0, 115.6, 115.2, 110.8, 107.9, 55.1, 21.4; HRMS (ESI-TOF) (*m/z*) calculated $C_{30}H_{27}N_4O_2^+$: 475.2134; found 475.2150 $[M+H]^+$.

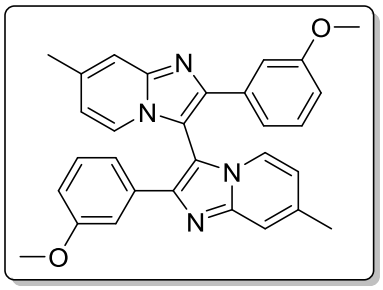

2,2'-Bis(4-methoxyphenyl)-8,8'-dimethyl-3,3'-biimidazo[1,2-*a*]pyridine (28o): White solid; yield: 54 mg (55%, Method B); mp: 244–247 °C; ^{1}H NMR (400 MHz, $CDCl_3$) δ 7.73 – 7.68 (m, 4H), 7.37 – 7.30 (m, 2H), 7.08 – 7.03 (m, 2H), 6.81 – 6.76 (m, 4H), 6.55 (t, J = 6.8 Hz, 2H), 3.76 (s, 6H), 2.77 (s, 6H); ^{13}C NMR (100 MHz, $CDCl_3$) δ 159.6, 146.8, 145.2, 128.0, 127.4, 126.4, 124.6, 121.7, 114.1, 112.6,

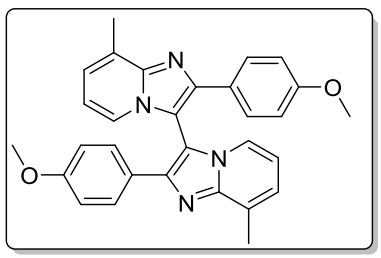

108.2, 55.2, 17.0; HRMS (ESI-TOF) (*m/z*) calculated $C_{30}H_{27}N_4O_2^+$: 475.2134; found 475.2145 $[M+H]^+$

6,6'-Diphenyl-5,5'-biimidazo[2,1-*b*]thiazole (30a): Yellow solid; yield: 56 mg (57%, Method A); mp: 268–270 °C; ^{1}H NMR (400 MHz, $CDCl_3$) δ 7.74 – 7.68 (m, 4H), 7.37 – 7.28 (m, 6H), 6.78 (d, J = 4.5 Hz, 2H), 6.70 (d, J = 4.5 Hz, 2H); ^{13}C NMR (100 MHz, $CDCl_3$) δ 150.8, 145.9, 133.6, 128.9, 127.9, 126.3, 118.1, 112.7, 110.8; HRMS (ESI-TOF) (*m/z*) calculated $C_{22}H_{15}N_4S_2^+$: 399.0738; found 399.0727 $[M+H]^+$.

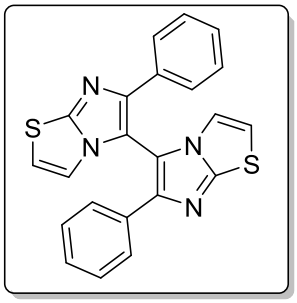

6,6'-Bis(4-methoxyphenyl)-5,5'-biimidazo[2,1-*b*]thiazole (30b): Yellow solid; yield: 67 mg (67%, Method B); mp: 271–273 °C; ^{1}H NMR (400 MHz, $CDCl_3$) δ 7.63 (d, J = 8.9 Hz, 4H), 6.85 (d, J = 8.9 Hz, 4H), 6.79 (d, J = 4.5 Hz, 2H), 6.68 (d, J = 4.5 Hz, 2H), 3.81 (s, 6H); ^{13}C NMR (100 MHz, $CDCl_3$) δ 159.3, 150.6, 145.9, 127.6, 126.3, 118.1, 114.3, 112.3, 109.9, 55.2; HRMS (ESI-TOF) (*m/z*) calculated $C_{24}H_{19}N_4O_2S_2^+$: 459.0949; found 459.0965 $[M+H]^+$.

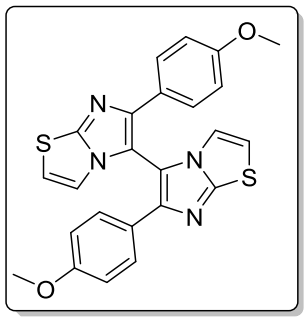

2,2'-Bis(3-methoxyphenyl)-3,3'-bibenzo[*d*]imidazo[2,1-*b*]thiazole (30c): White solid; yield: 63 mg (64%, Method A); mp: 260–262 °C; ^{1}H NMR (400 MHz, $CDCl_3$) δ 7.78 –7.64 (m, 2H), 7.37 – 7.32 (m, 4H), 7.27 – 7.21 (m, 2H), 7.17 – 7.10 (m, 4H), 6.83 – 6.74 (m, 4H), 3.62 (s, 6H); ^{13}C NMR (100 MHz, $CDCl_3$) δ 159.7, 149.7, 147.8, 134.3, 132.4, 130.2, 129.8, 126.8, 125.1, 124.3, 118.7, 114.9, 112.7, 111.0, 110.6, 55.0; HRMS (ESI-TOF) (*m/z*) calculated $C_{32}H_{23}N_4O_2S_2^+$: 559.1262; found 559.1275 $[M+H]^+$.

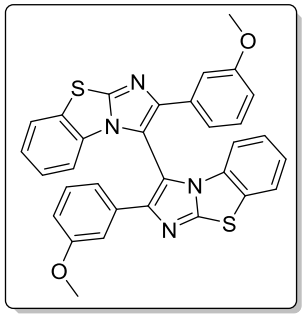

4A.4 X-ray Crystallography Studies

Initial crystal evaluation and data collection were performed on a Kappa APEX II diffractometer equipped with a CCD detector (with the crystal-to-detector distance fixed at 60 mm) and sealed-tube monochromated MoKα radiation using the program APEX2.[64] By using the program SAINT[64] for the integration of the data, reflection profiles were fitted, and values of F^2 and $\sigma(F^2)$ for each reflection were obtained. Data were also corrected for Lorentz and polarization effects. The subroutine XPREP[64] was used for the processing of data that included determination of space group, application of an absorption correction (SADABS)[64], merging of data, and

generation of files necessary for solution and refinement. The crystal structure was solved and refined using SHELX 97.[65] The space group was chosen based on systematic absences and confirmed by the successful refinement of the structure. Positions of most of the non-hydrogen atoms were obtained from a direct methods solution. There were two independent molecules of **30c** along with a lattice chloroform molecule in the asymmetric unit. Several full-matrix least-squares/difference Fourier cycles were performed, locating the remainder of the non-hydrogen atoms. All non-hydrogen atoms were refined with anisotropic displacement parameters. All hydrogen atoms except that for the disordered chloroform solvent (one of the chlorines was disordered over two positions with equal occupancies) were placed in ideal positions and refined as riding atoms with individual isotropic displacement parameters. All figures were drawn using MERCURY V 3.0[66] and Platon.[67]

4A.4.1 Crystallographic data for 30c (CCDC No. 1530436)

$0.5CHCl_3$. $C_{32.5}H_{23.5}N_4O_2S_2Cl_{1.5}$, M_r = 619.345, monoclinic, space group *P*21/*c*, a = 19.270(16) Å, b = 10.347(9) Å, c = 21.930(19) Å, α = 90°, β = 92.29(2)°, γ = 90°, V = 4369(6) Å^3, Z = 8, T = 296(2) K, D_{calcd} = 1.883 g/cm^3; Full matrix least-square on F^2; R_1 = 0.0719, wR_2 = 0.1816 for 4547 observed reflections [$I > 2\sigma(I)$] and R_1 = 0.1308, wR_2 = 0.2349 for all 7685 reflections; GOF = 1.002.

4A.5 References

(1) McMurray, L.; O'Hara, F.; Gaunt, M. J. *Chemical Society Reviews* **2011**, *40*, 1885-1898.

(2) Yamaguchi, J.; Yamaguchi, A. D.; Itami, K. *Angewandte Chemie International Edition* **2012**, *51*, 8960-9009.

(3) Saini, M. S.; Kumar, A.; Dwivedi, J.; Singh, R. *International Journal of Pharmaceutical Sciences and Research* **2013**, *4*, 66-77.

(4) Liu, C.; Yuan, J.; Gao, M.; Tang, S.; Li, W.; Shi, R.; Lei, A. *Chemical Reviews* **2015**, *115*, 12138-12204.

(5) Zhang, C.; Tang, C.; Jiao, N. *Chemical Society Reviews* **2012**, *41*, 3464-3484.

(6) Li, B. -J.; Shi, Z. -J. *Chemical Society Reviews* **2012**, *41*, 5588-5598.

(7) Liu, C.; Zhang, H.; Shi, W.; Lei, A. *Chemical Reviews* **2011**, *111*, 1780-1824.

(8) Ping, L.; Chung, D. S.; Bouffard, J.; Lee, S.-G. *Chemical Society Reviews* **2017**, *46*, 4299-4328.

(9) Kuhl, N.; Hopkinson, M. N.; Wencel-Delord, J. Glorius, F. *Angewandte Chemie International Edition* **2012**, *51*, 10236-10254.

(10) Cho, S. H.; Kim, J. Y.; Kwak, J.; Chang, S. *Chemical Society Reviews* **2011**, *40*, 5068-5083.

(11) Sun, C. -L.; Shi, Z. -J. *Chemical Reviews* **2014**, *114*, 9219-9280.

(12) Yang, Y.; Lan, J.; You, J. *Chemical Reviews* **2017**, *117*, 8787-8863.

(13) Narayan, R.; Matcha, K.; Antonchick, A. P. *Chemistry–A European Journal* **2015**, *21*, 14678-14693.

(14) Yoshimura, A.; Zhdankin, V. V. *Chemical Reviews* **2016**, *116*, 3328-3435.

(15) Zhdankin, V. V.; Stang, P. J. *Chemical Reviews* **2008**, *108*, 5299-5358.

(16) Murarka, S.; Antonchick, A. P. In *Hypervalent Iodine Chemistry*; Springer: **2015**, p 75-104.

(17) Zheng, Z.; Zhang-Negrerie, D.; Du, Y.; Zhao, K. *Science China Chemistry* **2014**, *57*, 189-214.

(18) Zhdankin, V. V. *Hypervalent iodine chemistry: preparation, structure, and synthetic applications of polyvalent iodine compounds*; John Wiley & Sons, **2013**.

(19) Zhdankin, V. V. *Arkivoc* **2009**, *1*, 1-62.

(20) Matveeva, E.; Proskurnina, M.; Zefirov, N. *Heteroatom Chemistry* **2006**, *17*, 595-617.

(21) Willgerodt, C. *Advanced Synthesis & Catalysis* **1886**, *33*, 154-160.

(22) Yusubov, M.; V Zhdankin, V. *Current Organic Synthesis* **2012**, *9*, 247-272.

(23) Zhdankin, V. V.; Stang, P. J. *Chemical Reviews* **2002**, *102*, 2523-2584.

(24) Ochiai, M.; Sueda, T.; Miyamoto, K.; Kiprof, P.; Zhdankin, V. V. *Angewandte Chemie International Edition* **2006**, *118*, 8383-8386.

(25) Kiprof, P. *Arkivoc* **2005**, *4*, 19-25.

(26) Samanta, R.; Matcha, K.; Antonchick, A. P. *European Journal of Organic Chemistry* **2013**, *2013*, 5769-5804.

(27) Tellitu, I.; Domínguez, E. *Synlett* **2012**, *23*, 2165-2175.

(28) Yu, W.; Du, Y.; Zhao, K. *Organic Letters* **2009**, *11*, 2417-2420.

(29) Chen, Y.; Ju, T.; Wang, J.; Yu, W.; Du, Y.; Zhao, K. *Synlett* **2010**, 231-234.

(30) Huang, J.; He, Y.; Wang, Y.; Zhu, Q. *Chemistry-A European Journal* **2012**, *18*, 13964-13967.

(31) Quideau, S.; Pouységu, L.; Avellan, A. -V.; Whelligan, D. K.; Looney, M. A. *Tetrahedron Letters* **2001**, *42*, 7393-7396.

(32) Merritt, E. A.; Olofsson, B. *Synthesis* **2011**, 517-538.

(33) Nocquet-Thibault, S.; Retailleau, P.; Cariou, K.; Dodd, R. H. *Organic Letters* **2013**, *15*, 42-1845.

(34) Li, X.; Yang, L.; Zhang, X.; Zhang-Negrerie, D.; Du, Y.; Zhao, K. *The Journal of Organic Chemistry* **2014**, *79*, 955-962.

(35) Manna, S.; Antonchick, A. P. *Angewandte Chemie International Edition* **2014**, *53*, 7324-7327.

(36) Manna, S.; Matcha, K.; Antonchick, A. P. *Angewandte Chemie International Edition* **2014**, *3*, 8163-8166.

(37) Hamamoto, H.; Umemoto, H.; Umemoto, M.; Ohta, C.; Dohshita, M.; Miki, Y. *Synlett* **2010**, 2593-2596.

(38) Dohi, T.; Ito, M.; Yamaoka, N.; Morimoto, K.; Fujioka, H.; Kita, Y. *Tetrahedron* **2009**, *65*, 10797-10815.

(39) Grzybowski, M.; Skonieczny, K.; Butenschön, H.; Gryko, D. T. *Angewandte Chemie International Edition* **2013**, *125*, 10084-10115.

(40) Kita, Y.; Gyoten, M.; Ohtsubo, M.; Tohma, H.; Takada, T. *Chemical Communications* **1996**, 1481-1482.

(41) Dohi, T.; Kita, Y. *Current Organic Chemistry* **2016**, *20*, 580-615.

(42) Kita, Y.; Takada, T.; Tohma, H. *Pure and Applied Chemistry* **1996**, *68*, 627-630.

(43) Dembitsky, V. *Citation: Dembitsky VM (2016) Chemistry, Origin, Antitumor and Other Activities of Fungal Homo-Dimeric Alkaloids. MJ Pharma* **2016**, *1*, 004

(44) Wirtanen, T.; Muuronen, M.; Hurmalainen, J.; Tuononen, H. M.; Nieger, M.; Helaja, J. *Organic Chemistry Frontiers* **2016**, *3*, 1738-1745.

(45)Masui, K.; Ikegami, H.; Mori, A. *Journal of the American Chemical Society* **2004**, *126*, 5074-5075.

(46) Takahashi, M.; Masui, K.; Sekiguchi, H.; Kobayashi, N.; Mori, A.; Funahashi, M.;Tamaoki, N. *Journal of the American Chemical Society* **2006**, *128*, 10930-10933.

(47) Kar, A.; Mangu, N.; Kaiser, H. M.; Beller, M.; Tse, M. K. *Chemical Communications* **2008**, 386-388.

(48) Li, N. -N.; Zhang, Y. -L.; Mao, S.; Gao, Y. -R.; Guo, D. -D.; Wang, Y. -Q. *Organic Letters* **2014**, *16*, 2732-2735.

(49) Liang, Z.; Zhao, J.; Zhang, Y. *The Journal of Organic Chemistry* **2009**, *75*, 170-177.

(50) Li, Y.; Wang, W. -H.; Yang, S. -D.; Li, B. -J.; Feng, C.; Shi, Z. -J. *Chemical Communications* **2010**, *46*, 4553-4555.

(51) Xia, J. -B.; Wang, X. -Q.; You, S. -L. *The Journal of Organic Chemistry* **2008**, *74*, 456-458.

(52) Monguchi, D.; Yamamura, A.; Fujiwara, T.; Somete, T.; Mori, A. *Tetrahedron Letters* **2010**, *51*, 850-852.

(53) Li, Y.; Jin, J.; Qian, W.; Bao, W. *Organic & Biomolecular Chemistry* **2010**, *8*, 326-330.

(54) Zhu, M.; Fujita, K. -I.; Yamaguchi, R. *Chemical Communications* **2011**, *47*, 12876-12878.

(55) Truong, T.; Alvarado, J.; Tran, L. D.; Daugulis, O. *Organic Letters* **2010**, *12*, 1200-1203.

(56) Dohi, T.; Morimoto, K.; Kiyono, Y.; Maruyama, A.; Tohma, H.; Kita.Y. *Chemical Communications* **2005**, 2930-2932.

(57) Morimoto, K.; Yamaoka, N.; Ogawa, C.; Nakae, T.; Fujioka, H.; Dohi, T.; Kita, Y. *Organic Letters* **2010**, *12*, 3804-3807.

(58) Dohi, T.; Morimoto, K.; Maruyama, A.; Kita, Y. *Organic Letters* **2006**, *8*, 2007-2010.

(59) Xie, W. W.; Liu, Y.; Yuan, R.; Zhao, D.; Yu, T. Z.; Zhang, J.; Da, C. S. *Advanced Synthesis & Catalysis* **2016**, *358*, 994-1002.

(60) Lei, S.; Cao, H.; Chen, L.; Liu, J.; Cai, H.; Tan, J. *Advanced Synthesis & Catalysis* **2015**, *357*, 3109-3114.

(61) Antonchick, A. P.; Samanta, R.; Kulikov, K.; Lategahn, J. *Angewandte Chemie International Edition* **2011**, *50*, 8605-8608.

(62) Ito, M.; Kubo, H.; Itani, I.; Morimoto, K.; Dohi, T.; Kita, Y. *Journal of the American Chemical Society* **2013**, *135*, 14078-14081.

(63) Manna, S.; Serebrennikova, P. O.; Utepova, I. A.; Antonchick, A. P.; Chupakhin, O. N. *Organic Letters* **2015**, *17*, 4588-4591.

(64) *APEX2, SADABS and SAINT*; Bruker AXS inc: Madison, WI, USA, **2008**.

(65) Sheldrick, G. M., *Acta Crystallographica* **2008**, *A64*, 112-122.

(66) Macrae, C. F.; Bruno, I. J.; Chisholm, J. A.; Edginton, P. R.; McCabe, P.; Pidocck, E.; Rodriguez Monge, L.; Taylor, T.; Van de Streek, J.; Wood, P. A *Journal of Applied Crystallography* **2008**, *41*, 466-470.

(67) Spek, A. L. *PLATON, Version 1.62*, University of Utrecht, **1999.**

CHAPTER 4B

Transition Metal-Free Homocoupling of Imidazo-Heterocycles Linked *via* Sulfur Bridges

4B.1 Introduction

Sulfur heterocycles and sulfur-derived functional groups constitute an integral part of numerous natural products and potential pharmaceuticals.[1-4] Over the years, the accountability of sulfur in about 362 FDA approved drugs has strongly contributed in building up its dominating repute, besides carbon and nitrogen.[5] In particular, sulfide and disulfide linkages are frequently observed in many drugs and bioactive alkaloids such as Discorhabdin B, Butoconazole, Axitinib, Disulfram, Epicorazin B, Emerthallicin E *etc.* (Figure 4B.1.1)[1,2,5,6] Disulfide linkages are also responsible for folding and stabilization of tertiary structure of proteins and enzymes.[7-9] Therefore, development of direct synthetic strategies for the construction of C-S-C and C-S-S-C linkages are highly valuable**.**

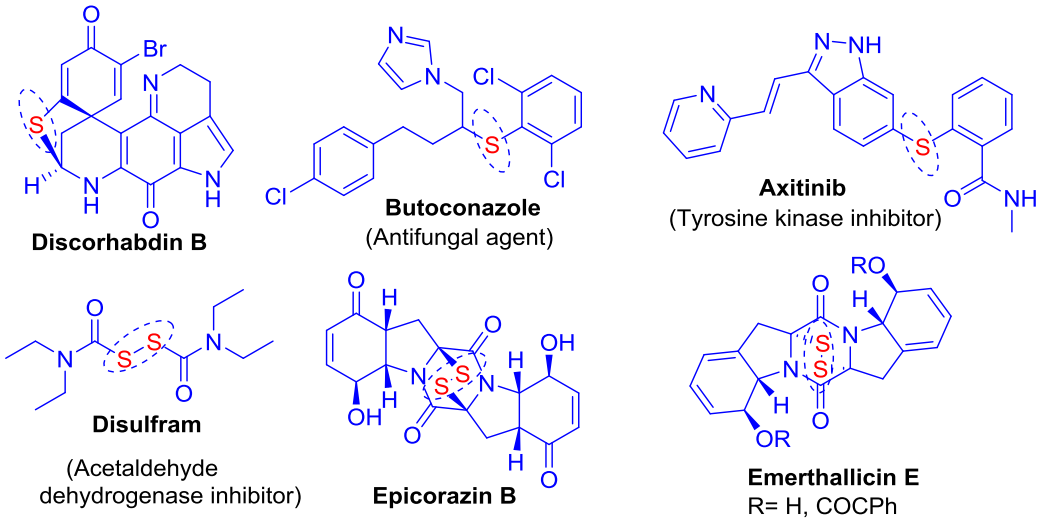

Figure 4B.1.1: Selective examples of drugs and natural alkaloids containing sulfide and disulfide linkages

With the increasing voice of sustainable chemistry, cross-dehydrogenative coupling strategies leading to the construction of C–C and C–X (X = N, S, O) bonds[10-13] have streamlined the chemical processes by providing shorter, atom-economical and environmentally benign protocols.[14-16] The oxidative C−S bond formation is a highly useful, and equally challenging approach for the construction of sulfur-containing frameworks.[17,18] In this regard, a number of transition-metal catalyzed[17,19-22] and metal-free[23-25] C–S bond forming strategies have been developed in recent years. In this context, molecular iodine has developed a significant repute due to its close resemblance in the reactivity pattern and structural features with various heavy transition metals complexes.[26-29] Iodine is one of the heaviest non-radioactive element in the

Periodic Table classified as a non-metal. It can form inorganic and organic derivatives in various oxidation states (−1, 0, +1, +3, +5, +7). Contentedly as an inexpensive, low-toxic and air insensitive reagent, molecular iodine has been actively involved in various oxidative C−C, C−N, C−O and C−S bond formation reactions.[23,30-34] Appreciable efforts have been devoted towards the oxidative C−S bond formation for sulfenylation/arylthiolation of different heterocyclic frameworks under molecular iodine-catalyzed/mediated conditions (briefly summarized in scheme 4B.1.1).[31,33,35-48]

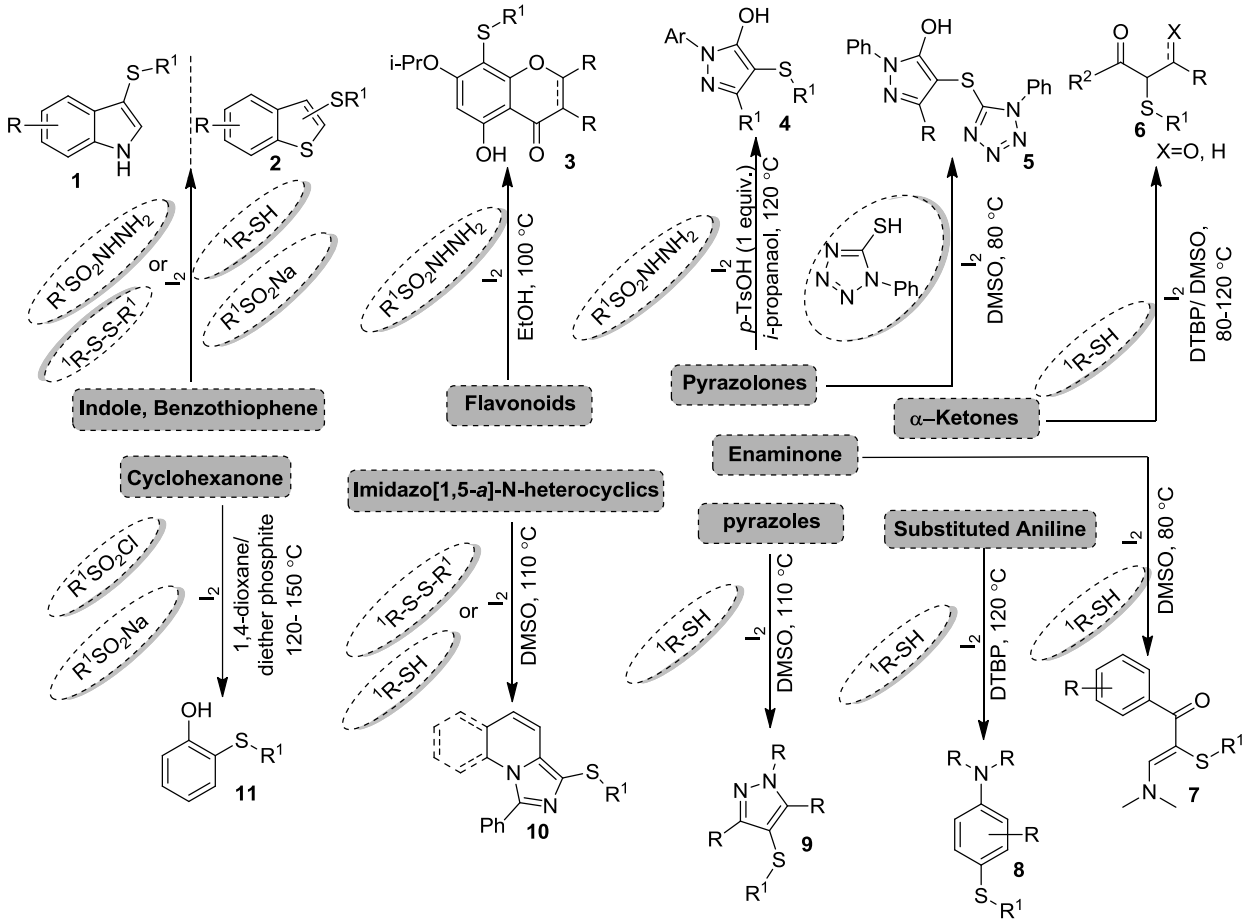

Scheme 4B.1.1: An overview of I_2-catalyzed/mediated arylthiolation of various organic motifs

On the other hand, looking into the eye-catching biological profile of imidazo-heterocycles and the occurrence of its core skeleton in various marketed drugs several efforts have been devoted by various research groups towards the C-3 functionalization. In particular, sulfur decorated imidazo[1,2-*a*]pyridines were synthesized using different sulfur source such as disulfides, thiols, sulfenyl chlorides, sulfonyl hydrazines, sodium thiosulfate, sodium sulfonate, and elemental sulfurs.[49-59] Molecular iodide has been extensively employed by various research group for the

regioselective C-3 aryl/heteroarylthiolation of imidazo[1,2-*a*]pyridine under different reaction condition.

Braga and co-workers prepared C-3 sulfenylated imidazo[1,2-*a*]pyridines **16** with various diaryl disulfides (**13**) using catalytic iodine and DMSO (Scheme 4B.1.2a). The author also extended the methodology with other thiolating reagents such as thiols **14** and aryl sulfonyl hydrazide (**15**) under the similar standardized condition to afford the corresponding sulfenylated products **13** in comparatively lower yields (Scheme 4B.1.2b,c).[49]

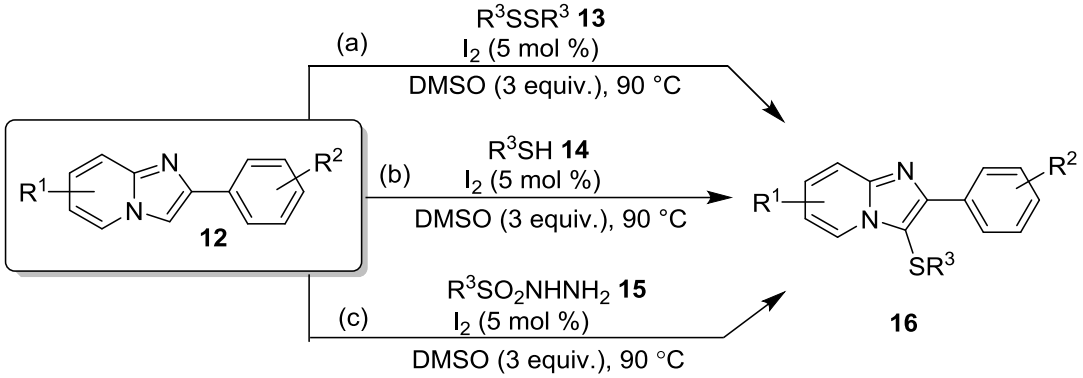

Scheme 4B.1.2: I_2-catalyzed regioselective C-3 thioarylation of imidazo[1,2-*a*]pyridine (**12**)

However, Hajra and co-worker used sulfonyl hydrazides (**15**) as a thiol surrogate for regioselective sulfenylation at C-3 position of imidazo[1,2-*a*]pyridine (**12**) under catalytic iodine condition in ethanol (Scheme 4B.1.3).[53]

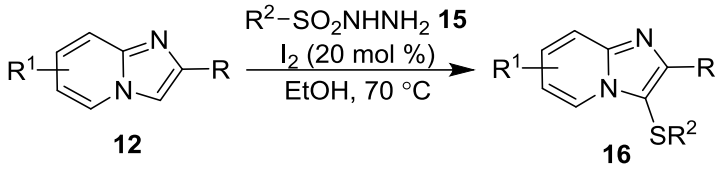

Scheme 4B.1.3: I_2-catalyzed regioselective C-3 thioarylation of imidazo[1,2-*a*]pyridine (**12**)

Recently, Li and coworkers documented an elegant and regioselective approach for the direct arylthiolation of imidazo[1,2-*a*]pyridines (**12**) with sodium sulfinates (**17**) using molecular iodine in presence of triphenylphosphine under DMF. Apart from aromatic and heteroaromatic sodium sulfinates, aliphatic sodium sulfinates were also reactive to produce the desired products in fairly good yields (Scheme 4B.1.4).[57]

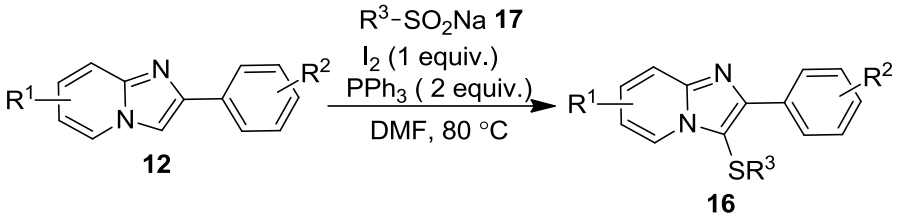

Scheme 4B.1.4: I_2-mediated regioselective C-3 thioarylation of imidazo[1,2-*a*]pyridine (**12**)

Very recently, Prabhu *et a.l* disclosed a convergent cross-dehydrogenative coupling strategy for the C-3 sulfenylation of 2-arylimidazo[1,2-*a*]pyridines (**12**) from a variety of easily available heterocyclic thiols or thiones (**18**), using iodine as catalyst and dimethyl sulfoxide as an oxidant in fairly good to excellent yields (Scheme 4B.1.5).[60] Similarly, Hiebel *et al.* also reported iodine-catalyzed regioselective sulfenylation of imidazo[1,2-*a*]pyridines with various thiophenols (**14**) in PEG-400, using hydrogen peroxide as an oxidizing agent (Scheme 4B.1.5).[50]

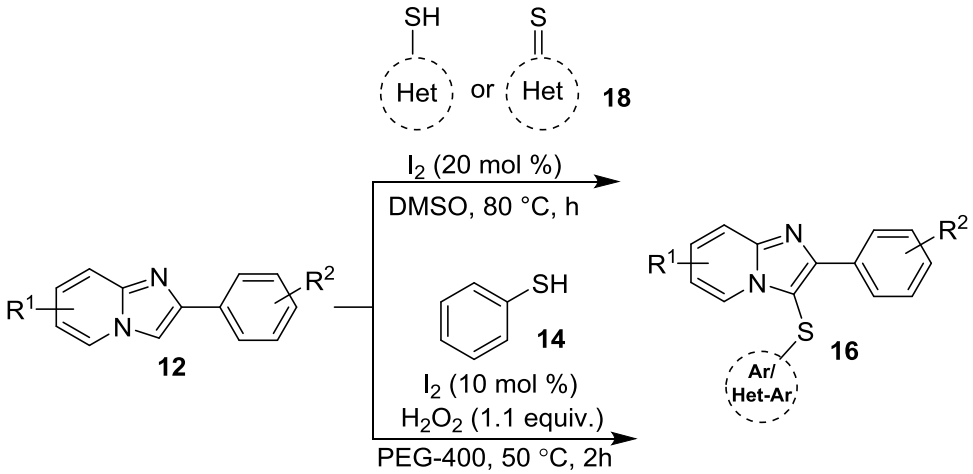

Scheme 4B.1.5: I_2-mediated regioselective C-3 thioarylation/heterothioarylation of imidazo[1,2-*a*]pyridine (**12**)

Interestingly, bis-heterocyclic compounds including; bis-indole, bis-(pyrimido)acridines, bis-(pyrazolo)acridine, bis-(benzothiazolylquinazoline), bis-(1*H*-imidazo[1,2-*a*]benzimidazole), bis-pyrrole, bis-quinoline, bis-azoles *etc.* were identified as potentially biologically active, showing anticancer, antibacterial, antifungal, antiviral activities. In this regard few noticeable efforts have been devoted by various research group's for the synthesis of methylene linked 3,3'-biimidazo[1,2-*a*]pyridine derivatives in recent times (Chapter 1, Scheme1.2.19).[61-66]

Janosik *et al.* synthesized 3,3'-bis(indolyl) disulfide (**19**) derivatives in an improved yield of 62-80 % simply by passing a stream of air through the reaction mixture, modifying the well established

Dougherty's process[67] of exposure of indoles to thiourea in the presence of iodine under basic medium (Scheme 4B.1.6).[68]

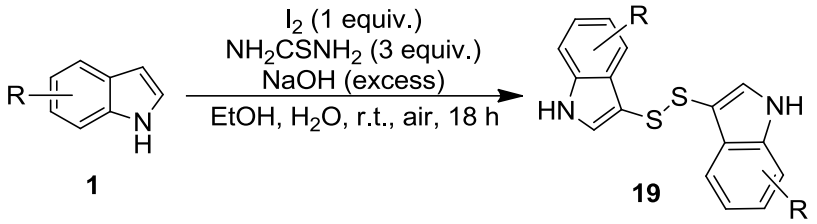

Scheme 4B.1.6: I_2-mediated synthesis of 3,3'-dithiobisindoles (**19**)

Janosik and coworker synthesized 3,3'-bis(indolyl) sulfide (**21**) in a multiple steps using *N*–protected 3,3'-bis(indolyl) disulfide (**20**) involving lithiated indole using *n*-butyl lithium giving unsymmetrically protected 3,3'-bis(indolyl) sulfide, which upon treatment with 1 M KOH (aq)-dioxane (1:1) at 80°C resulted in the formation of **21** (Scheme 4B.1.7).[69]

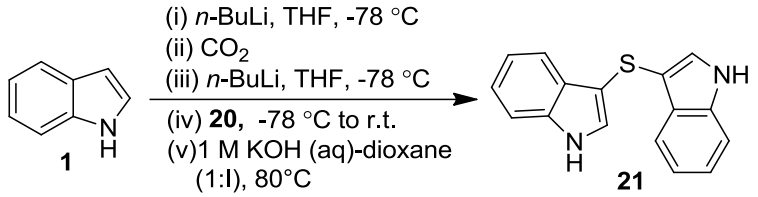

Scheme 4B.1.7: Multiple steps synthesis of 3,3'-bis(indolyl) sulfide (**21**)

Li and coworker disclosed a robust C-H activation strategy for the selective synthesis of 3,3'-indolyl sulfide (**21)** and 3,3'-indolyl disulfide (**19**) using nickel and iron catalyst respectively with stoichiometric amount of potassium iodide in DMF. The reaction showcased substantial compatibility with various substituent's including aldehydes, halides, ester, nitrile, and nitro (Scheme 4B.1.8).[70]

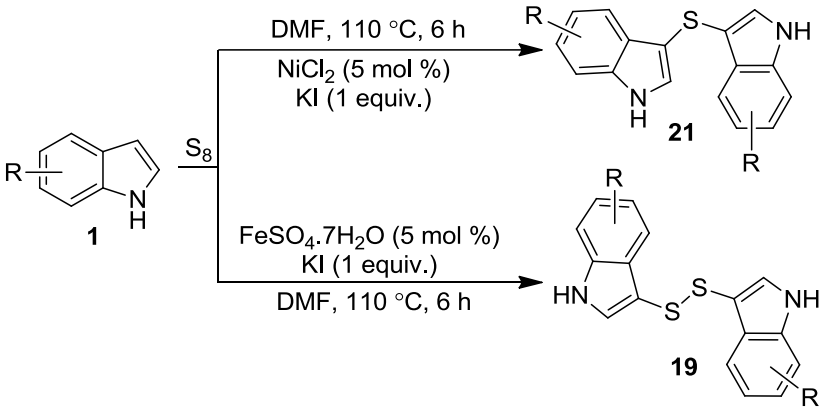

Scheme 4B.1.8: Ni-catalyzed synthesis of 3,3'-indolyl sulfide (**21)** & Fe-catalyzed 3,3'-indolyl disulfide (**19**)

Murai *et al* in 2014, demonstrated an efficient protocol for the synthesis of bis imidazo[1,5-*a*]pyridyl sulfides (**23**) in appreciable yields in presence of CuTC (copper(I) thiophenecarboxylate) by treating imidazo[1,5-*a*]pyridine (**22**) with elemental sulfur in DMSO at 90 °C under aerobic condition (Scheme 4B.1.9).[71]

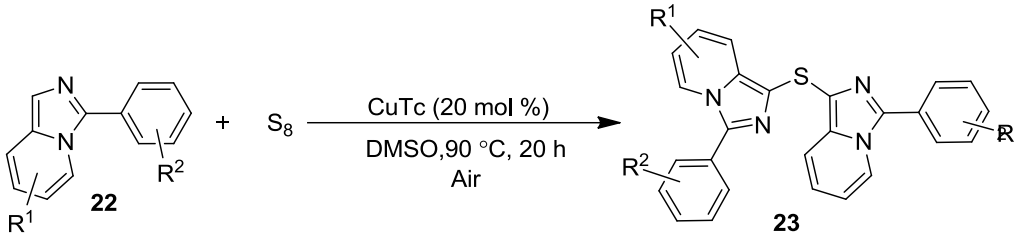

Scheme 4B.1.9: Cu-catalyzed Synthesis of bisimidazo[1,5-*a*]pyridyl sulfides derivatives (**23**)

To complement these reports, it became highly desirable to develop environmentally benign protocol for the construction of sulfur linked bis imidazo[1,2-*a*]pyridines as a potential pharmacological lead. With our advent interest of functionalizing IP,[66,72-74] herein we projected to synthesis bis(imidazo[1,2-*a*]pyridin-3-yl)sulfanes under metal-free using appropriate sulfur source.

4B.2 Results and Discussion

With an anticipation to synthesize sulfur-bridged dimeric imidazo-heterocycles and following a trail from previous chapter work, we attempted the reaction of 2-phenylimidazo[1,2-*a*]pyridine (**24a**) with 3 equiv. of sodium sulfide (Na_2S) as a model reaction under PIDA-mediated conditions (Table 4B.2.1, entry 1). Sodium sulfide failed to participate in the reaction, and consequently 3,3'-biimidazo[1,2-*a*]pyridine[61,63-65] was obtained in a variety of solvents under reflux conditions over the targeted 3,3′-bis(imidazo[1,2-*a*]pyridin-3-yl)sulfane (Table 4B.2.1, entry 1). Moreover, PIDA-mediated reaction of **24a** and Na_2S in dimethyl sulfoxide (DMSO) or *N*,*N*-dimethylacetamide (DMA) failed to yield any product at all. (Table 4B.2.1, entry 2). Interestingly, the desired product bis(imidazo[1,2-*a*]pyridin-3-yl)sulfane (**25a**) was first witnessed and isolated in 18% yield by replacing PIDA with molecular iodine in DCM under ambient conditions (Table 4B.2.1, entry 3). Interestingly, unexpected formation of bis disulfane **26a** in 10% yield was observed along with **25a** in 48%, when the model reaction was performed using 2 equiv. of iodine in DCM under reflux conditions for 20 h (Table 4B.2.1, entry 4). The structures of **25a** and **26a** were unambiguously confirmed by ^{1}H and ^{13}C NMR spectra and HRMS analysis. A further enhancement in the yield of **25a** up to 69% was observed by screening

solvents from DCM to DCE, and finally to chloroform under reflux conditions (Table 4B.2.1, entries 5-6). The reaction was further optimized by varying the number of equivalents of sodium sulfide and iodine. The results indicated that increasing the equivalents of sodium sulfide to five can yield **25a** in 75% yield (Table 4B.2 1, entry 7). Delightfully, the best result was obtained by using three and five equiv. of molecular iodine and sodium sulfide respectively, yielding 80% of **25a** with trace formation of **26a** (Table 4B.2.1, entry 8). Subsequently, a number of iodine source replacements such as KI or NH_4I were screened for the reaction, however comparatively lower yields of **25a** were obtained (Table 4B.2.1, entries 9-10). A marginal decrease in the yield of the **25a** was observed by replacing Na_2S with K_2S (Table 4B.2.1, entry 11). Attempt to optimize the reaction conditions using catalytic amount of iodine resulted in the formation of minor amount of **25a** (<10%) in chloroform upon refluxing up to 20 h (Table 4B.2.1, entry 12).

Table 4B.2.1: Selected optimization[a] of reaction conditions for synthesis of **25a** and **26a**

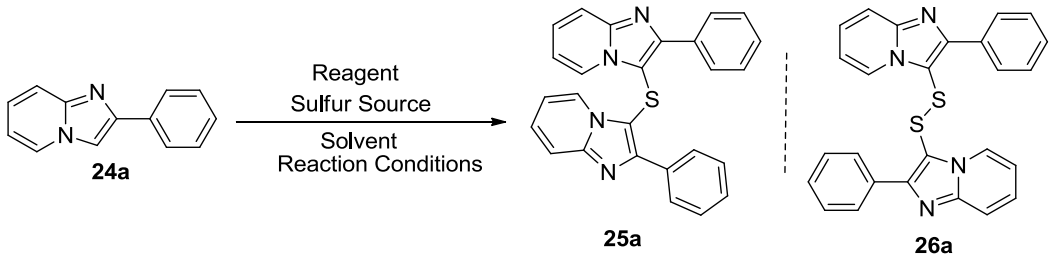

24a **25a** **26a**

Entry	Reagent (equiv.)	Sulfur Source (equiv.)	Solvent	Yield[b] (%)	
				25a	**26a**
1[c]	$PhI(OAc)_2$ (2)	Na_2S (3)	DCE/CH_3CN/ $CHCl_3$/DCM	-	-
2[d]	$PhI(OAc)_2$ (2)	Na_2S (3)	DMSO/DMA	-	-
3[e]	I_2 (2)	Na_2S (3)	DCM	18	-
4[a]	I_2 (2)	Na_2S (3)	DCM	48	10
5[a]	I_2 (2)	Na_2S (3)	DCE	61	<10
6[a]	I_2 (2)	Na_2S (3)	$CHCl_3$	69	<5
7[a]	I_2 (2)	Na_2S (5)	$CHCl_3$	75	<5
8[a]	**I_2 (3)**	**Na_2S (5)**	**$CHCl_3$**	**80**	**<5**
9[a]	KI (3)	Na_2S (5)	$CHCl_3$	41	<5
10[a]	NH_4I (3)	Na_2S (5)	$CHCl_3$	44	<5
11[a]	I_2 (3)	K_2S (5)	$CHCl_3$	78	<5
12[a]	I_2 (0.2)	Na_2S (5)	$CHCl_3$	<10	-
13[f]	I_2 (3)	Na_2S (5)	CH_3COOH	<5	47
14[g]	I_2 (3)	Na_2S (5)	CH_3COOH	<10	85

[a]Reaction conditions: **24a** (0.25 mmol), reagent (as indicated), sulfur Source (as indicated), solvent (5 mL), reflux, 20 h; [b]Isolated yield; [c]T = reflux for 20 h; [d]T = 110 °C (for 20 h); [e]r.t. for 30 h; [f]T = 100 °C for 20 h; [g]T = 100 °C for 48 h.

With the optimized reaction conditions in hand, the practical applicability of the methodology was systematically investigated using different substituted imidazo[1,2-*a*]pyridines bearing electron-donating and electron-withdrawing groups (Scheme 4B.2.1).

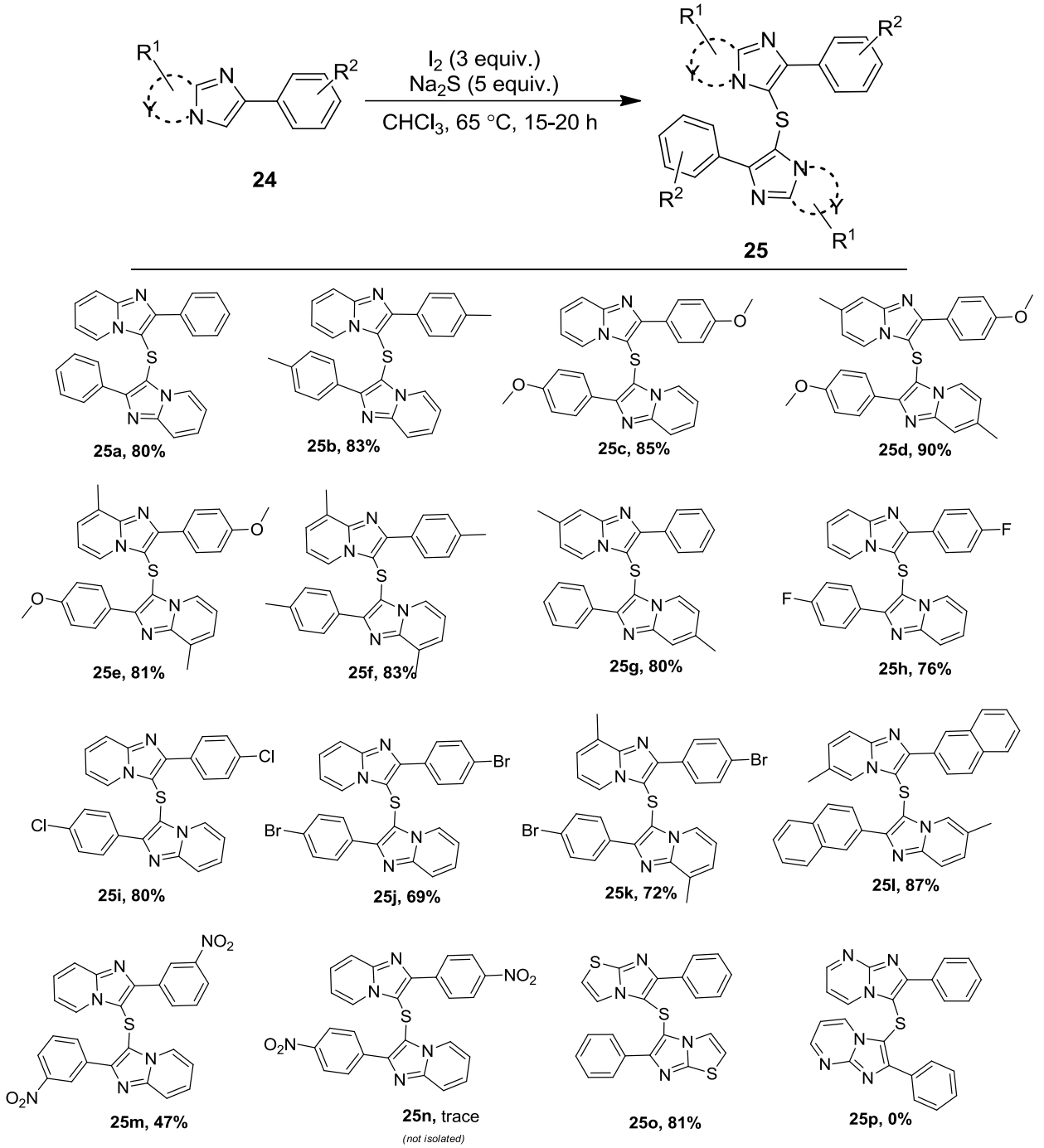

Scheme 4B.2.1: Substrate scope of substituted 2-arylimidazo-heterocycles (**24**) towards the synthesis of bis sulfane (**25**)

2-arylimidazo[1,2-*a*]pyridines possessing Me and OMe group on the aryl ring showcased excellent reactivity offering **25b** and **25c** in 83% and 85% yield, respectively. The presence of Me and OMe group on the pyridyl and aryl rings respectively proved **24d** to be the best substrate, producing the corresponding bis sulfane **25d** in 90% yield. Similarly, 2-arylimidazo[1,2-*a*]pyridine bearing Me group on both the pyridyl and phenyl rings yielded their desired bis sulfanes **25f** in 83% yield. Halogen (–F, Cl and Br) substituted 2-arylimidazo[1,2-*a*]pyridines (**24h-k**) afforded the corresponding products (**25h-k**) in 69-80% isolated yields. The reaction also tolerated bulkier naphthyl group (in place of aryl), yielding the expected bis sulfane (**25l**) in 87% yield. The *m*-nitro substituted 2-arylimidazo[1,2-*a*]pyridine (**24m**) showed slight sluggish behavior in reactivity offering **25m** in only 47% yield, whereas *p*-nitro substituted 2-arylimidazo[1,2-*a*]pyridine (**24n**) showed reluctance in reactivity, yielding only trace amount of bis sulfane that was not isolated. To our delight, the reaction was also successful with 2-arylimidazo[2,1-*b*]thiazole (**24o**) yielding bis(6-phenylimidazo[2,1-*b*]thiazol-5-yl)sulfane (**25o**) in 81% yield. Representative ^{1}H NMR and ^{13}C NMR spectra of **25h** are shown in figures 4B.2.1 and 4B.2.2.

Interestingly, during further solvent optimization, 3,3′-bis(imidazo[1,2-*a*]pyridin-3-yl)disulfane (**26a**) was obtained in 47% yield at 100 ^{0}C in acetic acid after 20 h (Table 4B.2.1, entry 13). Gratifyingly, increasing the reaction time to 48 h in acetic acid at 100 $^{\circ}$C predominantly resulted in formation of **26a** in 85% yield (Table 4B.2.1, entry 14). Within this realm, the substrate scope of imidazo-heterocycles bearing different electron-donating and electron-withdrawing groups on aryl and pyridyl rings were examined (Scheme 4B.2.2). In general, all 2-arylimidazo[1,2-*a*]pyridines exhibited admirable reactivity yielding their corresponding disulfanes in excellent yields. Interestingly, the nitro *m*/*p*-substituted 2-arylimidazo[1,2-*a*]pyridines (**24m-n**) comfortably delivered the desired products (**26m-n**) in 85% and 87% yields, respectively.

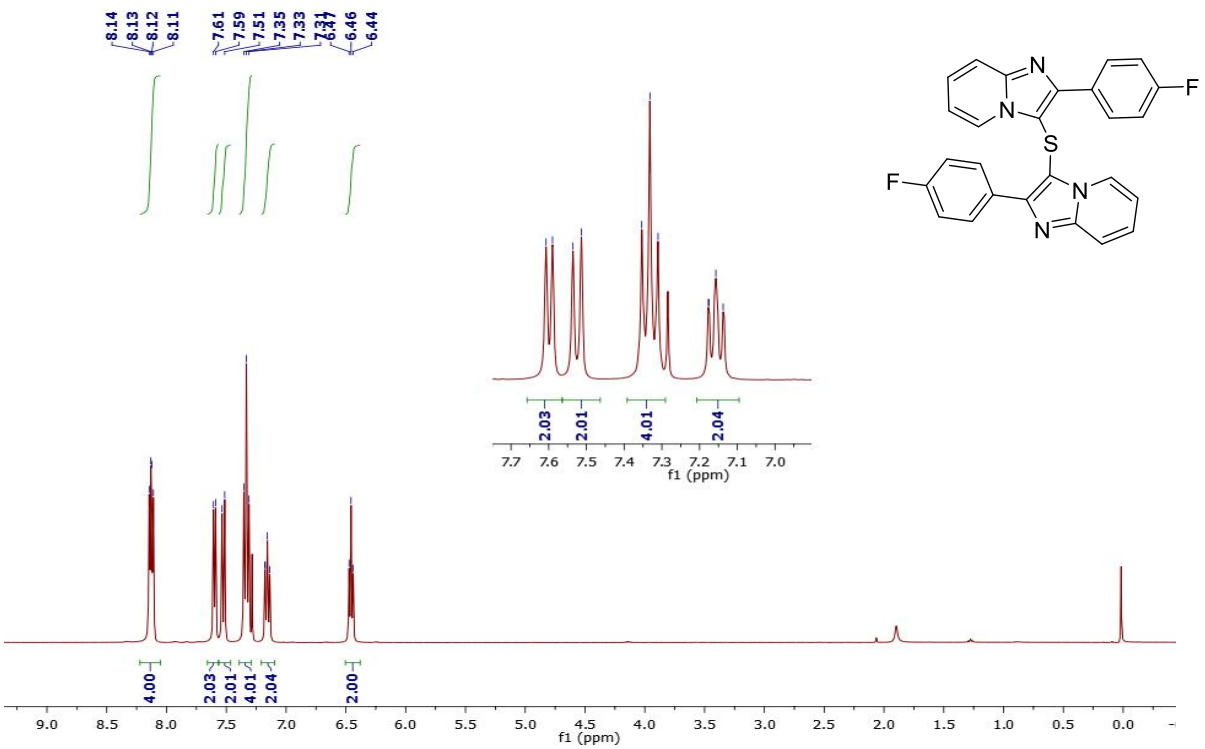

Figure 4B.2.1: ^{1}H NMR spectrum of **25h**

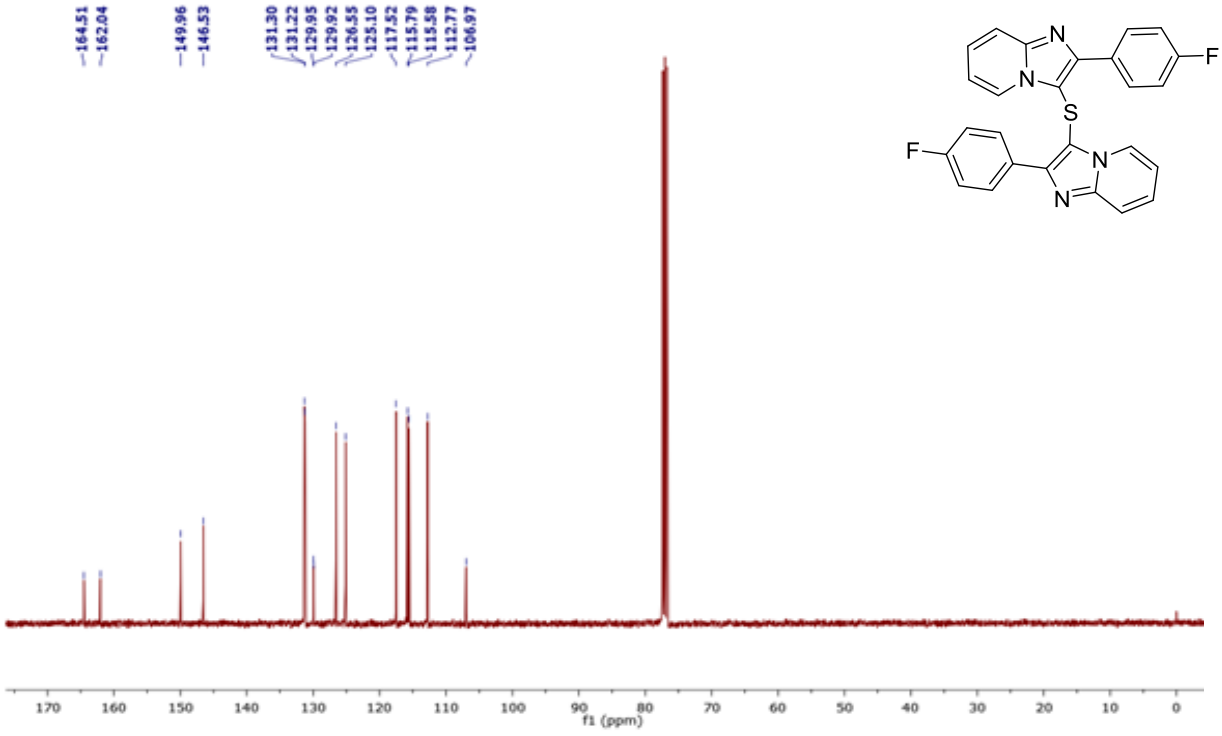

Figure 4B.2.2: ^{13}C NMR spectrum of **25h**

The methodology was also extended towards the synthesis of 1,2-bis(6-phenylimidazo[2,1-*b*]thiazol-5-yl)disulfane (**26o**) from imidazo[2,1-*b*]thiazole (**24o**) in appreciable yield. Unfortunaltely, 2-arylimidazo[1,2-*a*]pyrimidine (**24p**) failed to yield either bis sulfane (**25p**) or bis disulfane (**26p**) under optimized conditions. Representative ^{1}H NMR and ^{13}C NMR spectra of **26o** are shown in figures 4B.2.3 and 4B.2.4

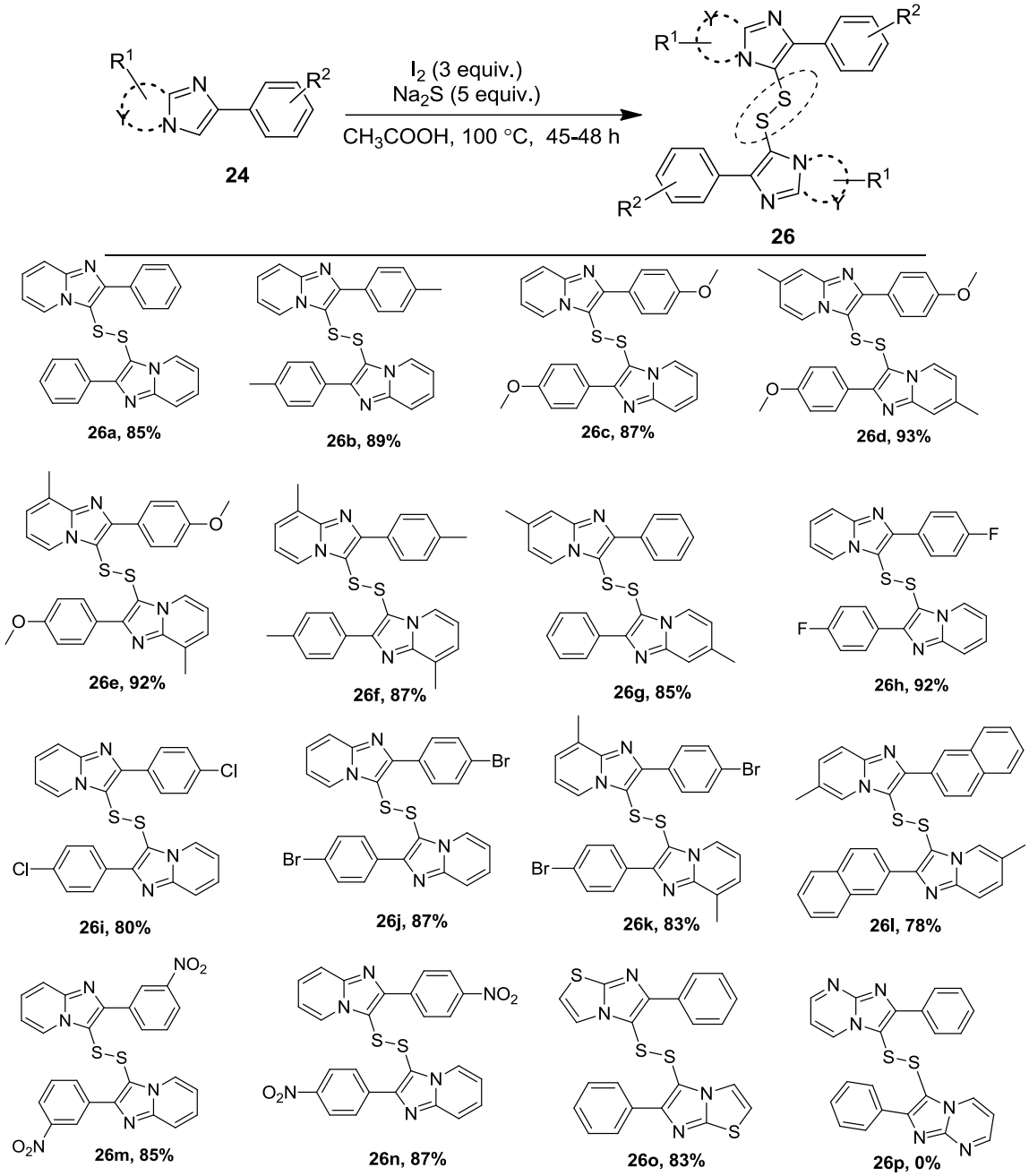

Scheme 4B.2.2: Substrate scope of 2-arylimidazo-heterocycles (**24**) towards the synthesis of bis-disulfane (**26**)

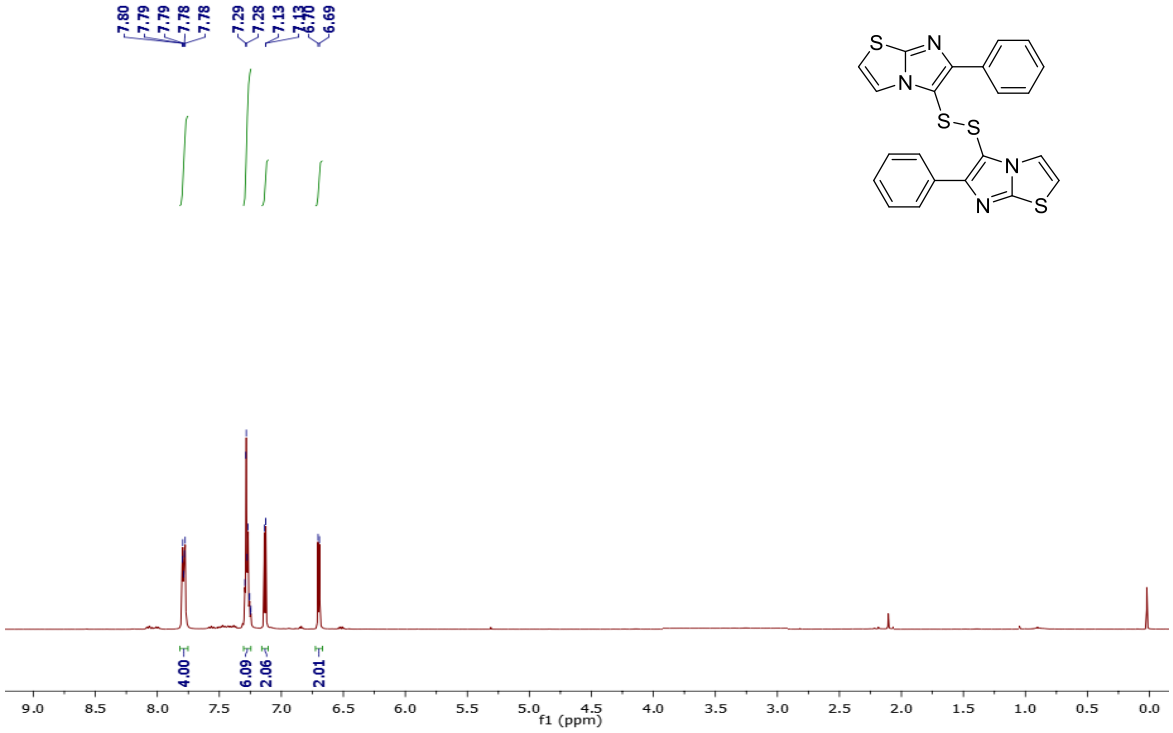

Figure 4B.2.3: ^{1}H NMR spectrum of **26o**

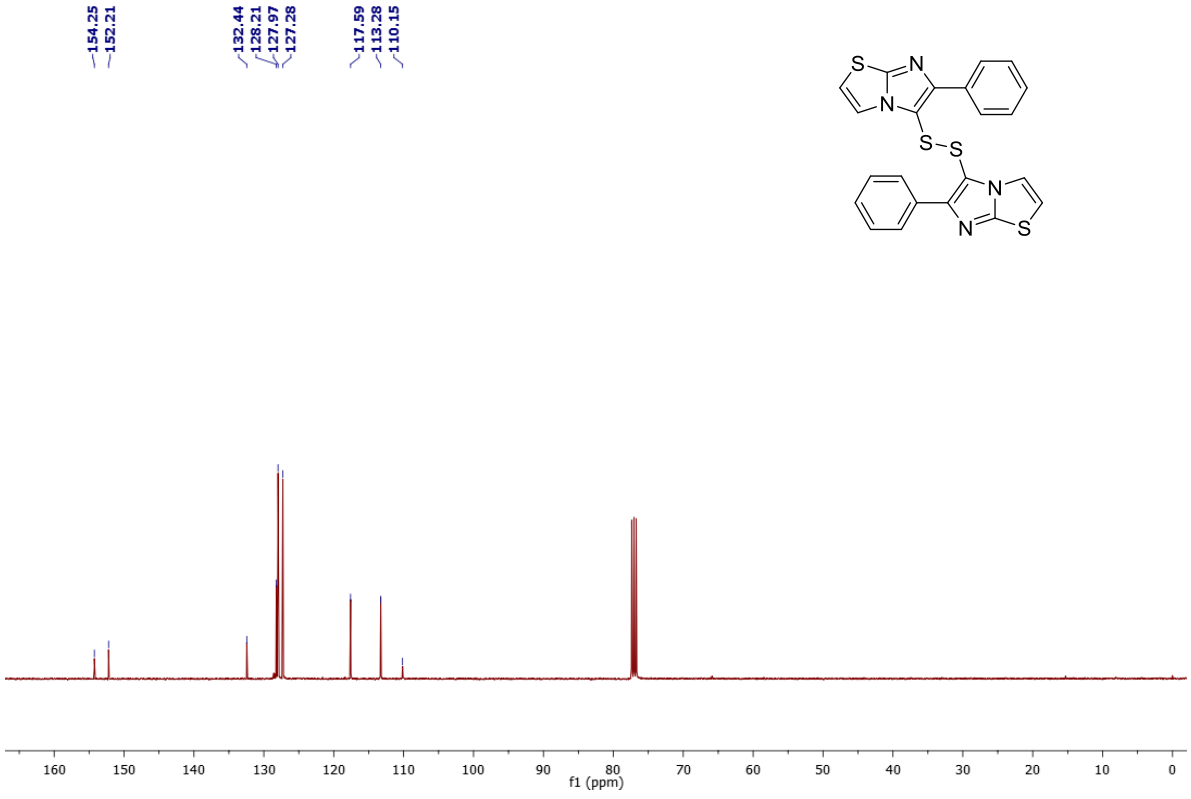

Figure 4B.2.4: ^{13}C NMR spectrum of **26o**

In order to further confirm the proposed structures, as representative examples single crystals of bis sulfane (**25h**) and bis disulfane (**26j** & **26o**) were grown by chloroform for the X-ray diffraction studies. Both **25h** & **26j** crystallize in the monoclinic C2/c space group, while **26o** crystallizes in the orthorhombic C2221 space group. ORTEP diagrams of **25h** (CCDC No. 1559710), **26j** (CCDC No. 1559711) and **26o** (CCDC No. 1559712), are shown in Figure 4.2.5. In addition, ^{1}H-^{13}C correlation (HETCOR) spectra was also recorded for bis sulfane (**25f**) and bis disulfane (**26f**) (Figures 4B.2.6 and 4B.2.7).

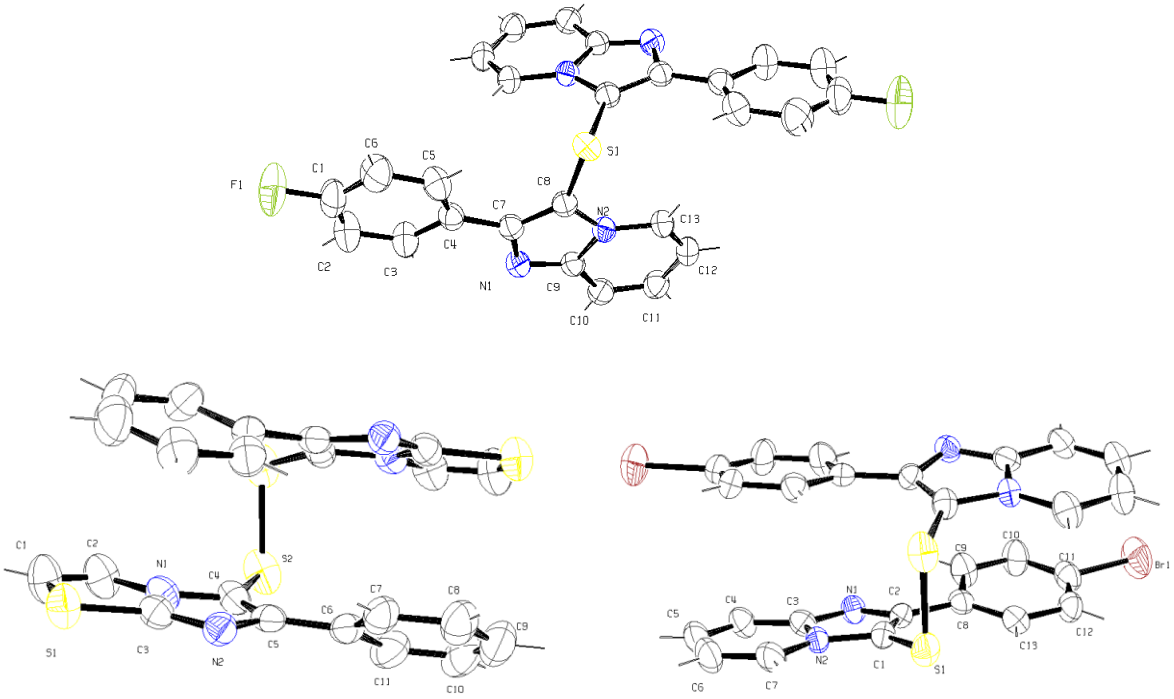

Figure 4B.2.5: ORTEP diagrams of **25h, 26j** and **26o**

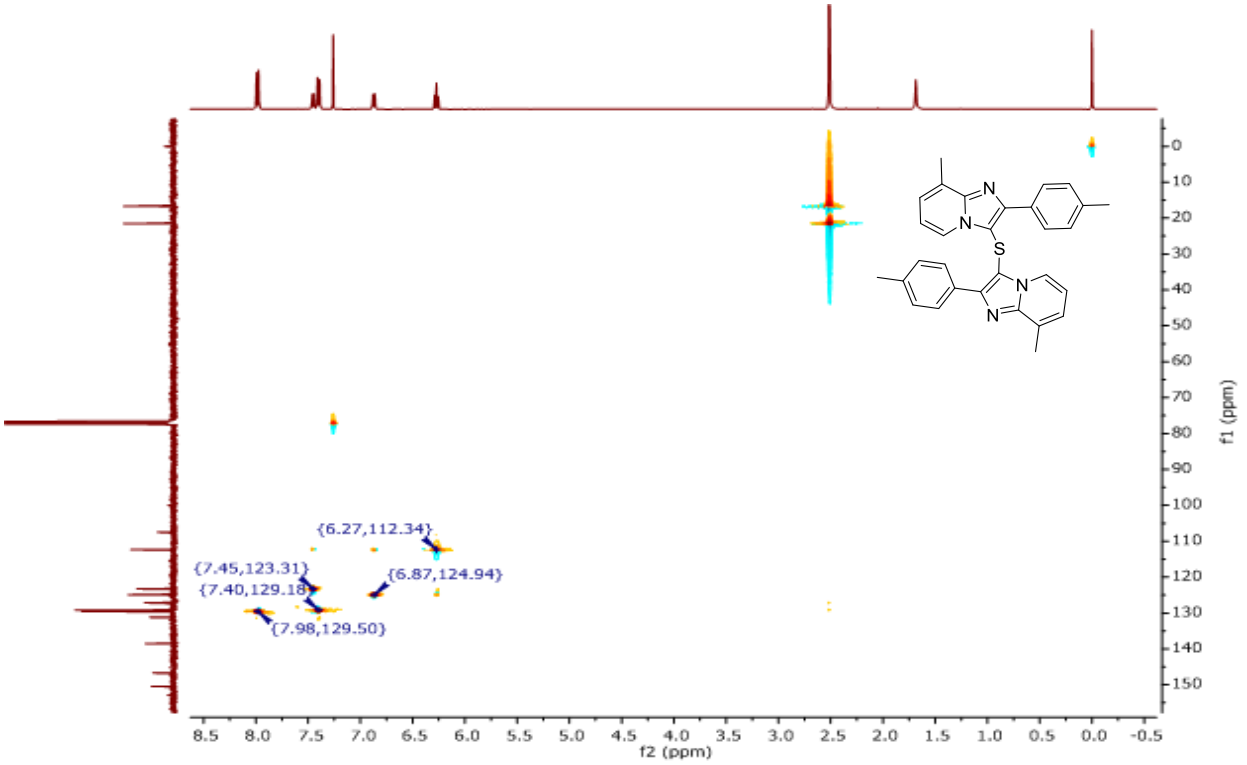

Figure 4B.2.6: ^{1}H-^{13}C correlation NMR spectrum of **25f**

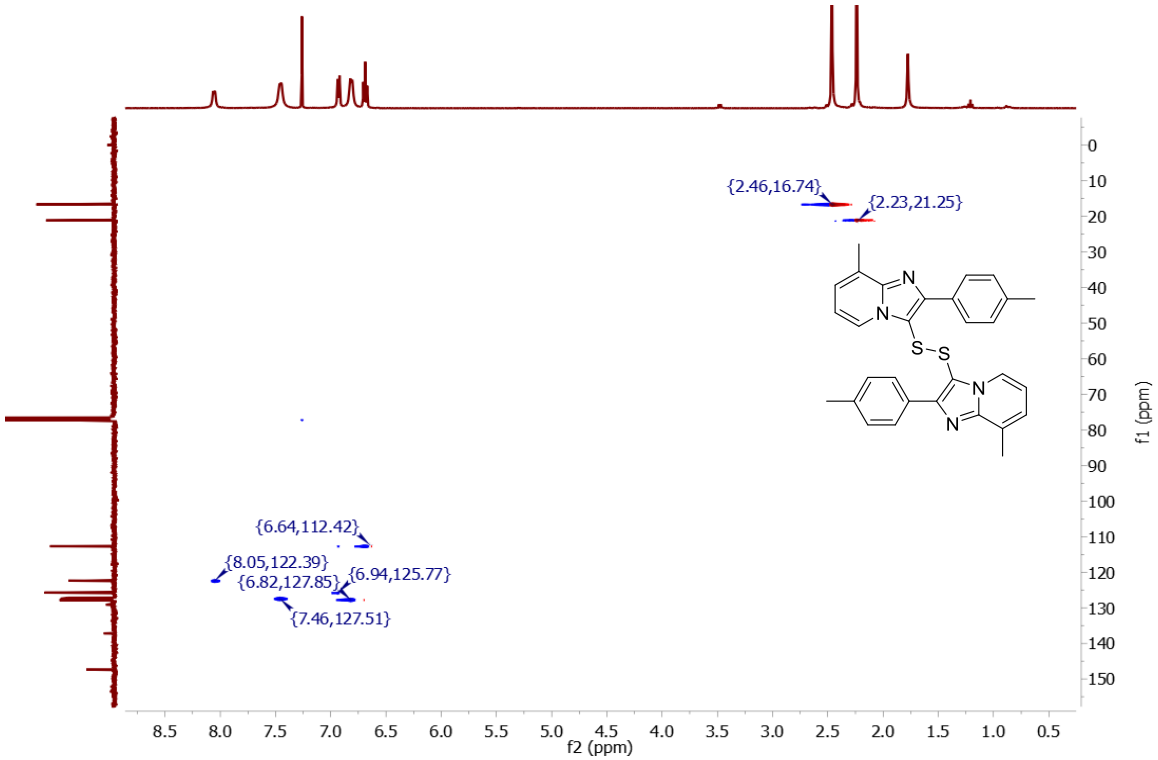

Figure 4B.2.7: ^{1}H-^{13}C correlation NMR spectrum of **26f**

To access the scalability of the developed synthetic strategies, 1 gram scale reactions of 2-(*p*-tolyl)imidazo[1,2-*a*]pyridine (**24b**) with 5 equivalents of sodium sulfide under optimized reaction conditions, yielded bis sulfane (**25b**) and bis disulfane (**26b**) in 65% (0.696 g) and 71% (0.815 g) yields, respectively (Scheme 4B.2.3).

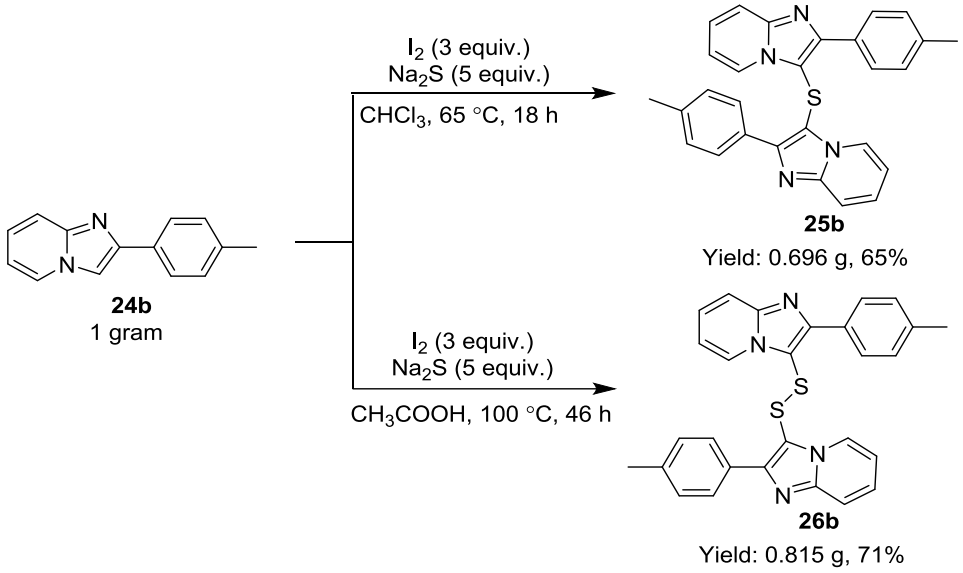

Scheme 4B.2.3: Gram scale synthesis of bis sulfane (**25b**) & bis disulfane (**26b**)

To probe the reaction mechanism, several preliminary experiments were performed (Scheme 4B.2.4). The non-involvement of free-radical species in the reaction pathway was ascertained by obtaining bis sulfane (**25f**) and disulfane (**26f**) from **24f** in 81% and 84% yields respectively, under optimized conditions in presence of 3 equiv. of a radical scavenger TEMPO (Scheme 4B.2.4i-ii). 3-iodo-8-methyl-2-(*p*-tolyl)imidazo[1,2-*a*]pyridine (**24f'**) was observed to be formed (& isolated) in almost quantitative yields (TLC) after refluxing **24f** and I_2 (3 equiv.) in chloroform within 4 h. **24f'** upon further reaction with Na_2S/I_2 in chloroform under reflux conditions resulted in the formation of bis(8-methyl-2-(*p*-tolyl)imidazo[1,2-*a*]pyridin-3-yl)sulfane **25f** in major amounts (Scheme 4B.2.4iii). It is noteworthy to mention that subsequent de-halogenation of **24f'** to **24f** was also observed during the progress of the reaction. Similarly, **24f'** upon reaction with Na_2S/I_2 in acetic acid resulted in the formation of 1,2-bis(8-methyl-2-(*p*-tolyl)imidazo[1,2-*a*]pyridin-3-yl)disulfane **36f** in major amounts, albeit the formation of **24f'** in acetic acid was observed to be a slow process and in lower yield (Scheme 4B.2.4iv).

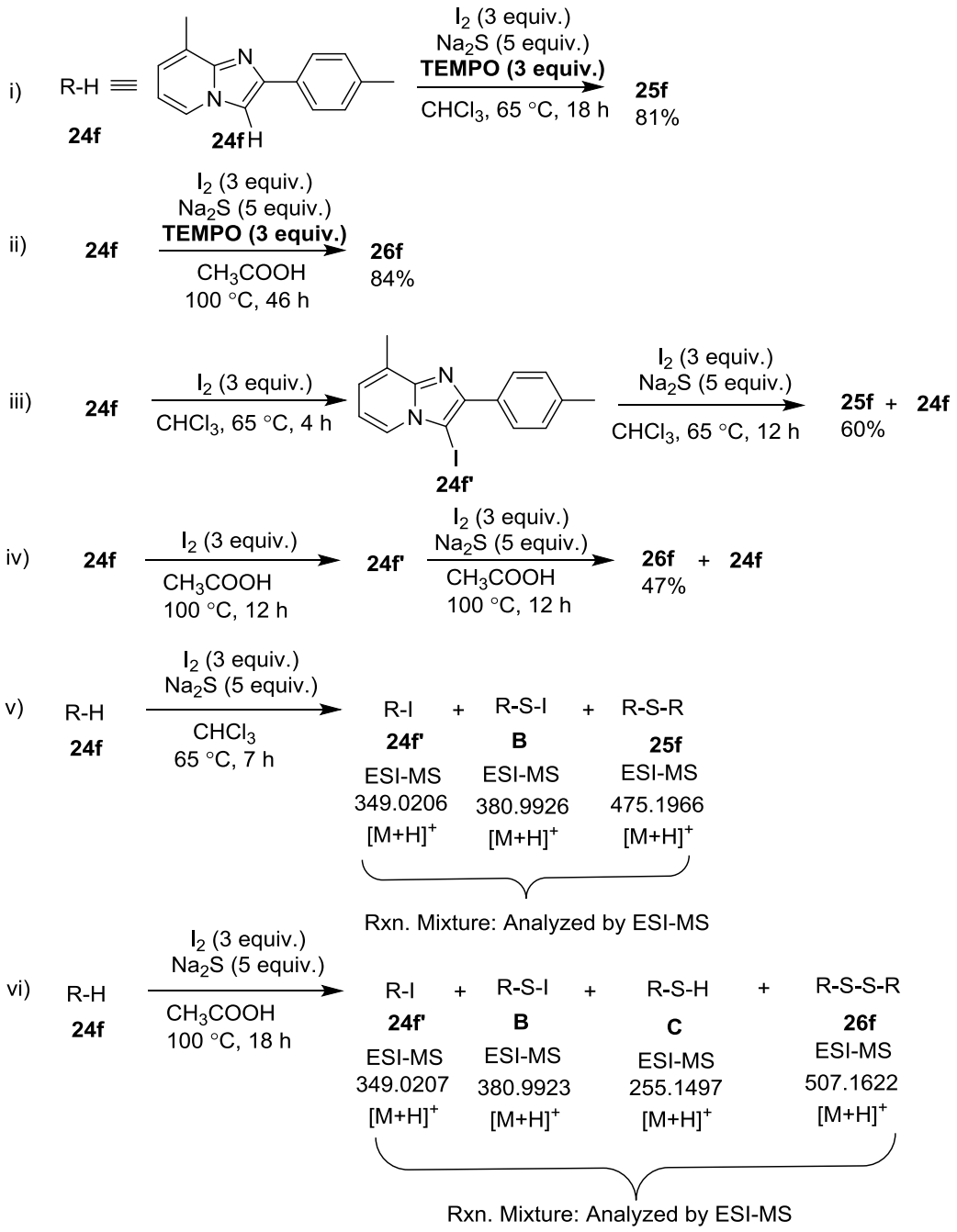

Scheme 4B.2.4: Preliminary mechanistic studies

The mass spectral studies (ESI-MS) of the reaction mixture obtained by reacting **24f** under optimized conditions in chloroform after 7 h affirmed the formation of **24f'**, **B** (R-S-I) and **25f**, thereby suggesting the possible involvement of **B** (R-S- I) intermediate in the reaction pathway (Scheme 4B.2.4v, Figure 4B.2.8). Similarly, the mass spectral studies (ESI-MS) of the reaction mixture obtained by reacting **24f** under optimized conditions in acetic acid after 18 h affirmed

the formation of **24f'**, **B,** **C** and **26f**, thereby suggesting the possible involvement of intermediates **B** (R-S- I) and **C** (R-S-H) in the reaction pathway (Scheme 4B.2.4vi, Figure 4B.2.9).

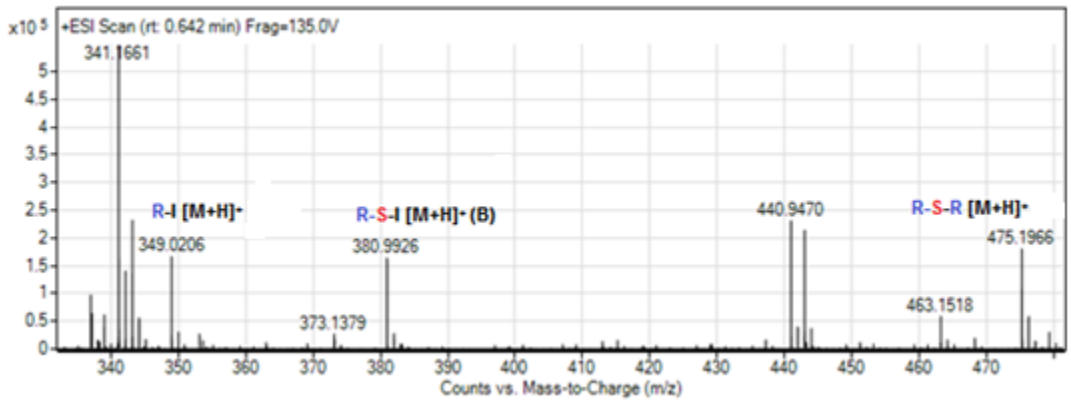

Figure 4B.2.8: ESI-MS data of reaction mixture (**24f** + Na_2S + I_2) in chloroform after 7 h

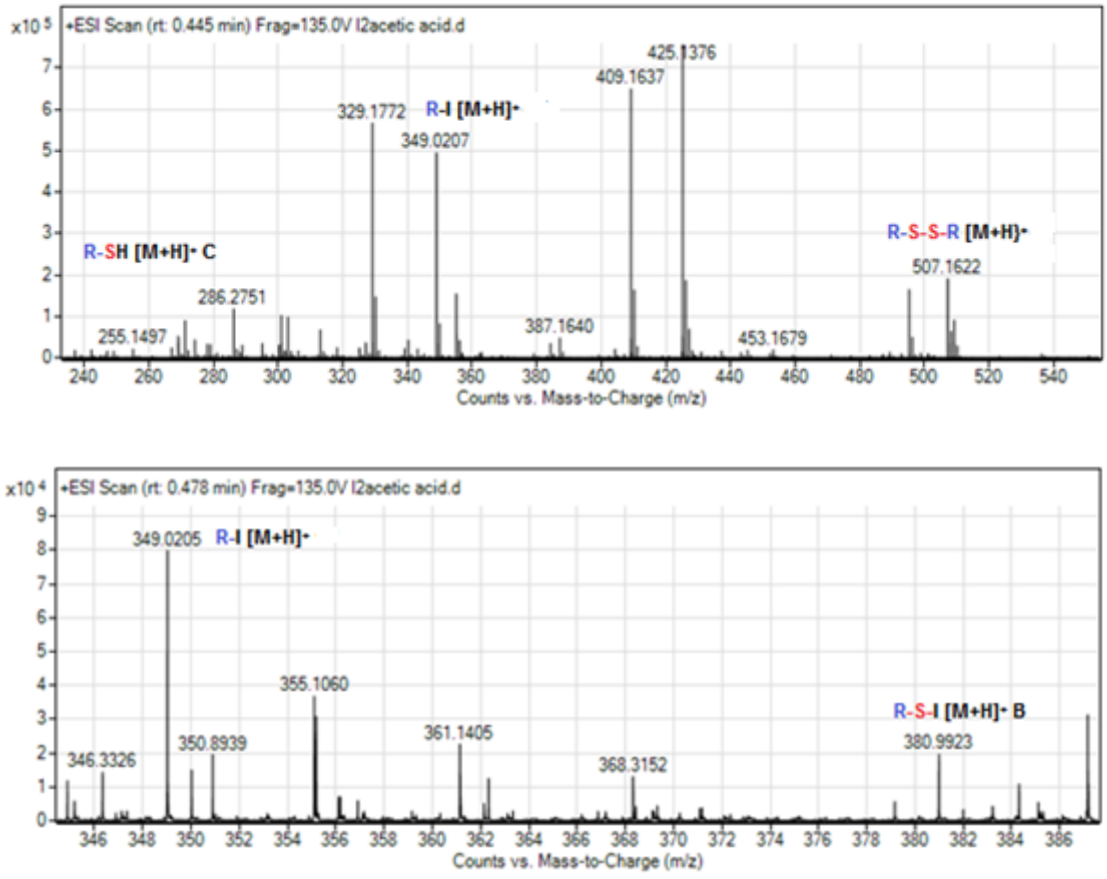

Figure 4B.2.9: ESI-MS data of reaction mixture (**24f** + Na_2S + I_2) in acetic acid after 18 h

On the basis of our current studies and available literature,[60] a plausible mechanism is proposed (Scheme 4B.2.5). The initial reaction (in chloroform or acetic acid) is believed to proceed *via* C-3 nucleophilic attack of imidazo[1,2-*a*]pyridine (**24f**) on I_2, forming intermediate **24f'**. In chloroform, nucleophilic attack of the sulfide ion on **24f'** possibly *via* SN2' pathway forms intermediate species **A** along with the de-iodination to generate **24f** in the reaction mixture. Thereafter, species **A** generates species **B** which on further reaction[60] with **24f** furnishes **25f** (Scheme 4B.2.5, Path a). On the other hand, due to possible conversion of S^{2-} to either SH^- or H_2S (existing in equilibrium with each other) in acetic acid, the reaction might proceed *via* nucleophilic substitution of I^- in **24f'** by SH^- (or H_2S) to generate thiol intermediate **C** (which is known to exist in equilibrium with **B**).[75,76] Subsequently, iodine-mediated oxidation of **C**[53,77] affords **26f** (Scheme 4B.2.5, Path b), Alternatively, the reaction in acetic acid could also proceed by the nucleophilic attack of *in-situ* generated S_2^- species (by I_2-mediated oxidation of S^{2-}) on **24f'** resulting in **D**, which eventual attacks another **24f'** to yield **26f** (Scheme 4B.2.5, Path b').

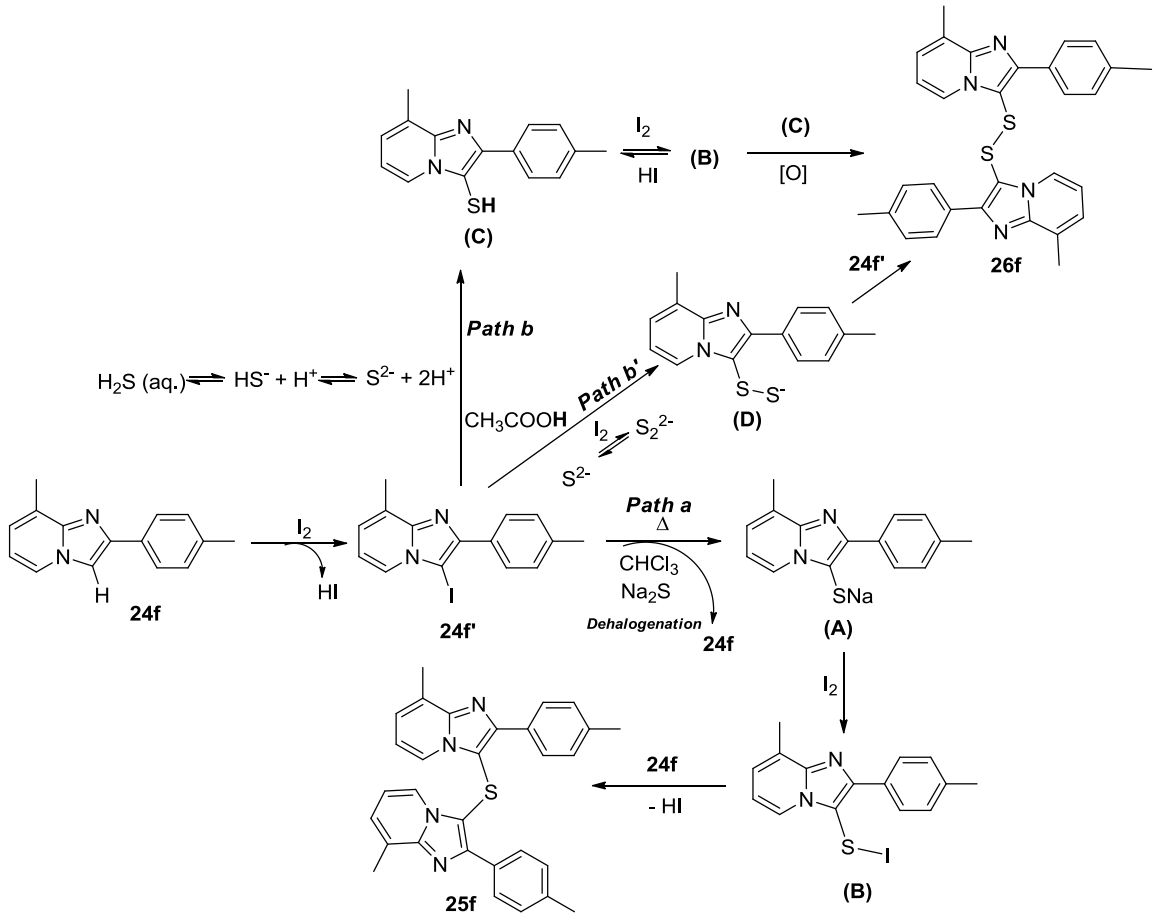

Scheme 4B.2.5: Plausible mechanism

In summary, we have successfully described solvent-driven straightforward, direct oxidative strategies for the synthesis of bis(imidazo[1,2-*a*]pyridin-3-yl)sulfanes and bis(imidazo[1,2-*a*]pyridin-3-yl)disulfanes using Na_2S as a sulfur source.

4B.3 Experimental Section

4B.3.1 General Materials and Methods

Commercially available reagents were used without purification. Commercially available solvents were dried by standard procedures prior to use. Nuclear magnetic resonance spectra were recorded on 400 MHz spectrometer and chemical shifts are reported in δ units, parts per million (ppm), relative to residual chloroform (7.26 ppm) or DMSO (2.5 ppm) in the deuterated solvent. The following abbreviations were used to describe peak splitting patterns when appropriate: s = singlet, d = doublet, t = triplet, dd = doublet of doublet and m = multiplet. Coupling constants *J* were reported in Hz. The ^{13}C NMR spectra were reported in ppm relative to deuterochloroform (77.0 ppm) or [d_6] DMSO (39.5 ppm). Melting points were determined on a capillary point apparatus equipped with a digital thermometer and are uncorrected. High resolution mass spectra were recorded with a TOF analyzer spectrometer by using electrospray mode.

General procedure for bis sulfane and bis disulfane

A mixture of imidazo-heterocycle (**24a-o**) (0.5 mmol), molecular iodine (1.5 mmol), sodium sulfide (2.5 mmol), in chloroform (10 mL) was refluxed at 65 °C under air atmosphere for 15-20 h. On completion of reaction as indicated by TLC, water was added to the reaction mixture. The organic layer was separated, and washed with a 20% sodium thiosulfate solution (30 mL × 2). The organic layer was concentrated under reduced pressure and the crude product was purified by silica gel column chromatography [SiO_2 (100–200 mesh), hexanes/EtOAc, 8:2 v/v], affording the corresponding bis sulfane (**25a-o**).

Similarly, a mixture of imidazo-heterocycle (**24a-o**) (0.5 mmol), molecular iodine (1.5 mmol), sodium sulfide (2.5 mmol), in acetic acid (10 mL) was heated at 100 °C under air atmosphere for 45-48 h. On completion of reaction as indicated by TLC, 10% sodium bicarbonate solution (20 smL) was added to the reaction mixture. Thereafter, the reaction mixture was extracted with ethyl acetate (20 mL × 2) and the organic layer was washed with a 20% sodium thiosulfate solution (30 mL × 2). Finally The organic layer was separated, concentrated under reduced

pressure and subjected to silica gel column chromatography [SiO_2 (100–200 mesh), hexanes/EtOAc, 3:7 v/v], affording bis sulfane (**26a-o**).

Bis(2-phenylimidazo[1,2-*a*]pyridin-3-yl)sulfane (25a): White solid; yield: 83 mg (80%); R_f = 0.41 (silica gel, hexanes/EtOAc, 6:4 v/v); mp > 250 °C; ^{1}H NMR (400 MHz, $CDCl_3$) ^{1}H NMR (400 MHz, $CDCl_3$) δ 8.19 – 8.08 (m, 4H), 7.68 – 7.62 (m, 4H), 7.61 – 7.55 (m, 4H), 7.53 (dt, J = 9.0, 1.0 Hz, 2H), 7.17 – 7.07 (m, 2H), 6.38 (td, J = 6.9, 1.1 Hz, 2H);^{13}C NMR (100 MHz, $CDCl_3$) δ 150.9, 146.5, 133.8, 129.6, 128.9, 126.4, 125.4, 117.4, 112.6, 107.5, 104.9; HRMS (ESI-TOF) (*m/z*) calculated $C_{26}H_{19}N_4S^+$: 419.1330; found 419.1343 $[M+H]^+$

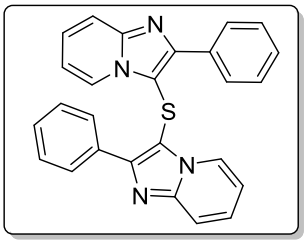

Bis(2-(*p*-tolyl)imidazo[1,2-*a*]pyridin-3-yl)sulfane (25b): White solid; yield: 93 mg (83%); R_f = 0.45 (silica gel, hexanes/EtOAc, 6:4 v/v); mp 244–245 °C; ^{1}H NMR (400 MHz, $CDCl_3$) δ 8.03 (d, J = 8.1 Hz, 4H), 7.63 – 7.58 (m, 2H), 7.54 – 7.48 (m, 2H), 7.44 (d, J = 7.9 Hz, 4H), 7.15 – 7.06 (m, 2H), 6.41 – 6.34 (m, 2H), 2.54 (s, 6H); ^{13}C NMR (100 MHz, $CDCl_3$) δ 150.9, 146.5, 138.8, 130.9, 129.4, 129.3, 126.2, 125.4, 117.2, 112.5, 106.9, 21.5; HRMS (ESI-TOF) (*m/z*) calculated $C_{28}H_{23}N_4S^+$: 447.1643; found 447.1657 $[M+H]^+$.

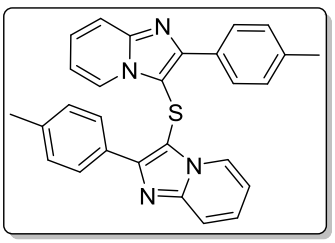

Bis(2-(4-methoxyphenyl)imidazo[1,2-*a*]pyridin-3-yl)sulfane (25c): White solid; yield: 95 mg (85%); R_f = 0.38 (silica gel, hexanes/EtOAc, 6:4 v/v); mp 220–222 °C; ^{1}H NMR (400 MHz, $CDCl_3$) δ 8.10 (d, J = 8.7 Hz, 4H), 7.64 (d, J = 6.9 Hz, 2H), 7.50 (d, J = 8.9 Hz, 2H), 7.16 (d, J = 8.7 Hz, 4H), 7.14 – 7.06 (m, 2H), 6.41 (t, J = 6.8 Hz, 2H), 3.97 (s, 6H); ^{13}C NMR (100 MHz, $CDCl_3$) δ 160.2, 150.6, 146.5, 130.7, 126.3, 126.2, 125.4, 117.2, 114.0, 112.5, 106.5, 55.4; HRMS (ESI-TOF) (*m/z*) calculated $C_{28}H_{23}N_4O_2S^+$: 479.1541; found 479.1538 $[M+H]^+$.

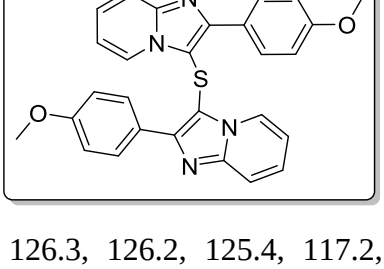

Bis(2-(4-methoxyphenyl)-7-methylimidazo[1,2-*a*]pyridin-3-yl)sulfane (25d): White solid; yield: 117 mg (90%); R_f = 0.35 (silica gel, hexanes/EtOAc, 6:4 v/v); mp 238–239 °C; ^{1}H NMR (400 MHz, $CDCl_3$) δ 8.17 – 8.06 (m, 4H), 7.47 (d, J = 7.0 Hz, 2H), 7.24 (s, 2H), 7.19 – 7.11 (m, 4H), 6.24 (dd, J = 7.0, 1.6 Hz, 2H), 3.97 (s, 6H), 2.27 (s, 6H); ^{13}C NMR (100 MHz, $CDCl_3$) δ 160.1, 150.3, 146.8, 137.4, 130.6,

126.46, 124.5, 115.7, 115.0, 113.9, 105.8, 55.4, 21.2; HRMS (ESI-TOF) (*m/z*) calculated $C_{30}H_{27}N_4O_2S^+$: 507.1854; found 507.1873 $[M+H]^+$.

Bis(2-(4-methoxyphenyl)-8-methylimidazo[1,2-*a*]pyridin-3-yl)sulfane (25e): White solid;

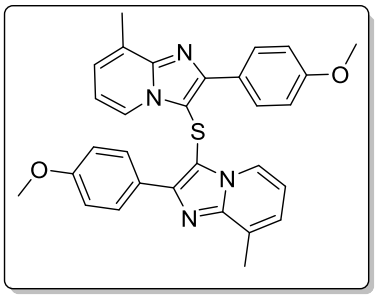

yield: 121 mg (81%); R_f = 0.36 (silica gel, hexanes/EtOAc, 6:4 v/v); mp 208-209 °C; ^{1}H NMR (400 MHz, $CDCl_3$) δ 8.15 – 8.03 (m, 4H), 7.56 – 7.45 (m, 2H), 7.21 – 7.10 (m, 4H), 6.94 – 6.86 (m, 2H), 6.33 (t, *J* = 6.9 Hz, 2H), 3.97 (s, 6H), 2.54 (s, 6H); ^{13}C NMR (100 MHz, $CDCl_3$) δ 160.1, 150.2, 146.7, 130.9, 127.1, 126.7, 124.9, 123.2, 113.9, 112.3, 107.0, 55.4, 16.7; HRMS (ESI-TOF) (*m/z*) calculated $C_{30}H_{27}N_4O_2S^+$: 507.1854; found 507.1859 $[M+H]^+$.

Bis(8-methyl-2-(*p*-tolyl)imidazo[1,2-*a*]pyridin-3-yl)sulfane (25f): White solid; yield: 98 mg

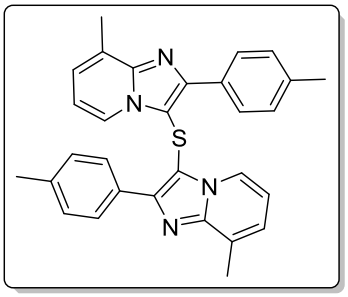

(83%); R_f = 0.44 (silica gel, hexanes/EtOAc, 6:4 v/v); mp 239–240 °C; ^{1}H NMR (400 MHz, $CDCl_3$) δ 8.00 (d, *J* = 8.1 Hz, 4H), 7.47 (d, *J* = 6.7 Hz, 2H), 7.42 (d, *J* = 7.9 Hz, 4H), 6.94 – 6.85 (m, 2H), 6.29 (t, *J* = 6.9 Hz, 2H), 2.53 (s, 12H); ^{13}C NMR (100 MHz, $CDCl_3$) δ 150.5, 146.7, 138.5, 131.2, 129.5, 129.2, 127.2, 124.9 123.3, 112.4, 107.5, 21.5, 16.7; HRMS (ESI-TOF) (*m/z*) calculated $C_{30}H_{27}N_4S^+$: 475.1956; found 475.1977 $[M+H]^+$.

Bis(7-methyl-2-phenylimidazo[1,2-*a*]pyridin-3-yl)sulfane (25g): White solid; yield: 88 mg

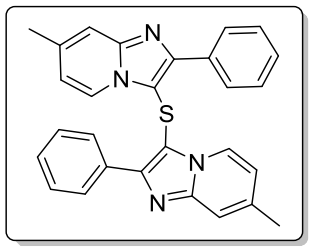

(80%); R_f = 0.46 (silica gel, hexanes/EtOAc, 6:4 v/v); mp 203–204 °C; ^{1}H NMR (400 MHz, DMSO-d_6) δ 8.10 – 8.04 (m, 4H), 7.60 – 7.55 (m, 6H), 7.40 (d, *J* = 7.0 Hz, 2H), 7.32 (s, 2H), 6.36 (dd, *J* = 7.0, 1.3 Hz, 2H), 2.21 (s, 6H); ^{13}C NMR (100 MHz, DMSO-d_6) δ 150.1, 146.5, 138.1, 133.9, 129.3, 129.3, 129.0, 123.9, 116.1, 115.7, 106.4, 20.9; HRMS (ESI-TOF) (*m/z*) calculated $C_{28}H_{23}N_4S^+$: 447.1643; found 447.1640 $[M+H]^+$.

Bis(2-(4-fluorophenyl)imidazo[1,2-*a*]pyridin-3-yl)sulfane (25h): White solid; yield: 86 mg

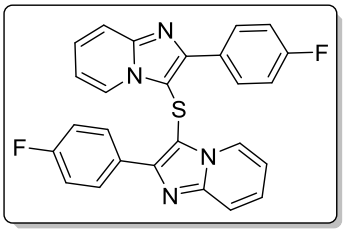

(76%); R_f = 0.52 (silica gel, hexanes/EtOAc, 6:4 v/v); mp >250 °C; ^{1}H NMR (400 MHz, $CDCl_3$) δ 8.13 (dd, *J* = 8.6, 5.5 Hz, 4H), 7.60 (d, *J* = 6.9 Hz, 2H), 7.52 (d, *J* = 9.0 Hz, 2H), 7.33 (t, *J* = 8.6 Hz, 4H), 7.20 – 7.12 (m, 2H), 6.46 (t, *J* = 6.6 Hz, 2H); ^{13}C NMR (100 MHz, $CDCl_3$) δ 164.5, 162.0, 149.9, 146.5, 131.3, 131.2, 129.9,

126.5, 125.1, 117.5, 115.8, 115.6, 112.7, 106.9; HRMS (ESI-TOF) (*m/z*) calculated $C_{26}H_{17}F_2N_4S^+$: 455.1141; found 455.1165 $[M+H]^+$.

Bis(2-(4-chlorophenyl)imidazo[1,2-*a*]pyridin-3-yl)sulfane (25i): White solid; yield: 97 mg (80%); R_f = 0.58 (silica gel, hexanes/EtOAc, 6:4 v/v); mp >250 °C; ^{1}H NMR (400 MHz, $CDCl_3$) δ 8.18 – 8.05 (m, 4H), 7.69 – 7.58 (m, 6H), 7.54 (d, *J* = 9.0 Hz, 2H), 7.21 – 7.14 (m, 2H), 6.49 (td, *J* = 6.9, 0.9 Hz, 2H); ^{13}C NMR (100 MHz, $CDCl_3$) δ 149.7, 146.6, 135.1, 132.2, 130.6, 128.9, 126.7, 125.1, 117.6, 112.9, 107.1; HRMS (ESI-TOF) (*m/z*) calculated $C_{26}H_{17}Cl_2N_4S^+$: 487.0551; found 487.0569 $[M+H]^+$ and 489.0704 $[M+H+2]^+$.

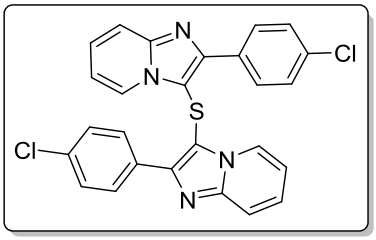

Bis(2-(4-bromophenyl)imidazo[1,2-*a*]pyridin-3-yl)sulfane (25j): White solid; yield: 99 mg (69%); R_f = 0.61 (silica gel, hexanes/EtOAc, 6:4 v/v); mp >250°C; ^{1}H NMR (400 MHz, $CDCl_3$) δ 8.03 (d, *J* = 8.4 Hz, 4H), 7.76 (d, *J* = 8.4 Hz, 4H), 7.63 (d, *J* = 6.9 Hz, 2H), 7.54 (d, *J* = 9.0 Hz, 2H), 7.23 – 7.12 (m, 2H), 6.49 (t, *J* = 6.7 Hz, 2H); ^{13}C NMR (100 MHz, $CDCl_3$) δ 149.7, 146.6, 132.7, 131.8, 130.9, 126.7, 125.1, 123.3, 117.6, 113.0, 107.1; HRMS (ESI-TOF) (*m/z*) calculated $C_{26}H_{17}Br_2N_4S^+$: 574.9541; found 574.9552 $[M+H]^+$ and 576.9696 $[M+H+2]^+$.

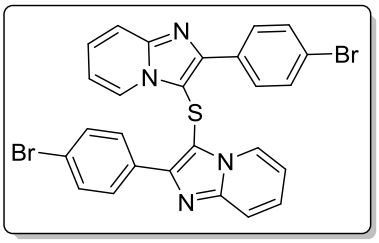

Bis(2-(4-bromophenyl)-8-methylimidazo[1,2-*a*]pyridin-3-yl)sulfane (25k): White solid; yield: 108 mg (72%); R_f = 0.64 (silica gel, hexanes/EtOAc, 6:4 v/v); mp 248-250 °C; ^{1}H NMR (400 MHz, $CDCl_3$) δ 8.07 – 7.98 (m, 4H), 7.78 – 7.70 (m, 4H), 7.49 (d, *J* = 6.6 Hz, 2H), 6.98 – 6.91 (m, 2H), 6.40 (t, *J* = 6.9 Hz, 2H), 2.54 (s, 6H); ^{13}C NMR (100 MHz, $CDCl_3$) δ 149.2, 146.8, 133.0, 131.7, 131.1, 127.6, 125.3, 123.1, 122.9, 112.9, 107.5, 16.6; HRMS (ESI-TOF) (*m/z*) calculated $C_{28}H_{21}Br_2N_4S^+$: 602.9854; found 602.9863 $[M+H]^+$ and 605.0006 $[M+H+2]^+$.

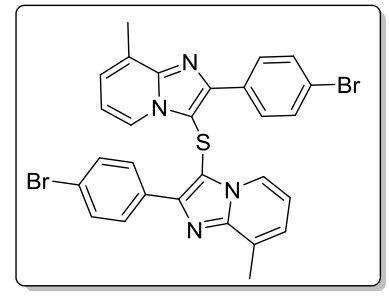

Bis(6-methyl-2-(naphthalen-2-yl)imidazo[1,2-*a*]pyridin-3-yl)sulfane (52l): White solid; yield: 123 mg (87%); R_f = 0.45 (silica gel, hexanes/EtOAc, 6:4 v/v); mp: >250 °C; ^{1}H NMR (400 MHz, $CDCl_3$) δ 8.67 (s, 2H), 8.33 (dd, *J* = 8.5, 1.4 Hz, 2H), 8.13 (d, *J* = 8.5 Hz, 2H), 8.70 – 7.97 (m, 4H), 7.61 (dd, *J* = 6.2, 3.2 Hz, 4H), 7.46 – 7.33 (m, 4H), 6.89

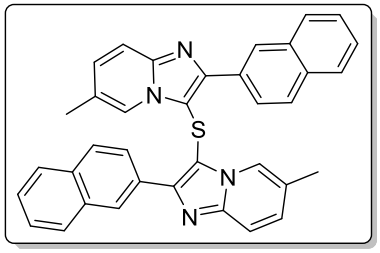

(dd, *J* = 9.0, 1.2 Hz, 2H), 1.34 (s, 6H); ^{13}C NMR (100 MHz, $CDCl_3$) δ 150.4, 145.6, 133.4, 131.5, 129.5, 128.6, 128.2, 127.8, 127.0, 126.7, 126.5, 123.6, 122.5, 116.5, 107.3, 17.3; HRMS (ESI-TOF) (*m/z*) calculated $C_{36}H_{27}N_4S^+$: 547.1956; found 547.1951 $[M+H]^+$.

Bis(2-(3-nitrophenyl)imidazo[1,2-*a*]pyridin-3-yl)sulfane (25m): Yellow solid; yield: 59 mg (47%); R_f = 0.60 (silica gel, hexanes/EtOAc, 6:4 v/v); mp: >250°C; ^{1}H NMR (400 MHz, $CDCl_3$) δ 9.03 (s, 2H), 8.47 (d, *J* = 7.6 Hz, 2H), 8.27 (d, *J* = 7.0 Hz, 4H), 7.68 (t, *J* = 8.1 Hz, 4H), 7.42 – 7.30 (m, 2H), 7.02 (t, *J* = 6.5 Hz, 2H); ^{13}C NMR (100 MHz, $CDCl_3$) δ 148.3, 145.4, 135.4, 134.2, 129.4, 126.7, 126.3, 123.2, 122.9, 117.9, 113.8; HRMS (ESI-TOF) (*m/z*) calculated $C_{26}H_{17}N_6O_4S^+$: 509.1032; found 509.1047 $[M+H]^+$.

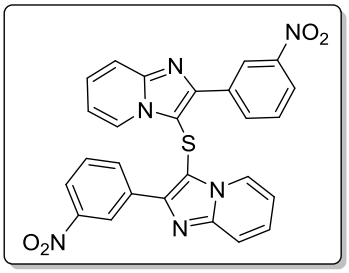

Bis(6-phenylimidazo[2,1-*b*]thiazol-5-yl)sulfane (25o): White solid; yield: 87 mg (81%); R_f = 0.70 (silica gel, hexanes/EtOAc, 6:4 v/v); mp 230–231 °C; δ 8.09 (dd, *J* = 5.2, 3.3 Hz, 4H), 7.60 – 7.52 (m, 4H), 7.51 – 7.45 (m, 2H), 6.54 (d, *J* = 4.5 Hz, 2H), 6.51 (d, *J* = 4.5 Hz, 2H); ^{13}C NMR (100 MHz, $CDCl_3$) δ 151.3, 151.2, 133.6, 128.6, 128.5, 118.4, 112.6, 109.4; HRMS (ESI-TOF) (*m/z*) calculated $C_{22}H_{15}N_4S_3^+$: 431.0458; found 431.0475 $[M+H]^+$.

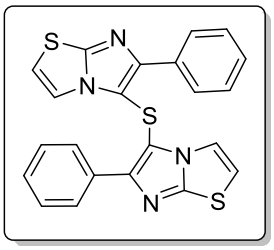

1,2-Bis(2-phenylimidazo[1,2-*a*]pyridin-3-yl)disulfane (26a): Yellow solid; yield: 96 mg (85%); R_f = 0.32 (silica gel, hexanes/EtOAc, 2:8 v/v); mp 242–243 °C; ^{1}H NMR (400 MHz, $CDCl_3$) δ 8.13 (d, *J* = 6.6 Hz, 2H), 7.78 – 7.50 (m, 4H), 7.40 (d, *J* = 8.6 Hz, 2H), 7.26 – 7.20 (m, 2H), 7.14 (dd, *J* = 12.5, 7.1 Hz, 6H), 6.78 (td, *J* = 6.8, 1.1 Hz, 2H); ^{13}C NMR (100 MHz, $CDCl_3$) δ 147.3, 131.9, 128.1, 127.9, 127.7, 127.0, 124.4, 117.3, 113.0; HRMS (ESI-TOF) (*m/z*) calculated $C_{26}H_{19}N_4S_2^+$: 451.1051; found 451.1075 $[M+H]^+$.

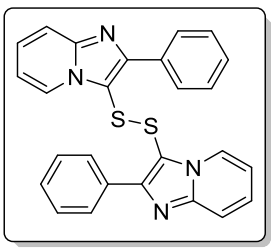

1,2-Bis(2-(*p*-tolyl)imidazo[1,2-*a*]pyridin-3-yl)disulfane (26b): White solid; yield: 106 mg (89%); R_f = 0.38 (silica gel, hexanes/EtOAc, 2:8 v/v); mp 203–204 °C; ^{1}H NMR (400 MHz, $CDCl_3$) δ 8.13 (d, *J* = 6.5 Hz, 2H), 7.70 – 7.47 (m, 4H), 7.35 (d, *J* = 8.0 Hz, 2H), 7.23 – 7.13 (m, 2H), 6.90 (d, *J* = 6.8 Hz, 4H), 6.77 (td, *J* = 6.8, 0.9 Hz, 2H), 2.29 (s, 6H); ^{13}C NMR (100 MHz, $CDCl_3$) δ 147.3, 138.0, 128.4, 127.7, 126.8, 124.4, 117.5, 112.9, 21.3; HRMS (ESI-TOF) (*m/z*) calculated $C_{28}H_{23}N_4S_2^+$: 479.1364; found 479.1387 $[M+H]^+$.

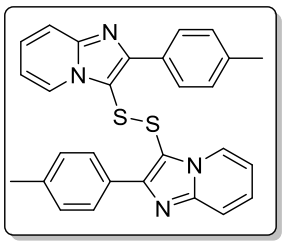

1,2-Bis(2-(4-methoxyphenyl)imidazo[1,2-*a*]pyridin-3-yl)disulfane (26c): Yellow solid; yield:

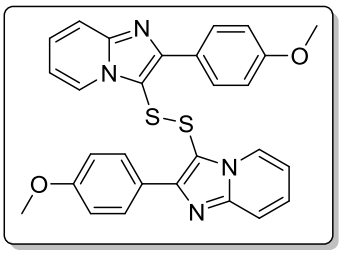

111 mg (87%); R_f = 0.34 (silica gel, hexanes/EtOAc, 2:8 v/v); mp 211–213 °C; ^{1}H NMR (400 MHz, $CDCl_3$) δ 8.15 (d, J = 6.1 Hz, 2H), 7.78 – 7.46 (s, 4H), 7.36 (d, J = 7.4 Hz, 2H), 7.25 – 7.18 (m, 2H), 6.79 (t, J = 6.7 Hz, 2H), 6.63 (d, J = 6.8 Hz, 4H), 3.81 (s, 6H); ^{13}C NMR (100 MHz, $CDCl_3$) δ 159.8, 147.3, 129.1, 127.0, 124.5, 117.3, 113.1, 112.9, 55.2; HRMS (ESI-TOF) (*m/z*) calculated $C_{28}H_{23}N_4O_2S_2^+$: 511.1262; found 511.1276 $[M+H]^+$.

1,2-Bis(2-(4-methoxyphenyl)-7-methylimidazo[1,2-*a*]pyridin-3-yl)disulfane (26d): Yellow

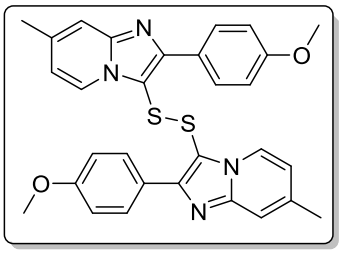

solid; yield: 125 mg (93%); R_f = 0.30 (silica gel, hexanes/EtOAc, 2:8 v/v); mp 219–220 °C; ^{1}H NMR (400 MHz, $CDCl_3$) δ 7.99 (d, J = 6.7 Hz, 2H), 7.78 – 7.39 (m, 4H), 7.17 – 6.92 (m, 2H), 6.75 – 6.45 (m, 6H), 3.81 (s, 6H), 2.39 (s, 6H); ^{13}C NMR (100 MHz, $CDCl_3$) δ 159.7, 147.6, 138.4, 129.1, 123.8, 115.9, 115.2, 112.8, 55.0, 21.2; HRMS (ESI-TOF) (*m/z*) calculated $C_{30}H_{27}N_4O_2S_2^+$: 539.1575 ; found 539.1573 $[M+H]^+$.

1,2-Bis(2-(4-methoxyphenyl)-8-methylimidazo[1,2-*a*]pyridin-3-yl)disulfane (26e): Yellow

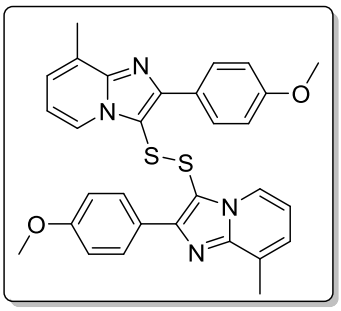

solid; yield: 123 mg (92%); R_f = 0.38 (silica gel, hexanes/EtOAc, 2:8 v/v); mp 221–223 °C; ^{1}H NMR (400 MHz, $CDCl_3$) δ 8.09 (d, J = 3.0 Hz, 2H), 7.75 – 7.70 (m, 4H), 6.97 (d, J = 6.8 Hz, 2H), 6.71 (t, J = 6.8 Hz, 2H), 6.57 (d, J = 5.8 Hz, 4H), 3.78 (s, 6H), 2.48 (s, 6H); ^{13}C NMR (100 MHz, $CDCl_3$) δ 159.3, 147.5, 128.8, 127.2, 125.7, 124.8, 122.4, 112.6, 112.5, 55.0, 16.7; HRMS (ESI-TOF) (*m/z*) calculated $C_{30}H_{27}N_4O_2S_2^+$: 539.1575 ; found 539.1572 $[M+H]^+$

1,2-Bis(8-methyl-2-(*p*-tolyl)imidazo[1,2-*a*]pyridin-3-yl)disulfane (26f): Yellow solid; yield:

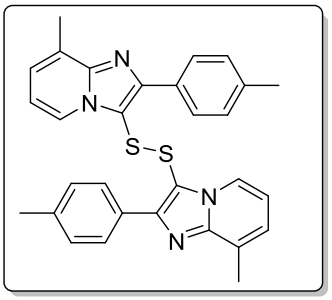

110 mg (87%); R_f = 0.51 (silica gel, hexanes/EtOAc, 2:8 v/v); mp 178–180 °C; ^{1}H NMR (400 MHz, $CDCl_3$) δ 8.15 – 8.02 (m, 2H), 7.48 (d, J = 7.6 Hz, 4H), 6.99 – 6.92 (m, 2H), 6.84 (d, J = 7.7 Hz, 4H), 6.71 (t, J = 6.8 Hz, 2H), 2.49 (s, 6H), 2.26 (s, 6H); ^{13}C NMR (100 MHz, $CDCl_3$) δ 147.4, 137.2, 129.2, 127.8, 127.5, 127.2, 125.8, 122.4, 112.7, 21.2, 16.7; HRMS (ESI-TOF) (*m/z*) calculated $C_{30}H_{27}N_4S_2^+$: 507.1677; found 507.1683 $[M+H]^+$.

1,2-Bis(7-methyl-2-phenylimidazo[1,2-*a*]pyridin-3-yl)disulfane (26g): Yellow solid; yield: 102 mg (85%); R_f = 0.46 (silica gel, hexanes/EtOAc, 2:8 v/v); mp 224–225 °C; ^{1}H NMR (400 MHz, $CDCl_3$) δ 7.95 (d, J = 6.9 Hz, 2H), 7.86 – 7.45 (m, 4H), 7.25 – 6.96 (m, 8H), 6.56 (dd, J = 6.9, 1.5 Hz, 2H), 2.40 (s, 6H); ^{13}C NMR (100 MHz, $CDCl_3$) δ 147.6, 138.3, 132.2, 127.9, 127.6, 123.6, 116.2, 115.5, 21.3; HRMS (ESI-TOF) (*m/z*) calculated $C_{28}H_{23}N_4S_2^+$: 479.1364; found 479.1371 $[M+H]^+$.

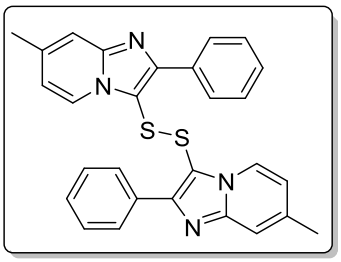

1,2-Bis(2-(4-fluorophenyl)imidazo[1,2-*a*]pyridin-3-yl)disulfane (26h): White solid; yield: 121 mg (92%); R_f = 0.56 (silica gel, hexanes/EtOAc, 2:8 v/v); mp 227–229 °C; ^{1}H NMR (400 MHz, DMSO-d_6) δ 8.60 (d, J = 6.8 Hz, 2H), 8.31 – 8.23 (m, 4H), 7.54 (d, J = 9.0 Hz, 2H), 7.34 – 7.28 (m, 2H), 7.14 – 7.07 (m, 4H), 6.95 (t, J = 6.8 Hz, 2H); ^{13}C NMR (100 MHz, DMSO-d_6 + $CDCl_3$) δ 161.4, 146.4, 130.2, 130.1, 126.9, 125.3, 117.2, 115.4, 115.2, 113.0, 108.5; HRMS (ESI-TOF) (*m/z*) calculated $C_{26}H_{17}F_2N_4S_2^+$: 487.0862; found 487.0880 $[M+H]^+$.

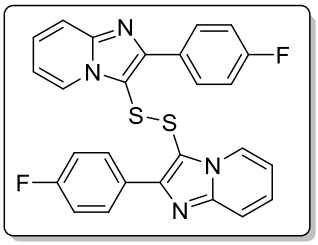

1,2-Bis(2-(4-chlorophenyl)imidazo[1,2-*a*]pyridin-3-yl)disulfane (26i): White solid; yield: 103 mg (80%); R_f = 0.53 (silica gel, hexanes/EtOAc, 2:8 v/v); mp 210–212 °C; ^{1}H NMR (400 MHz, DMSO-d_6) δ 8.61 (dd, J = 6.9, 1.1 Hz, 2H), 8.34 – 8.22 (m, 4H), 7.56 (dd, J = 9.0, 1.0 Hz, 2H), 7.45 – 7.37 (m, 4H), 7.35 – 7.30 (m, 2H), 6.99 (td, J = 6.8, 1.1 Hz, 2H); ^{13}C NMR (100 MHz, DMSO-d_6 + $CDCl_3$) δ 148.1, 146.5, 133.8, 132.6, 129.6, 128.5, 126.9, 125.3, 117.3, 113.1; HRMS (ESI-TOF) (*m/z*) calculated $C_{26}H_{17}Cl_2N_4S_2^+$: 519.0272; found 519.0285 $[M+H]^+$ and 521.0428 $[M+H+2]^+$.

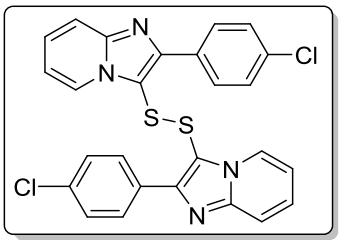

1,2-Bis(2-(4-bromophenyl)imidazo[1,2-*a*]pyridin-3-yl)disulfane (26j): Orange solid; yield: 116 mg (87%); R_f = 0.60 (silica gel, hexanes/EtOAc, 2:8 v/v); mp 235–236 °C; ^{1}H NMR (400 MHz, $CDCl_3$) δ 8.25 (d, J = 6.6 Hz, 2H), 7.49 – 7.29 (m, 8H), 7.10 (d, J = 8.1 Hz, 4H), 6.96 – 6.88 (m, 2H); ^{13}C NMR (100 MHz, $CDCl_3$) δ 147.4, 130.5, 128.9, 127.8, 124.7, 122.5, 117.9, 113.4; HRMS (ESI-TOF) (*m/z*) calculated $C_{26}H_{17}Br_2N_4S_2^+$: 606.9261; found 606.9274 $[M+H]^+$ and 608.9418 $[M+H+2]^+$.

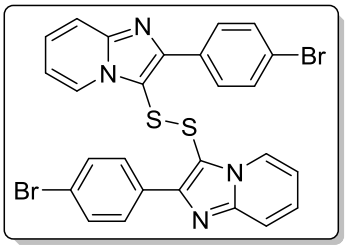

1,2-Bis(2-(4-bromophenyl)-8-methylimidazo[1,2-*a*]pyridin-3-yl)disulfane (26k): Yellow solid; yield: 132 mg (83%); R_f = 0.64 (silica gel, hexanes/EtOAc, 2:8 v/v); mp 184–186 °C; ^{1}H NMR (400 MHz, $CDCl_3$) δ 8.18 (d, J = 6.2 Hz, 2H), 7.42 (d, J = 7.8 Hz, 4H), 7.14 – 7.03 (m, 6H), 6.86 (t, J = 6.8 Hz, 2H), 2.51 (s, 6H); ^{13}C NMR (100 MHz, $CDCl_3$) δ 147.5, 130.5, 130.0, 128.7, 127.5, 127.0, 122.5, 121.8, 113.4, 16.7; HRMS (ESI-TOF) (*m/z*) calculated $C_{28}H_{21}Br_2N_4S_2^+$: 634.9574; found 634.9597 $[M+H]^+$ and 636.9731 $[M+H+2]^+$.

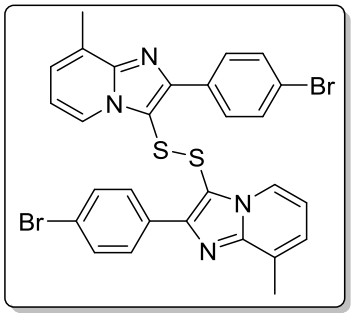

1,2-Bis(6-methyl-2-(naphthalen-2-yl)imidazo[1,2-*a*]pyridin-3-yl)disulfane (26l): Yellow solid; yield: 113 mg (78%); R_f = 0.47 (silica gel, hexanes/EtOAc, 2:8 v/v); mp 245–247 °C; ^{1}H NMR (400 MHz, $CDCl_3$) δ 8.05 (s, 2H), 7.81 (d, J = 7.7 Hz, 2H), 7.79 – 7.67 (m, 5H), 7.61 (d, J = 8.2 Hz, 2H), 7.56 – 7.36 (m, 5H), 6.74 (d, J = 8.4 Hz, 2H), 6.35 (d, J = 8.3 Hz, 2H), 2.13 (s, 6H); ^{13}C NMR (100 MHz, $CDCl_3$) δ 146.2, 133.1, 129.8, 128.6, 127.4, 126.9, 125.9, 125.7, 125.4, 122.8, 122.2, 116.1, 18.2; HRMS (ESI-TOF) (*m/z*) calculated $C_{36}H_{27}N_4S_2^+$: 579.1677; found 579.1673 $[M+H]^+$.

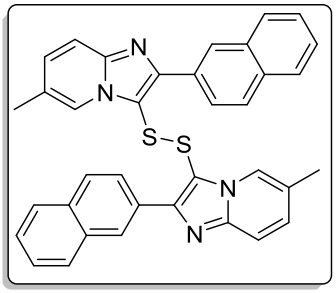

1,2-Bis(2-(3-nitrophenyl)imidazo[1,2-*a*]pyridin-3-yl)disulfane (26m): Yellow solid; yield: 115 mg (85%); R_f = 0.59 (silica gel, hexanes/EtOAc, 2:8 v/v); mp >250 °C; ^{1}H NMR (400 MHz, DMSO-d_6) δ 9.14 (s, 2H), 8.69 – 8.57 (m, 4H), 8.19 – 8.15 (m, 2H), 7.63 – 7.57 (m, 4H), 7.35 – 7.28 (m, 2H), 7.00 – 6.92 (m, 2H); ^{13}C NMR (100 MHz, DMSO-d_6 + $CDCl_3$) 148.4, 147.1, 146.7, 135.5, 134.1, 129.4, 127.2, 125.2, 122.9, 122.8, 117.5, 113.4, 109.8; HRMS (ESI-TOF) (*m/z*) calculated $C_{26}H_{17}N_6O_4S_2^+$: 541.0752 ; found 541.0769 $[M+H]^+$.

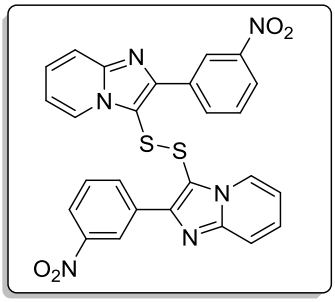

1,2-Bis(2-(4-nitrophenyl)imidazo[1,2-*a*]pyridin-3-yl)disulfane (26n): Orange solid; yield: 117 mg (87%); R_f = 0.60 (silica gel, hexanes/EtOAc, 2:8 v/v); mp >250 °C; ^{1}H NMR (400 MHz, DMSO-d_6) δ 8.65 (d, J = 6.9 Hz, 2H), 8.59 – 8.53 (m, 4H), 8.28 – 8.22 (m, 4H), 7.61 (d, J = 9.0 Hz, 2H), 7.43 – 7.35 (m, 2H), 7.04 (td, J = 6.8, 1.0 Hz, 2H); ^{13}C NMR (100 MHz, DMSO-d_6 + $CDCl_3$) δ 147.2, 146.8, 140.4, 128.9, 127.5,

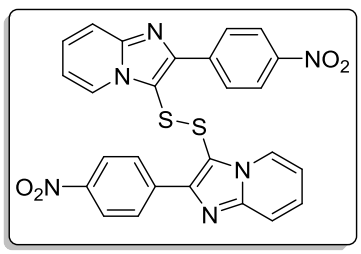

125.5, 123.6, 117.6, 113.6, 110.7; HRMS (ESI-TOF) (*m/z*) calculated $C_{26}H_{17}N_6O_4S_2^+$: 541.0752 ; found 541.0778 $[M+H]^+$.

2-Phenyl-3-((6-phenylimidazo[2,1-*b*]thiazol-5-yl)disulfanyl)imidazo[1,2-*b*]isothiazole (26o):

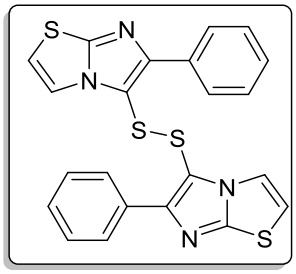

Pale yellow solid; yield: 96 mg (83%); R_f = 0.54 (silica gel, hexanes/EtOAc, 2:8 v/v); mp 177–179 °C; ^{1}H NMR (400 MHz, $CDCl_3$) δ 7.80 – 7.77 (m, 4H), 7. 29 – 7.24 (m, 6H), 7.13 (d, J = 4.4 Hz, 2H), 6.70 (d, J = 4.4 Hz, 2H); ^{13}C NMR (100 MHz, $CDCl_3$) δ 154.2, 152.2, 132.4, 128.2, 127.9, 127.3, 117.6, 113.3, 110.1; HRMS (ESI-TOF) (*m/z*) calculated $C_{22}H_{15}N_4S_4^+$: 463.0179; found 463.0164 $[M+H]^+$.

4B.4 X-ray Crystallography Studies

Crystals of the compounds were screened under a microscope for mounting in a nylon loop attached to a goniometer head. Initial crystal evaluation and data collection were performed on a Kappa APEX II diffractometer equipped with a CCD detector (with the crystal-to-detector distance fixed at 60 mm) and sealed-tube monochromated MoKα radiation using the program APEX2.[78] By using the program SAINT[78] for the integration of the data, reflection profiles were fitted, and values of F^2 and $\sigma(F^2)$ for each reflection were obtained. Data were also corrected for Lorentz and polarization effects. The subroutine XPREP[78] was used for the processing of data that included determination of space group, application of an absorption correction (SADABS),[78] merging of data, and generation of files necessary for solution and refinement. The crystal structure was solved and refined using SHELX 97.[79] In each case, the space group was chosen based on systematic absences and confirmed by the successful refinement of the structure. Positions of most of the non-hydrogen atoms were obtained from a direct methods solution. Several full-matrix least-squares/difference Fourier cycles were performed, locating the remainder of the non-hydrogen atoms. All non-hydrogen atoms were refined with anisotropic displacement parameters. All hydrogen atoms were placed in ideal positions and refined as riding atoms with individual isotropic displacement parameters. All figures were drawn using MERCURY V 3.0[80] and Platon.[81]

4B.4.1 Crystallographic data of 25h (CCDC No. 1559710)

$C_{26}H_{16}F_2N_4S$, M_r = 454.49 g/mol, monoclinic, space group *C*2/*c*, a = 25.7529(13) Å, b = 5.3952(3) Å, c = 16.9212(8) Å, α = 90°, β = 117.744(3)°, γ = 90°, V = 2080.8(2) Å^3, Z = 4, T = 296(2) K, D_{calcd} = 1.451 g/cm^3; Full matrix least-square on F^2; R_1 = 0.0375, wR_2 = 0.1067 for

1618 observed reflections [$I > 2\sigma(I)$] and R_1 = 0.0469, wR_2 = 0.1264 for all 1836 reflections; GOF = 1.158.

4B.4.2 Crystallographic data of 26j (CCDC No. 1559711)

$C_{22}H_{14}N_4S_4$, M_r = 462.61 g/mol, orthorhombic, space group $C222_1$, a = 11.2826(7) Å, b = 12.8551(7) Å, c = 14.4863(8) Å, α = 90°, β = 90°, γ = 90°, V = 2101.1(2) Å^3, Z = 4, T = 296(2) K, D_{calcd} = 1.462 g/cm^3; Full matrix least-square on F^2; R_1 = 0.0280, wR_2 = 0.0719 for 1799 observed reflections [$I > 2\sigma(I)$] and R_1 = 0.0292, wR_2 = 0.0726 for all 1861 reflections; GOF = 1.070.

4B.4.3 Crystallographic data of 26o (CCDC No. 1559712)

$C_{26}H_{16}Br_2N_4S_2$, M_r = 608.37 g/mol, monoclinic, space group $C2/c$, a = 18.39(5) Å, b = 13.05(4) Å, c = 12.22(3) Å, α = 90°, β = 126.33(4)°, γ = 90°, V = 2363(11) Å^3, Z = 4, T = 296(2) K, D_{calcd} = 1.711 g/cm^3; Full matrix least-square on F^2; R_1 = 0.0385, wR_2 = 0.0971 for 1568 observed reflections [$I > 2\sigma(I)$] and R_1 = 0.0543, wR_2 = 0.1043 for all 2076 reflections; GOF = 1.044.

4B.5 References

(1) Guo, H.; Sun, B.; Gao, H.; Chen, X.; Liu, S.; Yao, X.; Liu, X.; Che, Y. *Journal of Natural Products* **2009**, *72*, 2115-2119.

(2) Wang, J. -M.; Ding, G. -Z.; Fang, L.; Dai, J. -G.; Yu, S. -S.; Wang, Y. -H.; Chen, X. - G.; Ma, S. -G.; Qu, J.; Xu, S. *Journal of Natural Products* **2010**, *73*, 1240-1249.

(3) Madaan, C.; Saraf, S.; Priyadarshani, G.; Reddy, P. P.; Guchhait, S. K.; Kunwar, A.; Sridhar, B. *Synlett* **2012**, 1955-1959.

(4) Knerr, P. J.; Tzekou, A.; Ricklin, D.; Qu, H.; Chen, H.; van der Donk, W. A.; Lambris, J. D. *ACS Chemical Biology* **2011**, *6*, 753-760.

(5) Feng, M.; Tang, B.; Liang, S. H.; Jiang, X. *Current Topics in Medicinal Chemistry* **2016**, *16*, 1200-1216.

(6) Pola, S. In *Scope of Selective Heterocycles from Organic and Pharmaceutical Perspective*; Varala, R., Ed.; InTech: Rijeka, **2016**, Ch. 01.

(7) Bulaj, G. *Biotechnology Advances* **2005**, *23*, 87-92.

(8) Krawczyk, B.; Krawczyk, J. M.; Sussmuth, R. D. In *Drug Discovery from Natural Products*; The Royal Society of Chemistry: **2012**, p 42-57.

(9) Holmgren, A. *Journal of Biological Chemistry* **1989**, *264*, 13963-13966.

(10) Chen, X.; Engle, K. M.; Wang, D. H.; Yu, J. Q. *Angewandte Chemie International Edition* **2009**, *48*, 5094-5115.

(11) Guo, X. -X.; Gu, D. -W.; Wu, Z.; Zhang, W. *Chemical Reviews* **2014**, *115*, 1622-1651.

(12) Topczewski, J. J.; Sanford, M. S. *Chemical Science* **2015**, *6*, 70-76.

(13) Song, G.; Wang, F.; Li, X. *Chemical Society Reviews* **2012**, *41*, 3651-3678.

(14) Allen, S. E.; Walvoord, R. R.; Padilla-Salinas, R.; Kozlowski, M. C. *Chemical Reviews* **2013**, *113*, 6234-6458.

(15) Sun, C. -L.; Shi, Z. -J. *Chemical Reviews* **2014**, *114*, 9219-9280.

(16) Yang, Y.; Lan, J.; You, J. *Chemical Reviews* **2017**, *117*, 8787-8863.

(17) Kondo, T.; Mitsudo, T. -A. *Chemical Reviews* **2000**, *100*, 3205-3220.

(18) Liu, C.; Yuan, J.; Gao, M.; Tang, S.; Li, W.; Shi, R.; Lei, A. *Chemical Reviews* **2015**, *115*, 12138-12204.

(19) Li, J.; Li, C.; Yang, S.; An, Y.; Wu, W.; Jiang, H. *The Journal of Organic Chemistry* **2016**, *1*, 7771-7783.

(20) Yuan, B.; Zhuang, J.; Kirmess, K. M.; Bridgmohan, C. N.; Whalley, A. C.; Wang, L.; Plunkett, K. N. *The Journal of Organic Chemistry* **2016**, *81*, 8312-8318.

(21) Chen, F. -J.; Liao, G.; Li, X.; Wu, J.; Shi, B. -F. *Organic Letters* **2014**, *16*, 5644-5647.

(22) Zhou, Z.; Liu, Y.; Chen, J.; Yao, E.; Cheng, J. *Organic Letters* **2016**, *18*, 5268-5271.

(23) Gao, Y.; Wei, L.; Liu, Y.; Wan, J. -P. *Organic & Biomolecular Chemistry* **2017**, *15*, 4631-4634.

(24) Singh, N.; Singh, R.; Raghuvanshi, D. S.; Singh, K. N. *Organic Letters* **2013**, *15*, 5874-5877.

(25) Singh, R.; Raghuvanshi, D. S.; Singh, K. N. *Organic Letters* **2013**, *15*, 4202-4205.

(26) Yusubov, M. S.; Zhdankin, V. V. *Resource-Efficient Technologies* **2015**, *1*, 49-67.

(27) U Tekale, S.; S Kauthale, S.; A Dake, S.; R Sarda, S.; P Pawar, R. *Current Organic Chemistry* **2012**, *16*, 1485-1501.

(28) Liu, D.; Lei, A. *Chemistry–An Asian Journal* **2015**, *10*, 806-823.

(29) Zhao, X.; Zhang, L.; Lu, X.; Li, T.; Lu, K. *The Journal of Organic Chemistry* **2015**, *80*, 18-2924.

(30) Sun, J.; Qiu, J. -K.; Jiang, B.; Hao, W. -J.; Guo, C.; Tu, S. -J. *The Journal of Organic Chemistry* **2016**, *81*, 3321-3328.

(31) Siddaraju, Y.; Prabhu, K. R. *Organic & Biomolecular Chemistry* **2017**, *15*, 5191-5196 .

(32) Fan, W.; Yang, Z.; Jiang, B.; Li, G. *Organic Chemistry Frontiers* **2017**, *4*, 1091-1102.

(33) Yang, D.; Sun, P.; Wei, W.; Meng, L.; He, L.; Fang, B.; Jiang, W.; Wang, H. *Organic Chemistry Frontiers* **2016**, *3*, 1457-1461.

(34) Singh, R.; Allam, B. K.; Singh, N.; Kumari, K.; Singh, S. K.; Singh, K. N. *Organic Letters* **2015**, *17*, 2656-2659.

(35) Sang, P.; Chen, Z.; Zou, J.; Zhang, Y. *Green Chemistry* **2013**, *15*, 2096-2100.

(36) Siddaraju, Y.; Prabhu, K. R. *Organic Letters* **2016**, *18*, 6090-6093.

(37) Siddaraju, Y.; Prabhu, K. R. *The Journal of Organic Chemistry* **2017**, *82*, 3084-3093.

(38) Yang, D.; Yan, K.; Wei, W.; Zhao, J.; Zhang, M.; Sheng, X.; Li, G.; Lu, S.; Wang, H. *The Journal of Organic Chemistry* **2015**, *80*, 6083-6092.

(39) Wu, S. -S.; Feng, C. -T.; Hu, D.; Huang, Y. -K.; Li, Z.; Luo, Z. -G.; Ma, S. -T. *Organic & Biomolecular Chemistry* **2017**, *15*, 1680-1685.

(40) Raghuvanshi, D. S.; Verma, N. *RSC Advances* **2017**, *7*, 22860-22868.

(41) Cao, H.; Yuan, J.; Liu, C.; Hu, X.; Lei, A. *RSC Advances* **2015**, *5*, 41493-41496.

(42) Chen, Y.; Xiao, F.; Chen, H.; Liu, S.; Deng, G. -J. *RSC Advances* **2014**, *4*, 44621-44628.

(43) Zhao, X.; Li, T.; Zhang, L.; Lu, K. *Organic & Biomolecular Chemistry* **2016**, *14*, 1131-1137.

(44) Zhao, X.; Deng, Z.; Wei, A.; Li, B.; Lu, K. *Organic & Biomolecular Chemistry* **2016**, *14*,304-7312.

(45) Xiao, F.; Xie, H.; Liu, S.; Deng, G. J. *Advanced Synthesis & Catalysis* **2014**, *356*, 364-368.

(46) Yang, F. L.; Tian, S. K. *Angewandte Chemie International Edition* **2013**, *125*, 5029-5032.

(47) Zhao, X.; Zhang, L.; Li, T.; Liu, G.; Wang, H.; Lu, K. *Chemical Communications* **2014**, *50*, 13121-13123.

(48) Yi, S.; Li, M.; Mo, W.; Hu, X.; Hu, B.; Sun, N.; Jin, L.; Shen, Z. *Tetrahedron Letters* **2016**, *57*, 1912-1916.

(49) Rafique, J.; Saba, S.; Rosário, A. R.; Braga, A. L. *Chemistry-A European Journal* **2016**, *22*, 11854-11862.

(50) Hiebel, M. -A.; Berteina-Raboin, S. *Green Chemistry* **2015**, *17*, 937-944.

(51) Ravi, C.; Reddy, N. N. K.; Pappula, V.; Samanta, S.; Adimurthy, S. *The Journal of Organic Chemistry* **2016**, *81*, 9964-9972.

(52) Yang, D.; Yan, K.; Wei, W.; Li, G.; Lu, S.; Zhao, C.; Tian, L.; Wang, H. *The Journal of Organic Chemistry* **2015**, *80*, 11073-11079.

(53) Bagdi, A. K.; Mitra, S.; Ghosh, M.; Hajra, A. *Organic & Biomolecular Chemistry* **2015**, *13*, 3314-3320.

(54) Ravi, C.; Mohan, D. C.; Adimurthy, S. *Organic & Biomolecular Chemistry* **2016**, *14*, 2282-290.

(55) Ravi, C.; Chandra Mohan, D.; Adimurthy, S. *Organic Letters* **2014**, *16*, 2978-2981.

(56) Gao, Z.; Zhu, X.; Zhang, R. *RSC Advances* **2014**, *4*, 19891-19895.

(57) Huang, X.; Wang, S.; Li, B.; Wang, X.; Ge, Z.; Li, R. *RSC Advances* **2015**, *5*, 22654-22657.

(58) Wang, D.; Guo, S.; Zhang, R.; Lin, S.; Yan, Z. *RSC Advances* **2016**, *6*, 54377-54381.

(59) Li, Z.; Hong, J.; Zhou, X. *Tetrahedron* **2011**, *67*, 3690-3697.

(60) Siddaraju, Y.; Prabhu, K. R. *The Journal of Organic Chemistry* **2016**, *81*, 7838-7846.

(61) Kaswan, P.; Nandwana, N. K.; DeBoef, B.; Kumar, A. *Advanced Synthesis & Catalysis* **2016**, *358*, 2108-2115.

(62) Lei, S.; Cao, H.; Chen, L.; Liu, J.; Cai, H.; Tan, J. *Advanced Synthesis & Catalysis* **2015**, *357*, 3109-3114.

(63) Modi, A.; Ali, W.; Patel, B. K. *Advanced Synthesis & Catalysis* **2016**, *358*, 2100-2107.

(64) Patel, O. P.; Anand, D.; Maurya, R. K.; Yadav, P. P. *The Journal of Organic Chemistry* **2016**, *81*, 7626-7634.

(65) Liu, P.; Shen, Z.; Yuan, Y.; Sun, P. *Organic & Biomolecular Chemistry* **2016**, *14*, 6523-6530.

(66) Shakoor, S. M. A ; Mandal, S. K.; Sakhuja, R. *European Journal of Organic Chemistry* **2017**, 2596-2602.

(67) Woodbridge 3RD, R. G.; Dougherty, G. *Journal of the American Chemical Society* **1950**, *72*, 4320-4322.

(68) Shirani, H.; Janosik, T. *Synthesis* **2007**, 2690-2698.

(69) Shirani, H.; Stensland, B.; Bergman, J.; Janosik, T. *Synlett* **2006**, 2459-2463.

(70) Yang, Y.; Li, W.; Ying, B.; Liao, H.; Shen, C.; Zhang, P. *ChemCatChem* **2016**, *8*, 2916-2919.

(71) Shibahara, F.; Kanai, T.; Yamaguchi, E.; Kamei, A.; Yamauchi, T.; Murai, T. *Chemistry–An Asian Journal* **2014**, *9*, 237-244.

(72) Sakhuja, R.; Shakoor, S. M. A.; Kumari, S.; Kumar, A. *Journal of Heterocyclic Chemistry* **2015**, *52*, 773-779

(73) Shakoor, S. M. A.; Kumari, S.; Khullar, S.; Mandal, S. K.; Kumar, A.; Sakhuja, R. *The Journal of Organic Chemistry* **2016**, *81*, 12340-12349.

(74) Shakoor, S. M. A.; Agarwal, D. S.; Kumar, A.; Sakhuja, R. *Tetrahedron* **2016**, *72*, 645-652.

(75) Danehy, J. P.; Doherty, B. T.; Egan, C. P. *The Journal of Organic Chemistry* **1971**, *36*, 2525-2530.

(76) Okamura, T. A.; Kaga, T.; Yamashita, S.; Furuya, R.; Onitsuka, K. *The Journal of Organic Chemistry* **2017**, *82*, 2187-2192.

(77) Nakatani, A.; Hirano, K.; Satoh, T.; Miura, M. *The Journal of Organic Chemistry* **2014**, *79*, 1377-1385.

(78) *APEX2*, *SADABS and SAINT*; Bruker AXS inc: Madison, WI, USA, **2008**.

(79) Sheldrick, G. M., *Acta Crystallographica* **2008**, *A64*, 112-122.

(80) Macrae, C. F.; Bruno, I. J.; Chisholm, J. A.; Edginton, P. R.; McCabe, P.; Pidocck, E.; Rodriguez Monge, L.; Taylor, T.; Van de Streek, J.; Wood, P. A *Journal of Applied Crystallography* **2008**, *41*, 466-470.

(81) Spek, A. L. *PLATON, Version 1.62*, University of Utrecht, **1999.**

CHAPTER 5

Exploration of Imidazolium-Supported Benzotriazole Reagent for Selective Organic Transformations

5.1 Background

Ionic liquids (ILs) have streamlined the organic synthesis in the past two decades.[1-8] They have been used as environmentally benign reaction media due to their unique chemical and physical properties such as non-volatility, non-flammability, controlled miscibility, lack of measurable vapor pressure, high thermal and chemical stability. At present, they have been broadly used as (i) catalysts, (ii) reagents, and (iii) scavengers in various organic transformations.[6,7,9-11] Reactions in ionic liquids generally exhibit variable thermodynamic and kinetic behavior that often leads to improved process performance. Ionic liquids can be immobilized on a functionalized support that carries or contains one component of the ionic liquid, or a precursor to such a component.[12-14] Ionic liquid may be immobilized *via* the anion, by treating a support with an anion source, e.g. an inorganic halide, before the ionic liquid is applied or formed. Alternatively, the ionic liquid may be immobilized by having the cation covalently bounded to the support. Some of the commonly used cationic and anionic entities constituting various ionic liquids are shown below (Figure 5.1.1).[15]

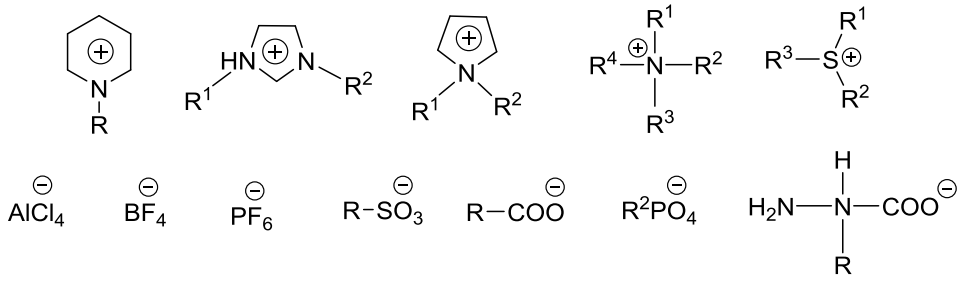

Figure 5.1.1: Typical molecular structures of cations and anions constituting ionic liquids

The concept of grafting or supporting small molecules on other surfaces was first disclosed by 'Merrifield' in 1963 using insoluble solid polymer resin for tetrapeptide synthesis.[16] Since then, polymer-supported strategy has been widely employed in combinatorial synthesis of various organic molecules. These traditional supported syntheses have employed heterogeneous materials such as cross-linked polystyrene to support one of the reactants. Unfortunately, various disadvantages have been allied with the solid phase synthesis technique including comparatively longer reaction times, low loading capacities of resins, and challenges in monitoring the reaction *via* TLC. To overcome these problems "liquid phase" techniques have been introduced, and continuously grown in various fields. The term, soluble-phase synthesis was first used to differentiate soluble polyethylene glycol (PEG)-supported synthesis from solid-phase peptide synthesis.[17-22] Since its introduction polyethylene glycol (PEG) polymers

have been enormously used as soluble support for the synthesis of numerous pharmacologically important compounds. These polyethylene glycol based supports have good stability, high compatibility and good swelling characteristic with non-polar solvents. Despite of few valuable advantages, the polyethylene glycol (PEG) polymer technique suffer from certain limitations such as swelling of polymer in polar solvents, low loading capacities, limited chemical stability to free radical, oxidative or strong acidic conditions. In conjunction to this, "fluorous phase" synthesis based on the concept that fluorinated compounds preferentially dissolves in a fluorous solvent was introduced a decade ago. However, the fluorous phase synthesis was unable to made synergy with the sustainable chemistry parameters due to the low solubility in organic solvents, and the requirement of expensive fluorinated solvents.[23,24] Thereafter, room-temperature ionic liquids (RTILs) provided a breakthrough in the field of modern organic and combinatorial chemistry (Figure 5.1.2). RTIL provides an easy purification process for the separating the soluble support from the reaction mixture by washing with appropriate solvent at each step. In addition, monitoring of the reactions fate by TLC and spectroscopic techniques, and high loading efficiency of the process have proved IL-phase synthesis as a leading technique to accelerate the drug-discovery process *via* the synthesis of chemical entities. Moreover, various imidazolium-supported reagents have been documented under the IL-phase synthesis frame in recent years.[2,6,8,15]

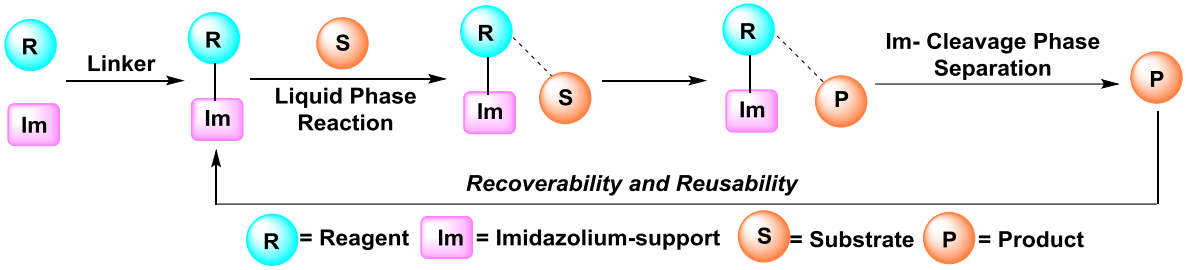

Figure 5.1.2: Typical flow diagram of ionic liquid supported organic synthesis

Interesting utilities of selective imidazolium-supported reagents are briefly described in the following section.

5.1.1 Imidazolium-supported organotin reagents

Legoupy and coworkers have reported the synthesis of novel imidazolium-supported organotin reagents **4**, and successfully utilized them in selective cross-coupling reactions. The synthesis of the reagents proceeded by the substitution reaction of **1** with stannane [(*n*-Bu)$_2$SnPhH] **2** affording **3** in the presence of Lithium diisopropyl amide (LDA) in THF. Thereafter reaction of

3 with alkyl iodides afforded the desired imidazolium–supported organotin reagents **4** (Scheme 5.1.1.1). The authors described the effective use of reagent **4** using catalytic $Pd_2dba_3.CHCl_3$ to furnish the desired products **6** and **8** from substituted aryl halides **5** and hetroaryl halides **7**, respectively (Scheme 5.1.1.1).[25-28] Notably, imidazolium-supported organotin compounds were recycled and reused after Stille cross-coupling reactions, exhibiting no loss in activity.

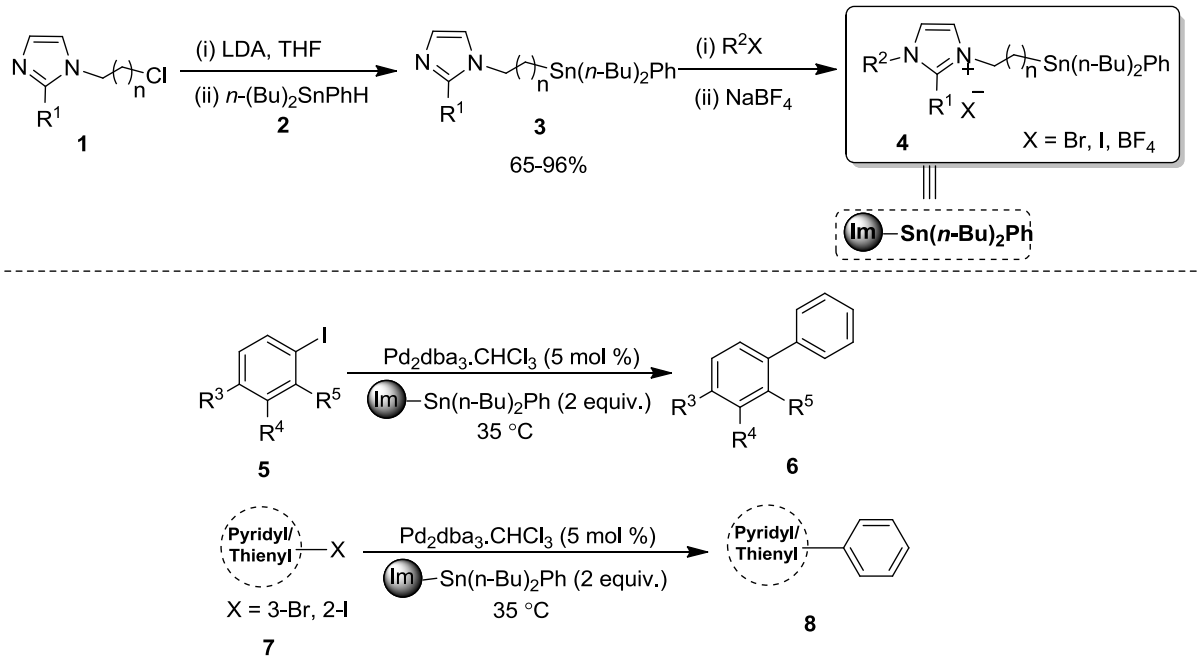

Scheme 5.1.1.1: Synthesis and application of imidazolium-supported organotin reagents **4**

Legoupy *et al.* further reported the utility of novel imidazolium-supported organotin reagents **9** and **10** for the reduction of alkyl and aryl halides **11** in presence of AIBN and $NaBH_4$ (Scheme 5.1.1.2).[27] AIBN was believed to form organotin radical, which promotes the reduction of alkyl and aryl halides.

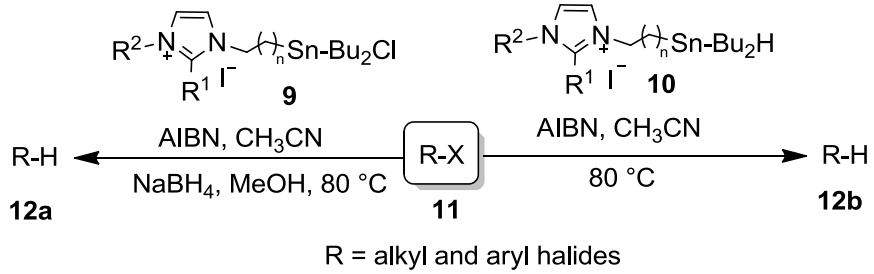

Scheme 5.1.1.2: Reduction of alkyl/aryl halides (**11**) using imidazolium-supported organotin reagents **9** and **10**

5.1.2 Imidazolium-supported iodobenzene and iodobenzene diacetate reagents

Togo group has documented the synthesis and application of several imidazolium-supported iodobenzenes.[29,30] The group developed an elegant and greener protocol for the synthesis of *α*-tosyloxylated ketones**14** from ketones **13** using *m*-CPBA/*p*-TsOH in the presence of a catalytic amount of imidazolium-supported iodobenzene thereby, avoiding the conventional use of HTIB-Koser's reagent. The *α*-tosyloxylation process was also explored towards the synthesis of thiazoles (**15**) *via in-situ* formation of **14** (Scheme 5.1.2.1).[29]

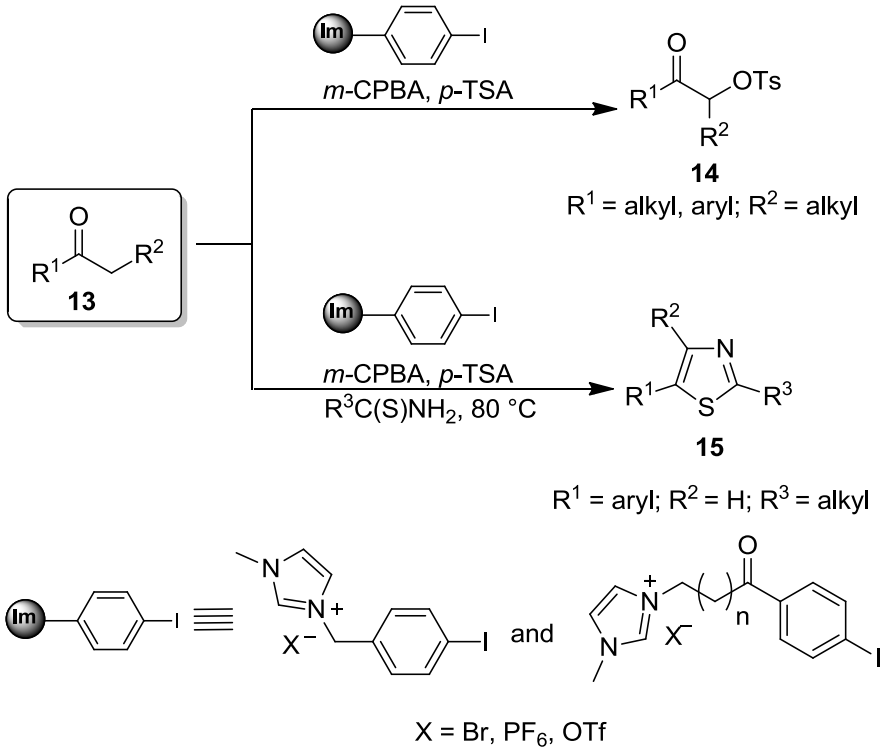

Scheme 5.1.2.1: Applications of imidazolium-supported iodobenzene reagents

With an anticipation to develop alternative hypervalent iodine(III) reagents, Zhang *et al.* prepared imidazolium-supported iodobenzene diacetate reagent [dibmim][BF_4] (**19)** by reacting 4-bromomethyliodobenzene (**16)** with 1-methylimidazole (**17),** followed by oxidation with peracetic acid *via* formation of **18** (scheme 5.1.2.2).[31] The reagent **19** was successfully employed for the oxidation of alcohols **20** to carbonyl compounds **21** in ionic liquid [emim][BF_4] (1-ethyl-3-methylimidazolium tetrafluoroborate), under mild conditions (Scheme 5.1.2.2a).[31] Qian *et al.* elaborately reported a successful oxidation of sulphides **22** using the imidazolium-supported iodobenzene diacetate (**19**) at room temperature in water (Scheme 5.1.2.2b)[32] Similarly, the reagent **19** was also used by Bao and coworkers for the oxidative amidation of aldehydes **24** with amines **25** offering various amidated products **26** in moderate-

to-good yields (Scheme 5.1.2.2c).[33] Although, the reagent was found to be less effective than commercial iodobenzene diacetate reagent, yet an ease in separation of the products and exceptional recyclability have added few valuable advantages.

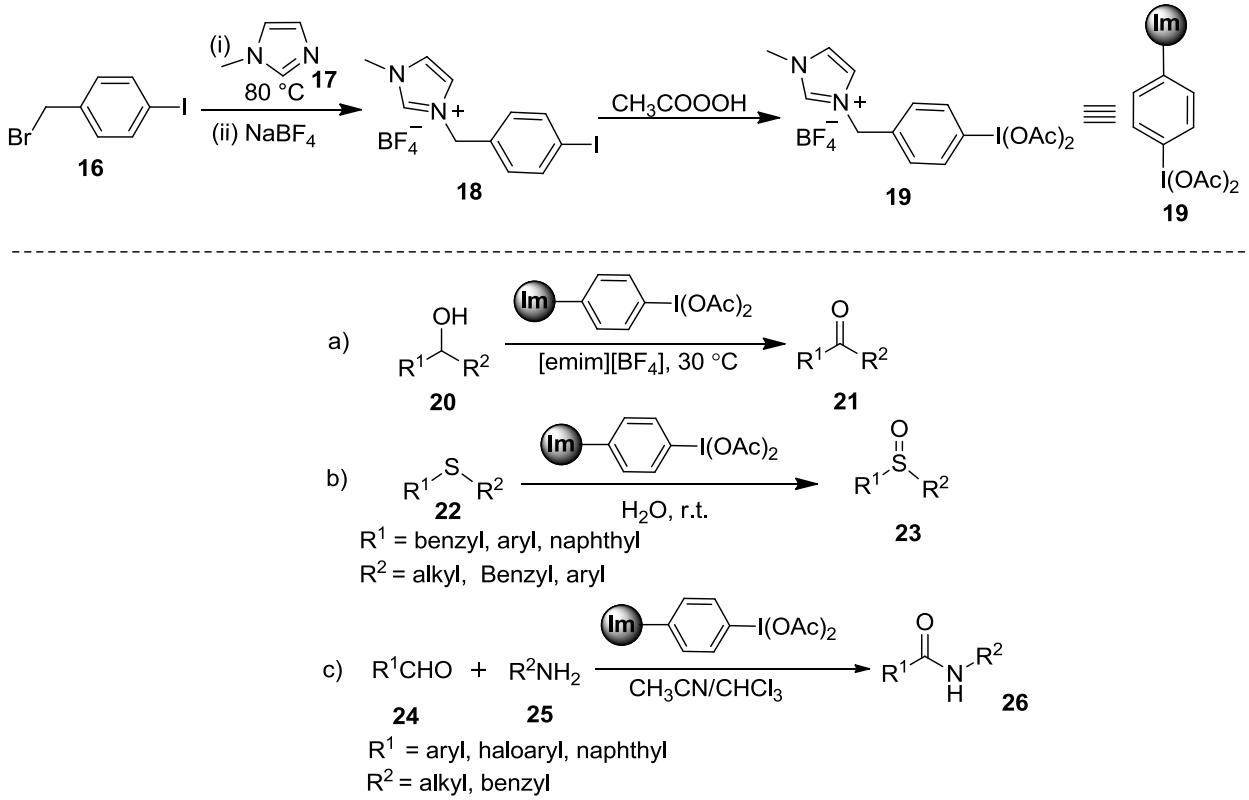

Scheme 5.1.2.2: Synthesis and application of imidazolium-supported iodobenzene diacetate (**19**)

5.1.3 Imidazolium-supported diaryliodonium salts

Due to the electron-deficient nature and excellent leaving-group ability of diaryliodonium salts, they have been used as a versatile arylating agent in modern organic synthesis.[34,35] However, the release of expensive iodobenzene as a waste, and frequent use of column chromatography has concealed the use of diaryliodonium salts in organic syntheses. To address some of these issues, Kumar *et al.* synthesized imidazolium-supported diaryliodonium salts **34** in multiple steps, from imidazolium-supported aryl **31** by using **32**.[36] This reagent was elegantly employed for the arylation of substituted carboxylic acids **35** and phenols **37**, affording their corresponding aryl esters **36** and diaryl ethers **38** in moderate-to-good yields (Scheme 5.1.3.1).

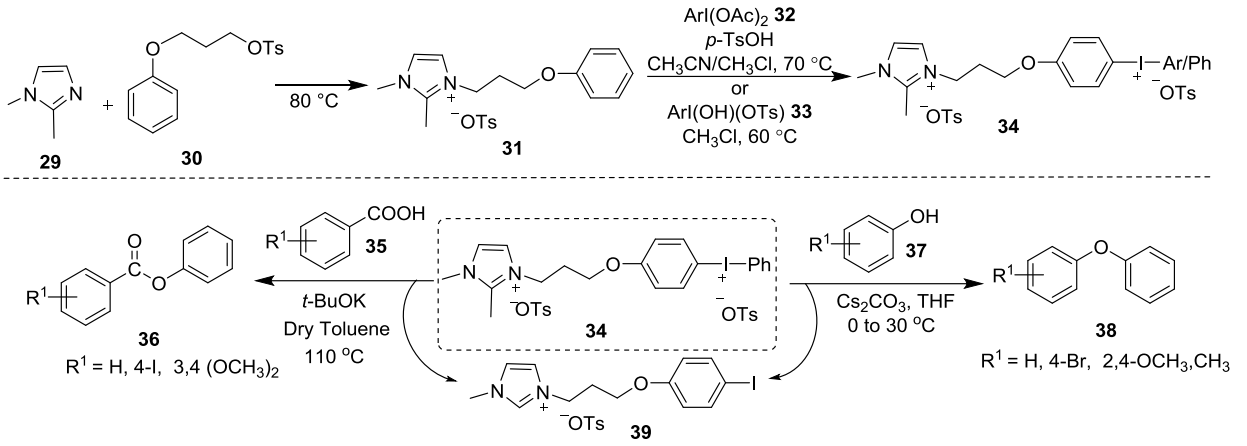

Scheme 5.1.3.1: Synthesis and application of imidazolium-supported diaryliodonium salts **34**

5.1.4 Imidazolium-supported hypervalent iodine derivatives as catch & release reagents

Recently, Kumar *et al.* synthesized a unique imidazolium-supported hypervalent iodine reagent **42** starting from 2,3-dimethylimidazole **29** and sultone sulfonic acid **40** to yield imidazolium-supported sulfonic acid **41** which upon reaction with iodobenzene diacetate **34** in acetonitrile afforded the reagent **42**.[37] **42** was further employed in a 'catch and release' strategy to generate various *α*-substituted acetophenones (**44a-c**) in a good-to-excellent yields, when reacted with various nucleophiles such as KSCN, NaN_3 and $PhSO_2Na$ (Scheme 5.1.4.1).

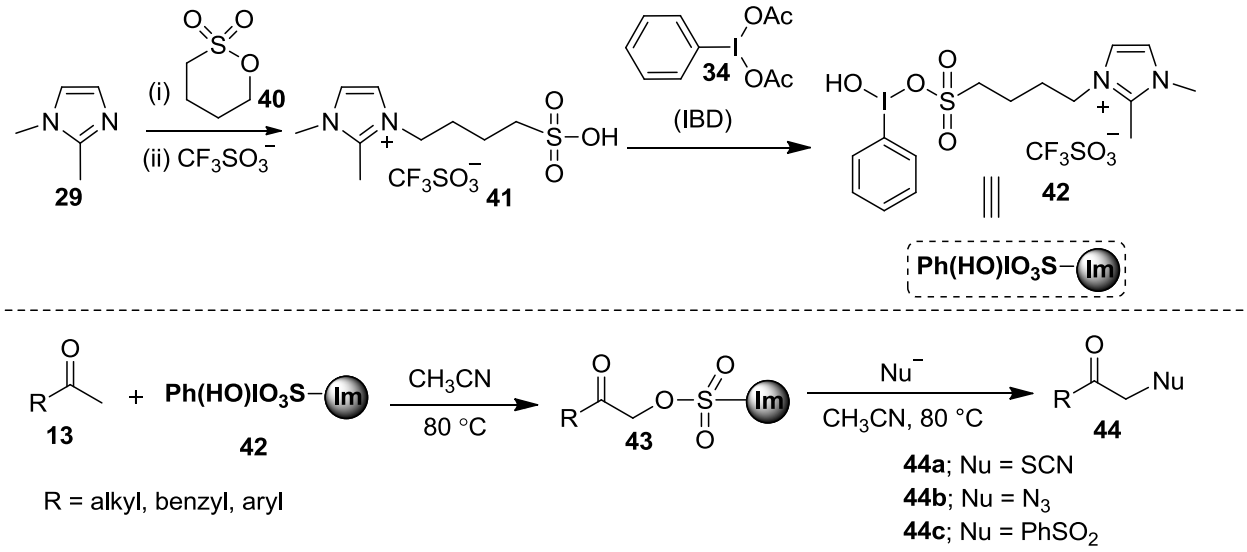

Scheme 5.1.4.1: Synthesis and application of imidazolium-supported hypervalent iodine reagent **44**

5.1.5 Imidazolium-supported TEMPO reagents

Several 2,2,6,6-tetramethylpiperidine-1-oxyl (TEMPO) radical bearing an imidazolium-type appendage have been prepared by various research groups, and successfully utilized for the oxidation of alcohols to carbonyl compounds. In this context, Wu, Tong, Fall, Qian and Zhdankin groups, independently reported the synthesis of different imidazolium-supported TEMPO reagents starting from 4-hydroxy-2,2,6,6-tetramethylpiperidin-1-oxyl (4-HOTEMPO) **45** in multiple steps as described in Scheme 5.1.5.1.[38-42] Wu *et al.* further used imidazolium-supported TEMPO **46a** as co-catalyst along with terminal oxidant sodium hypochlorite ($NaClO_4$) in [bmim][PF_6] water biphasic mixture for the oxidation of alcohols **20** to ketones **21** (Scheme 5.1.5.2a).[38]

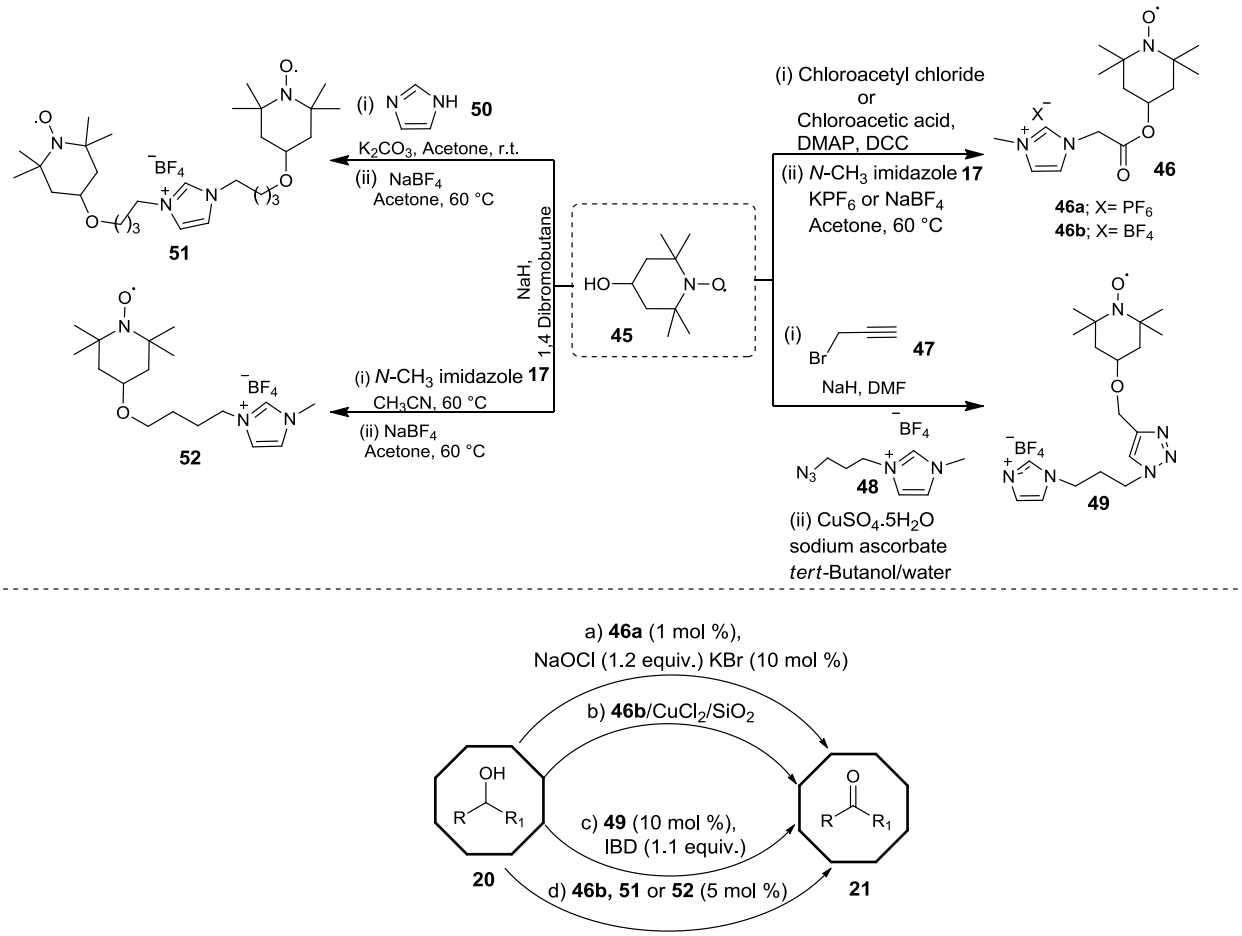

Scheme 5.1.5.1: Synthesis and application of different imidazolium-supported TEMPO reagents **46**, **49**, **51** and **52**

Similarly, Tong's group affixed the imidazolium-supported TEMPO **46b** and $CuCl_2$ on to various silica supports including SiO_2, MCM-41 and SBA-15, and applied it as oxidizing agent

for the same chemical transformation;[39] delightfully, these heterogeneous catalysts showed better catalytic activity over the imidazolium-supported TEMPO/$CuCl_2$ system (Scheme 5.1.5.2b). Likewise, Fall et al. explored imidazolium-supported TEMPO based triazole system **49** as a catalyst for same oxidation reaction in combination with $PhI(OAc)_2$ (Scheme 5.1.5.2c).[40] Qian et al. also employed different imidazolium-grafted TEMPO reagent **46b**/**51**/**52** for the described oxidation reactions.[41]

5.1.6 Imidazolium-based nucleophilic reagents

Nucleophilic ionic liquids (NILs), are a special class of highly reactive imidazolium-supported reagents that are prepared by nucleophilic displacement of halide ion with sodium or potassium salts of anions. For example, the reagent [bmim][N_3] **53** was used by Anna and coworkers for the nucleophilic aromatic substitution of aryl/heteroaryl halides to obtain the corresponding azides (Scheme 5.1.6.1a).[43]

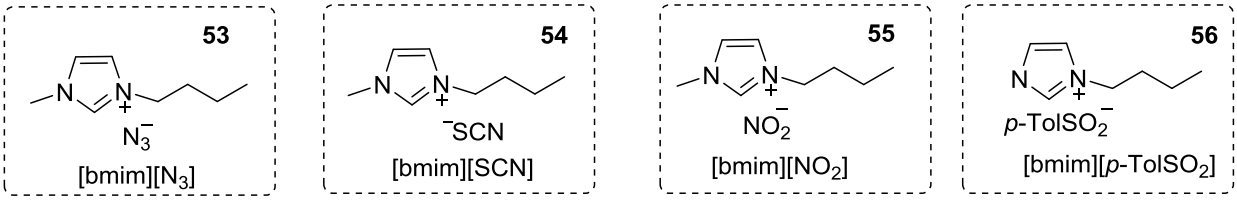

Figure 5.1.6.1: Application of imidazolium-based nucleophilic reagents

Chauhan *et al.* synthesized a novel NIL [bmim][SCN] **54** by the anion exchange of [bmim][Br] with KSCN in acetone, and used it for the thiocyanation of alkyl halides, and phenacyl bromides at room temperature under solvent-free conditions (Scheme 5.1.6.1b).[44] Subsequently, Yadav and team also used the reagent **54** for the conjugative hydro thiocyanation of chalcones, offering *β*–thiocyanato *α,β*-unsaturated ketones in appreciable yields (85-93%) as comparison to the earlier reports (Scheme 5.1.6.1c).[45] Valizadeh and Gholipour prepared [bmim][NO_2] reagent **55** and utilized as a nitronium ion source for the nitrosation of substituted arenes in presence of boric acid under microwave-assisted solvent-free conditions (Scheme 5.1.6.1d).[46] Recently, Kumar and coworkers prepared [bmim][*p*-$TolSO_2$] reagent **56** from [bmim][Br] with sodium *p*-toluenesulfinate (*p*-$TolSO_2Na$) in acetone, and used it for the transformation to sulfones and *β*-ketosulfones from alkyl/phenacyl bromides (Scheme 5.1.6.1e).[47]

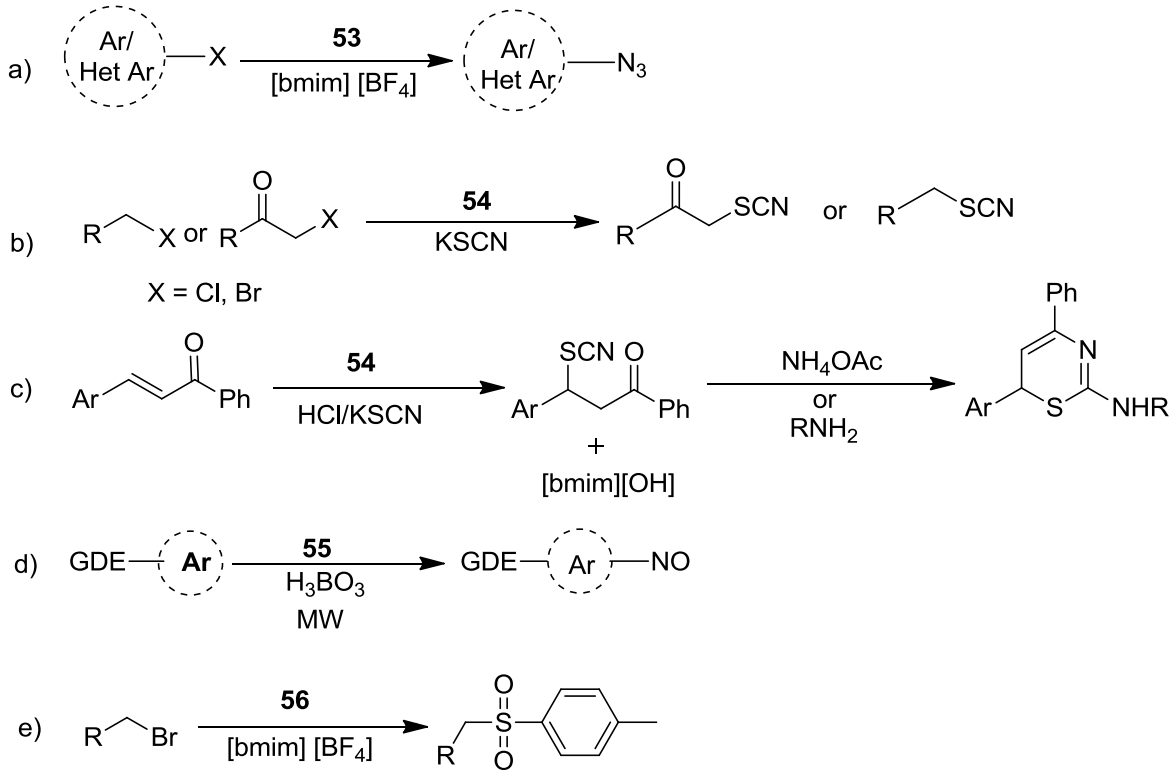

Scheme 5.1.6.1: Various nucleophilic substitution reactions by nucleophilic ionic liquid reagents (**53**, **54**, **55** & **56**)

5.1.7 Imidazolium-supported diphenylphosphinite salts (IL-OPPh$_2$)

Iranpoor *et al.* efficiently synthesized diphenylphosphinite-functionalized imidazolium salt **59** by reacting imidazolium-supported alcohol **57** with commercially available chlorodiphenylphosphine (**58**) in the presence of triethylamine (Scheme 5.1.7.1).[48,49] The reagent **59** was efficiently used as a reaction medium and ligand for the silylation, alkenylation *via* Heck reaction, arylation and dehalogenation of aryl halides (**5**) under Pd-catalyzed conditions to obtain corresponding aryl silanes (**60**), alkenyl arenes (**61**), biaryls (**62**) and arenes (**63**) respectively (Scheme 5.1.7.1).

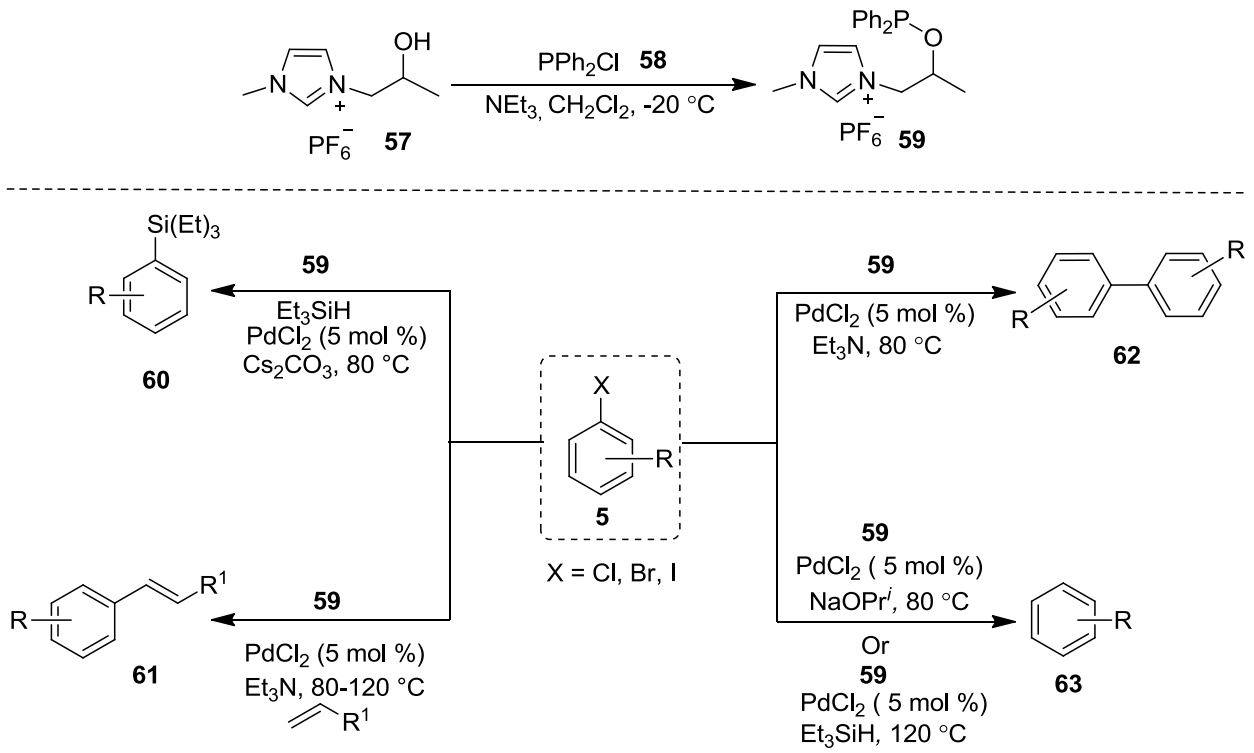

Scheme 5.1.7.1: Synthesis and application of imidazolium-supported diphenylphosphinite salt **59**

Moreover Valizadeh *et al.* efficiently used another imidazolium-supported diphenylphosphinite-fuctionalized reagent **65**, as a catalyst for the synthesis of substituted coumarins **66** from phenolic substrate **37** with di(methyl or ethyl) acetylenedicarboxylate **64** under microwave irradiaition.[50]

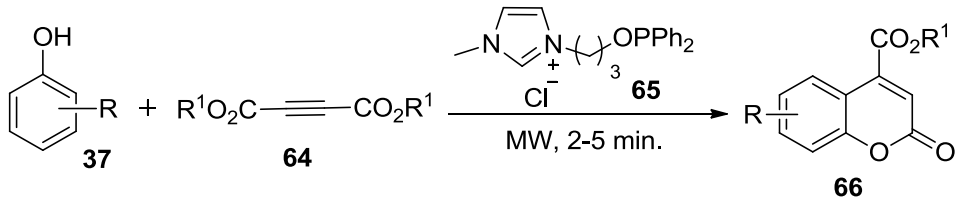

Scheme 5.1.7.2: Application of imidazolium-supported diphenylphosphinite-fuctionalized reagent (**65**) in the synthesis of coumarins

5.1.8 Imidazolium-supported Mukaiyama reagent

N-methyl-2-chloropyridinium iodide (Mukaiyama reagent) is an effective activating agent used for the formation of esters, carboxamides, ketenes, lactones and lactams from carboxylic acids. Despite its great success, it is associated with some issues of solubility, stability and purification of coupled products. To target these limitations, Kumar *et al.* anchored

imidazolium-support to Mukaiyama reagent **72** through a series of steps. The strategy involves the synthesis of *o*-chlorobutyl benzyl alcohol (**69**) from *p*-hydroxybenzaldehyde (**67**) and 4-chloro-1-bromobutane (**68**), which on further reaction with 1,2-dimethylimidazole (**29**) yielded **70**. Imidazolium-supported benzyl alcohol **70** upon reaction with 2-chloropyridine (**71**) using triflic anhydride resulted in the formation of **72** in 55% yield. Thereafter, the synthesized imidazolium-supported Mukaiyama reagent **72** was comfortably used for the coupling of various acids **35** and amine **25** to generate the corresponding amides **26** in good-to-excellent yields (Scheme 5.1.8.1).[51]

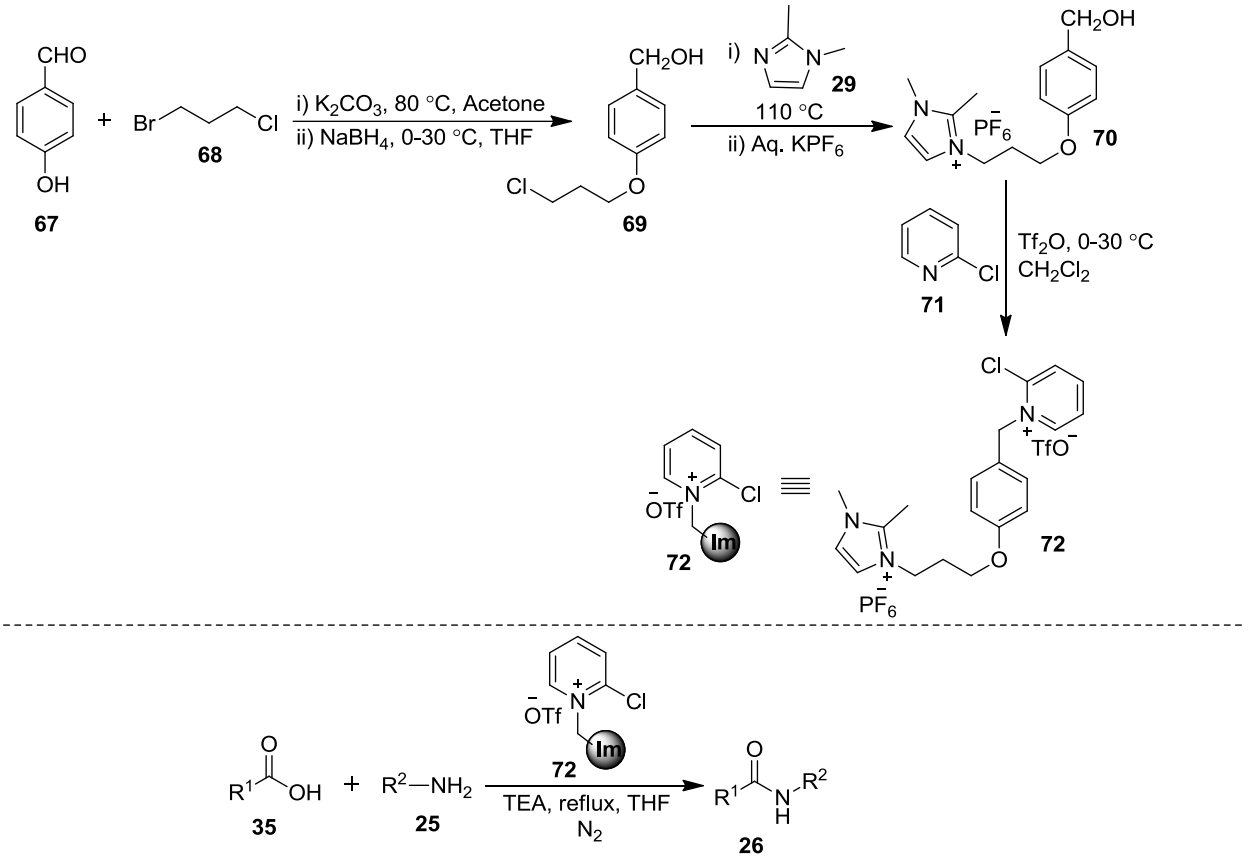

Scheme 5.1.8.1: Synthesis and application of imidazolium-supported Mukaiyama reagent **72**

5.2 Introduction

Amide, ester and thioesters functionalities are highly desirable synthetic targets that form an integral component of numerous natural products and biologically active synthetic molecules. Amide bond itself accounts its presence in more than 25% of known drugs as per the Comprehensive Medicinal Chemistry (CMC) database (Figure 5.2.1).[52-54] Amide and ester linkages have been introduced as an essential component to synthetic drugs such as Procaine, Lidocaine, Tocainide to increase their metabolic stability.[55] These groups have imposed degradable character and good thermal and mechanical characteristics to biodegradable poly(ester amide)s (PEAs) polymers.[56] Glycolamide esters of Aspirin,[57] Ibuprofen,[58] Niflumic acid,[59] Scutellarin[60] and Nimesulide[61] have also been used as biolabile prodrugs due to their ability to undergo quick cleavage in human plasma. Similarly, thioesters have been extensively used in native chemical ligation for the synthesis of many biologically active small and medium-sized peptides and proteins.[62,63] Selective examples of amide, ester and thioester containing commercialized drugs and prodrugs are shown in Figure 5.2.1

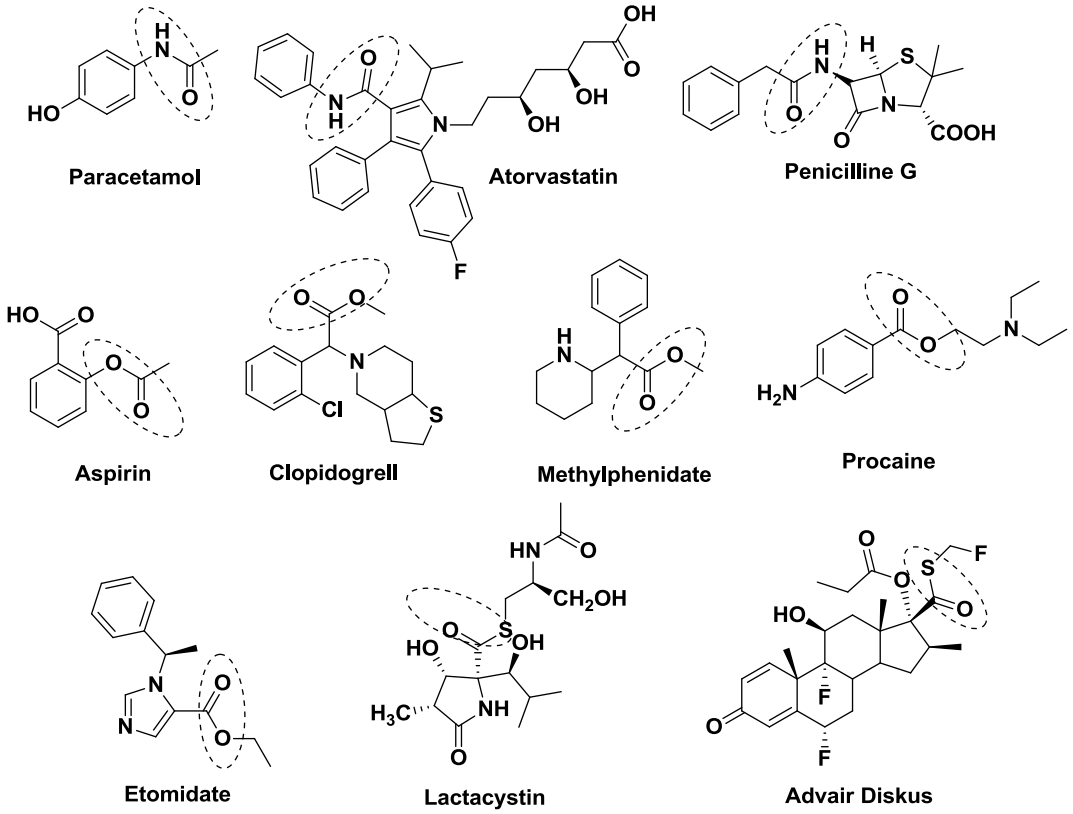

Figure 5.2.1: Selective examples of commercial available drugs and prodrugs containing amide, ester and thioester functionalities

Acid-activation as acyl halides, acyl azides, acylimidazoles, anhydrides, esters and acyl benzotriazoles, followed by nucleophilic substitution are among the most common strategies employed for construction of amide, ester and thioester bonds. Benzotriazole is a versatile synthetic auxiliary that impose multiple activating influences on neighboring groups, and its reactivity has been immensely exemplified by Katritzky and coworkers (Figure 5.2.2).[64-66] In the above aspect mentioned aspect, *N*-acyl benzotriazoles have surpasses most of the aforementioned reagents due to their relative stability, ease of formation, higher reactivity and high yields of the *N*-, *S*- and *O*-acylated products.[64,67] In addition, Katritzky's pioneer work on the applications of *N*-acyl benzotriazoles have led to the synthesis of libraries of novel heterocycles, peptides and peptidomimetics.[68]

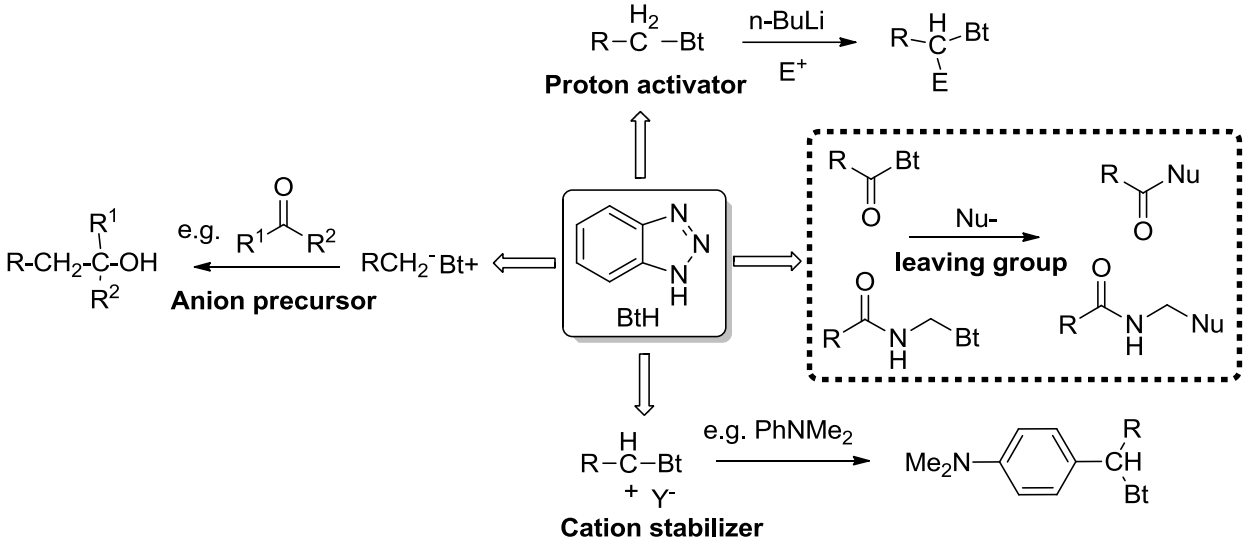

Figure 5.2.2: Multiple reactivity of benzotriazole reagent (BtH)

However, *N*-acyl benzotriazole methodology suffers one or more hindrances in term of green chemistry perspective, including the use of organic solvents in the acylation reaction, non-reusability of benzotriazole, and use of column chromatography for the purification of the acylated product.[69-71] Efforts to overcome some of these drawbacks have been undertaken by Paio, Showalter, Fang and Katritzky by synthesizing different polymer-supported benzotriazole reagents. For example, Katritzky and Paio *et al.* independently synthesized polymer-supported benzotriazole reagents from Merrifield resin bounded to 1,2-phenylenediamine in multistep protocol. Such grafting of benzotriazole onto different polymeric supports described the combinatorial approach for the synthesis of substituted amines **75** *via* mannich type reaction (Scheme 5.2.1)[72,73] In addition, Paio and coworkers also anchored benzotriazole on different

resin bound polymers such as; hydroxymethyl polystyrene (HMB-PS), chloromethyl polystyrene (CM-PS), aminomethyl polystyrene (AM-PS), Argogel-NH_2 (AG-NH_2), for executing the aforementioned application (Scheme 5.2.1).[73]

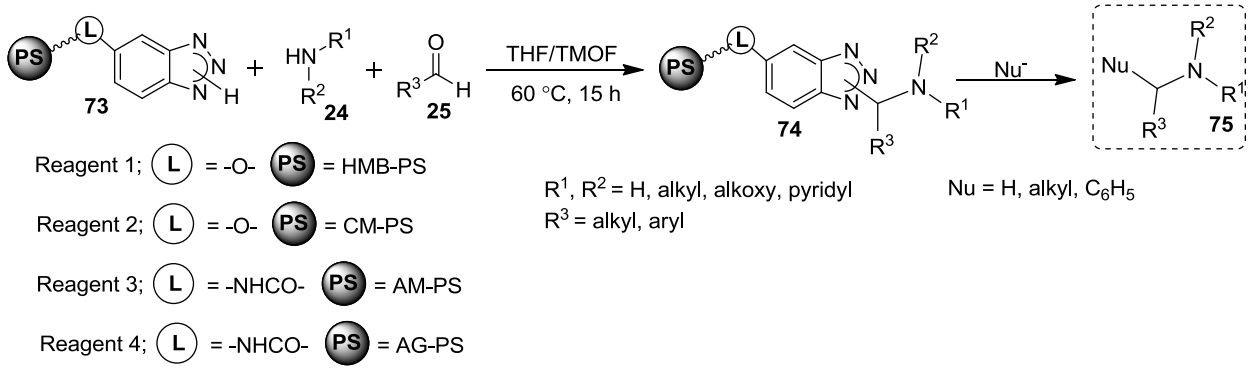

Scheme 5.2.1: Katritzky and Paio works; Synthesis of tertiary amines **75** by the cleavage of polymer-supported benzotriazole Mannich adducts

In continuation, Showalter and coworkers also developed a distinct methodology for the synthesis substituted amino methyl functionalized Merrifield resin anchored benzotriazole reagent. This polymer-supported benzotriazole reagents **76** upon reaction with grignard reagent also yielded a small library of homologated secondary and tertiary amines **75** (Scheme 5.2.2).[74]

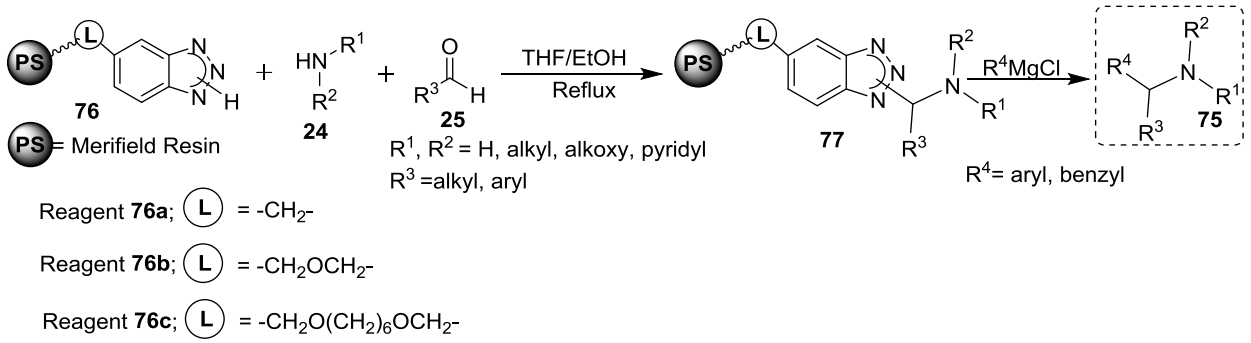

Scheme 5.2.2: Showalter's work; Synthesis of tertiary amines **75** by the cleavage of polymer-supported benzotriazole Mannich adducts

Later, in an extension to the aforementioned work, Paio *et al.* described an automated synthesis of unsymmetrical aryl ureas **83** from the synthesized, polymer supported benzotriazole adduct **80** by mean of coupling reaction between polystyrene-polyoxyethylene-amino (AG-NH_2) or aminomethyl-polystyrene (AM-PS) resins with benzotriazole-5-carboxylic acid (**79**) (Scheme 5.2.3).[75]

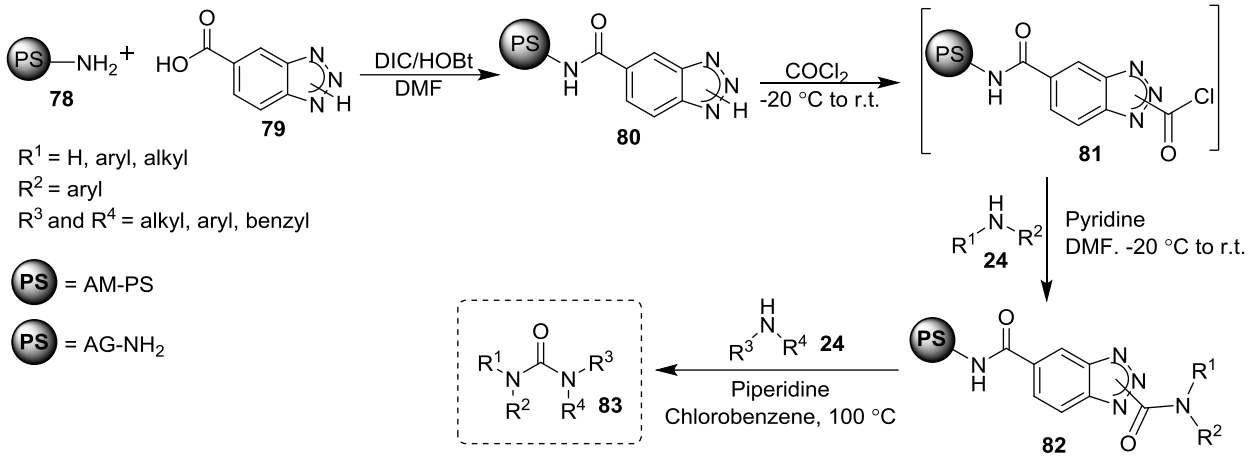

Scheme 5.2.3: Polymer-supported benzotriazole mediated synthesis of unsymmetrical aryl ureas **83**

In 2001, the leaving group ability of benzotriazole was elegantly explored with polymer decorated benzotriazole reagent **84** & **85** by Katritzky *et al*. towards the synthesis of synthetic useful diketones **88** from α-CH_2-ketones, *via* polymer azolides **87.** The derivatives of resins **85** afforded compounds **88** in 18-41% yields while polymer azolides based on resin **84** gave corresponding diketones **88** in 47-77% (Scheme 5.2.4).[76]

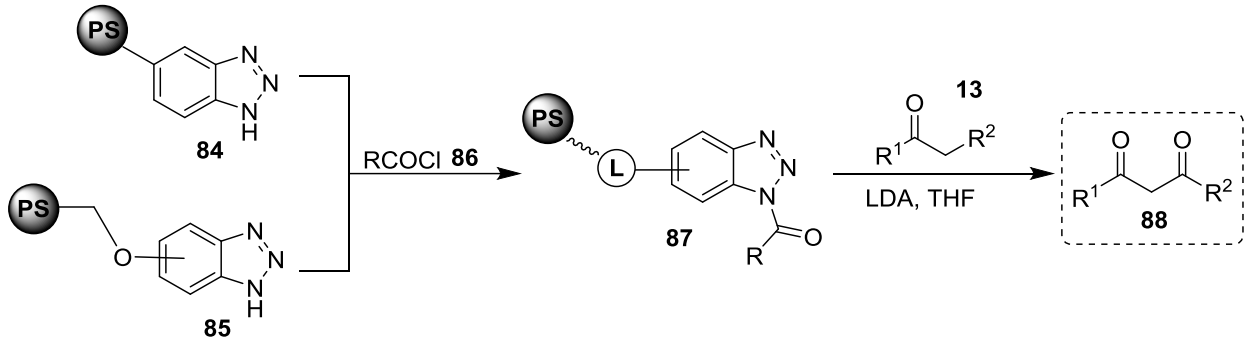

Scheme 5.2.4: *C*-acylation of ketones with polymer-supported azolides **87**

Polymer-supported benzotriazoles reagents (**P1-3**) were also prepared by Fang *et al.* by linking 5-(hydroxymethyl)benzotriazole and benzotriazole-5-carboxylic acid 7**9** with Wang resin, Merrifield resin, and (monomethoxy)poly(ethylene glycol). The aforementioned benzotriazole derivatives were effectively used as promoters for the condensation of anilines **24** with different phenyl acetaldehydes **89**, affording tetrahydroquinoline derivatives **90** in 84-89% yields (Scheme 5.2.5).[77]

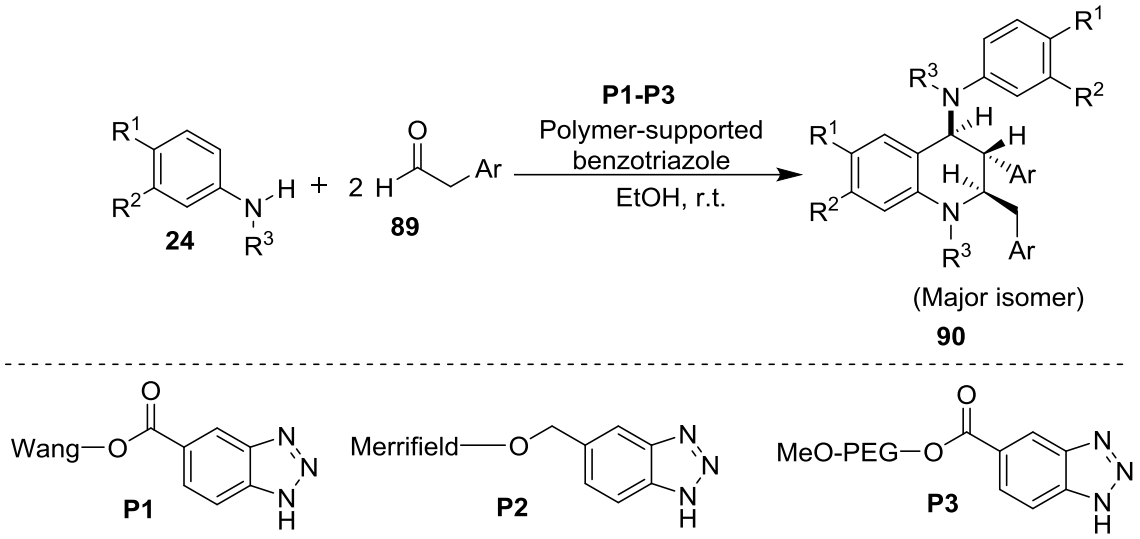

Scheme 5.2.5: Polymer-supported benzotriazole reagent as a promoter in the synthesis of tetrahydroquinoline derivatives **90**

Although, some of the limitations associated with benzotriazole chemistry were overcome by synthesizing polymer-supported benzotriazole auxiliaries, yet these reagents are associated with their own disadvantages of low loading capacity, elaborate purification procedures, low swelling properties, limited solubility and the scope of the reagents.

As described earlier, a great attention has been devoted on the synthesis of functionalized imidazolium-supported reagents, and their use in solution-phase parallel synthesis[1-8,78-80] and in facilitating the separation process.[81,82] Tuning chemical and physical properties, higher loading capacity, reactions under homogeneous conditions and use of conventional methods for the analysis of reaction progress have proved imidazolium entity to be ideal support[12,83] for the synthesis of small molecule libraries, peptides,[84,85] and oligosaccharides.[86,87] With our interest in application of benzotriazole in acylation reactions, we envisaged to affix benzotriazole on imidazolium-support to generate soluble-supported benzotriazole auxiliary that can have high efficiency and can be exemplified as a reusable carboxyl group activating reagent for amide, ester and thioester bonds formation in aqueous media.

5.3 Results and Discussion

The work commenced with the synthesis of imidazolium-supported benzotriazole reagent connected *via* methylene linker (Im-CH_2-BtH, **95**) as depicted in Scheme 5.3.1. Esterification of commercially available benzotriazole-5-carboxylic acid (**79**), followed by reduction with lithium aluminium hydride (LAH) in THF yielded 5-hydroxymethylbenzotriazole (**92**).[88] Chlorination of

92 with thionyl chloride in toluene furnished 5-chloromethylbenzotriazole (**93**) in 70% as a single isomer. Reaction of **93** with 1,2-dimethylimidazole under solvent-free heating condition afforded imidazolium methylene linked benzotriazole chloride salt (**94**), as a gummy product in 98% yield. Based on the ^{1}H NMR analysis, it was found that **94** is an isomeric mixture of N^1- and N^3-isomers with major amounts of N^1-isomer. **94** was used as such for the next step without further purification. For tuning the solubility, the counter anion in **94** was exchanged with PF_6 anion by reacting with KPF_6 in dry acetone under reflux condition to yield methylene linked imidazolium-supported benzotriazole potassium hexafluorophosphate (**95**) as a brown solid in 96% yield. Initially the exchange of Cl^- by PF_6^- was attempted in water at room temperature. The reaction did not goes to completion, and the product remains soluble along with **94** in water.

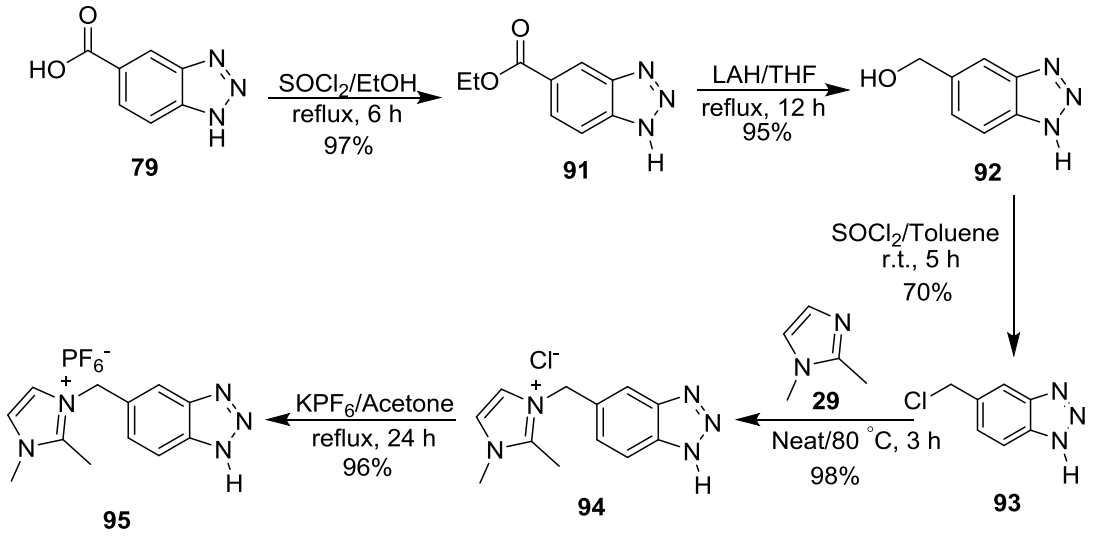

Scheme 5.3.1: Synthesis of imidazolium-supported benzotriazole (Im-CH_2-BtH) (**95**)

The ^{1}H NMR of **95** indicated the presence of N^1- and N^2-isomers in the ratio 2:1. Three characteristic singlets at δ 5.58, 3.76 and 2.64 for the methylene (2H), *N*-methyl (3H) and *C*-methyl (3H) protons were observed for N^1-isomer along with three singlets at δ 6.17, 3.66 and 2.44 for N^2-isomer. Peaks for equivalent aromatic protons were observed in the region δ 7.37-8.07 in the ^{1}H NMR of **95**. We were successful in isolating N^1-isomer by recrystallization of the brown solid using methanol. Thus, the overall strategy provides a straightforward high-yielding method for the synthesis of imidazolium-supported benzotriazole reagent, avoiding protection and de-protection steps as usually required in polymer-supported benzotriazole synthesis. The ^{1}H NMR and ^{13}C NMR of pure **95** are shown in figures 5.3.1 and 5.3.2.

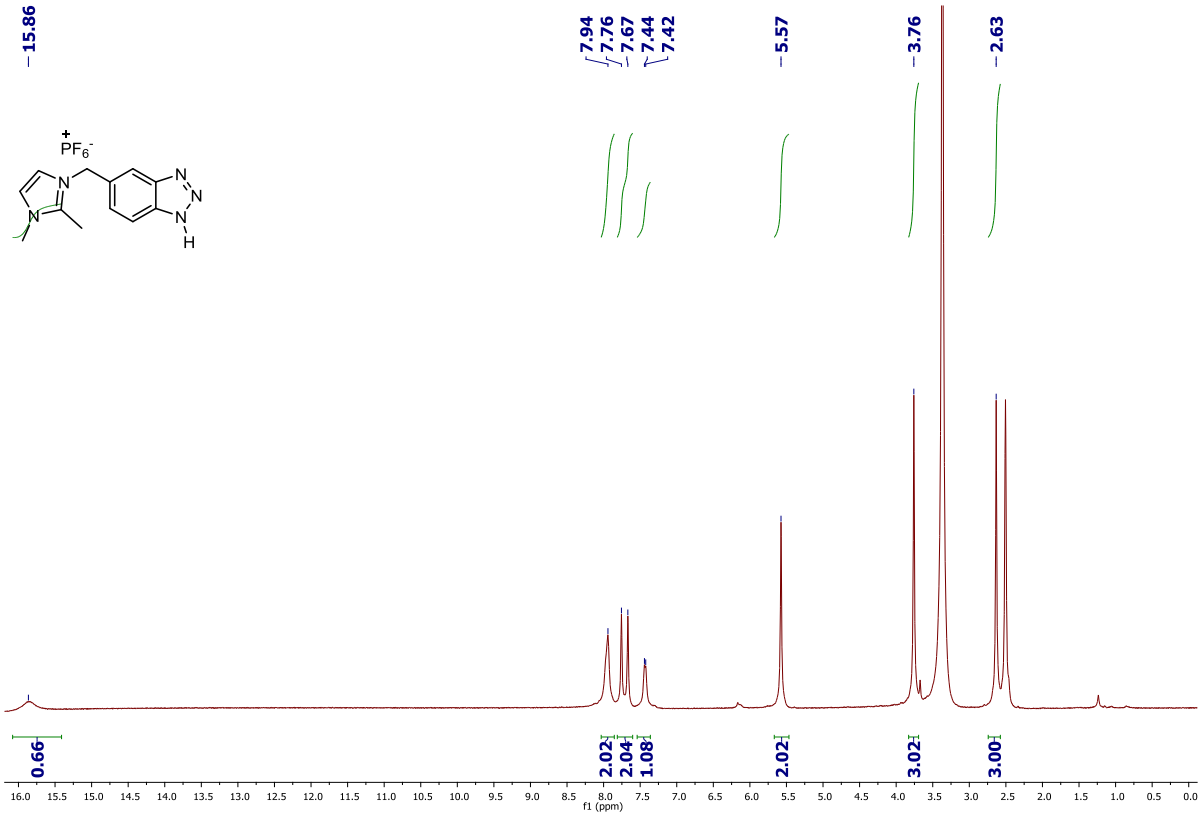

Figure 5.3.1: ^{1}H NMR spectrum of **95** (pure: N^{1} isomer)

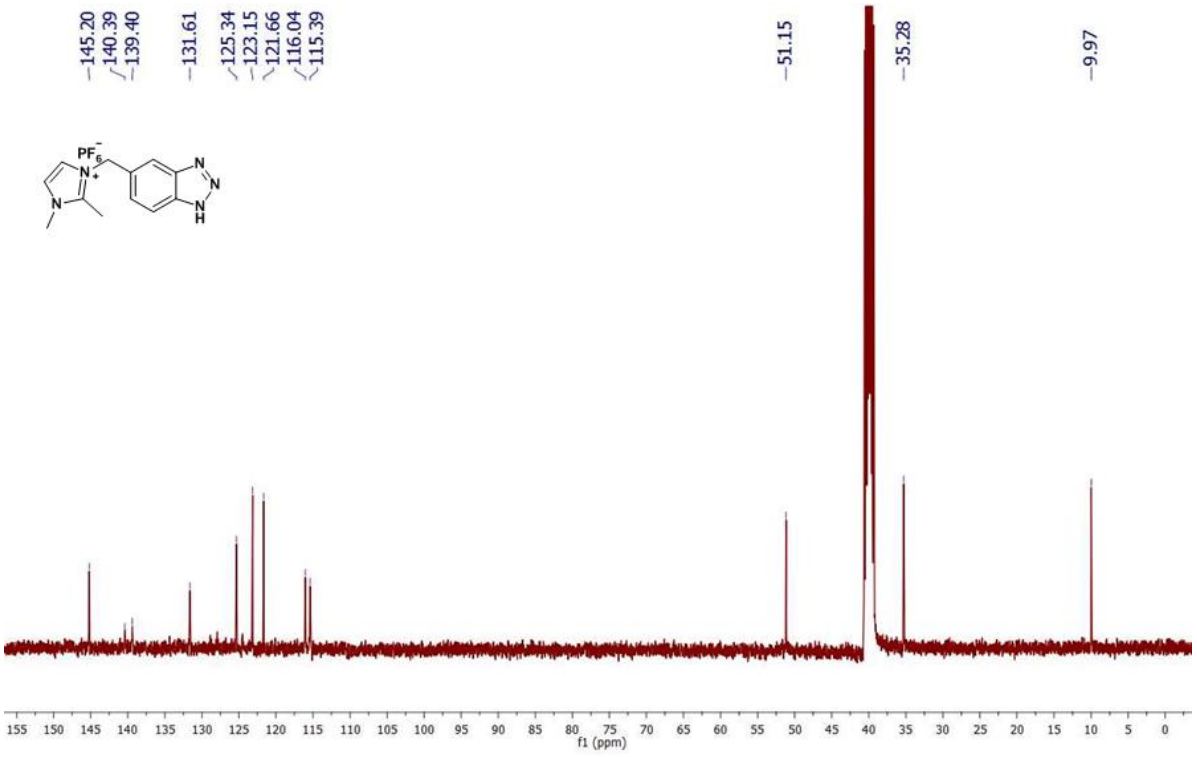

Figure 5.3.2: ^{13}C NMR spectrum of **95** (pure: N^{1} isomer)

The thermal stability profile of the synthesized reagent **95** was studied using differential scanning calorimetry (DSC) and thermogravimetric analysis (TGA). The DSC experiment showed that the exothermic decomposition temperature of **95** is above 150 °C (Figure 5.3.3, left curve) with an initiation temperature of 151.81 °C and end point at 185.81 °C. The compound **95** could be used well below its decomposition temperature. It is worth mentioning that **95** did not show any sign of decomposition or loss of reactivity even after storing for more than two month at room temperature. The TGA of **95** indicated the first weight loss to be around 254 °C, and the full degradation centred around 366 °C, (Figure 5.3.3, right curve) suggesting that **95** is quite thermally stable.

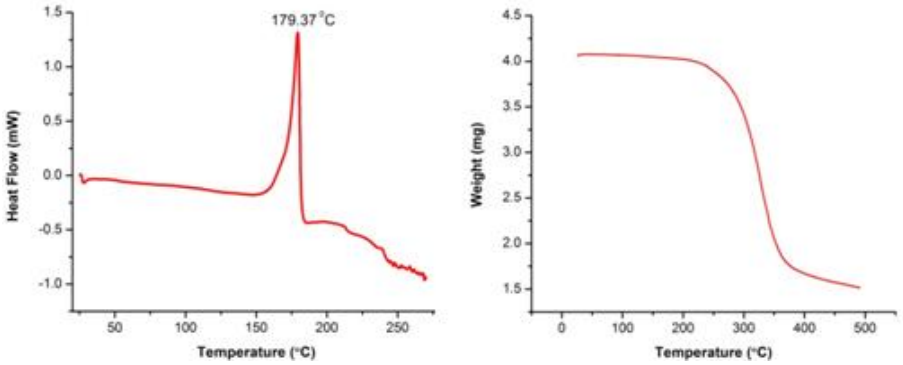

Figure 5.3.3: DSC and TGA curves of compound **95**

After successful synthesis and characterization of **95**, we focused our attention to investigate the carboxylic acid activating capability of **95** for preparing amides, esters and thioesters. Thus, we initially attempted the activation of benzoic acid (**96a**) with **95**. Prior to this, the activation of **96a** was initially attempted with the reagent **94** (Im-CH_2-BtH, Cl^- salt), however due to difficulty in the weighing due to its gummy nature and comparatively lower reactivity, we switched to activation of **96a** using **95** (Im-CH_2-BtH, PF_6^- salt**)**.

Various coupling reagents *viz*. DCC, EDC.HCl, HBTU and HATU were screened in tetrahydrofuran (THF) and acetonitrile (CH_3CN) for the activation of benzoic acid (**96a**) using **95** (Table 5.3.1). The use of polar solvents such as DMF and DMSO were discarded due to difficulty of removing them after the reaction. After screening different conditions, the use of DCC (1.2 eq.) in CH_3CN using a catalytic amounts of DMAP at room temperature gave imidazolium-supported *N*-benzoyl benzotriazole (**97a**) in 75% isolated yield (Table 5.3.1, entry 3). A number of spots were visible on the TLC when the reaction was carried under reflux conditions, and subsequently a declination in the isolated yield of **97a** was observed (Table 5.3.1, entry 5)**.** Interestingly due to

high polarity of **97a**, the generated DCU was easily removed from the reaction mixture by simple washing with ethyl acetate, and thereafter the precipitation with methanol yielded **97a** in pure form. A catalytic amount of DMAP was sufficient and necessary for the reaction as its absence leads to tremendous decrease in the yield of **97a** (Table 5.3.1, entry 4).

Table 5.3.1: Optimization of Reaction Conditions for the Synthesis of **97a**

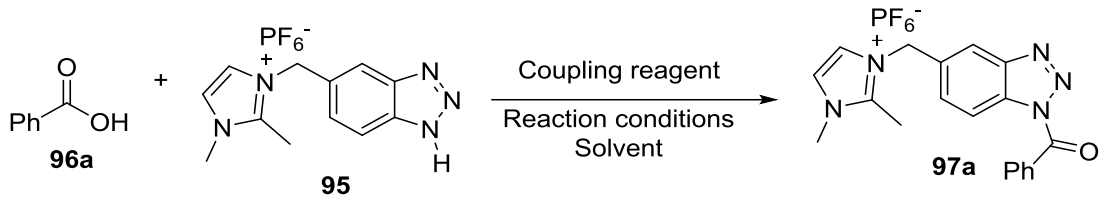

Entry	Coupling reagents	Solvent (mL)	Reaction conditions	Yield[b] of 97a (%)
1	DCC (1.2 eq.) /DMAP (cat.)	THF	r.t., 26 h	50
2	DCC (2 eq.)/DMAP (cat.)	CH_3CN	r.t., 20 h	76
3	**DCC (1.2 eq.)/DMAP (cat.)**	**CH_3CN**	**r.t., 20 h**	**75**
4	DCC (1.2 eq.)	CH_3CN	r.t., 20 h	40
5	DCC (1.2 eq.)/DMAP (cat.)	CH_3CN	reflux, 8 h	55[a]
5	EDC.HCl (1.5 eq.)/DMAP (cat.)	CH_3CN	r.t., 20 h	65
6	HBTU (1.5 eq.)/DMAP (cat.)	CH_3CN	r.t., 20 h	45
7	HATU (1 eq.)/DMAP (cat.)	CH_3CN	r.t., 20 h	52

[a]A number of spots on TLC appeared on refluxing and subsequently the yield of **97a** decreased; [b]Isolated yield.

With optimized conditions in hand, the substrate scope of this reaction was studied and six more aromatic and heteroaromatic acids (**96b-g**) were successfully activated using imidazolium-supported benzotriazole reagent (**95**), yielding their corresponding imidazolium-supported *N*-acyl benzotriazole reagents (Im-CH_2-Bt-COAr, **97b-g**) in 65-80% yields (Scheme 5.3.2). The compounds **97a-g** were obtained either in pure N^1-isomeric form or as enriched N^1-isomer with small amounts of N^3-isomer. Apart from aromatic and heteroaromatic acids, acetic acid also got efficiently activated by **95** yielding imidazolium-supported benzotriazole acetyl reagent (**97h**) in 85% isolated yield. It is noteworthy that the loss in yield of **97** is solely during the isolation process due to its partial solubility in methanol. A representative ^{1}H NMR and ^{13}C NMR of **97f** are shown in figures 5.3.4 and 5.3.5.

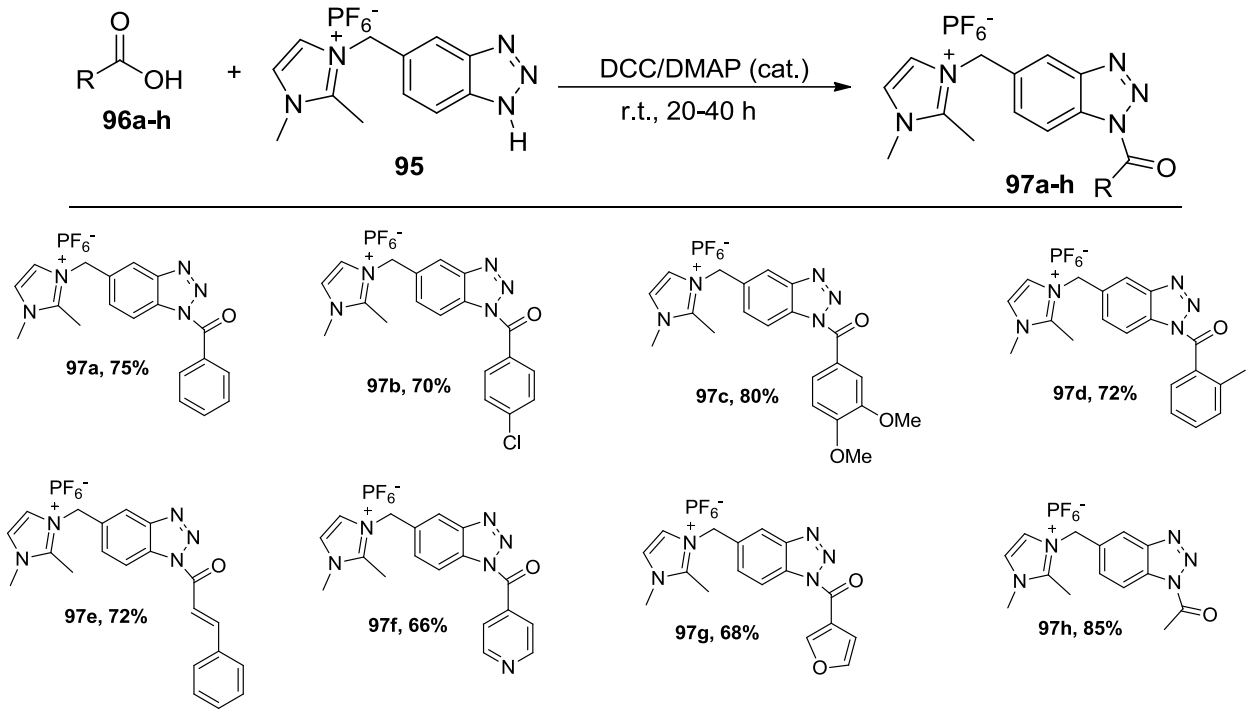

Scheme 5.3.2: Synthesis of imidazolium-supported *N*-acyl benzotriazole reagents (Im-CH_2-Bt-COR) (**97a-h**)

We next investigated the benzoylation of *p*-toluidine (**98A**) using imidazolium-supported *N*-benzoyl benzotriazole (**97a**) in the presence of base (DMAP and K_2CO_3) under classical and microwave conditions in a number of solvents including CH_3CN, THF, EtOH and water. To our delight, the reaction in CH_3CN and water proceeded smoothly under microwave irradiation giving **99aA** in 85% and 90% yields, respectively in 15 minutes (Scheme 5.3.3). On the other hand, 12-14 h was required for completion of reaction under reflux condition in acetonitrile and water yielding **99aA** in comparable yields. The substrate scope of other imidazolium-supported *N*-acyl benzotriazoles (**97b-g**) was explored under similar conditions with a variety of *N*-nucleophilic substrates such as aliphatic, aromatic and heteroaromatic amines (**98A-E**). For all substrates, the reaction comfortably proceeded smoothly in water by applying microwave irradiation for 15-30 minutes, yielding the corresponding amides **99** in 80-95% isolated yields (Scheme 5.3.3).

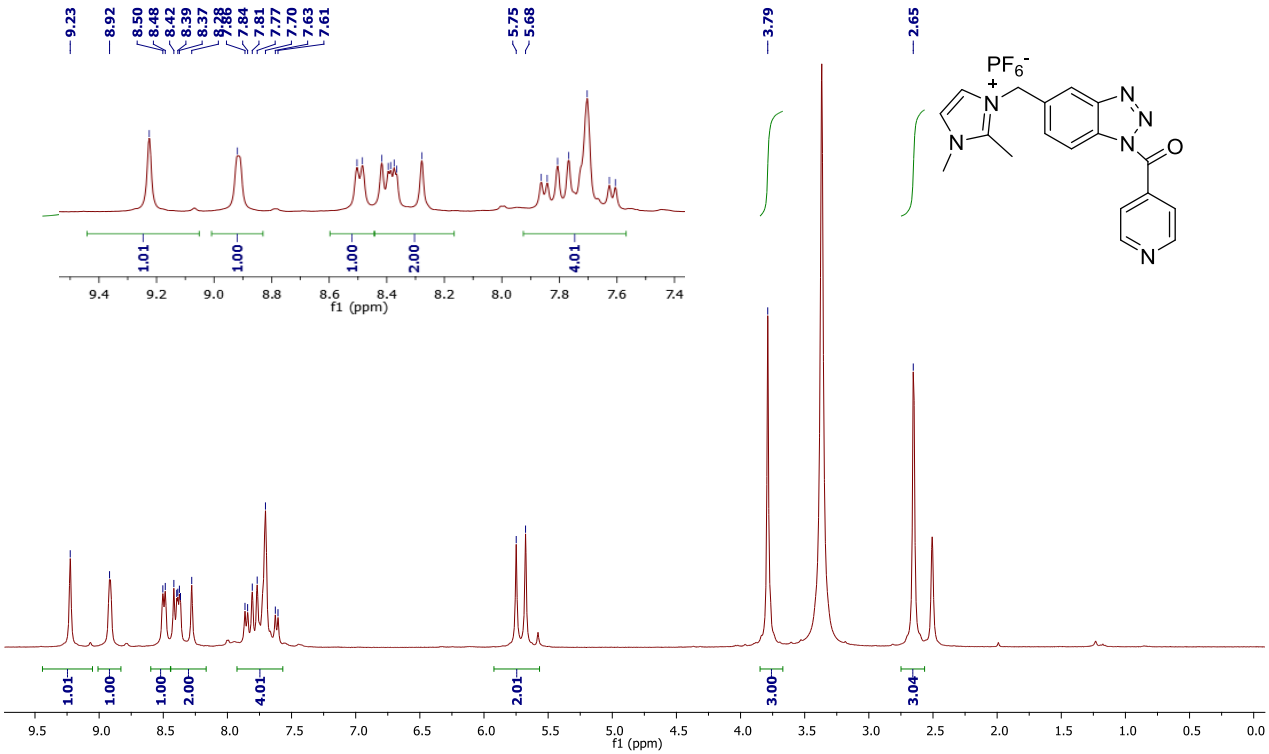

Figure 5.3.4: ^{1}H NMR spectrum of **97f**

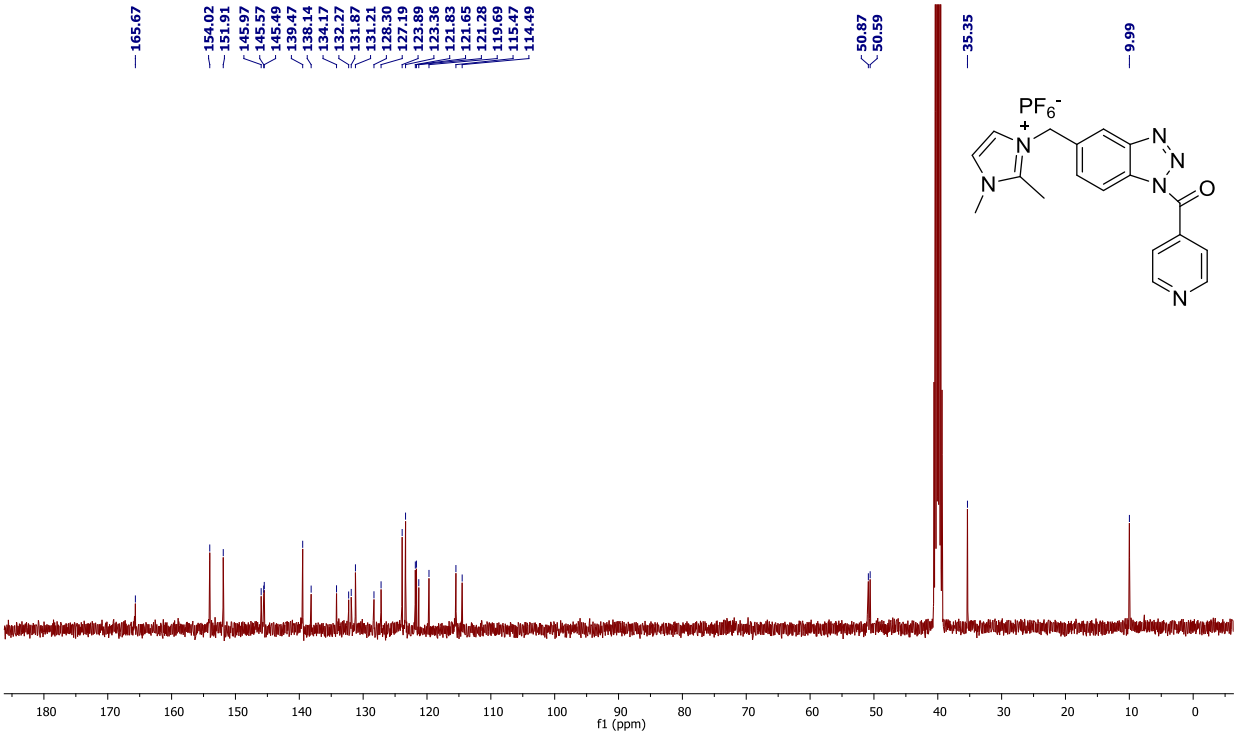

Figure 5.3.5: ^{13}C NMR spectrum of **97f**

Interestingly, extraction of the concentrated reaction mixture with ethyl acetate followed by washing with 1N HCl (to remove the un-reacted *N*-nucleophilic substrate and DMAP) yielded pure amides **99**, thereby avoiding the use of column chromatography.

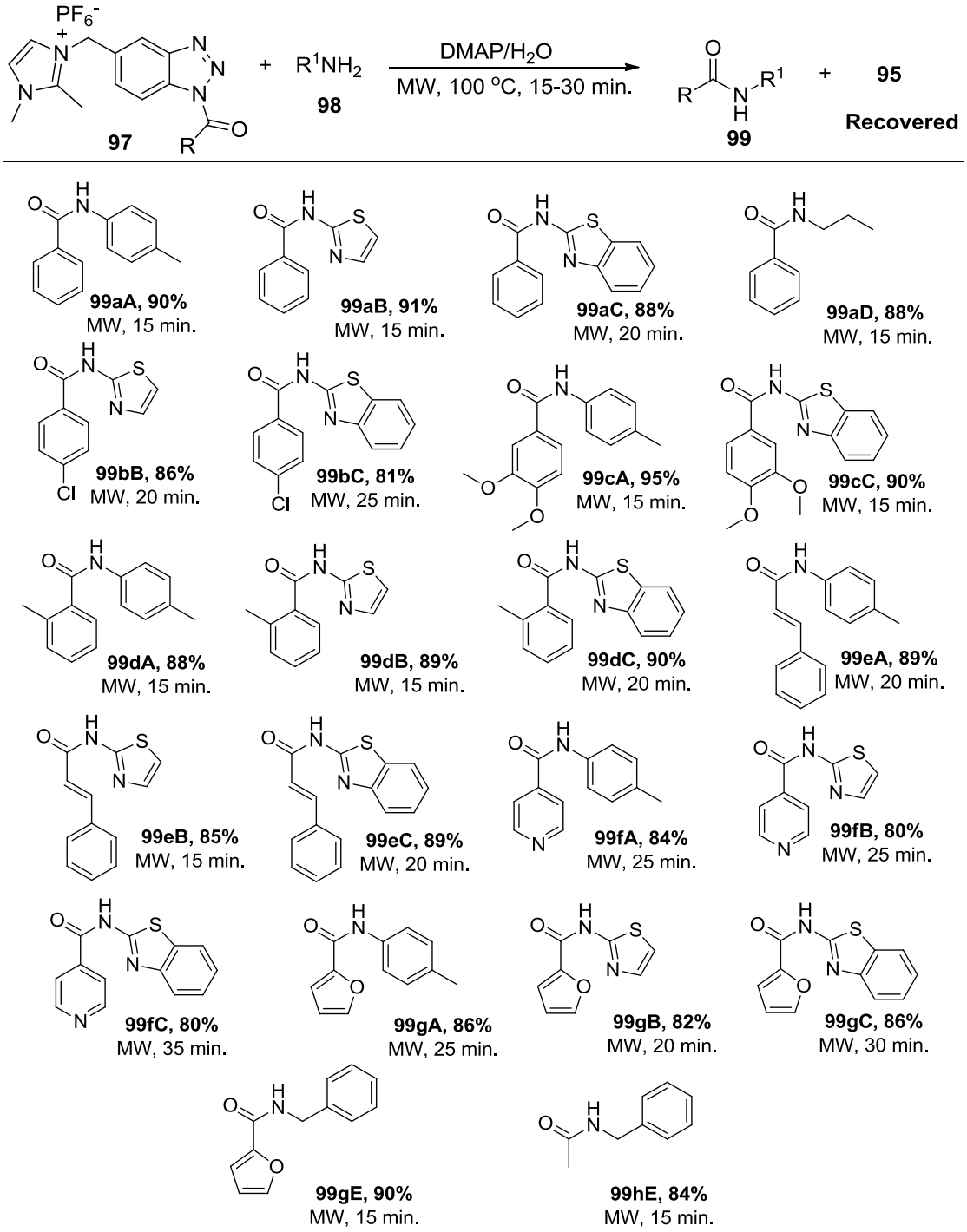

Scheme 5.3.3: Imidazolium-supported *N*-acyl benzotriazoles (**97a-g**)-mediated synthesis of amides (**99**) in aqueous media under MW irradiation

Apart from aromatic and heteroaromatic *N*-nucleophiles, the acylation with **97** worked quite well with aliphatic amines such as propyl amine (**99D**) and benzyl amine (**99E**) in water, yielding the corresponding amides **99aD** and **99gE** in 88% and 90% yields, respectively. The acetylation of benzyl amine (**98E**) with **97h** yielded **99hE** in 84% yield in 15 minutes under the described reaction conditions.

We further utilized imidazolium-supported *N*-acyl benzotriazoles **(97a-g)** for the thioester bond formation by reacting with thiophenol (**100A**) and 2-naphthalenethiol (**100B**) under similar conditions **(**Scheme 5.3.4**)**. Here again, DMAP was found to be the ideal base for the desired transformation in water and acetonitrile, while the reaction worked comparatively slower with K_2CO_3. Longer reaction time and lower yield of the product (**101aA**) was obtained under classical reflux conditions in water and acetonitrile. Both thiophenols (**100A-B**) reacted smoothly with **97** and the reaction completed in 10-30 minute of microwave irradiation. Extraction of the concentrated reaction mixture with ethyl acetate followed by washing of organic filtrate with water (to remove DMAP), and thereafter recrystallization with hexanes yielded pure thioesters (**101**) in 85-96% yields.

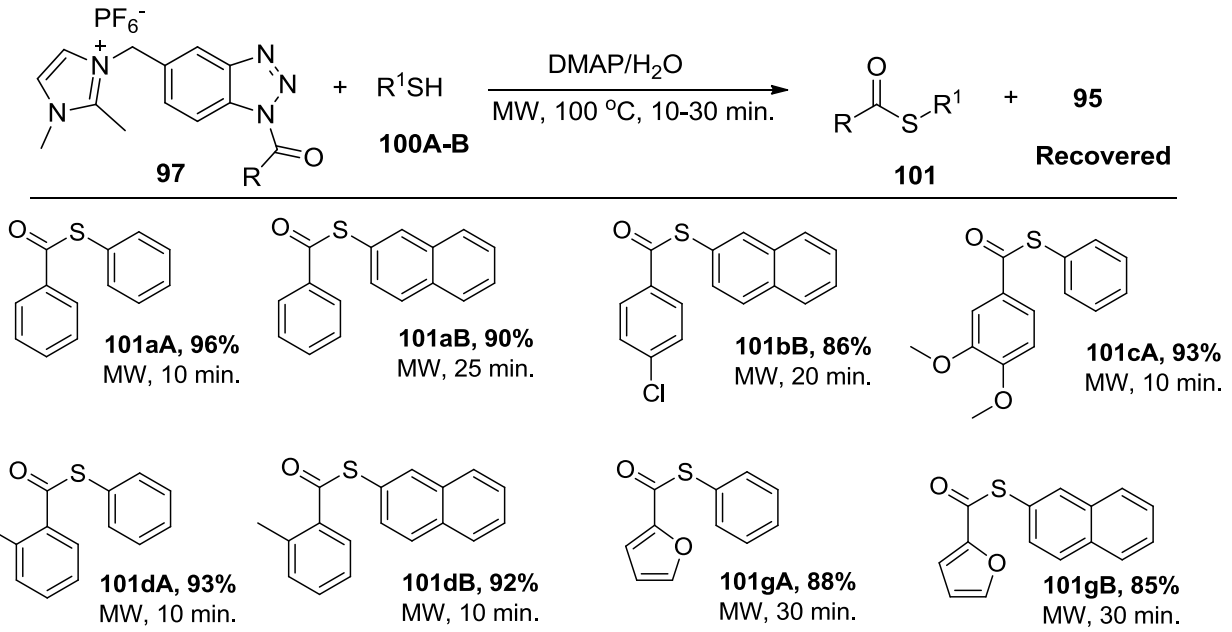

Scheme 5.3.4: Imidazolium-supported *N*-acyl benzotriazoles (**97a-g**)-mediated synthesis of thioesters (**101**) in aqueous media under MW irradiation

After the success of amide and thioester bond formation in aqueous medium, we turned our attention towards ester bond formation using imidazolium-supported *N*-acyl benzotriazoles

(**97a-g**). When 3-methoxyphenol (**102**) was allowed to react with **97a** under the standardized conditions for amide bond formation, the corresponding ester **103a** was only formed in 26% yield. Interestingly, the use of *t*-BuOK in-place of DMAP resulted in formation of **103a** in 80% isolated yield after 40 minutes of MW irradiation. Similarly, other imidazolium-supported *N*-acyl benzotriazoles (**97b-g)** upon reaction with 3-methoxyphenol (**102A**) in water under microwave irradiation using *t*-BuOK as base yielded their corresponding esters **103aA-gA** (Scheme 5.3.5). In this case, extraction of the concentrated reaction mixture with ethyl acetate followed by washing of organic filtrate with 2N NaOH yielded pure esters (**103aA-gA)** in 70-84% isolated yields.

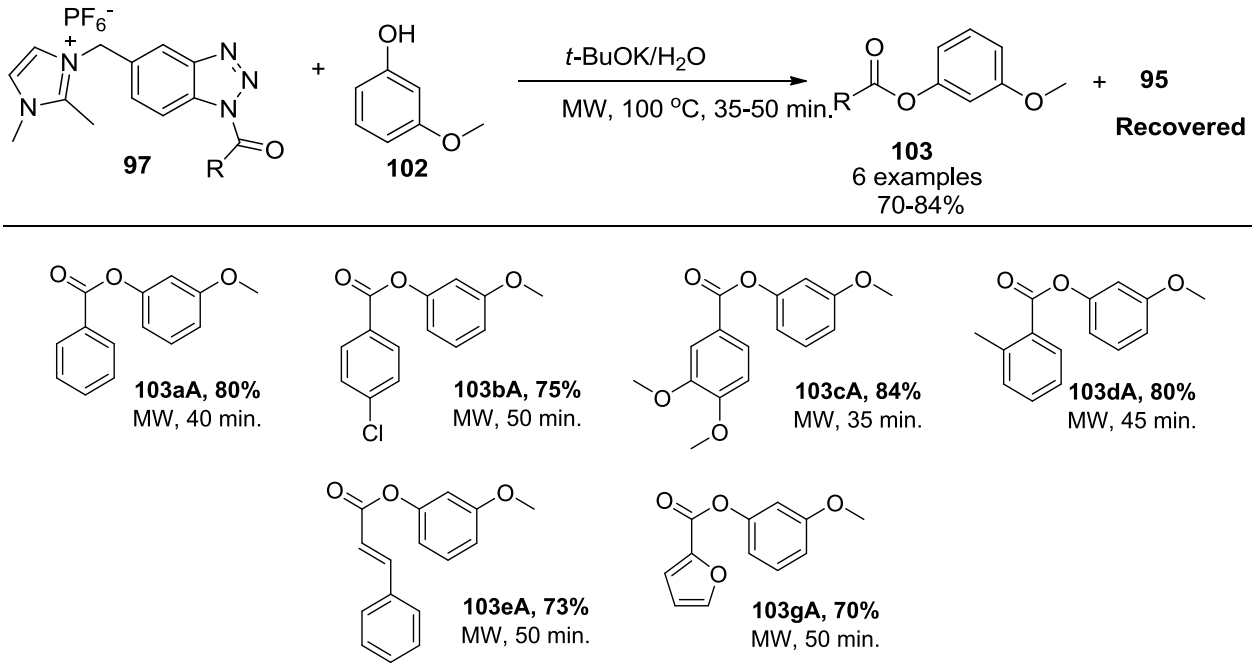

Scheme 5.3.5: Imidazolium-supported *N*-acyl benzotriazoles (**97a-g**)-mediated synthesis of esters (**103**) in aqueous media under MW irradiation

Recovery and reusability of imidazolium-supported benzotriazole reagent

Recoverability of Im-CH_2-BtH was attempted in all the three cases of reactions. The insolubility of Im-CH_2-BtH (**95**) in ethyl acetate provided a simple procedure for separating it from crude reaction mixture. In case of amide and thioester synthesis, pure Im-CH_2-BtH (**95**) was obtained after washing of concentrated reaction mass with ethyl acetate followed by high vacuum drying. In case of ester synthesis, an additional washing with water was required to remove *t*-BuOK to yield pure **95**. Comparison of the ^{1}H NMR of the recovered Im-CH_2-BtH (**95**) reagent with that

of initially synthesized reagent (**95**) is shown in Figure 5.3.6. From the ^{1}H NMR it is evident that the recovered Im-CH_2-BtH was obtained in pure form.

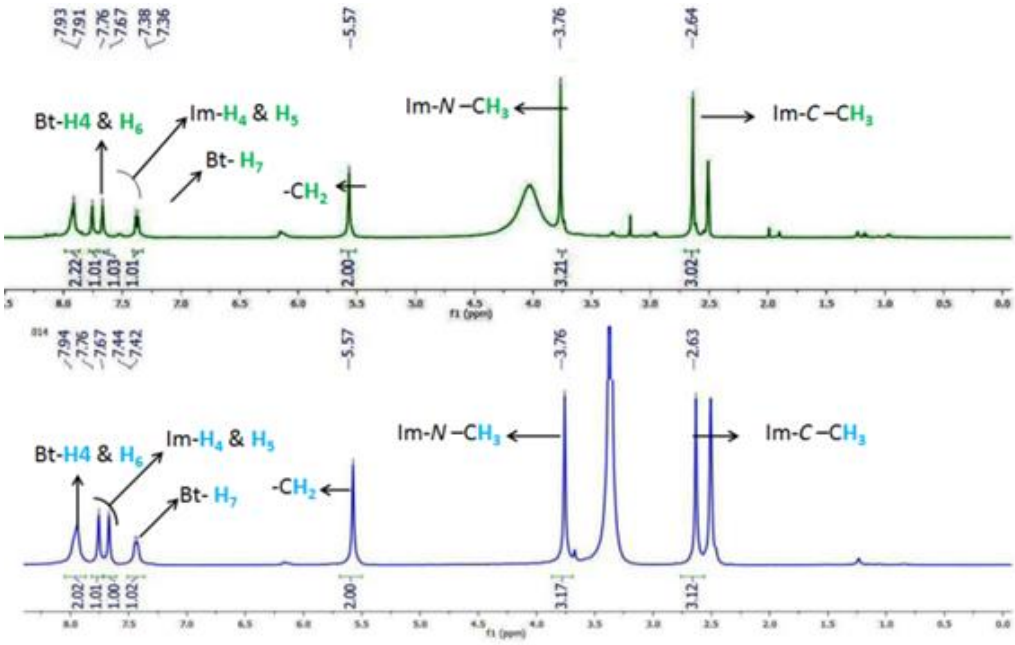

Figure 5.3.6: Comparison of ^{1}H NMR of Im-CH_2-BtH (**95**) and recovered **95**

The reusability of the recovered reagent (**95**) was further evaluated towards the synthesis of **97a**. Delightfully the recovered reagent (**95**) did not show any significant change in the chemical reactivity, and for five cycles 75%, 75%, 73%, 72% and 70% isolated yield of **97a** were obtained based on the amount of recovered Im-CH_2-BtH (**95**) **(**Figure 5.3.7). It is worth mentioning that the recovery process is very simple and less arduous. However, due to inevitable loss of Im-CH_2-BtH (**95**) during the activation step, the amount of amide (**99aA**) formed in each subsequent cycle's decreases (percentage yield remain same) due to use of lesser amount of nucleophile in the subsequent cycles.

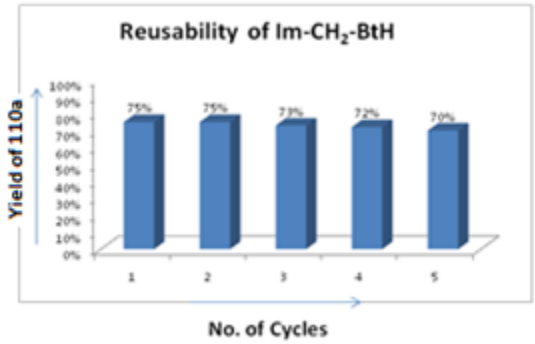

Figure 5.3.7: Recyclability and reusability of Im-CH_2-BtH (**95**)

One-pot and sequential synthesis of amide without isolating Im-CH_2-BtCOR

To overcome the loss in yield during the purification of imidazolium-supported *N*-acyl benzotriazole reagents (Im-CH_2-Bt-COR) (**97**) and to make the process more efficient and economical, we planned to perform the synthesis of amide (**99aA**) in one-pot fashion. Since the activation step does not proceed in water, therefore benzoic acid (**96a**) and Im-CH_2-BtH (**95**) were allowed to react in acetonitrile at room temperature for 20 h using DCC (1.2 eq.)/DMAP (5 mol %). After this *p*-toluidine (1.0 equiv.), additional DMAP (1.2 eq.) were added to the same pot, and the reaction mixture was subjected to microwave irradiation for 20 minutes. After the two sequential reactions in one-pot, the reagent Im-CH_2-BtH (**95**) was almost completely recovered (97% of its starting amount) by washing the concentrated and dried reaction mixture with ethyl acetate and decanting the organic filtrate to separate the amide product along with by-products such as DCU, DMAP and un-reacted acid from **95**. However, the isolation of the amide product **99aA** in 82% yield from this organic filtrate (ethyl acetate) required tedious separation procedure including acid-base workup followed by column chromatography.

In order to explore the synthetic utility of Im-CH_2-BtCOR towards acylation in water, we also attempted the sequential synthesis of amide (**99aA**) by (i) carrying the activation step in acetonitrile in the usual manner at room temperature, (ii) removing the side products (DCU) by washing the concentrated and dried residue with ethyl acetate, and (iii) using this concentrated residue for the benzoylation of *p*-toluidine in water using DMAP (1.2 equiv.) under microwave irradiation. In this case, amide (**99aA**) was isolated in 92% yield by usual work up procedure without employing column chromatography, along with almost recovery of Im-CH_2-BtH (**95**) (98% of its starting material). Thus, the step-wise synthetic strategy leads to the synthesis of **a**mide (**99aA**) in comparable yields, with or without the isolation of Im-CH_2-BtCOPh (Scheme 5.3.6).

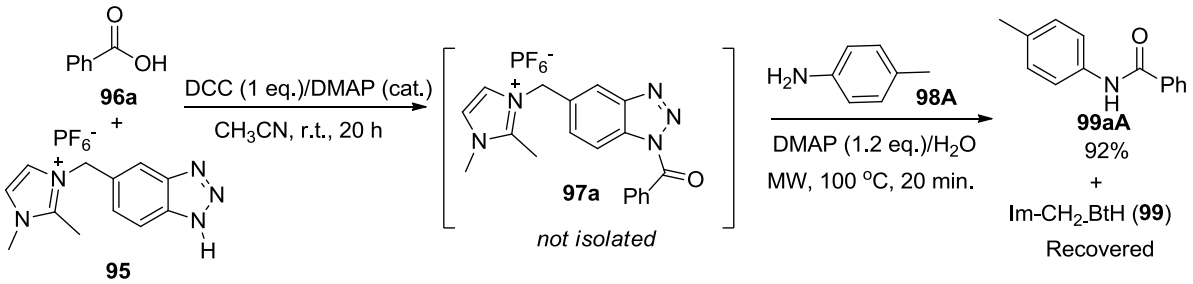

Scheme 5.3.6: Sequential synthesis of amide (**99aA**) without isolating *N*-acyl imidazolium-supported acyl benzotriazole (**97a**)

Application of imidazolium-supported *N*-acetyl benzotriazole (97h) for the synthesis of paracetamol

Finally, we applied the chemical utility of imidazolium-supported benzotriazole reagent towards the synthesis of paracetamol. Paracetamol (*N*-(4-hydroxyphenyl)acetamide) is a mild painkiller and reduces the temperature of patients with fever, and thus widely used OTC drug in many countries either in different pharmaceutical formulations, alone or in combination with other active pharmaceutical ingredients. Many synthetic routes have been explored for the paracetamol production, however majority of them involve acetylation of *p*-aminophenol using acetic anhydride at the final stage. We attempted to substitute corrosive acetic anhydride by imidazolium-supported *N*-acetyl benzotriazole **97h** for preparing paracetamol in a cleaner and safer way. Pleasingly, **97h** effectively and selectively acetylated amino group of *p*-aminophenol (**98F**) using DMAP in water under microwave irradiation in 15 minutes, yielding paracetamol (**99hF**) in 93% yield, along with the easy recovery of Im-CH_2-BtH (**95**). In order to evaluate the potential of this process on a larger scale, a one gram batch production of paracetamol from 3.95 g of **97h** and 1.0 g of *p*-aminophenol was successfully achieved under optimized conditions (Scheme 5.3.7).

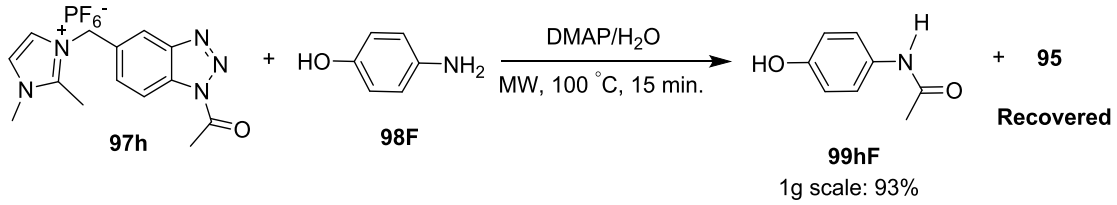

Scheme 5.3.7: Gram scale synthesis of paracetamol (**99hF**) from Im-CH_2-$BtCOCH_3$ (**97h**)

In summary, we have developed an efficient imidazolium-supported benzotriazole reagent as a novel synthetic auxiliary, and exemplified its applicability in the formation of amides, esters, thioesters under microwave irradiation bonds in water. Pleasingly, the methodology was also employed for the synthesis of paracetamol at gram level.

5.4 Experimental Section

5.4.1 General Materials and Methods

Commercially available reagents were used without purification. Commercially available solvents were dried by standard procedures prior to use. Reactions were monitored by using thin layer chromatography (TLC) on 0.2 mm silica gel F254 plates. Nuclear magnetic resonance spectra were recorded on 400 MHz spectrometer and the chemical shifts are reported in δ units,

parts per million (ppm), relative to residual chloroform (7.26 ppm) or DMSO (2.5 ppm) in the deuterated solvent. The following abbreviations were used to describe peak splitting patterns when appropriate: s = singlet, d = doublet, t = triplet, dd = doublet of doublet and m = multiplet. Coupling constants *J* were reported in Hz. The ^{13}C NMR spectra were reported in ppm relative to deuterochloroform (77.0 ppm) or [d_6] DMSO (39.5 ppm). Melting points were determined on a capillary point apparatus equipped with a digital thermometer and are uncorrected. High resolution mass spectra were recorded with a TOF analyzer spectrometer by using electrospray mode.

Synthesis of ethyl 1*H*-benzo[*d*][1,2,3]triazole-5-carboxylate (91)

To a solution of benzotriazole-5-carboxylic acid (0.1 mol) (**79**) in ethanol (80 mL), thionyl chloride (0.3 mol) was added drop-wise, at 0 ^{o}C. The reaction mixture was refluxed for about 6 h until the consumption of the starting material. The reaction mixture was concentrated under reduced pressure and extracted with ethyl acetate and water (100 mL × 3). The combined organic layer was dried over Na_2SO_4 and concentrated to yield **91** in 97% yield. m.p: 106-108 ^{o}C (Lit[88] m.p: 108-109 ^{o}C).

Synthesis of 1*H*-benzo[*d*][1,2,3]triazol-5-yl)methanol (92)

To a suspension of lithium aluminium hydride (0.09 mol) in dry THF (100 mL) in a round-bottom flask, ethyl 1*H*-benzo[*d*][1,2,3]triazole-5-carboxylate (**91**) (0.03 mol) was slowly added from a dropping funnel at 0 °C under an atmosphere of nitrogen. The reaction mixture was refluxed for 12 h. The reaction mixture was then quenched in ice-cold water, acidified with 1N HCl, filtered through celite and extracted with ethyl acetate (100 mL × 4). Drying and concentrating the organic layer under reduced pressure afforded **92** in 95% yield. m.p: 147-149 °C (Lit.[88] m.p: 149-150 ^{o}C).

Synthesis of 5-(chloromethyl)-1*H*-benzo[*d*][1,2,3]triazole (93)

Thionyl chloride (0.36 mol) was slowly added to a solution of (1*H*-benzo[*d*][1,2,3]triazol-5-yl)methanol (**92**) (0.026 mol) in toluene (100 mL), and the mixture was stirred vigorously for 5 h. The resulting solid was filtered and washed with hexanes to give pure **93**.

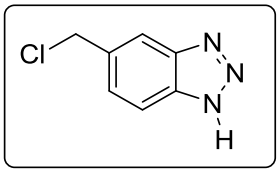

White solid; yield: 3 g (70%); mp 162-163 ^{o}C; ^{1}H NMR (400 MHz, $CDCl_3$ + DMSO-d_6) δ 7.86 (s, 1H), 7.80 (d, J = 8.5 Hz, 1H), 7.41 (dd, J = 8.6, 1.3 Hz, 1H), 4.79 (s, 2H); ^{13}C NMR (100 MHz, $CDCl_3$ + DMSO-d_6) δ 143.3, 143.0, 140.3, 131.7, 120.1, 119.5, 51.0.

Synthesis of 3-((1*H*-benzo[*d*][1,2,3]triazol-5-yl)methyl)-1,2-dimethyl-1*H*-imidazol-3-ium chloride (94)

A mixture of 1,2–dimethylimidazole (**29**) (0.019 mol) and 5-(chloromethyl)-1*H*-benzo[*d*][1,2,3]triazole (**93**) (0.017 mol) were heated at 80 °C for 3 h. Upon completion of reaction, the reaction mixture was washed with ethyl acetate (25 mL × 3) yielding **94**.

Brown gummy semi-solid (N^1 + N^3 isomers); yield: 4.4 g (98%); ^{1}H NMR (400 MHz, $CDCl_3$ + DMSO-d_6) δ 16.08 (s, 1H), 7.95 (s, 1H), 7.91 (d, J = 8.5 Hz, 1H), 7.81 (d, J = 2.0 Hz, 1H), 7.71 (d, J = 1.9 Hz, 1H), 7.43 (d, J = 8.3 Hz, 1H), 5.62 (s, 2H), 3.79 (s, 3H), 2.66 (s, 3H); ^{13}C NMR (100 MHz, $CDCl_3$ + DMSO-d_6) δ 144.5, 144.1, 132.7, 131.2, 125.2, 122.6, 121.2, 117.7, 50.8, 33.7, 9.4.

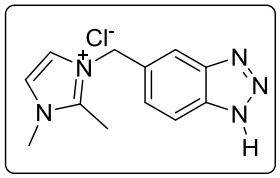

Synthesis of 3-((1*H*-benzo[*d*][1,2,3]triazol-5-yl)methyl)-1,2-dimethyl-1*H*-imidazol-3-ium hexafluorophosphate (95)

In a round-bottom flask, 3-((1*H*-benzo[*d*][1,2,3]triazol-5-yl)methyl)-1,2-dimethyl-1*H*-imidazol-3-ium chloride (**94**) (0.017 mol) was refluxed with potassium hexafluorophosphate (0.018 mol) in dry acetone (40 mL) for 24 h under an inert atmosphere of nitrogen gas. Upon completion of reaction, the excess potassium hexafluorophosphate was filtered-off. The mother liquor was concentrated under reduced pressure, dried under high vacuum and precipitated with methanol to yield compound **95**.

Brown solid (N^1 + N^2 isomers); yield: 6.1 g (96%); ^{1}H NMR (400 MHz, DMSO-d_6) δ 8.07 (s, 1H), 7.96 (d, J = 10.6 Hz, 2H), 7.90 (s, 0.5H), 7.75 (s, 1H), 7.67 (s, 1H), 7.44 (d, J = 7.6 Hz, 1H), 7.37 (s, 1H), 6.17 (s, 1H, CH_2-N^2-isomer), 5.58 (s, 2H, CH_2-N^2-isomer), 3.76 (s, 3H, *N*-CH_3-N^1-isomer), 3.66 (s, 1.5H, *N*-CH_3-N^2-isomer), 2.64 (s, 3H, *C*-CH_3-N^1-isomer), 2.44 (s, 1.5H, *C*-CH_3-N^2-isomer); ^{13}C NMR (100 MHz, DMSO-d_6) δ 145.3, 139.7, 138.7, 132.4, 126.0, 123.2, 121.6, 116.0, 115.6, 51.5 (**C**H_2-N^3-isomer), 51.0 (**C**H_2-N^1-isomer), 35.2 (*N*-**C**H_3-N^1-isomer), 33.7 (*N*-**C**H_3-N^2-isomer), 11.3 (*C*-**C**H_3-N^2-isomer), 9.9 (*C*-**C**H_3-N^1-isomer).

Recrystallization in methanol yielded pure N^1-isomer of **95**. White solid (N^1-isomer); mp 172-173 °C; ^{1}H NMR (400 MHz, DMSO-d_6) δ 15.86 (s, 1H), 7.94 (s, 2H), 7.71 (d, J = 34.9 Hz, 2H), 7.43 (d, J = 7.0 Hz, 1H), 5.57 (s, 2H), 3.76 (s, 3H), 2.63 (s, 3H); ^{13}C NMR (100 MHz, DMSO-d_6) δ 145.2, 140.4, 139.4, 131.6, 125.3, 123.1, 121.7, 116.0, 115.4, 51.1, 35.3, 9.9; HRMS (ESI-

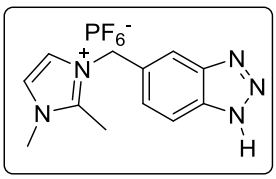

TOF) (*m/z*) calculated for $C_{12}H_{15}N_5^+$: 229.1327; found 229.1326 $[M+1-PF_6]^+$.

General procedure for synthesis of imidazolium-supported *N*-acyl benzotriazoles

A 50 mL round-bottom flask containing a mixture of DCC (1.2 mmol), carboxylic acid (**96a-h**) (1.2 mmol), **95** (1 mmol) and dimethylaminopyridine (5 mol %) in dry acetonitrile (20 mL) was stirred for 20-40 h under ambient conditions. After the completion of reaction, the solvent was concentrated under reduced pressure, and the crude reaction mixture was washed with ethyl acetate (50 mL). The residue was dried under high vacuum, and the washing of the residual solid with minimum amount of methanol yielded pure product (**97a-h**). The compounds **97a-h** were obtained either in pure N^1-isomeric form or as enriched N^1-isomer with trace amount of N^3-isomer.

3-(1-Benzoyl-1*H*-benzo[*d*][1,2,3]triazol-5-yl)methyl)-1,2-dimethyl-1*H*-imidazol-3-ium hexaflurophosphate (97a): White solid (N^1-isomer); yield: 358 mg (75%); mp 164-166 °C; ^{1}H NMR (400 MHz, DMSO-d_6 + $CDCl_3$) δ 8.37 (d, J = 8.6 Hz, 1H), 8.25 (s, 1H), 8.16 – 8.12 (m, 2H), 7.84 – 7.79 (m, 1H), 7.77 (dd, J = 4.8, 2.6 Hz, 2H), 7.68 (d, J = 2.1 Hz, 1H), 7.65 (t, J = 7.8 Hz, 2H), 5.68 (s, 2H), 3.82 (s, 3H), 2.68 (s, 3H); ^{13}C NMR (100 MHz, DMSO-d_6 + $CDCl_3$) δ 166.5, 145.4, 133.6, 133.0, 131.3, 130.9, 130.3, 128.3, 122.8, 121.2, 119.2, 114.9, 50.3, 34.8, 9.5; HRMS (ESI-TOF) (*m/z*) calculated for $C_{19}H_{19}N_5O^+$: 333.1589; found 333.1614 $[M+1-PF_6]^+$.

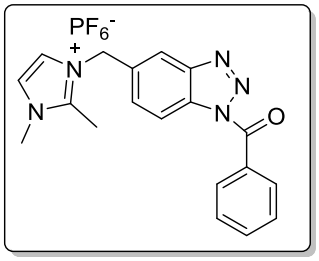

3-((1-(4-Chlorobenzoyl)-1*H*-benzo[*d*][1,2,3]triazol-5-yl)methyl)-1,2-dimethyl-1*H*-imidazol-3-ium hexaflurophosphate (97b): Brown solid (N^1 + N^3-isomers); yield: 358 mg (70%); mp 142-146 °C ; ^{1}H NMR (400 MHz, DMSO-d_6) δ 8.37 (dd, J = 9.8, 6.5 Hz, 1H), 8.27 (s, 1H), 8.15 (d, J = 8.3 Hz, 2H), 7.86 – 7.80 (m, 1H), 7.76 (d, J = 8.4 Hz, 2H), 7.70 (s, 1H), 7.60 (d, J = 8.3 Hz, 1H), 5.75 – 5.65 (m, 2H), 3.78 (s, 3H), 2.65 (s, 3H); ^{13}C NMR (100 MHz, DMSO-d_6) δ 166.0, 145.4, 139.2, 133.8, 131.6, 131.1, 130.6, 129.1, 123.3, 121.7, 121.2, 119.6, 115.5, 114.6, 50.9, 50.6, 35.3, 10.2; HRMS (ESI-TOF) (*m/z*) calculated for $C_{19}H_{18}ClN_5O^+$: 367.1199; found 367.1219 $[M+1-PF_6]^+$.

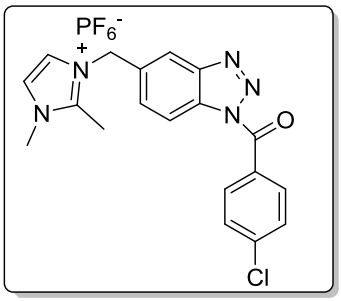

3-((1-(3,4-Dimethoxybenzoyl)-1*H*-benzo[*d*][1,2,3]triazol-5-yl)methyl)-1,2-dimethyl-1*H*-imidazol-3-ium (97c): White Solid (N^1 + N^3-isomers); yield: 429 mg (80%); mp 223-227 °C;

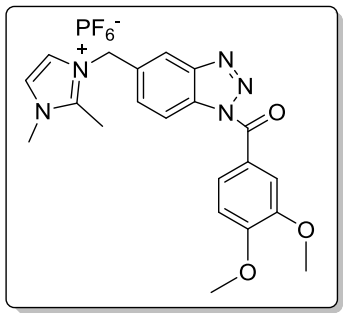

^{1}H NMR (400 MHz, DMSO-d_6) δ 8.33 (dd, J = 15.0, 6.3 Hz, 1H), 8.28 (d, J = 11.0 Hz, 1H), 7.86 (dd, J = 8.5, 1.8 Hz, 1H), 7.83 – 7.73 (m, 2H), 7.71 (s, 2H), 7.23 (d, J = 8.7 Hz, 1H), 5.73 – 5.65 (m, 2H), 3.92 (s, 3H), 3.85 (s, 3H), 3.78 (s, 3H), 2.64 (d, J = 7.3 Hz, 3H); ^{13}C NMR (100 MHz, DMSO-d_6) δ 165.7, 154.3, 148.8, 145.7, 145.4, 137.7, 133.7, 132.8, 132.4, 130.8, 127.4, 126.8, 123.4, 123.2, 121.7, 121.1, 119.6, 115.5, 114.5, 111.5, 56.4, 56.2, 50.9, 50.6, 35.3, 9.9; HRMS (ESI-TOF) (*m/z*) calculated for $C_{21}H_{23}N_5O_3^+$: 393.1800; found 393.1827 $[M+1-PF_6]^+$.

1,2-Dimethyl-3-((1-(2-methylbenzoyl)-1*H*-benzo[*d*][1,2,3]triazol-5-yl)methyl)-1*H*-imidazol-3-ium hexafluorophosphate (97d): White solid (N^1 + N^3-isomers); yield: 354 mg (72%); mp

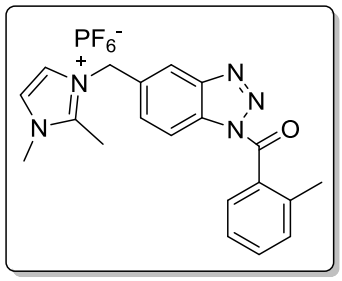

122-124 °C; ^{1}H NMR (400 MHz, DMSO-d_6) δ 8.43 – 8.23 (m, 2H), 7.83 (dd, J = 17.4, 5.1 Hz, 1H), 7.78 – 7.64 (m, 3H), 7.59 (t, J = 8.4 Hz, 1H), 7.49 – 7.38 (m, 2H), 5.74 – 5.66 (m, 2H), 3.79 (s, 3H), 2.66 (s, 3H), 2.37 (2s, 3H total, for N^1+N^3-isomers); ^{13}C NMR (100 MHz, DMSO-d_6) δ 168.1, 146.2, 145.8, 145.5, 138.0, 137.7, 134.0, 132.4, 131.6, 131.2, 130.6, 127.1, 125.9, 121.7, 121.2, 119.7, 115.4, 114.5, 51.1, 50.7, 35.3, 19.8, 10.0, 9.9; HRMS (ESI-TOF) (*m/z*) calculated for $C_{20}H_{21}N_5O^+$: 347.1746; found 347.1764 $[M+1-PF_6]^+$.

(*E*)-3-((1-Cinnamoyl-1*H*-benzo[*d*][1,2,3]triazol-5-yl)methyl)-1,2-dimethyl-1*H*-imidazol-3-ium hexaflurophosphate (97e): Brown solid (N^1-isomer); yield: 362 mg (72%); mp 214-216 °C;

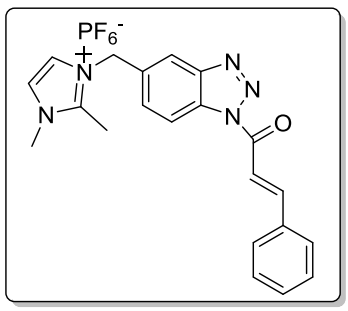

^{1}H NMR (400 MHz, DMSO-d_6) δ 8.36 (d, J = 8.5 Hz, 1H), 8.13 (brs, 1H), 8.09 (s, 1H), 8.01 (dd, J = 16.3, 2.9 Hz, 1H), 7.82 (d, J = 3.7 Hz, 1H), 7.75 – 7.60 (m, 4H), 7.56 (brs, 1H), 7.46 (brs, 2H), 5.62 (s, 2H), 3.81 (s, 3H), 2.65 (s, 3H); ^{13}C NMR (100 MHz, DMSO-d_6) δ 163.8, 158.9, 149.0, 146.4, 145.5, 134.2, 133.9, 132.2, 131.2, 129.7, 123.3, 121.7, 119.7, 116.3, 115.4, 50.6, 35.3, 34.6, 10.0; HRMS (ESI-TOF) (*m/z*) calculated for $C_{21}H_{21}N_5O^+$: 359.1746; found 359.1767 $[M+1-PF_6]^+$.

3-((1-Isonicotinoyl-1*H*-benzo[*d*][1,2,3]triazol-5-yl)methyl)-1,2-dimethyl-1*H*-imidazol-3-ium hexafluorophosphate (97f): White solid (N^1 + N^3-isomers); yield: 325 mg (66%); mp 181-184 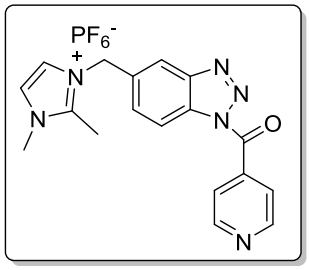

°C; ^{1}H NMR (400 MHz, DMSO-d_6) δ 9.23 (s, 1H), 8.92 (d, J = 2.7 Hz, 1H), 8.49 (d, J = 7.5 Hz, 1H), 8.44 – 8.24 (m, 2H), 7.89 – 7.58 (m, 4H), 5.75 – 5.67 (m, 2H), 3.79 (s, 3H), 2.65 (s, 3H); ^{13}C NMR (100 MHz, DMSO-d_6) δ 165.7, 154.0, 151.9, 146.2, 145.3, 139.5, 138.1, 134.2, 131.9, 131.2, 128.3, 127.2, 123.9, 123.4, 121.7, 121.3, 119.7, 115.5, 114.5, 50.9, 50.6, 35.3, 9.9; HRMS (ESI-TOF) (*m/z*) calculated for $C_{18}H_{18}N_6O^+$: 334.1542; found 334.1561 $[M+1-PF_6]^+$.

3-((1-(Furan-2-carbonyl)-1*H*-benzo[*d*][1,2,3]triazol-5-yl)methyl)-1,2-dimethyl-1*H*-imidazol-3-ium hexafluorophosphate (97g): White solid (N^1 + N^3-isomers); yield: 318 mg (68%); mp 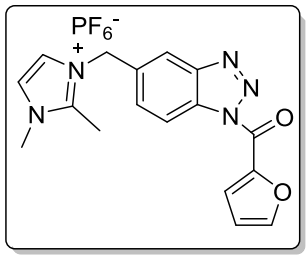

220-224 °C; ^{1}H NMR (400 MHz, DMSO-d_6) δ 8.34 (dd, J = 13.0, 8.6 Hz, 2H), 8.27 (brs, 1H), 8.07 (d, J = 3.5 Hz, 1H), 7.86 – 7.74 (m, 2H), 7.69 (s, 1H), 6.94 (dd, J = 3.6, 1.6 Hz, 1H), 5.73 – 5.64 (m, 2H), 3.79 (s, 3H), 2.65 (s, 3H); ^{13}C NMR (100 MHz, DMSO-d_6) δ 154.8, 151.0, 145.6, 145.4, 144.2, 137.9, 133.9, 132.4, 132.0, 131.1, 126.9, 125.6, 123.3, 121.7, 121.3, 119.7, 115.3, 114.4, 113.9, 50.9, 50.6, 35.3, 9.9; HRMS (ESI-TOF) (*m/z*) calculated for $C_{17}H_{17}N_5O_2^+$: 323.1382; found 323.1410 $[M+1-PF_6]^+$.

3-((1-acetyl-1H-benzo[*d*][1,2,3]triazol-5-yl)methyl)-1,2-dimethyl-1*H*-imidazol-3-ium hexafluorophosphate (97h): White solid (N^1-isomer); yield: 353 mg (85%); mp 198-200 °C; ^{1}H 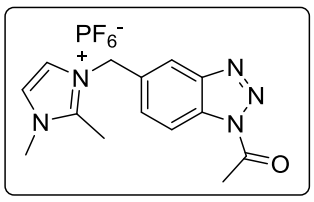

NMR (400 MHz, DMSO-d_6) δ 8.26 (d, J = 7.5 Hz, 1H), 8.21 (s, 1H), 7.75 (brs, 2H), 7.69 (brs, 1H), 5.66 (s, 2H), 3.77 (s, 3H), 2.94 (s, 3H), 2.63 (s, 3H); ^{13}C NMR (100 MHz, DMSO-d_6) δ 170.3, 146.2, 145.8, 145.5, 137.8, 133.6, 130.9, 126.7, 123.3, 121.6, 121.1, 119.6, 115.1, 114.2, 50.7, 35.3, 23.6, 9.9.

General procedure for the synthesis of amides, thioesters, esters and recovery of reagent (95)

In a microwave capped tube, *N*, *S*- or *O*-nucleophilic aromatic/heteroaromatic substrate (1.2 mmol), imidazolium-supported *N*-acyl benzotriazole reagent (**97a-g**) (1 mmol) and DMAP (1.5 mmol) (*t*-BuOK for *O*-nucleophilic substrate) were mixed in water (2 mL). The tube was irradiated in a CEM microwave synthesizer for 10-50 minutes at 100 °C, 50 W, and the progress of the reaction was monitored *via* TLC. After completion of the

reaction, the mixture was concentrated to yield a gummy reaction mass. Subsequently, ethyl acetate (20 mL × 2) was added and the mixture was stirred for 15 minutes and decanted. The product (amide, thioester and ester) got dissolved in organic filtrate leaving behind the regenerated reagent **95** as semi-solid (in case of *N*- & *S*-nucleophilc substrates. While in case of *O*-nucleophlic substrates, washing with water (5 mL) was additionally required to remove *t*-BuOK to regenerate pure **95.**

For *N*-nucleophilic substrates, the organic filtrate was washed with 1N HCl, dried with Na_2SO_4 and concentrated to yield pure amides **99.**

For *S*-nucleophilic substrates, the organic filtrate was washed with water, concentrated and recrystallized with hexanes to yield pure thioesters **101.**

For *O*-nucleophilic substrates, the organic filtrate was washed with 2N NaOH, dried with Na_2SO_4 and concentrated to yield pure esters **103.**

***N*-*p*-Tolylbenzamide (99aA):** White solid; yield: 190 mg (90%); mp 154-157 °C (Lit.[89,90] mp 158 °C); ^{1}H NMR (400 MHz, DMSO-d_6 + $CDCl_3$) δ 10.08 (s, 1H), 7.98 – 7.92 (m, 2H), 7.66 (d, J = 8.4 Hz, 2H), 7.56 – 7.52 (m, 1H), 7.48 (dd, J = 10.0, 4.5 Hz, 2H), 7.12 (d, J = 8.3 Hz, 2H), 2.30 (s, 3H); ^{13}C NMR (100 MHz, DMSO-d_6 + $CDCl_3$) δ 165.3, 136.5, 135.1, 132.4, 131.1, 128.7, 128.0, 127.5, 120.3, 39.6, 20.5.

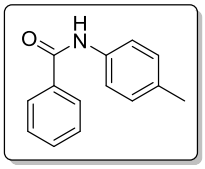

***N*-(Thiazol-2-yl)benzamide (99aB):** Brown solid; yield: 185 mg (91%); mp 143-145 °C (Lit.[91] mp 144 °C); ^{1}H NMR (400 MHz, $CDCl_3$) δ 12.61 (s, 1H), 8.05 (dt, J = 8.5, 1.6 Hz, 2H), 7.68 – 7.63 (m, 1H), 7.58 – 7.52 (m, 2H), 7.03 (d, J = 3.6 Hz, 1H), 6.96 (d, J = 3.6 Hz, 1H); ^{13}C NMR (100 MHz, $CDCl_3$) δ 166.1, 160.5, 137.1, 132.8, 128.8, 128.2, 113.4.

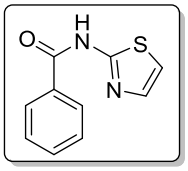

***N*-(Benzo[*d*]thiazol-2-yl)benzamide (99aC):** White solid; yield: 223 mg (88%); mp 185-187 °C (Lit.[92] mp 186- 187 °C); ^{1}H NMR (400 MHz, $CDCl_3$) δ 12.26 (s, 1H), 8.04 (d, J = 7.2 Hz, 2H), 7.80 (dd, J = 6.3, 2.2 Hz, 1H), 7.51 (t, J = 7.3 Hz, 1H), 7.40 (d, J = 7.8 Hz, 2H), 7.37 – 7.33 (m, 1H), 7.29 – 7.22 (m, 2H); ^{13}C NMR (100 MHz, $CDCl_3$ + DMSO-d_6) δ 166.3, 159.7, 148.1, 132.9, 132.0, 128.8, 128.2, 125.9, 123.8, 121.3, 120.6.

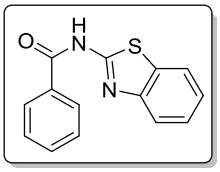

***N*-Propylbenzamide (99aD):** Yellow solid; yield: 144 mg (88%); mp 82-84 ^{o}C; ^{1}H NMR (400

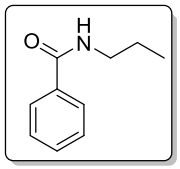

MHz, $CDCl_3$) δ 7.78 (dd, J = 5.2, 3.3 Hz, 2H), 7.55 – 7.47 (m, 1H), 7.47 – 7.39 (m, 2H), 6.24 (s, 1H), 3.44 (dt, J = 7.2, 6.1 Hz, 2H), 1.71 – 1.60 (m, 2H), 1.01 (t, J = 7.4 Hz, 3H); ^{13}C NMR (100 MHz, $CDCl_3$) δ 167.6, 134.9, 131.3, 128.5, 126.8, 41.8, 22.9, 11.4.

4-Chloro-*N*-(thiazol-2-yl)benzamide (99bB): Off-white solid; yield: 205 mg (86%); mp 208-

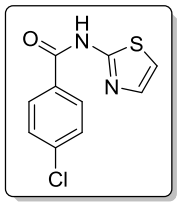

210 °C (Lit.[93] mp 211- 212 °C); ^{1}H NMR (400 MHz, $CDCl_3$) δ 8.22 (d, J = 8.7, Hz, 2H), 7.84 (d, J = 4.3 Hz, 1H), 7.65 (d, J = 8.7 Hz, 2H), 7.31 (d, J = 4.3 Hz, 1H). ^{13}C NMR (100 MHz, $CDCl_3$) δ 164.8, 162.8, 161.2, 141.1, 130.1, 129.5, 127.9, 114.3.

***N*-(Benzo[*d*]thiazol-2-yl)-4-chlorobenzamide (99bC):** White solid; yield: 234 mg (81%); mp

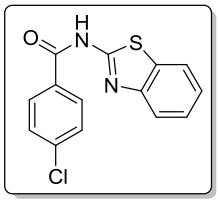

>280 °C (Lit.[92,94] mp 304 °C); ^{1}H NMR (400 MHz, $CDCl_3$) δ 11.82 – 11.09 (m, 1H), 7.95 (d, J = 8.5 Hz, 2H), 7.89 (dd, J = 6.0, 2.9 Hz, 1H), 7.42 (d, J = 8.6 Hz, 2H), 7.39 (t, J = 4.7 Hz, 1H), 7.38 – 7.32 (m, 2H); ^{13}C NMR (100 MHz, $CDCl_3$ + DMSO-d_6) δ 165.4, 159.4, 148.4, 138.9, 132.1, 131.3, 129.8, 128.8, 125.9, 123.6, 121.3, 120.4.

3,4-Dimethoxy-*N*-(*p*-tolyl)benzamide (99cA): White solid; yield: 258 mg (95%); mp 160-161

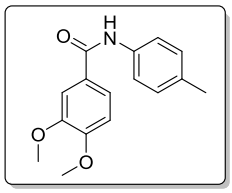

°C (Lit.[95] mp 157-158 °C); ^{1}H NMR (400 MHz, $CDCl_3$) δ 7.90 (s, 1H), 7.53 (d, J = 8.4 Hz, 2H), 7.50 (d, J = 2.0 Hz, 1H), 7.41 (dd, J = 8.3, 2.0 Hz, 1H), 7.18 (d, J = 8.2 Hz, 2H), 6.89 (d, J = 8.4 Hz, 1H), 3.95 (s, 3H), 3.94 (s, 3H), 2.35 (s, 3H); ^{13}C NMR (100 MHz, $CDCl_3$ + DMSO-d_6) δ 165.5, 151.4, 136.2, 133.1, 129.0, 127.5, 120.7, 110.8, 110.1, 55.8, 20.7.

***N*-(Benzo[*d*]thiazol-2-yl)-3,4-dimethoxybenzamide (99cC):** White Solid; yield: 283 mg (90%);

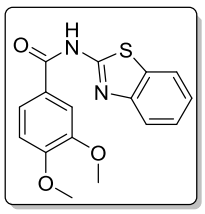

mp 98-100 °C; ^{1}H NMR (400 MHz, $CDCl_3$) δ 11.52 (s, 1H), 7.92 – 7.85 (m, 1H), 7.60 (dd, J = 5.3, 1.9 Hz, 2H), 7.45 – 7.40 (m, 1H), 7.37 – 7.29 (m, 2H), 6.82 (d, J = 8.9 Hz, 1H), 3.92 (s, 3H), 3.86 (s, 3H) ^{13}C NMR (100 MHz, $CDCl_3$ + DMSO-d_6) δ 165.6, 160.3, 153.1, 149.2, 147.7, 131.8, 126.1, 124.3, 123.9, 121.5 120.6, 110.9, 110.5, 56.1, 55.8.

2-Methyl-*N*-*p*-tolylbenzamide (99dA): White Solid, yield: 196 mg (88%); mp 143-146 °C

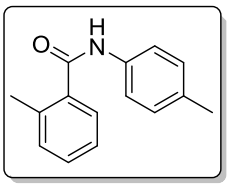

(Lit.[96] mp 147-148 °C); ^{1}H NMR (400 MHz, $CDCl_3$) δ 7.55 – 7.45 (m, 4H), 7.38 (t, *J* = 7.2 Hz, 1H), 7.28 (t, *J* = 4.7 Hz, 2H), 7.18 (s, 1H), 2.52 (s, 3H), 2.37 (s, 3H); ^{13}C NMR (100 MHz, $CDCl_3$) δ 167.9, 136.4, 135.4, 134.2, 131.2, 130.2, 129.6, 126.6, 125.9, 119.9, 20.9, 19.8.

2-Methyl-*N*-(thiazol-2-yl)benzamide (99dB): White solid; yield: 194 mg (89%); mp 177-180

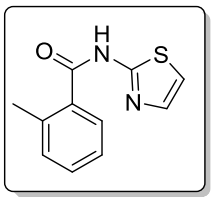

°C (Lit.[97] mp 178 -179 °C); ^{1}H NMR (400 MHz, $CDCl_3$) δ 13.20 (s, 1H), 7.62 – 7.57 (m, 1H), 7.49 (td, *J* = 7.6, 1.2 Hz, 1H), 7.34 (dd, *J* = 16.7, 8.0 Hz, 2H), 6.82 (d, *J* = 3.7 Hz, 1H), 6.30 (d, *J* = 3.7 Hz, 1H), 2.52 (s, 3H); ^{13}C NMR (100 MHz, $CDCl_3$) δ 167.9, 160.2, 137.0, 136.4, 134.5, 130.9, 127.7, 125.9, 112.9, 19.8.

***N*-(Benzo[*d*]thiazol-2-yl)-2-methylbenzamide (99dC):** Off-white solid; yield: 241 mg (90%);

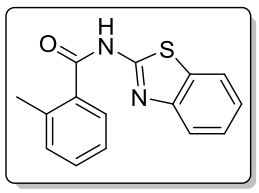

mp 144-147 °C; ^{1}H NMR (400 MHz, $CDCl_3$) δ 12.60 (s, 1H), 7.89 (d, *J* = 7.7 Hz, 1H), 7.67 (d, *J* = 7.3 Hz, 1H), 7.46 – 7.31 (m, 3H), 7.17 (dd, *J* = 18.5, 7.6 Hz, 2H), 6.71 (d, *J* = 7.9 Hz, 1H), 2.70 (s, 3H); ^{13}C NMR (100 MHz, $CDCl_3$) δ 168.2, 159.9, 147.4, 137.6, 133.2, 131.4, 127.9, 126.2, 125.9, 123.7, 121.1, 120.1, 20.2.

***N*-(*p*-Tolyl)cinnamamide (99eA):** Brown solid; yield: 211 mg (89%); mp 155-157 °C (Lit.[89] mp

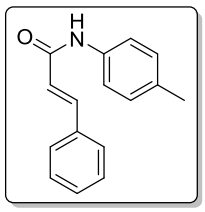

161 °C); ^{1}H NMR (400 MHz, $CDCl_3$) δ 7.77 (d, *J* = 15.5 Hz, 1H), 7.60 – 7.49 (m, 4H), 7.48 (s, 1H), 7.42 – 7.37 (m, 3H), 7.17 (d, *J* = 8.2 Hz, 2H), 6.58 (d, *J* = 15.5 Hz, 1H), 2.35 (s, 3H); ^{13}C NMR (100 MHz, $CDCl_3$) δ 159.3, 137.3, 130.8, 129.9, 129.3, 125.1, 124.8, 124.1, 123.2, 116.3, 115.4, 16.2.

***N*-(Thiazol-2-yl)cinnamamide (99eB):** White solid; yield: 196 mg (85%); mp 235-238 °C; ^{1}H

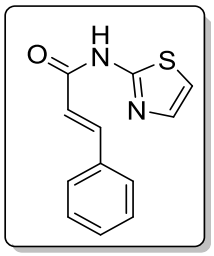

NMR (400 MHz, $CDCl_3$) δ 7.67 (d, *J* = 15.8 Hz, 1H), 7.56 – 7.50 (m, 2H), 7.41 (dd, *J* = 3.5, 1.1 Hz, 1H), 7.37 (brs, 1H), 7.36 (brs, 2H), 7.01 (dd, *J* = 3.5, 1.0 Hz, 1H), 6.87 (d, *J* = 15.8 Hz, 1H); ^{13}C NMR (100 MHz, $CDCl_3$ + DMSO-d_6) δ 168.3, 163.4, 147.3, 142.8, 139.4, 135.1, 133.9, 132.9, 124.7, 118.3.

***N*-(Benzo[*d*]thiazol-2-yl)cinnamamide (99eC):** White solid; yield: 249 mg (89%); mp 150-152 °C (Lit.[98] mp 149-151 °C); ^{1}H NMR (400 MHz, $CDCl_3$) δ 8.14 (d, J = 15.7 Hz, 1H), 7.97 – 7.94 (m, 1H), 7.85 – 7.72 (m, 3H), 7.71 – 7.62 (m, 2H), 7.62 – 7.51 (m, 3H), 6.92 (d, J = 15.7 Hz, 1H); ^{13}C NMR (100 MHz, $CDCl_3$) δ 164.9, 163.6, 160.9, 160.5, 160.1, 149.2, 135.9, 133.3, 131.8, 129.1, 126.7, 122.5, 116.3, 113.4.

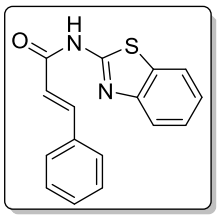

***N*-(*p*-Tolyl)isonicotinamide (99fA):** White solid; yield: 178 mg (84%); mp 157-159 °C; (Lit.[99] mp 160 °C); ^{1}H NMR (400 MHz, $CDCl_3$) δ 8.85 (s, 1H), 8.73 (d, J = 6.0 Hz, 2H), 7.75 (d, J = 5.8 Hz, 2H), 7.59 (d, J = 8.2 Hz, 2H), 7.22 (d, J = 8.2 Hz, 2H), 2.42 (s, 3H); ^{13}C NMR (100 MHz, $CDCl_3$) δ 164.0, 150.3, 142.3, 134.9, 134.7, 129.6, 121.1, 120.8, 20.9.

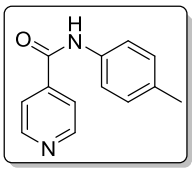

***N*-(Thiazol-2-yl)isonicotinamide (99fB):** Brown solid; yield: 164 mg (80%); mp 186-188 °C; ^{1}H NMR (400 MHz, $CDCl_3$) δ 8.95 (s, 2H), 8.00 (d, J = 2.9 Hz, 2H), 7.17 (d, J = 17.6 Hz, 2H); ^{13}C NMR (100 MHz, $CDCl_3$) δ 164.2, 160.3, 150.6, 139.8, 135.9, 121.8, 114.4.

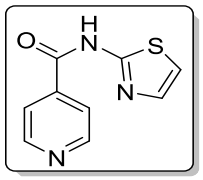

***N*-(Benzo[d]thiazol-yl)isonicotinamide (99fC):** White solid; yield: 204 mg (80%); mp >250 °C; ^{1}H NMR (400 MHz, $CDCl_3$) δ 8.71 (dd, J = 7.9, 4.5 Hz, 2H), 8.02 (dd, J = 7.8, 5.0 Hz, 2H), 7.78 (d, J = 6.2 Hz, 1H), 7.69 (t, J = 8.3 Hz, 1H), 7.36 (dd, J = 15.8, 8.0 Hz, 1H), 7.23 (dd, J = 15.8, 7.8 Hz, 1H); ^{13}C NMR (100 MHz, DMSO-d_6) δ 172.1, 168.9, 155.3, 153.9, 148.1, 137.2, 130.7, 127.6, 127.4, 126.6, 124.6.

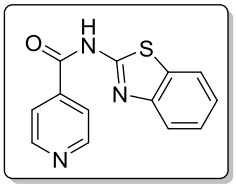

***N*-(*p*-Tolyl)furan-2-carboxamide (99gA):** White solid; yield: 173 mg (86%); mp 108-109 °C (Lit.[100] mp 107-108 °C); ^{1}H NMR (400 MHz, $CDCl_3$) δ 8.20 (s, 1H), 7.67 – 7.62 (m, 2H), 7.59 (dd, J = 1.7, 0.8 Hz, 1H), 7.32 (dd, J = 3.5, 0.8 Hz, 1H), 7.26 (d, J = 8.2 Hz, 2H), 6.64 (dd, J = 3.5, 1.8 Hz, 1H), 2.43 (s, 3H); ^{13}C NMR (100 MHz, $CDCl_3$) δ 156.0, 147.9, 144.1, 134.8, 134.1, 129.6, 119.9, 115.0, 112.6, 20.8.

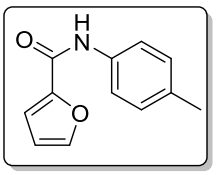

***N*-(Thiazol-2-yl)furan-2-carboxamide (99gB):** White solid; yield: 159 mg (82%); mp 108-110 °C; ^{1}H NMR (400 MHz, $CDCl_3$) δ 12.34 (s, 1H), 7.67 – 7.62 (m, 1H), 7.61 (d, J = 3.6 Hz, 1H), 7.44 (d, J = 3.5 Hz, 1H), 7.13 (d, J = 3.6 Hz, 1H), 6.69 (dd, J = 3.5, 1.7 Hz, 1H); ^{13}C NMR (100 MHz, $CDCl_3$) δ 154.4, 151.1, 141.6, 140.4, 132.7, 112.3, 108.9, 108.1.

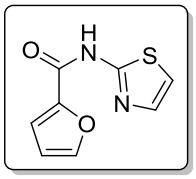

***N*-(Benzo[*d*]thiazol-2-yl)furan-2-carboxamide (99gC):** White solid; yield: 210 mg (86%); mp 165-167 °C (Lit.[100] mp 188-190 °C); ^{1}H NMR (400 MHz, $CDCl_3$) δ 11.33 (s, 1H), 7.96 (d, J = 7.8 Hz, 1H), 7.82 (d, J = 8.0 Hz, 1H), 7.55 – 7.40 (m, 3H), 7.31 (s, 1H), 6.66 – 6.59 (m, 1H); ^{13}C NMR (100 MHz, $CDCl_3$) δ 158.5, 155.9, 148.2, 145.7, 132.1, 126.1, 124.0, 121.2, 117.7, 112.9.

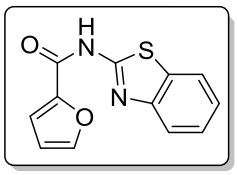

***N*-Benzylfuran-2-carboxamide (99gE):** White solid; yield: 181 mg (90%); mp 111-112 °C; ^{1}H NMR (400 MHz, $CDCl_3$) δ 7.44 (brs, 1H), 7.38 (brs, 1H), 7.37 (brs, 2H), 7.32 (dt, J = 9.0, 4.4 Hz, 1H), 7.17 (d, J = 3.3 Hz, 1H), 6.70 (brs, 1H), 6.52 (dd, J = 3.3, 1.6 Hz, 1H), 4.64 (d, J = 5.9 Hz, 2H); ^{13}C NMR (100 MHz, $CDCl_3$) δ 158.3, 147.9, 143.9, 138.0, 128.8, 127.9, 127.6, 114.2, 112.2, 43.2.

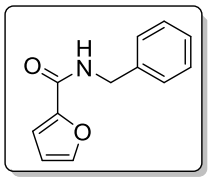

***N*-Benzylacetamide (99hE):** Brown solid; yield: 124 mg (84%); mp 50-52 °C; ^{1}H NMR (400 MHz, $CDCl_3$) δ 7.39 – 7.35 (m, 1H), 7.34 (s, 1H), 7.31 (t, J = 3.0 Hz, 2H), 7.29 (s, 1H), 5.88 (s, 1H), 4.45 (d, J = 5.7 Hz, 2H), 2.04 (s, 3H); ^{13}C NMR (100 MHz, $CDCl_3$) δ 170.1, 138.2, 128.7, 127.8, 127.5, 4.7, 23.2.

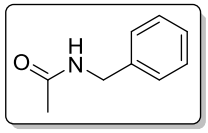

***N*-(4-Hydroxyphenyl)acetamide [Paracetamol] (99hF)** White solid; yield: 140 mg (93%); mp 165-168 °C (Lit.[100] mp 166-168 °C); ^{1}H NMR (400 MHz, DMSO-d_6 + $CDCl_3$); δ 9.06 (s, 1H), 7.25 (dd, J = 6.8, 2.0 Hz, 2H), 6.65 (dd, J = 6.8, 2.0 Hz, 2H), 1.99 (s, 3H); ^{13}C NMR (100 MHz, DMSO-d_6 + $CDCl_3$) δ 166.9, 152.2, 129., 120.2, 113.9, 22.7.

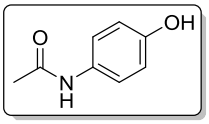

***S*-Phenyl benzothioate (101aA):** White crystalline solid; yield: 204 mg (96%); mp 54-56 °C (Lit.[101] mp 55-56 °C); ^{1}H NMR (400 MHz, $CDCl_3$) δ 8.08 – 8.06 (m, 1H), 8.05 (t, J = 1.7 Hz, 1H), 7.67 – 7.61 (m, 1H), 7.58 – 7.55 (m, 1H), 7.55 – 7.52 (m, 2H), 7.52 (s, 1H), 7.51 – 7.47 (m, 3H); ^{13}C NMR (100 MHz, $CDCl_3$) δ 190.16, 136.7, 135.1, 133.7, 129.5, 129.3, 128.8, 127.4.

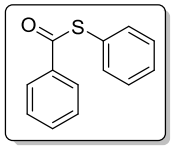

***S*-Naphthalen-2-yl benzothioate (101aB):** White solid; yield: 293 mg (90%); mp 104-105 °C

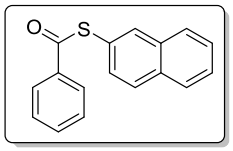

(Lit.[102] mp 107 °C); ^{1}H NMR (400 MHz, $CDCl_3$) δ 8.10 (d, J = 1.0 Hz, 1H), 8.08 (d, J = 1.3 Hz, 2H), 7.95 (d, J = 8.6 Hz, 1H), 7.93 – 7.87 (m, 2H), 7.69 – 7.62 (m, 1H), 7.61 – 7.55 (m, 3H), 7.53 (dd, J = 9.8, 4.0 Hz, 2H); ^{13}C NMR (100 MHz, $CDCl_3$) δ 190.4, 136.7, 135.0, 133.8, 131.4, 128.8, 127.9, 127.5, 127.2, 126.5, 125.9, 125.8, 120.8.

***S*-Naphthalen-2-yl-4-chlorobenzothioate (101bB):** White solid; yield: 257 mg (86%); mp 130-

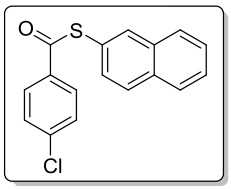

131 °C; ^{1}H NMR (400 MHz, $CDCl_3$) δ 8.08 (s, 1H), 8.03 (d, J = 8.6 Hz, 2H), 7.95 (d, J = 8.5 Hz, 1H), 7.93 – 7.85 (m, 2H), 7.62 – 7.53 (m, 3H), 7.51 (d, J = 8.6 Hz, 2H); ^{13}C NMR (100 MHz, $CDCl_3$) δ 189.3, 140.1, 135.0, 133.6, 131.3, 129.3 – 128.8, 127.9, 127.3, 126.6, 124.2.

***S*-Phenyl 3,4-dimethoxybenzothioate (101cA):** White solid; yield: 255 mg (93%); mp 98-

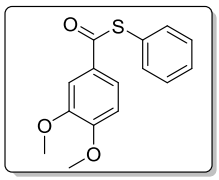

101°C (Lit.[103,104] mp 102-103 °C); ^{1}H NMR (400 MHz, $CDCl_3$) δ 7.77 (dd, J = 8.4, 2.1 Hz, 1H), 7.58 – 7.54 (m, 1H), 7.53 (dd, J = 3.1, 1.4 Hz, 2H), 7.51 – 7.45 (m, 3H), 6.95 (d, J = 8.5 Hz, 1H), 3.99 (s, 3H), 3.96 (s, 3H); ^{13}C NMR (100 MHz, $CDCl_3$) δ 188.8, 153.7, 149.0, 135.2, 129.5, 129.1, 127.6, 122.0, 110.3, 109.7, 56.1, 56.0.

***S*-Phenyl 2-methyl benzothioate (101dA):** White crystalline solid; yield: 212 mg (93%); mp

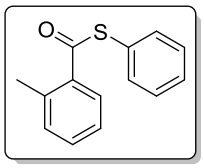

45-46 °C (Lit. [103,105] mp 50-51 °C); ^{1}H NMR (400 MHz, $CDCl_3$) δ 7.97 (d, J = 7.7 Hz, 1H), 7.59 – 7.53 (m, 2H), 7.51 – 7.47 (m, 3H), 7.45 (dd, J = 7.5, 1.2 Hz, 1H), 7.34 (d, J = 7.6 Hz, 1H), 7.30 (d, J = 8.2 Hz, 1H), 2.52 (s, 3H); ^{13}C NMR (100 MHz, $CDCl_3$) δ 192.2, 137.4, 136.8, 134.9, 132.0, 131.7, 129.4, 128.6, 128.2, 125.8, 20.8.

***S*-(Naphthalen-2-yl) 2-methylbenzothioate (101dB):** White solid; yield: 256 mg (92%); mp 71-

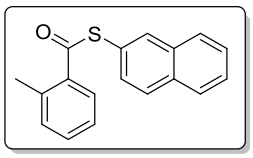

73 °C; ^{1}H NMR (400 MHz, $CDCl_3$) δ 8.09 (d, J = 0.8 Hz, 1H), 8.03 (dd, J = 7.7, 1.0 Hz, 1H), 7.96 (d, J = 8.6 Hz, 1H), 7.93 – 7.88 (m, 2H), 7.62 – 7.53 (m, 3H), 7.47 (td, J = 7.5, 1.2 Hz, 1H), 7.39 – 7.30 (m, 2H), 2.54 (s, 3H); ^{13}C NMR (100 MHz, $CDCl_3$) δ 192.4, 137.5, 136.8, 134.8, 133.7, 133.4, 132.1, 131.8, 131.3, 128.8, 128.0, 127.8, 127.2, 126.5, 125.9, 125.6, 20.8.

***S*-Phenyl furan-2-carbothioate (101gA):** White Solid; yield: 180 mg (88%); mp 102-104 °C ^{1}H

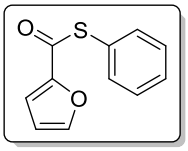

NMR (400 MHz, $CDCl_3$) δ 7.65 (brs, 1H), 7.58 – 7.51 (m, 2H), 7.50 – 7.45 (m, 3H), 7.29 (d, J = 3.6 Hz, 1H), 6.60 (dd, J = 3.5, 1.6 Hz, 1H); ^{13}C NMR (100 MHz, $CDCl_3$) δ 178.7, 150.4, 146.5, 135.2, 129.7, 129.3, 126.2, 116.3, 112.4.

***S*-Naphthalen-2-yl furan-2-carbothioate (101gB):** White Solid; yield: 101 mg (85%); mp 92-

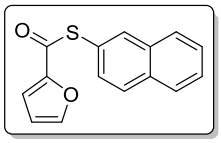

95 °C; ^{1}H NMR (400 MHz, $CDCl_3$) δ 8.08 (s, 1H), 7.97 – 7.86 (m, 3H), 7.68 (s, 1H), 7.60 – 7.53 (m, 3H), 7.32 (d, J = 3.4 Hz, 1H), 6.62 (dd, J = 3.5, 1.7 Hz, 1H); ^{13}C NMR (100 MHz, $CDCl_3$) δ 178.9, 150.4, 146.5, 135.1, 133.6, 131.4, 128.8, 127.9, 127.2, 126.6, 123.5, 116.3, 112.5.

3-Methoxyphenyl benzoate (103aA): Colourless oil; yield: 182 mg (80%); ^{1}H NMR (400 MHz,

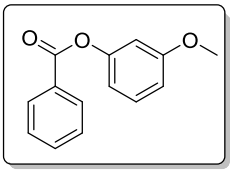

$CDCl_3$) δ 8.36 – 8.23 (m, 2H), 7.72 – 7.64 (m, 1H), 7.54 (dd, J = 11.1, 4.2 Hz, 2H), 7.36 (dd, J = 10.5, 5.8 Hz, 1H), 6.95 – 6.82 (m, 3H), 3.85 (d, J = 3.7 Hz, 3H); ^{13}C NMR (100 MHz, $CDCl_3$) δ 165.1, 160.6, 151.9, 133.6, 130.2, 129.9, 129.6, 128.6, 113.9, 111.9, 107.7, 55.4.

3-Methoxyphenyl 4-chlorobenzoate (103bA): Colourless oil; yield: 197 mg (75%); ^{1}H NMR

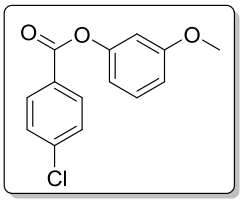

(400 MHz, $CDCl_3$) δ 8.18 – 8.14 (m, 2H), 7.51 (d, J = 8.5 Hz, 2H), 7.35 (t, J = 8.2 Hz, 1H), 6.89 – 6.82 (m, 2H), 6.81 – 6.78 (m, 1H), 3.84 (s, 3H); ^{13}C NMR (100 MHz, $CDCl_3$) δ 164.2, 160.6, 151.7, 140.1, 131.5, 129.9, 128.9, 128.7, 113.8, 111.9, 107.6, 55.5.

3-Methoxyphenyl 3,4-dimethoxybenzoate (103cA): Colourless oil; yield: 242 mg (84%); ^{1}H

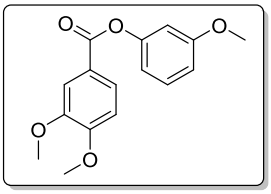

NMR (400 MHz, $CDCl_3$) δ 7.88 (dd, J = 8.4, 2.0 Hz, 1H), 7.69 (d, J = 1.9 Hz, 1H), 7.34 (t, J = 8.2 Hz, 1H), 6.98 (d, J = 8.5 Hz, 1H), 6.87 – 6.81 (m, 2H), 6.79 (t, J = 2.2 Hz, 1H), 4.00 (s, 3H), 3.99 (s, 3H), 3.84 (s, 3H); ^{13}C NMR (100 MHz, $CDCl_3$) δ 164.9, 160.5, 153.6, 152.0, 148.8, 129.8, 124.4, 121.9, 114.0, 112.4, 111.8, 110.4, 107.7.

3-Methoxyphenyl 2-methylbenzoate (103dA): Colourless oil; yield: 194 mg (80%); ^{1}H NMR

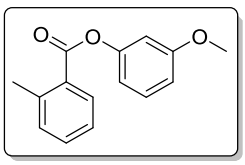

(400 MHz, $CDCl_3$) δ 8.18 (d, J = 7.5 Hz, 1H), 7.51 (t, J = 7.0 Hz, 1H), 7.36 (dd, J = 12.4, 5.1 Hz, 3H), 6.90 – 6.82 (m, 2H), 6.80 (d, J = 2.1 Hz, 1H), 3.85 (s, 3H), 2.71 (s, 3H); ^{13}C NMR (100 MHz, $CDCl_3$) δ 165.7, 160.6, 151.9, 141.3, 132.7, 131.9, 131.2, 129.9, 128.5, 125.9, 114.1, 111.7, 107.8, 55.4, 29.7.

3-Methoxyphenylcinnamate (103eA): Colourless oil; yield: 185 mg (73%); ^{1}H NMR (400 MHz, $CDCl_3$) δ 7.90 (d, J = 16.0 Hz, 1H), 7.65 – 7.59 (m, 2H), 7.48 – 7.43 (m, 3H), 7.33 (dd, J = 10.6, 5.8 Hz, 1H), 6.73 – 6.64 (m, 2H), 6.76 (t, J = 2.2 Hz, 1H), 6.65 (d, J = 16.0 Hz, 1H), 3.84 (s, 3H); ^{13}C NMR (100 MHz, $CDCl_3$) δ 165.3, 160.5, 151.7, 146.6, 134.2, 130.7, 129.8, 129.0, 128.3, 117.3, 113.8, 111.7, 107.6, 55.4.

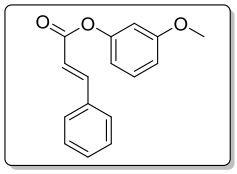

3-Methoxyphenyl benzoate (103gA): Colourless liquid; yield: 152 mg (70%); ^{1}H NMR (400 MHz, $CDCl_3$) δ 7.70 (dd, J = 1.6, 0.8 Hz, 1H), 7.40 (dd, J = 3.5, 0.7 Hz, 1H), 7.34 (t, J = 8.2 Hz, 1H), 6.88 – 6.82 (m, 2H), 6.80 (t, J = 2.2 Hz, 1H), 6.62 (dd, J = 3.5, 1.7 Hz, 1H), 3.83 (s, 3H); ^{13}C NMR (100 MHz, $CDCl_3$) δ 160.5, 156.8, 151.1, 147.2, 143.9, 129.9, 119.5, 113.8, 112.1, 107.6, 55.4.

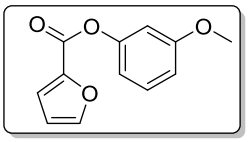

Reusability of 3-((1*H*-benzo[*d*][1,2,3]triazol-5-yl)methyl)-1,2-dimethyl-1*H*-imidazol-3-ium hexafluorophosphate (95)

After the first run of the reaction and following the above mentioned the work-up procedure, the regenerated semi-solid **95** was dried under vacuum for 4-5 h and was reused for the next cycle of the reaction.

Procedure for one-pot synthesis of amide (99aA) without isolating Im-CH$_2$-BtCOR (97a)

A 25 mL round-bottom flask containing a mixture of DCC (1.2 mmol), benzoic acid (1.2 mmol), **95** (1 mmol) and DMAP (5 mol %) in dry acetonitrile (8 mL) were stirred for 20 h under ambient condition. After the completion of reaction, *p*-toluidine (1.2 mmol), additional DMAP (1.2 mmol) were added to the above pot, and the reaction mixture was subjected to microwave irradiation for 20 minutes. After the two sequential reactions, the reaction mixture was concentrated and dried under high vacuum for 5-6 h and the residue was washed with ethyl acetate (20 mL × 2). The organic filtrate was decanted to separate the product along with by-products (DCU, DMAP and un-reacted acid) from **95**. The un-dissolved semi-solid was dried under vacuum to regenerate pure Im-CH$_2$-BtH (**95**) (97% of its starting amount). The organic filtrate was washed with 1N HCl and then with 2N NaOH. Purification of this residue by column chromatography over silica gel using EtOAc: hexanes (1: 9, v/v) yielded **99aA** in 82% yield.

Procedure for sequential synthesis of amide (99aA) without isolating Im-CH$_2$-BtCOR (97a)

A 25 mL round-bottom flask containing a mixture of DCC (1.2 mmol), benzoic acid (1.2 mmol), **95** (1 mmol) and DMAP (5 mol %) in dry acetonitrile (8 mL) was stirred for 20 h at 20 ^{o}C. After the completion of reaction, the mixture was concentrated and dried under vacuum and washed with ethyl acetate (20 mL × 2) to remove DCU, DMAP and un-reacted acid. The residue was charged with *p*-toluidine (1.2 mmol), additional DMAP (1.2 mmol) and water (4 mL) and the mixture was subjected to microwave irradiation for 20 minutes. After completion of the reaction, reaction mixture was concentrated, dried and washed with ethyl acetate (20 mL × 2). The organic filtrate was decanted and washed with 1N HCl, dried using Na_2SO_4 and concentrated to yield pure amide **99aA** in 92% yield. The left over residue was dried using under vacuum to give pure Im-CH_2-BtH (**95**) (98% of its starting material).

5.5 References

(1) Azadi, R.; Shams, L. *Letters in Organic Chemistry* **2017**, *14*, 141-145.

(2) Fraga-Dubreuil, J.; Bazureau, J. P. *Tetrahedron Letters* **2001**, *42*, 6097-6100.

(3) Fraga-Dubreuil, J.; Bazureau, J. P. *Tetrahedron* **2003**, *59*, 6121-6130.

(4) Fraga-Dubreuil, J.; Famelart, M. -H.; Bazureau, J. P *Organic Process Research & Development* **2002**, *6*, 374-378.

(5) Hakkou, H.; Eynde, J. J. V.; Hamelin, J.; Bazureau, J. P. *Tetrahedron* **2004**, *60*, 3745-3753.

(6) Martins, M. A.; Frizzo, C. P.; Moreira, D. N.; Zanatta, N.; Bonacorso, H. G. *Chemical Reviews* **2008**, *108*, 2015-2050.

(7) Welton, T. *Chemical Reviews* **1999**, *99*, 2071-2084.

(8) Martins, M. A.; Frizzo, C. P.; Tier, A. Z.; Moreira, D. N.; Zanatta, N.; Bonacorso, H. G. *Chemical Reviews* **2014**, *114*, PR1-PR70.

(9) Hallett, J. P.; Welton, T. *Chemical Reviews* **2011**, *111*, 3508-3576.

(10) Petkovic, M.; Seddon, K. R.; Rebelo, L. P. N.; Pereira, C. S. *Chemical Society Reviews* **2011**, *40*, 1383-1403.

(11) Welton, T. *Green Chemistry* **2011**, *13*, 225-225.

(12) Miao, W.; Chan, T. H. *Accounts of Chemical Research* **2006**, *39*, 897-908.

(13) H. Davis, J., James *Chemistry Letters* **2004**, *33*, 1072-1077.

(14) Visser, A. E.; Swatloski, R. P.; Reichert, W. M.; Mayton, R.; Sheff, S.; Wierzbicki, A.; Davis Jr, J. H.; Rogers, R. D. *Chemical Communications* **2001**, 135-136.

(15) Brahmachari, G. *Green synthetic approaches for biologically relevant heterocycles*; Elsevier, **2014**.

(16) Merrifield, R. B. *Journal of the American Chemical Society* **1963**, *85*, 2149-2154.

(17) Bayer, E.; Mutter, M. *Nature* **1972**, *237*, 512-513.

(18) Bergbreiter, D. E. *Chemical Reviews* **2002**, *102*, 3345-3384.

(19) Bonora, G. M.; Scremin, C. L.; Colonna, F. P.; Garbesi, A. *Nucleic Acids Research* **1990**, *18*, 3155-3159.

(20) Dickerson, T. J.; Reed, N. N.; Janda, K. D. *Chemical Reviews* **2002**, *102*, 3325-3344.

(21) Douglas, S. P.; Whitfield, D. M.; Krepinsky, J. J. *Journal of the American Chemical Society* **1991**, *113*, 5095-5097.

(22) Toy, P. H.; Janda, K. D. *Accounts of Chemical Research* **2000**, *33*, 546-554.

(23) Mizuno, M.; Goto, K.; Miura, T.; Matsuura, T.; Inazu, T. *Tetrahedron Letters* **2004**, *45*, 3425-3428.

(24) Studer, A.; Hadida, S.; Ferritto, R.; Kim, S.-Y.; Jeger, P.; Wipf, P.; Curran, D. P. *Science* **1997**, *275*, 823-826.

(25) Dien Pham, P.; Vitz, J.; Chamignon, C.; Martel, A.; Legoupy, S. *European Journal of Organic Chemistry* **2009**, 3249-3257.

(26) Louaisil, N.; Pham, P. D.; Boeda, F.; Faye, D.; Castanet, A. S.; Legoupy, S. *European Journal of Organic Chemistry* **2011**, *2011*, 143-149.

(27) Pham, P. D.; Legoupy, S. *Tetrahedron Letters* **2009**, *50*, 3780-3782.

(28) Vitz, J.; Mac, D. H.; Legoupy, S. *Green Chemistry* **2007**, *9*, 431-433.

(29) Akiike, J.; Yamamoto, Y.; Togo, H. *Synlett* **2008**, 2529-2531.

(30) Kawano, Y.; Togo, H. *Tetrahedron* **2007**, *65*, 2168-2172.

(31) Qian, W.; Jin, E.; Bao, W.; Zhang, Y. *Angewandte Chemie International Edition* **2005**, *44*, 952-955.

(32) Qian, W.; Pei, L. *Synlett* **2006**, 709-712.

(33) Fang, C.; Qian, W.; Bao, W. *Synlett* **2008**, 2529-2531.

(34) Merritt, E. A.; Olofsson, B. *Angewandte Chemie International Edition* **2009**, *48*, 9052-9070.

(35) Yoshimura, A.; Zhdankin, V. V. *Chemical Review* **2016**, *116*, 3328-3435.

(36) Kumar Muthyala, M.; Choudhary, S.; Pandey, K.; Shelke, G. M.; Jha, M.; Kumar, A. *European Journal of Organic Chemistry* **2014**, 2365-2370.

(37) Muthyala, M. K.; Choudhary, S.; Kumar, A. *RSC Advances* **2014**, *4*, 14297-14303.

(38) Wu, X. -E.; Ma, L.; Ding, M. -X.; Gao, L. -X. *Synlett* **2005**, 607-610.

(39) Liu, L.; Ma, J.; Sun, Z.; Zhang, J.; Huang, J.; Li, S.; Tong, Z. *Canadian Journal of Chemistry* **2010**, *89*, 68-71.

(40) Fall, A.; Sene, M.; Gaye, M.; Gómez, G.; Fall, Y. *Tetrahedron Letters* **2010**, *51*, 4501-4504.

(41) Qian, W.; Jin, E.; Bao, W.; Zhang, Y. *Tetrahedron* **2006**, *62*, 556-562.

(42) Zhu, C.; Yoshimura, A.; Wei, Y.; Nemykin, V. N.; Zhdankin, V. V. *Tetrahedron Letters* **2012**, *53*, 1438-1444.

(43) D'Anna, F.; Marullo, S.; Noto, R. *The Journal of Organic Chemistry* **2008**, *73*, 6224-6228.

(44) Kamal, A.; Chouhan, G. *Tetrahedron Letters* **2005**, *46*, 1489-1491.

(45) Yadav, L. D. S.; Patel, R.; Rai, V. K.; Srivastava, V. P. *Tetrahedron Letters* **2007**, *48*, 7793-7795.

(46) Valizadeh, H.; Gholipour, H. *Comptes Rendus Chimie* **2011**, *14*, 963-966.

(47) Kumar, A.; Muthyala, M. K. *Tetrahedron Letters* **2011**, *52*, 5368-5370.

(48) Iranpoor, N.; Firouzabadi, H.; Azadi, R. *European Journal of Organic Chemistry* **2007**, 2197-2201.

(49) Iranpoor, N.; Firouzabadi, H.; Azadi, R. *Tetrahedron Letters* **2006**, *47*, 5531-5534.

(50) Valizadeh, H.; Gholipour, H.; Mahmoudian, M. *Journal of the Iranian Chemical Society* **2011**, *8*, 862-871.

(51) Pandey, K.; Muthyala, M. K.; Choudhary, S.; Kumar, A. *RSC Advances* **2015**, *5*, 13797-13804.

(52) Ghose, A. K.; Viswanadhan, V. N.; Wendoloski, J. J. *Journal of Combinatorial Chemistry* **1999**, *1*, 55-68.

(53) Andrews, P.; Craik, D.; Martin, J. *Journal of Medicinal Chemistry* **1984**, *27*, 1648-1657.

(54) Andrews, P. *Trends in Pharmacological Sciences* **1986**, *7*, 148-151.

(55) Nogrady, T.; Weaver, D. F. *Medicinal chemistry: a molecular and biochemical approach*; Oxford University Press, **2005**.

(56) Rodriguez-Galan, A.; Franco, L.; Puiggali, J. *Polymers* **2010**, *3*, 65-99.

(57) Moerk, N. N.; Bundgaard, H. *Journal of Medicinal Chemistry* **1989**, *32*, 727-734.

(58) Bansal, A. K.; Khar, R. K.; Dubey, R.; Sharma, A. K. *Drug Development and Industrial Pharmacy* **2001**, *27*, 63-70.

(59) Gadad, A. K.; Bhat, S.; Tegeli, V. S.; Redasani, V. V. *Arzneimittelforschung* **2002**, *52*, 817-821.

(60) Cao, F.; Guo, J.-X.; Ping, Q.-N.; Liao, Z.-G. *European Journal of Pharmaceutical Sciences***2006**, *29*, 385-393.

(61) Kankanala, K.; Reddy, V. R.; Devi, Y. P.; Mangamoori, L. N.; Mukkanti, K.; Pal, S. *Journal of Chemistry* **2013**, 1-8.

(62) Dawson, P. E.; Kent, S. B. *Annual Review of Biochemistry* **2000**, *69*, 923-960.

(63) Clark, R. J.; Craik, D. J. *Peptide Science* **2010**, *94*, 414-422.

(64) Katritzky, A. R.; Lan, X.; Yang, J. Z.; Denisko, O. V. *Chemical Reviews* **1998**, *98*, 409-548.

(65) Katritzky, A. R.; Rachwal, S. *Chemical Reviews* **2009**, *110*, 1564-1610.

(66) Katritzky, A. R.; Rachwal, S. *Chemical Reviews* **2011**, *111*, 7063-7120.

(67) Katritzky, A. R.; Suzuki, K.; Wang, Z. *Synlett* **2005**, 1656-1665.

(68) Panda, S. S.; Hall, C. D.; Scriven, E.; Katritzky, A. R. *Aldrichimica Acta* **2013**, *46*, 43-45.

(69) Katritzky, A. R.; He, H.-Y.; Suzuki, K. *The Journal of Organic Chemistry* **2000**, *65*, 8210-8213.

(70) Lin, S. -M.; Zhang, J.-L.; Chen, J. -X.; Gao, W. -X.; Ding, J. -C.; Su, W. -K.; Wu, H. -Y. *Journal of the Brazilian Chemical Society* **2010**, *21*, 1616-1620.

(71) Katritzky, A. R.; Shestopalov, A. A.; Suzuki, K. *Synthesis* **2004**, 1806-1813.

(72) Katritzky, A. R.; Belyakov, S. A.; Tymoshenko, D. O. *Journal of Combinatorial Chemistry* **1999**, *1*, 173-176.

(73) Paio, A.; Zaramella, A.; Ferritto, R.; Conti, N.; Marchioro, C.; Seneci, P. *Journal of Combinatorial Chemistry* **1999**, *1*, 317-325.

(74) Schiemann, K.; Showalter, H. D. H, *The Journal of Organic Chemistry* **1999**, *64*, 4972-4975.

(75) Paio, A.; Crespo, R. F.; Seneci, P.; Ciraco, M. *Journal of Combinatorial Chemistry* **2001**, *3*, 354-359.

(76) Katritzky, A. R.; Pastor, A.; Voronkov, M.; Tymoshenko, D. *Journal of Combinatorial Chemistry* **2001**, *3*, 167-170.

(77) Talukdar, S.; Chen, R. -J.; Chen, C. -T.; Lo, L. -C.; Fang, J. -M. *Journal of Combinatorial Chemistry* **2001**, *3*, 341-345.

(78) Peng, Y.; Yi, F.; Song, G.; Zhang, Y. *Monatshefte für Chemie* **2005**, *136*, 1751-1755.

(79) De Kort, M.; Tuin, A. W.; Kuiper, S.; Overkleeft, H. S.; van der Marel, G. A.; Buijsman, R. C. *Tetrahedron Letters* **2004**, *45*, 2171-2175.

(80) Miao, W.; Chan, T. H. *Organic Letters* **2003**, *5*, 5003-5005.

(81) Bösmann, A.; Datsevich, L.; Jess, A.; Lauter, A.; Schmitz, C.; Wasserscheid, P. *Chemical Communications* **2001**, 2494-2495.

(82) Anthony, J. L.; Maginn, E. J.; Brennecke, J. F. *The Journal of Physical Chemistry B* **2002**, *106*, 7315-7320.

(83) Pucheault, M.; Vaultier, M. *In Ionic Liquids*; Springer: **2009**, p 83-126.

(84) He, X.; Chan, T. H. *Organic Letters* **2007**, *9*, 2681-2684.

(85) Han, S. -Y.; Kim, Y.-A. *Tetrahedron* **2004**, *60*, 2447-2467.

(86) Li, C.; Zhang, Z.; Duan, Q.; Li, X. *Organic Letters* **2014**, *16*, 3008-3011.

(87) Yerneni, C. K.; Pathak, V.; Pathak, A. K. *The Journal of Organic Chemistry* **2009**, *74*, 6307-6310.

(88) Katritzky, A. R.; Ji, F. -B.; Fan, W. -Q.; Delprato, I. *Synthetic Communications* **1993**, *23*, 2019-2025.

(89) Sheng, G.; Wu, X.; Cai, X.; Zhang, W. *Synthesis* **2015**, *47*, 949-954.

(90) Kumar, S.; Vanjari, R.; Guntreddi, T.; Singh, K. N. *RSC Advances* **2015**, *5*, 9920-9924.

(91) Devine, S. M.; Mulcair, M. D.; Debono, C. O.; Leung, E. W.; Nissink, J. W. M.; Lim, S. S.; Chandrashekaran, I. R.; Vazirani, M.; Mohanty, B.; Simpson, J. S. *Journal of Medicinal Chemistry* **2015**, *58*, 1205-1214.

(92) Kim, S.-G.; Jung, S. -L.; Lee, G. -H.; Gong, Y. -D. *ACS Combinatorial Science* **2012**, *15*, 29-40.

(93) Kaye, I. A.; Parris, C. L. *The Journal of Organic Chemistry* **1951**, *16*, 1761-1763.

(94) Meshram, H.; Reddy, G. S.; Reddy, M. M.; Yadav, J. *Tetrahedron Letters* **1998**, *39*, 4103-4106.

(95) Narasimhan, B.; Ohlan, S.; Ohlan, R.; Judge, V.; Narang, R. *European Journal of Medicinal Chemistry* **2009**, *44*, 689-700.

(96) Verma, A.; Patel, S.; Kumar, A.; Yadav, A.; Kumar, S.; Jana, S.; Sharma, S.; Prasad, C. D.; Kumar, S. *Chemical Communications* **2015**, *51*, 1371-1374.

(97) Wannberg, J.; Larhed, M. *The Journal of Organic Chemistry* **2003**, *68*, 5750-5753.

(98) Amnerkar, N. D.; Bhusari, K. P. *European Journal of Medicinal Chemistry* **2010**, *45*, 149-159.

(99) Shang, Y.; Jie, X.; Zhao, H.; Hu, P.; Su, W. *Organic Letters* **2014**, *16*, 416-419.

(100) Wang, F.; Song, G.; Li, X. *Organic Letters* **2010**, *12*, 5430-5433.

(101) Prajapti, S. K.; Nagarsenkar, A.; Babu, B. N. *Tetrahedron Letters* **2014**, *55*, 1784-1787.

(102) Cao, H.; McNamee, L.; Alper, H. *The Journal of Organic Chemistry* **2008**, *73*, 3530-534.

(103) Burhardt, M. N.; Ahlburg, A.; Skrydstrup, T. *The Journal of Organic Chemistry* **2014**, *9*, 11830-11840.

(104) Burhardt, M. N.; Taaning, R. H.; Skrydstrup, T. *Organic Letters* **2013**, *15*, 948-951.

(105) Badsara, S. S.; Liu, Y. -C.; Hsieh, P. -A.; Zeng, J. -W.; Lu, S. -Y.; Liu, Y. -W.; Lee, C. -F. *Chemical Communications* **2014**, *50*, 11374-11377.

CHAPTER 6

Conclusions of the Thesis

6.1 General conclusions

Imidazo[1,2-*a*]pyridine (IP) has been recognized as premium aza-heterocyclic system. In its functionalized forms it exhibits numerous biological applications, and found its presence in several commercialized drugs. Thus, functionalizing imidazo[1,2-*a*]pyridine under environmentally benign reaction conditions is in high demand. Development of methodologies for the formation of nascent chemical bonds under metal-catalyzed or metal-free conditions have become the foremost task of synthetic organic chemists in recent years. In particular, development of new methodologies by overcoming the demand of pre-activated starting materials have proved to be effective and advantageous protocols towards the construction of plethora of pharmaceutical leads and natural products. The ongoing periodical documentation of on imidazo[1,2-*a*]pyridines allude our interest towards developing novel metal-catalyzed and metal-free strategies for functionalizing imidazo-heterocycles.

Coequally, the upsurge concern for minimizing the waste and providing an environmental being reaction process, has endorsed the exploration of different imidazolium-supported reagents for the liquid-phase synthesis of small aromatics and heteroaromatics. Such strategies have offered unique advantages in organic synthesis by retaining the supremacy of product purification along with the solubility benefits of the reagents. In this regard, we have developed a novel imidazolium–supported benzotriazole reagent and exemplified its applicability in selective organic transformations. The present work was successfully executed in due diligence of sustainable chemistry, and the thesis has been divided into six chapters (Figure 6.1.1).

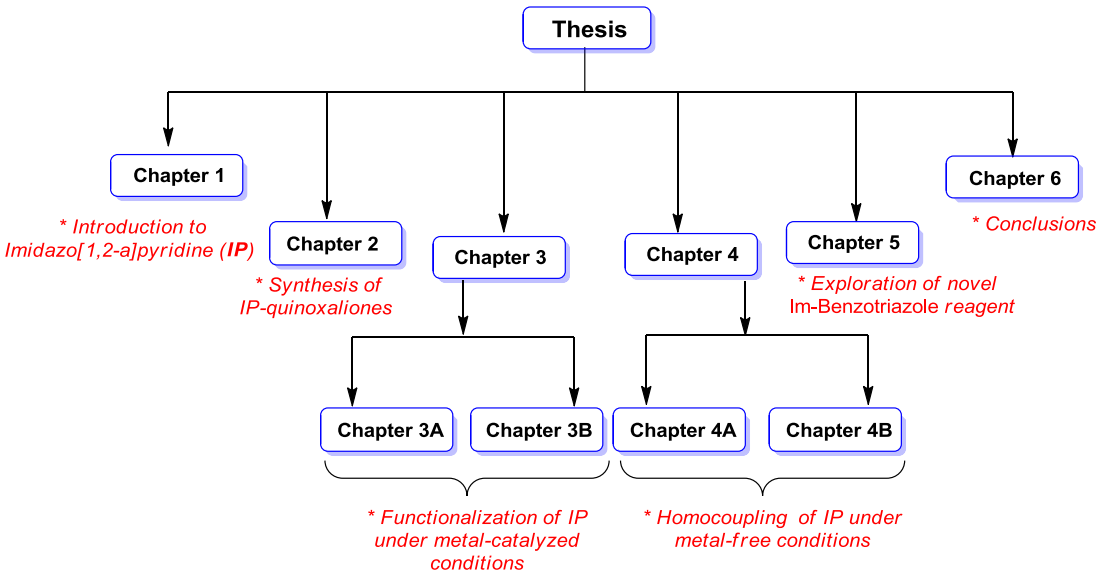

Figure 6.1.1: A diagram describing the systematic division of the thesis

The present thesis entitled **"C-H Functionalization of Imidazo-Heterocycles and Exploration of Imidazolium-Supported Benzotriazole Reagent for Selective Organic Transformations"** deals with the functionalization of imidazo[1,2-*a*]pyridine (IP) scaffold *via* conventional heterocyclization, metal-catalyzed C-H activation and metal-free oxidative coupling reactions. In addition the thesis systematically documents the synthesis and exploration of novel imidazolium-supported benzotriazole reagent as carboxylic acid activator. A chapter wise summary is presented below:

6.2 Specific conclusions

In chapter 1, of the thesis, we have described the importance and chemical reactivity of imidazo[1,2-*a*]pyridine skeleton as an introductory chapter to provide a background on imidazo[1,2-*a*]pyridine based works conducted by synthetic chemists in the past (Figure 6.2.1).

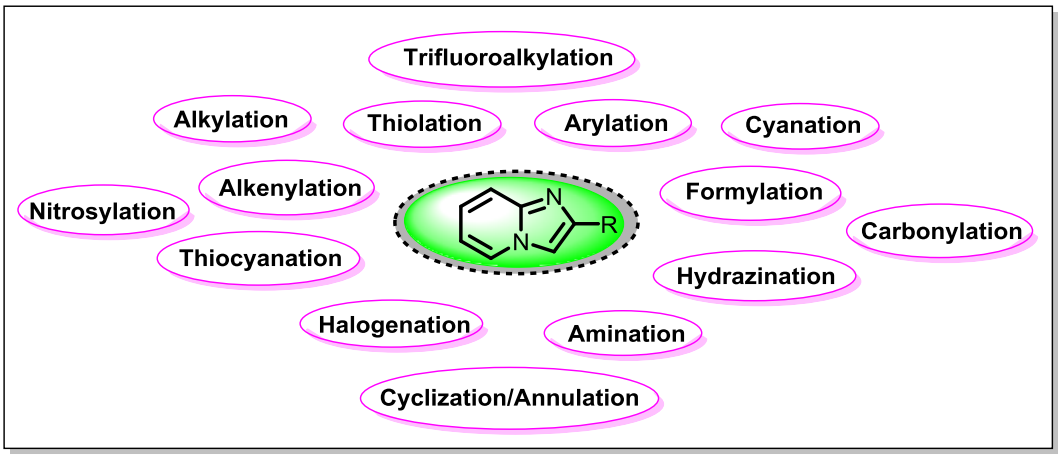

Figure 6.2.1: A graphical representation on the functionalization of imidazo[1,2-*a*]pyridines

Chapter 2: Microwave-Assisted Expedite Synthesis of Imidazo[1,2-*a*]pyridyl Quinoxalin-2(1*H*)-ones

Inspired from the valuable medicinal importance of different imidazo[1,2-*a*]pyridyl-heterocyclic conjugates, and the profound biological profile of quinoxalines derivatives. **In this chapter** we have described a microwave-assisted strategy for the synthesis of imidazo[1,2-*a*]pyridyl appended quinoxalin-2(1*H*)-ones. The desired product were synthesized by reacting prior synthesized imidazo[1,2-*a*]pyridine-3-glyoxalates and *ortho*-phenylene diamine using montmorillonite K-10 under solvent-free condition or $Yb(OTf)_3$ in THF. This Hinsberg heterocyclization reaction showcased good compatibility with a wide variety of substituted

imidazo[1,2-*a*]pyridines resulting in the formation of described products in 20-82% yields under environmentally being reaction conditions (Scheme 6.2.1).

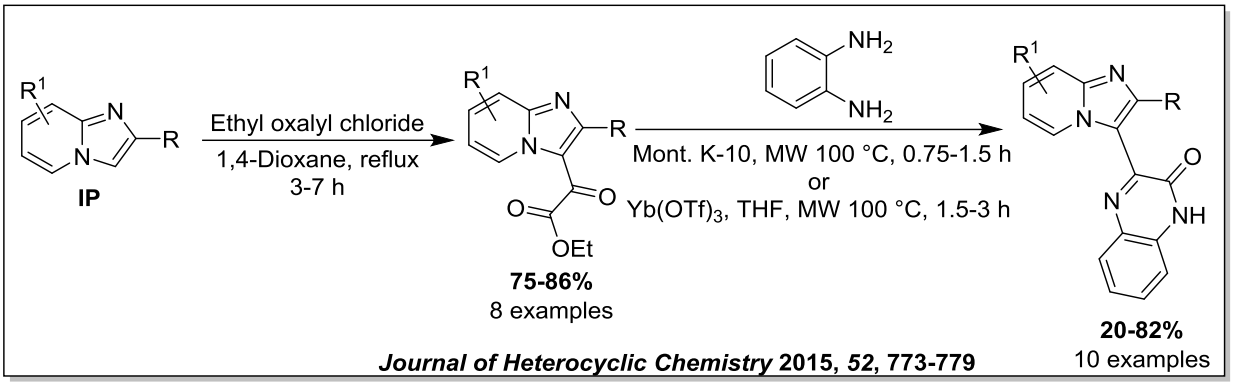

Scheme 6.2.1: Montmorillonite K-10 or $Yb(OTf)_3$-catalyzed synthesis of imidazo[1,2-*a*]pyridyl quinoxalinones

The synthesized imidazo[1,2-*a*]pyridine-3-glyoxalates and imidazo[1,2-*a*]pyridyl appended quinoxalin-2(1*H*)-ones were well characterized by ^{1}H NMR, ^{13}C NMR and mass-spectrometry analysis

The third chapter of the thesis describes a significant exploration of transition metal-catalyzed strategies towards the direct synthesis of functionalized imidazo-heterocycles. The chapter is divided into two parts:

Chapter 3A: Copper-Catalyzed Direct Dicarbonylation of Imidazo-Heterocycles *via* C-H Bond Activation

Chapter 3A, of the thesis is focused on the development of an oxidative coupling strategy for the formation of C-3 dicarbonylated imidazo-heterocycles using aryl actaldehydes under Cu-catalyzed conditions without the prior activation of Csp^2-H bond of imidazo-heterocycles in the presence of aerial oxygen. This methodology is proposed to proceed by means of cleavage of sp^2-H and sp^3-H bonds between imidazo-heterocycles and aryl acetaldehyde, whereby oxidative cross-dehydrogenative coupling and oxidation of α-methylene of aryl acetaldehydes proceeds in a cumulative manner (Scheme 6.2.2). The versatility of the reaction was generalized with differently substituted electron-rich and electron-deficient imidazo[1,2-*a*]pyridines and aryl acetaldehydes. A detailed mechanistic pathway was proposed by performing a set of control experiments and mass-spectrometry study of the reaction mixture. The mechanism was believed to proceed *via* single electron transfer process (SET) with eventual introduction of oxygen atom

from atmospheric air. The synthesized C-3 dicarbonylated imidazo[1,2-*a*]pyridines completely characterized by ^{1}H NMR, ^{13}C NMR and mass spectrometry analysis.

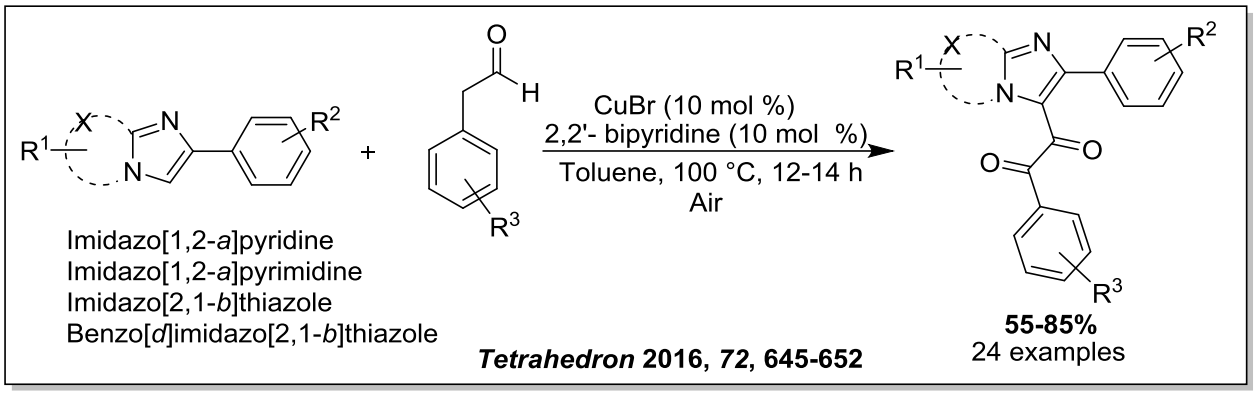

Scheme 6.2.2: Cu-catalyzed aerobic C-3 dicarbonylation of imidazo[1,2-*a*]pyridines

Chapter 3B: Ruthenium(II)-Catalyzed Regioselective *o*-Amidation of 2-Arylimidazo-Heterocycles *via* C-H Bond Activation

In Chapter 3B, we have described a regioselective Ru(II)-catalyzed strategy for *ortho*-amidation of 2-arylimidazo[1,2-*a*]pyridines with aryl isocyanates *via* Csp^2–H bond activation. An array of *ortho*-amidated 2-arylimidazo[1,2-*a*]pyridines with different functionalities on aryl and pyridyl rings were synthesized in good-to-excellent yields (Scheme 6.2.3). The developed protocol was also applicable to the selective *ortho*-amidation of other 2-arylimidazo-heterocycles such as 2-phenylimidazo[2,1-*b*]thiazole, 2-phenylbenzo[*d*]imidazo[2,1-*b*]thiazole, and 2-phenyl imidazo[1,2-*a*]pyrimidine. Delightfully, the methodology was scalable at gram scale without any noticeable declination in the yield. This is the first method for the coupling of aryl isocyanates with the imidazo[1,2-*a*]pyridine system *via* a pentacyclometalated intermediate. Contentedly, the mechanistic pathway of the reaction was advocated by several control experiments and by ESI-MS study of the reaction mixture. The cationic pentacyclometalated intermediate complex was synthesized, and utilized for the catalytic and stoichiometric transformation of targeted product, justifying the formation of described complex in the catalytic cycle. All of the synthesized *ortho*-amidated 2-arylimidazo[1,2-*a*]pyridines were detailed characterized by detailed spectroscopic analysis. In addition, the X-ray crystal structure of one of the synthesized derivative provides a transparent spectroscopic support.

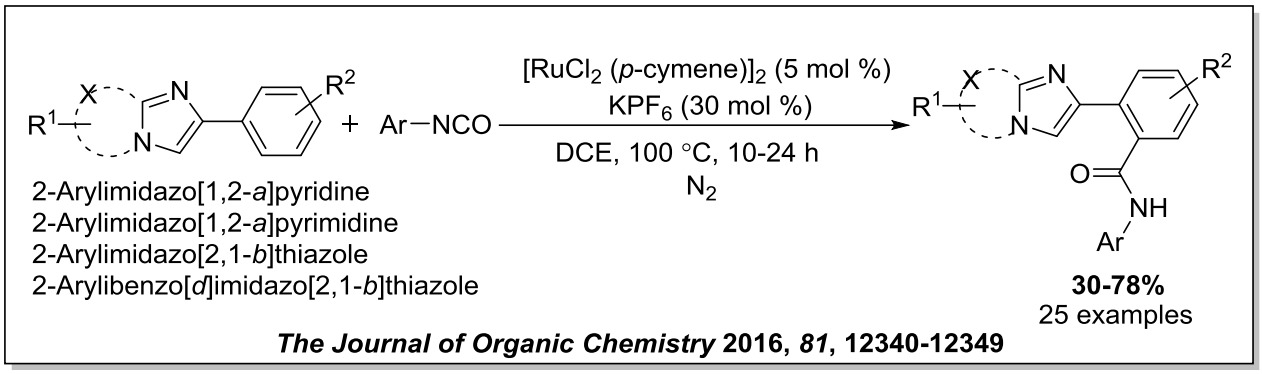

Scheme 6.2.3: Ru(II)-catalyzed *ortho*-amidation of 2-arylimidazo[1,2-*a*]pyridines

The fourth chapter of the thesis describes the significant exploration of metal-free strategies towards the homocoupling of imidazo-heterocycles. This chapter is also divided into two parts:

Chapter 4A: Transition Metal-Free Homocoupling of Imidazo-Heterocycles *via* Csp^2–Csp^2 Bond Formation

In chapter 4A, we have described a iodobenzene diacetate (PIDA)-mediated synthesis of 3,3′-biimidazo[1,2-*a*]pyridines by the oxidative homocoupling of 2-arylimidazo[1,2-*a*]pyridines under ambient condition (Scheme 6.2.4a). A series of homocoupled 2,2′-diaryl-3,3′-biimidazo[1,2-*a*]pyridines were synthesized from wide range of electronically rich imidazo[1,2-*a*]pyridyl substrates in moderate-to-good yields. This hypervalent iodine(III) mediated cross-dehydrogenative protocol was also applicable towards the homocoupling of other imidazo-heterocycles, such as imidazo[2,1-*b*]thiazoles and benzo[*d*]imidazo[2,1-*b*]thiazoles.

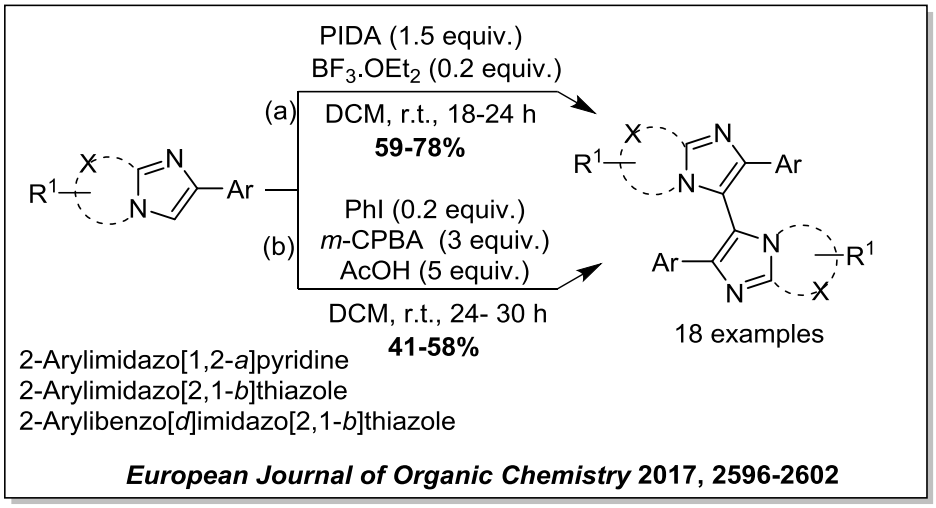

Scheme 6.2.4: PIDA/PhI-mediated/catalyzed synthesis of 2,2′-diaryl-3,3′-biimidazo[1,2-*a*]pyridines

The reaction mechanism was believed to proceed with the reversal of the polarity at the C-3 position of imidazo[1,2-*a*]pyridine in the presence of stoichiometric amount of iodobenzene diacetate, followed by $SN^{2'}$ nucleophilic substitution with another molecule of imidazo[1,2-*a*]pyridine. All of the synthesized homocoupled biimidazo-heterocycles were detailed characterized by spectroscopic analysis including ^{1}H NMR, ^{13}C NMR and mass spectrometry. In addition, the X-ray crystal structure of one of the synthesized compound provides a clear evidence for the formation of described products. In addition, an organocatalytic approach for the desired transformation employing catalytic amount of iodobenzene with *m*-CPBA/AcOH was also executed (Scheme 6.2.4b).

Chapter 4B: Transition Metal-Free Homocoupling of Imidazo-Heterocycles Linked *via* Sulfur Bridges

In chapter 4B` we have explored the utility of molecular iodine for the oxidative direct homocoupling of imidazo-heterocycles using Na_2S as a sulfur source for predominant synthesis of bis(imidazo[1,2-*a*]pyridin-3-yl)sulfanes and bis(imidazo[1,2-*a*]pyridin-3-yl)disulfanes. The methodology was efficiently controlled under variable solvent conditions in straightforward manner. These direct oxidative strategies for the synthesis of bis-sulfanes and bis-disulfanes were well exemplified with a broad range of substituted 2-arylimidazo[1,2-*a*]pyridines (Scheme 6.2.5). The detailed mechanistic pathway for the synthesis of bis-sulfanes and bis-disulfanes is been properly advocated through a series of control experiments and ESI-MS studies. Intriguingly, 2-arylimidazo[2,1-*b*]thiazole were also explored towards the formation of bis-sulfanes and bis-disulfanes in fairly good yields. All of the synthesized bis(imidazo[1,2-*a*]pyridin-3-yl)sulfanes and bis(imidazo[1,2-*a*]pyridin-3-yl)disulfanes were well characterized by ^{1}H NMR, ^{13}C NMR and mass spectrometry analysis. The structures of both sulfur bridge homocoupled products were unambiguously confirmed by X-ray crystallographic studies.

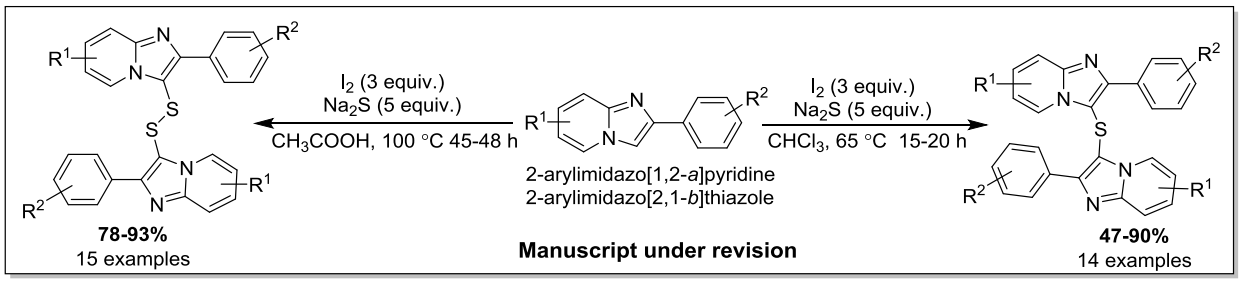

Scheme 6.2.5: I_2-mediated synthesis of bis(imidazo[1,2-*a*]pyridin-3-yl)sulfanes and bis(imidazo[1,2-*a*]pyridin-3-yl)disulfanes

Chapter 5: Exploration of Imidazolium-Supported Benzotriazole Reagent for Selective Organic Transformations

In Chapter 5, we have presented a brief background of different imidazolium-supported reagents, and their application in various organic transformations. Later on, the chapter deals with a detailed synthetic protocol for the synthesis of imidazolium-supported benzotriazole reagent (Im-BtH) as a novel synthetic auxiliary. Thereafter, eight different *N*-acylated imidazolium-supported benzotriazole reagents (Im-BtCOR) were prepared and exemplified as greener carboxyl group activating reagents for the synthesis of library of amides, esters and thioesters in aqueous medium under microwave irradiation (Scheme 6.2.6). Gratifyingly, Im-BtH was efficiently used in one-pot fashion for the synthesis of an amide in comparable yield as a representative example. The application of imidazolium-supported *N*-acetyl benzotriazole (Im-BtCOCH$_3$) leads to synthesis of Paracetamol on the gram scale under green conditions in 93% yield. The reagent was successfully reused five times without any noticeable loss in activity

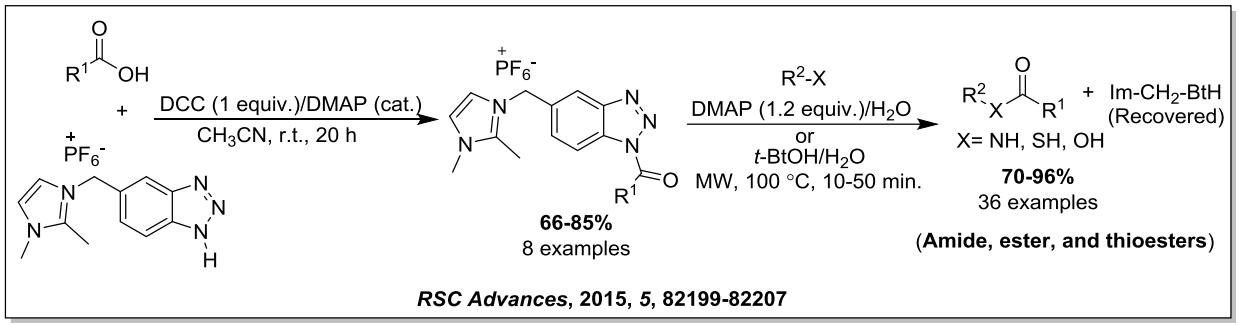

Scheme 6.2.6: Synthesis of amides, esters and thioesters, using novel imidazolium-supported benzotriazole reagent.

6.3 Future Scope

The current thesis reflects the development of new methodology for the synthesis of biologically active compounds under metal-catalyzed and metal-free conditions. Although the thesis mainly focused on the exploration of chemistry on imidazo[1,2-*a*]pyridine scaffold, yet there exist enormous scope for developing different imidazo[1,2-*a*]pyridyl fused heterocyclic frameworks. In addition, introducing other nascent functionalities, at the expense of chelation-assistance of nitrogen of IP is an area left to explore for further the tandem cyclization reactions under appropriate reaction conditions. In concordance with the literatures precedence, we can expect to perceive good bioactivity of all functionalized imidazo-heterocycles.

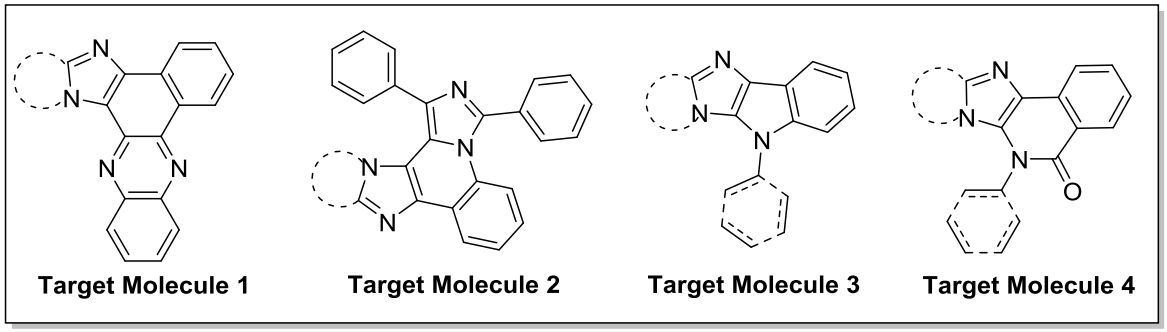

On the other hand the broad range applications of benzotriazole chemistry, further provides a strong need for the exploration of imidazolium-supported benzotriazole reagent (ImBtH) to achieve various organic molecules in constantly greener approaches.

Appendices

List of Publications *[A-1]*

1. **S. M. A. Shakoor**, D. S. Agarwal, S. Khullar, S. K. Mandal, R. Sakhuja "Solvent-driven iodine-mediated oxidative strategies for the synthesis of bis(imidazo[1,2-*a*]pyridin-3-yl)sulfanes and disulfanes" Manuscript under revision.
2. **S. M. A. Shakoor**, S. Mandal, R. Sakhuja "An articulate oxidative transition metal-free homocoupling of imidazo-heterocycles *via* $C(sp^2)$-$C(sp^2)$ bond formation" *European Journal of Organic Chemistry* **2017**, 2596-2602.
3. **S. M. A. Shakoor**, S. Kumari, S. Khullar, S. Mandal, A Kumar, R. Sakhuja "Ruthenium(II)-catalyzed regioselective *ortho*-amidation of imidazo-heterocycles with isocyanates" *The Journal of Organic Chemistry* **2016**, *81*, 12340-12349.
4. **S. M. A. Shakoor**, D. S. Agarwal, A Kumar, R. Sakhuja "Copper catalyzed direct aerobic double-oxidative cross-dehydrogenative coupling of imidazo-heterocycles with aryl acetaldehydes: an articulate approach for dicarbonylation at C-3 position" *Tetrahedron* **2016**, *72*, 645-652.
5. S. Kumari, **S. M. A. Shakoor**, K. Bajaj, S. H. Nanjegowda, P. Mall, R. Sakhuja "Copper-catalysed C-N/C-O coupling in water: a facile access to *N*-coumaryl amino acids and fluorescent tyrosine & lysine labels" *Tetrahedron Letters* **2016**, *57*, 2732-2736.
6. **S. M. A. Shakoor**, K. Bajaj, S. Choudhary, M. K. Muthyala, A Kumar, R. Sakhuja "Imidazolium-supported benzotriazole: An efficient and recoverable activating reagent for amide, ester and thioester bond formation in water" *RSC Advances*, **2015**, *5*, 82199-82207.
7. S. Kumari, S. Joshi, **S. M. A. Shakoor**, D. S. Agarwal, S. S. Panda, D. D. Pant, R. Sakhuja "Synthesis, absorption, and fluorescence studies of coumaryl-labelled amino acids and dipeptides linked *via* triazole ring" *Australian Journal of Chemistry* **2015**, *68*, 1415-1426.
8. R. Sakhuja, **S. M. A. Shakoor**, S. Kumari, A. Kumar "Microwave-assisted expedite synthesis of 2-phenylimidazo[1,2-*a*]pyridyl quinoxalin-2(1*H*)-ones" *Journal of Heterocyclic Chemistry* **2015**, *52*, 773-779
9. R. Sakhuja, K. Bajaj, **S. M. A. Shakoor**, A. Kumar "Microwave-assisted synthesis of benzo-fused seven-membered azaheterocycles" *Mini Review in Organic Chemistry* **2014**, *11*, 55-72.

List of Presentations in Conferences *[A-2]*

Oral:

1. **S. M A. Shakoor**, R. Sakhuja "Ruthenium(II)-catalyzed regioselective *ortho*-amidation of imidazo-heterocycles with isocyanates" at NVCR-2017 organized by Department of Chemistry, The IIS University, Jaipur: January 18-19, 2017. (***Received first prize***)

Poster:

1. **S. M A. Shakoor**, D. S. Agarwal, R. Sakhuja "Copper catalyzed direct aerobic double-oxidative cross-dehydrogenative coupling of imidazo-heterocycles with aryl acetaldehydes: an articulate approach for dicarbonylation at C-3 position" at OCSD-2016 organized by Department of Chemistry, Birla Institute of Technology and Science Pilani, Pilani Campus, Pilani: August 29-30, 2016.
2. **S. M A. Shakoor**, D. S. Agarwal, R. Sakhuja "Copper catalyzed direct aerobic double-oxidative cross-dehydrogenative coupling of imidazo-heterocycles with aryl acetaldehydes: an articulate approach for dicarbonylation at C-3 position" at NDCS-2015 organized by Department of chemistry, Birla Institute of Technology and Science Pilani, Pilani Campus, Pilani: October 16-18, 2015.
3. **S. M A. Shakoor**, A Kumar, R. Sakhuja "Imidazolium-supported benzotriazole: An efficient and recoverable activating reagent for amide, ester and thioester bond formation in water" at NFCFA-2015 organized by Department of Chemistry, Birla Institute of Technology and Science Pilani, Goa Campus, Goa: December 18-19, 2015.
4. **S. M A. Shakoor**, A Kumar, R. Sakhuja "Imidazolium-supported benzotriazole: An efficient and recoverable activating reagent for amide, ester and thioester bond formation in water" at 21st ISCBC-2015 organized by Department of Chemistry, CDRI Lucknow, Lucknow: February 25-28, 2015.
5. **S. M A. Shakoor**, A Kumar, R. Sakhuja "Microwave-assisted expedite synthesis of 2-phenylimidazo[1,2-*a*]pyridylquinoxalin-2(1*H*)-ones' at 19th ISCBC-2013 organized by Department of Chemistry, Mohanlal Sukhadia University, Udaipur: March 2-5, 2013.

Brief Bibliography of the Candidate *[A-3]*

S M Abdul Shakoor obtained his master degree in Organic Chemistry from VIT University, Vellore, India during 2009-11. In June 2012, he cleared the Joint CSIR-UGC NET for Lectureship (LS) by CSIR, New Delhi. He joined Department of Chemistry, BITS Pilani, Pilani Campus for Ph.D. program in august 2012 under the guidance of Dr. Rajeev Sakhuja with the financial assistance ship from BITS Pilani. However in January 2014 he has been selected for UGC-BSR fellowship. During the tenure of Ph.D he was actively involved in the synthesis and functionalization of imidazo[1,2-*a*]pyridines skeletons. In addition, he has also developed a novel imidazolium-supported reagent which was efficiently used in selected organic transformations. He has published eight research articles in peer reviewed international journals and presented papers in three national and three international conferences.

His main research interest lies in the development of new methods towards the formation of nascent chemical bonds using novel C−H activation/functionalizations strategies under metal-catalyzed and metal free conditions.

Brief Bibliography of the Supervisor *[A-4]*

Dr. Rajeev Sakhuja obtained his M.Phil. and Ph.D. degrees from the Department of Chemistry, University of Delhi, New Delhi in the area of heterocyclic chemistry. Following this, he pursued his postdoctoral research with Prof. Alan R. Katritzky at the Center of Heterocyclic Compounds, University of Florida, Gainesville, and thereafter with Professor Raymond Booth at Department of Medicinal Chemistry, University of Florida from 2009-2012. After returning, he joined the Department of Chemistry, BITS Pilani, Pilani Campus as an Assistant Professor in March 2012. Following Ph.D., he has ten years of post-PhD research experience in the broad field of organic synthesis. Dr. Sakhuja is presently leading an independent research group at Birla Institute of Technology & Science, Pilani where his current area of research interests lies in the development of metal-catalyzed and metal-free strategies for the functionalization of heterocycles, synthesis of biologically important heterocyclic scaffolds, along with the development of organic materials with sensing and gelation abilities. His effective contribution in these areas has fetched him 39 research articles, 4 reviews in peer-reviewed journals of international repute. He has successfully completely four sponsored projects funded by government agencies (DST & UGC), and private organization (BITS seed grant & additional research grant) in the past five years.